ISSN 0021-9673

VOL. 523 DECEMBER 7, 1990

COMPLETE IN ONE ISSUE

including

7th Int. Symp. on Preparative Chromatography, Ghent, April 8–11, 1990

JOURNAL OF CHROMATOGRAPHY

INTERNATIONAL JOURNAL ON CHROMATOGRAPHY, ELECTROPHORESIS AND RELATED METHODS

ELSEVIER

JOURNAL OF CHROMATOGRAPHY

Scope. The *Journal of Chromatography* publishes papers on all aspects of chromatography, electrophoresis and related methods. Contributions consist mainly of research papers dealing with chromatographic theory, instrumental development and their applications. The section *Biomedical Applications*, which is under separate editorship, deals with the following aspects: developments in and applications of chromatographic and electrophoretic techniques related to clinical diagnosis or alterations during medical treatment; screening and profiling of body fluids or tissues with special reference to metabolic disorders; results from basic medical research with direct consequences in clinical practice; drug level monitoring and pharmacokinetic studies; clinical toxicology; analytical studies in occupational medicine.

Submission of Papers. Manuscripts (in English; *four* copies are required) should be submitted to: Editorial Office of *Journal of Chromatography*, P.O. Box 681, 1000 AR Amsterdam, The Netherlands, Telefax (+31-20) 5862 304, or to: The Editor of *Journal of Chromatography, Biomedical Applications*, P.O. Box 681, 1000 AR Amsterdam, The Netherlands. Review articles are invited or proposed by letter to the Editors. An outline of the proposed review should first be forwarded to the Editors for preliminary discussion prior to preparation. Submission of an article is understood to imply that the article is original and unpublished and is not being considered for publication elsewhere. For copyright regulations, see below.

Subscription Orders. Subscription orders should be sent to: Elsevier Science Publishers B.V., P.O. Box 211, 1000 AE Amsterdam, The Netherlands, Tel. (+31-20) 5803 911, Telex 18582 ESPA NL, Telefax (+31-20) 5803 598. The *Journal of Chromatography* and the *Biomedical Applications* section can be subscribed to separately.

Publication. The *Journal of Chromatography* (incl. *Biomedical Applications*) has 37 volumes in 1990. The subscription prices for 1990 are:

J. Chromatogr. (incl. *Cum. Indexes, Vols. 451–500*) + *Biomed. Appl.* (Vols. 498–534):
Dfl. 6734.00 plus Dfl. 1036.00 (p.p.h.) (total *ca.* US$ 4365.25)

J. Chromatogr. (incl. *Cum. Indexes, Vols. 451–500*) only (Vols. 498–524):
Dfl. 5616.00 plus Dfl. 756.00 (p.p.h.) (total *ca.* US$ 3579.75)

Biomed. Appl. only (Vols. 525–534):
Dfl. 2080.00 plus Dfl. 280.00 (p.p.h.) (total *ca.* US$ 1325.75).

Our p.p.h. (postage, package and handling) charge includes surface delivery of all issues, except to subscribers in Argentina, Australia, Brasil, Canada, China, Hong Kong, India, Israel, Malaysia, Mexico, New Zealand, Pakistan, Singapore, South Africa, South Korea, Taiwan, Thailand and the U.S.A. who receive all issues by air delivery (S.A.L. — Surface Air Lifted) at no extra cost. For Japan, air delivery requires 50% additional charge; for all other countries airmail and S.A.L. charges are available upon request. Back volumes of the *Journal of Chromatography* (Vols. 1–497) are available at Dfl. 195.00 (plus postage). Claims for missing issues will be honoured, free of charge, within three months after publication of the issue. Customers in the U.S.A. and Canada wishing information on this and other Elsevier journals, please contact Journal Information Center, Elsevier Science Publishing Co. Inc., 655 Avenue of the Americas, New York, NY 10010, U.S.A., Tel. (+1-212) 633 3750, Telefax (+1-212) 633 3990.

Abstracts/Contents Lists published in Analytical Abstracts, Biochemical Abstracts, Biological Abstracts, Chemical Abstracts, Chemical Titles, Chromatography Abstracts, Clinical Chemistry Lookout, Current Contents/Life Sciences, Current Contents/Physical, Chemical & Earth Sciences, Deep-Sea Research/Part B: Oceanographic Literature Review, Excerpta Medica, Index Medicus, Mass Spectrometry Bulletin, PASCAL-CNRS, Pharmaceutical Abstracts, Referativnyi Zhurnal, Research Alert, Science Citation Index and Trends in Biotechnology.

See inside back cover for Publication Schedule, Information for Authors and information on Advertisements.

0021-9673/90/$03.50

This issue is printed on acid-free paper.

Printed in The Netherlands

CONTENTS

(Abstracts/Contents Lists published in Analytical Abstracts, Biochemical Abstracts, Biological Abstracts, Chemical Abstracts, Chemical Titles, Chromatography Abstracts, Current Contents/Life Sciences, Current Contents/Physical, Chemical & Earth Sciences, Deep-Sea Research/Part B: Oceanographic Literature Review, Excerpta Medica, Index Medicus, Mass Spectrometry Bulletin, PASCAL-CNRS, Referativnyi Zhurnal, Research Alert and Science Citation Index)

7TH INTERNATIONAL SYMPOSIUM ON PREPARATIVE CHROMATOGRAPHY, GHENT, APRIL 8–11, 1990

(Continued overleaf)

In articles with more than one author, the name of the author to whom correspondence should be addressed is indicated in the article heading by a 6-pointed asterisk (*)

JOURNAL OF CHROMATOGRAPHY
VOL. 523 (1990)

JOURNAL *of* CHROMATOGRAPHY

INTERNATIONAL JOURNAL ON CHROMATOGRAPHY,
ELECTROPHORESIS AND RELATED METHODS

ELSEVIER
AMSTERDAM — OXFORD — NEW YORK — TOKYO

J. Chromatogr., Vol. 523 (1990)

0021-9673/90/$03.50

Printed in The Netherlands

SYMPOSIUM ISSUE

SEVENTH INTERNATIONAL SYMPOSIUM ON PREPARATIVE CHROMATOGRAPHY

Ghent (Belgium), April 8–11, 1990

SYMPOSIUM VOLUMES

Guest Editor

M. VERZELE

(Ghent, Belgium)

Symposium participants.

CONTENTS

7TH INTERNATIONAL SYMPOSIUM ON PREPARATIVE CHROMATOGRAPHY, GHENT, APRIL 8–11, 1990

Journal of Chromatography, 523 (1990) 1–10
Elsevier Science Publishers B.V., Amsterdam

CHROM. 22 657

Dependence of the production rate on the relative retention of two components in preparative chromatography

SADRODDIN GOLSHAN-SHIRAZI and GEORGES GUIOCHON*

* *Department of Chemistry, University of Tennessee, Knoxville, TN 37996-1600 and Division of Analytical Chemistry, Oak Ridge National Laboratory, Oak Ridge, TN 37831-6120 (U.S.A.)*

ABSTRACT

The maximum possible production rate which can be obtained with a given chromatographic system, under optimized conditions, increases approximately as the third power of $(\alpha - 1)/\alpha$. The optimum conditions themselves depend also on the relative retention. In contrast, the production rate of a given column (constant column length, L, and particle size, d_p) increases more slowly, nearly in proportion to the square of $(\alpha - 1)/\alpha$ when the ratio d_p^2/L is lower than its optimum value. These relationships are valid under both touching band and overlapping band conditions.

INTRODUCTION

There has been considerable interest recently in the optimization of the experimental conditions for maximum production rate, and hence in theoretical investigations of the dependence of the production rate on the parameters of a separation [1–6]. As in all chromatographic applications, the most critical factor controlling the difficulty of a separation is $\Delta(\Delta G^0) = \Delta G_2^0 - \Delta G_1^0$, the difference between the molar Gibbs free energies ΔG_1^0 and ΔG_2^0 of transfer from one phase to the other of the chromatographic system used, for the two components of a mixture. In linear chromatography [7]

$$\Delta(\Delta G^0) = -RT \ln \alpha \tag{1}$$

where α is the relative retention of the two components, *i.e.*, the ratio of their column capacity factors at infinite dilution, $\alpha = k'_{0,2}/k'_{0,1}$, or the ratio of the slopes of their equilibrium isotherms at the concentration origin, $\alpha = a_2/a_1$, and R and T are the ideal gas constant and the temperature, respectively. Although preparative chromatography is carried out at high concentrations, theory shows that the production rate depends on α and on the column saturation capacities for the two components [5,8,9].

Admittedly, most mixtures whose separation is of practical interest contain more than two components. A separation procedure may involve several successive chromatographic steps using different modes of chromatography. In addition to the separation of enantiomers for which it is directly relevant, the theory of binary mixture

0021-9673/90/$03.50

separations can be applied to the most important pairs of components of the mixture, including those involving the main compound to be purified and the impurities eluted close by. It gives critical information regarding the need for a multi-step procedure. Therefore, it is important to distinguish two separate problems, the dependence of the production rate on the relative retention of two components on a given column and the dependence of the maximum possible production rate on α. In the former case, the column characteristics are given. In the latter, these characteristics result from the optimization procedure and vary with α.

We briefly review here the relevant results. In both instances two separation objectives are discussed, touching bands and overlapping bands. The former permits a nearly total recovery yield, whereas the latter allows a higher production rate, but at the cost of recycling part of the throughput. In all the following, for the sake of simplicity, we make two assumptions. First, we assume with Knox and Pyper [1] that the reduced plate height equation of the column is $h = Cv$. It has shown previously [5,9,10] that, in order to achieve the maximum production rate with any constraint of recovery yield or fraction purity, preparative columns should always be operated at high reduced velocities (*i.e.*, at velocities between one and two orders of magnitude higher than the velocity providing the maximum column efficiency). Hence this assumption provides a very good and useful approximation. If needed, a simple numerical calculation permits the determination of the optimum conditions with any plate-height equation [5,9,10]. Second, we assume that the equilibrium isotherms of the two components follow the competitive Langmuir isotherm model [5,9,10].

MAXIMUM PRODUCTION RATE

In this section, we summarize previous results relating the maximum production rate to the column saturation capacities and α in the two extreme strategies, touching bands and overlapping bands. The column length, the particle size and the mobile phase velocity are optimized in both instances.

Touching bands

We have shown in a previous paper that the maximum production rate of the second component, Pr_2 (moles per unit time), is given by the following equation (ref. 9, eqn. 38):

$$\frac{Pr_2}{(1-\varepsilon)S} = (\text{constant}_1)\left[\frac{\alpha-1}{\alpha}\right]^3 \frac{q_{s,2}}{1+k'_{0,2}} \tag{2}$$

where $q_{s,2}$ is the ratio a_2/b_2 of the two coefficients of the Langmuir isotherm of the second component. $q_{s,2}$ is the saturation capacity for the second component. The column saturation capacity is the product of $q_{s,2}$ and the amount of packing material in the column. In this equation, ε is the packing porosity and S the column cross-sectional area. The constant is independent of the isotherm parameters, but depends on the mass transfer parameters (molecular diffusion coefficient of solutes, mobile phase viscosity, C coefficient of the plate-height equation) and on the maximum pressure available. Eqn. 2 is correct if we ignore the competitive behavior of the two-component

adsorption, as was done by Knox and Pyper [1]. It remains a good approximation if we assume that the equilibrium isotherms of the two components are given by the competitive Langmuir isotherm model, as we have done in our work. The value of the constant is different in the two cases, however. In the case where competitive interactions are neglected, it is

$$(\text{constant}_1) = \frac{1}{24}\sqrt{\frac{\Delta P D_m}{3\phi\eta C}} \tag{2a}$$

where ΔP is the maximum pressure available, D_m the molecular diffusion coefficient of the second component, ϕ the column-specific permeability, η the mobile phase viscosity and C the third coefficient of the plate-height equation. In the case where competitive interactions are taken into account the constant has a different numerical coefficient.

Eqn. 2 assumes that the cycle time, t_c, is equal to $t_{R0.2} - t_0$, where $t_{R0.2}$ and t_0 are the limiting retention time at infinite dilution and the hold-up time, respectively. With the value assumed by Knox and Pyper [1] and by Snyder *et al.* [6], $t_c = t_{R0,2}$, the equation becomes

$$\frac{Pr_2}{(1-\varepsilon)S} = (\text{constant}_1)\left[\frac{\alpha - 1}{\alpha}\right]^3 \frac{q_{s,2}k'_{0,2}}{(1 + k'_{0,2})^2} \tag{3}$$

This equation provides for the dependence of the production rate on the isotherm parameters, and more specifically on the relative retention and the limit column capacity factor of the last component.

Overlapping bands

In a previous paper [4], we showed that the production rate is given by

$$\frac{Pr_2}{(1-\varepsilon)S} = \frac{R_2 q_{s,2} L_{f,2} u t_0}{t_c} \tag{4}$$

where u is the mobile phase velocity and $L_{f,2}$ is the loading factor for the second component, *i.e.*, the ratio of the amount of second component in the sample to the column saturation capacity. The recovery yield, R_2, is near 60% under the experimental conditions giving the maximum production rate, regardless of α [3,5]. The optimum loading factor for the second component is given by [4]

$$L_{f,2} = \frac{1}{1+y}\left[\frac{\alpha - 1}{\alpha(1-x)}\right]^2 \tag{5}$$

where

$$x = \sqrt{\frac{1 - Pu_2}{Pu_2 \alpha r_1}} \tag{6a}$$

and

$$y = \frac{q_{s,2} r_1}{\alpha q_{s,1}} \approx \frac{q_{s,2} C_{0,1}}{\alpha q_{s,1} C_{0,2}} \approx \frac{L_{f,1}}{\alpha L_{f,2}} \tag{6b}$$

Pu_2 is the required purity of the more retained component and r_1 is almost equal to the ratio of the concentrations of the two components in the feed, $C_{0,1}/C_{0,2}$. Eqn. 5 has been derived for the ideal model (infinitely efficient column). It has been shown that it remains valid also in the semi-ideal model, for real columns [5]. Although the use of the sample size given by eqn. 5 permits the achievement of the maximum possible production rate for a given purity requirement, the recovery yield will be merely *ca.* 60% [5], which may be considered too low. Higher recovery yields may be achieved by multiplying the sample size by $0.60/R_2$, where R_2 is the required recovery yield [10].

The linear velocity of the mobile phase is related to the column efficiency through the plate-height equation ($h = Cv$, with $H = hd_p$ and $v = ud_p/D_m$). On the other hand, it is related to the pressure drop, ΔP, the mobile phase viscosity, η, and the specific permeability, ϕ, by

$$u = \frac{\Delta P d_p^2}{\phi \eta L} \tag{7}$$

This leads to the following equation:

$$N_0 = \frac{L}{C v d_p} = \frac{L D_m}{C u d_p^2} = \frac{\phi \eta D_m}{\Delta P C} \left[\frac{L}{d_p^2}\right]^2 \tag{8}$$

where N_0 is the column efficiency under linear conditions. Elimination of L/d_p^2 between eqns. 7 and 8 gives

$$u = \sqrt{\frac{\Delta P D_m}{\phi \eta C N_0}} \tag{9}$$

In analytical chromatography, the resolution between two bands is related to the number of theoretical plates, the relative retention and the column capacity factor by the classical Purnell equation:

$$R_s = \frac{\sqrt{N_0}}{4} \cdot \frac{\alpha - 1}{\alpha} \cdot \frac{k'_{0,2}}{1 + k'_{0,2}} \tag{10}$$

Combination of eqns. 9 and 10 gives

$$u = (\text{constant}_2) \cdot \frac{\alpha - 1}{R_s \alpha} \cdot \frac{k'_{0,2}}{1 + k'_{0,2}} \tag{11}$$

with $(\text{constant}_2) = 0.25\sqrt{(\Delta P D_m)/(\phi \eta C)}$. Combination of eqns. 4–6 and 11, with a cycle time equal to $t_{R0,2} - t_0$, gives

$$\frac{Pr_2}{(1-\varepsilon)S} = (\text{constant}_2)\left(\frac{\alpha-1}{\alpha}\right)^3 \frac{R_2 q_{s,2}}{R_s(1-x)^2(1+k'_{0,2})(1+y)} \tag{12a}$$

where R_s is the resolution between the bands of an infinitely dilute sample of the feed. The difference with the touching band case, previously discussed, is that R_s, x and y depend on α [5]. The dependence of x is especially strong when the relative concentration of the second component is high (*i.e.*, under conditions where the displacement effect predominates) [4].

If the cycle time is equal to $t_{R0,2}$, we have

$$Pr_2 = (\text{constant}_2)\left(\frac{\alpha-1}{\alpha}\right)^3 \frac{R_2 k'_{0,2} q_{s,2}}{R_s(1-x)^2(1+k'_{0,2})^2(1+y)} \tag{12b}$$

Eqns. 12a and 12b are valid for overlapping bands, with or without a recovery yield constraint. However, the value of the constant and of the necessary resolution depend on the required recovery yield. In the case of a required yield R_2^*, it becomes $(\text{constant}_2 \cdot 0.6/R_2^*)$.

PRODUCTION RATE OF A GIVEN COLUMN

In many instances, the optimum column cannot be used, either because it is unavailable or, more generally, because it is impractical to order a new column for each new separation. The relevant equations can be summarized as follows.

Touching bands

In a previous paper on this topic, we have shown that the production rate is given by the following equation (ref. 9, eqn. 21):

$$Pr_2 = (\text{constant}_3)\frac{u q_{s,2}(\alpha-1)^2}{k'_{0,2}}\left\{2 - \frac{1}{\alpha} - \sqrt{4\cdot\frac{\alpha-1}{\alpha} + \frac{16}{N_0}\left[\frac{k'_{0,2}+1}{k'_{0,2}(\alpha-1)}\right]^2}\right\} \tag{13}$$

In this equation, N_0 is given by eqn. 8. Eqn. 13 is valid only for moderate values of the optimum loading factor (exactly when $L_{f,2}$ is negligible compared to $\sqrt{L_{f,2}}$), which usually corresponds to cases when α is close to unity. Eqn. 13 takes the competitive interaction of the two components with the stationary phase into account by using competitive Langmuir isotherms in the derivation. If we neglect this interaction with Knox and Pyper [1], we have (see ref. 9, eqn. 23):

$$\frac{Pr_2}{(1-\varepsilon)S} = \frac{u q_{s,2}}{4k'_{0,2}}\left[\left(\frac{\alpha-1}{\alpha}\right)^2 - \frac{16\left(\frac{k'_{0,2}+1}{k'_{0,2}}\right)^2}{N_0}\right] \tag{14}$$

From the Purnell equation [11], we see that the production rate is positive and different from zero only if the analytical resolution is larger than unity. Given the assumptions of the touching band case, this is an expected result.

We have shown previously, in agreement with Knox and Pyper [1], that there is an optimum value for the ratio d_p^2/L as long as the HETP equation is limited to its third term ($h = Cv$; *cf.*, eqn. 8) [5,9]. If the column characteristics (*i.e.*, its length and the average particle size of the packing) are such that the value of the ratio d_p^2/L is smaller than the optimum value, we cannot operate that column at the optimum mobile phase velocity: the maximum pressure available is not high enough. In this case, the velocity is given by eqn. 7, the plate number, N_0, is given by eqn. 8 and, according to eqns. 13 and 14, the production rate exhibits a primary dependence on $[(\alpha - 1)/\alpha]^2$. Eqns. 13 and 14, however, include corrective terms which may lead to a different dependence in some instances.

If, on the contrary, the column characteristics are such that the ratio d_p^2/L is larger than the optimum value for maximum production rate, there is an optimum mobile phase velocity. This optimum, however, corresponds to an inlet pressure which is lower than the maximum available. The production rate increases nearly in proportion to $[(\alpha - 1)/\alpha]^3$. The decision as to whether to change the column depends in part on the possible gain in production rate. This gain is approximately proportional to the square root of the ratio of the maximum available pressure to the operating pressure of the column considered.

Overlapping bands

Eqn. 4 is also valid in this case if we use the optimum value of the sample size, corresponding to the maximum production rate possible with the given column. Combination with eqn. 5 and a cycle time of $t_{R0,2} - t_0$, gives

$$\frac{Pr_2}{(1-\varepsilon)S} = \frac{uR_2q_{s,2}}{(1+y)k'_{0,2}}\left[\frac{\alpha - 1}{\alpha(1-x)}\right]^2 \tag{15}$$

As the column is given, L and d_p are now constant. If these values are such that the ratio d_p^2/L is smaller than the optimum value (corresponding to the maximum possible production rate), we cannot operate this column at its optimum velocity: the pressure would exceed the maximum acceptable. The velocity is given by eqn. 7. Then the production rate is approximately proportional to $[(\alpha - 1)/\alpha]^2$, because x, y and R_2 depend also on α.

If the column length and the particle size are such that the ratio d_p^2/L is larger than the optimum value, the column can be operated at its optimum velocity, but this velocity corresponds to a pressure lower than the maximum available. The maximum production rate which can be obtained with this column increases approximately in proportion to $[(\alpha - 1)/\alpha]^3$. As the column is operated at a pressure lower than the maximum possible, the production rate achieved is not the largest possible. The decision regarding whether the column should be changed or not depends on the economics of the choice.

DISCUSSION

Whether a touching band or an overlapping band strategy is adopted, the production rate which can be achieved with a given column is proportional at least to the square of $(\alpha - 1)/\alpha$ and sometimes to the cube of this ratio. This is a strong dependence [5].

In contrast, the maximum production rate which can be achieved with an optimized column, designed to be operated at the maximum pressure available, increases still more rapidly (see Table IV in ref. 5), as the third power of $(\alpha - 1)/\alpha$, a result which happens to be in agreement with previous work [6]. This means that the maximum production rate doubles when α is increased from 1.1 to 1.13 or from 1.2 to

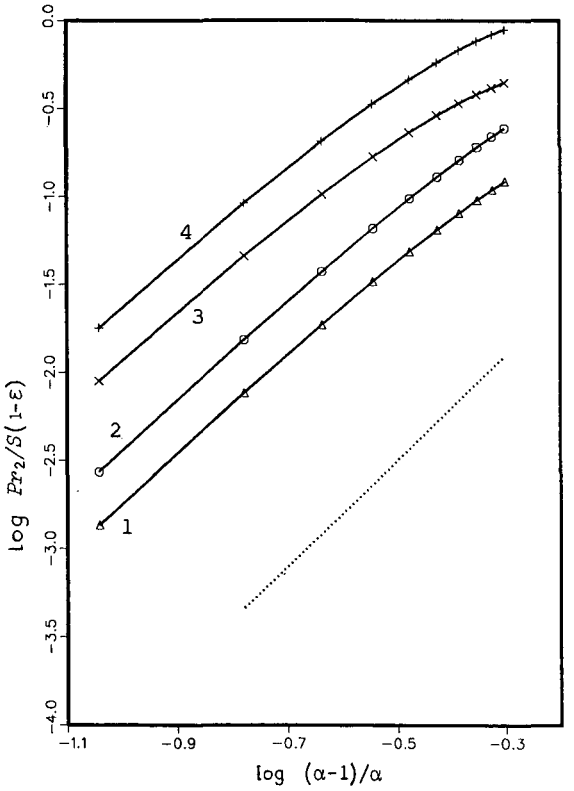

Fig. 1. Plot of the logarithm of the maximum possible production rate per unit column cross-sectional area $[Pr_2/S(1 - \varepsilon)]$ with a given chromatographic phase system *versus* the logarithm of $(\alpha - 1)/\alpha$. The column length and the optimum mobile phase velocity are optimized for each value of α. (The values of α corresponding to the abscissa markers, *i.e.*, $\log[(\alpha - 1)/\alpha]$ equal to -1.1, -0.9, -0.7, -0.5 and -0.3, are 1.086, 1.144, 1.25, 1.46 and 2.0, respectively.) Relative composition of the feed, 1:9; phase ratio, 0.25; column capacity factor, $k'_{0,1} = 6$; column saturation capacity, $q_{s,1} = q_{s,2} = 10$; eluent viscosity, $\eta = 1$ cP; molecular diffusion coefficient, $D_m = 1 \cdot 10^{-5}$ cm^2/s; plate-height equation, $h = 0.1v$; cycle time, $t_{R0,2} - t_0$. Curve 1: touching bands, $\Delta P = 50$ atm. Curve 2: touching bands, $\Delta P = 200$ atm. Curve 3: overlapping bands, $\Delta P = 50$ atm. Required degree of purity: 99%. The recovery yield is about 60%. Curve 4: overlapping bands, $\Delta P = 200$ atm. Required degree of purity: 99%. The recovery yield is about 60%. Dotted line: a straight line with a slope equal to 3.

1.27 or from 1.4 to 1.56. The production rate is increased ten-fold if α increases from 1.05 to 1.11 or from 1.1 to 1.24 or from 1.2 to 1.56. If an adjustment of the mobile phase composition permits an increase in α from 1.1 to 1.3, the production rate can be multiplied by 16. These numbers illustrate how the choice of the stationary phase and of the composition of the mobile phase are of paramount importance.

The production rates and their relative retention dependence are different in the four situations discussed here. To illustrate these differences, Figs. 1 and 2 show plots of the production rate versus the ratio $(\alpha - 1)/\alpha$ in double logarithmic coordinates. A production rate dependence on the square or cube of this ratio would result in straight lines with slopes of 2 or 3, respectively, as indicated by the dotted line in Fig. 1 and the two dotted lines in Fig. 2. The actual dependences are as follows.

In Fig. 1, we have plotted the maximum production rate which can be achieved with a given chromatographic system (*i.e.*, for a given value of α) *versus* the ratio

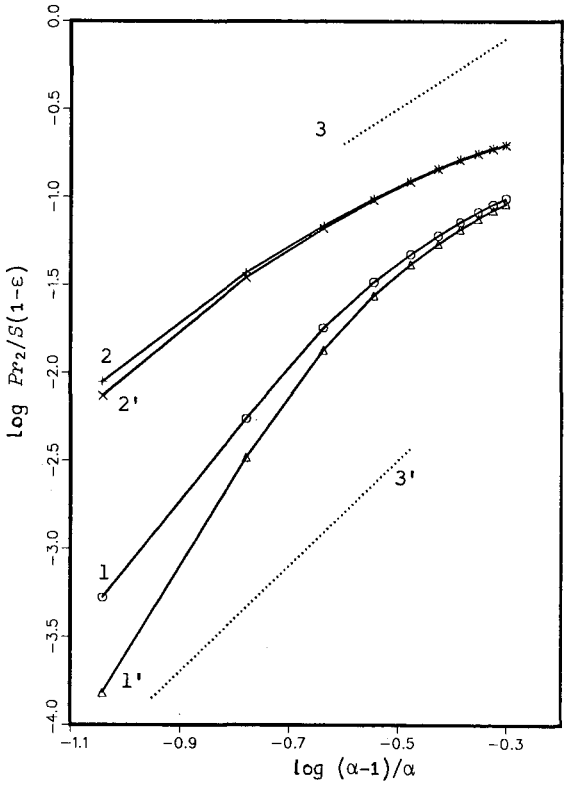

Fig. 2. Plot of the logarithm of the maximum production rate per unit column cross-sectional area $[Pr_2/S(1 - \varepsilon)]$ with a given chromatographic phase system *versus* the logarithm of $(\alpha - 1)/\alpha$ for a given column. Same conditions as in Fig. 1, except column length 30 cm and particle size 20 μm. Curve 1: touching bands, $\Delta P = 50$ atm. Plate-height equation: $h = 0.1\nu$. Curve 1′: touching bands, $\Delta P = 50$ atm. Plate-height equation: $h = 2/\nu + \nu^{0.33} + 0.1\nu$. Curve 2: overlapping bands, $\Delta P = 50$ atm. Required degree of purity: 99%. Plate-height equation: $h = 0.1\nu$. Curve 2′ = overlapping bands, $\Delta P = 50$ atm. Required degree of purity: 99%. Plate-height equation: $h = 2/\nu + \nu^{0.33} + 0.1\nu$. Dotted lines: 3, a straight line with a slope equal to 2; 3′, a straight line with a slope equal to 3.

$(\alpha - 1)/\alpha$. In this case, the column length and the mobile phase velocity are optimized for each value of α. We have considered both the overlapping and the touching band conditions. For each condition, two curves correspond to two different values of the inlet pressure, 50 and 200 atm, respectively. Eqns. 4 and 13 show that for each condition, the maximum production rate is proportional to the velocity used, whereas eqn. 9 shows that this velocity is proportional to the square root of the maximum pressure available. Hence the two curves which correspond to the same condition are shifted by log 2. As can be seen in Fig. 1, the production rate increases nearly as the cube of $(\alpha - 1)/\alpha$ at values of α close to one, and more slowly when α becomes large.

In Fig. 2, we have plotted the maximum production rate which can be achieved with a given column. The choice of the exact conditions (*i.e.*, $L = 30$ cm and $d_p = 20$ μm) is more arbitrary than in the previous instance. In Fig. 2, we show two examples, corresponding to touching band (curves 1 and 1′) and overlapping band (curves 2 and 2′) conditions. In both instances we carried out the calculations using the complete Knox plate-height equation [12] and a simplified plate-height equation. The difference between the results obtained with these two plate-height equations is very small, except at values of the relative retention close to unity, in the touching band case. This is because at values of α close to 1 a high column efficiency is needed and the reduced velocity is low, *e.g.*, 12 for $\alpha = 1.10$.

We observe in Fig. 2 that in both the touching and the overlapping band cases, the production rate at low values of α increases more rapidly with increasing α than what would correspond to the square of $(\alpha - 1)/\alpha$ (see the dotted lines). This is because in this region the column characteristics are such that d_p^2/L is larger than the optimum value of this ratio for the maximum production rate. We must operate the column at a pressure which is below the maximum allowed by the equipment. When α increases, the optimum value of the ratio d_p^2/L increases, the column can be operated at an increasingly high velocity, corresponding to an inlet pressure closer and closer to the maximum available and the production rate increases very rapidly. The dimensions of the column chosen for this discussion give a value of d_p^2/L which is optimum for a relative retention equal to *ca.* 1.4. For this value, curves 1 and 2 in Fig. 2 are tangential to curves 1 and 3 in Fig. 1, respectively. For higher values of α, the ratio d_p^2/L becomes smaller than the optimum, the column must be operated at the maximum available pressure, but the corresponding velocity is below the optimum value and the production rate increases more and more slowly with increasing value of α, approximately as $[(\alpha - 1)/\alpha]^2$.

These results are only valid, however, as far as one critical assumption remains satisfied. We have assumed all along that the column saturation capacity is unchanged by the adjustments made to the composition of the mobile phase. When we compare the production rates for different separations, we tend to emphasize the role of α and to play down the role of the column saturation capacity. Both are important. For example, in the separation of enantiomers on chiral phases, we have observed that the production rate is orders of magnitude smaller than that achieved with less closely related isomers with a comparable relative retention [13]. The column saturation capacity for the chiral recognition sites of immobilized bovine serum albumin is very much smaller than the capacity for the non-specific interaction sites. There are reported cases when the column saturation capacity and the relative retention of proteins vary with the mobile phase composition in opposite directions [14].

Obviously, in such cases the optimum mobile phase composition for preparative chromatography will be different from that for analytical separation.

Finally, we know that most users of preparative chromatography prefer normal-phase to reversed-phase chromatography. The capacity of the mobile phase is higher with the former, because the solubility of most organics is higher in organic solvents than in water-rich solutions. The use of an additive which causes a large increase in the mobile phase solubility of the feed components while decreasing slightly the relative retention may lead to a higher production rate.

ACKNOWLEDGEMENTS

This work was supported in part by Grant CHE-8901382 of the National Science Foundation and by the cooperative agreement between the University of Tennessee and the Oak Ridge National Laboratory. We acknowledge support of our computational effort by the University of Tennessee Computing Center.

REFERENCES

1 J. H. Knox and H. M. Pyper, *J. Chromatogr.*, 363 (1986) 1.
2 G. Guiochon and H. Colin, *Chromatogr. Forum*, 1, No. 3 (1986) 21.
3 S. Ghodbane and G. Guiochon, *Chromatographia*, 26 (1988) 53.
4 S. Golshan-Shirazi and G. Guiochon, *Anal. Chem.*, 61 (1989) 1276.
5 S. Golshan-Shirazi and G. Guiochon, *Anal. Chem.*, 61 (1989) 1368.
6 L. R. Snyder, J. W. Dolan and G. B. Cox, *J. Chromatogr.*, 483 (1989) 63.
7 B. L. Karger, *Anal. Chem.*, 39 (1967) 24A.
8 A. W. J. de Jong, H. Poppe and J. C. Kraak, *J. Chromatogr.*, 148 (1978) 127.
9 S. Golshan-Shirazi and G. Guiochon, *J. Chromatogr.*, 517 (1990) 229.
10 S. Golshan-Shirazi and G. Guiochon, *J. Chromatogr.*, in press.
11 J. H. Purnell, *J. Chem. Soc.*, (1960) 1268.
12 J. H. Knox, *J. Chromatogr. Sci.*, 15 (1977) 352.
13 S. Jacobson, S. Golshan-Shirazi and G. Guiochon, *J. Am. Chem. Soc.*, 112 (1990) 6492.
14 J.-X. Huang, J. V. H. Schudel and G. Guiochon, *J. Chromatogr. Sci.*, in press.

Journal of Chromatography, 523 (1990) 11–21
Elsevier Science Publishers B.V., Amsterdam

CHROMSYMP. 1998

Frontal chromatographic techniques in preparative chromatography

DEREK A. HILL*, PAUL MACE and DONALD MOORE
Chemical Development Laboratories, The Wellcome Foundation Ltd., Temple Hill, Dartford, Kent DA1 5AH (U.K.)

ABSTRACT

This paper describes the use of frontal chromatography as a preparative method and its application to large-scale purifications, demonstrating that it can provide a useful alternative to the more familiar elution and displacement modes of operation of a chromatographic column.

INTRODUCTION

Although the operation of a chromatographic column in the frontal mode was first described by Tiselius [1] in 1943, the method does not appear to have been developed as a preparative technique. Tiselius [1] defined three distinct modes in which a chromatographic column may be operated, namely elution, displacement and frontal. Whilst elution chromatography has found widespread use in preparative chromatography and displacement chromatography has, more recently, been revived as a preparative technique by Horváth *et al.* [2] and by Verzele *et al.* [3], frontal chromatography appears to have been largely ignored. Guiochon and Katti [4] suggested that this may be attributable to the method not appearing well suited to the preparation of pure compounds. However, although the method is not universally applicable, in those cases where it can be applied, it provides a cost-effective alternative to either elution or displacement.

THEORY

Consider a chromatographic system in which the combination of stationary and mobile phases is such that the capacity factor, k', for a particular analyte is infinite. If a solution of the analyte in mobile phase is continuously loaded onto the column the solute will be adsorbed, occupying all adsorption sites sequentially and forming a narrow band which broadens until, when all the adsorption sites on the column are occupied, it begins to elute in a concentration which rapidly increases until it is equal to the loading concentration. The resulting chromatogram will appear as in Fig. 1.

Now consider a three-component mixture, A, B and C, where k' for each

0021-9673/90/$03.50

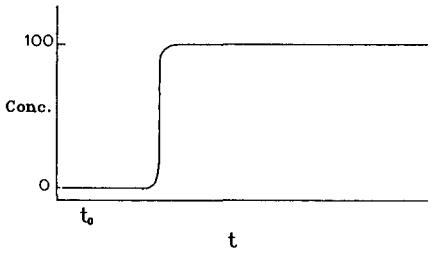

Fig. 1. Frontal chromatogram, single solute. Concentration (Conc.) is expressed as a percentage of the loading concentration. t = Time; t_0 = dead time.

component is infinite, but where the adsorption isotherms of the components are different so that their affinity for the stationary phase is C > B > A. In the ideal case, where the difference between the adsorption isotherms is large, if a solution of the mixture is continuously loaded onto the column, all three components will be adsorbed, but the most strongly adsorbed component C will displace the other components whilst B will displace A, resulting in the formation of three distinct bands. As loading is continued, these bands will broaden until, when all adsorption sites are occupied, component A will start to elute in a concentration equal to the sum of the loading concentration and the amount of A being displaced from the column by B and C. When all component A has been displaced from the column, its elution concentration falls towards its loading concentration and B starts to co-elute in a concentration which rapidly increases until it is equal to the sum of its loading concentration and the amount being displaced from the column by component C. When all component B has been displaced from the column, its elution concentration falls towards its loading concentration and component C starts to co-elute with A and B in a concentration which rapidly increases to its loading concentration *i.e.* the column eluate has the same composition as the solution being loaded. The resulting chromatogram will appear as in Fig. 2 whilst the on-column situation will be as diagramatically represented in Fig. 3. In practice, the difference between the

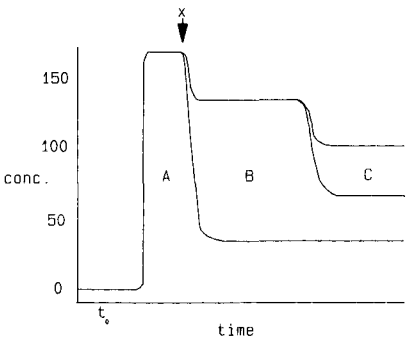

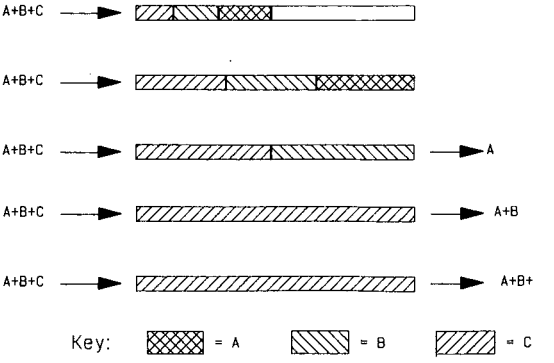

Fig. 2. Frontal chromatogram, three solutes (A, B and C). Concentration is expressed as a percentage of the loading concentration. For point X, see text.

Fig. 3. Diagramatic representation of the on-column situation during the development of a frontal chromatogram with three solutes (A, B and C).

adsorption isotherms is not always large and the analytes compete with each other for the available active sites on the stationary phase, resulting in the boundary between adjacently eluting analytes being less sharp, its sharpness depending upon the relative magnitudes of the adsorption isotherms of the analytes. The material adsorbed onto the column at the point where the composition of the feed solution and the eluate become equal will not be pure component C, but will be contaminated with component B and possibly with some component A, the degree of contamination being determined by the relative magnitudes of the adsorption isotherms. Slow mass transfer kinetics of the system would also lead to the boundaries between successively eluting components being less well defined.

Thus, there exist two situations during the development of a frontal chromatogram which may potentially be exploited in a preparative role:

(1) The least retained component is eluted in a pure form up to the point where the next component starts to elute (point X, Fig. 2)

(2) When most of the adsorption sites on the column are occupied by the most strongly retained component. In this case the column may be washed free of non-adsorbed compounds and the material on the column desorbed into a "stronger" solvent. The relative magnitude(s) of the adsorption isotherms of the most strongly retained component and of the component(s) preceding it will determine the degree of purity obtainable in this case.

Where the required component of a multi-component mixture is not either the most or the least retained component (as is usually the case), it is still possible to use frontal chromatography for its isolation, but a two-column process is required. The mixture is treated as if it consists of three components, the component of interest, all less strongly retained components and all more strongly retained components. The mixture is loaded onto a column until all the component of interest along with the less retained components have eluted, but elution of the more strongly retained components has not yet started. The eluate from the first column is then loaded to a second column until the less strongly retained components have eluted, but the component of interest has not. The component of interest can then be obtained by desorption into a "stronger" solvent. Once the optimum loading for each of the columns has been determined, provided that the composition of the feedstock remains constant and column performance does not deteriorate, the process may be represented thus:

Column 1

(1) Load an aliquot of feedstock solution.

(2) Wash column free of non-adsorbed compounds.

(3) Desorb the more strongly retained components into a "strong" solvent.

(4) Regenerate column with original mobile phase.

Column 2

(1) Load an aliquot of the partially purified feedstock solution.

(2) Wash column free of non-adsorbed compounds.

(3) Desorb the required component into a "strong" solvent.

(4) Regenerate column with the original mobile phase.

The purity obtainable for any given component will depend upon the sharpness of the boundaries between the eluting components of any mixture (*i.e.* the relative magnitude of the adsorption isotherms of the components) and the applicability of the method will thus be limited to those cases where there are large differences in the isotherms or where the purity requirements of the products are less stringent.

EXPERIMENTAL, RESULTS AND DISCUSSION

Instrumentation

A Prep 500 instrument (Waters Assoc., Milford, MA, U.S.A.) was modified by removing the radial compression module and fitting a 250 mm × 75 mm Annular Expansion column (Separations Technology, Wakefield, RI, U.S.A.) or a 500 mm × 50 mm axially compressed column (Amicon, Stonehouse, U.K.). The spare port on the flow splitter of the Prep 500 was connected to a Model 7520 injection valve (Rheodyne, Cotati, CA, U.S.A.) fitted with a 0.5-μl internal sample loop, this valve being connected to an analytical h.p.l.c. instrument comprising a Model 6000A pump and Model 440 detector (Waters Assoc.) and a Model PM8251 chart recorder (Phillips, Cambridge, U.K.), so that by operating the valve an analysis of the eluent could be made at any point during the preparative run (Fig. 4). Larger-scale work was carried out on a Model K'3000 instrument fitted with a 500 mm × 200 mm axially compressed column (Amicon).

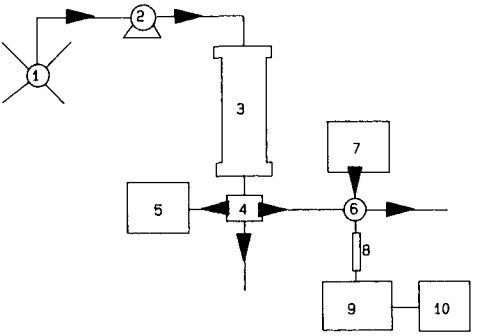

Fig. 4. Diagramatic representation of the preparative instrumentation. 1 = Five-way valve; 2 = preparative pump; 3 = preparative column; 4 = flow splitter; 5 = refractive index detector; 6 = injection valve; 7 = analytical pump; 8 = analytical column; 9 = UV detector; 10 = chart recorder.

Example 1

Deprotection of a protected synthetic pentapeptide using trifluoroacetic acid in the presence of anisole, gave a crude product containing 75% of the required pentapeptide and 25% of related impurities. Additionally, the product contained anisole and anisole derivatives and was obtained as the trifluoroacetate salt. The product was required as the free base with an assay of >96%. A solution of the crude product in water (4%, w/v) was prepared, the pH was adjusted to 5.9 (sodium carbonate) and the solution was extracted with dichloromethane to remove anisole related compounds. The resulting solution (Fig. 5a) was pumped at a flow-rate of 100 $cm^3\ min^{-1}$ onto the 250 mm × 75 mm Annular Expansion column packed with 500 g of 20-45 μm irregular C_8 bonded silica (Amicon), and the column eluate was monitored by high-performance liquid chromatography (HPLC) simply by operating the injection valve when required. Fig. 6 shows the analytical chromatograms collected during the course of a preparative run. At the point where the breakthrough of

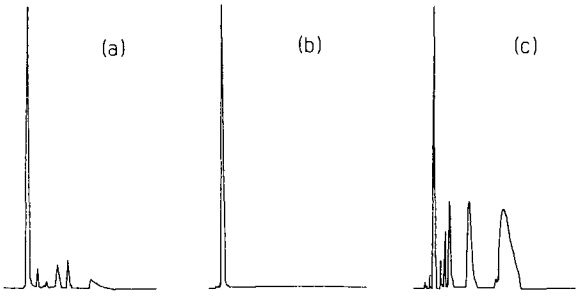

Fig. 5. Analyses of fractions, example 1. (a) Crude product, (b) purified product, (c) methanol solution. Analytical conditions: water–acetonitrile–phosphoric acid (400:100:5), 2.0 cm^3 min^{-1} on 250 mm × 4.6 mm Partisil 5 ODS 3. Detection, UV at 254 nm.

impurities commenced (Fig. 6f), loading was stopped and the column was washed sequentially with water (500 cm^3), methanol (2000 cm^3) and water (500 cm^3) at a flow-rate of 200 cm^3 min^{-1}. The analytical chromatogram Fig. 6h shows a decrease in concentration as the water wash elutes and Fig. 6i shows the methanol wash. The aqueous eluate was examined by HPLC (Fig. 5b), and found to contain product with a purity of >98% whilst the methanol solution (Fig. 5c), contained mainly impurities. Once the optimum load volume had been determined on the first run, subsequent runs were effected by loading the predetermined volume of crude product solution then using the above wash sequence before recommencing loading. This cycle was conveniently carried out by using a five-port valve fitted to the pump inlet to switch between sample, water, methanol and water. Fraction cut points were determined with the aid of the refractive index detector on the Prep 500 instrument. A total of 25 cycles was carried out. The chromatogram of the first preparative run is given in Fig. 7, this having been constructed from the analyses taken during the run. It should be noted that this is not the full frontal chromatogram of the separation, but only of that part which is required to obtain the required purification, the washes being added before complete development of the frontal chromatogram has occurred. An aliquot of the aqueous solution containing purified product was then loaded onto the column so that breakthrough did not occur, the column was washed free of salts with water and the

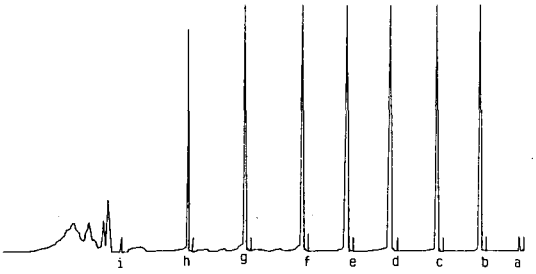

Fig. 6. Monitoring of the eluate from the purification step in example 1. The letters indicate the points at which injections were made during the preparative run. Analytical conditions: water–acetonitrile–phosphoric acid (400:100:5), 4.0 cm^3 min^{-1} on 50 mm × 4.6 mm Hypersil 3 ODS. Detection, UV at 254 nm (2.0 a.u.f.s.). Injection 0.5 μl of column eluate.

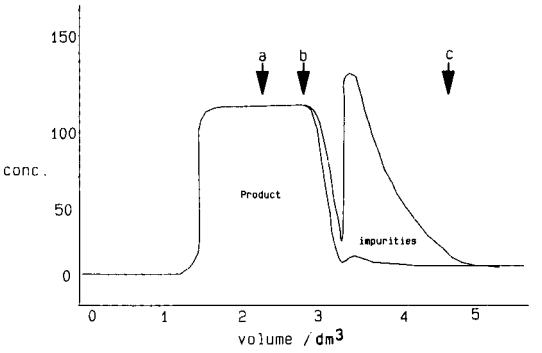

Fig. 7. Preparative chromatogram for the purification step in example 1, constructed from the analyses taken during the run. Point a: water wash started; point b: methanol wash started; point c: column regeneration wash started.

product was desorbed into methanol. After regeneration of the column with a water wash, the cycle was repeated. Treatment of the total batch required 140 cycles. The methanol eluate from these runs was combined, evaporated to dryness, the residue was dissolved in a minimum volume of methanol and the product precipitated with acetone. The precipitate was collected by filtration and dried *in vacuo* to give 3.14 kg of product which assayed at 98.5%.

In this case the required compound was the fastest running component of the crude product and, therefore provides an example of the simplest form of frontal chromatography in preparative applications, although a second step was required to effect the desalt. From analyses of the crude product and of the methanol solution from the first step the yield for the purification step was estimated at 97% whilst the yield for the desalt step was close to 100%. No deterioration of the column performance was found during this work. Each kilogram of purified product obtained used a total of 109.5 dm^3 of methanol (16 dm^3 for purification, 93.5 dm^3 for desalt) and required 21 h of instrument time (5.5 h for purification, 15.5 h for desalt). Projecting this to a large scale, assuming a high degree of automation, recovery of solvent and a column lifetime allowing the purification of 60 kg of product per kg of stationary phase, it was shown that, had it been possible to use recrystallisation to purify this material, a recovery of >95% would have been required to obtain an equivalent purification cost. A limited study of elution chromatography for this purification on the same size column used for this work showed that the purification would have required 33 h/kg (*cf.* 5.5 h/kg), considerably more solvent and a desalt step would still have been necessary. The processing cost would have been an order of magnitude higher and, although the cost differential is somewhat smaller when product recovery is included in the calculation, the lower throughput would require larger equipment and consequent capital investment in order to achieve an equivalent production rate.

Example 2

Fluorination of an anhydronucleoside with hydrofluoric acid resulted in a complex mixture in which the required product was present at a level of 20–25%. In addition to the unwanted products shown by HPLC (Fig. 8a) (the required material is

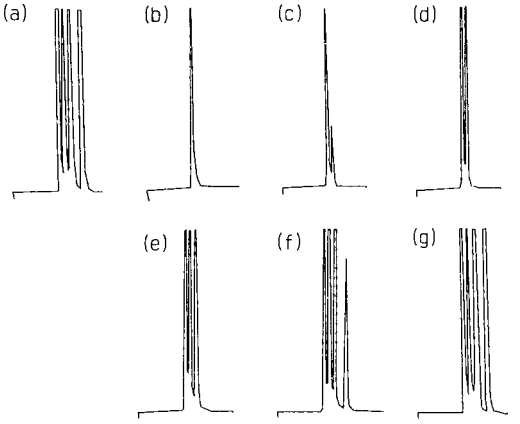

Fig. 8. Analyses of fractions from the small-scale frontal experiment, example 2. For explanation see text. Analytical conditions: water–tetrahydrofuran (80:20), 2.0 cm^3 min^{-1} on 250 mm × 4.6 mm Partisil 10 ODS. Detection, UV at 254 nm (2.0 a.u.f.s.). Injection 5.0 μl of column eluate.

the fourth major peak), late-running impurities were present which were not detected by UV or were not eluted in the mobile phase used for the analysis. Numerous attempts to isolate the product by crystallisation were unsuccessful. A solution of the reaction product in water (4%, w/v) was pumped onto a 250 mm × 4.6 mm Partisil 10 ODS column (Whatman, Maidstone, U.K.) at a flow-rate of 1.0 cm^3 min^{-1} and 1.0-cm^3 fractions were collected and analysed, Fig. 8b–g show the analyses of fractions 10, 15, 20, 25, 30 and 35, respectively, and demonstrated that frontal chromatography was likely to be successful preparatively. A solution of the mixture (627 g) in water (15 l) was divided into ten aliquots and an aliquot was pumped onto a 250 mm × 75 mm Annular Expansion column containing 500 g of 20–45-μm C_8 bonded silica (Amicon) at a flow-rate of 100 cm^3 min^{-1}. The column was then washed sequentially with water (500 cm^3), methanol (2000 cm^3) and water (500 cm^3) before the next aliquot was loaded. The aqueous solution containing the required product and the less strongly adsorbed impurities, was divided into twenty aliquots, an aliquot was loaded onto the column, and the column was subjected to the same wash sequence as above before loading the next aliquot. The methanol washes were collected and combined. On each of these runs a small fraction of the aqueous eluent (100 cm^3) immediately before the methanol began to elute, contained some impure product. These fractions were combined and rechromatographed in a single run, the methanol eluate from which was combined with the other methanol fractions and the solvent was evaporated to dryness to give 126 g of product which assayed at >95%. The chromatogram of the preparative separation for the second step of the purification is given in Fig. 9, this having been constructed from analyses of collected fractions. Sufficient data were not available to determine the individual elution profiles of the three impurities within the impurity fraction.

In this example, the required component was the slowest running on the analytical system used, which suggested that a single stage process might be used for its isolation, since the required purity of the product was not high (95%) and, once the

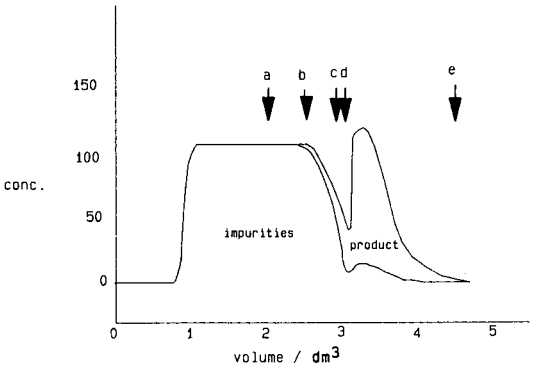

Fig. 9. Preparative chromatogram from the second purification step, example 2, constructed from the analyses of collected fractions. Point a: water wash started; point b: methanol wash started; point c: collect aqueous fraction; point d: collect methanol fraction; point e: column regeneration water wash started.

product had been isolated from the bulk of the impurities, its purity could, if necessary, be improved by recrystallisation. However, on commencement of the preparative work, it soon became apparent that other, slow-running, impurities were present which either did not elute on the analytical system or were not detectable by UV and it was therefore necessary to use a two stage purification. Evaporation of the methanol from the first step of the purification yielded a black tarry residue which contained only a trace of the required product. A small amount of product was lost in the aqueous liquors from the second purification step. The overall yield of product from the two stage purification was estimated to be 95%. This example demonstrates the use of frontal chromatography on a small column in order to predict the likelihood of success on a larger scale.

Example 3

Recrystallisation of a crude product from 10% brine gave good quality product plus mother liquors which, in addition to various impurities, contained approximately 2% (w/w) of the product which represented a loss of about 10% of the process yield. Evaporation of the liquors and second cropping recovered only a small proportion of the available material because of decomposition during the evaporation step. Frontal chromatography was therefore investigated as a recovery method. The mother liquors were passed down a 500 mm × 200 mm axially compressed column packed with 10 kg of 20–45-μm C_8-bonded silica at a flow-rate of 1.2 dm^3 min^{-1}, which effectively removed the bulk of the late-running impurities including highly coloured materials, with a minimum loss of the required product. Approximately 800 dm^3 of liquors could be treated before the breakthrough of impurities in a concentration high enough to affect the quality of the product after subsequent crystallisation occurred and the column required regeneration by washing with methanol (40 dm^3) and water (20 dm^3). Experiments were then conducted on either a 250 mm × 75 mm Annular Expansion column or on a 500 mm × 50 mm axially compressed column, both containing 500 g of 20–45-μm C_8-bonded silica, to determine optimum loading and flow-rate, each

experiment being carried out by loading an aliquot of partially purified liquors then washing the column sequentially with water, methanol and water. The first water wash and the methanol wash were then examined by analytical HPLC to determine if product was being lost in the water and the purification efficiency. When the optimum conditions had been determined, the process was transferred to the 500 mm × 200 mm axially compressed column. A proportion of the water wash which followed the methanol wash was combined with the methanol wash, the methanol was stripped off and the purified product was obtained by adding strong brine to the residual aqueous solution and cooling to effect crystallisation.

Since large amounts of mother liquor were available in this instance, it was possible to carry out a more detailed examination of conditions and hence to optimise the process. Table I shows the results obtained during the optimisation experiments. The initial experiments on each column determined the optimum load volume, showing that too low a load gave a product of inferior quality whilst too large a load led to product being lost through breakthrough. Of the two columns used, the 500 mm × 50 mm gave either a higher recovery of product at the same purity or a higher purity for the same recovery when using an equivalent linear flow-rate, 200 $cm^3\ min^{-1}$ on the 75 mm diameter column being equivalent to 100 $cm^3\ min^{-1}$ on the 50 mm diameter column since the effective diameter of the former is reduced by the tapered rod used to produce the Annular Expansion effect. An investigation into loading flow-rate carried out on the 50 mm diameter column showed that, up to 125 $cm^3\ min^{-1}$ there was no effect on the separation efficiency, but above this point efficiency

TABLE I

RESULTS OF OPTIMISATION EXPERIMENTS (EXAMPLE 3)

The 75 mm diameter column was an Annular Expansion type and the 50 mm column an axially compressed type. Assay is the externally standardised assay of the residue obtained from evaporation of the methanol eluate. Breakthrough indicates whether the aqueous eluate immediately preceding the methanol eluate contained product.

Column diameter (mm)	Load volume (dm^3)	Flow-rate ($cm^3\ min^{-1}$)	Assay (%)	Breakthrough
75	2.50	200	56	No
75	2.75	200	64	No
75	3.00	200	73	No
75	3.50	200	82	Slight
75	4.00	200	85	Yes
50	3.50	100	69	No
50	4.00	100	77	No
50	4.25	100	88	No
50	4.50	100	91	Slight
50	4.75	100	92	Yes
50	4.25	50	89	No
50	4.25	125	90	No
50	4.25	150	86	Slight
50	4.25	175	83	Slight

diminished with increasing flow, albeit slightly, up to 170 cm^3 min^{-1}, the highest flow obtainable within the pressure constraints of the instrumentation. This decrease in efficiency at higher flows would be predicted on the basis of mass transfer kinetics. From experiments on the isolation of product from methanol solution, it was found that the final crystallisation gave product of acceptable quality provided that the material in the methanol assayed at >85%. The wash volumes determined by experiment were: water 100 cm^3; methanol 2000 cm^3; water 500 cm^3, and were the minimum required to obtain optimum recovery/purity whilst minimising solvent usage and thus maximising throughput.

Having optimised conditions on the small scale, the method was transferred to the 200 mm diameter column without difficulty. Several hundred litres of liquors were processed and the overall economics of the process were determined. Because of the high recoveries as compared to the existing recovery method, chromatographic recovery was found to be cost effective.

General discussion

A general stratagem for investigating the possibility of using frontal chromatography for any particular preparative separation is first to find a combination of stationary phase and mobile phase which gives infinite k' for the components of the mixture and where the components are all soluble in the mobile phase. Running a small-scale experiment as in example 2 will then rapidly show whether further work is likely to be justified, taking into consideration the purity requirements for the product to be isolated.

Example 1 stands out as one of the very rare cases where it is possible to obtain a high purity product directly by frontal chromatography. In the majority of cases, as Guiochon and Katti [4] state, the technique is not well suited to the production of pure materials. It can, however, as demonstrated in examples 2 and 3 be extremely useful in the rapid and cost effective isolation of materials from a crude mixture where either the purity requirements of the product are less stringent, or where subsequent further purification is to be used.

The use of preparative chromatography in production can often be justified economically since the higher yields obtained compensate for the higher processing costs involved, particularly with high value products, even in those cases where a simple alternative such as recrystallisation is feasible. However, a combination of techniques can often prove most cost effective. Taking the example of recrystallisation, product will be lost in the mother liquors. This material can be chromatographically purified in one of two ways, either by using chromatography directly to obtain pure material or by using chromatography to enhance the quality of the material to that of the crude product thus allowing good quality material to be obtained by recrystallisation. Since the purity requirements are less stringent in the second case, much higher throughputs can be achieved and an additional advantage is that all product will be produced via an identical last step, *i.e.* recrystallisation. In this way overall yields close to 100% can be obtained, thereby more than compensating for the cost of the chromatographic step, even with low to moderate value products. In this context, the technique of frontal chromatography shows considerable promise.

CONCLUSION

In the examples studied here, frontal chromatography has been shown to be a simple and cost-effective purification technique, but further work will be required to determine whether its use will be restricted to a few very specific examples or if it can be improved as a more general preparative method. In view of the promise shown thus far, it would seem worth the effort in studying the effect of such parameters as loading concentration and the nature of the stationary phase (shape and particle size), as well as its application in normal-phase and ion-exchange chromatography.

REFERENCES

1 A. Tiselius, *Ark. Kemi Mineral. Geol.*, 16a (1943) 1.
2 C. Horváth, A. Nahum and J. Frenz, *J. Chromatogr.*, 218 (1981) 365.
3 M. Verzele, C. Dewaele, J. Van Dyck and D. Van Haver, *J. Chromatogr.*, 249 (1982) 231.
4 G. Guiochon and A. Katti, *Chromatographia*, 24 (1987) 165.

Journal of Chromatography, 523 (1990) 23–34
Elsevier Science Publishers B.V., Amsterdam

CHROMSYMP. 2022

Packing of preparative high-performance liquid chromatography columns by sedimentation

TIANSONG WANG and RICHARD A. HARTWICK*
Department of Chemistry, State University of New York at Binghamton, Binghamton, NY 13901 (U.S.A.)
NEIL T. MILLER
The PQ Corporation, Conshohocken, PA 19428 (U.S.A.)
and
DENNIS C. SHELLY
Department of Chemistry, Texas Institute of Technology, Lubbock, TX 79409 (U.S.A.)

ABSTRACT

Based on the colloid chemistry of a suspension of ODS packing material, a new packing technique using particle sedimentation has been developed. With this approach, a slurry consisting of the packing and a deflocculating solvent is poured into the column, the bed was formed by sedimentation. The bed is then solidified by a flocculating solvent. Using acetone as the slurry solvent and methanol–water (1:1) as the solidification solvent, high-quality columns (150 mm × 21 mm I.D., 16-μm C_{18}-silica packing) were successfully packed with reduced plate heights of 2.5–3.6 and typical A terms in the Knox plot below 1.0. The normalized sedimentation volume is introduced as a basis for the selection of sedimentation and solidification solvents. Various experimental factors, including slurry concentration, solidification flow-rate programming and temperature, are studied and discussed.

INTRODUCTION

In the last several years, there has been a considerable increase of interest in preparative liquid chromatography (LC). Many chromatographers are conducting research on the theory and the application of preparative LC, such as overloading and band interactions [1,2], throughput [3], injection [4,5], particle size [6], column design [7] and column performance evaluation [8]. The research of column packing technique still remains one of the important aspects in the development of preparative LC, as evidenced by numerous techniques being developed, patented and commercialized.

The current packing methods may be classified into three groups: dry packing, high-pressure slurry packing and compression slurry packing.

Dry packing

In this technique, the dry packing material is slowly poured into the column and the bed is formed under the action of vibration, rotation, and/or tamping. Dry packing is suitable for large particles with particle diameter (d_p) > 30 μm. For particles with d_p < 20 μm, this technique usually is poor, because the high surface free energy of

0021-9673/90/$03.50

small particles causes agglomeration and the particles can not be well dispersed by the mechanical action applied in packing. Even for large particles, the column efficiency and its reproducibility often are not very good [9].

High-pressure slurry packing

In this technique, the suspension of packing materials, *i.e.*, the slurry, is stored in a reservoir which is connected to the column. A packing solvent is then introduced under high pressure (usually above 5000 p.s.i.) and at high flow-rate into the reservoir to push the slurry into the column to form the bed by filtration. The high pressure slurry packing is the most successful and the most popular method for particles with $d_p < 20$ μm and columns with 20 mm internal diameter or smaller. Although larger columns can be packed by this method [9,10], the technical requirements (*e.g.*, the mechanical strength of the column and the pump capacity) of this method become more and more difficult.

Compression slurry packing

The compression can be axial or radial or both [9,11]. Typically, radial compression is accomplished by applying gas or liquid pressure on a flexible-walled cartridge which is filled with packing material [11,12]. Axial compression is achieved by moving a piston in the column, which is filled with slurry, to force the solvent out of the end frit and make a filtration bed in the column [13,14]. This technique seems perfect for packing large columns because of the low packing pressure required (5–20 atm) and the excellent column efficiency obtained (reduced plate height of about 2) [9]. Annular expension, *i.e.*, compression in both axial and radial directions, is available by insertion of a plunger in the center of a column [11]. The major shortcoming of the compression slurry packing is the requirement of special equipment, which can be expensive.

The selection of solvents in slurry packing methods is very important. From the viewpoint of colloid chemistry, there are two kinds of solvents: flocculating and deflocculating solvents [15,16]. In flocculating solvents, the attraction between particles is stronger than repulsion, causing the particles to agglomerate and to form a loose sedimentation cake. In deflocculating solvents, the repulsion between particles is stronger than the attraction, the particles are well dispersed, and can form a dense sedimentation cake. The properties of the slurry made from flocculating and deflocculating solvents are compared in Table I [16]. Recently, the importance of colloid chemistry and rheology in packing technique has been emphasized and a new high pressure slurry packing method has been developed which combines a deflocculating slurry solvent with a flocculating packing solvent [17–19].

TABLE I

PROPERTIES OF FLOCCULATING AND DEFLOCCULATING SLURRY

Deflocculating slurry	Flocculating slurry
Particles are well dispersed	Particles agglomerate
Sedimentation rate is slow	Sedimentation rate is high
Sediment is dense	Sediment is loose

In this research, a new packing technique, sedimentation packing, based on the colloid chemistry properties of the suspension of ODS packing material, is developed. Various experimental factors are studied and discussed.

EXPERIMENTAL

Instrumentation

A Waters Prep LC 3000 chromatograph (Millipore, Milford, MA, U.S.A.) was used for packing and conditioning of columns. The chromatograph used for column evaluation was composed of a HP-1084A liquid chromatograph (Hewlett-Packard, Boblingen, F.R.G.), a Lambda-Max Model 481 spectrophotometer (Millipore), and a Waters 740 data module.

The column hardware (150 mm and 500 mm × 21 mm I.D. columns) was supplied by PQ (Conshohocken, PA, U.S.A.).

Packing material and chemicals

The irregular C_{18}-silica with average particle size 16 μm and the test compounds uracil, caffeine and phenol were supplied by PQ. The test compound propiophenone was obtained from Aldrich (Milwaukee, WI, U.S.A.), the solvent isooctane from Burdick & Jackson Labs. (Muskegon, MI, U.S.A.), other solvents from Fisher Scientific (Fair Lawn, NJ, U.S.A.).

Sedimentation volume measurement

Typically, 1.5 g of packing material were put into a 10-ml graduated cylinder, manually bounced on the table to make a dry packing bed, and its volume was recorded. Then 8–9 ml of solvent were added and a suspension was made by hand shaking. After a few minutes, the total volume was adjusted to 8.6 ml (concentration 17%) by removal of the supernatant. Then, the suspension was reshaken, allowed to settle and the volume of the sediment was recorded until no change was noted.

Packing procedure

New and reused packing materials were filter-washed with acetone or methyl ethyl ketone and dried under reduced pressure at room temperature. For 150 mm × 21 mm I.D. column, 37 g silica was put into a 500 ml erlenmeyer flask with about 200 ml of a slurry solvent, acetone (AT) or methyl ethyl ketone (MEK). Fines were removed by sonicating the content for 1–2 min and decanting the supernatant after settlement of particles. This operation was repeated 2–3 times.

The 150-mm column was terminated with an end-fitting and frit, and was then connected to a reservoir, *i.e.*, a 500-mm column with the same internal diameter. The suspension prepared above was poured into the column, and allowed to sediment overnight.

After sedimentation, the supernatant was poured off, and the reservoir was filled with methanol. The inlet was sealed with an end-fitting, and then a solution of methanol–water (1:1) was passed through the assembly to solidify the column.

Soon after sodification, the column was disconnected gently from the reservoir and was sealed with an end-fitting and a frit. The column was conditioned with methanol–water (1:1) at 50 ml/min for 20–30 min with recording of the pressure drop.

Column evaluation

The test mixture was composed of uracil (capacity factor, $k' = 0$), caffeine, phenol and propiophenone ($k' = 6$) in the individual concentrations of 0.05–0.4 mg/ml (20 μl injected). The mobile phase was methanol–water (1:1). The column performance was evaluated by the propiophenone at a flow-rate of 10 ml/min (reduced velocity, $v = 24$) in terms of reduced plate height h, asymmetry factor b/a, flow resistance ϕ and the Knox plot (see ref. 20).

The peak width and the asymmetry factor were manually measured at 10% peak height from the chromagrams. The column efficiency was calculated using eqn. 1:

$$N = 18.5(t_R/w_{0.1})^2 \quad (1)$$

where N is the theoretical plate number, t_R is the retention time and $w_{0.1}$ is the peak width at 10% peak height. The standard deviation of measurement is ± 50 for N (corresponding to ± 0.09 for h when $n = 2300$), ± 0.05 for b/a.

Two typical columns were conditioned by recirculation with methanol–water (1:1) or pure methanol at 50 ml/min for 109 h in order to observe their stability. The solvent volume passed during this conditioning was 6300 column volumes.

RESULTS AND DISCUSSION

Selection of solvents

Particle interactions play a very important role in determining the bed structure, and these interactions are strongly controlled by solvents. The principle of sedimentation packing is simple: firstly, the particles in a deflocculating solvent freely participate to form a uniform and dense bed in a column; and secondly, a flocculating solvent is passed through the column to consolidate the bed. Therefore, solvent selection plays the predominant role in sedimentation packing.

The flocculation property of a solvent can be measured by the sedimentation volume SV [16] at equilibrium

$$\text{SV} = \text{volume of sediment/volume of suspension} \quad (2)$$

or the sedimentation quotient SQ [17,18]

$$\text{SQ} = 1000(\text{height of sediment/height of slurry}) \quad (3)$$

However, SV and SQ values only make sense if each suspension has the same concentration, and such relative values can not be used to predict the real density of the sediment. Therefore, a normalized sedimentation volume is introduced:

$$\text{SV}_n = \text{volume of sedimentation bed/volume of dry bed} \quad (4)$$

The SV_n value is relative to the real density of the sediment and does not depend on the concentration of the suspension. The SV_n values of some solvents commonly used in packing are tabulated in Table II.

From Table II it can seen that both strongly polar (methanol, acetonitrile and

TABLE II

NORMALIZED SEDIMENTATION VOLUME OF SOME SOLVENTS

MA–W = methanol–water (75:25); MA = methanol; ACN = acetonitrile; IPA = isopropanol; AT = acetone; EA = ethyl acetate; THF = tetrahydrofuran; OCT = isooctane; MEK = methyl ethyl ketone.

	Solvent								
	MA–W	MA	ACN	IPA	AT	EA	THF	OCT	MEK
SV_n [a]	–	1.29	1.24	1.19	1.02	1.00	1.00	1.18	1.05
SV_n [b]	1.46	1.36	1.32	1.21	1.02	1.00	0.98	1.13	1.11

[a] Packing material lot p89-146-1.
[b] Packing material lot p87-183-2.

isopropanol) and non-polar (isooctane) solvents have high SV_n values (1.18–1.36), that is, they are flocculating solvents and are not suitable as the slurry solvent, but may be good as the solidification solvent. The addition of water to methanol makes the solvent more flocculating. In contrast, acetone, ethyl acetate and tetrahydrofuran are deflocculating solvents, and their SV_n values are almost equal to unity, *i.e.*, the sedimentation bed formed in such solvents is as dense as that formed in dry packing. According to this research, solvent with SV_n values smaller than 1.05 were suitable as the slurry solvents.

Besides the SV_n value, the particle settling rate also should be considered in order to save settling time. It can be seen in Fig. 1 that acetone has a higher settling rate than that of either ethyl acetate or tetrahydrofuran, and is therefore chosen as the slurry solvent although the three solvents have a similar SV_n value.

Slurry concentration

The SV_n value of acetone slurries was measured in the concentration range 9–31% (w/v), and there was no change in the SV_n values measured. However, the

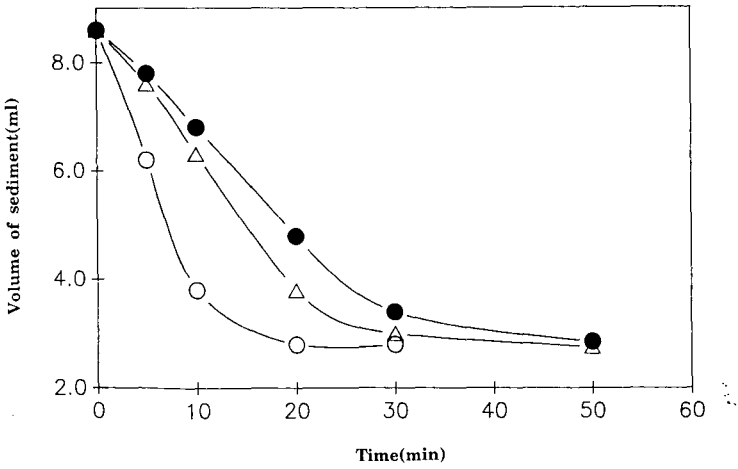

Fig. 1. Sedimentation rate of slurry made of acetone (○), tetrahydrofuran (△) and ethyl acetate (●).

TABLE III

EFFECT OF SLURRY CONCENTRATION ON COLUMN PERFORMANCE

Column[a]	Concentration	N	h (v = 24)	b/a	ϕ
32AT	26% (w/v) or 49% (v/v)	2130	4.4	0.82 (leading)	1100
27AT	17% (w/v) or 31% (v/v)	2650	3.5	0.85 (leading)	1070
33AT	9% (w/v) or 17% (v/v)	1850	5.1	0.96 (leading)	1070

[a] Used packing material; AT = acetone used as slurry solvent.

column performance was affected by the slurry concentration. The columns listed in Table III were packed using the acetone slurry and the best solidification condition (see below). The highest column efficiency was obtained with a slurry concentration of 17% (w/v); either increasing or decreasing the concentration lowered the column efficiency.

Solidification condition

The settled bed is not ready to be used. Firstly, the settled bed is not dense enough to give very good column performance. Secondly, the bed is not stable enough to maintain the column performance. The purpose of solidification is to increase the attraction between particles. The solidification solvents should be strongly flocculating solvents such as methanol and water in order to encourage particle-particle interactions. The selection of the condition includes the flow-rate profile, the final flow-rate, the gradient and the total volume of solvent passed through the bed.

Flow-profile. Three flow-rate profiles were studied. Program I is a constant flow-rate in the range of 50–100 ml/min for 10–60 min. Using program I, columns gave either a very low column efficiency (see Table IV) with low conditioning flow-rate or split peaks with conditioning flow-rate greater than 70 ml/min.

The flow-rate in program II is started at 10 ml/min for 30 min, then is increased to 100 ml/min via a linear gradient of 5 (ml/min)/min and is held for 10 min. Using program II, the column efficiency is slightly improved. The average reduced plate height of five columns is 6.6 at v = 24 (see Table IV), but the peaks are obviously tailed with b/a values 1.3–1.6.

TABLE IV

EFFECT OF FLOW-RATE PROGRAM ON THE COLUMN PERFORMANCE

Slurry	Flow-rate program[a]	N	h (v = 24)	b/a	ϕ
MEK (1 column)	I	1280	7.3	1.17	–
MEK (5 columns)	II	1420 ± 68	6.6 ± 0.3	1.3–1.6	750 ± 98
MEK (4 columns)	III	2380 ± 190	3.9 ± 0.3	0.84–0.95	1140 ± 86
AT (5 columns)	III	2590 ± 250	3.6 ± 0.3	0.82–0.98	1090 ± 28

[a] Program I: methanol–water (1:1), 70 ml/min, 20 min.
Program II: same solvent, 10 ml/min 30 min, 5 (ml/min)/min to 100 ml/min, hold 10 min.
Program III: same solvent, 1–5 (ml/min)/min from 1 to 50 or 75 ml/min, hold 5–20 min.

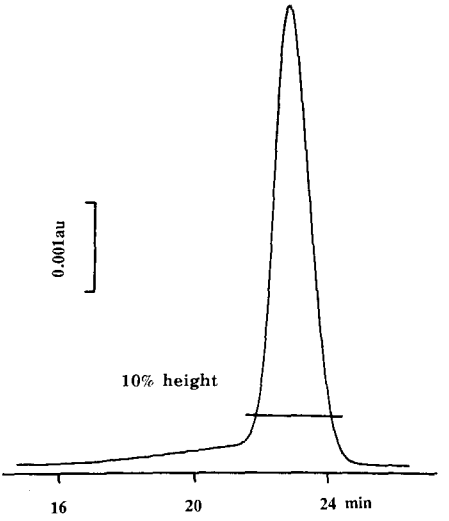

Fig. 2. Leading peak (propiophenone).

In program III, the flow-rate is started at 1 ml/min, then is increased to a final value ranging from 30 to 90 ml/min via a linear gradient varied from 1 to 10 (ml/min)/min with a final hold for 5–30 min. Using program III with suitable parameters (discussed below), very good columns are obtained. The average reduced plate height is 3.9 for the methyl ethyl ketone slurry and 3.6 for the acetone slurry at $v = 24$ (see Table IV).

When using program III to consolidate columns, a unusual leading peak often appears. Fig. 2 shows a typical leading peak. It is not a normal fronting peak but looks like a combination of a normal peak and a drifting baseline. The inflection point is usually below 10% height. In this paper, the term "leading peak" refers to that observed as in Fig. 2. The cause of such peak is currently unknown, but it may be due to short channels between the packing bed and the column wall. Columns packed with reused packing material almost always produce such leading peaks.

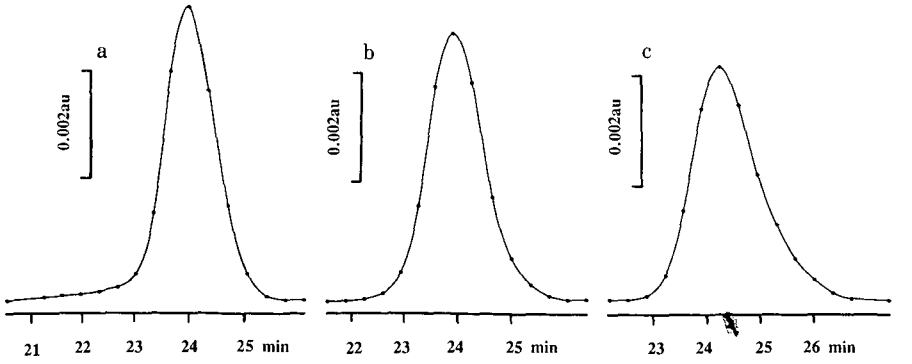

Fig. 3. Effect of final flow-rate on the peak shape (propiophenone, replotted and normalized). (a) 70 ml/min; (b) 50 ml/min; (c) 30 ml/min.

TABLE V

EFFECT OF FINAL FLOW-RATE ON COLUMN PERFORMANCE

Column[a]	Final flow-rate (ml/min)[b]	N	h ($v = 24$)	b/a	ϕ
5AT	90	1780	5.3	0.94 (leading)	1030
2AT	70	2730	3.4	1.04 (leading)	1070
3AT	50	2060	4.6	1.21	920
4AT	30	1460	6.4	1.57	–

[a] New packing material.
[b] Program III, gradient 2 (ml/min)/min.

Final flow-rate. When using program III, the final flow-rate is very important in the control of column efficiency and peak shape. The effect of the final flow-rate can be seen from Fig. 3 and Table V. At high final flow-rate (70 ml/min, corresponding to 1400–1500 p.s.i.), the column efficiency is very good, but the peak is leading (2AT). At low final flow-rate (30 ml/min, 400–500 p.s.i.), the column efficiency is low (4AT, $h = 6.4$ at $v = 24$) and a seriously tailing peak appears. The best final flow-rate is 50 ml/min (corresponding to 800–900 p.s.i.). Similar trends were obtained using the methyl ethyl ketone slurry except a best final flow-rate of 75 ml/min (1400–1500 p.s.i.) was ascertained.

Flow-rate gradient. The major effect of flow-rate gradient is on the peak shape as can be seen from Table VI. As the flow-rate gradient is increased from 2 to 5 and then to 10 (ml/min)/min, the peak shape is changed from slightly tailing (3AT) to almost symmetric (6AT) to leading (14AT), respectively. The column efficiency shows minor changes. Although the 5 (ml/min)/min gradient can give good columns, this gradient seems to be a critical point and a slightly leading peak sometimes appears using the 5 (ml/min)/min gradient. Therefore, the 2 (ml/min)/min gradient is prefered.

Total solvent volume. The total solvent volume passed through the column in solidification seems not to be very important. By changing the hold-time at final flow-rate (see Table VII), the total solvent volume was altered from 750 to 1250 ml (6AT, 8AT) or from 1500 to 2600 ml (53MEK, 50MEK), and no significant change in column performance was observed. However, when the hold-time was increased to 30 min, the column efficiency deteriorated (7AT).

Finally, the best solidification condition established for columns packed with the

TABLE VI

EFFECT OF FLOW-RATE GRADIENT ON COLUMN PERFORMANCE

Column[a]	Gradient [(ml/min)/min][b]	N	h ($v = 24$)	b/a	ϕ
3AT	2	2060	4.6	1.21	920
6AT	5	2390	3.9	0.95	1020
14AT	10	2460	3.8	0.87 (leading)	1020

[a] New packing material.
[b] Program III, final flow-rate 50 ml/min.

TABLE VII

EFFECT OF TOTAL SOLVENT VOLUME ON COLUMN PERFORMANCE

Column	Final flow-rate hold time (min)	Total solvent volume (ml)[a]	N	h (v = 24)	b/a	ϕ
6AT	10	750	2390	3.9	0.95	1020
8AT	20	1250	2270	4.1	1.13	1020
7AT	30	1750	1330	7.0	1.02 (leading)	1050
53MEK	5	1500	2150	4.4	0.84 (leading)	1070
50MEK	20	2600	2300	4.1	0.91 (leading)	1070

[a] Program III.

acetone slurry and the methanol–water (1:1) solidification solvent was: program III, start at 1 ml/min, 2 (ml/min)/min gradient to 50 ml/min, then hold for 10 min. Fig. 4 presents a chromatogram obtained from a typical column (35AT) packed according to these conditions and the reduced plate height is 3.1 (v = 24). This column provides an optimum reduced plate height of 2.5 at v = 12 (flow-rate 5 ml/min), with asymmetry factor 1.00 and flow resistance 990.

To the best of the authors' knowledge, the best preparative columns obtained with high-pressure slurry packing gave a reduced plate height of 1.8 [9,10]. In terms of reduced plate height, although sedimentation packing does not yet equal high-pressure slurry packing, these preliminary results are satisfactory. Moreover, according to Dewaele *et al.* [8], the column efficiency at one flow-rate is affected not only by packing procedures, but also by the properties of the packing materials and chromatographic system. Therefore, measurement of efficiency *vs.* flow-rate is necessary (see below).

Stability and Knox plot

The column performance of two columns (8AT and 25AT) was examined before and after 109 h of conditioning. Figs. 5 and 6 are the Knox plots obtained from the 8AT and 25AT columns, respectively. According to the plots, the coefficients of the Knox equation (see ref. 20)

$$h = B/v + Av^{0.33} + Cv \tag{5}$$

TABLE VIII

COEFFICIENTS OF KNOX EQUATION

Column	Status	B	A	C	r^2
8AT	New	9.80	0.90	0.05	0.997
8AT	After conditioning[a]	10.80	0.75	0.05	0.995
25AT	New	15.39	0.84	0.04	0.97
25AT	After conditioning[b]	12.31	1.00	0.02	0.95

[a] Methanol–water (1:1), 50 ml/min for 109 h.

[b] Methanol, 50 ml/min for 109 h.

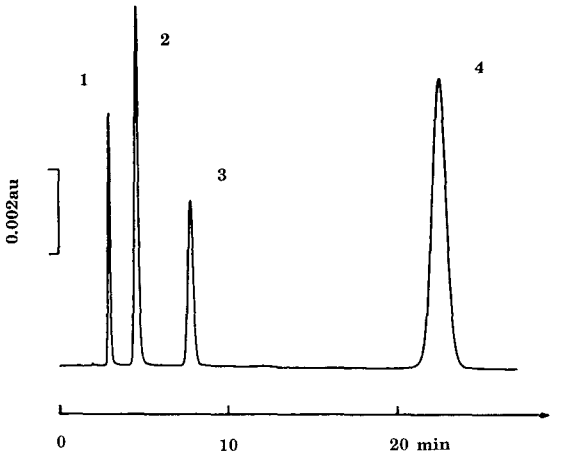

Fig. 4. Separation of test mixture. Column, 150 mm × 21 mm I.D. (35AT), methanol–water (1:1), 10 ml/min (v = 24). Peaks: 1 = uracil; 2 = caffeine; 3 = phenol; 4 = propiophenone.

are calculated and listed in Table VIII. From Figs. 5 and 6, it can be seen that the column performance of both columns is stable, with no obvious change after 6300 column volumes of solvent conditioning. For 8AT which was conditioned by the same condition of solidification [methanol–water (1:1), 50 ml/min], the long time of conditioning even leads to a slight improvement of the column performance. According to Dewaele *et al.* [8], the A term in eqn. 5 is the best parameter to justify the packing quality, and a well-packed column should have an A value < 2 and the lower the better. In Table VIII, the A terms of columns 8AT and 25AT are 0.75–0.90 and 0.84–1.0, respectively, indicating the two columns are packed to an excellent degree by sedimentation packing technique.

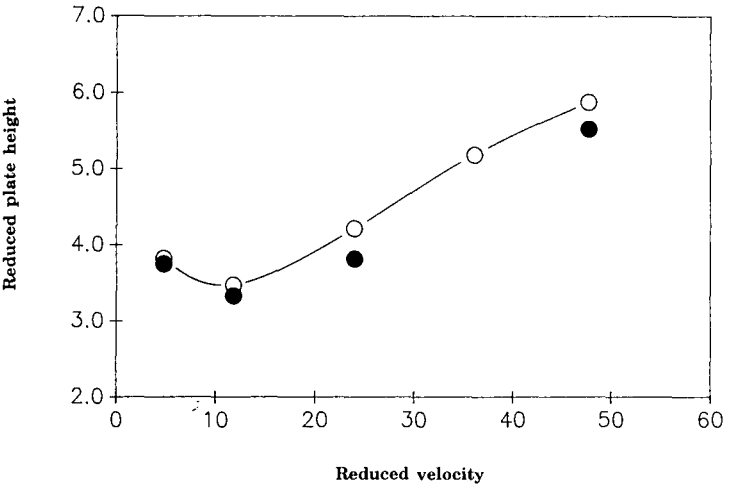

Fig. 5. Knox plot from 8AT before (○) and after (●) conditioning (see text).

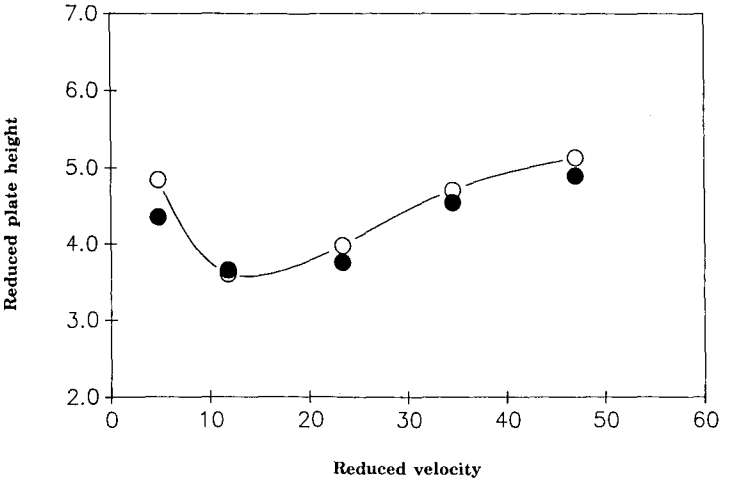

Fig. 6. Knox plot from 25AT before (○) and after (●) conditioning (see text).

Temperature effect

In order to obtain high column efficiency in sedimentation packing, the sedimentation temperature and the solidification temperature should be under control. The temperature effect on column performance can be seen from Table IX. The highest column efficiency is obtained when the sedimentation temperature is 3–5°C higher than that of solidification (19AT). The reason for this temperature effect is unclear at present, but the thermal effect of solvent mixing may play an important role. The bed seems to need to be kept at constant temperature during the sedimentation and the solidification. However, the mixing of methanol and acetone is endothermic, and the mixing of methanol and water is exothermic. During solidification, the bed temperature will decrease first (methanol + acetone) and then increase [methanol–water (1:1) + methanol]. Therefore, a warm bed will compensate somewhat the temperature change created by solvent mixing. In addition, the sedimentation temperature also should be stable.

TABLE IX

EFFECT OF TEMPERATURE ON COLUMN PERFORMANCE

Column[a]	Temperature control	N	h (v = 24)	b/a	ϕ
19AT	25°C sedimentation 22°C solidification	2990	3.1	0.91 (leading)	1140
20AT	20°C sedimentation 24°C solidification	2050	4.6	0.86 (leading)	1100
21AT	24°C sedimentation 24°C solidification	2430	3.9	0.89 (leading)	1100

[a] Used packing material, solidification gradient 5 (ml/min)/min, final flow-rate 50 ml/min and hold 15 min.

CONCLUSION

Based on the colloid chemistry properties of the suspension of ODS packing material, the sedimentation packing technique has been developed. Using acetone as the slurry solvent and methanol–water (1:1) as the solidification solvent, high-quality columns (150 mm × 21 mm I.D.) were obtained with reduced plate heights of 2.5 – 3.6 and stable column performance. The typical A term in the Knox plot was below 1.0. Although the best columns produced using sedimentation packing do not equal the best columns produced with high-pressure slurry packing in term of reduced plate heights, the new method shows obvious promise because of its simplicity. The normalized sedimentation volume was introduced in order to easily select sedimentation and solidification solvents. Various experimental factors were studied, such as the slurry concentration, the flow-rate profile in solidification, the final flow-rate, the flow-rate gradient, the total solvent volume and the temperature effect. These studies provide valuable guidelines for the preparation of packed large bore columns.

REFERENCES

1 S. Ghodbane and G. Guiochon, *J. Chromatogr.*, 450 (1988) 27.
2 G. Guiochon, S. Golshan-Shirazi and A. Jaulmes, *Anal. Chem.*, 60 (1988) 1856.
3 J. H. Knox and H. M. Pyper, *J. Chromatogr.*, 363 (1986) 1.
4 P. Gareil and R. Rosset, *J. Chromatogr.*, 450 (1988) 13.
5 G. Cretier and J. L. Rocca, *Sep. Sci. Technol.*, 22 (1987) 1881.
6 J. Newburger, L. Liebes, H. Colin and G. Guiochon, *Sep. Sci. Technol.*, 22 (1987) 1933.
7 H. Colin, *Sep. Sci. Technol.*, 22 (1987) 1851.
8 C. Dewaele, M. De Coninck and M. Verzele, *Sep. Sci. Technol.*, 22 (1987) 1919.
9 G. Guiochon and A. Katti, *Chromatographia*, 24 (1987) 165.
10 T. J. Gentilucci, S. I. Sivakoff, G. B. Cox, S. D. Stearns and M. W. Hutchinson, *J. Chromatogr.*, 461 (1989) 63.
11 M. Verzele, M. De Coninck, J. Vindevogel and C. Dewaele, *J. Chromatogr.*, 450 (1988) 47.
12 J. W. Little, R. L. Cotton, J. A. Pendergast and P. D. McDonald, *J. Chromatogr.*, 126 (1976) 439.
13 E. Godbille and P. Devaux, *J. Chromatogr. Sci.*, 12 (1974) 564.
14 E. Godbille and P. Devaux, *J. Chromatogr.*, 122 (1976) 317.
15 P. A. Bristow, *Liquid Chromatography in Practice*, hetp, Wilmslow, 1976, p. 34.
16 W. I. Higuchi, J. Swarbrick, N. F. H. Ho, A. P. Simonelli and A. Martin, in A. R. Gennaro (Editor), *Remington's Pharmaceutical Sciences*, Mack, Easton, PA, 17th ed., 1985, Ch. 20.
17 R. F. Meyer, *Ph.D. Dissertation*, Rutgers University, New Brunswick, NJ, 1986.
18 D. C. Shelly and T. J. Edkins, *J. Chromatogr.*, 411 (1987) 185.
19 D. C. Shelly, V. L. Antonucci, T. J. Edkins and T. J. Dalton, *J. Chromatogr.*, 458 (1989) 267.
20 P. A. Bristow and J. H. Knox, *Chromatographia*, 10 (1977) 279.

Journal of Chromatography, 523 (1990) 35–42
Elsevier Science Publishers B.V., Amsterdam

CHROMSYMP. 2037

Silica–dextran sorbent composites and their cleaning in place

E. BOSCHETTI*, P. GIROT and L. GUERRIER
IBF-Biotechnics, 35 Avenue Jean Jaurès, F-92390 Villeneuve la Garenne (France)

ABSTRACT

Large-scale liquid chromatography requires sorbents that are mechanically stable in order to ensure repeated cycles without shrinkage. The industrial separation of biological materials moreover implies working in apyrogenic and sterile conditions. Dextran-coated silica used as a chromatographic sorbent was treated with different sanitizing solutions after bacterial contamination. It was demonstrated that most of the strains used were inactivated by using alkaline solutions or ethanolic acetic acid. However, the sporulated form of *Bacillus subtilis*, which seemed more resistant than other strains, was inactivated only when alkaline solutions contained more than 40% ethanol. All these treatments were also very effective for pyrogen removal and did not indicate significant degradation of the silica moiety or the chromatographic performance of the sorbent.

INTRODUCTION

Among the different hydrophilic coated silicas that have been described, silica–dextran composites undoubtedly represent one of the major recent accomplishments in the design of solid sorbents for the liquid chromatography of proteins. Their superiority is the result of the association of a mineral skeleton with a biohydrocolloid, the first conferring remarkable mechanical resistance and the second avoiding the non-specific adsorption of proteins and bringing in the approriate chemical group. By this principle, ion-exchange sorbents [1,2], affinity sorbents [3,4] and hydrophobic sorbents have been synthesized and used in the separation of protein mixtures.

As one of the weaknesses of silica-based sorbents is their sensitivity at alkaline pH, a dextran coating seemed to be an appropriate solution to prevent too rapid solubilization of silica. In this respect, opinions on the stability of silica towards alkaline conditions did not seem very consistent in the literature and probably differed as a consequence of the variable nature of silica and of the coating (grafted silica). Some authors indicate that at pH > 7 the life of the packing material could be seriously reduced [5], whereas others [6,7] claimed that reversed-phase silica could remain stable at pH up to 9–10. Wehrli *et al.* [8] demonstrated that the rate of dissolution of silica by strongly alkaline solutions was very dependent on the content of organic modifiers. More recently, Law and Chan [9] concluded that, contrary to popular belief, silica-based packing materials can show excellent stability with certain alkaline eluents.

0021-9673/90/$03.50

The resistance of a sorbent against alkaline attack is in any case an important concern when the sorbents must be repeatedly used in clean conditions for preparative biological applications. The dextran moiety, widely used for more than 30 years, is well known for its good stability in sanitizing conditions (salt, temperature, strong alkaline solutions, etc.). In this paper, we first describe the fundamental properties of silica–dextran composites and their derivatives for use in liquid chromatography. A study focused on cleaning in place and sanitization is also reported, with particular reference to sterilization possibilities and their influence on the physico-chemical properties of the alkali-treated sorbent.

EXPERIMENTAL

Silica was obtained from IBF-Biotechnics (Villeneuve la Garenne, France) and dextran and dextran ionic derivatives from Sigma, (St. Louis, MO, U.S.A.). All other chemicals were of analytical-reagent grade from Sigma or from Aldrich (Beerse, Belgium). Silica–dextran composite materials were synthesized according to previously described techniques [1,3,4].

Coating of porous silica with dextran

Dry silica beads with a pore volume of 1 cm^3/g and a mean pore size of 1200 Å were coated with cationic or anionic dextran. The dextran used had a molecular weight between 70 and 500 kilodalton and possessed a certain amount of ionic groups (about 0.5–1% for the synthesis of non-ionic derivatives and about 10% for the preparation of ion exchangers). Briefly, the coating was performed as follows: 25 g of dextran derivative were dissolved in 150 ml of 0.2 *M* carbonate buffer (pH 10.5), then 5 ml of butanediol diglycidyl ether were added with stirring. Finally 100 g of dry silica beads were added (specific surface area 25 m^2/g; pore diameter 1250 Å). The suspension was then filtered under vacuum to remove the excess of the dextran solution. The gel was placed in a ventilated oven and kept at 80°C for 24 h. The dry product obtained was repeatedly washed with water and with acidic and alkaline solutions, and finally stored in the presence of 1 *M* sodium chloride.

Sanitization treatments

Dextran-coated silica was first contaminated with a large amount of a defined microorganism (*Escherichia coli, Staphylococcus aureus, Candida albicans* and the sporulated form of *Bacillus subtilis*) and then decontaminated by washing with appropriate solutions.

The solutions used were sodium hydroxide at different concentrations, 60% ethanol–0.5 *M* acetic acid with different incubation times and mixtures of 0.2 *M* sodium hydroxide with ethanol in different proportions.

After contamination, the sorbents were treated with three volumes of the appropriate sanitizing solution (up to 24 h at 25°C). The remaining germs were then detected on the neutralized sorbent slurry using a standard culture. Tests were performed in diluted tryptase–soya sterile broth in triplicate per dilution. Each tube was incubated at 33°C for 14 days with daily observations; the number of germs was determined classically according to the original Sperman–Karber method [10,11] as recommended by the World Health Organization [12].

Stability studies of silica–dextran sorbents

Two kind of studies were performed: (i) physico-chemical modifications of the silica-dextran matrix with ion exchangers and (ii) modification of the performance of a packed column after numerous strong alkali treatments.

In the former instance, ion-exchange dextran-coated silica was treated in a stirred suspension with sodium hydroxide from 0.1 to 1 *M* for 1 to 24 h. Each sample was then tested in order to determine the amount of leached silica (in the supernatant) and to measure the modifications of the specific surface area (BET) and the pore diameter (mercury porosimetry). Leached silicon was determined by elemental analysis.

In the latter instance, an analytical column of 8 ml (10 cm × 1 cm I.D.) of dextran sulphate-coated silica was submitted to 250 washings with 2 *M* sodium hydroxide at room temperature. The volume of alkaline solution injected was 0.5 ml per cycle. These treatments were followed by equilibration with 0.05 *M* acetate buffer (pH 4.5) and by the chromatographic separation of a mixture of β-lactoglubulin and cytochrome *c*. Then proteins were eluted under a salt gradient up to 0.8 *M*. To determine the possible influence of these sodium hydroxide washings, the chromatographic resolution was calculated.

RESULTS AND DISCUSSION

Sorbent synthesis and properties

Coating porous silica beads with dextran or ionic dextran derivatives is necessary for eliminating the well know non-specific protein adsorptions or to introduce ion-exchange properties. Indeed, on native silica, most proteins are tightly adsorbed and frequently denatured. As the synthesis of silica ion exchangers and their properties have been extensively described elsewhere [1,2], our study was focused on non-ionic silica–dextran composites.

It should be noted that a complete coating with a polysaccharide prevented direct contact between the protein and the silanol groups; this is clearly evidenced (Table I) by the progressive decrease in the adsorption of a cationic protein such as cytochrome *c*. An increase in the dextran content lowered to zero the interaction between cytochrome *c* and the silica gel. The dextran layer also contributes to making the silica more resistant to strongly alkaline media and further makes easy the acti-

TABLE I

EFFECT OF DEXTRAN COATING ON THE SORPTION CAPACITY OF CYTOCHROME *c* AND ON THE V_e/V_t RATIO OR BSA

Amount of dextran (g per 100 g silica)	Cytochrome *c* sorption capacity (mg/ml)	V_e/V_t[a] (BSA)
5	3.7	0.77
10	2.5	0.71
15	1.1	N.D.
20	0.2	0.60

[a] Experiments performed on-column (V_t = total volume of the column; V_e = elution volume).

vation of polysaccharide-based supports involving the classical reagents used in affinity chromatography. Altough a high concentration of dextran is beneficial to the elimination of non-specific adsorptions, it also diminishes the porosity of the support. The value of V_e/V_t (ratio of the elution volume for bovine serum albumin (BSA) to the total column volume) descreased when the amount of dextran increased. This decrease is linked with the progressive reduction of the pore size inside the silica network. The degree of cross-linking (different amounts of cross-linking agent) did not significantly modify the behaviour of the silica–dextran composite towards cytochrome *c* and BSA (data not shown).

Non-ionic derivatives can be easily used in affinity chromatography after activation and immobilization of biologically active substances such as concanavalin A and protein A [3,4,13].

Sterilization results

It was found that the inactivation of germs by sodium hydroxide washing was dependent on the nature of the strains used (see Table II). This is the reason why we used the strain that covers fairly well the range of common microorganisms such as bacteria, fungi and other sporulated standard forms (*e.g., Bacillus subtilis*). The latter is recommended by pharmacopoeias for validating cleaning operations. In this study, *Escherichia coli* seemed the most sensitive to alkaline media; it was in fact totally inactivated by sodium hydroxide at concentrations as low as 0.05 *M*. *Candida albicans* and *Staphylococcus aureus* were also sensitive to sodium hydroxide treatment but their total inactivation was observed when the sodium hydroxide concentration was 0.1 *M* or higher. However, sodium hydroxide at any concentration (and at temperatures of 20–25°C for 3 h) was not found to be very effective in the inactivation of the sporulated form of *Bacillus subtilis*, even when the sodium hydroxide treatment was extended up to 24 h. In the best instances, the decrease in the amount of *Bacillus subtilis* was about five $\log_{10}$, which means that, from an initial concentration of about 10^7 germs/ml, about 100 germs/ml were still present at the end of the treatment (0.2 and 1 *M* sodium hydroxide).

TABLE II

GERM IN ACTIVATION USING DIFFERENT CLEANING SOLUTIONS (3 h, ROOM TEMPERATURE)

Washing solution	*E. coli* (Germs/ml gel)	*S. aureus* (germs/ml gel)	*C. albicans* (germs/ml gel)	*B. subtilis* (germs/ml gel)
Before washing	10^7	10^7	10^7	10^7
0.2 *M* NaOH	0	0	0	200
1 *M* NaOH	0	0	0	70
60% Ethanol–0.5 *M* acetic acid	0	0	0	800
20% Ethanol–0.2 *M* sodium hydroxide	0	0	0	20
40% Ethanol–0.2 *M* sodium hydroxide	0	0	0	3
60% Ethanol–0.2 *M* sodium hydroxide	0	0	0	0

The treatment of contaminated supports with 60% ethanol–0.5 *M* acetic acid indicated an extreme sensitivity of all the strains studied, except *Bacillus subtilis* (see Table II). Whereas with ethanol–acetic acid treatment for less than 1 h *E. coli, C. albicans* and *S. aureus* germs were quantitatively inactivated, the number of *B. subtilis* decreased greatly during the first few hours of treatment (four $\log_{10}$) and then very slowly so that after 24 h of treatment a significant level of contamination (180 germs/ml) still persisted (data not shown).

These results are in accordance with those presented by Whitehouse and Clegg [14], who reported a strong resistance of *B. subtilis* towards treatment with sodium hydroxide. It was demonstrated that at 22°C, 1 *M* sodium hydroxide decreased the initial amount of *B. subtilis* by about four $\log_{10}$ in 12 h whereas under the same conditions it took 25, 49 and about 70 h to obtain similar results with 0.6, 0.4 and 0.2 *M* sodium hydroxide, respectively.

It was found, however, that alternate treatment of a contaminated sorbent for 1.5 h each with 0.2 *M* sodium hydroxide and ethanol–acetic acid totally inactivated *B. subtilis*. These results led us to investigate treatment with a solution composed of 0.2 *M* sodium hydroxide and ethanol at concentrations between 20 and 60% for 3 h. When the ethanol concentration was above 40%, the inactivation of sporulated *B. subtilis* was total. However, with an ethanol concentration of 20%, although sterilization of contaminated sorbents was very good for *E. coli, C. albicans* and *S. aureus, B. subtilis* was not totally destroyed (see Table II). From these results, it can be concluded that, if total elimination of germs in a chromatographic support is to be achieved, it is necessary to apply either alternate treatment with 0.2 *M* sodium hydroxide and ethanol–acetic acid or an alkaline treatment at low concentration in the presence of ethanol.

When simple elimination of pyrogens is required, all the above-mentioned methods could be used. In this situation, three general problems could occur on the practical level: (1) with such treatments in the presence of ethanol, soft or semi-rigid gels may shrink to various extents, thus making operation on-column very difficult; (ii) the solid matrix could be damaged during the treatments; (iii) the stability of the biologically active ligand attached to the sorbents may be affected. It is clear that with rigid sorbents such as dextran-coated silica, all treatments with high concentrations of ethanol could be applied without any shrinkage or channelling.

Sodium hydroxide resistance of silica–dextran composites

The resistance of dextran-coated silica was studied when using alkaline solutions. It is known that silica is particularly stable in acidic media. Further, in the presence of 0.5 *M* acetic acid, the cross-linked dextran moiety, whether chemically derivatized or not, is also fairly stable.

It is currently considered that silica-based material will be progressively destroyed by the use of strongly alkaline aqueous solutions. However, only a few papers have reported experimental results on the behaviour of the silica packing when washed at alkaline pH [5–9].

In most instances, the packing material was a reversed-phase silica with C_8 and C_{18} aliphatic chains chemically bonded on the silica material and the degradation was determined by the loss of organic coating. The use of organic modifiers such as acetonitrile or methanol in the alkaline solution showed that the dissolution was reduced for non-bonded silica [8].

In this study, silica was coated with a cross-linked cationic macromolecule, the association between the two entities being dependent on the strong ionic multi-point exchange. To determine the degradation of this particular sorbent, we used the elemental analysis of the released silicon because the organic layer was neither hydrolysed nor solubilized or dissociated from the matrix.

Experimental data showed that an alkaline treatment released small amounts of silicon from the sorbent. This limited silica solubilization was dependent on the sodium hydroxide concentration and on the treatment time (see Table III). It was found that 0.2 *M* sodium hydroxide, classically used in the sanitization of these sorbents (see above), induced the solubilization of about 0.3% of silica after a 2-h treatment. When the treatment was continued for 10 h, the silica solubilization was *ca.* 2%.

These chemical phenomena did not indicate any modification of the chromatographic behaviour, *e.g.*, sorption capacity, titration curve and separation efficiency of ion exchangers based on silica–dextran composite materials, which are all dependent on the properties of the coating material.

The specific surface area varied only very slightly when the sodium hydroxide concentration was below 0.1 *M*; at 0.2 *M* sodium hydroxide, it increased by *ca.* 5–10% and then remained constant. This was checked with treatments of 1 and 24 h (Table IV).

The pore diameter remained almost constant when the alkaline treatment was limited (*e.g.*, 1 h). For 24-h treatment, the pore diameter was modified when the sodium hydroxide concentration was increased from 0.1 to 0.2 *M*; higher concentrations did not show any clear modification of this parameter, except at 1 *M* for 24 h.

In summary, the specific surface area seemed not to be significantly affected by sodium hydroxide treatments (Table IV). Beyond 16-h pefusion, silica-dextran composites can be progressively damaged particularly when the sodium hydroxide concentration is very high. It should be kept in mind, however, that sodium hydroxide concentrations above 0.2 *M* are not necessarily suitable for the total sanitization of the sorbents (see above). On the other hand, for cleaning purposes only, when the sorbent becomes contaminated owing to the injection of very crude samples, sodium hydroxide at concentrations up to 2 *M* could be the sole means of regenerating correctly.

Under these conditions, it was demonstrated that very numerous repeated sodium hydroxide treatments did not significantly decrease the chromatographic effi-

TABLE III

EFFECT OF SODIUM HYDROXIDE TREATMENT ON THE SOLUBILIZATION OF SILICON FROM DEXTRAN-COATED SILICA

Sodium hydroxide concentration (*M*)	Silicon solubilized (%)		
	after 1 h	after 5 h	after 15 h
0.1	10.18	–	–
0.2	0.40	0.98	2.78
0.5	0.41	–	–
1.0	0.52	–	–

TABLE IV

VARIATION OF THE SPECIFIC SURFACE AREA AND OF THE MEAN PORE DIAMETER AS A FUNCTION OF SODIUM HYDROXIDE TREATMENT OF DEXTRAN-COATED SILICA

Sodium hydroxide concentration (*M*)	Specific surface area (m^2/g)		Mean pore diameter (Å)	
	1 h	24 h	1 h	24 h
Before treatment	24	24	1000	1000
0.1	24	25	1000	1220
0.2	25	26.5	980	1250
0.4	25.5	27	980	1250
0.8	25.5	27	1000	1300
1.0	25.3	27	1050	1600

ciency of the sorbent. Fig. 1 shows that the reslution decreased slightly after each cycle. After 250 cycles of washing with 2 *M* sodium hydroxide for 8–10 minutes each (this corresponds to a total time of treatment of 33–42 h at room temperature) the total decrease in resolution was only 16–18% and was approximately 0.07% per cycle (average). During this very drastic treatment the column back-pressure did not change significantly and the length of the column bed decreased only by less than 1%. Even though this last comment is not related to the inactivation protocols, it shows that when a sterilized chromatographic packing is not totally cleaned up (adsorbed material), additional washings with 1–2 *M* sodium hydroxide can be performed. Conversely, these treatments are not efficient enough for proper sterilization even after several hours.

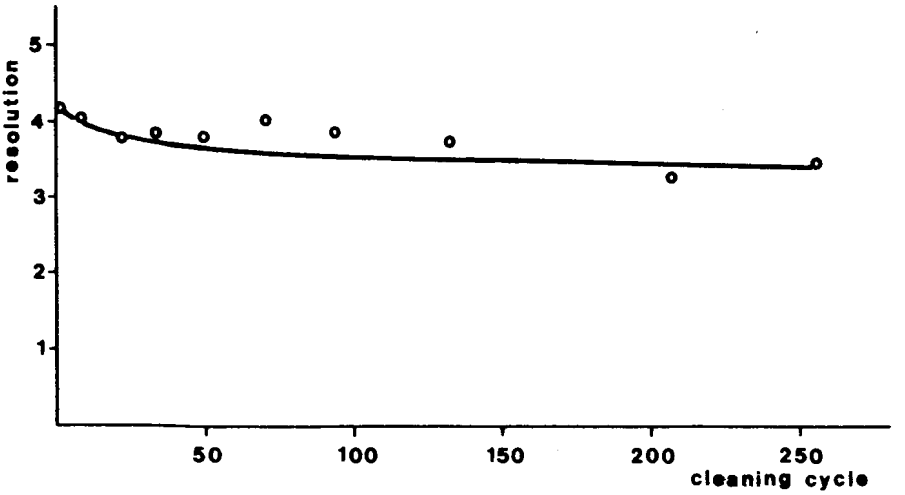

Fig. 1. Influence of 2 *M* sodium hydroxide cleaning in place on the resolution of a column of dextran sulphate–silica packing (S-Zephyr). Column, 10 cm × 1 cm I.D. (7.8 ml); particle size, 20 ± 5 μm; buffer, 0.05 *M* acetate (pH 4.5) (sodium chloride gradient); protein separated, β-lactoglobulin and cytochrome *c*; separation time, 25 min (including 8–10 min of cleaning with 2 *M* sodium hydroxide); working pressure, 15 bar.

CONCLUSIONS

Although the necessity to clean all types of sorbent (ion exchangers, gel filtration and affinity media) is undoubtedly admitted, the real efficiency and the consequences of the chemical treatments were not clearly known in the past. This study has demonstrated that sodium hydroxide treatment does not guarantee good sterilization. *Bacillus subtilis* was in fact not totally inactivated by alkaline treatment, whatever the period of contact or the sodium hydroxide concentration, and an additional ethanol–acetic acid treatment was necessary to eliminate any germs. This result was also achieved when the sterilization was effected with a mixture of sodium hydroxide and ethanol.

These treatments are particularly suitable for dextran-coated silica, which is incompressible in the presence of any amount of ethanol. It was in addition demonstrated that these sorbents were particularly stable when treated with alkaline solutions. Only a very small amount of silica was dissolved, permitting repeated concentrated (2 *M*) sodium hydroxide washings without significant modification of the chromatographic properties of the sorbents.

REFERENCES

1 J. L. Tayot, M. Tardy, T. Gattel, R. Plan and M. Roumiantzeff, in R. Epton (Editor), *Chromatography of Synthetic and Biological Polymers*, Vol. 2, Ellis Horwood, Chichester, 1978, p. 95.
2 J. L. Tayot, M. Tardy, T. Gattel, G. Cueille and Liautaud, in *Dev. Biol. Stand.*, 67 (1987) 15.
3 X. Santarelli, D. Muller and J. Jozefonvicz, *J. Chromatogr.*, 443 (1988) 55.
4 P. Girot, Y. Morous, X. P. Duteil, C. Nguyen and E. Boschetti, *J. Chromatogr.*, 510 (1990) 213.
5 C. Horvath, W. Melander and I. Molnar, *Anal. Chem.*, 49 (1977) 142.
6 R. V. Vivilecchia, R. L. Cotter, R. J. Limpert, N. Z. Thimot and J. N. Little, *J. Chromatogr.*, 99 (1974) 407.
7 A. Pryde, *J. Chromatogr. Sci.*, 12 (1976) 486.
8 A. Wehrli, J. C. Hildenbrand, H. P. Keller and R. Stampli, *J. Chromatogr.*, 149 (1978) 199.
9 B. Law and P. F. Chan, *J. Chromatogr.*, 467 (1989) 267.
10 C. Spearman, *Br. J. Psychol.*, 2 (1908) 227.
11 G. Karber, *Naunyn-Schmiedebergs Arch. Exp. Pathol. Pharmakol.*, 162 (1931) 480.
12 J. Sperman, in M. M. Kaplan and H. Koprowesky (Editors), *WHO Monography*, Vol. 23, 3rd. ed., 1973, p. 321.
13 J. L. Lorne, M. Allary and E. Boschetti, *Rev. Fr. Transfus. Hemobiol.*, 32 (1989) 391.
14 R. L. Whitehouse and L. F. L. Clegg, *J. Dairy Res.*, 30 (1963) 315.

Journal of Chromatography, 523 (1990) 43–52
Elsevier Science Publishers B.V., Amsterdam

CHROMSYMP. 2027

Forced-flow multi-phase liquid extraction, a separation method based on relative and absolute counter-current distribution

I. Description of the method and basic possibilities

Sz. NYIREDY, L. BOTZ and O. STICHER*

Department of Pharmacy, Swiss Federal Institute of Technology (ETH) Zurich, CH-8092 Zürich (Switzerland)

ABSTRACT

A novel variant of continuous relative and absolute counter-current distribution (CCD), called forced-flow multi-phase liquid extraction (FFMLE), is introduced as a new separation method. This method is a special case of liquid–liquid extraction requiring three immiscible liquid phases and movement of inert gas bubbles through the three liquid phases as the fourth constituent of the multi-phase system.

On using three immiscible liquid phases, two basic situations prevail: two phases may be stationary and one mobile, or one stationary and two mobile. Among the five basic possibilities, four belong to relative CCD in the ascending and descending modes. The extraction columns are filled with the immiscible stationary phase or phases and mobile phase or phases are forced through the stationary phase or phases by means of pumps. For the fifth possibility, the two mobile phases move in opposite directions as very small droplets. This method constitutes absolute CCD, and results in exhaustive and rapid extraction. The efficiency of FFMLE is achieved not just because the mobile phases move in opposite directions, but is also a result of three other effects that are discussed. The different types of relative and absolute CCD methods may also be varied by connecting two or more columns together.

A typical three-phase system can be obtained on mixing *n*-hexane, acetonitrile and water as the basic ternary system, with one of diethyl ether, dichloromethane, toluene or chloroform as the fourth solvent (auxiliary solvent). A virtual solvent strength (S_v) value is introduced for characterization of the three-phase liquid system. The solvent and phase ratio of some three-phase systems are given for different S_v values and selectivity.

The method can be used for the rapid purification of various substance classes occurring as complex matrices. Experiments carried out with a laboratory extraction column (3.5 l) show that the separation of *ca.* 10 g of raw extract into two or more fractions requires less than 1 h.

INTRODUCTION

The separation of molecules as a result of their differential solubility between two immiscible phases has provided the basis for various separation techniques. Martin and Synge [1] first reported liquid–liquid chromatography: one liquid was used as a sorbent and another liquid was allowed to percolate through the former, thus

0021-9673/90/$03.50

making the method a chromatographic process [Martin–Synge distribution (MSD)]. Craig invented countercurrent distribution (CCD) [2] and performed such separations with CCD instruments [3,4]. The selectivity of CCD arises from the fact that the partition coefficient basically reflects the intermolecular forces, which can be strongly influenced by phase composition and by selection of a suitable temperature.

The development of CCD methods leads to liquid–liquid chromatography, called countercurrent chromatography (CCC). The theory and advantages of CCC have recently been summarized in detail by Mandava and Ito [5] and by Conway [6]. The application of CCC to natural product isolation was summarized by Hostettmann *et al.* [7]. All of the CCC methods are concerned with two immiscible phases; therefore, relative CCD was generally carried out. Recently, Lee *et al.* [8] reported the application of dual CCC. In this method, the separation system used a combination of centrifugal and planetary motion to produce an unique hydrodynamic effect which allows two immiscible phases to flow countercurrently through the coiled column. This method constitutes absolute CCD, working continously with two phases.

The other direction of development of CCD leads to liquid–liquid extraction, where the aim of the process is not to separate substances with closely related structures, but to divide a given matrix into different fractions or to isolate a pure compound from a complex mixture. Generally, modern liquid–liquid extraction methods are carried out in the relative CCD mode using two immiscible phases [9–11].

Discontinuous CCD using three immiscible liquid phases has been known for many years [3]. The efficiency of discontinuous three-phase CCD was clearly demonstrated as long ago as 1958 for the isolation of brain lipids by Meltzer [12] and Meltzer *et al.* [13]. However, this relative three-phase CCD has not found widespread use either for extraction or for chromatography, because of experimental difficulties encountered both in the selection of suitable solvents for the preparation of immiscible multi-phase systems and in the development of convenient phase separation devices. Advances in multiple liquid–liquid partition systems have not gone beyond three-phase systems.

Combining the advantage of relative and absolute CCD, the forced-flow technique with a continuous operating mode, and the three-phase solvent systems which ensure the fractionation and purification of a given biological matrix or the isolation of pure compounds from a complex mixture, we recently developed a new separation method, called forced-flow multi-phase liquid extraction (FFMLE) [14,15]. In this paper we report the principle of FFMLE, the design of the prototype apparatus and the preparation of basic three-phase liquid systems, and also describe the fundamental operating possibilities.

EXPERIMENTAL

Glass extraction columns (1500 × 60 mm I.D. and 1000 × 40 mm I.D.) were obtained from Möller (Zürich, Switzerland). The mobile phases were delivered with two Lewa lab® (Leonberg, F.R.G.) M 5 pumps.

Analytical-reagent grade solvents were used for the preparation of the three-phase solvent systems. Saturation of the multi-phase systems was always carried out for over 3 h in a shaker.

The furocoumarin-containing raw extract of *Heracleum sphondylium* was ob-

tained using chloroform as extraction solvent. The flavonoid glycoside-containing raw extract from Betulae folium was extracted with ethyl acetate. For monitoring of the extraction process, 250-ml fractions were obtained. Samples of the effluents were applied with a Linomat IV TLC spotter from Camag, (Muttenz, Switzerland). Process monitoring was by thin-layer chromatography (TLC) on silica gel 60 F_{254} TLC alufoils from Merck (Darmstadt, F.R.G.) in unsaturated chromatographic chambers. The mobile phase for TLC checks on the extraction of furocoumarins consisted of *n*-hexane–dichloromethane–tetrahydrofuran–chloroform (72.8:10.8:8.3:8.1) [16] and for the flavonoids ethyl acetate–tetrahydrofuran–*n*-hexane–ethanol–water–formic acid (70:20:15:10:5:2) [17]. The densitograms in the absorption mode were recorded at 313 nm for furocoumarins and 254 nm for the flavonoid glycosides with a Camag TLC scanner II coupled with an HP 9000-216 computer.

RESULTS AND DISCUSSION

Description of the method

The separation of a certain sample into fractions of different polarity can be achieved with the new multi-phase extraction technique. Successful separation requires that the equilibrium between the phases be maintained constantly, which means that sufficient time must be allowed for mass transfer between the phases.

On using three immiscible liquid phases, two basic situations prevail: two phases may be stationary and one mobile, or one stationary and two mobile. The five basic possibilities are shown in Fig. 1. The first four cases (Fig. 1a–d) belong to relative CCD; cases (a) and (c) represent the descending mode and cases (b) and (d) the ascending mode. The extraction columns are filled with the immiscible stationary phase or phases and mobile phase or phases are forced through the stationary phase or phases by means of one or two pumps. The directions of movement of the mobile

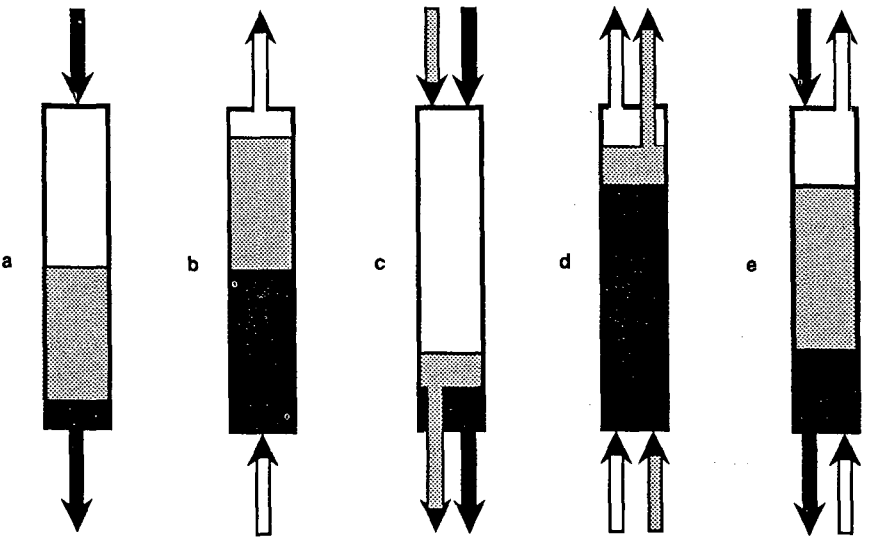

Fig. 1. Basic possibilities for extraction with three liquid phases.

phase or phases are marked with arrows. For the fifth possibility (Fig. 1e), the two mobile phases move in opposite directions as very small droplets. This method constitutes absolute CCD.

The operating principle and design of the FFMLE set-up in the absolute CCD operating mode are shown schematically in Fig. 2. The extraction column is filled with an appropriate volume of the stationary phase (shown in grey, Fig. 2). The lowest of the three immiscible liquid phases, shown in black, is pumped through the stationary (middle) phase. It moves as droplets from the top of the column to the bottom, where it is collected and removed from the system. The uppermost of the three immiscible phases (white) is pumped from the bottom to the top of the extractor, where it is collected and removed from the extraction column. The driving force for movement of the droplets is, in addition to the forced flow, the difference between the specific gravities of the phases travelling in opposite directions.

The extraction column can be thermostated; the whole system is made of inert materials. Both ends of the glass column are closed with a PTFE stopper unit. The lower unit incorporates an injector system for the upper phase, a lower phase outlet and an inlet for inert gas. The top unit consists of the lower phase injector, the upper

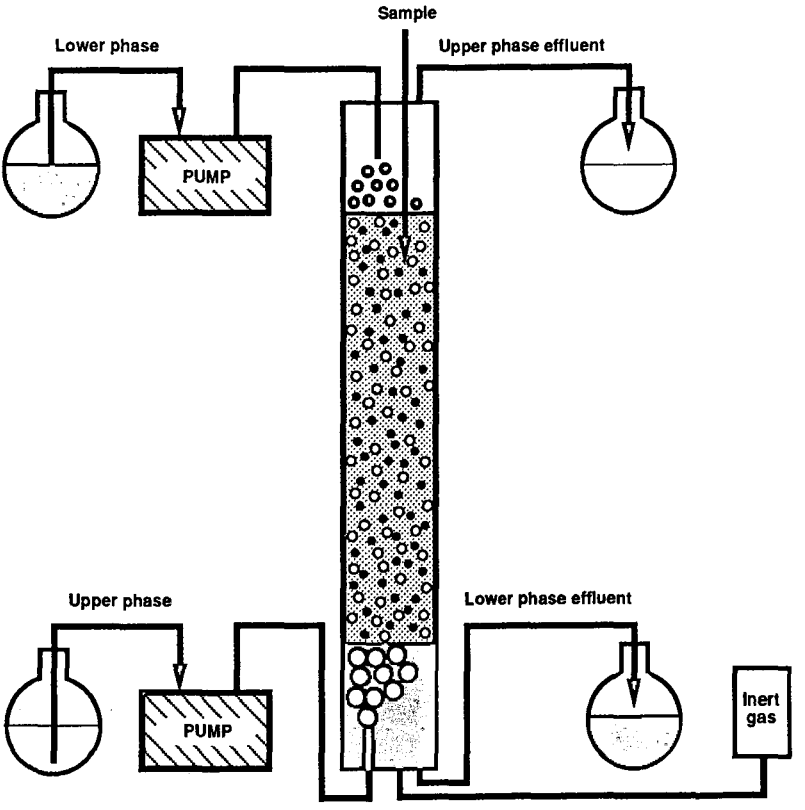

Fig. 2. Operating principle and design of the FFMLE set-up in the absolute CCD operating mode. Upper (mobile) phase is white, middle (stationary phase) is grey and the lower (mobile) phase is black.

phase outlet, a sensor for recording the level of the middle and upper phases and the sample inlet. The two mobile phases are forced through the injector systems with a programmed pump system. This is connected to an electronic sensor, which ensures that the same volume of mobile phases leave the extraction column at each end.

The high velocity (10–50 ml/min) of the mobile phases and the small diameter (0.3 mm) of the injectors ensure that both mobile phases enter the system in the form of an extremely fine spray. In the absolute CCD operating mode, the adjustable injector systems are located such that the upper phase is injected into the lower phase and the lower phase into the upper phase. At the phase boundary the droplets can be disintegrated into numerous much smaller droplets, thus significantly increasing the surface area of the droplets. In the middle phase millions of tiny droplets are present; these droplets can only be shown schematically in Fig. 2. The distance travelled by such a droplet is much longer than the length of the column, because both mobile phases move in opposite directions and therefore the droplets do not move in a straight line but, owing to the many collisions, in a zig-zag manner. The movement of inert gas (e.g., nitrogen) bubbles through the three liquid phases further enhances this effect.

The length and the inside diameter of the extraction column determine its capacity; therefore, both dimensions should be selected according to the separation problem. In the absolute CCD operating mode, the sample is always injected into the middle phase; however, the ratio of the three phases can be chosen freely.

Among the main features of FFMLE, the variety of possible operating modes, which include relative and absolute CCD and also the descending and ascending modes, warrants particular mention. Other operating factors are the geometry of the extraction column, the physico-chemical properties of the three-phase liquid system, the ratio of the phases, the flow-rate of the mobile phase(s), extraction time, pressure and temperature and amount of sample.

Needless to say, the different types of relative and absolute distribution methods may also be varied by connecting different columns together. For example, for the isolation of alkaloids after a three-phase absolute CCD the upper phase may contain alkaloids in addition to other compounds. These may then be passed through a second extraction column operating in the relative CCD mode, in which the middle stationary phase has been modified with 2% sulphuric acid; the purified alkaloid fraction is concentrated in the modified middle phase of the second column. Further, various other variations of the extraction columns are also possible. With suitable selection of three-phase liquid systems, one of the mobile phases can be passed through a second or third three-phase liquid system, with a similar solvent composition to the first.

Preparation of multi-phase solvent systems

FFMLE is a special case of liquid–liquid extraction requiring three immiscible phases which are generally obtained from three or four solvents. A three-phase liquid system can be achieved on mixing three suitable solvents, *e.g.*, a 1:1:1 mixture of *n*-hexane or *n*-octanol, water and nitromethane or nitrobenzene. However, from the practical point of view, the uses of these mixtures are limited.

Based on our experience, the solvent strength values of the individual solvents (S_i) and Snyder's solvent classification [18] seem to be helpful for selection of suitable

three-phase liquid systems. Snyder classified the commonly used solvents into eight groups (I–VIII) according to their properties with regard to proton-acceptor, proton-donor and dipole interactions. Typical three-phase systems can be obtained on mixing hexane, acetonitrile (VI) and water (VIII) as the basic ternary system, with one of the following as the fourth (auxiliary) solvent: the basic ternary system, with one of the following as the fourth (auxiliary) solvent: diethyl ether (II), dichloromethane (V), toluene (VII) or chloroform (VIII). Some of the possible three-phase liquid systems are given in Table I, together with the ratio of the upper, middle and lower phases.

TABLE I

TYPICAL TERNARY AND QUATERNARY SOLVENT SYSTEMS

	Solvent mixture	Solvent strength	Selectivity group	Solvent ratio	Phase ratio[a]
(A)	*n*-Hexane	0.1	–	1	1:1:1
	Water	10.2	VIII	1	
	Nitromethane	6.0	VII	1	
	$S_v = 5.43$				
(B)	*n*-Octanol	3.4	II	1	1:1:1
	Water	10.2	VIII	1	
	Nitromethane	6.0	VII	1	
	$S_v = 6.53$				
(C)	*n*-Butanol	3.9	II	1	23:36:41
	n-Hexane	0.1	–	1	
	Water	10.2	VI	1	
	Nitromethane	6.0	VIII	1	
	$S_v = 4.17$				
(D)	Diethyl ether	2.8	I	1	19:37:44
	n-Hexane	0.1	–	2	
	Acetonitrile	5.8	VIII	2	
	Water	10.2	VII	1	
	$S_v = 4.13$				
(E)	Dichloromethane	3.1	V	1	23:32:45
	n-Hexane	0.1	–	2	
	Acetonitrile	5.8	VI	2	
	Water	10.2	VIII	1	
	$S_v = 4.18$				
(F)	Toluene	2.4	VII	1	21:51:58
	n-Hexane	0.1	–	2	
	Acetonitrile	5.8	VI	2	
	Water	10.2	VIII	1	
	$S_v = 4.07$				
(G)	Chloroform	4.1	VIII	1	21:51:58
	n-Hexane	0.1	–	2	
	Acetonitrile	5.8	VI	2	
	Water	10.2	VIII	1	
	$S_v = 4.35$				

[a] Lower phase:middle phase:upper phase.

To the best of our knowledge, no value exists for the characterization of three-phase liquid systems. It appeared to us that the solvent strength values serve this purpose with a certain modification indicating that the total solvent strength (S_T) of the system is divided among three phases. Theoretically, all three phases may be characterized by an S_T value and the solvent strength of the system would be the average of these three S_T values. However, as the calculation of these values would be complicated, we propose the introduction of the virtual solvent strength (S_v) value for the characterization of three-phase liquid systems.

The S_v of a three-phase liquid system is the arithmetic average of the solvent strengths of the pure solvents (S_i) in the system, weighted according to the volume fraction (φ) of each solvent. For a quaternary three-phase liquid system composed of solvents A, B, C and D, the S_v can be defined as

$$S_v = \varphi_A S_A + \varphi_B S_B + \varphi_C S_C + \varphi_D S_D$$

As shown in Table I, the three-phase liquid systems always have various S_v values, which indicate the different polarities. All the mixtures presented also have different selectivities. Three-phase liquid systems can be obtained from three solvents (see Table I, mixtures A and B) or more solvents (see Table I, mixtures C–G). In four of these cases (D, E, F and G) the ratio of all the solvents in each system is the same, but there is a difference in the quality of the fourth. Diethyl ether, as a representative of group I (see in Table I), is a proton acceptor, whereas in mixture G, the fourth solvent, chloroform (group VIII), is a typical proton-donor solvent. In the other two examples the fourth solvent is from group V (mixture E), whereas toluene is from group VII (mixture F). Despite these general combinations, it has been possible to formulate a large number of three-phase solvent systems that appear to be useful for the separation of complex mixtures.

It should be noted that the selectivity can be further increased by adding a fifth solvent. A three-phase system containing eight solvents, *e.g.*, of *n*-hexane–diethyl ether–methanol–tetrahydrofuran–dichloromethane–acetonitrile–chloroform–water (68.2:3.6:4.4:7.7:25.8:50:2.4:37.8), is also known.

In Fig. 3 the ratios of the three basic solvents (water, acetonitrile and *n*-hexane) are represented in a triangular diagram, where the volume fractions of the three solvents are given as three-digit numbers, called combination points (P_c). The fourth solvent (chloroform) is added (5–25%) to achieve the three immiscible phases. The combination points, where three phases could be obtained, are shown by black circles. It is clearly seen that three-phase liquid systems can be achieved only at given P_c. These difficulties could be one of the reasons why liquid–liquid partition systems have not been exploited beyond three-phase systems.

The ratio of the solvents determines not only the selectivity, but also the volume ratio of the three immiscible phases, as is shown in Fig. 4, where the three-digit numbers represent the same three-phase solvent combinations as in Fig. 3b. The linear relationship found is always valid in the horizontal direction if the amounts of two of the four solvents (forming the three-phase system) are constant, *e.g.*, along the lines between $P_c = 127$ and 172 the volumes of water and chloroform were constant and only the ratio of acetonitrile and *n*-hexane was varied. The same is valid, *e.g.*, between $P_c = 613$ and 253, where the amount of *n*-hexane was constant (30%) and the added volume was always 10%.

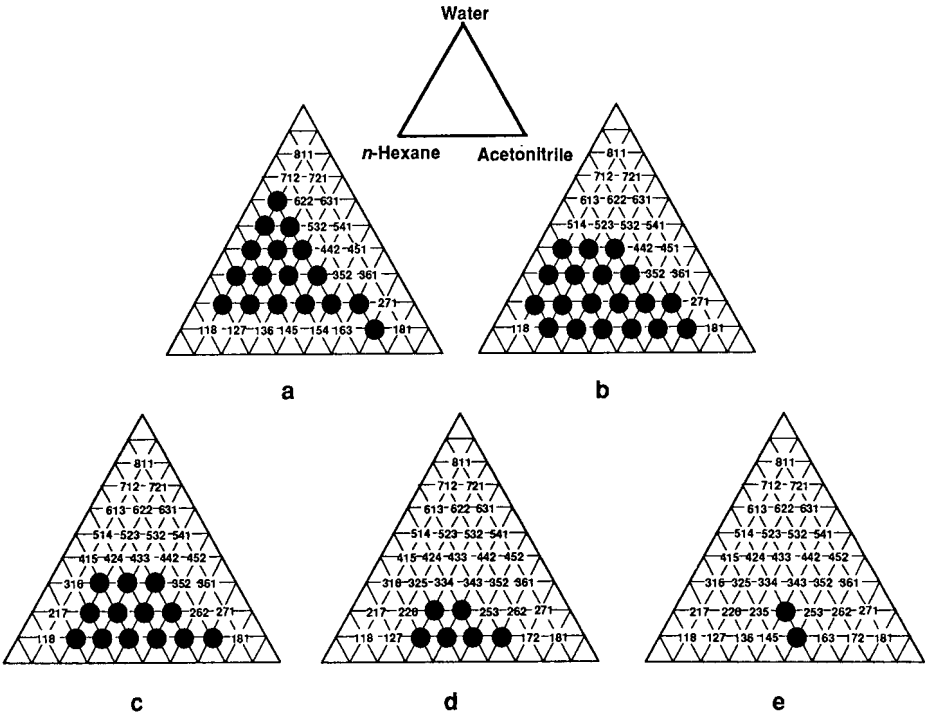

Fig. 3. Preparation of three immiscible phases for FFMLE from the three basic solvents (water, acetonitrile and *n*-hexane) and from a fourth, auxiliary solvent (chloroform). The volume fractions of the three basic solvents are given as three-digit numbers. The solvent compositions where three phases could be obtained are shown by black circles.

At a given P_c there also exists a vertical function between the fourth (auxiliary) solvent and the proportion of phases. Fig. 4b shows the connections of the amount of chloroform (5–25%) and the ratio of the three immiscible phases at $P_c = 244$. It should be noted that the change of lower phase is small and almost linear, whereas the middle and upper phases show quadratic relationships. Increasing the content of chloroform causes the volume of upper phase to decrease. At the critical volume of chloroform, where the curves of two phases meet, the third phase is eliminated.

Separation examples

Pimpinella saxifraga was selected as an example of purification for non-polar compounds containing eight furocoumarin isomers in various ratios [19]. A 860-g sample of plant material was subjected to exhaustive forced-flow solid–liquid extraction [20] with chloroform for a combined solution and diffusion time [21] of 6 h. The residue of the extract was dissolved in the middle phase of the saturated three-phase system, which consisted of chloroform–*n*-hexane–acetonitrile–water (5:20:60:20). The extraction column was filled with 10% of lower phase, 80% of middle phase and 10% of upper phase. The sample was injected into the middle layer of the three-phase system. FFMLE was carried out in the absolute CCD operating mode at a velocity of

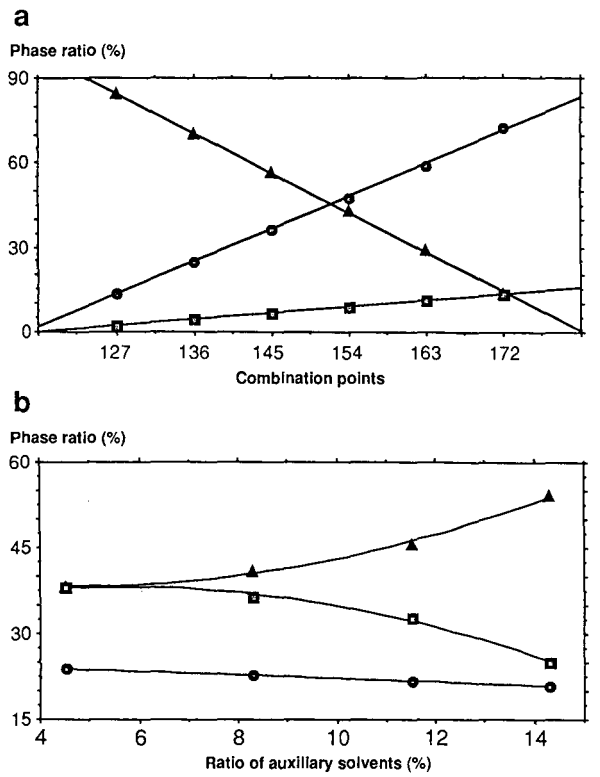

Fig. 4. Ratio of three immiscible phases using the solvent composition from Fig. 3b. ● = Upper phase; ▲ = middle phase; ■ = lower phase. (a) The horizontal linear relationship for a quaternary solvent system. The amounts of any two solvents (water and chloroform shown) are constant; only the ratio of the others (acetonitrile and *n*-hexane shown) are varied. (b) The vertical relationship for a quaternary solvent system. Only the amount of the auxiliary solvent (chloroform shown) is varied.

23 ml/min for both mobile phases. Upper phase fractions of 250 ml were monitored by TLC; the total area of the densitograms between 0.1 and 0.8 was determined at 313 nm. The extraction was complete in 40 min. After the process was finished, the two other (middle and lower) phases were also checked by analytical methods [22]. It could be stated that the extraction was exhaustive.

As an example of the extraction of polar compounds, flavonoid glycosides were separated from Betulae folium. The forced-flow solid–liquid extraction was started with chloroform to purify the plant material (1650 g) from non-polar compounds. Extraction of flavonoid glycosides was subsequently carried out with ethyl acetate for a combined solution and diffusion time [21] of 8 h. The residue of the extract was dissolved in the middle phase of the three-phase liquid system [chloroform–*n*-hexane–acetonitrile–water (13:26:4:13)]. FFMLE was carried out in the absolute CCD operating mode at a velocity of 10 ml/min for both mobile phases. The lower phase fractions containing the flavonoid glycosides were evaporated and the amount of flavonoid glycosides was determined in each fraction by analytical methods [23]. The two other immiscible phases were also checked. The exhaustive extraction of flavonoid glycosides was completely finished in 65 min.

CONCLUSIONS

This novel CCD method permits the rapid and complete extraction of various substance classes from complex matrices. It utilizes the forced-flow technique and works with three immiscible liquid phases within an extraction column. The whole process is continuous, including the sample application and the outlet of effluents.

The most important advantage of this separation technique, as with other liquid–liquid partition methods, lies in the absence of solid supports. Additionally, it can be applied as a thorough yet mild purification and/or isolation method owing to the permanent present of inert gas in the extraction column.

The technique can be used on both the micropreparative and preparative scales by variation of the column size, is more readily applied to separations of polar compounds, is applicable to both small and macromolecules and operates at low pressure (< 10 p.s.i.). The equipment is simple to operate, comparatively inexpensive, requiring minimum bench space, and is easily cleaned between runs. Also macromolecules that have been purified by the slower CCD procedure may be efficiently separated by FFMLE. It is perhaps best regarded as being complementary to, rather than competitive with, other purification and/or extraction methods.

ACKNOWLEDGEMENTS

The authors thank Petazon (Zug, Switzerland) for producing a prototype of the multi-phase liquid extraction device. Financial support from the Swiss KWF Commission is gratefully acknowledged.

REFERENCES

1 A. J. P. Martin and R. L. M. Synge, *Biochem. J.*, 35 (1941) 1358.
2 L. C. Craig, *J. Biol. Chem.*, 155 (1944) 519.
3 L. C. Craig, W. Hausmann, E. H. Ahrens, Jr., and E. J. Harbenist. *Anal. Chem.*, 23 (1951) 1326.
4 L. C. Craig and D. Craig, in A. Weissberger (Editor), *Technique of Organic Chemistry* Vol. 3, Interscience, New York, 2nd ed., 1956, p. 149.
5 N. B. Mandava and Y. Ito (Editors), *Countercurrent Chromatography*, Theory and Practice, Marcel Dekker, New York, 1988.
6 W. D. Conway, *Countercurrent Chromatography —Apparatus, Theory and Applications*, Verlag Chemie, Weinheim, 1990.
7 K. Hostettmann, M. Hostettmann and A. Marston, *Preparative Chromatography Techniques, Applications in Natural Product Isolation*, Springer, Berlin, 1986.
8 Y.-W. Lee, C. E. Cook and Y. Ito, *J. Liq. Chromatogr.*, 11 (1988) 37.
9 R. Blumberg, *Liquid–Liquid Extraction*, Academic Press, London, 1988.
10 K. Najuin, *Control of Liquid–Liquid Extraction Columns*, Gordon and Breach, New York, 1988.
11 M. Brenner, C. Moirandat and R. Schlimme, *J. Chromatogr.*, 499 (1990) 721.
12 H. L. Meltzer, *J. Biol. Chem.*, 233 (1958) 1327.
13 H. L. Meltzer, J. Buchler and Z. Frank, *Anal. Chem.*, 37 (1965) 721.
14 Sz. Nyiredy, L. Botz and O. Sticher, *Swiss Pat.*, 673405, 1990; *Patent Cooperation Treaty Pat. Appl.* PCT/CH 89/ 00028, 1989.
15 Sz. Nyiredy, L. Botz and O. Sticher, *Planta Med.*, 55 (1989) 585.
16 Sz. Nyiredy, L. Botz and O. Sticher, *J. Planar Chromatogr.*, 2 (1989) 53.
17 Sz. Nyiredy, S. Y. Mészáros, K. Dallenbach-Tölke, K. Nyiredy-Mikita and O. Sticher, *J. Planar Chromatogr.*, 1 (1988) 54.
18 L. R. Snyder, *J. Chromatogr. Sci.*, 16 (1978) 223.
19 G. C. Zogg, Sz. Nyiredy and O. Sticher, *Dtsch. Apoth.-Ztg.*, 129 (1989) 717.
20 Sz. Nyiredy, L. Botz and O. Sticher, *Swiss Pat. Appl.*, 03 197/89-7, 1989.
21 Sz. Nyiredy, L. Botz and O. Sticher, in preparation.
22 G. C. Zogg, Sz. Nyiredy and O. Sticher, *J. Planar Chromatogr.*, 1 (1988) 351.
23 K. Dallenbach-Tölke, Sz. Nyiredy and O. Sticher, *Dtsch. Apoth.-Ztg.*, 127 (1987) 1167.

Journal of Chromatography, 523 (1990) 53–60
Elsevier Science Publishers B.V., Amsterdam

CHROMSYMP. 2021

Improved methods for the purification of enzymes of the folate pathway in *Escherichia coli*

I. Chromatographic methods

RAINER BARTELS and LOTHAR BOCK*
Forschungsinstitut Borstel, Medizinisch-Pharmazeutische Chemie, Parkallee 4a, D-2061 Borstel (F.R.G.)

ABSTRACT

A sequence of chromatographic procedures is described for the isolation of three consecutive enzymes of the folate pathway in *Escherichia coli*: hydroxymethyldihydropteridine pyrophosphokinase (E.C. 2.7.6.3) (I), 7,8-dihydropteroate synthase (E.C. 2.5.1.15) (II) and 7,8-dihydrofolate reductase, (E.C. 1.5.1.3) (III). Starting with the crude extract, ion-exchange chromatography on a DEAE-Sepharose CL-6B column with a salt gradient completely separated I, II and III. I and II were further purified by hydrophobic-interaction chromatography on Phenyl-Sepharose CL-4B, followed by size-exclusion chromatography on Ultrogel AcA 54. For III only size-exclusion chromatography was used. The overall enrichment factors, on the basis of protein, were 13 700-fold for I, 280-fold for II and 500-fold for III. Bacterial batches of more than 500 g were handled.

INTRODUCTION

For special assignments in enzymology, the availability of purified enzymes, acting sequentially in a biochemical pathway, is sometimes necessary. We were interested in the properties of the enzymes of the folate pathway of *E. coli, i.e.*, hydroxymethyldihydropteridine pyrophosphokinase (E.C. 2.7.6.3) (I), 7,8-dihydropteroate synthase (E.C. 2.5.1.15) (II) and 7,8-dihydrofolate reductase (E.C. 1.5.1.3) (III), which catalyse the reactions shown in Fig. 1. For this a purification procedure combining different efficient chromatographic methods was selected, starting from whole cells of *Escherichia coli*.

Classical strategies in protein purification recommend adsorptive media with high load capacities at the beginning, followed by volume- or mass-limited techniques toward the end of the procedure. Under some circumstances, this strategy must be abandoned, *e.g.*, if unsuccessful separation efficiencies compel changes in this sequence. This seemed to be the case in the purification method for enzymes I and II, published by Richey and Brown [1]. According to their paper, size-exclusion chromatography (SEC) rather than ion-exchange chromatography (IEC) is performed first. However, in such a procedure there is a bottle-neck in the economical accumulation of sufficient amounts of enzyme.

0021-9673/90/$03.50

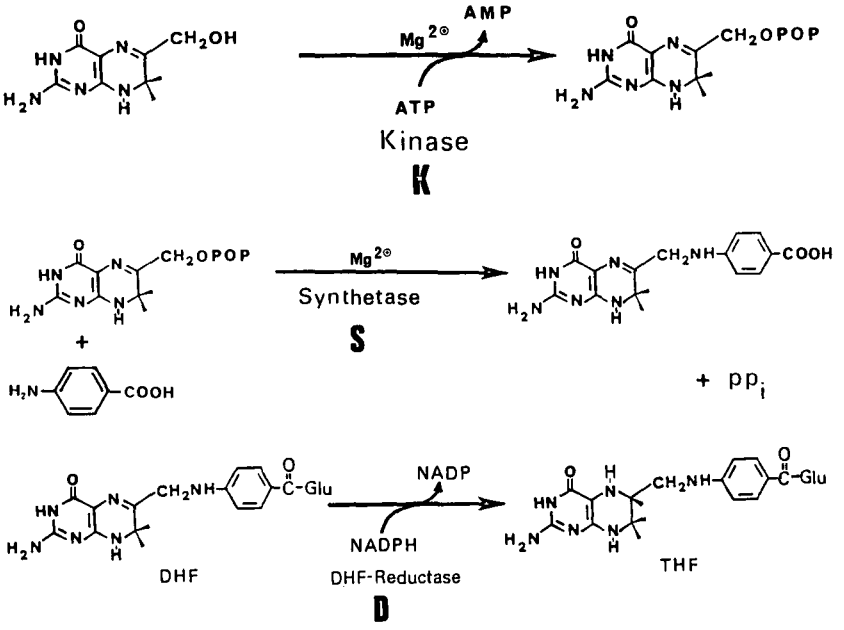

Fig. 1. Enzyme reactions.

In our procedure, the classical strategies mentioned above are used and III is additionally obtained.

EXPERIMENTAL

Materials

The column materials DEAE-Sepharose CL-6B and Phenyl-Sepharose CL-4B, were purchased from Pharmacia (Freiburg, F.R.G.) and Ultrogel AcA-54 from LKB (Bromma, Sweden). The glass columns (50 × 10 cm I.D., 30 × 5 cm I.D. and 90 × 5 cm I.D.) were obtained from Kranich (Göttingen, F.R.G.). The preparation of substrates for the tests of I and II and the sources of chemical supplies were described in ref. 2 and those for III in ref. 3. The cell mass was fermented by E. Merck (Darmstadt, F.R.G.) using *E. coli* ATCC, strain 11.7775, from the American Type Culture Collection (Rockville, MD, U.S.A.). Thin-layer chromatographic (TLC) plates, trishydroxymethyl aminomethane (Tris) and all other chemicals were purchased from E. Merck. Equipment for ultrafiltration with membrane type PM 10 was from Amicon, [Witten (Ruhr), F.R.G.].

Methods

All enzyme purifiation steps were carried out at 4°C, unless stated otherwise. The salt gradients were monitored by conductivity measurements. The enzyme activities of I and II were determined by a TLC method [2], following the increase in products fluorimetrically at an excitation wavelength of 365 nm. The activity of III was

determined photometrically according to ref. 3 by following the decrease in absorbance of the substrates NADPH and dihydrofolic acid at 340 nm. Two buffer concentrations were used (pH 7.7): buffer A, 0.1 *M* Tris–HCl and buffer B, 0.01 *M* Tris–HCl.

The protein content of fraction I was determined by the method of Lowry *et al.* [4], while the one in the chromatographic fractions was estimated by the method of Warburg and Christians [5]. If storage was necessary after separation, the pooled fractions were concentrated, dialyzed against buffer B by ultrafiltration, and lyophilized.

Crude extract

Usually, 550 g of frozen cells were thawed and suspended in 370 ml of buffer A, resulting in a total volume of 855 ml. For easier handling, this cell suspension was divided into two parts. Each part was subjected to twenty ultrasonication intervals of 2 min each (Branson B12 sonifier, output control: 10; Heinemann, Schwäbisch Gmünd, F.R.G.). The temperature was held between 3 and 10°C. The DNA of the broken cells was digested by treatment with DNase I (27 mg of DNase I per 20 ml of buffer A) for 30 min at room temperature with stirring. Cell debris was separated by ultracentrifugation (2 h at 145000 *g*; MSE Superspeed 65 centrifuge, Colora, Lorch/Württ., F.R.G.). The supernatant of *ca.* 640 ml was subjected to fractional precipitation by addition of solid ammonium sulphate, 20–70% saturation at 4°C. A pH of 7.7 was maintained by dropwise addition of 1.0 *M* NaOH. Both precipitations were accomplished by stirring the suspension for *ca.* 1 h. The precipitated proteins were collected by centrifugation in a Beckman (Munich, F.R.G.) J2-21 centrifuge (30 min at 22000 *g*). In the 20% fraction the three enzymes remained in the supernatant whereas in the 70% step they precipitated together with the bulk of the protein. The pellet was suspended in *ca.* 210 ml of buffer A and dialysed once against 2 l of buffer A followed by 5-l batches of buffer B until the electric conductivity after the last buffer change corresponded to that of buffer B. Insoluble material was removed by centrifugation. With the aid of 4 *M* NaCl in buffer B, the clear dark yellow supernatant was adapted to the equilibration buffer of the ion-exchange column (55 m*M* NaCl in buffer B) (pH and conductivity control). If necessary, the protein concentration of this solution was adjusted to *ca.* 30 mg/ml with equilibration buffer (fraction I).

Ion-exchange chromatography

A DEAE-Sepharose CL-6B column (47 × 10 cm I.D.) was prepared and equilibrated with 55 m*M* NaCl in buffer B. The column was run with a flow-rate of *ca.* 3 ml/min. After fraction I (28.6 g of protein in 905 ml of equilibration buffer, 31.6 mg/ml) had been applied to the column, unbound material was washed out with starting buffer until the absorbance of the eluent matched the baseline. The column was developed with the aid of an increasing salt gradient (8.5 l of 55 m*M* NaCl in buffer B against 8.5 l of 360 m*M* NaCl in buffer B) and finally flushed with 0.8 *M* NaCl in buffer B. Fractions of 26.5 ml were collected. The activities of enzymes I, II and III, were located according to refs. 2 and 3 and pooled in fractions K, S and D, respectively (Fig. 2). The fractions K and S were further purified by HIC, whereas fraction D was submitted to SEC.

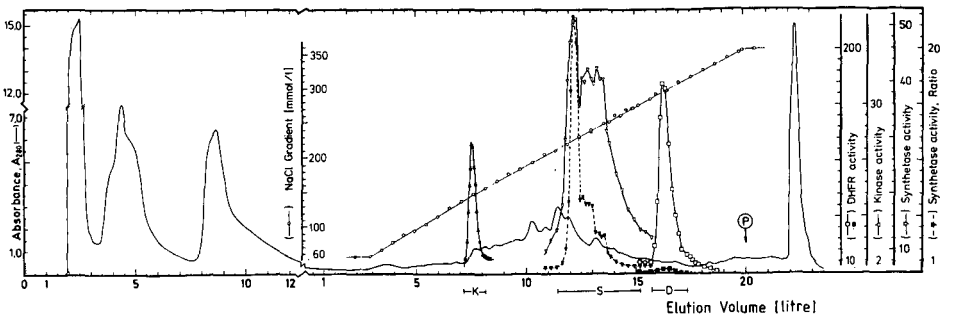

Fig. 2. Ion-exchange chromatography of fraction I on DEAE-Sepharose CL-6B. Activity of enzyme I (△) expressed in arbitrary area units. Activity of enzyme II expressed in arbitrary area units (▽) and the product/substrate ratio (▼). (□) Activity of enzyme III. Control: + 1 m*M* methotrexate (■), expressed as $-\Delta A_{340} \times 10^{-3}$/min corresponding to $81.3 \cdot 10^{-6}$ units/ml [6].

Hydrophobic-interaction chromatography (HIC)

Fractions K and S from the ion-exchange chromatography were separately loaded onto a Phenyl-Sepharose Cl-4B column (27 × 5 cm I.D.). To attain adequate binding and separation of the desired enzymes the total loading of protein should be lower than 10 mg/ml column material (a load of *ca.* 3 g of protein and a concentration of 4 mg/ml in each instance were successful). The flow-rate was 2 ml/min. Fractions of 27 ml were collected during the gradient. Enzyme activities were located using a previously described method [2].

For purification of enzyme I, the column was equilibrated with 3 *M* NaCl in buffer B and fraction K from IEC was adjusted to this salt concentration. After the protein solution (2.9 g of protein in 750 ml) had been applied, the column was washed with equilibration buffer. Normally, after a 9–10-l wash all of the unattached protein was eluted and the decreasing salt gradient was started (2.5 l of 3 *M* NaCl in buffer B down to 2.84 l of buffer B). The activity of I was pooled (fraction K) and finally purified by SEC (Fig. 5).

For purification of enzyme II, the column was equilibrated with 2 *M* NaCl in buffer B. Fraction S from IEC was adjusted to this salt concentration and loaded onto the column (2.6 g of protein in 612 ml). Unbound material was washed out with the equilibration buffer. Normally, after a 9–10-l wash the absorbance matched the baseline and a decreasing salt gradient in combination with an increasing alcohol gradient was started (2.5 l of 2 *M* NaCl in buffer B against 2.74 l of an aqueous solution of 5% ethanol). The activity of enzyme II was located in fraction S, which was finally purified by SEC (Fig. 6).

Size-exclusion chromatography

Fractions K and S from HIC and fraction D from IEC were applied separately onto an Ultrogel AcA-54 column (84 × 5 cm I.D.), equilibrated with 80 m*M* NaCl in buffer B. The flow-rate was *ca.* 1 ml/min and fractions of 20 ml were collected.

The samples applied were as follows: enzyme I, fraction K from HIC (88.5 mg in 24.7 ml); enzyme II, fraction S from HIC (248 mg in 38 ml) and enzyme III, fraction D from IEC (654 mg in 28 ml). Enzyme activities were located as indicated above.

RESULTS AND DISCUSSION

Our aim was the development of an efficient preparation procedure to obtain the enzymes I, II and III of the folate pathway in *E. coli* in both sufficient quantity and purity.

Fig. 2 shows that a DEAE-Sepharose CL-6B column clearly separates these three enzymes under the conditions described under Experimental. The enzymes I and III were eluted as single sharp peaks centred at NaCl concentrations of 145 and 285 m*M*, respectively. Because of the favourable elution pattern of the proteins in this range of the gradient, the purification effects calculated on the basis of protein content were 25- and 40-fold for I and III, respectively.

However, the elution pattern of enzyme II is complicated and shows at least two peaks of activity, as determined by the enzymatic product, covering a range from about 210 to 270 m*M* NaCl near the bulk of the protein. Thus the purification effect of this step is only *ca.* 5-fold. We observed this phenomenon always when the separation techniques had been based on differences in charge and adsorption behaviour, no matter whether a crude sample preparation [7] or a highly purified enzyme had been used [8]. Therefore, we assume dynamic changes in the conformation(s) of enzyme II during the separation process comparable to the behaviour in binding of this enzyme to an affinity matrix [9]. This hypothesis is supported by kinetic studies of Ferone and Webb [10].

If the enzyme activity of II is determined on the basis of the product/substrate ratio (H_2-pteroate/H_2-ptCH_2OPOP)[a], the main activity centres in the first peak of fraction S correspond to 225 m*M* NaCl. In this peak an overproportional consumption of the pyrophosphate substrate is observed, whereas a corresponding formation of the product H_2-pteroate is missing. In accordance with the observations of Ferone and Webb [10], this behaviour may be explained by a product inhibition of the H_2-pteroate which is synthesized to a sufficient level in these enzymatically most active fractions. Additionally, there seems to be a pyrophosphorylase activity in these fractions, probably caused by a contaminating enzyme [1] and/or by the enzyme II itself, despite its inhibition by its product H_2-pteroate. This effect was also noticed when more purified samples of II were used [11]. Therefore, we speculate on a pyrophosphorylase activity associated with a distinctive conformation of enzyme II. More experiments have to be carried out to clarify this phenomenon of pyrophosphorylase activity.

Figs. 3 and 4 show the HIC of the enzymes I and II. There are significant differences in the hydrophobic properties of these enzymes. I is less hydrophobic than II and therefore different NaCl concentrations are recommended for binding each enzyme on the Phenyl-Sepharose column. Furthermore, special conditions for the elutions are necessary.

As shown in Fig. 3, enzyme I is eluted from the column in the range 1.6–1.3 *M* NaCl. The absorbance pattern at 280 nm indicates an efficient separation effect. Finally, this enzyme was highly purified by SEC (Fig. 5) with an overall purification effect of *ca.* 13 700-fold as calculated on the basis of its protein balance.

---

[a] H_2-ptCH_2OPOP = Hydroxymethyldihydropteridine pyrophosphate, see also Fig. 1.

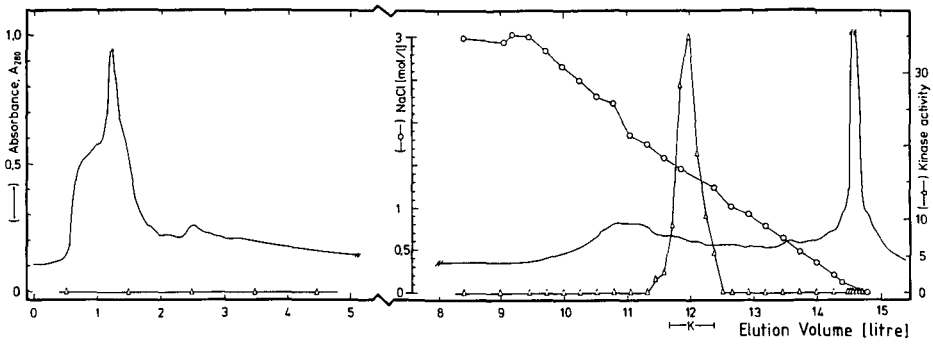

Fig. 3. Hydrophobic-interaction chromatography of fraction K from the IEC column on Phenyl-Sepharose CL-4B. Activity of enzyme I (△) expressed in arbitrary area units.

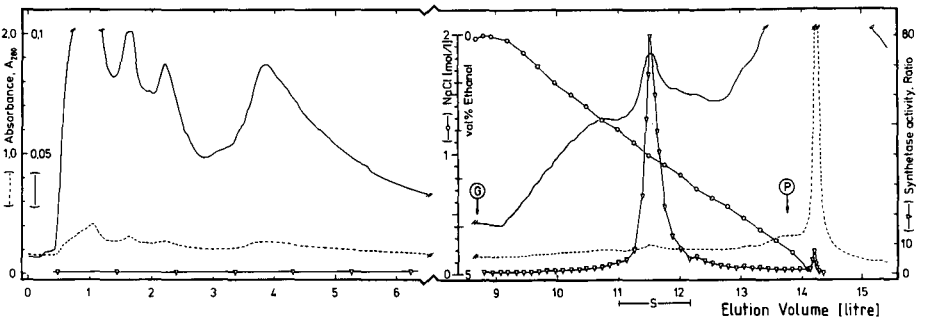

Fig. 4. Hydrophobic-interaction chromatography of fraction S from the IEC column on Phenyl-Sepharose CL-4B. Activity of enzyme II (▽) expressed as the product/substrate ratio.

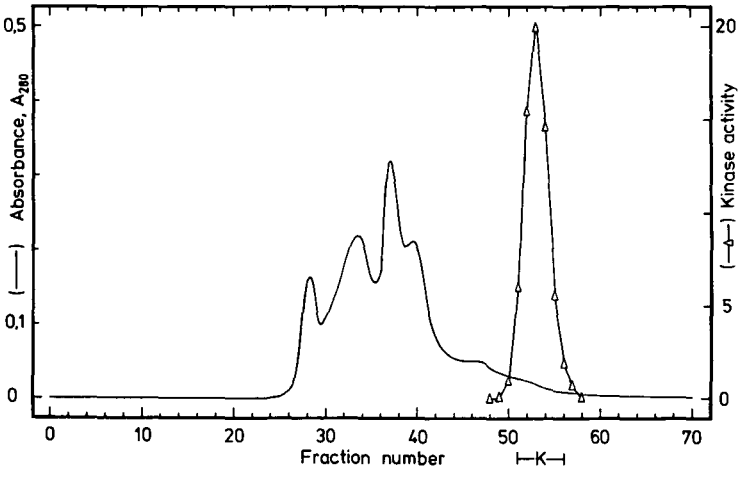

Fig. 5. Size-exclusion chromatography of fraction K from HIC on Ultrogel AcA-54. Activity of enzyme I (△) expressed in arbitrary area units.

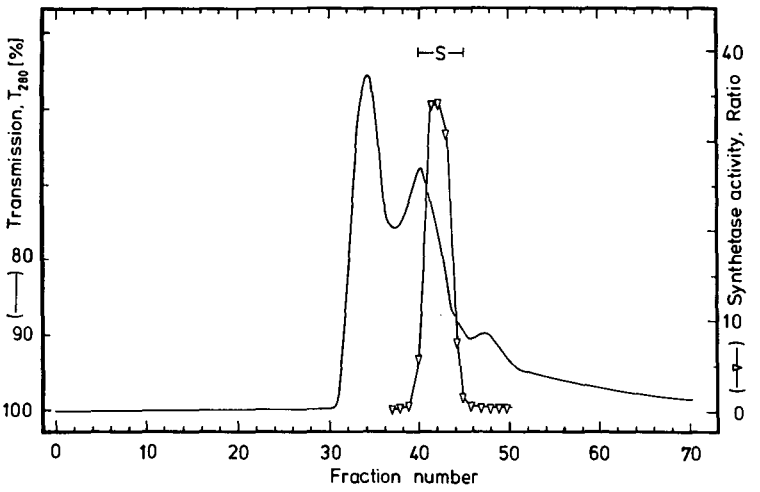

Fig. 6. Size-exclusion chromatography of fraction S from HIC on Ultrogel AcA-54. Activity of enzyme II (▽) expressed in arbitrary area units.

Fig. 4 shows the binding and elution conditions of enzyme II on the same column material, but equilibrated with a low concentration of NaCl. Because enzyme II seems to expose a hydrophobic domain, a decreasing salt gradient was run simultaneously against an increasing gradient of ethanol. Enzyme II is detached in a peak corresponding to 1 *M* NaCl and 2.5% ethanol together with a distinct peak of protein. Finally, after SEC (Fig. 6), the total purification effect was *ca.* 280-fold. This material is a suitable sample for application of an electrophoretic purification process such as preparative isoelectric focusing [8].

Fraction D from the IEC experiment was purified only by SEC (Fig. 7), yielding

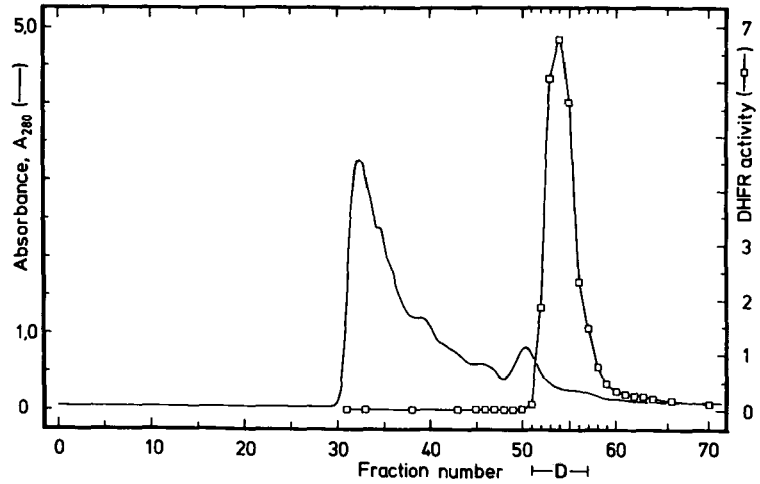

Fig. 7. Size-exclusion chromatography of fraction D from IEC on Ultrogel AcA-54. Activity of enzyme III (□) expressed as described for Fig. 1.

a purification effect of *ca.* 500-fold by these two steps. In this enzyme preparation an unspecific background consumption of the substrate NADPH of only 1% was observed, as determined by the inhibitory effect of methotrexate (data not shown) which was tolerable for our purposes.

In conclusion, ion-exchange chromatography is useful for a high loading capacity at the beginning and further is not restricted by the sample volume by special procedures. As the salt concentration of the samples obtained increases during this separation procedure, HIC should be the next step. For this task only a further increase in the salt concentration is necessary, *ie.*, by addition of solid NaCl. There is no need to reduce the sample volume. Finally, SEC separates proteins of different size and simultaneously eliminates high salt concentrations. These methods of purification were repeated several times and showed high reproducibility. Before the samples are ready for storage they have to be dialysed, concentrated by ultrafiltration and lyophilized. In our hands, bacterial masses of more than 500 g have been processed, but scaling up is easily possible.

REFERENCES

1 D. P. Richey and G. M. Brown, *J. Biol. Chem.*, 244 (1969) 1582–1592.
2 L. Bock, W. Butte, M. Richter and J. K. Seydel, *Anal. Biochem.*, 86 (1978) 238–251.
3 M. Wiese, M. Kansy, B. Kunz, K.-J. Schaper and J. K. Seydel, in H.-Ch. Curtius, S. Ghisla and N. Blau (Editors), *Proc. 9th Int. Symp. on the Chemistry and Biology of Pteridines*, 1989, Walter de Gruyter, Berlin, New York, 1990, in press.
4 O. H. Lowry, N. J. Rosebrough, A. L. Farr and R. J. Randall, *J. Biol. Chem.*, 193 (1951) 265–275.
5 O. Warburg and W. Christians, *Biochem. Z.*, 310 (1941) 384.
6 B. L. Hillcoat, P. F. Nixon and R. L. Blakley, *Anal. Biochem.*, 21 (1967) 178.
7 L. Bock and R. Bartels, in D. Stathakos (Editor), *Electrophoresis '82, Advanced Methods, Biochemical and Clinical Applications, Athens (Greece), 1982*, Walter de Gruyter, Berlin, New York, 1983, pp. 485–489.
8 R. Bartels and L. Bock, in C. Schafer-Nielsen (Editor), *Electrophoresis '88, Proceedings of the 6th Meeting of the International Electrophoresis Society, Copenhagen, 1988*, VCH, Weinheim, 1988, pp. 289–294.
9 C. J. Suckling, J. R. Sweeney and H. C. S. Wood, in W. Pfleiderer (Editor), *Proc. 5th Int. Symp. on the Chemistry and Biology of Pteridines, 1975*, Walter de Gruyter, Berlin, 1975, pp. 61–71.
10 R. Ferone and S. R. Webb, in W. Pfleiderer (Editor), *Proc. 5th Int. Symp. on the Chemistry and Biology of Pteridines, 1975*, Walter de Gruyter, Berlin, 1975, pp. 73–83.
11 R. Bartels and L. Bock, unpublished results.

Journal of Chromatography, 523 (1990) 63–80
Elsevier Science Publishers B.V., Amsterdam

CHROM. 22 746

Utility of the displacement effect in the routine optimization of separations by preparative liquid chromatography

JOAN NEWBURGER
Squibb Institute for Medical Research, P.O. Box 4000, Princeton, NJ 08543-4000 (U.S.A.)
and
GEORGES GUIOCHON*
* *Department of Chemistry, University of Tennessee, Knoxville, TN 37996-1600 and Division of Analytical Chemistry, Oak Ridge National Laboratory, Oak Ridge, TN 37831-6120 (U.S.A.)*
(First received February 7th, 1990; revised manuscript received June 8th, 1990)

ABSTRACT

The utility of the displacement effect, previously observed between the first- and the second-eluted components of a particular binary mixture ("sample self-displacement effect"), is demonstrated by a further series of experiments. The use of this phenomenon is shown to be an effective, general approach for the separation of a binary mixture. When practical, it considerably facilitates the optimization of experimental conditions for a high production rate of very pure fractions, while permitting the achievement of high recovery yields. Using a 750 × 21.4 mm I.D. silica column, separations of several two-component mixtures were achieved for loads as high as 6 g per injection. A good recovery of the first-eluting component with a purity higher than 99% is easily achieved. As the loading increases, tailing of the first component into the second band can reduce the production of the second component. Nevertheless, the recoveries for both components can be substantially greater than those achieved with conventional elution chromatography. Factors found to influence recovery yield are α, k' and the mobile phase flow-rate. Guidelines are presented that can be used routinely to induce the self-displacement separation mode.

INTRODUCTION

Displacement chromatography is an attractive separation method [1]. Sharp boundaries form between successive bands in an isotachic displacement train and provide for very strong concentration gradients of closely eluted compounds, *i.e.*, for high-concentration fractions. Large productions per run and good recovery yields make the method extremely attractive. Its use at the laboratory level for multi-batch separations is hampered, however, by the long development time and by the lengthy and tedious regeneration steps after each injection to remove the strongly retained displacing agent. In contrast, the ability to induce a displacement effect between two closely eluted components of a mixture without resorting to an external displacer is a very attractive feature of high-concentration elution chromatography. This induction is possible, as we have shown previously, in a particular case [2–4].

When the sample size of a binary mixture is increased, and if the concentration

0021-9673/90/$03.50

of the second component in the feed is of the same order as or larger than that of the first component, displacement by the second band of the first band takes place and can be very strong. The second component pushes the first one in front of it, a shock layer appears between the two components and the mixed band between the two zones of almost pure compounds can be narrow if the experimental conditions are properly adjusted [2,3]. As noted above, the addition of a displacer is not necessary to achieve this result and a considerable increase in production rate can be easily achieved. We have termed this phenomenon "sample self-displacement", to emphasize the concept of interaction between the sample components during their overloaded elution.

Previous work was done with a mixture of epimers, having a relative retention near unity [2,3]. Accordingly, the generality of the phenomenon, in spite of strongly supportive theoretical evidence [5], was not proved. This work demonstrates experimentally that the phenomenon is general and can be used to increase production for any two-component batch purified using preparative liquid chromatography. Further, we show that the method can be used routinely and that it is easy to find the experimental conditions under which the phenomenon of sample self-displacement takes place.

EXPERIMENTAL

Apparatus

Preparative experiments were carried out on a Waters Assoc. (Milford, MA, U.S.A.) Model 3000 preparative liquid chromatograph, equipped with a Waters Assoc. Model 480 variable-wavelength absorbance detector and a Kipp & Zonen (Delft, The Netherlands) Model BD40 strip-chart recorder.

Isomer ratios were determined on an analytical high-performance liquid chromatographic (HPLC) system consisting of a Perkin-Elmer (Norwalk, CT, U.S.A.) Series 4 liquid chromatograph, an Applied Biosystems (Foster City, CA, U.S.A.) Model 783a variable-wavelength absorbance detector, a Perkin-Elmer ISS-100 autosampler and a Perkin-Elmer Model 7700 data collection system.

Reagents

Solvents were of HPLC grade, purchased from J. T. Baker (Phillipsburg, NJ, U.S.A.). Diethyl phthalate, dimethyl phthalate, α-tetralone, β-tetralone and benzosuberone were of 99% + purity from Aldrich (Milwaukee, WI, U.S.A.).

Preparative chromatographic conditions

The preparative column consisted of three identical 250 × 21.4 mm I.D. Dynamax 8-μm silica columns (Rainin Instruments, Woburn, MA, U.S.A.) connected in series with the minimum length of 0.040-in. tubing. For the experiment on the separation of a mixture of dimethyl and diethyl phthalate, one column or two columns in series were also used.

Prior to use, each column was washed with the following series of solvents: 100 ml of tetrahydrofuran (THF)–hexane (30:70), 300 ml of THF–hexane–ethyl acetate (10:75:15) and 1 l of ethyl acetate–hexane (15:85). This procedure was found to be necessary to remove any trace of silica-deactivating solvents (*e.g.*, water) present in

the shipping solvent. Failure to wash the columns resulted in a substantial reduction of the displacement effect.

For the β-tetralone–diethyl phthalate and the diethyl phthalate–dimethyl phthalate experiments, the mobile phase was ethyl acetate–hexane (4:96). The flow-rate was 40 ml/min (0.25 cm/s), except as noted in the flow-rate study. Peaks were monitored at 300 nm.

For the β-tetralone–benzosuberone self-displacement experiments, the mobile phase was ethyl acetate–hexane (2:98) for the loading study or ethyl acetate–hexane (2:98), (3:97) or (3.85:96.15) for the k' study. For the elution chromatographic experiment, the mobile phase was ethyl acetate–hexane (0.5:99.5). The flow-rate was 50 ml/min and peaks were monitored at 310 nm.

Procedures

Test compounds were weighed out according to the desired ratio (25:75) and loadings, added to volumetric flasks and dissolved in mobile phase at concentrations of 0.3–3 g per 5 ml, 4-5 g per 7 ml or 6 g per 9 ml. If necessary, ethyl acetate was added to improve the solubility. Sample mixtures were injected onto the column by filling a 5-, 7- or 9-ml injection loop (Rheodyne, Cotati, CA, U.S.A.).

For each injection, fractionation began as soon as a slope change was noted. Fraction volumes were monitored indirectly by counting chart paper units. Most of the fraction volumes were 10 and 16 ml in the α-tetralone and β-tetralone experiments, respectively. Multiple volumes were collected for the first one or two and the last two or three fractions.

The fractions were analyzed to determine component ratios using a Waters Assoc. Nova-Pak 4-μm silica column (150 mm × 3.9 I.D.). In all studies, a mobile phase of ethyl acetate–hexane (2:98) was used and the peaks were monitored at 254 nm. Owing to the difference in molar absorptivities for the components of each mixture, it was not possible to obtain component ratios in the fractions by taking a simple ratio of integration area counts. Instead, masses for each compound per injection were determined by comparison with known standards. A standard of each component was made up fresh and injected several times for every fraction set analysis. The absorbance was linear for most of the concentration range, although for very small and very large amounts the fit was poorer.

Calculations

Recovery yields were calculated for each chromatogram by counting the number of chart paper units under the curve. This procedure was reproducible to within a few percent. The criteria for 95% and 99% pure materials required that all fractions of less than 94% and 98.5% purity, respectively, be discarded. The chromatogram areas of the impure, mixed fractions were discounted in determining the total pure material recovered.

The yields determined by this method are only approximate as the molar absorptivities for each component of the particular fractions are different. Yields from the different sets of mixtures should not be compared; however, reasonable conclusions regarding relative behavior can be drawn from injections of the same mixture. The reported "total yield combined" is the sum of the recoveries at the required purity for the first and the second components.

RESULTS AND DISCUSSION

Successful extension of the overload phenomenon, sample self-displacement, from the original laboratory application to a practical preparative tool has been predicted only in modeling studies [5–9]. A non-linear phenomenon was inferred from some published data [2,3,10,11], but actual band profile data were still lacking for confirmation at the beginning of this study. Therefore, at the outset of this study, chromatographic conditions were designed to mimic as closely as possible those used in the prior epimer study. Nevertheless, potential sample compounds were chosen at random from the Aldrich catalog to prove the generality of the overload technique. We have systematically investigated the effect of sample size and several other experimental parameters on the batch production of pure material from multi-gram injections of three selected mixtures. Detailed investigations of band profiles under overloaded conditions have been published recently [12–14]. In contrast to this work, however, they do not focus on the influence of the experimental conditions on the recovery yield and production rate.

Effect of sample size on the recovery of β-tetralone

In a previous study [3], the retention factor for the first component of the epimer pair, k', was 7 and the relative retention at infinite dilution, α, was 1.04. Of the compounds chosen from the Aldrich catalogue, a mixture of diethyl phthalate and β-tetralone came closest to matching those parameters, having k' and α equal to 6 and 1.1, respectively (see Fig. 1).

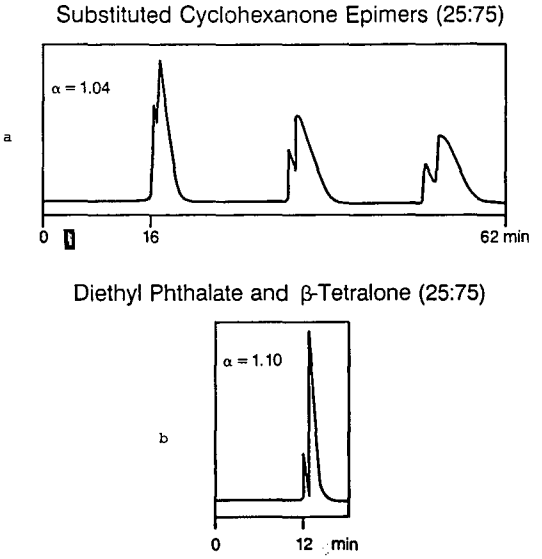

Fig. 1. Initial development of self-displacement chromatographic conditions. (a) Chromatogram of a 60-mg mixture of methyl *cis*- and *trans*-1-ethyl-2-oxo-4-(2-propenyl)cyclohexaneacetate. Three passes on one 250 × 21.4 mm I.D. column with recycling. Mobile phase, ethyl acetate–hexane (2.5:97.5); flow-rate, 40 ml/min (velocity, 0.25 cm/s). Relative retention calculated for the first pass. (b) Similar chromatogram obtained for a 60-mg mixture of diethyl phthalate and β-tetralone on a 250 × 21.4 mm I.D. silica column. Mobile phase, ethyl acetate–hexane (4:96); flow-rate, 40 ml/min.

The analytical separation of a 15-mg mixture of diethyl phthalate and β-tetralone (1:1) is shown in Fig. 2. The relative retention is 1.1 and near baseline resolution is achieved. Based on this chromatogram, practical experience with elution chromatography would suggest that a sample load of 50 mg might be reasonable if the separation is to be carried out under conditions of linear chromatography, with touching bands. However, these chromatographic conditions were developed specifically to induce the displacement effect.

Samples of 0.3–5 g were injected under the same experimental conditions as in Figs. 1 and 2. The chromatograms are shown in Figs. 3 and 4. In contrast to results expected in the linear elution mode, the compounds are resolved to the baseline when 300 mg are injected. The resolution is still excellent when the load is more than tripled to 1 g. When the injection size is increased to 3 g, very sharp fronts are recorded for the two components and differentiation between the two bands can be observed. Visually, however, the resolution is poor. The recovery yield and production are also given in Fig. 4 for the three sample sizes. Surprisingly, with the 3-g injection, there is only a narrow mixed zone behind the front of the second component band. The composition profile of the mixed zone is reported Fig. 5 for the three chromatograms shown in Fig. 4. The curves in Fig. 5 give the relative concentration of diethyl phthalate in the β-tetralone fraction collected after the sharp front (see the next section). The mixed zone is weakly polluted by a slight tail of the first component, but its purity exceeds 95%. If it is not essential that the purity of the collected fractions of the two purified components exceeds 95%, the recovery is nearly total. If the purity of the material recovered must exceed 99%, the yield is still high (67%).

With larger samples the yield decreases, but for a 5-g sample it is still 74% when combining fractions that are 95% pure. In practice, for the maximum production of purified material of the two individual components, each having a purity of 95 or 99%, sample sizes of 3 or 5 g, respectively, would be optimum.

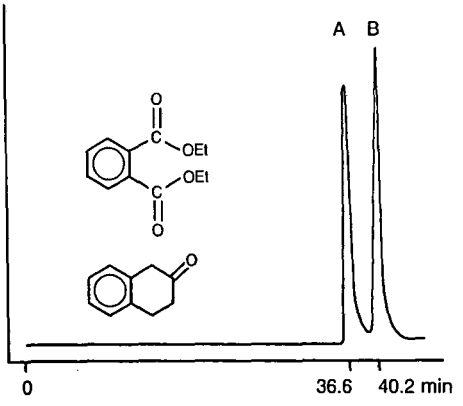

Fig. 2. Analytical separation of a 25:75 mixture of diethyl phthalate (A) and β-tetralone (B). Chromatograms for different sample sizes. Column, 750 × 21.4 mm I.D., packed with 10-μm silica particles. Mobile phase, ethyl acetate–hexane (4:96); flow-rate, 40 ml/min; sample size, 15 mg (1:1 mixture).

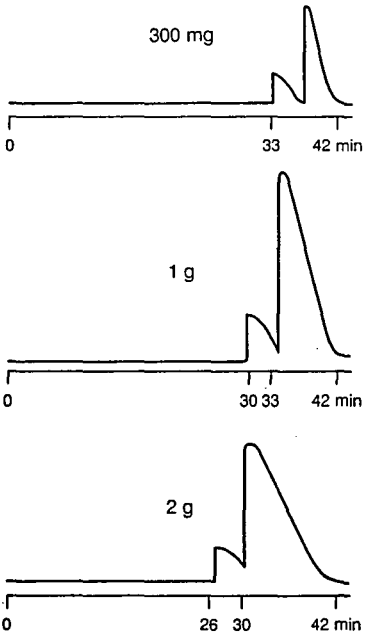

Fig. 3. Effect of sample size on the elution profile of a 25:75 mixture of diethyl phthalate and β-tetralone. Experimental conditions as in Fig. 2, except for sample sizes: 0.3, 1 and 2 g. Complete or near-complete resolution is achieved for sample sizes below 2 g.

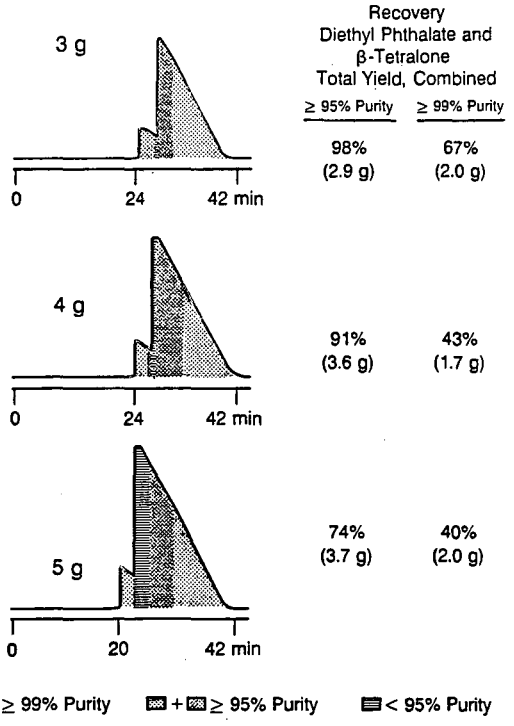

Fig. 4. Effect of sample size on the elution profile and the recovery yields for a 25:75 mixture of diethyl phthalate and β-tetralone. Experimental conditions as in Fig. 2, except for sample sizes: 3, 4 and 5 g.

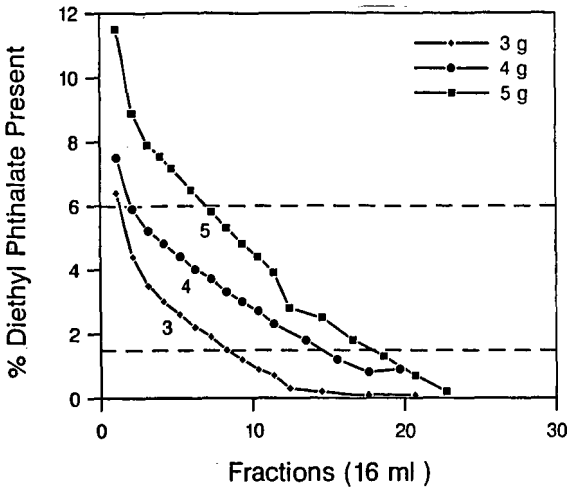

Fig. 5. Effect of sample size on the purity of fractions of β-tetralone collected during the elution of samples of increasing size of a 25:75 mixture of diethyl phthalate and β-tetralone. Plot of the diethyl phthalate concentration in collected fractions *versus* the fraction number. The collection of the first 16-ml fraction starts 16 ml after the front of β-tetralone appears in the chromatogram (Fig. 4).

Effect of sample size on the purity of β-tetralone

Although it would be valuable to draw the elution profile of diethyl phthalate, this is not possible because of differences in the molar absorptivities of the two compounds. Information about the elution behavior of the first component can still be obtained by plotting the percentage of diethyl phthalate present in the β-tetralone fractions. The fractions collected before the nearly vertical front of β-tetralone all consisted of diethyl phthalate in greater than 99.9% purity. The composition of the 16-ml fractions collected during the elution of the mixed zone, behind the steep front of the second component (see Fig. 3), is shown in Fig. 5. The concentration decay of diethyl phthalate behind the steep front of the β-tetralone band takes place as predicted by theory [5,6]. This explains the decrease in recovery of the two compounds when the sample size increases.

To obtain material that is 95% pure, only one or two fractions must be discarded from the 3-g injection, two or three fractions must be eliminated from the 4-g injection and six fractions must be removed from the 5-g injection. Further, it is evident from the plot that the overall purity of the combined material designated as 95% pure will be greater for the 3-g injection than for the 4- and 5-g injections.

The purity of the individual fractions of diethyl phthalate collected before the elution of the front of the β-tetralone band (not shown) exceeds 99% in all three instances. The loss in recovery yield is due solely to the tailing of the diethyl phthalate peak into the β-tetralone band and not to possible fronting of the β-tetralone band into the diethyl phthalate. Such fronting of the second component has never been observed [2,3].

Confirmation of the displacement effect

The observations made in the previous two sections are in excellent agreement

with our previous experimental results [2,3] and with the predictions of the theory of non-linear chromatography [5,6]. They seem to indicate the occurrence of a displacement effect. Proof of the strong degree of interaction between the two bands of this binary mixture is shown in Fig. 6. The top chromatogram shows the elution of the 3-g sample of the 1:3 binary mixture discussed above. The bottom part shows the superimposition of two chromatograms, corresponding to 0.75 g of pure diethyl phthalate and 2.25 g of pure β-tetralone. Both chromatograms exhibit triangular profiles with steep, almost vertical fronts, which are typical of an overloaded column. Because the sample size for β-tetralone is three times larger than that for diethyl phthalate, the retention time of the front of the former compound has become shorter than that of the latter. Based on consideration of these individual chromatograms, a reasonable degree of separation for the mixture, permitting the production of important amounts of purified fractions with a high recovery yield, would be ruled out by most chemists.

However, the retention times of the fronts on the two pure compound chromatograms are substantially different from those of the two fronts in the chromatogram of the mixture. In the previous section, we have shown that (i) the first front corresponds to the beginning of the elution of a pure band of the lesser retained component, (ii) the concentration of the first component in the eluate drops off abruptly at

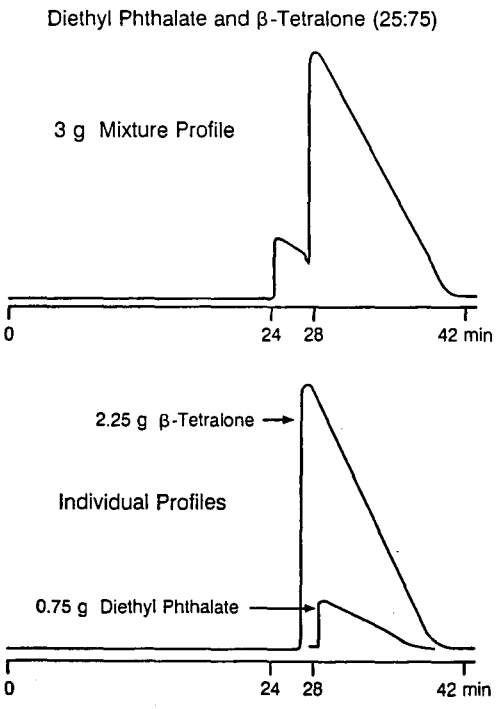

Fig. 6. Confirmation of the self-displacement effect. Comparison between the chromatogram of a 3-g sample of a 25:75 mixture of diethyl phthalate and β-tetralone with the chromatograms obtained from individual injections of the same relative amounts of the two pure compounds. Experimental conditions as in Fig. 2.

the second front, when the second component suddenly surges out of the column, and (iii) a thin mixed zone is eluted just after the second front. The 3-g line in Fig. 5 shows the tail of the elution profile of diethyl phthalate behind the β-tetralone band front. This tail lasts for only about 4 min and decays rapidly, from 6.5% in the first fraction to less than 1% in the tenth.

Clearly, the behavior of the two compounds during the elution of the mixture is not independent, in spite of their lack of structural similarity. Because it is more strongly absorbed, β-tetralone displaces diethyl phthalate, forcing the elution of the diethyl phthalate as an earlier band and permitting the collection of purified products. As we have shown previously [3], for this displacement effect to take place, it is important that the concentration of the second component in the feed is substantial; preferably, it should be comparable to or larger than the concentration of the first component [14]. Experimental results involving the detailed comparison between individual elution profiles obtained experimentally and calculated from the equilibrium isotherms, using the semi-ideal model [5,6,9], have demonstrated the reality of this effect and the importance of the relative composition of the feed on the magnitude of the displacement effect [12,13].

Effect of sample size on the recovery yield of α-tetralone

A second example of the displacement of the first component by the second is given by the separation of a mixture of benzosuberone (first-eluted component) and α-tetralone. The relative retention of the two compounds at very low concentration is 1.3, and higher loadings can be used. Fig. 7 shows two chromatograms, obtained on the injection of 4- and 6-g feed samples. The profile of the benzosuberone tail behind the front of the α-tetralone band is discussed in the next section. The resolution between the two bands is much better than that for the chromatograms in Fig. 4, owing to the better selectivity of the stationary phase. Accordingly, the recovery yields and the production of pure fractions are higher. The difference is greater for 99% than for 95% pure fractions. Absolute comparisons between the chromatograms obtained for this mixture and the previous mixture cannot be made because the molar absorptivities of the four compounds in question are different.

It is interesting to compare the performance of this separation with that achieved under more conventional conditions, with larger values of k' but using a shorter column, 1/3 in length (see Fig. 8). The production per run achieved under the present conditions, which promote the sample self-displacement effect, is much greater than those corresponding to slightly overloaded, but still quasi-linear elution. This result confirms that the production rate is increased by actions which promote the importance of the displacement effect. It is in agreement with independent theoretical work [9] showing that there is an optimum column length, corresponding to a low value of the column efficiency, and that the optimum retention factor, k', is small [9,15].

Effect of sample size on the purity of α-tetralone

The composition of the fractions collected during the elution of the mixed zone of the chromatograms shown in Fig. 7 is plotted in Fig. 9 *versus* the fraction number. The purity of the benzosuberone fractions eluted before the α-tetralone front always exceeds 99%. This is a general result. The second component front is nearly vertical

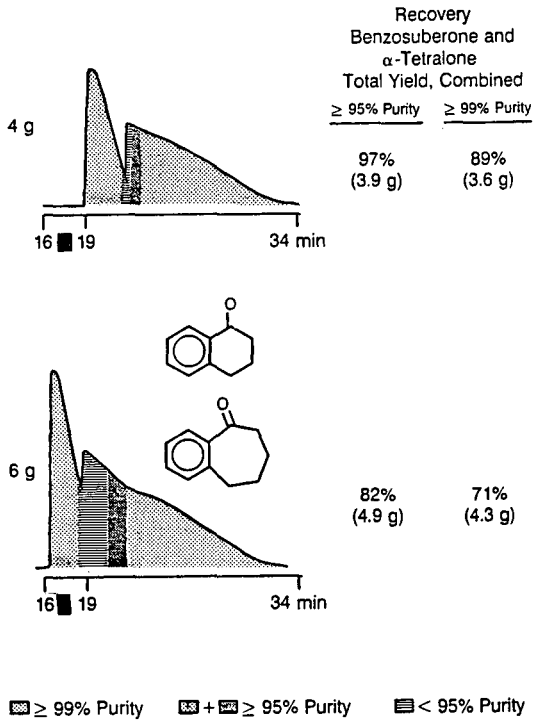

Fig. 7. Effect of sample size on the elution profile of a 25:75 mixture of benzosuberone and α-tetralone and on the recovery yield and production of pure material. Chromatograms for 4- and 6-g injections. Mobile phase, ethyl acetate–hexane (2:98); flow-rate, 50 ml/min (velocity, 0.32 cm/s); column length, 75 cm.

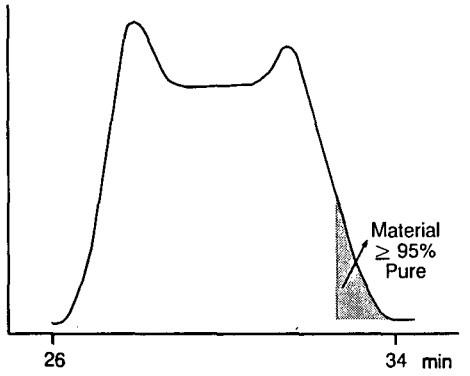

Fig. 8. Elution profile, recovery yield and production of pure material for a small sample (250 mg) of a 25:75 mixture of benzosuberone and α-tetralone, eluted with a weak mobile phase, under quasi-linear conditions, in the absence of self-displacement effect. Mobile phase, ethyl acetate–hexane (0.5:99.5); flow-rate, 50 ml/min (velocity, 0.32 cm/s); column length, 25 cm.

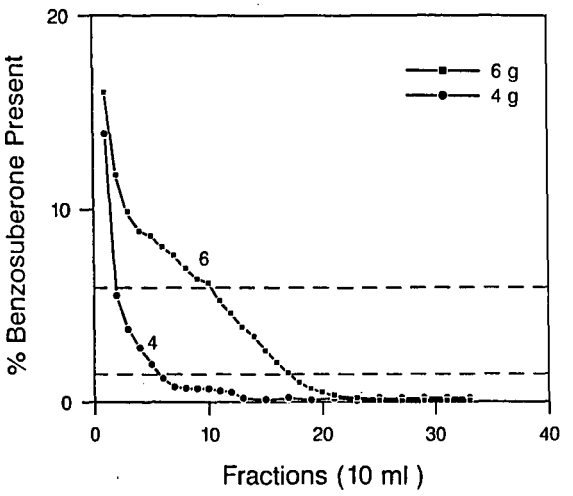

Fig. 9. Effect of sample size on the elution profile of a 25:75 mixture of benzosuberone and α-tetralone. Plot of the benzosuberone concentration in collected fractions *versus* the fraction rank. The collection of the first 10-ml fraction starts 10 ml after the front of α-tetralone appears in the chromatogram (Fig. 7).

and the fraction purity of the first component eluted before that front is usually much more than 99%.

Tailing of the first component (benzosuberone) into the second component band accounts for nearly all the lost production and the recovery yields fall below 100%. With a 4-g sample size, only one fraction has to be rejected to prepare 95% pure β-tetralone and five fractions if 99% compound purity is required. For a 6-g sample the number of fractions to be discarded is ten in order to prepare 95% pure α-tetralone and seventeen for 99% pure material. Using either purity criterion, the 6-g injection would result in a better production rate if absolute recovery is not an issue.

Effect of column length on the separation of diethyl and dimethyl phthalates

A third separation was developed with two homologous phthalate esters. The relative retention of the two components of this mixture is extremely high, 1.7, and the separation is very easy (see Fig. 10). With a 4-g sample, the resolution between the two bands greatly exceeds unity on the three-column series used in this experiment and also in all the previous experiments. The separation is total and any loss in recovery would not arise from overlapping chromatographic bands.

On the two-column series, the retention time decreased by one third, as expected. Although the resolution is lower, it still exceeds unity and the recovery yields are again total (Fig. 10). Comparing the top two chromatograms in Fig. 10, we note that the elution times of the two fronts are reduced by slightly more than one third. As the column is shorter, the extent of dilution is less and the bands are taller. The migration velocity of a front increases with its concentration [6,7]. From the second chromatogram, it does not seem that a significant further reduction of the column length will produce a marked improvement in the production rate. On the contrary, we expect that the two bands will interfere strongly, thereby leading to a drop in the recovery yield.

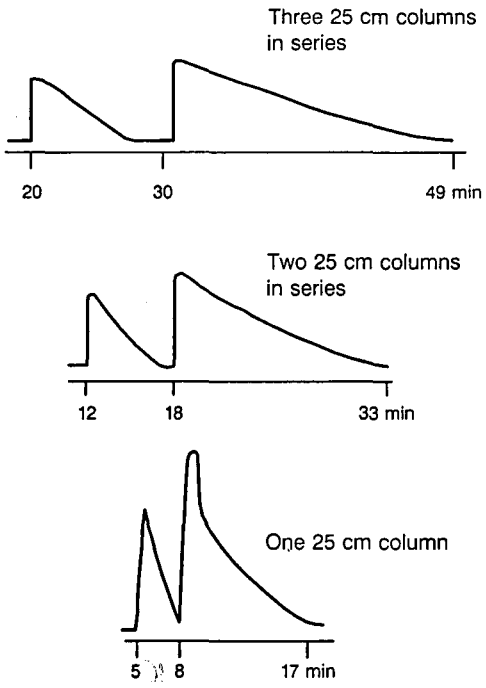

Fig. 10. Effect of sample size on the elution profile of a 25:75 mixture of dimethyl and diethyl phthalates. Chromatograms for a 4-g sample size on columns of different lengths. Experimental conditions as in Fig. 2.

The third chromatogram in Fig. 10 shows that the opposite of this expectation is true. Reducing the column length to one third of the original value leads to a chromatogram that exhibits touching bands. The resolution is nearly total and the separation is still complete. Pure fractions (99%) of both components can be collected with a recovery exceeding 99%. As the flow velocity was kept constant while the column length was reduced from 75 to 25 cm, the production rate has been effectively tripled, which is a noteworthy improvement.

The atypical elution profile of the two components on the third chromatogram must be considered carefully. The first component band is much narrower than in the previous two chromatograms and it is much taller. Again, the retention times of the two fronts have decreased more than proportionally to the decrease in the column length because the velocity of the fronts increases with their concentration. The second component band is now much taller than the first and exhibits a front "tower". All these non-classical features of the elution bands are evidence for the interaction that took place in the column during the progressive separation between the two bands and from which the profiles, just resolved, have not had time to recover completely [6].

Finally, a note of caution is appropriate when comparing the chromatograms in Figs. 4, 7 and 10. The compounds are different and so are the relative responses of the UV detector for the two components. Because of a variable degree of saturation of the detector during elution, the relative response is not even constant. The chroma-

tograms shown are absorbance profiles of the eluate during the elution of the sample and are not true chromatograms, *i.e.*, not true concentration profiles.

Effect of a change in k' on yield and purity

Fig. 11 shows a series of chromatograms corresponding to a 6-g feed sample of the benzosuberone–α-tetralone mixture already discussed (Figs. 7 and 8). The composition of the mobile phase has been changed by increasing the concentration of the strong solvent, ethyl acetate, from 2 to 3.85% (v/v), thereby decreasing the retention of the two components. The run time decreases from 33 to 21 min and the retention time of the first front from 16 to 11.5 min. (Note that the attenuation was different for the third chromatogram, which explains the shorter band height). The relative retention of the two components does not change significantly: α is equal to 1.21, 1.23 and 1.24 for ethyl acetate concentrations of 2, 3 and 3.85%, respectively. Thus, any change observed in the production rate cannot be due to a variation of the relative retention {theory predicts that the production rate with a given column is proportional to $[(1 - \alpha)/\alpha]^2$, *i.e.*, it predicts a change of 5% in the present instance, which is a negligible effect [15,16]}.

A significant increase in the recovery yield is observed, from 10% for 95% pure fractions to 13% for 99% pure fractions. Accordingly, the production rate increases

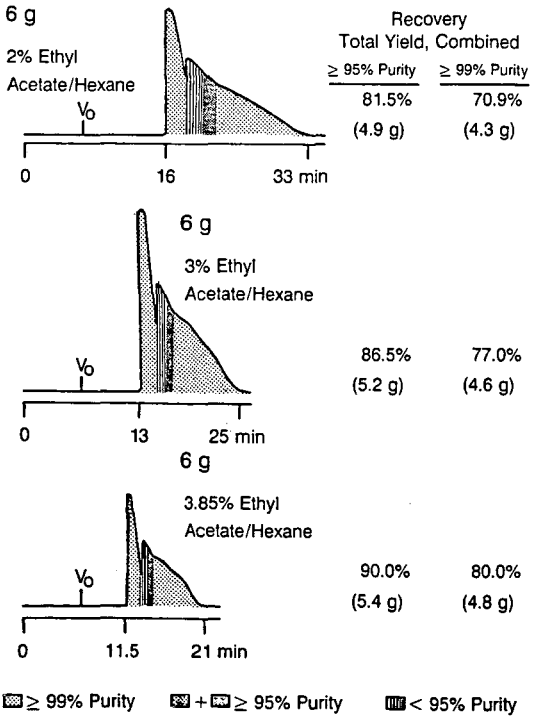

Fig. 11. Effect of mobile phase composition on the elution profile of a 6-g sample of a 25:75 mixture of benzosuberone and α-tetralone. Chromatograms, recovery and production for different concentrations of ethyl acetate in *n*-hexane (2%, 3% and 3.85%). Flow-rate, 50 ml/min.

considerably, as it is proportional both to the recovery yield and to the reverse of the run time. Assuming what is probable, *viz.*, that the change in the composition of the mobile phase does not modify the column saturation capacity, the enhancement of the displacement effect is due to the lesser dilution of the sample, in relation to faster elution. In contrast to the development of separations in the non-overload elution mode, the data suggest that the mobile phase composition should be adjusted so that the capacity factor for the first component, k', is low. For the third chromatogram in Fig. 11, k' for the first-eluted component is only 1.5. This conclusion is in agreement with theoretical results [7–9].

The composition of the fractions collected systematically after the elution of the second component front is plotted in Fig. 12 for the three chromatograms given in Fig. 11. The reason for the increase in recovery yield with decreasing retention is obvious. The number of fractions to be discarded to recover 95% pure products decreases from 10 (2% strong solvent) to 4 (3%) and to 3 (3.85%). The volume of the fractions to be discarded decreases much faster than the volume of eluate occupied by the band system at the column exit (see Fig. 11). Similarly, the number of fractions eliminated in order to prepare 99% pure products decreases from 17 (2%) to 8 (3%) and to 6 (3.85%). Comparable conclusions would be derived by considering the area under the curves in Fig. 12 (total amount of benzosuberone discarded) and the area of the α-tetralone band which has to be discarded.

In order to investigate in greater detail the influence of retention on production, another experiment was performed. The concentration of the strong solvent was decreased to 0.5% ethyl acetate and the column length was reduced to 25 cm to keep the run time comparable to the other experiments (34 min). These conditions correspond to what many consider to be the optimum for preparative elution chromatography. A 250-mg sample was injected (Fig. 8). The band profile is consistent with

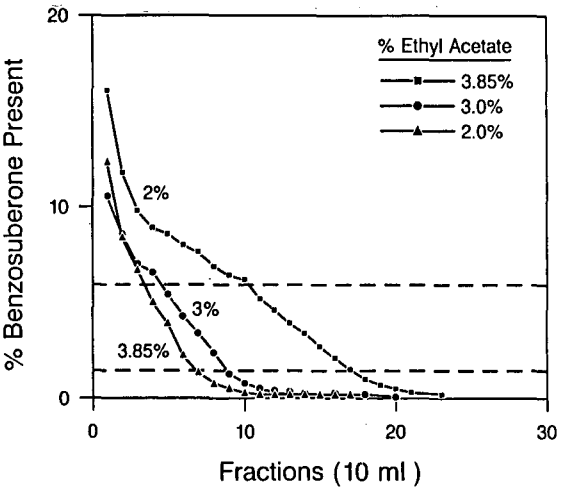

Fig. 12. Effect of mobile phase composition on the elution profile of a 6-g sample of a 25:75 mixture of benzosuberone and α-tetralone. Plot of the benzosuberone concentration in collected fractions *versus* the fraction number. The collection of the first 10-ml fraction starts 10 ml after the front of α-tetralone appears on the chromatogram (Fig. 11).

conventional linear elution chromatography. Unlike the chromatograms obtained under experimental conditions permitting the displacement effect to take place, a sharp boundary between the two component bands does not exist. Only a small amount of pure material can be recovered from this 250-mg injection, compared with almost total recovery for a 4-g injection under conditions promoting a strong displacement effect (see Fig. 7).

Clearly, in this example the self-displacement mode is superior for production.

Effect of mobile phase flow-rate on production

In two recent papers, it was predicted through modeling that the optimum value of the mobile phase velocity for maximum production rate is relatively very high, much higher than the optimum velocity for maximum column efficiency [8,9]. We investigated this phenomenon experimentally by repeating the separation of the mixture of diethyl phthalate and β-tetralone at three different flow-rates, 20, 40 and 60 ml/min. Because the flow resistance of the long column used (75 cm) reached the maximum operating pressure of the chromatograph, it was not practical to use higher values of the flow-rate. The results are reported in Figs. 13 and 14.

In Fig. 13, we see that the elution times of the main features of the chromatogram decrease approximately in proportion to the reverse of the flow-rate, as expected. As the sample (4 g) is large, the influence of the column efficiency on the elution profile is moderate and can be neglected as a first approximation. The recovery for 95% pure products increases slightly with increasing flow-rate, from 86% to 90%. The differences are of questionable significance. The recovery for the preparation of 99% pure fractions seems to remain approximately constant (49, 44 and 49%). Plotting the composition of the intermediate fractions *versus* their rank (Fig. 14) again shows only slight differences. The number of fractions to be discarded in order to prepare 99% pure material is nearly the same in all three instances, *i.e.*, eleven or twelve. These numbers reflect minor fluctuations of experimental conditions

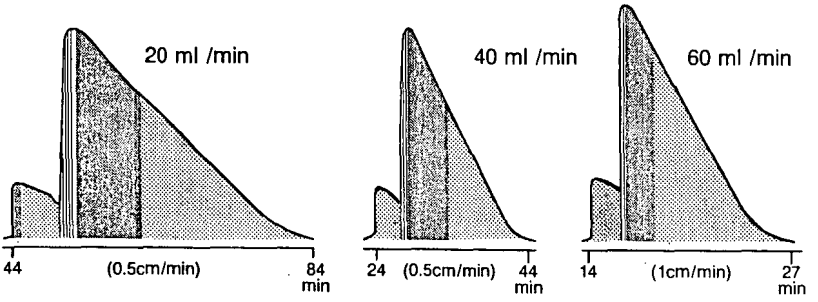

Recovery Total Yield, Combined			
≥ 95% Purity	86% (3.4 g)	91% (3.6 g)	90% (3.6 g)
≥ 99% Purity	49% (2.0 g)	44% (1.7 g)	49% (2.0 g)

≥ 99% Purity + ≥ 95% Purity < 95% Purity

Fig. 13. Effect of mobile phase flow-rate on the elution profile of a 4-g sample of a 25:75 mixture of diethyl phthalate and β-tetralone. Chromatograms, recovery and production obtained at different flow-rates. Mobile phase as in Fig. 2.

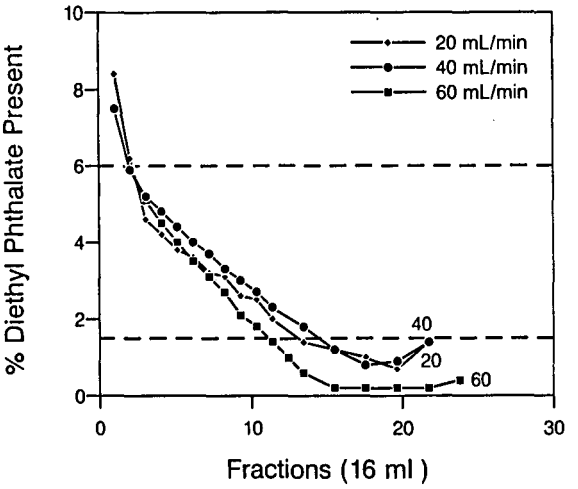

Fig. 14. Effect of mobile phase flow-rate on the elution profile of a 4-g sample of a 25:75 mixture of diethyl phthalate and β-tetralone. Plot of the diethyl phthalate concentration in collected fractions of β-tetralone *versus* the fraction number. The collection of the first 16-ml fraction starts 16 ml after the front of β-tetralone appears in the chromatogram (Fig. 13).

rather than a meaningful distinction. It is seen in Fig. 14, however, that the purity of the usable fractions with 60 ml/min flow-rate is systematically better than in the other two instances.

As the recovery yield and the production per run remain essentially independent of the flow-rate in the range investigated, we may conclude that the production rate increases as the flow-rate increases (*i.e.*, the amount produced per unit volume of mobile phase used is constant) and that the trend may be extrapolated to some extent, as suggested by theory. Obviously, the pressure capacity of the pump and the column tubing used may set limits much lower than the maximum production rate.

Guidelines for method development

The production amounts and rates presented in these studies have major ramifications for the practical purification laboratory. Fortunately, it is easy to induce the self-displacement effect. As one conclusion of this work, we summarize in the following set of guidelines the systematic optimization procedure that has been developed and is being applied routinely in the laboratory to a variety of problems involving compounds that cannot be discussed here. First, however, we should point out that these rules are valid for small production scales, when a small batch of a pure or very pure chemical has to be prepared rapidly, on an intermittent basis. Optimization of preparative processes for the large-scale production of commercial compounds would require and could support more quantitative and systematic investigations.

(1) Using an analytical-scale column, approximate conditions permitting the resolution of the components of interest are generated. A relative retention exceeding 1.1 is highly desirable but not essential. It is not necessary to use exactly matched column sets for scale-up, but it is helpful to select a packing material from the same manufacturer, having the same average particle size as the material in the preparative

column whose use is intended. We have found the optimum particle size to be about 10 μm or smaller. As a general rule, it is better to elute the minor component first, unless the relative retention under conditions where the major component is eluted first is extremely high. Strategies have been developed where the displacement effect can be used to advantage only if the concentration of the second component in the feed is comparable to or larger than that of the first component [17].

(2) A 25-cm long preparative column is equilibrated with the mobile phase of the selected composition. The column should be packed with particles of average size 10 μm or smaller and the flow-rate should be approximately one column volume every 2 min.

(3) Using a sample size of 10–40 mg (larger if the column diameter exceeds 20 mm), the mobile phase composition is adjusted for a capacity factor between 3 and 7 for the first component, if possible. Larger values of k' are acceptable but the recovery and/or the production will be lower. If a choice must be made between conditions giving maximum relative retention or an adequate value of k', the optimization of the former parameter is more important.

(4) A series of three 25-cm preparative columns are equilibrated with the mobile phase selected. Alternatively, one column is used in the recycle mode.

(5) the maximum load depends on the relative retention and the relative composition of the feed mixture. In most instances it will exceed several grams on a standard 21.5 mm I.D. column (conventional 1 in. O.D.) when α is greater than 1.1.

(6) The conditions obtained by following the procedure just described are not truly optimized, but they should provide good recoveries and excellent production rates. It may prove useful to experiment further with the flow-rate and the mobile phase composition to reduce the retention while keeping a high value of the relative retention.

CONCLUSIONS

The results of this study confirm the generality of the sample self-displacement effect. It takes place in all the preparative separations we have tried, provided that the sample size is large enough and that the bands of the components of the mixture interact during the separation. The displacement effect is stronger at high concentrations (large sample size, moderate retention factors) and high relative retention of the two components involved. Using the guidelines we have established, it is easy to develop separation methods where this effect is enhanced and used to advantage. High recovery yields can be achieved in spite of a poor-looking chromatogram and production rates are obtained which far exceed those possible under the more classical conditions corresponding to nearly linear behavior. The use of a high flow-rate does not reduce the yield significantly and further enhances the production rate.

The advantages of separations carried out under conditions that maximize the self-displacement effect are important and obvious in the case of the first component. For this reason, the compound of greatest interest in a feed should be eluted as early as possible. When the production of purified fractions of the second component is desired, the choice is less clear. This production must be balanced against losses in yield. Purity and, consequently, recovery are diminished by the tailing of the first component into the band of the second. In most instances, it may be better to reduce

the sample size, compared with the size preferred for purification of the first component. However, significantly large yields can sometimes be obtained and production rates of the second component may be substantially greater overall in comparison with those arising from conventional "touching bands" methodology. Even when complete resolution between two high concentration bands is achieved (Fig. 10), the displacement effect has been used with advantage, effectively compressing the first component band and increasing the resolution [9].

As a general rule, the production rate is much increased by operating the column under non-linear conditions.

ACKNOWLEDGEMENTS

We thank Mr. Norman Cole and Dr. Philip Funke (Squibb Institute for Medical Research, Princeton, NJ) for their support of this project. This work was supported in part by grant CHE-8901382 of the National Science Foundation and by the cooperative agreement between the University of Tennessee and the Oak Ridge National Laboratory.

REFERENCES

1 Cs. Horváth, J. Frenz and Z. El Rassi, *J. Chromatogr.*, 255 (1983) 273.
2 J. Newburger, L. Liebes, H. Colin and G. Guiochon, *Sep. Sci. Technol.*, 22 (1987) 1933.
3 J. Newburger and G. Guiochon, *J. Chromatogr.*, 484 (1989) 153.
4 *Proceedings of the 6th International Symposium on Preparative Liquid Chromatography, Washington, DC, May 1989, J. Chromatogr.*, 484 (1989).
5 G. Guiochon and S. Ghodbane, *J. Phys. Chem.*, 92 (1988) 3682.
6 S. Golshan-Shirazi and G. Guiochon, *J. Phys. Chem.*, 93 (1989) 4143.
7 S. Golshan-Shirazi and G. Guiochon, *Anal. Chem.*, 60 (1988) 2364.
8 S. Ghodbane and G. Guiochon, *Chromatographia*, 26 (1988) 53.
9 S. Golshan-Shirazi and G. Guiochon, *Anal. Chem.*, 61 (1989) 1368.
10 J. M. R. Parker, C. T. Mant and R. S. Hodges, *Chromatographia*, 24 (1987) 832.
11 J. E. Eble, R. L. Grob, P. E. Antle and L. R. Snyder, *J. Chromatogr.*, 405 (1987) 31.
12 A. M. Katti and G. Guiochon, *J. Chromatogr.*, 499 (1990) 5.
13 S. Jacobson, S. Golshan-Shirazi and G. Guiochon, *J. Am. Chem. Soc.*, 112 (1990) 6492.
14 S. Golshan-Shirazi and G. Guiochon, *Anal. Chem.*, 62 (1990) 217.
15 S. Golshan-Shirazi and G. Guiochon, *Am. Biotechnol. Lab.*, 8 (1990) 26.
16 S. Golshan-Shirazi and G. Guiochon, *J. Chromatogr.*, 523 (1990) 1.
17 J. Newburger, S. Taylor and G. Guiochon, presented at the *7th International Symposium on Preparative Liquid Chromatography, Ghent, April 1990*, in preparation.

Journal of Chromatography, 523 (1990) 81–89
Elsevier Science Publishers B.V., Amsterdam

CHROM. 22 749

Computer simulation for optimization of high-performance liquid chromatography of some phenolic pollutants

W. MARKOWSKI*, T. H. DZIDO and E. SOCZEWIŃSKI
Department of Inorganic and Analytical Chemistry, Medical Academy, Staszica 6, 20-081 Lublin (Poland)
(First received June 7th, 1990; revised manuscript received August 1st, 1990)

ABSTRACT

Computer simulation was used to optimize high-performance liquid chromatography of phenol and its chloro and nitro derivatives. On the basis of two linear gradient runs of different steepness (RP-18–water + methanol + 1% acetic acid), several simulated gradient runs allowed the optimum gradient programme and flow-rate to be chosen so that the time of analysis could be considerably shortened. Good agreement between simulated and experimental chromatograms was obtained in spite of changes in experimental conditions.

INTRODUCTION

The increasing application of computers in the optimization of chromatographic systems, including gradient elution, is reflected by the recent publication of several books [1–3] and special issues of chromatographic journals [4,5]. The well developed theory of gradient elution [6–8] permits the prediction of the relationships between resolution (R_s) and the gradient programme and other experimental variables.

Advanced computer programs for the simulation and optimization of high-performance liquid chromatography (HPLC) separations have recently been reported by Snyder and co-workers [9,10]: these programs, Drylab I (isocratic) and Drylab G (gradient), analyse the resolution of all pairs of components for various eluent compositions (Drylab I) or gradient programs (Drylab G) on the basis of a few experimental data, *i.e.*, capacity factors (k') for two eluent compositions or two linear gradient runs of various steepness. After the choice of the optimum conditions (good resolution in the shortest possible time), the simulated chromatogram is displayed. The experimental variables can then be further adapted (column length, particle size of the packing, flow-rate, gradient profile) and the modified simulated chromatogram checked for optimum separation.

In this study, the conditions for the HPLC of a group of chloro- and nitrophenols, frequently occurring as water and air pollutants, were optimized using the Drylab G expert system.

0021-9673/90/$03.50

TABLE I

CHLORO- AND NITROPHENOLS STUDIED

Compound	Code No.	Compound	Code No.
Phenol	1	4-Chloro-3-methylphenol	6
4-Nitrophenol	2	2,4-Dichlorophenol	7
2,4-Dinitrophenol	3	2,4,6-Trichlorophenol	8
2-Nitrophenol	4	Pentachlorophenol	9
2,3-Dimethylphenol	5		

EXPERIMENTAL

An HP-1050 gradient liquid chromatograph (Hewlett-Packard, Palo Alto, CA, U.S.A.) equipped with a 20-μl sample injector (Rheodyne, Cotati, CA, U.S.A.) and a variable-wavelength UV detector (HP 1050) operated at 280 nm was used. The chromatograms were recorded with a Hewlett-Packard Model 3396A reporting integrator. The stainless-steel column, 150 × 4.6 mm I.D., was packed with 10-μm C_{18}-bonded silica gel (based on Si 100, 18% carbon) additionally silanized with hexamethyldisilazane. The column was prepared and kindly supplied by prof. H. Engelhardt's laboratory (Department of Applied Physical Chemistry, University of Saarland, Saarbrücken, F.R.G.) and had an efficiency of 2300 plates, as determined using toluene as the test solute, eluted with methanol–water (60:40) at a flow-rate of 1.0 ml/min. The column dead volume ($V_m = t_0F$, where t_0 is the column dead time and F is the flow-rate), determined using pure water as the sample with methanol–water (50:50) as mobile phase, was $V_m = 1.4$ ml.

The dwell volume of the equipment, $V_D = t_DF$ (where t_D is the dwell time), was determined by running a blank gradient without the column [11]; it was found to be $V_D = 0.45$ ml. The estimated extra-column band broadening was $\sigma_{ext} = 0.020$.

In gradient runs, methanol (E. Merck, Darmstad, F.R.G.) and water (doubly distilled) were used as components of the mobile phase; both solvents contained 1% (v/v) of acetic acid. The sample was a mixture of nine components (see Table I) dissolved in methanol. The volume of sample injected was 10 μl, which corresponded to *ca.* 50 μg of each component.

RESULTS AND DISCUSSION

As indicated in the Drylab G instruction manual [11], two linear gradients of various slopes were run (gradient times, $t_g = 15$ and 45 min, the methanol content being varied in the range 5–100%. The retention times and peak areas are given in Table II and the chromatograms in Fig. 1a and b.

Comparison of these chromatograms indicates that at $t_g = 15$ some drift of the baseline is obtained. For $t_g = 45$ min all component pairs have $R_s > 1.5$ and the stability of the baseline is satisfactory. Comparison of the peaks in Fig. 1a and b shows that the sequence of peaks is the same.

The next step is to introduce the retention data to the computer in accordance with the Drylab G program. The optimization can be carried out assuming the rou-

TABLE II

RETENTION VALUES FOR TWO GRADIENT RUNS

t_R = Retention time. t_g = 15 and 45 min. Note: Table II and Figs. 1c, 2a and 3a are copies of Drylab G displays.

Code No.	Run 1		Run 2: t_R (min)
	t_R (min)	Area	
1	7.58	104 010	10.58
2	9.04	276 487	15.28
3	9.56	441 062	16.92
4	10.26	167 457	18.75
5	11.01	232 109	21.95
6	11.88	177 688	24.97
7	12.37	334 442	26.32
8	13.77	85 657	30.63
9	15.85	127 520	38.25

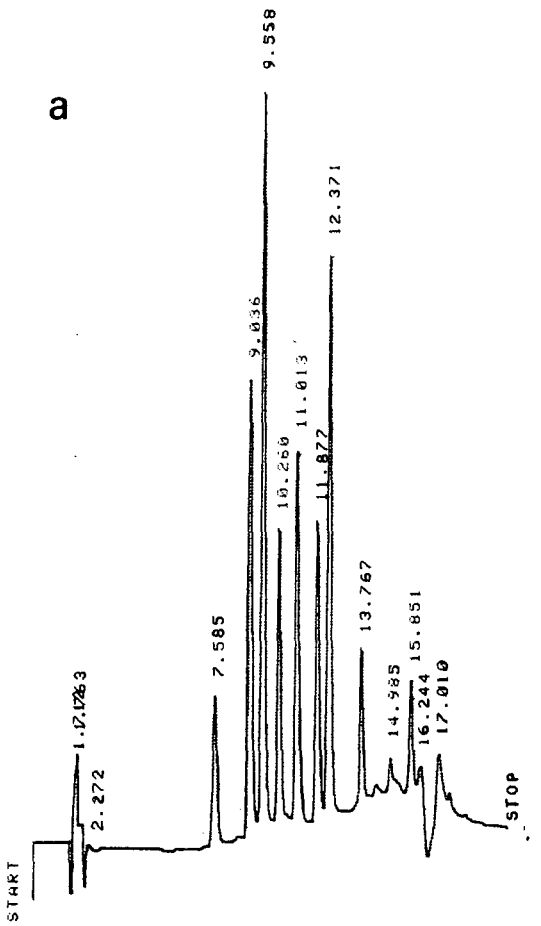

Fig. 1.

(Continued on p. 84)

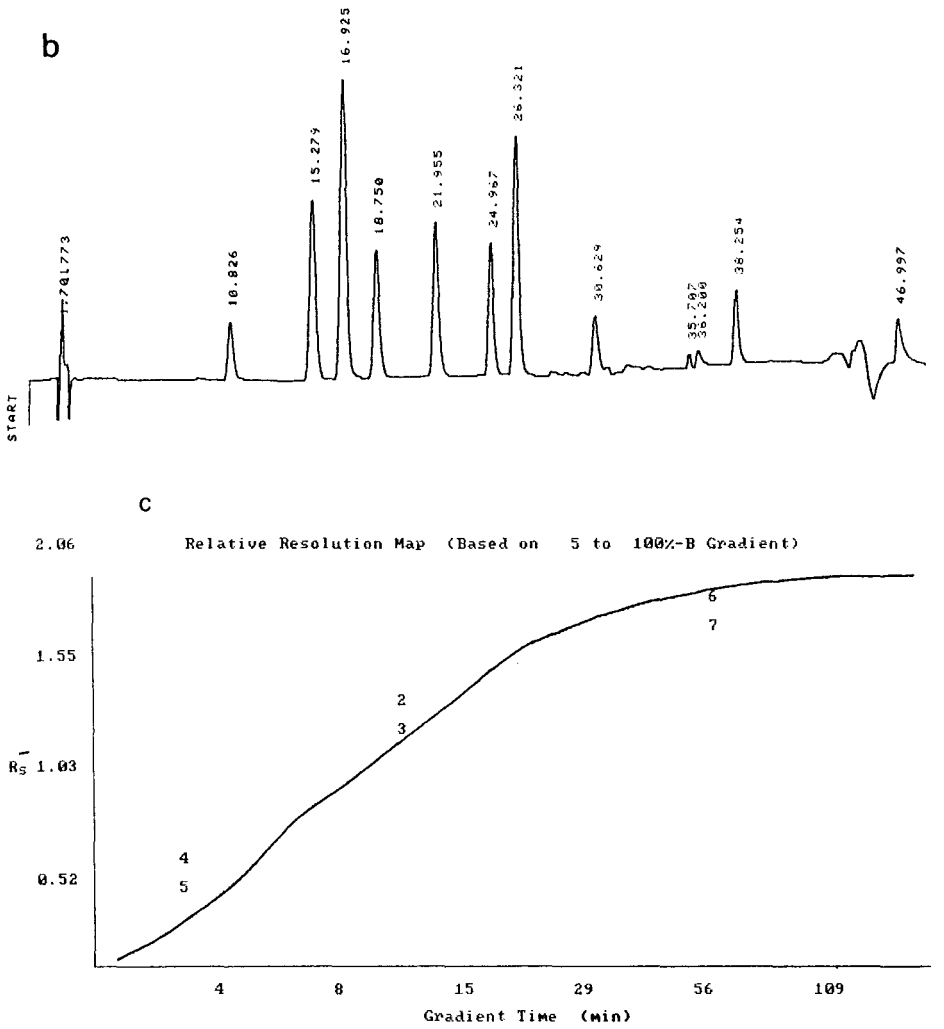

Fig. 1. Separation of chloro- and nitrophenols by gradient elution with 5–100% methanol–water (a) Gradient time t_g = 15 min; (b) t_g = 45 min; (c) R_s *vs.* t_g plot. Values at peaks are retention times in min.

tine efficiency (plate number, $N = 10^4$) or introducing the actual efficiency; in our experiment we chose the latter option ($N = 2302$); the column efficiency was corrected using option 6.6 of the Drylab G manual. The R_s of the critical pair was decreased from 4.023 to 1.93.

The next step consists in the selection of the minimum gradient time for which R_s for the critical pair is above 1.5 and all components are eluted from the column. This step could be done on the basis of the R_s *vs.* t_g relationship [10,11] (Fig. 1c) or from results presented by option 2 in table form (run time, resolution *vs.* gradient time). The optimum t_g was found to be 24 min. For these conditions the retention

TABLE III

RESULTS FOR OPTION 6.5: MULTI-SEGMENTED GRADIENT FOR NINE BANDS IN A 31.0–100.0% MULTI-SEGMENTED GRADIENT RUN OVER 20 min IN TWO SEGMENTS

Gradient: 0 min, 31.0% B; 9 min, 50% B; 20 min, 100% B.

Band No.	$t_{R(calc.)}$	$t_{R(exp.)}$ [a]	Band width	Average k'	R_s [b]
1	5.352	5.04	0.435	4.178	3.67
2	7.091	6.95	0.512	5.272	1.65
3	7.963	7.87	0.543	5.722	2.27
4	9.253	9.38	0.594	6.444	3.16
5	11.153	11.58	0.596	6.478	3.57
6	13.078	13.62	0.492	4.987	1.77
7	13.932	14.43	0.475	4.746	5.14
8	16.259	16.61	0.431	4.120	8.60
9	19.619	19.72	0.351	2.993	

[a] Average error in $t_R = \pm 0.29$ min ($= \pm 2.4\%$).
[b] Average error in R_s (difference in t_R) $= \pm 9\%$.

time of the first peak was too long, 8.96 min (Fig. 1c), so further optimization consisted in finding the maximum initial concentration of methanol at which the earlier obtained separation would be retained. Several simulations, using linear and segmented gradients, permitted the reduction of the retention time of the first peak to 5 min, keeping $R_s > 1.5$ (Table III).

The gradient run simulated for these conditions is shown in Fig. 2a and compared with the experimental run (Fig. 2b, with a blank run for the water–methanol system, Fig. 2c). A comparison of the simulated and experimental chromatograms

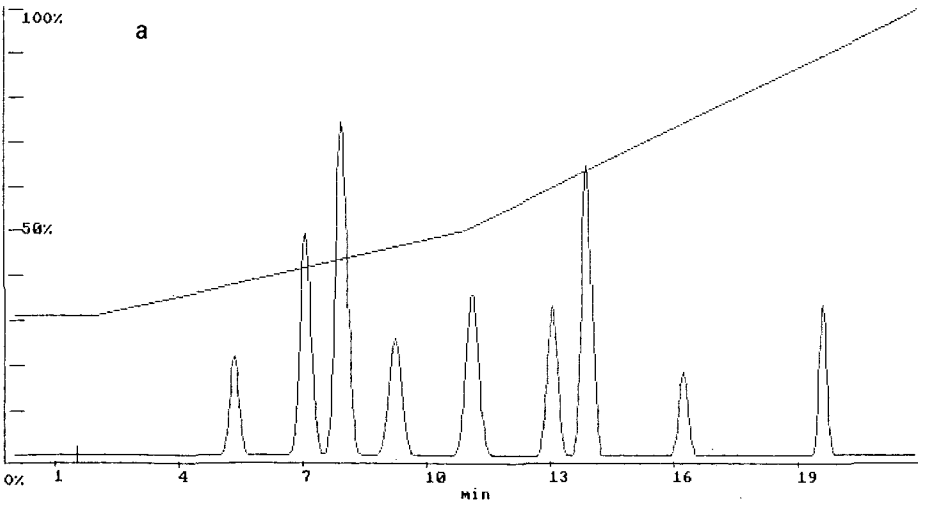

Fig. 2.

(Continued on p. 86)

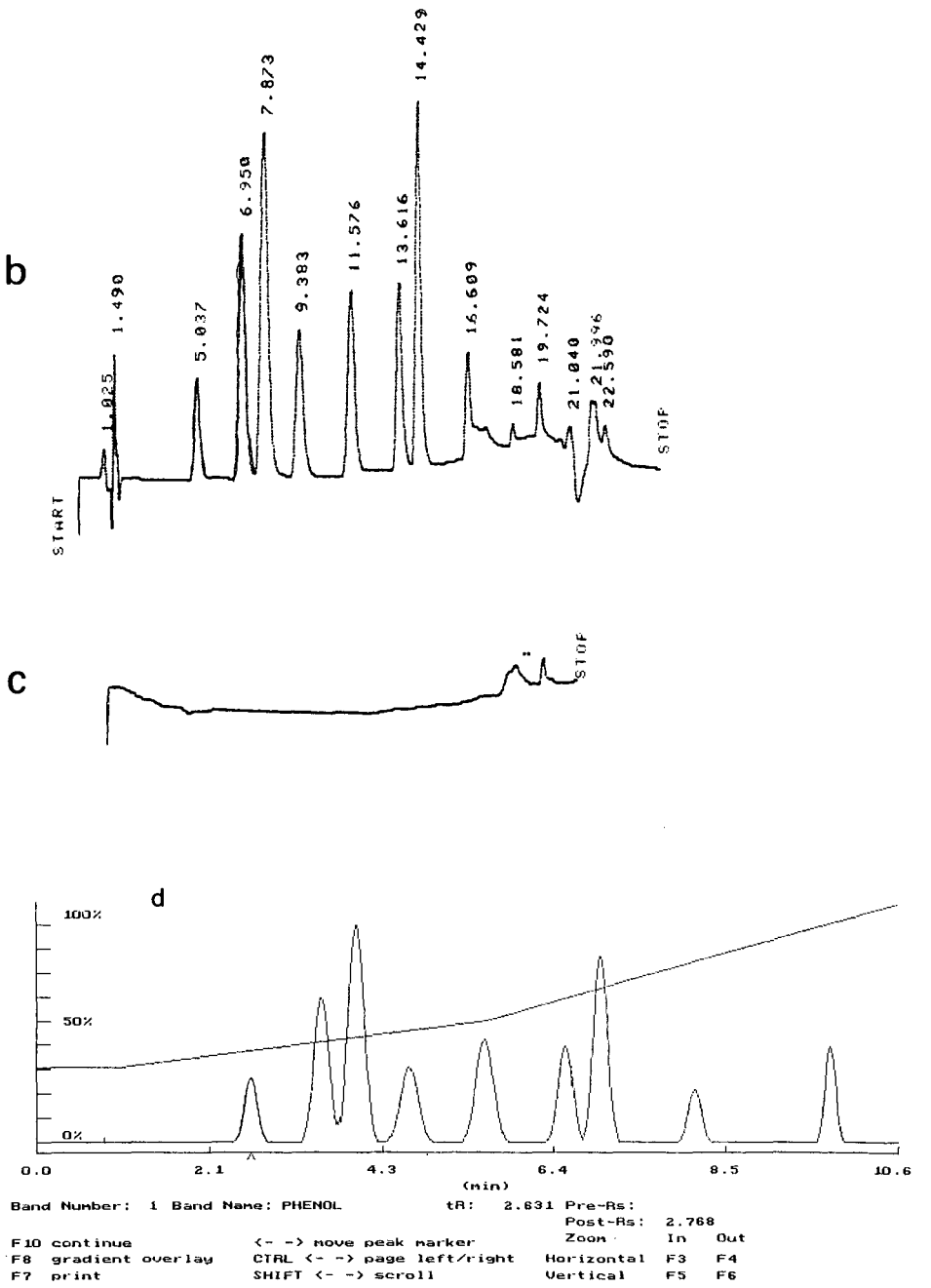

Fig. 2 (a) Computer-simulated chromatogram (Drylab G). Sample as in Fig. 1a and b. The gradient is indicated by the dashed curve. (b) Experimental chromatograms. Sample as in Fig. 1a and b and conditions as in (a). (c) Blank gradient run with methanol–water at 280 nm. (d) Computer-simulated chromatogram (Drylab G). Sample as in Fig. 2a. The gradient is indicated by the dashed curve. The column efficiency decreased to $N = 1900$.

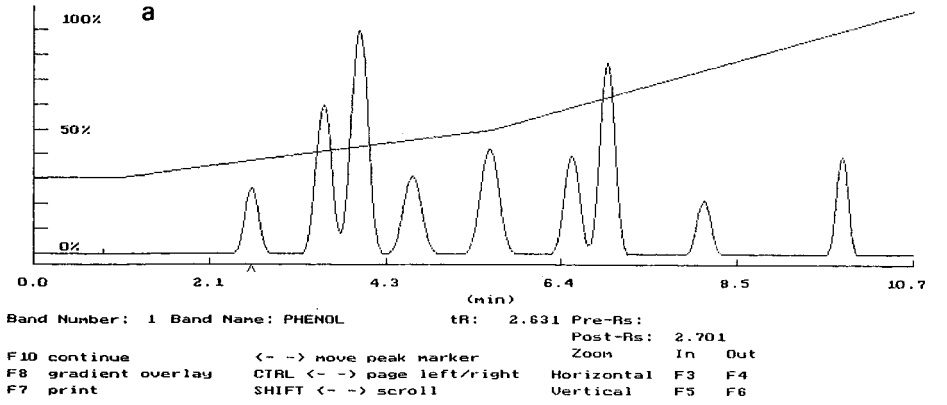

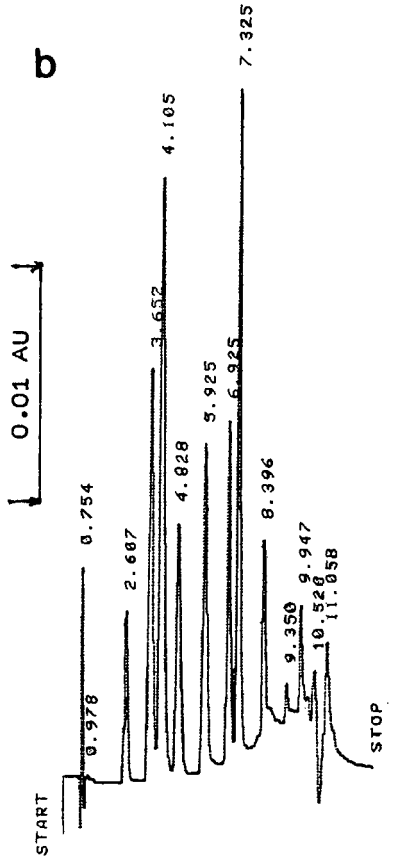

Fig. 3. (a) Computer-simulated chromatogram (Drylab G). Conditions as in Fig. 2a except flow-rate = 2 ml/min and the column efficiency decreased to N = 1008. (b) Experimental chromatogram. Conditions as in (a).

TABLE IV

RESULTS FOR OPTION 3: DATA FOR PRESENT SEPARATION FOR NINE BANDS IN A 31.0–100.0% MULTI-SEGMENTED GRADIENT RUN OVER 10.0 min IN TWO SEGMENTS

Gradient: 0 min, 31.0% B; 4.5 min, 50% B; 10 min, 100% B.

Band No.	$t_{R(calc.)}$	$t_{R(exp.)}$ [a]	Band width	R_s [b]
1	2.68	2.607	0.151	5.38
2	3.55	3.652	0.172	2.48
3	3.98	4.105	0.180	3.45
4	4.63	4.828	0.194	4.84
5	5.57	5.925	0.195	5.39
6	6.54	6.925	0.166	2.60
7	6.97	7.325	0.162	7.45
8	8.13	8.396	0.150	11.96
9	9.81	9.947	0.131	

[a] Average error in $t_R = \pm 0.22$ min ($= \pm 3.7\%$).
[b] Average in R_s (difference in t_R) $= \pm 9\%$.

confirmed the accuracy of the predictions (Table IV) of retention times, the experimental R_s values being lower. When the R_s value of the critical pair was decreased to 1.50, even better agreement was obtained (Fig. 2d).

The conditions were further optimized by changing the column parameters. Retaining the same column (length, particle size), the flow-rate was changed to 2.0 ml/min. This resulted in some decrease in column efficiency (to $N = 1008$), which Drylab G took into account from its routine Knox relationship. The calcualted data are given in Table IV and the simulated and experimental chromatograms in Fig. 3. Here also the agreement is good; the time of analysis was reduced to 10 min.

CONCLUSIONS

The conditions for the gradient HPLC of phenol and eight derivatives were optimized using the Drylab G computer program. only a few experimental results were needed to choose a gradient programme that gave a satisfactory separation of all components in a short time. Good resolution of most pairs of of components indicated that the method is suitable also for the separation of mixtures containing varying relative amounts of the components. The chromatograms simulated by the computer were very similar to the experimental chromatograms.

ACKNOWLEDGEMENT

The donation of a Hewlett-Packard 1050 liquid chromatograph by the Alexander von Humboldt Foundation (Bonn, F.R.G.) to T.H.D. is gratefully acknowledged.

REFERENCES

1 J. C. Berridge, *Techniques for the Automated Optimization of HPLC Separations*, Wiley, New York, 1985.
2 P. J. Schoenmakers, *Optimization of Chromatographic Selectivity*, Elsevier, Amsterdam, 1986.
3 L. R. Snyder, J. L. Glajch and J. J. Kirkland, *Practical HPLC Method Development*, Wiley-Interscience, New York, 1988.
4 J. L. Glajch and L. R. Snyder (Editors), *J. Chromatogr.*, 485 (1989).
5 Sz. Nyiredy (Editor), *J. Liq. Chromatogr.*, 12, Nos. 1 and 2 (1989).
6 P. Jandera and J. Churaček, *Gradient Elution in Column Liquid Chromatography*, Elsevier, Amsterdam, 1985.
7 L. R. Snyder, in Cs. Horváth (Editor), *High-Performance Liquid Chromatography —Advances and Perspectives*, Vol. 1, Academic Press, New York, 1980, p. 207.
8 M. A. Stadalius and L. R. Snyder, in Cs. Horváth (Editor), *High-Performance Liquid Chromatography – Advances and Perspectives*, Vol. 4, Academic Press, New York, 1986, p. 195.
9 L. R. Snyder, J. W. Dolan and D. C. Lommen, *J. Chromatogr.*, 485 (1989) 65.
10 J. W. Dolan, D. C. Lommen and L. R. Snyder, *J. Chromatogr.*, 485 (1989) 91; and references cited therein.
11 L. R. Snyder and J. W. Dolan, *Drylab G Instruction Manual*, L. C. Resources, Lafayette, CA, 1987.

Journal of Chromatography, 523 (1990) 91–102
Elsevier Science Publishers B.V., Amsterdam

CHROM. 22 708

Chromatographic investigations of macromolecules in the "critical range" of liquid chromatography

I. Functionality type and composition distribution in polyethylene oxide and polypropylene oxide copolymers

A. V. GORSHKOV
Institute of Chemical Physics, U.S.S.R. Academy of Sciences, Kosygina 4, 117977 Moscow (U.S.S.R.)
H. MUCH*, H. BECKER and H. PASCH
Academy of Sciences of the G.D.R., Central Institute of Organic Chemistry, Division of Macromolecular Chemistry, Rudower Chaussee 5, 1199 Berlin (G.D.R.)
and
V. V. EVREINOV and S. G. ENTELIS
Institute of Chemical Physics, U.S.S.R. Academy of Sciences, Kosygina 4, 117977 Moscow (U.S.S.R.)
(First received February 1st, 1990; revised manuscript received July 16th, 1990)

ABSTRACT

Polyethers obtained from ethylene oxide (EO) and propylene oxide (PO) and corresponding copolyethers were analysed by liquid chromatography under critical conditions (near the critical point of polymer adsorption) to obtain information on the functionality type distribution and structural inhomogeneity of copolymers. Homopolyether species were separated according to the number and type of their end groups. Copolymers of EO and PO (random and block) were split into groups depending on chemical composition, block length and the character of order in the monomer distribution. The experimental results are explained by considering the theory of polymer adsorption.

INTRODUCTION

The problem of determining functionality type distribution (FTD) is a classical one in the chemistry of reactive oligomers (telechelics) [1]. We have recently developed a method for the chromatography of macromolecules in the critical region close to the critical point of adsorption of macromolecules [2]. In this region, located at the boundary of the exclusion and adsorption separation modes, the dependence of the retention volumes V_R of homopolymers on their size (molecular weight) disappears, and separation is accomplished by other criteria, *e.g.*, by the number and type of terminal groups. The theory of this method has been described [1,2,11]. The method has subsequently been successfully used to investigate the FTD of a wide class of polyethers and polyesters [3,4], polycondensation oligomers [5–8] and oligobutadienes [9].

0021-9673/90/$03.50

The problem of analysing the FTD of copolymers is much more complex than that of homopolymers. In the general case, the separation by functionality types will be superimposed by the separation according to copolymer composition and structure. Therefore, to solve the problem of the FTD of copolymers, it is first necessary to investigate their heterogeneity in composition and the nature of the disordering of different monomers in the chain. This work was devoted to the analysis of the FTD of polypropylene oxide (PPO) and polyethylene oxide (PEO) and the structure of copolymers based on them.

THEORY AND METHOD

Separation in chromatography is defined by the distribution coefficient K_d, associated with a change in free energy when the macromolecule passes from the mobile phase (interparticle space) into the stationary phase pores:

$$K_d = \exp(-\Delta G)$$

(all the energy values will be expressed in kJ K^{-1} units). The variation of ΔG depends on the macromolecule size, R, pore size, D, and the energy of the interaction of monomers with the surface, $\varepsilon(x)$. The $\varepsilon(x)$ value depends on the chemical structures of the monomer and solvent, solvent composition and temperature and constitutes the effective potential of monomer interaction with the pore surface. The laws governing chromatography in the critical region can only be understood on the basis of the theory of the adsorption of macromolecules. Despite the great complexity of the current theory of macromolecule adsorption [10], requiring the application of the concepts of statistical physics unknown to most chromatographers, the final conclusions of this theory are simple, and can be easily used for the chromatographic analysis of heterogeneous macromolecules.

A fundamental consequence of the adsorption theory is the existence of a finite, critical depth of potential, ε_c, starting with which the adsorption of macromolecules in the pores takes place. If $\varepsilon > \varepsilon_c$ the energy of the interaction of monomers with the surface exceeds the entropy losses, and the macromolecule is adsorbed. If $\varepsilon < \varepsilon_c$ we have the reverse relationship, and the macromolecule is almost unabsorbed and remains in the interparticle space all the time. At $\varepsilon = \varepsilon_c$ the energy of interaction exactly compensates the entropy losses.

Corresponding to these three cases are the three modes in the chromatography of macromolecules: adsorption, exclusion and critical, differing in the sequence in which macromolecules of different size elute. The existence of these modes has been confirmed experimentally and well studied [1,2].

In the adsorption mode, K_d is exponentially dependent on the degree of polymerization, N. The adsorption of macromolecules soon becomes irreversible, and so the adsorption mode is appreciably limited from above with respect to molecular weight.

In the exclusion mode, K_d values for a Gaussian model of the chain are given by

$$K_d \approx \exp(-R^2/D^2); \qquad R > D$$

$$K_d \approx 1 - (2R/D); \qquad R < D$$

At the critical point, ΔG is zero irrespective of the size of the macromolecule and the pore size. In this case $K_d = 1$. Such a "disappearance" of the effect of the size of the macromolecules and their molar mass distribution (MMD) in the critical region opens up new possibilities for investigating the structure of heteropolymers such as telechelics and copolymers.

Polymers with functional groups

The simplest type of a heteropolymer is a telechelic, *i.e.*, a macromolecule containing terminal groups. The presence of these groups causes a difference in the interaction with the pore surface. If a binary solvent is chosen, corresponding to the critical conditions of adsorption for the polymer chain, the polymer chain itself will not contribute to any variations of ΔG. For a monofunctional macromolecule, the contribution to the ΔG variations will only be made by the terminal unit. This contribution is easy to find and thereby the determination of $K_d^{(1)}$, which numerically coincides with the statistical sum for a monofunctional macromolecule:

$$K_d^{(1)} = 1 - \frac{2a}{D} + \frac{2a}{D} \cdot \exp(\varepsilon_f - \varepsilon_c) = 1 + \frac{2a}{D}[\exp(\varepsilon_f - \varepsilon_c) - 1] \quad (1)$$

where ε_f is the energy of interaction of the terminal unit with the pore surface and a is the unit size. Let us now consider a bifunctional macromolecule with two terminal units (joined by an "invisible" filament that makes no contribution to ΔG). For such a macromolecule one can obtain

$$K_d^{(2)} = \left\{1 + \frac{2a}{D}[\exp(\varepsilon_f - \varepsilon_c) - 1]\right\}^2 = [K_d^{(1)}]^2; \qquad R > D \quad (2)$$

and

$$K_d^{(2)} = 1 - \frac{2R}{D} + \frac{2R}{D}\left\{1 + \frac{a}{R}[\exp(\varepsilon_f - \varepsilon_c) - 1]\right\}^2; \qquad R < D \quad (3)$$

These equations reflect the fact that at $R > D$ the macromolecule does not undergo any interactions with the pore surface. At $R \approx D$ the interaction of the solvated macromolecule with the pore surface takes place with one terminal unit only (*cf.*, eqn. 2).

At $R < D$ (*cf.*, eqn. 3), the ends of the chain are assumed to be statistically independent and make an additive contribution to free energy variations. Within the accuracy of a numerical coefficient of the order of unity, the equations coincide with strict dependences obtained for a Gaussian model [12].

Note that even at the critical point, when the chain joining the terminal groups becomes "invisible", the dependence of $K_d^{(2)}$ ($R < D$) on the size or molecular weight does not disappear. However, $K_d^{(2)} > [K_d^{(1)}]^2$ and the zones of different functionality under these conditions cannot overlap.

A macromolecule containing several functional units in the chain is "polyfunctional", turning in the critical region into a new one, a "chain of functional groups" joined by "invisible" Gaussian filaments of size l_i. As distinct from the usual

model of a polymer chain, the length of these filaments is different and reflects the nature of the ordering of defects in the chain. The distribution coefficient $K_d^{(n)}$ for such macromolecules can be estimated similarly to the derivation of eqns. 2 and 3. For instance, when all $l_i > D$ the defects are statistically independent [2], and

$$K_d^{(n)} = [K_d^{(1)}]^n \tag{4}$$

Regularities of the chromatography of block copolymers

Let us consider block copolymers of the AB and ABA′ types in the critical region. This problem is similar to a mono- and a bifunctional telechelic, where the role of a functional group is played by the block A. Let us define $\varepsilon_A < \varepsilon_B$. It is obvious that at the critical solvent composition for the block A one should observe separation according to the size of block B, and *vice versa* [13]. The distribution coefficients K_d^{AB} in this instance will be

$$K_d^{AB} = K_d^B; \qquad \varepsilon = (\varepsilon_A)_c \tag{5}$$

$$K_d^{AB} = K_d^A; \qquad \varepsilon = (\varepsilon_B)_c \tag{6}$$

where K_d^B and K_d^A are the distribution coefficients of the corresponding homopolymers.

For a three-block copolymer ABA′ under the critical conditions, for the outer blocks A, irrespective of their MMD functions, only the inner block B is seen in the adsorption mode and

$$K_d^{ABA'} = K_d^B; \qquad \varepsilon = (\varepsilon_A)_c \tag{7}$$

When the critical conditions are assigned for the inner block B, similarly to a bifunctional molecule, $K_d^{ABA'}$ depends on the ratio between the sizes of block B and the pores, R_B and D. If $R_B > D$ blocks A and A′ are statistically independent, and

$$K_d^{ABA'} = K_d^A K_d^{A'}; \qquad \varepsilon = (\varepsilon_B)_c \tag{8}$$

When $R_B < D$ and $R_{ABA'} < D$, we can, similarly to eqn. 3, determine $K_d^{ABA'}$ as

$$K_d^{ABA'} = 1 + \frac{2\,R_{ABA'}}{D}\left[\left(1 - \frac{R_A}{R_{ABA'}}\right)\left(1 - \frac{R_{A'}}{R_{ABA'}}\right) - 1\right] \tag{9}$$

The $K_d^{ABA'}$ value is a minimum when $R_A = R_{A'}$ and a maximum when the size of one of the blocks tends to zero (however, $R_{ABA'}^2 = R_A^2 + R_B^2 + R_{A'}^2 = \text{constant}$). In principle, this makes it possible to separate two- and three-block macromolecules of the same composition.

In the general case the relationship between K_d and the homopolymer structure is extremely complex and reflects the interrelation of such factors as its size and composition and the nature of the ordering of monomers in the chain. These aspects are beyond the scope of this work.

EXPERIMENTAL

Apparatus

A DuPont System 8800 high-performance liquid chromatograph consisting of a Model 8770 pump, a column oven and a manually operated Rheodyne Model 7125 injection valve with a 20-μl loop, together with an RIDK 101 differential refractive index detector from Laboratorní Přístroje (Prague, Czechoslovakia), was used. The separation was performed on a 250 × 4.6 mm I.D. Chrompak RP-18 C_{18} column at 298 K using acetonitrile–water or tetrahydrofuran–water as the mobile phase. A flow-rate of 1 ml min^{-1} was used in the isocratic mode.

Materials

PEO with number-average molecular weights of M_n = 150, 600, 2000, 6000 and 20 000 and PPO with M_n = 425, 1025 and 2000 were obtained from Merck (Darmstadt, F.R.G.). The following polymers were synthesized by anionic polymerization at 110°C using the corresponding potassium alcoholates and glycolates as initiators:

Monofunctional polyethers:

$HO(CH_2CH_2O)_{40}CH=CH_2$;
$HO(CH_2CH_2O)_{40}C_4H_9$;
$HO(CH_2CH_2O)_m[CH(CH_3)CH_2O]_nC_4H_9$ (n = 10; m = 10 or 30);

difunctional block copolyethers:

$HO(EO)_m(PO)_n(EO)_mOH$ (n = 11; m = 5, 10, 15 or 20);

difunctional random copolyether:

$HO(PEO)_{30}(PPO)_{11}OH$.

RESULTS AND DISCUSSION

Characteristic functions of the telechelic and block copolymer of the AB type are given in Fig. 1. For the telechelic it is a set of MMD functions for different functionalities (FTD), and for the block copolymer the surface in composition–molecular weight coordinates. These functions fully determine the properties of the given macromolecules.

The problem of determining the FTD for the telechelic is easily solved. In the critical mode, the separation is performed exclusively by the functionality types and the selected fractions are then defined by their molecular weights in the exclusion mode. The second part of this analysis is trivial and will not be dealt with here.

For PPO homopolymers with terminal OH groups the problem of separation by functionality types was previously solved using silica with ethyl acetate–methyl ethyl ketone [4]. The separation of PEO with terminal HO---OH, HO---OC_4H_9 and $CH_2=CH$---OH groups is considered in this work.

Corresponding to the critical conditions for PEO on the Chrompak RP-18 phase is the composition acetonitrile–water (42:58). In this instance the retention volume *versus* macromolecule size dependence disappears up to a molecular weight of 20 000 (Fig. 2). These conditions are optimum for the separation of PEO according to the

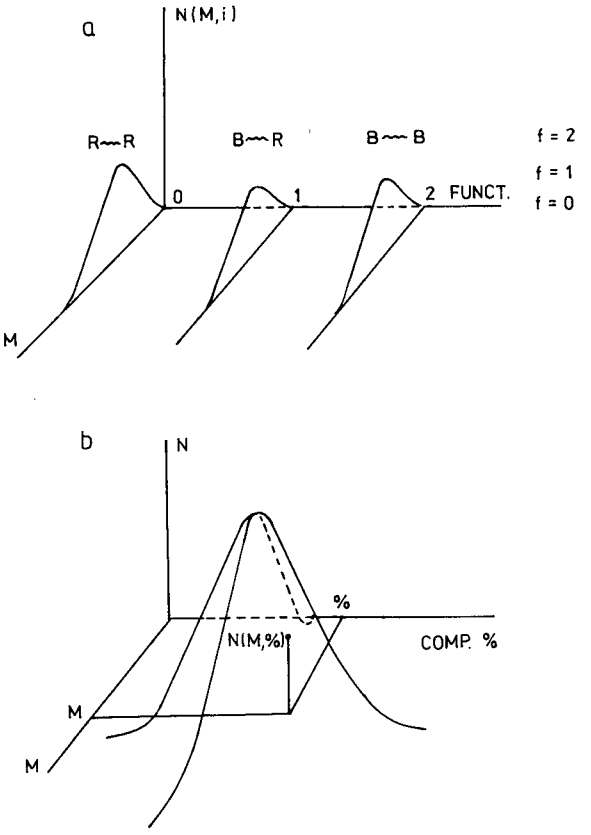

Fig. 1. Distribution functions (FTD, MMD) of (a) the telechelic and (b) the two-block copolymer.

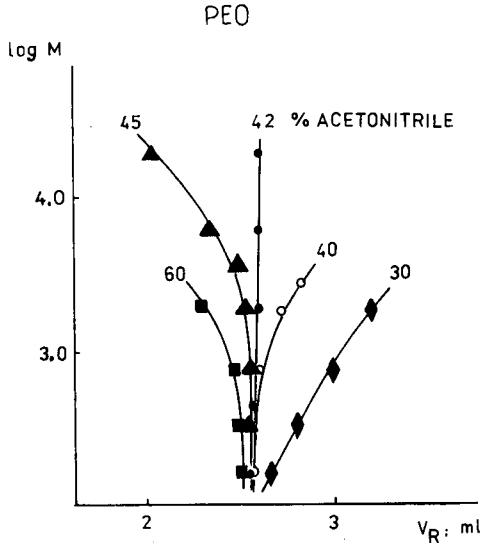

Fig. 2. Realization of the critical conditions for PEO. Column, RP-18; eluent, water–acetonitrile of different compositions. V_R = retention volume.

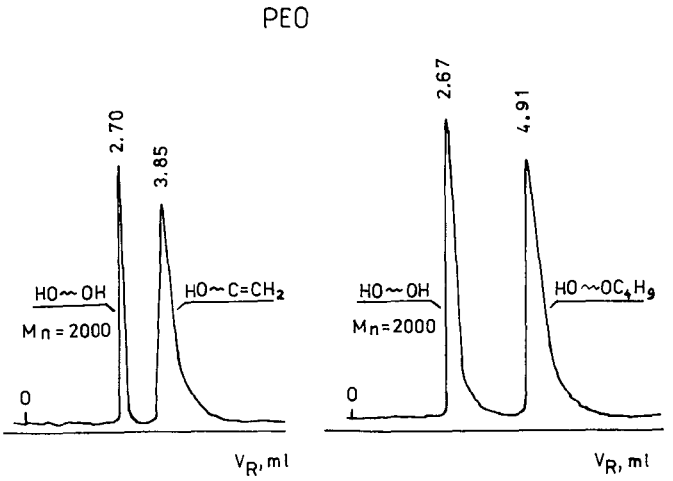

Fig. 3. PEO separation by functionality types under critical conditions. Column, RP-18; eluent, water–acetonitrile (58:42, v/v); flow-rate, 1 ml min^{-1}; loop volume, 20 μl; refractometric detection.

types of terminal groups (Fig. 3). As was to be expected, for the reversed phase the retention of macromolecules with the aliphatic end RO is stronger than that with a double bond. As follows from eqns. 2 and 3, the scale of retention volumes can be effectively changed by changing the pore size D. An increase in pore size leads to a decrease in retention volumes, as the fraction of conformations in which the end interacts with the surface decreases. Under the conditions established it is therefore very easy to determine the defectiveness of PEO in HO---OC_4H_9 or $CH_2=CH$---OH functionality over a wide range of molecular weights.

To solve a similar problem for PPO on a reversed phase it is necessary to choose a different mixture, *e.g.*, water–tetrahydrofuran (THF), as in 100% acetonitrile a weak adsorption regime occurs with PPO.

Let us consider the regularities characterizing the chromatography of PPO and PEO block copolymers. The copolymer composition and the nature of the ordering of different molecules in its chain (randon, block, regular, etc.) exert a decisive influence on its properties.

The simplest type of AB copolymer, $(PEO)_m(PPO)_n$, in our samples contained also a terminal aliphatic group, $-OC_4H_9$, which complicates the simple picture of the PPO block separation by size under the critical conditions for PEO (Fig. 4) by increasing the retention volumes. However, this example shows that the disappearance of the PEO tail does not depend on its length. In accordance with eqn. 6,

$$K_d^{AB}(-OC_4H_9) = K_d^{B}(-OC_4H_9)$$

Let us now consider a three-block copolymer, ABA'. At the critical point for PEO the outer blocks disappear, irrespective of their length, and therefore

$$K_d^{ABA'} = K_d^{B}$$

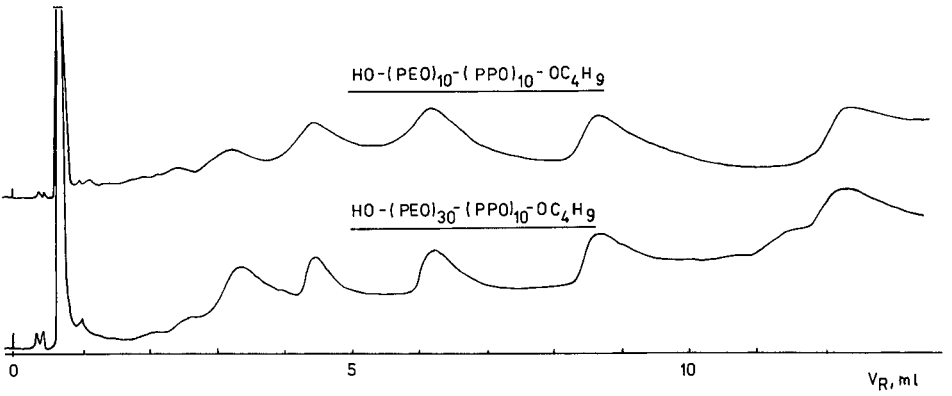

Fig. 4. Disappearance of PEO blocks and the MWD of PPO blocks for two-block PEO–PPO copolymers of different size and composition. Conditions as in Fig. 3.

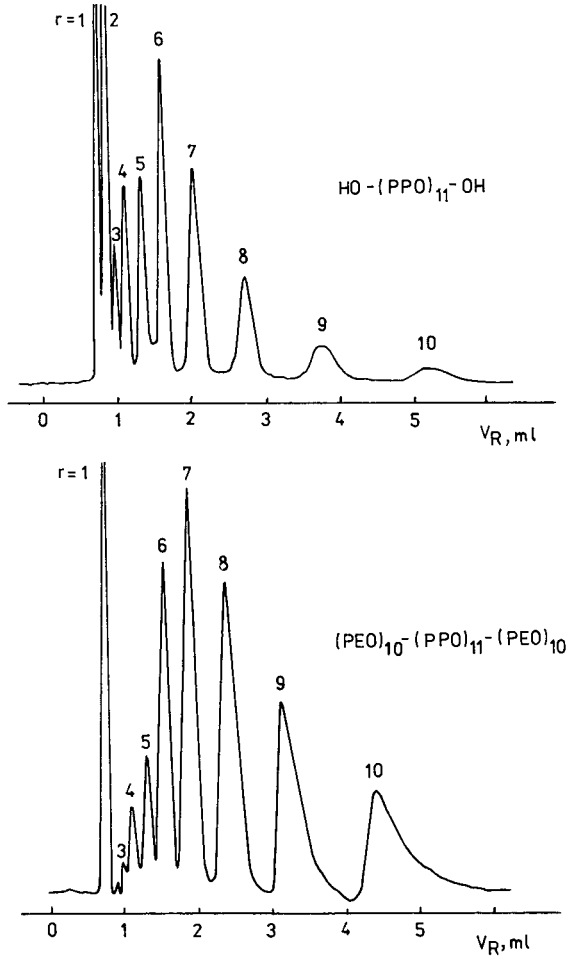

Fig. 5. Chromatograms of PPO and three-block PPO–PEO copolymer, obtained under the critical conditions for PEO. Conditions as in Fig. 3.

This phenomenon is illustrated in Figs. 5 and 6. Note the correspondence between the PPO homopolymer homologues and the macromolecules with a different degree of polymerization in the inner block B in the copolymer. As with functional molecules, one can decrease the scale of retention volumes of the copolymer by increasing the pore size.

It is now of interest to find the critical point for the inner PPO block in a three-block copolymer. For the outer blocks we would then have the exclusion mode and, depending on the ratio between the size of the PPO block and the pore size, the separation would be described by eqns. 8 and 9. Unfortunately, it proved impossible to do this on the chosen phase. The critical point occurs on PPO in a THF–water mixture with a small water content. Under these conditions the unmodified sites of the reversed phase, containing–SiOH groups, become significant. Because of the extremely strong interaction of PEO with these sites, the chromatograms, even for the PEO homopolymer, are strongly distorted by elongated tails. In other words, under the critical conditions for the inner PPO block, the exclusion mode for the outer PEO blocks cannot be realized on this phase.

In order to understand the differences in the chromatographic behaviour of a block copolymer and a random polymer of the same composition, let us consider

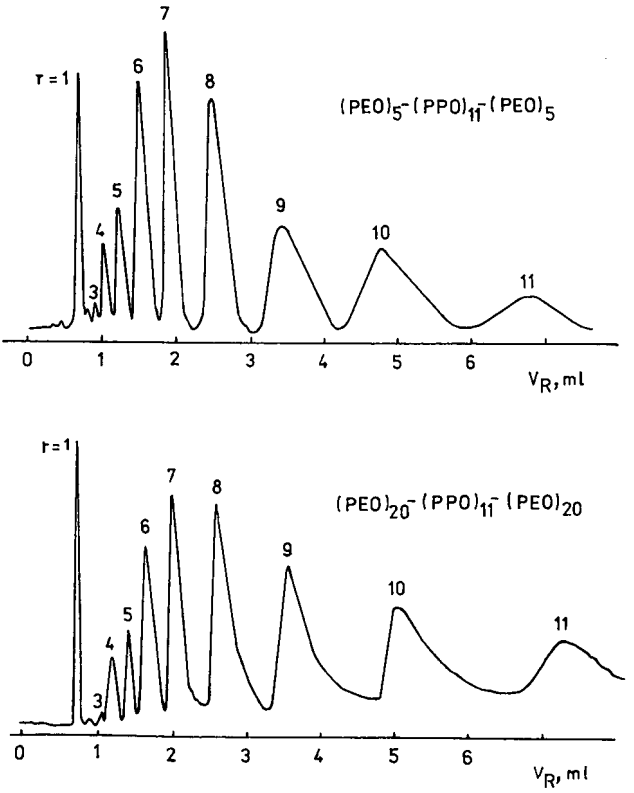

Fig. 6. Disappearance of PEO blocks and the MWD of visible PPO blocks of different size and compositions under the critical conditions for PEO. Conditions as in Fig. 3.

a simple example. Let us take two macromolecules of the same length and composition (number of PPO monomers). For the first chain we shall distribute the PPO monomers along the whole length of the chain at a scale 1 (Fig. 7). Under the critical conditions for PEO the parts of the chain joining the PPO monomers do not interact. To calculate $K_d^{(n)}$ it is only necessary to take into account the interaction of PPO monomers with the surface at a scale R in the first instance and at a scale $l \ll R$ in the second. Calculation according to eqn. 5 yields

$$K_d \text{ (block)} \approx 1 - \frac{2l}{D} + \frac{2l}{D}\left\{1 + \frac{a}{l}[\exp(\varepsilon_B) - 1]\right\}^n$$

$$K_d \text{ (random)} \approx 1 - \frac{2R}{D} + \frac{2R}{D}\left\{1 + \frac{a}{R}[\exp(\varepsilon_B) - 1]\right\}^n \qquad (10)$$

As seen from eqn. 10, the "random" copolymer with PPO situated along the whole chain must be eluted earlier than the "block copolymer" of the corresponding composition. This conclusion is confirmed by the experimental chromatogram in Fig. 7. On average, a random polymer emerges sooner than a block copolymer of the corresponding composition.

The chromatogram of a random polymer contains information on the nature of the ordering of monomers in its chain, not taken into account in the calculation of the

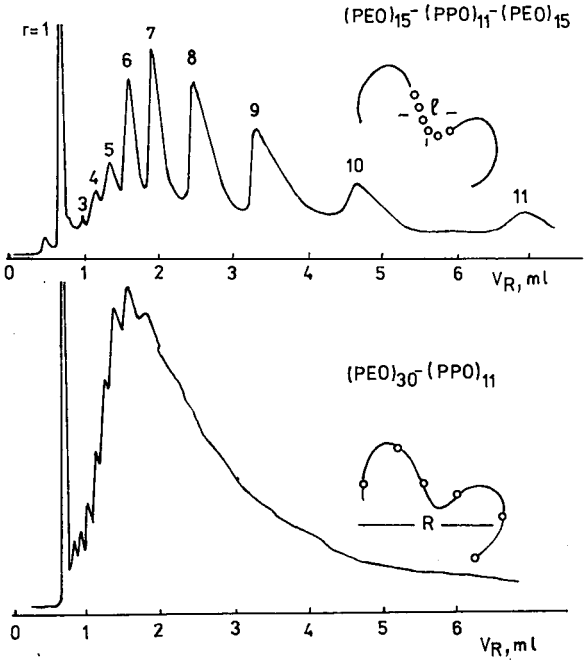

Fig. 7. Chromatograms of a block and a random copolymer of similar overall composition under the critical conditions for one of the PEO homopolymers. Separation conditions as in Fig. 3.

type in eqn. 10. Note that in the general case the chromatograms of heteropolymers close to the critical point should apparently reflect the fine differences from the truly random distribution, microblock parameters, etc. However, the qualitative difference in the form of the chromatogram of a random and a block copolymer of the same composition already allows the unambiguous attribution of the investigated polymer to one of these types of ordering.

When we return to the functionality of copolymers, it must now be obvious that separation according to functionality types in the critical region is superimposed by the polymer structure separation. To solve this problem it is necessary to choose a phase that gives a minimum difference in the interaction with the surface of PO and EO monomers. For the given system such a possibility seems to exist. On an RP-1 phase with a shorter aliphatic chain cross-linked to the surface, the sequence of emergence of PPO and PEO polymers is inverted in comparison with the C_{18} phase. Therefore, by changing the length of this tail one can choose a length for which the difference in PPO and PEO interactions is a minimum.

The heterogeneity of the reversed phase based on silica gel and the anomalously strong PEO interaction with the unmodified sites of this phase did not allow us to solve definitively the problem of determining the structure of the block copolymer and to construct the characteristic surface of the type shown in Fig. 4. Polymeric reversed phases have recently appeared that are free from the shortcomings of modified silica gels, in particular of residual –SiOH groups [14]. These phases, when critial conditions are realized on them, seem to be ideally suited for the analysis of the structure of PPO and PEO copolymers.

CONCLUSIONS

The questions of the chromatography of PPO and PEO macromolecules and their copolymers in the critical region have been considered theoretically and experimentally. The critical conditions for PEO have been established, making it possible to separate PEO according to the types of terminal groups, and copolymers according to the molecular weights of PPO blocks and the nature of their ordering in the chain. The method of chromatography in the critical region thus allows unique information to be obtained on the structure of macromolecules.

Some of the questions relating to the analysis of block copolymers have not been completely solved in this work. The same is true of questions regarding the functionality of block copolymers. However, we first wanted to demonstrate new opportunities in the analysis of the structures of heteropolymers offered by the method of chromatography near the critical point of adsorption.

REFERENCES

1 S. G. Entelis, V. V. Evreinov and A. I. Kuzaev, *Reactive Oligomers*, Khimiya, Moscow, 1985.
2 S. G. Entelis, V. V. Evreinov and A. V. Gorshkov, *Adv. Polym. Sci.*, 76 (1987) 129.
3 A. V. Gorshkov, V. V. Evreinov and S. G. Entelis, *Zh. Fiz. Khim.*, 59 (1985) 958.
4 A. V. Gorshkov, V. V. Evreinov, B. Lausecker, H. Pasch, H. Becker and G. Wagner, *Acta Polym. Berlin*, 37 (1986) 740.
5 V. V. Evreinov, A. V. Gorshkov, T. N. Prudskova, V. V. Gur'yaova, A. V. Pavlov, A. Ya. Malkin and S. G. Entelis, *Polym. Bull.*, 14 (1985) 131.

6 T. N. Prudskova, A. V. Gorshkov, V. V. Evreinov, V. V. Gur'yanova, A. V. Pavlov and C. G. Entelis, *Vysokomol. Soedin. Ser. B*, 28 (1986) 329.
7 A. V. Gorshkov, T. N. Prudskova, V. V. Gur'yanova and V. V. Evreinov, *Polym. Bull.*, 15 (1986) 465.
8 T. N. Prudskova, V. V. Gur'yanova, A. V. Gorshkov, V. V. Evreinov and A. V. Pavlov, *Vysokomol Soedin. Ser. B*, 28 (1986) 757.
9 A. V. Gorshkov, V. V. Evreinov and S. G. Entelis, *Zh. Fiz. Khim.*, 57 (1983) 2665.
10 E. Eisenrigler, K. Kremer and K. Binder, *J. Chem. Phys.*, 77 (1982) 6296.
11 P. G. De Gennes, *Scaling Concepts in Polymer Physics*, Cornell University Press, Ithaca, 1979, p. 352.
12 A. A. Gorbunov and A. M. Skvortsov, *Vysokomol. Soedin. Ser. A*, 26 (1984) 946.
13 A. M. Skvortsov and A. A. Gorbunov, *Vysokomol Soedin. Ser. A*, 21 (1979) 339.
14 F. Nevejans and M. Verzele, *J. Chromatogr.*, 406 (1987) 325.

Journal of Chromatography, 523 (1990) 103–117
Elsevier Science Publishers B.V., Amsterdam

CHROM. 22 744

Investigation of affinity partition chromatography using formate dehydrogenase as a model[a]

A. WALSDORF
Institut für Enzymtechnologie der Heinrich Heine Universität Düsseldorf, Postfach 2050, D-5170 Jülich (F.R.G.)
D. FORCINITI
Department of Chemical Engineering, North Carolina State University, Raleigh, NC 27695 (U.S.A.)
and
M. R. KULA*
Institut für Enzymtechnologie der Heinrich Heine Universität Düsseldorf, Postfach 2050, D-5170 Jülich (F.R.G.)
(First received March 21st, 1990; revised manuscript received August 7th, 1990)

ABSTRACT

The enzyme formate dehydrogenase (FDH) was purified from the crude extract of *Candida boidinii* by affinity partition chromatography. The partition coefficient, K, of the enzyme was selectively increased by adding polyethylene glycol–Procion Red HE3b as an affinity ligand to the mobile phase in the chromatographic column. The increased K value led to early elution of the enzyme–ligand complex and separated the target protein from the main peak of the contaminants.

INTRODUCTION

Partitioning in aqueous two-phase systems was introduced by Albertsson [1] as a mild method for separating cell organelles and macromolecules. The selectivity of extraction may be increased by adding biospecific ligands covalently bound to one of the phase-forming polymers. This approach has been successfully employed for the purification of enzymes [2–9] and nucleic acids and oligonucleotides [10,11]. Commonly used general ligands for enzyme extraction are the triazine dyes [12,13], which are cheaply available commercially. Application of polyethylene glycol (PEG)–Procion Red HE3b has been investigated for the large-scale extraction of formate dehydrogenase from *Candida boidinii* [14,15].

Newly developed matrices for liquid–liquid partition chromatography (LLPC) with aqueous two-phase systems [16] combine the favourable properties of partitioning with the advantages of column chromatography. It also offers the possibility of a convenient purification method: affinity partition chromatography. Incorporation

[a] The results presented in this paper are part of the Doctoral Thesis of A. Walsdorf, submitted to the Heinrich Heine Universität Düsseldorf.

0021-9673/90/$03.50

of ligands into the PEG–dextran system will lead to the formation of protein–ligand complexes depending on the ligand concentration and ionic strength. Fig. 1 shows schematically the simplest form of a 1:1 complex. A detailed analysis of the linked equilibria involved has been published [15]. The complex formation will selectively increase the partition coefficient and therefore change the elution volume of the target protein.

The fractionation of DNA restriction fragments has been accomplished, including base-specific DNA ligands, covalently bound to PEG in the mobile phase of a partition column [11,17], making use of the concept of affinity partition chromatography for the separation of very similar macromolecules.

In this work we investigated the application of affinity partition chromatography for the purification of formate dehydrogenase (FDH) from the crude extract of *Candida boidinii* as a model using Procion Red HE3b as the ligand. This enzyme and ligand were chosen as the system is well documented in the literature [14,18]. The method is appealing because in principle it allows the selective and early elution of the desired product from a partition column. Three methods to enhance the partition coefficient of the FDH in the partition column were investigated: first, the PEG–Procion Red HE3b was added to the sample only; second, the PEG–Procion Red HE3b was present in the sample and also at a constant, low concentration in the mobile phase, so that non-equilibrium conditions prevail and the elution volume will depend on the local concentration, dissociation rates and column length; and third, the influence of the ligand concentration in the mobile phase was tested.

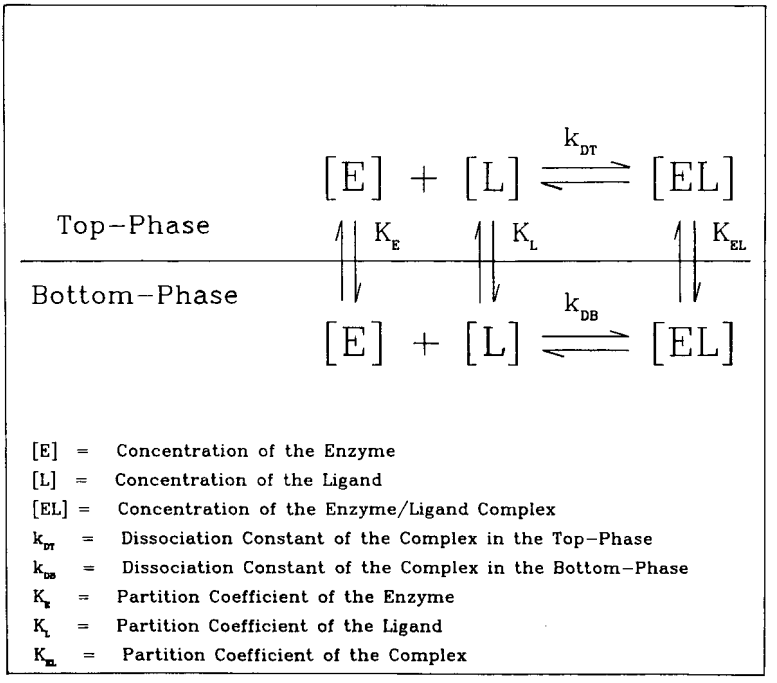

Fig. 1. Schematic representation of the linked equilibria of partition and enzyme–ligand association for the simplest case of a 1:1 complex.

EXPERIMENTAL

Materials

The support material LiParGel 750 was a gift from E. Merck (Darmstadt, F.R.G.). The triazine dye Procion Red HE3b was a gift from ICI Germany (F.R.G.). PEG 20000 was obtained from Merck Schuchard (München/Hohenbrunn, F.R.G.). Dextran Pl 500 (nominal molecular weight, MW = 500 000 dalton) and Vc 40 (MW = 40 000 dalton) were bought from Pfeifer und Langen (Dormagen, F.R.G.). The proteins were purchased from the following sources: albumin and peroxidase from E. Merck, ferritin from Pharmacia (Uppsala, Sweden), transferrin and myoglobin from Serva (Heidelberg, F.R.G.), α-chymotrypsinogen A Type II from Sigma (St. Louis, MO, U.S.A.) and formate dehydrogenase from Boehringer (Mannheim, F.R.G.).

All other chemicals were of analytical-reagent grade.

Preparation of the affinity ligand

The triazine dye Procion Red HE3b was coupled to PEG 20 000 according to Cordes and Kula [14].

Phase preparation

The concentrations of PEG and dextran in the various phase systems used for partition chromatography were taken from phase diagrams established by Albertsson [1], corresponding to a phase ratio of 1:1. The PEG- and dextran-rich phases were prepared with stirring, mixing the polymers with water and salts in the appropriate amounts for 1 h. The pH was adjusted by adding concentrated phosphoric acid or potassium hydroxide solutions. The phases were allowed to settle under gravity in a separating funnel; after 1–2 h the phases were separated. The PEG-rich phase was allowed to stand in order to obtain a totally clear top phase, removing the small amount of bottom phase after settling for several days.

The mobile phase containing the affinity ligand Procion Red HE3b was obtained by dissolving solid PEG–Procion Red HE3b in the top phase of an appropriate system. The concentration of ligand was determined spectrophotometrically at 542 nm, using a laboratory-determined molar absorption coefficient of 36 200 l $mmol^{-1}$ cm^{-1}. In order to prevent oxidative degradation of the PEG, the mobile phase was stored under nitrogen.

Preparation of columns

The LiParGel 750 support was equilibrated with the phase system and packed into the chromatographic columns (Superformance system; E. Merck) according to Müller [16].

Column chromatography

The chromatographic columns were integrated into a Pharmacia FPLC system. Fractions of 1 or 0.5 ml were collected using a Frac 100 fraction collector (Pharmacia).

Sample preparation

Exactly weighed amounts of the analyte substances were dissolved in the mobile

phase and centrifuged (3000 *g*, 5 min), removing undissolved solid material. The samples were applied to the column using an MV 7 valve (Pharmacia) and the programme was started.

Determination of partition coefficient

The partition coefficients of pure proteins were determined by mixing the sample with equal volumes of top and bottom phase, separating the phases by low-speed centrifugation (1800 *g*, 10 min) and measuring the absorbance at 280 nm (Shimadzu UV 160) in each phase. The activity of formate dehydrogenase was determined according to Schütte *et al.* [19] by an enzymatic assay. The partition coefficient, K, was calculated as the ratio of the absorbance or enzyme activity in the top to that in the bottom phase according to

$$\frac{C_T}{C_B} = \frac{f_T}{f_B} = K = \text{constant} \tag{1}$$

where C_T and C_B are the concentrations of the component in the top and bottom phase and f_T and f_B are the activities of the component in the top and bottom phases.

Determination of protein concentration

The protein concentration was determined according to Bradford [20] using bovine serum albumin for calibration.

Determination of the column parameters V_s and V_m

The physical parameters of the column were obtained as described previously [21] using a special set of calibration standards. Their elution volumes from the column and the K values measured by independent batch experiments were fitted to eqn. 2 [21] derived by Martin and Synge [22]. This fit, correlating elution volumes and K values, yields sufficiently accurate values for V_s and V_m:

$$V_e = V_s/K + V_m \tag{2}$$

where V_e = elution volume, V_s = volume of the stationary phase, V_m = volume of the mobile phase and K = partition coefficient.

The results shown in Fig. 2 were obtained for the column equilibrated with a phase system of PEG 20 000 and dextran 500. V_s was found to be 5.75 ml and V_m 10.0 ml. The broken line in Fig. 2 illustrates the relationship between the partition coefficient and elution volume in the given column.

Stabilization of eluents and column against microbial degradation

Sodium azide is commonly used to protect phase components against microbial contamination. Formate dehydrogenase is completely inhibited by sodium azide [19]. Therefore, we searched for a substitute and eventually selected chloroacetamide. The addition of 5 g/l of chloroacetamide has prevented contamination of the column and the mobile phases for more than 2 years already, although storage and operation were carried out at ambient temperature.

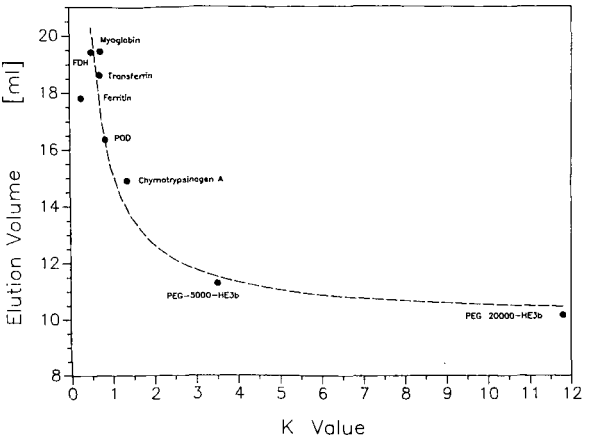

Fig. 2. Elution volume of a set of standard proteins, PEG 5000 and PEG 20 000 triazine dye derivatives in a LiParGel 750 column (30 × 1 cm I.D.). System composition, 2.7% PEG 20 000, 4.5% dextran 500, 75 m*M* potassium bromide, 10 m*M* phosphate buffer (pH 7); temperature, 30°C; flow-rate 1 ml/min. The graph illustrates the relationship between the partition coefficient and the elution volume in the given column. V_s = 5.75 ml; V_m = 10.0 ml.

Cell cultivation and harvesting

The cultivation of *Candida boidinii* on methanol as carbon and energy source was carried out according to Sahm and Wagner [23] in a 10-l Biostat E bioreactor (Braun Melsungen, Melsungen, F.R.G.) under maximum aeration. The cells were harvested using a KA2-06-075 chamber centrifuge (Westfalia Separator, Oelde, F.R.G.).

Preparation of crude extracts

The cells were suspended in 0.05 *M* potassium phosphate buffer (pH 7.5) to give a 40% (w/v) suspension and disrupted by wet milling in a Netsch LME 0.5 mill (Netsch Feinmahltechnik, Selb, F.R.G.) for 5 min at 2500 rpm using 80% (v/v) glass beads of 0.75 mm diameter. After addition of 0.5% (v/v) of a polyethyleneimine (PEI) solution [10% (w/v), pH 7.0, adjusted with HCl], the homogenate was centrifuged 10 min at 2000 *g* at 4°C and the sediment discarded. By treatment with PEI, nucleic acids are precipitated and the removal of cell debris is improved. The result was a crude extract free from solid material, which could be passed without problems through a microporous filter of 0.45-μm pore size. The crude extract was stored in aliquots at −20°C for the experiments described below.

RESULTS AND DISCUSSION

First series: addition of ligand to the sample

Addition of ligand only to the sample loaded on the column would be a cost-effective way of bringing about affinity partition chromatography and simple to operate with changing products. The ligand concentration in the sample should saturate the enzyme at the start of the chromatographic run. Multi-stage partitioning in the column will lead to dissociation and separation of the complex on the column, depending on K_L and K_{EL} (Fig. 1) and the kinetics of dissociation.

First we used a column equilibrated with a phase system of 5.45% PEG 6000 and 9.75% dextran 40 (MW = 40 000 dalton), 4 m*M* potassium bromide and 6.3 m*M* phosphate buffer (pH 7.5). The low salt concentration was chosen in order to obtain the highest efficiency of the affinity partitioning while keeping the dissociation constant of the enzyme–ligand complex small. The temperature of the column was adjusted to 23°C. To examine the general properties of the enzyme–ligand interaction in the column a partially purified formate dehydrogenase (4.8 U/mg; 12 U/ml) was used. In the absence of ligand, FDH activity was detected in the second peak in the chromatogram (Fig. 3a) at an elution volume of 25.4 ml, corresponding to a partition coefficient of 0.33. On adding increasing amounts of the affinity ligand PEG 20 000–Procion Red HE3b (PEG–Red) to the enzyme solution applied to the column,

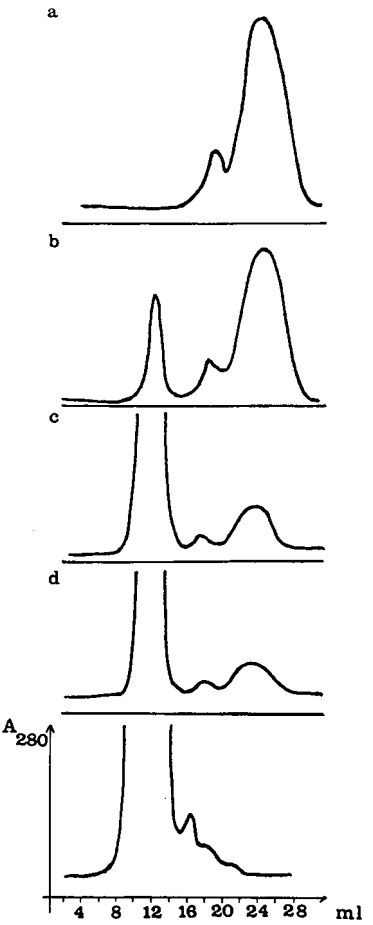

Fig. 3. Elution patterns of prepurified FDH with 12 U/ml enzymatic activity. Sample size, 100 μl. System composition, 5.45% PEG 6000, 9.75% dextran 40, 4 m*M* potassium bromide, 6.3 m*M* phosphate (pH 7.5); temperature, 23°C; flow-rate, 0.3 ml/min. The decrease in the FDH peak with increasing amounts of PEG–Red added to the sample is illustrated: PEG–Red concentration, (a) 0, (b) $0.146 \cdot 10^{-3}$, (c) $0.511 \cdot 10^{-3}$, (d) $1.022 \cdot 10^{-3}$, (e) $3.651 \cdot 10^{-3}$ *M*.

TABLE I

YIELD OF FDH IN THE ENZYME–LIGAND PEAK AND THE FDH PEAK ON INCREASING THE CONCENTRATION OF PEG–RED IN THE SAMPLE

System composition: 5.45% PEG 6000, 9.75% dextran 40, 4 m*M* potassium bromide, 6.3 m*M* phosphate buffer (pH 7.5), 23°C, flow-rate 0.3 ml/min, column size 30 × 1 cm I.D., sample size 100 μl; sample, prepurified FDH, 12 U/ml.

Concentration of PEG–Red (10^{-3} *M*)	Yield of FDH in the PEG–Red peak (%)	Yield of FDH in the FDH peak (%)	Total recovery (%)
0.146	7.8	90.2	98.0
0.511	29.2	68.7	97.9
1.022	47.4	46.6	94.0
3.651	77.0	13.9	90.9

the elution volume of the enzyme changed as illustrated in Fig. 3 b–e and quantified in Table I. Owing to the shift of the enzyme activity into the PEG-Red peak the FDH main peak decreased. However, with increasing concentration of the ligand in the sample the peak corresponding to PEG–Red becomes wider and wider and overlaps with the peak of the contaminants. Even with the highest amount of PEG–Red in the sample it was not possible to shift the FDH activity completely into the PEG–Red peak. A further increase in the concentration was not desirable owing to the increasing viscosity of the sample.

Because under the conditions employed the enzymatic activity could not be shifted completely into the PEG–Red peak and the ligand peak was not totally separated from the contaminants, we changed the system composition in order to increase the *K* value of the ligand. The higher *K* value should lead to earlier elution of the enzyme–ligand peak. On the basis of previous work we selected a phase system of PEG 20 000 and dextran 500 [24].

To find the optimum concentration of the polymers with respect to the *K* value of the PEG–Red we determined the partition coefficient of the affinity ligand as a function of the polymer concentration. The results are shown in Fig. 4. The ratio of the PEG concentration to dextran concentration was 1.0:1.5. At PEG concentrations above 5% the upper phase was difficult to clarify completely owing to the very small droplets of dextran retained in the top phase. Employing a UV monitor at 280 nm a totally clear eluate was needed in order to analyse the elution profile reproducibly. For the following experiments a system containing 4.5% PEG 20 000, 6% dextran 500, 5.5 m*M* potassium bromide and 6.3 m*M* phosphate buffer (pH 7.5) was selected. The *K* value of the PEG–Red was increased to 35 and the elution volume in the freshly prepared column was 7.5 ml, very close to the void volume.

On adding $1 \cdot 10^{-4}$ *M* PEG–Red to the enzyme sample, 38% of the FDH emerged in the enzyme–ligand peak and 62% in the main FDH peak. The yield was 100%. This is a significant improvement compared to the result given in Table I; nevertheless, the enzyme is eluted in two positions and the dissociation of the enzyme–ligand complex during the chromatographic run apparently cannot be suppressed sufficiently.

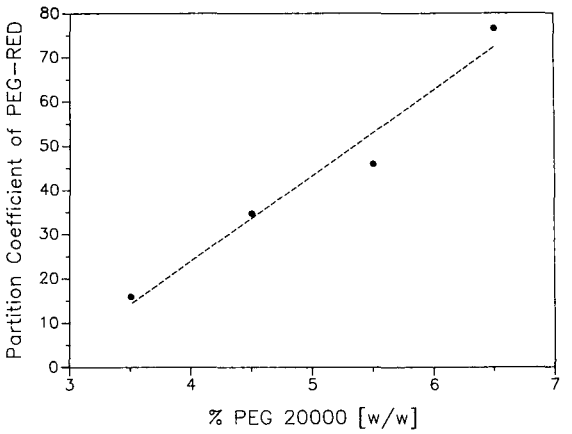

Fig. 4. Partition coefficient of the affinity ligand PEG 20 000–Procion Red HE3b as a function of the concentration of phase-forming polymers. The ratio of PEG to dextran concentration was 1:1.5.

Second series: addition of ligand to the sample and mobile phase

For the next series of experiments a crude extract of *C. boidinii* with 2.3 U/ml activity of FDH was employed. We added PEG–Red in various amounts to the sample and equilibrated and maintained PEG–Red at a low concentration of $2 \cdot 10^{-5}$ *M* in the mobile phase in the column. In this way, dissociation of the enzyme–ligand complex due to the changing concentrations of the free ligand should be minimized during the chromatography. Quantitative data are summarized in Table II.

The elution profiles are shown in Fig. 5a–c. At a PEG–Red concentration of $50 \cdot 10^{-5}$ *M* in the sample and $2 \cdot 10^{-5}$ *M* in the mobile phase the enzyme activity is shifted completely to the enzyme–ligand peak. The experiment was repeated twice to determine the reproducibility and the purification of the enzyme from the crude extract. The data are presented in Table III.

If the crude extract is heated for 10 min at 55°C in a water-bath to denature other

TABLE II

YIELD OF FDH IN THE ENZYME–LIGAND PEAK AND THE FDH PEAK USING DIFFERENT PEG–RED CONCENTRATIONS IN THE SAMPLE AND A CONSTANT CONCENTRATION OF $2 \cdot 10^{-5}$ *M* IN THE MOBILE PHASE

System composition: 4.5% PEG 20 000, 6% dextran 500, 5.5 m*M* potassium bromide, 6.3 m*M* phosphate buffer (pH 7.5), 23°C, column size 30 × 1 cm I.D., sample size 100 µl; sample, crude extract of *Candida boidinii*, 2.3 U/ml.

Concentration of PEG–Red in the sample (10^{-5} *M*)	Yield of FDH in the enzyme–ligand peak (%)	Yield of FDH in in the FDH main peak (%)	Total recovery (%)
2	40	60	100
10	63	37	100
50	100	–	93

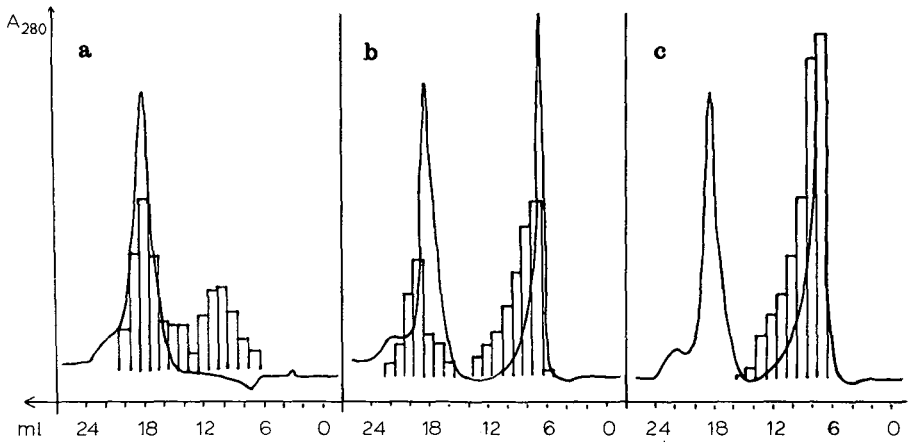

Fig. 5. Elution of FDH with increasing PEG–Red concentration in the sample (crude extract of *Candida boidinii*). The enzymatic activity in the peaks is indicated by histograms of the activity in the collected fractions. System composition, 4.5% PEG 20 000, 6% dextran 500, $2 \cdot 10^{-5}$ *M* PEG–Red, 5.5 m*M* potassium bromide, 6.3 m*M* phosphate buffer (pH 7.5); temperature, 23°C; column size, 30 × 1 cm I.D. PEG–Red ligand concentration in the sample: (a) $2 \cdot 10^{-5}$; (b) $1 \cdot 10^{-4}$; (c) $5 \cdot 10^{-4}$ *M*.

dehydrogenases and kinases competing for the ligand Procion Red HE3b [18,24], a higher specific activity is reached after the chromatography, 3.6 U/mg compared with 2.7 U/mg in the unheated sample. The yield decreased slightly to 78% after heat conditioning.

Third series: addition of ligand to the mobile phase

In a third series of experiments the ligand concentration in the mobile phase was varied while the sample was introduced without added ligand. The elution of the FDH was determined by an enzymatic test of the fractions collected. Fig. 6 shows the results. Because of the nature of partition chromatography, the elution volume is very sensitive to small changes in the *K* value in the range 0.2–3 (Fig. 2). Owing to the ligand binding

TABLE III

PURIFICATION OF FORMATE DEHYDROGENASE FROM THE CRUDE EXTRACT OF *CANDIDA BOIDINII* IN LIQUID–LIQUID PARTITION CHROMATOGRAPHY

System composition: 4.5% PEG 20 000, 6% dextran 500, 5.5 m*M* potassium bromide, 6.3 m*M* phosphate buffer (pH 7.5), 23°C, column size 30 × 1 cm I.D.; sample, 500 µl of crude extract of *C. boidinii* adjusted to a ligand concentration of $5 \cdot 10^{-4}$ *M* PEG–Red, the concentration of ligand in the mobile phase was $2 \cdot 10^{-5}$ *M*.

Specific activity of FDH in the crude extract (U/mg)	Specific activity of FDH in the enzyme–ligand peak (U/mg)	Purification factor	Yield (%)
0.58	2.62	4.5	100
0.64	2.94	4.6	84
0.54	2.48	4.6	92

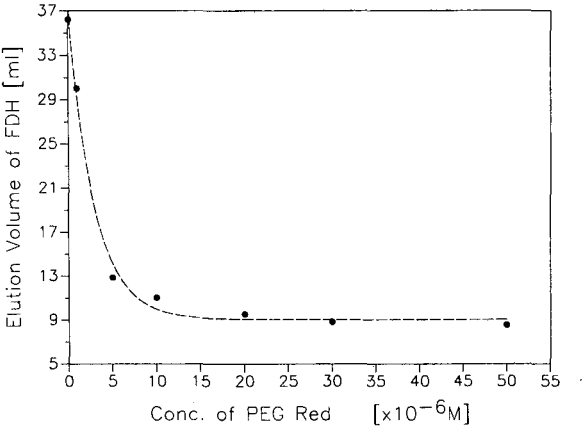

Fig. 6. Influence of the concentration of PEG 20 000–Procion Red HE3b in the mobile phase on the elution volume of FDH. Sample, 500 µl crude extract of *Candida boidinii*. System composition, 4.5% PEG 20 000, 6% dextran 500, 5.5 m*M* potassium bromide, 6.3 m*M* phosphate buffer (pH 7.5); temperature, 23°C; column size, 30 × 1 cm I.D. The elution volume of the FDH was determined by an enzymatic assay of the collected fractions.

and the resulting changes in the partition coefficient, the elution volume of the FDH decreases very rapidly until a ligand concentration of $5 \cdot 10^{-6}$ *M* and then more slowly, approaching the void volume of the column at $50 \cdot 10^{-6}$ *M* PEG–Red. The FDH activity obtained after the chromatographic separation is summarized in Table IV.

The low recovery is related to the decreasing stability of diluted FDH with time. The lowest yield is obtained in the most diluted fraction eluted from the column after 75 min. With decreasing dilution and a shorter time between injection and assay, the recovered amount of FDH increased. The fraction with 83% recovery was only 17 min in the column and three times more concentrated. The influence of dilution and time on the stability of FDH is also demonstrated with independent experiments in Fig. 7.

TABLE IV

ELUTION VOLUME AND ACTIVITY OF FDH WITH INCREASING PEG–RED CONCENTRATION IN THE MOBILE PHASE

System composition: 4.5% PEG 20 000, 6% dextran 500, 5.5 m*M* potassium bromide, 6.3 m*M* phosphate buffer (pH 7.5), 23°C, column size 30 × 1 cm I.D.; sample: 500 µl of crude extract of *C. boidinii*, 3 U/ml.

Concentration of PEG–Red (10^6 *M*)	Elution volume of the FDH (ml)	Volume of the FDH peak (ml)	Yield (%)
0	36	18	23
1	30	15	n.d.
5	13	16	43
10	11	9	n.d.
20	9.5	7	50
30	8.8	7	68
50	8.5	5	77

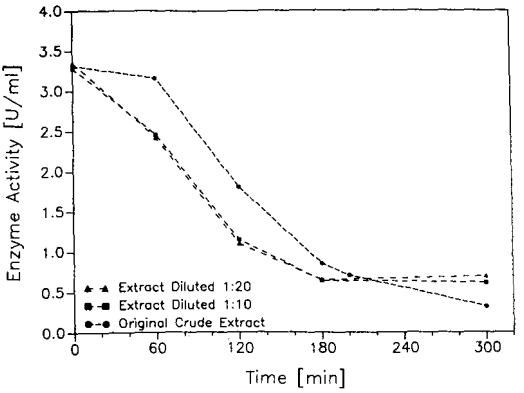

Fig. 7. Stability of FDH in the crude extract of *Candida boidinii* as a function of time at 23°C, pH 7.5 and three concentrations.

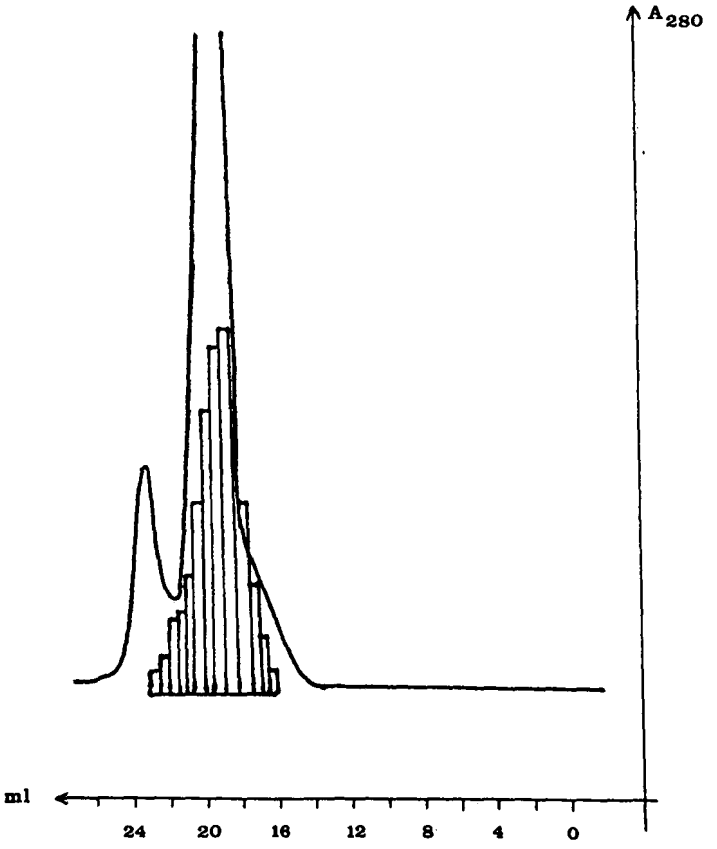

Fig. 8. Elution pattern of the crude extract of *Candida boidinii*. The elution volume of FDH indicated by the histogram of enzymatic activity in the collected fractions is 19.0 ml, which corresponds to a K value of 0.58. System composition, 2.7% PEG 20 000, 4.5% dextran 500, 75 mM potassium bromide, 12 mM phosphate buffer (pH 7.0); temperature, 30°C; column size, 30 × 1 cm I.D.; sample size, 100 μl; flow-rate, 0.6 ml/min.

In order to shorten the chromatographic separation, the viscosity of the phases was reduced by changing the concentration of the phase forming polymers and the temperature of the column was increased to 30°C. According to Fig. 5, 2.7% PEG 20 000 and 4.5% dextran 500 were selected in order to maintain a sufficiently high K value for the ligand. Further, the ionic strength was increased by adding 75 mM potassium bromide to the phase system to minimize the influence of the negatively charged groups of the support material [21]. Potassium bromide was chosen because it has a partition coefficient close to 1.0 and does not influence the elution of FDH and the ligand PEG–Red (see Fig. 10).

The elution pattern of the crude extract of *C. boidinii* under these conditions is shown in Fig. 8. The elution volume of FDH was 19.0 ml, which corresponds in this column (V_s = 5.25 ml, V_m = 10.0 ml) to a K value of 0.58. The ligand PEG–Red eluted at 10.13 ml, corresponding to a K value of 11.8. With $5 \cdot 10^{-5}$ M PEG–Red in the mobile phase, the elution volume of the FDH was reduced to 10.76 ml, corresponding to a K value of 6.9.

In order to find the maximum sample load, 100, 500 and 1000 µl of the heat-denatured crude extract were injected. The results are shown in Fig. 9. The elution volume of the enzyme–ligand complex increases with increasing sample size and eventually overlaps with the second peak. Therefore, the sample size was reduced to 500 µl in order to obtain a good separation for the purification of FDH from the crude extract. Table V gives the results.

To separate the PEG–Red from the FDH after the chromatographic run, solid potassium phosphate was added to the fractions containing FDH [14] to form a second PEG–salt phase system. A mixture of K_2HPO_4 and KH_2PO_4 was formulated to adjust the pH of the system to 7. To obtain a high yield of FDH, the influence of the

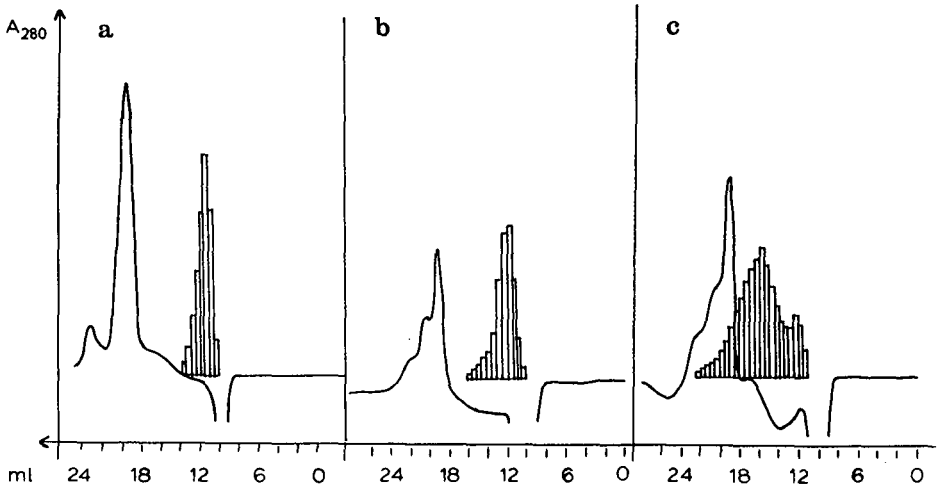

Fig. 9. Elution pattern of the crude extract of *Candida boidinii* under the conditions as in Fig. 8 but with $5 \cdot 10^{-5}$ M PEG–Red in the mobile phase. The elution volume of FDH increases with increasing sample size: (a) sample size = 100 µl, V_e (FDH) = 10.75 ml, K_{FDH} = 6.9; (b) sample size = 500 µl, V_e (FDH) = 11.97 ml, K_{FDH} = 2.7; (c) sample size = 1000 µl, V_e (FDH) = 15.8 ml, K_{FDH} = 0.9.

TABLE V

PURIFICATION OF FDH WITH PEG-RED IN THE MOBILE PHASE

System composition: 2.7% PEG 20 000, 4.5% dextran 500, 75 m*M* potassium bromide, 12 m*M* phosphate buffer (pH 7.5), 30°C, column size 30 × 1 cm I.D.; sample, 500 µl of crude extract of *C. boidinii*, heated for 10 min at 55°C, and with a concentration of $5 \cdot 10^{-5}$ *M* PEG–Red in the mobile phase.

Specific activity of FDH after heat conditioning (U/mg)	Specific activity of FDH after chromatography (U/mg)	Purification factor	Yield (%)
0.72	4.2	5.8	83
0.77	4.7	6.1	70

concentration of the phosphate on the volume ratio of the phases and the *K* value of the FDH were determined. The results are given in Table VI.

To avoid overlapping peaks with increasing sample size and to improve the separation, $5 \cdot 10^{-5}$ *M* PEG–Red was added to the sample. As in former experiments, the elution volume of the complex was reduced, but the maximum of the FDH activity emerged slightly later than the PEG–Red peak. This might be a consequence of the higher ionic strength of the phase system compared with the results reported in Figs. 2–6. To test the influence of the ionic strength on the dissociation constant of the enzyme–ligand complex, first the *K* values of FDH and PEG–Red were determined at various salt concentrations as shown in Fig. 10. An increasing concentration of potassium bromide did not change the *K* value of the PEG–Red and the *K*-value of FDH was slightly increased (elution volume decreased).

The elution volume of the enzyme–ligand complex was then investigated as a function of the salt concentration. The results are presented in Fig. 11. Using the scheme shown in Fig. 1, the following conclusion can be drawn: as the value of K_L was not affected by an increase in potassium bromide concentration (Fig. 10) and K_F varied

TABLE VI

VOLUME RATIO OF TOP AND BOTTOM PHASES AND PARTITION COEFFICIENT OF FDH AS A FUNCTION OF PHOSPHATE CONCENTRATION

Solid potassium phosphate was added to the eluate containing the FDH–ligand complex and a phase system (PEG–salt) formed. The volume ratio was determined after centrifugation (10 min, 2000 *g*) and the *K* value of FDH was determined by an enzymatic assay. Temperature, 25°C.

Concentration of potassium phosphate (%, w/w)	Volume of upper phase (ml)	Volume of lower phase (ml)	Volume ratio (top/bottom)	*K* value of FDH	Yield in the lower phase (%)
8[a]	–	–	–	–	–
9	1.1	3.5	1:3.18	0.0051	98
10	0.9	3.8	1:4.22	0.0028	99
12	0.7	4.0	1:5.71	[b]	n.d.
15	0.5	3.9	1:7.80	[b]	n.d.

[a] System remained homogeneous at this phosphate concentration.
[b] Precipitates formed at interphase.

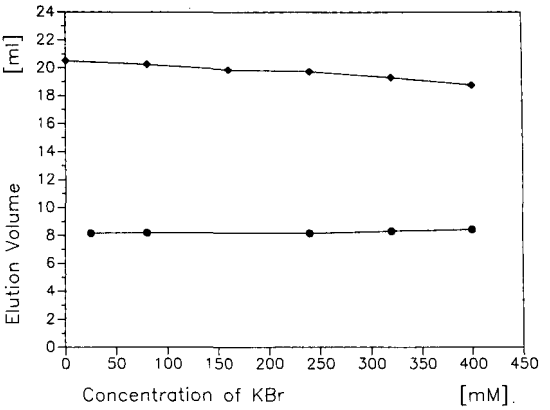

Fig. 10. Elution volume of PEG 20 000–Procion Red HE3b (●) and FDH (◆) as a function of potassium bromide concentration. System composition, 2.7% PEG 20 000, 4.5% dextran 500, 12 m*M* phosphate buffer (pH 7.0); temperature 30°C; column size, 30 × 1 cm I.D.

only slightly, the only way to explain the decrease in the partition coefficient of the enzyme–ligand complex, K_{EL}, at a given ligand concentration (corresponding to an increase in the elution volume) is a change in the dissociation constant of the complex.

It is obvious from the results presented that liquid–liquid partition chromatography incorporating affinity ligands is able to purify selectively the target protein even from fairly crude mixtures. Compared with affinity partitioning of FDH in batch systems [14], the main advantage of the partition column is the two orders of magnitude lower concentration of ligand required to achieve the desired result. This is a consequence of the nature of partition chromatography, because the elution volume is very sensitive to small changes in K values below 3 (Fig. 2). This sensitivity can be

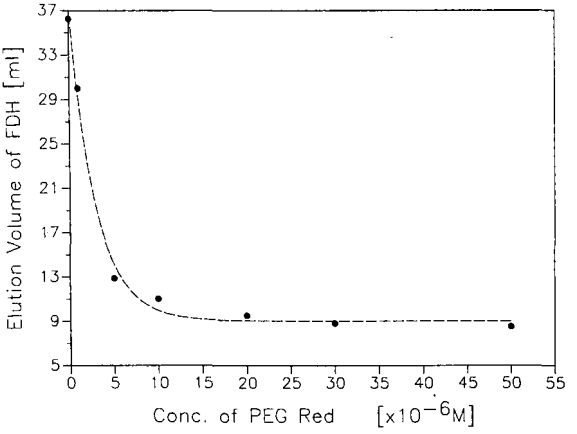

Fig. 11. Elution volume of FDH as a function of PEG–Red and potassium bromide concentration in the mobile phase. System composition, 2.7% PEG 20 000, 4.5% dextran 500, 12 m*M* phosphate buffer (pH 7.0); temperature, 30°C; column size, 30 × 1 cm I.D.

used in two directions. To separate the main peak of the contaminants of the crude extract from the enzyme–ligand peak, it is possible not only to shift the enzyme–ligand peak to the void volume of the column, but also to increase the elution volume of the contaminants by decreasing their partition coefficient through appropriate changes in the phase composition. A second advantage is that the amount of dextran required is much lower, as the column can be operated with no apparent loss of dextran over long periods of time. Uncontaminated PEG phase can be recycled directly. It also appears possible to recycle the affinity ligand after the separation from the enzyme–ligand complex [14]. As the ligand concentration is very low, this may not be worthwhile. The scale-up of liquid–liquid partition chromatography may be accomplished by increasing the diameter of the column.

ACKNOWLEDGEMENTS

We thank Professor W. Müller for stimulating discussions and E. Merck for the Superformance system and the supply of LiParGel. A.W. was supported by a fellowship within the BMFT Program "Applied Biology and Biotechnology" administered by DECHEMA. D.F. was supported by the U.S. National Institutes of Health (Grant No. 1RO1-GM40023-02) and the North Carolina Board of Science and Technology.

REFERENCES

1 P. A. Albertsson, *Partition of Cell Particles and Macromolecules*, Wiley-Interscience, New York, 3rd ed., 1986.
2 S. D. Flanagan and S. H. Barondes, *J. Biol. Chem.*, 250 (1975) 1484.
3 G. Kopperschläger and G. Johansson, *Anal. Biochem.*, 124 (1982) 117.
4 K. H. Kroner, A. Cordes, A. Schelper, M. Morr, A. F. Bückmann and M.-R. Kula, in T. C. J. Gribnau, J. Visser and R. J. F. Nivard (Editors), *Affinity Chromatography and Related Techniques*, Elsevier, Amsterdam, 1982, p. 491.
5 G. Kopperschläger, G. Lorenz and E. Usbeck, *J. Chromatogr.*, 259 (1983) 97.
6 G. Johansson, G. Kopperschläger and P. A. Albertsson, *Eur. J. Biochem.*, 131 (1983) 589.
7 G. Johansson and M. Andersson, *J. Chromatogr.*, 291 (1984) 175.
8 G. Johansson, M. Andersson and H. E. Akerlund, *J. Chromatogr.*, 298 (1984) 483.
9 G. Johansson and M. Andersson, *J. Chromatogr.*, 303 (1984) 39.
10 W. Müller and A. Eigel, *Anal. Biochem.*, 118 (1981) 269.
11 W. Müller, H. Bühnemann, H. J. Schütz and A. Eigel, in T. C. J. Gribnau, J. Visser and R. J. F. Nivard (Editors), *Affinity Chromatography and Related Techniques*, Elsevier, Amsterdam, 1982, p. 437.
12 A. Atkinson, J. E. McArdell, M. D. Scawen, R. F. Sherwood and D. A. P. Small, in T. C. J. Gribnau, J. Visser and R. J. F. Nivard (Editors), *Affinity Chromatography and Related Techniques*, Elsevier, Amsterdam, 1982, p. 399.
13 F. Qadri, *Trends Biotechnol.*, 3 (1985) 7.
14 A. Cordes and M.-R. Kula, *J. Chromatogr.*, 376 (1986) 375.
15 A. Cordes, J. Flossdorf and M.-R. Kula, *Biotechnol. Bioeng.*, 30 (1987) 514.
16 W. Müller, *Eur. J. Biochem.*, 155 (1986) 213.
17 W. Müller, in H. Walter, D. E. Brooks and D. Fisher (Editors), *Partition in Aqueous Two Phase Systems*, Academic Press, New York, 1985, Ch. 7, p. 248.
18 M. R. Kula, A. Walsdorf and C. Cordes, *Ber. Bunsenges. Phys. Chem.*, 93 (1989) 968.
19 H. Schütte, J. Flossdorf, H. Sahm and M.-R. Kula, *Eur. J. Biochem.*, 62 (1976) 151.
20 M. Bradford, *Anal. Biochem.*, 72 (1976) 248.
21 A. Walsdorf and M.-R. Kula, *J. Chromatogr.*, submitted for publication.
22 A. J. P. Martin and R. L. M. Synge, *Biochem. J.*, 35 (1941) 1358.
23 H. Sahm and F. Wagner, *Arch. Mikrobiol.*, 84 (1972) 29.
24 A. Cordes, *Thesis*, University of Braunschweig, Braunschweig, 1985.

Journal of Chromatography, 523 (1990) 119–130
Elsevier Science Publishers B.V., Amsterdam

CHROM. 22 741

Combination of polymer-bound charged groups and affinity ligands for extraction of enzymes by partitioning in aqueous two-phase systems[a]

LÜLING CHENG, MONICA JOELSSON and GÖTE JOHANSSON*
Department of Biochemistry, Chemical Centre, University of Lund, P.O. Box 124, S-221 00 Lund (Sweden)
(First received February 9th, 1990; revised manuscript received July 31st, 1990)

ABSTRACT

The partition of glucose-6-phosphate dehydrogenase in a water–dextran–polyethylene glycol two-phase system was influenced by the mutual addition of polymers carrying charged groups and affinity ligands. These polymers included DEAE-dextran, dextran sulphate, ligand–dextran, ligand–polyethylene glycol, ligand–Ficoll and ligand–DEAE-dextran, where the ligands used were the dyes Cibacron Blue F3G-A and Procion Yellow HE-3G. Some of these two-phase systems were also used for the counter-current distribution of yeast proteins, demonstrating the separation of several enzymes.

INTRODUCTION

It is well known that the partition of proteins within aqueous two-phase systems can be strongly influenced by either charged groups or affinity ligands restricted to one of the phases [1–8]. This location is achieved by binding these chemical groups to one of the phase-forming polymers. The most popular two-phase system is that containing dextran and polyethylene glycol (PEG). In this work a combination of both affinity and charged groups was tested on the partitioning of glucose-6-phosphate dehydrogenase (E.C. 1.1.1.49, from baker's yeast) and of a protein extract from baker's yeast.

EXPERIMENTAL

Chemicals

Dextran T-500 and T-2000, DEAE-dextran 500 (2.5% nitrogen), dextran sulphate 500 (27% sulphur) and Ficoll 400 were purchased from Pharmacia (Uppsala, Sweden). PEGs with M_r 3400 and 8000 were obtained from BP Chemicals (Hythe, U.K.). Procion Yellow HE-3G–dextran 2000 (46 μmol dye g^{-1}), Procion Yellow HE-3G–PEG 8000 (106 μmol dye g^{-1}), Cibacron Blue F-3GA–PEG 8000 (127 μmol

[a] This paper is dedicated to Professor Per-Åke Albertsson on the occasion of his 60th birthday.

0021-9673/90/$03.50

dye g^{-1}), and Procion Yellow HE-3G–Ficoll 400 (6 μmol dye g^{-1}) were synthesized as described elsewere [9–11]. Fresh baker's yeast (*Saccharomyces cerevisiae*) was purchased from Jästbolaget (Sollentuna, Sweden). Glucose-6-phosphate dehydrogenase and 3-phosphoglycerate kinase, from yeast, together with biochemicals for enzyme assays were purchased from Sigma (St. Louis, MO, U.S.A.). All other chemicals were of analytical-reagent grade. The distilled water used was first passed through a mixed ion exchanger.

Synthesis of dye–DEAE-dextran 500

A 1-g amount DEAE-dextran was dissolved in 20 ml of water together with 0.2 g of Procion Yellow HE-3G. To start the reaction, 2 ml of 1 *M* sodium hydroxide solution containing 0.5 *M* sodium sulphate were added. The mixture was kept at 70°C for 45 min and then 0.25 ml acetic acid was added to stop the reaction. The polymer was precipitated with 30 ml of ethanol and the precipitate was dissolved in 20 ml of water. The precipitation procedure was repeated twice. The yellow DEAE-dextran was dissolved in 10 ml of water and dialysed overnight against water, filtered and the dye content (by measurement of the absorbance at 400 nm) as well as the dextran content (measured polarimetrically [12]) were determined. The polymer contained 50 μmol dye g^{-1}.

Extract of baker's yeast

Baker's yeast (100 g) was suspended in 100 ml of 100 m*M* triethanolamine (TEA)–HCl buffer (pH 7.6) and sonicated in an ice-bath in two portions with a Benson B50 sonifier for 20 min using 40% pulses and an output setting of 7 (final temperature <12°C). The mixture obtained was centrifuged for 8 min at 1500 *g* at 0°C. Solid PEG 8000 was dissolved in the supernatant at 0°C to a final concentration of 7% (w/w) and the mixture was incubated for 10 min on ice. The precipitate was removed by centrifugation (8 min at 1500 *g* at 0°C) and the PEG 8000 content of the supernatant was adjusted to 17% (w/w) by addition of solid PEG. After incubation and centrifugation as above, the protein "pellet" was collected and dissolved in 5 ml of 50 m*M* TEA–HCl buffer (pH 7.6).

Two-phase systems

The systems were prepared by weighing out the required amounts of solutions of 40% (w/w) PEG 3400 and 25% (w/w) dextran 500, together with salt, buffer and enzyme solution, plus water to the final weight (normally 4 g). The systems were equilibrated at 25°C, centrifuged for 5 min at 700 *g* and samples of known volume were withdrawn and analysed. The partition coefficient of the enzyme, *K*, defined as the ratio of the concentrations of enzyme (obtained by activity measurements) in the upper and lower phases, was calculated. The partition coefficients of the free dye and of dye–dextran were determined by absorbance measurements at 400 nm using equally diluted phases without dye as blanks.

Centrifugal counter-current distribution

The apparatus for counter-current distribution has been described in detail elsewhere [13]. The operating unit consists of an inner plate with 60 cavities for the upper phases surrounded by an outer ring containing corresponding cavities for the

lower phases. The volume of each of the outer cavities was 0.96 ml. All operations were carried out at 3°C. The apparatus was loaded with 1.7 ml of phase system (of which 0.85 ml was the lower phase) in each chamber formed by the disk and the ring. The systems in chambers 0–2 were loaded with yeast extract in the phase system. Fifty-six partitioning steps were carried out automatically with shaking for 1.5 min followed by centrifugation for 15 min after each transfer. When the distribution was complete, 1.7 ml of 10 m*M* TEA–HCl buffer (pH 7.6) containing 1.5 m*M* 2-mercaptoethanol were added to each chamber, giving one-phase systems which were analysed for protein and enzyme activities.

Enzyme assays

The enzyme activities were determined spectrophotometrically at 340 or 240 nm (enolase) and 22°C using a Hitachi 100-60 double-beam spectrophotometer connected to an LKB 2210 potentiometric recorder. Descriptions of the assays can be found elsewhere: glucose-6-phosphate dehydrogenase [14], enolase [15], hexokinase [16] and glyceraldehydephosphate dehydrogenase [17]. Samples (phases, mixed systems or diluted systems from counter-current distribution experiments) of 25–100 μl were mixed with assay solution to a final volume of 2.9 ml. The polymers present in the sample had no detectable effect on the activity measurements.

Protein assay

Protein was assayed by using Coomassie Brilliant Blue G according to Bradford [18] at 595 nm with bovine serum albumin as standard.

RESULTS AND DISCUSSION

It is well known that the addition of salts to aqueous (two polymers) two-phase systems affects the partitioning of polyelectrolytes [8,10,12,19]. This salt effect was studied earlier by partitioning of proteins of various charges. This influence is assumed to be connected with the relative affinities of the two ions of the salt for the phases and it has been related to the presence of an interfacial potential [12,19]. In the two-phase system used below, based on dextran and PEG, anions such as chloride, bromide and iodide have an increasing affinity (in that order) for the PEG-rich upper phase. Likewise, the cations lithium, sodium and potassium show increasing affinity for the lower dextran-rich phase. The relative affinity for the anion and the cation of the salt for the two phases can be expressed by hypothetical partition coefficients, K_- and K_+, describing the partitions that the ions should have if they could partition independently of each other [19]. When the salt is a 1:1 electrolyte, the partition coefficient, K, of a polyelectrolyte with net charge Z is given by

$$K = K_0 (K_-/K_+)^{Z/2} \quad (1)$$

were K_0 is the partition coefficient of the polyelectrolyte in a system with no interfacial potential [19].

TABLE I

PARTITION COEFFICIENTS, K, OF DEAE-DEXTRAN, LABELLED WITH PROCION YELLOW HE-3G, IN THE PRESENCE OF KBr OR K_2SO_4

System composition: 8% dextran 500, 8% PEG 3400, 0.33% Procion Yellow HE-3G–DEAE-dextran 500, and various amounts of salt. The dye–DEAE-dextran was treated beforehand with the same salt used for the partitioning and dialysed against water. Temperature, 25°C; pH, 7.3.

Concentration of salt (mmol kg^{-1})	Log K	
	With KBr	With K_2SO_4
0	−0.27	−0.94
0.5	0.16	−1.45
5	1.11	−2.06
10	1.69	−2.10
25	1.67	−2.11
50	1.74	−1.49

Partition of dye-labelled DEAE-dextran

The effect of two salts, potassium bromide and potassium sulphate, on the partition of the dye–DEAE-dextran derivative is shown in Table I. The DEAE-dextran was "labelled' with covalently bound Procion Yellow HE-3G (PrY), which made it possible to determine the partitioning of the polyelectrolyte. The positive charge of the DEAE-dextran, 1.8 mmol g^{-1}, was reduced by around 25% owing to the presence of negatively charged groups on the dye, 0.4–0.5 mmol g^{-1}. Partitioning in salt-free systems was effected with DEAE-dextran that had been in contact with either potassium bromide or sulphate followed by dialysis. The polyelectrolyte can therefore be assumed to carry either bromide or sulphate, respectively, as counter ions, which affects the partition (Table I). The partition coefficient of the positively charged dextran was changed by as much as 7000-fold by exchanging the salt from 25 mM potassium sulphate (K = 0.0078) to 50 mM potassium bromide K = 55). For full effect the salt concentration had to be at least double the concentration of (net) positive charges on the dextran, which was 4.4–4.7 mmole kg^{-1} as calculated from the degree of substitution and the concentration of the dextran derivative in the system (3.3 g kg^{-1}). Therefore, salts can be used to adjust the partitioning of strongly charged polyelectrolytes.

Effect of DEAE-dextran on partitioning of an enzyme

The presence of DEAE-dextran in a system affected the partitioning of proteins which, if negatively charged, could be assumed to interact with the positive polyelectrolyte. This was studied by using a pure enzyme, glucose-6-phosphate dehydrogenase (G6PDH, from yeast), which has an isoelectric point [20] of 5.5–6.0 and therefore had a negative net charge at the pH value used, 7.6 (Table II). In systems without DEAE-dextran the G6PDH had a low partition coefficient of $\leqslant$ 0.1 (except for phosphate), which varied with the type of salt used. By addition of DEAE-dextran the K value of the enzyme could be changed as much as 1700-fold (with potassium iodide) (Table II). The two salts used in Table I, potassium sulphate and bromide,

TABLE II

PARTITION COEFFICIENTS, K_{G6PDH}, OF GLUCOSE-6-PHOSPHATE DEHYDROGENASE IN SYSTEMS CONTAINING DIFFERENT SALTS AND WITH OR WITHOUT DYE–POLYMERS AND/OR CHARGED DEXTRAN

Enzyme (G6PDH, 2 U ml^{-1}) was partitioned in systems containing 8% (w/w) dextran 500, 8% (w/w) PEG 3400, 2.5 m*M* TEA–HCl buffer (pH 7.6), salts, 20 m*M* (K_2SO_4 or Li_2SO_4) or 50 m*M* (other salts), and with or without 0.33% DEAE-dextran 500 (DEAE-Dx), 0.33% Procion Yellow HE-3G–DEAE-dextran 500 (PrY–DEAE-Dx), 0.004% dextran sulphate 500 or 0.004% dextran sulphate with 0.1% Procion Yellow HE-3G–PEG 8000 (PrY–PEG). Temperature, 25°C; pH, 7.6.

Salt	Log K_{G6PDH}				
	No additional	DEAE-Dx	PrY–DEAE-Dx	Dx sulphate	PrY–PEG + Dx sulphate
KH_2PO_4/K_2HPO_4	−0.68	−2.25	−2.96	−1.18	−0.08
Li_2SO_4	−0.95	−2.70	−2.15	1.28	2.22
K_2SO_4	−1.25	−2.66	−1.98	−1.96	−0.13
$KHCO_3$	−1.67	−0.24	0.58	–	–
$NaClO_4$	−2.08	0.13	1.37	−1.77	–
KI	−2.10	1.13	1.87	–	–
LiCl	−2.24	−0.25	1.07	−0.21	0.46
$NaNO_3$	−2.25	0.70	1.89	−2.52	−1.53
CH_3COOK	−2.32	−0.66	1.00	−2.05	−0.97
KBr	−2.41	0.28	1.81	−1.69	−0.87
KCl	−2.39	0.08	1.86	−1.61	−0.94

changed the partitioning of the dye–DEAE-dextran by −1.1 (K_2SO_4) or +1.9 (KBr) log *K* units on changing from a system without salt to one containing 25 mmole kg^{-1}. The change in the partitioning of the G6PDH by introducing DEAE-dextran in the systems was −1.4 (for K_2SO_4) and +2.7 (for KBr) log *K* units, respectively. This shows that the partitioning of the enzyme changed in the same order as the DEAE-dextran was assumed to do, estimated from the salt effects on the dye-labelled DEAE-dextran. When Procion Yellow HE-3G (PrY) was bound to the DEAE-dextran additional effects were observed on the partitioning of G6PDH. This dye is known to be an affinity ligand for G6PDH and therefore should support the interaction between the enzyme and the polyelectrolyte. This was also found to be true in most instances with the exception of sulphates. The additional change was in the range 0.6–1.8 log *K* units. The strongest total change in the partition coefficient was 17 800-fold (with KCl, $\Delta \log K = 4.25$).

Effect of dextran sulphate on partitioning of G6PDH

The salts which gave high partition coefficients for positively charged polyelectrolytes, such as DEAE-dextran, should give low *K* values to a negatively charged polyelectrolyte such as dextran sulphate. As both the polyelectrolyte and the G6PDH in this case are negatively charged, the enzyme should be excluded from the phase containing dextran sulphate. Consequently, dextran sulphate should change the *K* value of G6PDH in the same direction as DEAE-dextran does. This effect was also obtained in most instances (Table II), and the log *K* value of G6PDH changed in the

predicted direction. However, the change was, with one exception, less than that with DEAE-dextran. Lithium sulphate and sodium nitrate gave changes in the partition opposite to the predicted directions, which may indicate strong ion-pair formation. Addition of PrY–PEG, which was concentrated in the upper phase, to the system containing dextran sulphate increased the log K value by 0.7–1.8 unit (Table II). The use of another PEG-bound ligand, Cibacron Blue F3G-A together with dextran sulphate showed a considerably smaller effect on the partition coefficient of G6PDH, with an increase of only 0–0.8 log K units.

Combination of charged dextran and affinity ligand

The method of binding the ligand to one polymer and the charged groups to another polymer may be a fruitful means of increasing the selectivity in the partitioning of proteins. By using, *e.g.*, potassium phosphate buffer as the steering salt the DEAE-dextran can be located in the lower phase while dye–PEG is confined in the upper phase. In such a system the ligand is extracting the enzyme towards one phase while the positively charged dextran attracts proteins with a negative net charge to the other phase. The partitioning of G6PDH was shown to depend on the concentrations of salt, polymer-bound dye and DEAE-dextran (Table III). A high salt concentration eliminated both the binding between the ligand and enzyme and the electrostatic action of the DEAE-groups.

Another possibility is to use DEAE-dextran and highly substituted PrY–dextran. As the PrY is strongly negatively charged, the dye–dextran becomes a negative polyelectrolyte. By using potassium chloride in the system, DEAE-dextran was concentrated in the upper phase and the dye–dextran in the lower phase. The partitioning of G6PDH in such systems is shown in Fig. 1. Considerable precipitation and formation of a small third (intense yellow) phase was observed. This was probably due to complex formation between the two polyelectrolytes. More than 50% of PrY–dextran and enzyme were removed from the bulk phases (Fig. 1).

The relative effects of dextran sulphate and PrY–PEG (in a system with potassi-

TABLE III

PARTITIONING OF G6PDH WITH PrY–PEG 8000 AT VARIOUS CONCENTRATIONS OF POTASSIUM PHOSPHATE BUFFER AND DEAE-DEXTRAN 500

G6PDH (3.0 U ml^{-1}) was partitioned in the system containing 8% dextran 500, 7.6% PEG 3400, 0.4% PrY–PEG 8000, 2.5 mM TEA–HCl buffer (pH 7.6), potassium phosphate buffer (pH 7.6) and DEAE-dextran 500. Temperature, 25°C.

Concentration of phosphate buffer (mM)	Concentration of DEAE-dextran (%)	Log K_{G6PDH}
0	0.066	0.28
2	0.013	0.48
5	0.000	1.75
5	0.041	0.39
5	0.330	0.04
10	0.066	2.61
50	0.000	−0.99
50	0.206	−0.84
50	0.330	−0.91

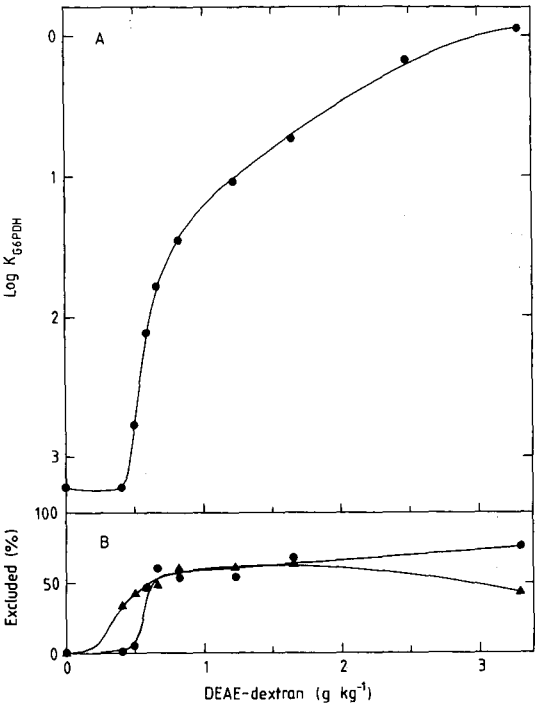

Fig. 1. Effect of DEAE-dextran concentration (given in g DEAE-dextran per kg system) on (A) the partitioning of G6PDH and (B) the amount of (●) G6PDH and (▲) PrY–dextran excluded from the phases (as a percentage of the total amount in the system) and recovered at the interface. System composition: G6PDH (2.3 U ml^{-1}), 8% (w/w) dextran 500, 8% (w/w) PEG 3400, 50 m*M* KCl, 2.5 m*M* TEA–HCl buffer (pH 7.6), 0.12% Procion Yellow HE-3G–dextran 2000 and various concentrations of DEAE-dextran 500. Temperature, 25°C.

um phosphate) were tested on a crude protein extract from baker's yeast (Table IV). In this system both ligand–PEG and dextran sulphate are in the upper phase. Very low concentrations of the dextran sulphate were sufficient to counteract the effect of the ligand. By using other ligand carriers or by increasing their concentrations, the K values of the enzyme could be increased again (Table IV). The strongest effect was found for ligand–Ficoll.

When the other combination of ligand and charged dextran was used (dye–PEG, DEAE-dextran, phosphate buffer) for partitioning of yeast extract, the enzyme G6PDH (Fig. 2) was effected by the concentration of DEAE-dextran. The partition coefficient of the protein, in general, decreased gradually from log $K = -0.1$ (no DEAE-dextran) to log $K = -1.1$ (2.5 g DEAE-dextran kg^{-1}).

Counter-current distribution

The combination of dextran sulphate and the ligand PEG was used to study the separation of enzymes, present in an extract of yeast, by counter-current distribution (CCD) (Fig. 3). The system contained sodium phosphate buffer, which caused both of the "steering" polymers to be in the upper phase. With solely dextran sulphate the

TABLE IV

PARTITIONING OF PROTEIN EXTRACT FROM BAKER'S YEAST IN SYSTEMS AT VARIOUS CONCENTRATIONS OF DEXTRAN SULPHATE WITH DIFFERENT POLYMERS CARRYING PROCION YELLOW HE-3G (PrY)

Yeast extract (containing 0.29 U ml^{-1} G6PDH) was partitioned in systems containing 8% (w/w) dextran, 7.6% (w/w) PEG 3400, various concentrations of dextran sulphate and 25 m*M* potassium phosphate (pH 7.0), with or without PrY–PEG 8000 (PrY–PEG), PrY–dextran 2000 (PrY–Dx), PrY–DEAE-dextran 500 (PrY–DEAE-Dx), or PrY–Ficoll 400 (PrY–Ficoll). Temperature, 25°C.

Dx sulphate (%)	Additional dye–polymer	Log K_{G6PDH}
0.0000	PrY–PEG, 0.40%	0.32
0.0025	PrY–PEG, 0.40%	0.07
0.0050	PrY–PEG, 0.40%	−0.25
0.0125	PrY–PEG, 0.40%	−0.77
0.0250	PrY–PEG, 0.40%	−1.14
0.0500	PrY–PEG, 0,40%	−1.45
0.1000	PrY–PEG, 0.40%	−1.55
0.0125	PrY–PEG, 0.65%	0.05
0.0125	PrY–Dx, 0.25%	−0.34
0.0125	PrY–DEAE-Dx, 0.33%	−0.98
0.0125	PrY–Ficoll, 1.75%	0.70

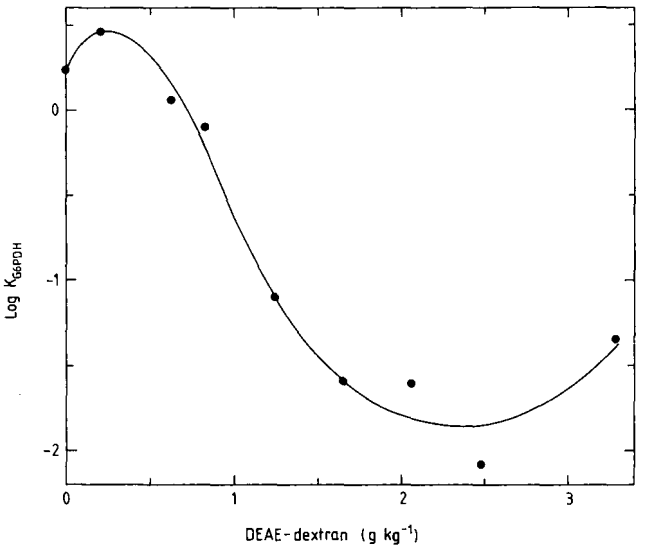

Fig. 2. Partitioning of protein extract from baker's yeast in systems at various concentrations of DEAE-dextran 500 (as a percentage of the total amount in the system). Yeast extract (containing 0.14 U ml^{-1} G6PDH) was partitioned in the system composed of 8% dextran 500, 7.6% PEG 3400, 0.4% Procion Yellow HE-3G–PEG 8000, 2.5 m*M* TEA–HCl buffer (pH 7.6) and 5 m*M* potassium phosphate buffer (pH 7.6). Temperature, 25°C.

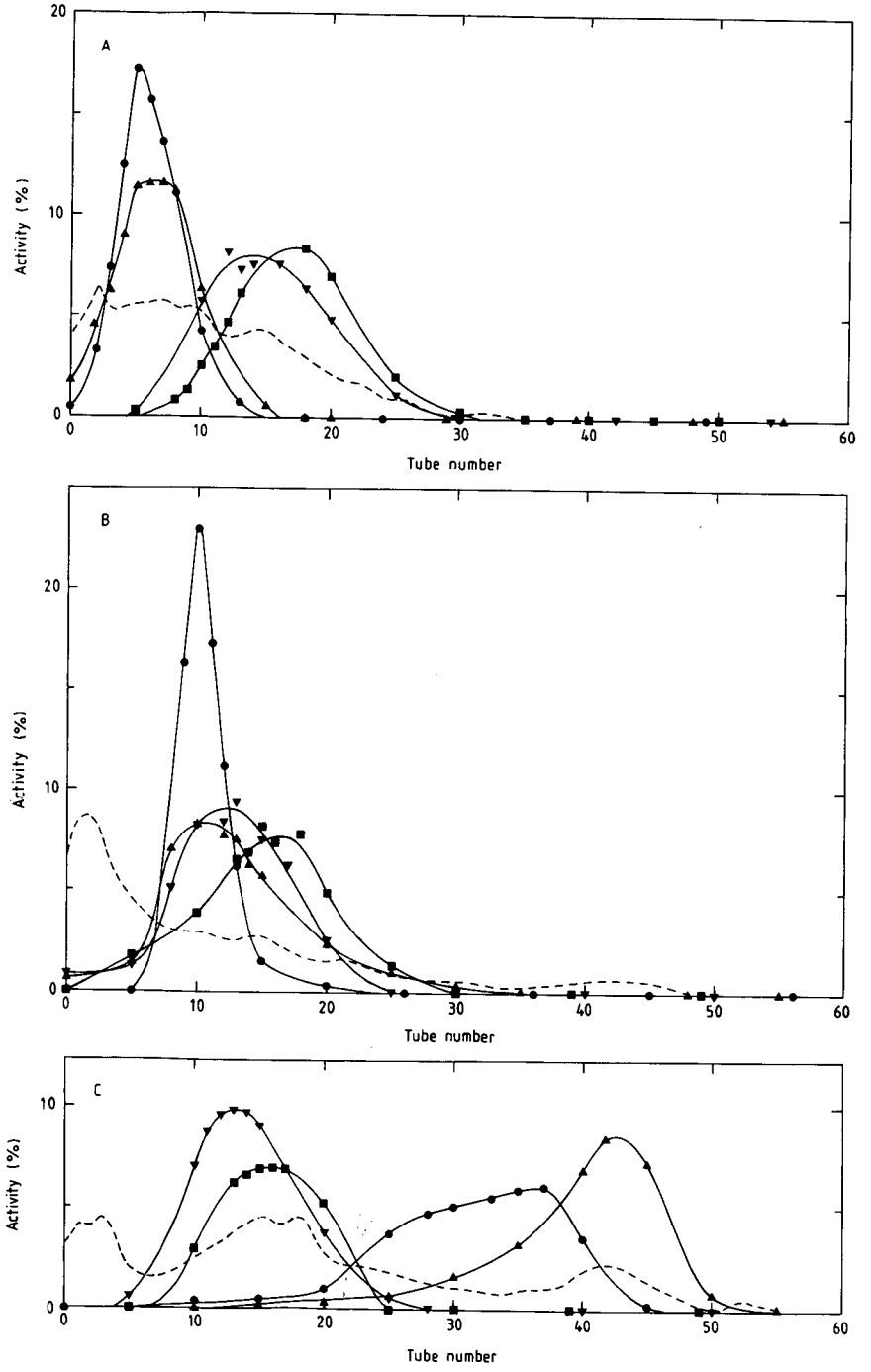

Fig. 3.

(Continued on p. 128)

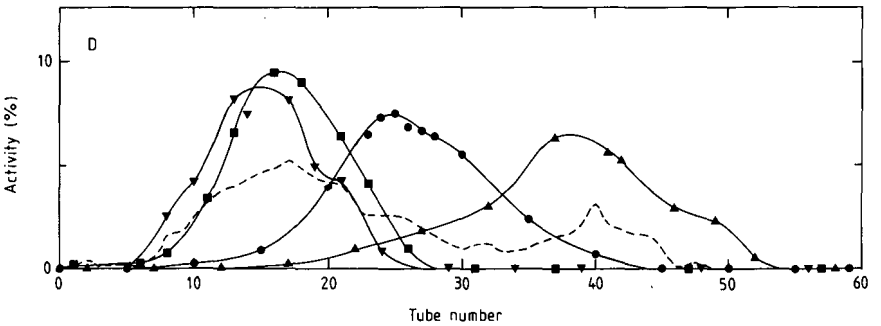

Fig. 3. Counter-current distribution of extract from baker's yeast. (A) The biphasic system contained 10% dextran 500, 5.4% PEG 3400, 0.004% dextran sulphate, 25 m*M* potassium phosphate buffer (pH 7.0), 5 m*M* glucose-6-phosphate and 9 m*M* dithiothreitol. (B) System as in A but it also contained 0.3% Cibacron Blue F3G-A–PEG 8000 and the concentration of PEG 3400 was reduced to 5.1%. (C) System as in A but with 0.1% Procion Yellow HE-3G–PEG 8000 and the concentration of PEG 3400 was 5.3%. (D) As in C but with 0.015% dextran sulphate. The diagrams show the distribution of (●) G6PDH, (▼) enolase, (■) hexokinase, (▲) glyceraldehyde phosphate dehydrogenase and (- - -) protein. Temperature, 4°C.

measured enzymes, glucose-6-phosphate dehydrogenase (G6PDH), glyceraldehyde-phosphate dehydrogenase (GAPDH), hexokinase (HK) and enolase, moved only slowly in the CCD process (Fig. 3A). Addition of Cibacron Blue–PEG to the system moved both G6PDH and GAPDH slightly towards higher tube numbers whereas the two other enzymes remained in their positions (Fig. 3B). This CCD experiment demonstrates a weak interaction between the two dehydrogenases and Cibacron Blue despite the negative results obtained in single-partition experiments above. Procion Yellow–PEG showed much stronger effect (Fig. 3C). No significant difference in the CCD patterns was found if the system contained no or 0.004% of dextran sulphate. Both G6PDH and GAPDH travelled ahead of the two other enzymes and were also partly separated. By increasing the concentration of dextran sulphate both G6PDH and GAPDH moved less to the right (Fig. 3D). The form of the CCD curves shows that these enzymes do not behave as homogeneous substances. Whether this is due to interactions between the enzymes and dextran sulphate or if the enzymes are present in multiple forms is not clear. The counter-current distribution machine gives nearly perfect distribution profiles with pure substances [13], which excludes technical errors.

The parameter G (partition ratio defined as the ratio of homogeneous enzyme in the mobile and stationary parts of the system [21]) of the most dominant region of the activity peaks was calculated from the position of the peak, $\hat{\imath}$, using the relationship [21] $G = \hat{\imath}/(n-\hat{\imath})$, where n is the number of transfers (Table V). From the G values and the volumes of the phases the K values were also calculated. To obtain a good separation of two (homogeneous) enzymes in CCD, the ratio, β, between their respective G values should be >3 or <0.33. This requirement is fulfilled for the peak components of the pair of enzymes GAPDH and enolase without dye–PEG (β = 0.32), and with the two concentrations of PrY–PEG (β = 10 and 6, respectively), as calculated from the G values in Table V. The optimum separation, which corresponds to CCD with no stationary upper phase, can be seen from the ratio between the K values (Table V) of the enzymes in the latter two systems giving β = 16 and 8. For the

TABLE V

PARTITION RATIOS (G VALUES) AND PARTITION COEFFICIENTS (K VALUES) OF THE MAIN ENZYME PEAKS IN THE COUNTER-CURRENT DISTRIBUTIONS PRESENTED IN FIG. 3A–D

The enzymes are G6PDH, enolase, hexokinase (HK) and glyceraldehyde phosphate dehydrogenase (GAPDH). The G values descibe the relative mobility of the peak along the counter-current distribution train [21] and they are related to the K values by the equation $G = 0.75K/(0.1K + 0.85)$ using the volumes of stationary and mobile phases given under Experimental. Cb–PEG = Cibacron Blue F3G-A–PEG 8000.

Figure	Dextran sulphate (%)	Dye–PEG (%)	G6PDH		Enolase		HK		GAPDH	
			G	K	G	K	G	K	G	K
3A	0.004	None	0.077	0.088	0.31	0.37	0.45	0.54	0.10	0.11
3B	0.004	Cb–PEG, 0.3	0.20	0.23	0.28	0.33	0.34	0.40	0.20	0.23
3C	0.004	PrY–PEG, 0.1	1.50	2.1	0.28	0.33	0.38	0.45	2.9	5.4
3D	0.015	PrY–PEG, 0.1	0.77	0.97	0.34	0.40	0.41	0.49	2.1	3.3

pair of (homogeneous) G6PDH and GAPDH, the combination of PrY–PEG and 0.004% dextran sulphate gave a less useful β value (1.9), whereas an increase in the dextran sulphate level to 0.015% gave a higher β value (2.7). The optimum conditions established from the β values obtained from the K values (Table V) show that good separations could be obtained with CCD avoiding the stationary part of the upper phase. In this instance the β values were 3.6 and 4.3, respectively.

CONCLUSIONS

The results show that polyelectrolytes, forced into one of the phases of the two-phase system by the choice of salt, can be used to affect strongly the partitioning of proteins. The polyelectrolytes can also be used simultaneously in an antagonistic or cooperative way with phase-localized (polymer-bound) affinity ligands.

ACKNOWLEDGEMENTS

This work was supported by grants from the Technical Research Council of the National Swedish Board for Technical Development (STUF) and the Nordic Industrial Foundation.

REFERENCES

1 S. D. Flanagan and S. H. Barondes, *J. Biol. Chem.*, 250 (1975) 1484.
2 G. Johansson, *J. Biotechnol.*, 3 (1985) 11.
3 H. K. Kroner, A. Cordes, A. Schelper, M. Morr, A. F. Bückmann and M.-R. Kula, in T. C. J. Gribnau, J. Visser and R. J. F. Nivard (Editors), *Affinity Chromatography and Related Techniques*, Elsevier, Amsterdam, 1982, p. 491.
4 G. Johansson and M. Joelsson, *Enzyme Microb. Technol.*, 7 (1985) 629.
5 G. Johansson, *Biochim. Biophys. Acta*, 222 (1970) 381.
6 G. Johansson, A. Hartman and P.-Å. Albertsson, *Eur. J. Biochem.*, 33 (1973) 379.

7 H. Walter and G. Johansson, *Anal. Biochem.*, 155 (1986) 215.
8 H. Walter, R. Garza and R. P. Coyle, *Biochim. Biophys. Acta*, 156 (1968) 409.
9 G. Johansson and M. Joelsson, *Biotechnol. Bioeng.*, 27 (1985) 621.
10 G. Johansson and M. Joelsson, *J. Chromatogr.*, 393 (1987) 195.
11 G. Johansson and M. Joelsson, *J. Chromatogr.*, 411 (1987) 161.
12 P.-Å. Albertsson, *Partition of Cell Particles and Marcomolecules*, Wiley, New York, 3rd ed., 1986.
13 H.-E. Åkerlund, *J. Biochem. Biophys. Methods*, 9 (1984) 133.
14 E. A. Noltmann, C. J. Gubler and S. A. Kuby, *J. Biol. Chem.*, 236 (1961) 1225.
15 E. W. Westhead, *Methods Enzymol.*, 9 (1966) 670.
16 P. K. Maitra, *Methods Enzymol.*, 42 (1975) 25.
17 H. U. Bergmeyer, *Methoden der enzymatischen Analyse*, Vol. 1, Verlag Chemie, Weinheim/Bergstr., 2nd ed., 1970, p. 425.
18 M. M. Bradford, *Anal. Biochem.*, 72 (1976) 248.
19 G. Johansson, *Mol. Cell. Biochem.*, 4 (1974) 169.
20 R. H. Yue, E. A. Noltman and S. A. Kuby, *Biochemistry*, 6 (1967) 1174.
21 T. E. Treffry, P. T. Sharpe, H. Walter and D. E. Brooks, in H. Walter, D. E. Brooks and D. Fisher (Editors), *Partitioning in Aqueous Two-Phase Systems*, Academic Press, Orlando, 1985, p. 131.

Journal of Chromatography, 523 (1990) 131–138
Elsevier Science Publishers B.V., Amsterdam

CHROM. 22 717

Hydrophobic interaction chromatography of proteins on Separon HEMA

II. Influence of sorbent modification on efficiency of separation

PETR ŠMÍDL, IMRICH KLEINMANN, JAN PLICKA and VRATISLAV SVOBODA*
Institute for Research, Production and Application of Radioisotopes, Radiová 1, 102 27 Prague 10 (Czechoslovakia)
(First received August 28th, 1989; revised manuscript received July 23rd, 1990)

ABSTRACT

Macroporous rigid hydrophilic Separon HEMA sorbents have been used in the hydrophobic interaction chromatography of proteins without any additional chemical modification but the efficiency of unmodified Separons is not very high. Simple chemical modification by reaction with benzoyl chloride and especially with 1,2-epoxy-3-phenoxypropane increases their efficiency and selectivity for the separation of proteins. As the concentrations of benzoyl and 2-hydroxy-3-phenoxypropyl groups on the surface of the sorbents were nearly identical, direct comparison of both materials was possible, showing that the best results were obtained with a spacer-containing derivatizing agent. The separation potential of this sorbent is demonstrated with the purification of β_2-microglobulin and immunoglobulin.

INTRODUCTION

Hydrophobic interaction chromatography (HIC) is widely used in the separation of proteins. The principle is based on hydrophobic interactions between the hydrophobic areas of proteins and isolated hydrophobic sites on the hydrophilic surface of sorbents. In comparison with reversed-phase high-performance liquid chromatography (RP-HPLC), operating on the same principle but with a much higher density of hydrophobic sites on the sorbent surface, milder elution conditions (usually a descending gradient of salt in buffer of pH *ca.* 7) are needed. This results in a higher mass recovery and also in a substantially higher recovery of biological activity of separated proteins in comparison with RP-HPLC [1–3].

Sorbents for HIC are usually based on hydrophilic organic matrices which are suitably hydrophobized [4–8] or on modified silica gels [2,3,9–16]. In addition to porous packings non-porous sorbents have also been described [17,18]. Silica gels and some organic gels are rigid enough for use in high-performance hydrophobic interaction chromatography (HP-HIC).

0021-9673/90/$03.50

Separon HEMA materials, which are copolymers of 2-hydroxyethyl methacrylate (HEMA) and ethylene dimethacrylate (EDMA), are rigid and hydrophilic products that can be commonly used under HPLC conditions. Whereas the organic sorbents usually applied in HP-HIC (TSKgel Phenyl of Superose Phenyl) are modified by chemical bonding of hydrocarboneous ligands, Separon HEMA materials have been used in HIC without any modification with interesting results [17–23]. In the case of Separon HEMA only the hydrophobic sites on the surface of proteins can interact with hydrophobic areas on the support of the sorbent whereas the hydrocarboneous ligands of the sorbents mentioned above are able to penetrate into the "pockets" in the structure of proteins. This results in the specific selectivity of Separon HEMA in some instances [20].

The drawback of unmodified Separon HEMA is a low efficiency in comparison with comercial organic materials even if small particles (10 μm) are used [23].

The aim of this work was to examine whether simple chemical modification of Separon HEMA (esterification [24] and reaction with an epoxy derivative [25]) can improve the efficiency of the separation of proteins by HIC on this material.

EXPERIMENTAL

Sorbents and chemicals

Separon HEMA 1000 H (10 μm) and Separon HEMA 1000 DEAE (10 μm) was obtained from Tessek (Prague, Czechoslovakia), Sephadex G-100 from Pharmacia (Uppsala, Sweden) and 1,2-epoxy-3-phenoxypropane (EPP) from Aldrich (Steinheim, F.R.G.). Boron trifluoride (BF_3) etherate (40%) and ammonium sulphate (for biochemical use) were purchased from Merck (Darmstadt, F.R.G.). Benzoyl chloride, disodium hydrogenphosphate, dioxane, toluene, acetone and methanol were from Lachema (Brno, Czechoslovakia).

Chicken egg-white lysozyme (LYS), horse skeletal muscle myoglobin (MYO), and bovine pancreas ribonuclease A (RNase) were purchased from Sigma (St. Louis, MO, U.S.A.) and bovine pancreas chymotrypsin (CHYT) from Reanal (Budapest, Hungary).

Chromatography

All experiments were performed with a Model 2150 HPLC pump, a low-pressure gradient mixer, a Model 2152 LC controller, a Model C6W-HC injector, a Model 2140 rapid spectral detector and a Data Print computer (Pharmacia–LKB, Bromma, Sweden).

Sorbents were packed into a stainless-steel column (50 × 4 mm I.D.) or a titanium column (50 × 8 mm I.D.). A 2 *M* solution of ammonium sulphate was used as the slurrying and packing solvent. A pressure of 2 MPa was maintained during the whole operation.

Preparation of Separon 1000 G benzoyl

A 5-g amount of Separon HEMA 1000 H, dried overnight at 348 K, was suspended in 50 ml of dry toluene, then 0.23 g of benzoyl chloride was added. The suspension was refluxed for 5 h under anhydrous conditions. The sorbent was filtered, washed thoroughly with methanol and acetone and dried at 348 K for 6 h. The

concentration of benzoyl ligands was calculated from the difference between the amount of hydroxyl groups presented on the surface of the sorbent before and after the modification [24]. This content was 0.3 mmol of benzoyl ligands per gram of dry sorbent in this instance.

Preparation of Separon HEMA 1000 H phenyl

A 2.5-g amount of Separon HEMA 1000 h (dried overnight at 348 K) was suspended in 10 ml of dry dioxane, then 0.15 g of BF_3 etherate and 0.188 g of EPP were added. The suspension was stirred at room temperature for 45 min under anhydrous conditions. The sorbent was filtered and washed thoroughly with dioxane, methanol and acetone and dried at 348 K for 6 h. The concentration of 2-hydroxy-3-phenoxypropyl ligands was determined by the photometric measurement of unreacted EPP at 270 nm, and was 0.25 mmol of ligand per gram of dry sorbent.

RESULTS AND DISCUSSION

Separon HEMA 1000 H (unmodified matrix) and its derivatives were compared. The concentrations of benzoyl and 2-hydroxy-3-phenoxypropyl ligands were 0.30 and 0.25 mmol/g, respectively. These substituent concentrations were found to be optimum from the point of view of the efficiency and selectivity of the separation of a model mixture of proteins (MYO, RNase, LYS, CHYT). Several concentrations of both ligands were prepared and tested (results not shown). In Figs. 1–3 the separations of the model mixture of proteins are demonstrated. Separon HEMA 1000 H benzoyl and phenyl were tested under the same conditions. With the unmodified matrix the starting concentration of salt was higher to compensate for the too high hydrophilicity of the sorbent. It can be clearly seen from Figs. 1–3 that a retention which should be proportional to the character of the hydrophobic interactions be-

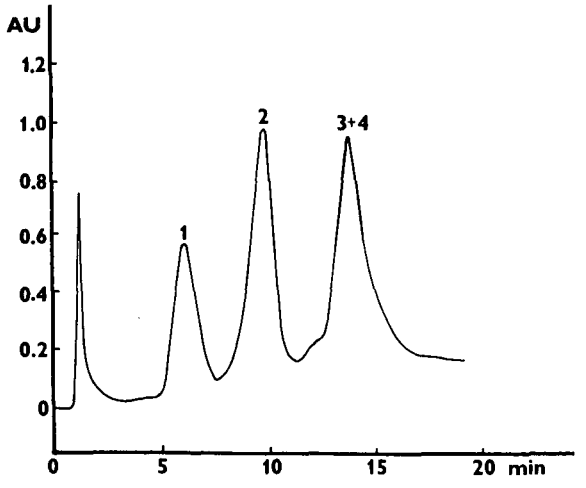

Fig. 1. Separation of model proteins on Separon HEMA 1000 H. Column: 50 × 4 mm I.D. Flow-rate: 0.5 ml/min. Gradient: from 2.4 to 0 *M* $(NH_4)_2SO_4$ in 0.1 *M* Na_2HPO_4 (pH 7.0) in 30 min. Proteins: 1 = MYO; 2 = RNase; 3 = LYS; 4 = CHYT.

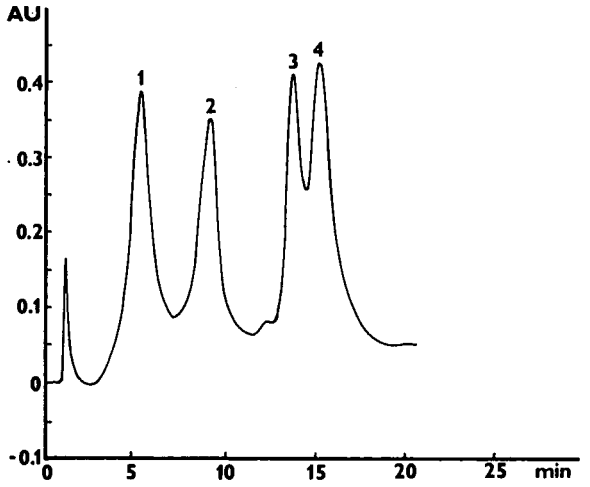

Fig. 2. Separation of model proteins on Separon HEMA 1000 H benzoyl. Conditions and proteins as in Fig. 1, except the gradient started from 2.2 *M* $(NH_4)_2SO_4$.

tween the sorbent and protein arose on going from the unmodified matrix to the phenyl derivative. The selectivity of the benzoylated sorbent is better than that of the the basic material, but the phenyl derivative showed the best selectivity of the three sorbents.

The important factor is the difference in the peak widths (W). W was calculated from well known relationship [26] $W = 1.7\ W_{1/2}$, where $W_{1/2}$ is the peak width at half-height). Results are given in Table I. It is evident that the efficiency of the phenyl derivative is substantially better the that of the two other materials.

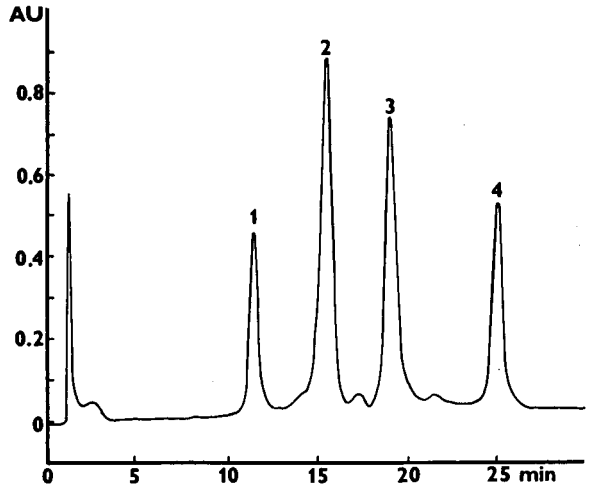

Fig. 3. Separation of model proteins on Separon HEMA 1000 H phenyl. Conditions and proteins as in Fig. 2.

TABLE I

PEAK WIDTHS (W) OF MODEL PROTEINS ON DIFFERENT SEPARON HEMA MATERIALS

For conditions, see Figs. 1–3

Sorbent	W (ml)			
	MYO	RNase	LYS	CHYT
Separon HEMA 1000 H	1.14	1.22	1.58	–
Separon HEMA 1000 H benzoyl	1.05	1.08	1.00	1.20
Separon HEMA 1000 H phenyl	0.47	0.62	0.60	0.58

The separation potential of Separon HEMA 1000 H phenyl is demonstrated on two examples. The first is the purification of β_2-microglobulin (β_2-m). A complex mixture of proteins from the urine of patients with kidney disfunction was obtained by precipitation with ammonium sulphate. This mixture was preseparated by size-exclusion chromatography on Sephadex G-100 and ion-exchange chromatography on Separon HEMA 1000 DEAE (see Fig. 4). Two fractions were obtained containing β_2-m which were separated by HIC on Separon HEMA 1000 H phenyl. The pertinent chromatograms are demonstrated in Figs. 5 and 6. The retention time of β_2-m was 26.5 min and both separations gave a product of high purity which was monitored by sodium dodecyl sulphate–polyacylamide gel electrophoresis (SDS-Page) (results not shown).

The second example is the purification of monoclonal antibody against prolactin. Mouse ascitic fluid was preseparated on Separon HEMA 1000 DEAE and the immunoglobulin G (IgG) containing fraction was then separated on Separon HEMA

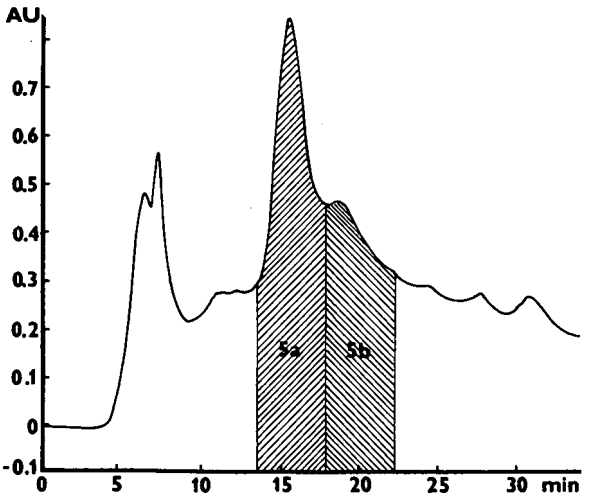

Fig. 4. Preparative separation of β_2-microglobulin fraction on Separon HEMA 1000 DEAE (in the marked area the presence of β_2-m was indicated by an ELISA test) Column: 100 × 8 mm I.D. Flow-rate: 0.5 ml/min. Gradient: from 0 to 1 M NaCl in 0.01 M Tris–HCl (pH 7.4) in 60 min.

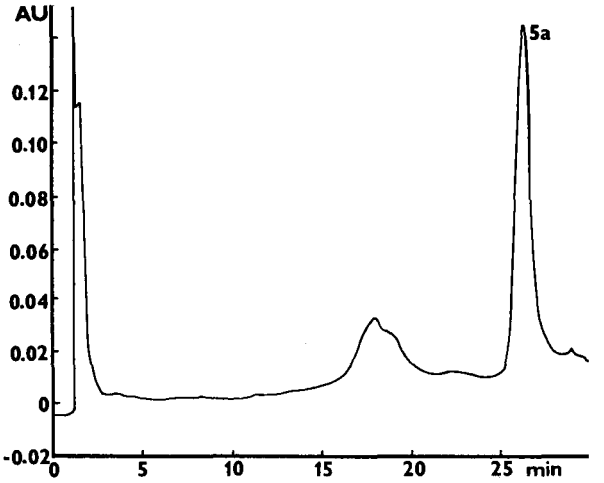

Fig. 5. Preparative separation of fraction 5a (Fig. 4) on Separon HEMA 1000 H phenyl. Conditions as in Fig. 1, except the gradient started from 2.0 *M* $(NH_4)_2SO_4$.

1000 H phenyl (Fig. 7). The complete separation of transferrin and IgG was achieved and the high purity of both proteins was verified by SDS-PAGE. The recovery of imunoactivity of IgG was determined to be 80% by a radioimmunoassay test with ^{125}I-labelled prolactine.

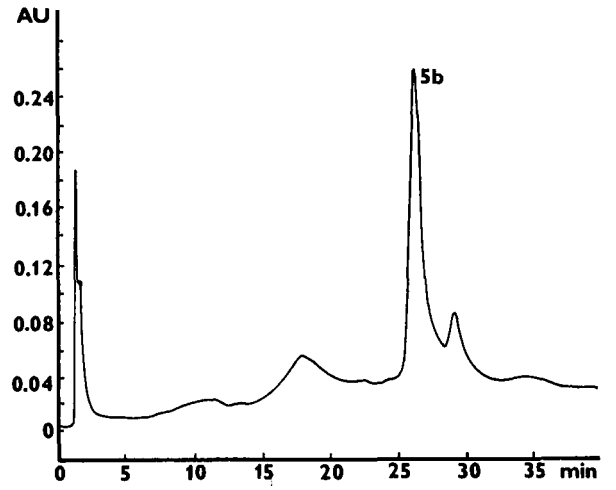

Fig. 6. Preparative separation of fraction 5b (Fig. 4) on Separon HEMA 1000 H phenyl. Conditions as in Fig. 5.

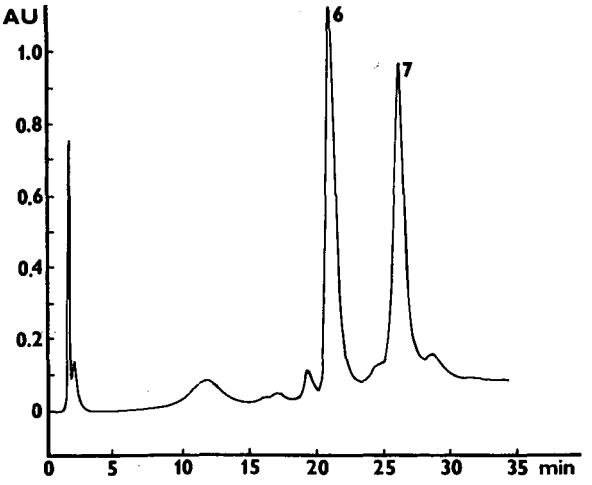

Fig. 7. Separation of IgG fraction (obtained from ascites fluid by gradient separation on Separon HEMA 1000 DEAE) on Separon HEMA 1000 H phenyl. Column: 50 × 8 mm I.D. Flow-rate: 0.5 ml/min. Gradient: from 1.8 to 0 *M* $(NH_4)_2SO_4$ in 0.1 *M* Na_2HPO_4 (pH 7.0) in 25 min.

CONCLUSIONS

The results support the hypothesis given in the Introduction that chemical modification of Separon HEMA can improve its selectivity and efficiency in the HIC of proteins. The comparison of benzoyl and 2-hydroxy-3-phenoxypropyl derivatives showed that a phenoxy group bonded via a 2-hydroxypropyl spacer gives the better results than a benzoyl group anchored directly on the sorbent surface. The small distance between the phenyl group and the sorbent surface with the benzoyl derivative is the probable cause of the unfavourable interactions between hydrophobic sites on the sorbent surface and the protein. The evidence for is the pour chromatographic characteristics of the unmodified matrix. On the other hand, the 2-hydroxypropyl spacer seems to be sufficient to prevent or minimize these unfavourable interactions.

The separation potential of EPP-derivatized Separon HEMA 1000 H was demonstrated by the purification of two proteins, β_2-microglobulin and immunoglobulin, routinely used in our department. The results obtained show that this sorbent is comparable to commercially available sorbents for HP-HIC.

REFERENCES

1 J. L. Fasnaugh, L. A. Kennedy and F. E. Regnier, *J. Chromatogr.*, 317 (1984) 141.
2 Y. Kato, T. Kitamura and T. Hashimoto, *J. Chromatogr.*, 266 (1983) 49.
3 J.-P. Chang, Z. El Rassi and C. Horváth, *J. Chromatogr.*, 319 (1985) 396.
4 S. Hjertén, J. Rosengren and S. Pahlman, *J. Chromatogr.*, 101 (1974) 281.
5 J. Rosengren, S. Pahlman, M. Glad and S. Hjertén, *Biochim. Biophys. Acta*, 412 (1975) 51.
6 G. Halperin, M. Breitenbach, M. Tauber-Finkelstein and S. Shaltiel, *J. Chromatogr.*, 215 (1981) 211.
7 S. Hjertén, K. Yao, Z.-Q. Liu, D. Yang and B.-L. Wu, *J. Chromatogr.*, 354 (1986) 203.

8 Y. Kato, T. Kitamura and T. Hashimoto, *J. Chromatogr.*, 292 (1984) 418.
9 J. L. Fausnaugh, E. Pfankoch, S. Gupta and F. E. Regnier, *Anal. Biochem.*, 137 (1984) 464.
10 Z. El Rassi and C. Horváth, *Chromatographia*, 19 (1984) 9.
11 A. L. Alpert, *J. Chromatogr.*, 359 (1986) 85.
12 L. A. Kennedy, W. Kopaciewicz and F. E. Regnier, *J. Chromatogr.*, 359 (1986) 61.
13 T. Ueda, Y. Yasui and Y. Ishida, *Chromatographia*, 24 (1987) 427.
14 H. Engelhardt and D. Mathes, *J. Chromatogr.*, 185 (1979) 305.
15 M. Czok and H. Engelhardt, *Fresenius' Z. Anal. Chem.*, 327 (1987) 305.
16 N. T. Miller, B. Feibusch and B. L. Karger, *J. Chromatogr.*, 316 (1984) 519.
17 S. Hjertén and J.-L. Liao, *J. Chromatogr.*, 457 (1988) 165.
18 R. Janzen, K. K. Unger, H. Giesche, J. N. Kinkel and M. T. W. Hearn, *J. Chromatogr.*, 397 (1987) 91.
19 P. Štrop, F. Mikeš and Z. Chytilová, *J. Chromatogr.*, 156 (1987) 239.
20 P. Štrop and D. Čechová, *J. Chromatogr.*, 207 (1981) 55.
21 P. Štrop, D. Čechová and V. Tomášek, *J. Chromatogr.*, 259 (1983) 255.
22. P. Štrop, *J. Chromatogr.*, 294 (1984) 213.
23 I. Kleinmann, J. Plicka, P. Šmídl and V. Svoboda, *J. Chromatogr.*, 479 (1989) 334.
24 K. Pecka, P. Šmídl, M. Vávra, S. Hála and Z. Havel, *Sci. Pap. Prague Inst. Chem. Tech.*, D46 (1982) 49.
25 S. Hjertén, J. Rosengren and S. Pahlman, *J. Chromatogr.*, 101 (1974) 281.
26 L. R. Snyder and J. J. Kirkland, *Introduction to Modern Liquid Chromatography*, Wiley-Interscience, New York, 2nd ed., 1979, Ch. 6.

Journal of Chromatography, 523 (1990) 139–150
Elsevier Science Publishers B.V., Amsterdam

CHROM. 22 739

Hydrophobic interaction chromatography of proteins on Separon HEMA

III. Selection of suitable gradient conditions for the separation of proteins by hydrophobic interaction chromatography

J. PLICKA, P. ŠMÍDL, I. KLEINMANN* and V. SVOBODA
Institute for Research, Production and Application of Radioisotopes, Radiová 1, 102 27 Prague 10 (Czechoslovakia)
(First received November 21st, 1989; revised manuscript received May 16th, 1990)

ABSTRACT

The aim of this work was to verify the possibility of the application of the simple approach to the prediction of the peak maximum position and peak width. The system studied was based on the sorbent Separon HEMA 1000 H benzoyl and on several proteins which were eluted with a decreasing concentration of ammonium sulphate. It was established that the relationships based on the approach according to Yamamoto *et al.* required correction, because a "limit" concentration of salt exists. A protein leaves the column at this "limit" concentration always if the initial concentration of salt in the gradient is higher than this "limit" value. A knowledge of the "limit" values of salt concentrations together with a knowledge of mutual ln k' *vs.* $[(NH_4)_2SO_4]$ dependences of the mixture of proteins (determined from isocratic experiments) is necessary in order to choose the elution conditions, *e.g.*, the gradient time, initial and final salt concentrations and in some instances even the length of the column.

INTRODUCTION

In previous work [1] we studied hydrophobic interaction chromatography (HIC) on unmodified Separons HEMA and determined the influence of the initial concentration of salt (φ_0) on gradient separations and of the mutual position of the isocratic dependences ln $k' \approx \varphi$ on the separation of a mixture of standard proteins. In subsequent work [2], we achieved a substantial improvement in separation efficiency by chemical modification of Separon HEMA 1000 H. In this work, we investigated the possibility of utilizing isocratic ln $k' = f(\varphi)$ data for the selection of the optimum separation conditions.

The theory of gradient elution was developed by various groups [3–11]. A number of Snyder and co-workers' papers [4–9] are devoted to the application of this theory in the chromatography of proteins, especially in the area of reversed-phase

0021-9673/90/$03.50

chromatography (RPC). Considering the calculation of retention time, t_R, and retention volume, V_R, the method is based on a simple integral equation balancing the volume of mobile phase passing through the centre of a peak during its movement along the column. The analytical solution of this equation has frequently been published with respect to the linear dependence of the logarithm of the capacity factor on the concentration of salt and with respect to the linear course of a gradient [5]. The calculation of the number of plates is based on Knox's equation, the coefficients of which are determined from empirical equations [6]. On the basis of the relationships obtained it is possible to establish an optimization strategy for gradient parameters.

Katti *et al.* [12] tried to predict the retention times of protein peaks in hydrophobic interaction chromatography (HIC) with the help of a mathematical model. In our own work we applied the ideas published by Yamamoto *et al.* [13] on ion-exchange chromatography (IEC) in the field of HIC. Our aim was to determine not only the retention time but also the peak width so as to follow the optimization of the separation of a model pair of proteins by HIC.

THEORY

Concerning the calculation of t_R, Yamamoto *et al.*'s [13] model began with an equation expressing the velocity of the peak movement along a column which is valid for equilibrium chromatography:

$$\frac{dz_p}{dt} = \frac{u}{1 + k'} \tag{1}$$

where z_p is the coordinate of the peak maximum ($z_p \in \langle 0,L \rangle$, where L is the column length), t is time, u is the linear velocity of eluent, k' is the capacity factor [for gradient conditions $k' = f(\varphi)$, where φ is the concentration of salt]. The steepness of the linear gradient of salt concentration is defined by

$$g = \frac{\varphi_0 - \varphi_t}{t_g} \tag{2}$$

where φ_t is the terminal concentration of salt and t_g is the duration of the gradient. Considering a gradient mixer delay t_D and zero salt retention, the course of salt concentration behind the column is expressed by

$$\varphi(t) = \varphi_0 - g(t - t_0 - t_D) \tag{3}$$

where t_0 is the dead time of the column, $t_0 = L/u$.

The salt concentration (φ) at the peak maximum during its movement along the column is described by the function

$$\varphi(t,z_p) = \varphi_0 - g\left(t - \frac{z_p}{u} - t_D\right) \tag{4}$$

and the following relationship describes its change:

$$\frac{d\varphi}{dz_p} = -g\left(\frac{dt}{dz_p} - \frac{1}{u}\right) \tag{5}$$

Combining eqns. 1 and 5, we obtain

$$\frac{d\varphi}{dz_p} = -g\left[\frac{k'(\varphi)}{u} + \frac{1}{u} - \frac{1}{u}\right] = -g \cdot \frac{k'(\varphi)}{u} \tag{6}$$

and in an integral form

$$\int_{\varphi_0}^{\varphi_e} \frac{d\varphi}{k'(\varphi)} = -g \cdot \frac{1}{u} \int_0^L dz_p \tag{7}$$

$$\int_{\varphi_e}^{\varphi_0} \frac{d\varphi}{k'(\varphi)} = gt_0 \tag{8}$$

The value of φ_e results from the numerical solution of eqn. 8; then, t_R can easily be calculated:

$$t_R = \frac{\varphi_0 - \varphi_e}{g} + t_0 + t_D \tag{9}$$

Yamamoto *et al.* [13] assumed that so-called "steady state" is reached, *i.e.*, the state when the peak broadening caused by its movement along the column is in equilibrium with its sharpening which is a consequence of the faster movement of the rear edge of peak in comparison with the front edge. If we accept this assumption, the solution of the fundamental mathematical model based on the Plate theory [13] gives the relationships for the number of plates, N_p, and σ^2:

$$N_p = \frac{L}{\frac{2D_L}{u} + \frac{d_p^2\, u\, k'_e}{30\bar{D}_e(1 + k'_e)^2}} \tag{10}$$

$$\sigma_\theta^2\, N_p = -\frac{1}{2} \cdot \frac{(1 + k'_e)^3}{gt_0\left(\frac{dk'}{d\varphi}\right)_e} \tag{11}$$

where D_L is the coefficient of axial dispersion, $\bar{D}$ is the coefficient of diffusion inside the particle, the subscript e indicates the values of the salt concentration equal to that at which a protein leaves the column and θ is non-dimensional time or volume ($\theta = t/t_0$ or V/V_0).

EXPERIMENTAL

Ribonuclease A (RIB), lysozyme (LYS), chymotrypsin (CHYM), soybean trypsin inhibitor (STI) and bovine serum albumin (BSA) were purchased from Sigma (St. Louis, MO, U.S.A.). Proteins were dissolved in 0.1 *M* phosphate buffer (pH 7.0) containing the initial concentration of ammonium sulphate chosen for a given gradient. A volume of 20–60 μl of each protein solution was injected onto the column. The stainless-steel columns (50 × 4 mm I.D., void volume 0.5 ml) were packed with Separon HEMA 1000 H (10 μm) (Tessek, Prague, Czechoslovakia) modified by esterification with benzoyl chloride [2].

All experiments were performed at room temperature using an LKB (Bromma, Sweden) high-performance liquid chromatographic system consisting of a pump (Model 2150), a diode-array detector (Model 2140), a controller (Model 2152) and an AT computer with LKB evaluation software.

RESULTS

To utilize the relationships given above, a knowledge of the dependence k' *vs.* φ is necessary. Hence it is necessary to carry out and to evaluate isocratic experiments. The relationships between ln k' and φ in the isocratic HIC of proteins are known frequently to be linear. Analogous relationships were used to describe the dependence σ^2 *vs.* φ:

$$\ln k' = A + B\varphi \quad (12)$$

$$\ln \sigma^2 = a + b\varphi \quad (13)$$

The parameters A, B, a and b were calculated from experimental data by linear regression. The results are summarized in Table I, including correlation coefficients. The experimental data for ln $k' \approx \varphi$ for the proteins studied are shown in Fig. 1.

Several gradient experiments were carried out with STI and the concentration of salt, φ_e (concentration of salt at which protein left the column), was found to be almost constant over a wide range of g (g = 0.02–0.1 mol dm^{-3} min^{-1}). The value of φ_e calculated according to eqn. 8 was also nearly constant (the parameters from Table I were used); however this value was significantly lower than that obtained from the experimental results. Similar results were obtained with the other proteins. To achieve

TABLE I

THE PARAMETERS OF EQNS. 12 AND 13

Protein	Ln $k' = A + B\varphi$			Ln $\sigma^2 = a + b\varphi$		
	A	B	Correlation coefficient	a	b	Correlation coefficient
STI	−8.3464	8.4988	0.9952	−6.419	12.66	0.9967
LYS	−7.4092	5.8509	0.9930	−3.1929	7.1571	0.9838
CHYT	−10.0397	8.2847	0.9983	−6.0483	10.5500	0.9995
RIB	−9.1737	5.8085	0.9978	−7.9846	8.5036	0.9577
BSA	−16.7388	1.4250	0.9995	−21.508	19.5000	0.9863

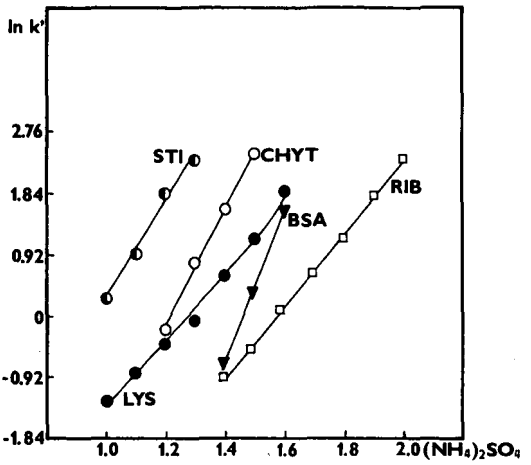

Fig. 1. Experimental dependences of ln k' on concentration of ammonium sulphate, φ. Sorbent: Separon HEMA 1000 H benzoyl. Concentration in mol dm^{-3}.

agreement between the two sets of values we introduced a correction parameter k'' into eqn. 8:

$$\int_{\varphi_e}^{\varphi_0} \frac{d\varphi}{k' - k''} = gt_0 \tag{14}$$

It would have been advantageous if one could have put instead of k'' the value of k' for φ corresponding to the experimentally determined constant φ mentioned above. Considering the course of the exponential functions on the left-hand sides of eqns. 8 and 14, it is clear that this simplification will not produce great differences. The values of φ_e for the proteins studied are given in Table II.

The concentration of salt at which a protein leaves the column was almost constant if the starting concentration of salt was chosen to be higher than the value $(\varphi_e)_{lim}$. Then the solution of eqn. 10 indicates that the number of theoretical plates, N_p, is also constant provided that the column length and the mobile phase velocity are also

TABLE II

THE VALUES OF k'' AND φ_e FOR THE STUDIED PROTEINS

Protein	k''	φ_e (mol dm^{-3})
STI	6.0	1.19
LYS	4.5	1.52
CHYT	5.0	1.41
RIB	6.0	1.89
BSA	6.0	1.62

constant. In addition, the relationship for σ_θ^2 at two different gradients follows from eqn. 11:

$$\frac{(\sigma_\theta^2)_1}{(\sigma_\theta^2)_2} = \frac{g_2}{g_1} \tag{15}$$

The applicability of eqn. 15 in HIC systems has been shown by Miller and Karger [10], as peak height is inversely proportional to peak area.

Using parameters a and b we could determine σ^2 for $\varphi = (\varphi_e)_{lim}$ under isocratic conditions. In addition, we assumed this value of σ^2 to be the same even for a very gentle gradient with $\varphi_0 > (\varphi_e)_{lim}$, *i.e.*, for very small g. However, if g reaches a certain value (critical value), σ^2 will fall according to eqn. 15. The values of these g_{crit} for individual proteins were determined from eqn. 15 utilizing the value of σ^2 for $(\varphi_e)_{lim}$ and the results of gradient experiments for $\varphi_0 > (\varphi_e)_{lim}$. These calculations resulted in average values of g_{crit} for the proteins studied (see Table III). Utilizing the parameters A, B, a, b, k'' and g_{crit}, the calculations of t_R and $W_{1/2}$ ($W_{1/2} = 2.35\sigma$) were carried out for gradient experiments. Calculated t_R and $W_{1/2}$ values for LYS and RIB are given in Tables IV and V as examples, together with the experimental results.

The other results were obtained when LSS theory [5] was applied to the calculations of some retention times and the values of φ_e are given in the Tables VI–VIII. The experimental isocratic data were employed (see Fig. 1). The following equations were used in t_R calculations [5]:

$$t_R = \frac{t_0}{b} \cdot \log\left(2.3\, k_0' b \cdot \frac{t_{sec}}{t_0} + 1\right) + t_{sec} + t_D \tag{16}$$

where $k_0' = k'$ for φ_0 (see eqn. 10), $b = (B/2.303)\Delta\varphi t_0/t_g$ ($\Delta\varphi = \varphi_0 - \varphi_{final}$), $t_0 = V_0/F = 0.515/0.5 = 1.03$ min, t_{sec} is the elution time of the excluded proteins and $t_D = V_D/F = 4$ min.

DISCUSSION

It is difficult to explain the existence of $(\varphi_e)_{lim}$ and consequently the necessity for the correction of eqn. 8 with the parameter k''. Applying the isocratic data in eqn. 8, one would have to obtain values of t_R close to the experimental values. We did not

TABLE III

THE VALUES OF g_{crit} FOR STUDIED PROTEINS

Protein	g_{crit} (mol dm^{-3} min^{-1})
STI	0.02
LYS	0.02
CHYT	0.012
RIB	0.013
BSA	0.0022

TABLE IV

CALCULATED AND EXPERIMENTAL DATA FOR LYS

t_0 (min)	t_g (min)	φ (mol dm^{-3})	g (mol dm^{-3} min^{-1})	t_R (min)		φ_e (mol dm^{-3})		$W_{1/2}$ (ml)	
				Exp.	Calc.	Exp.	Calc.	Exp.	Calc.
1.03	30	2.0	0.0667	11.77	11.75	1.55	1.552	0.62	0.56
1.03	20	2.0	0.100	9.50	9.69	1.55	1.534	0.40	0.46
1.03	20	1.8	0.090	7.82	7.96	1.55	1.536	0.52	0.48
1.03	30	1.8	0.060	9.17	9.15	1.55	1.553	0.65	0.59
1.03	30	1.6	0.053	6.12	6.17	1.54	1.539	0.62	0.63
1.03	20	1.6	0.080	5.62	5.89	1.55	1.531	0.46	0.51
1.03	20	1.4	0.070	3.23	3.28	1.40	1.40	0.54	0.59
1.03	30	1.4	0.0467	3.23	3.28	1.40	1.40	0.55	0.59
1.03	20	1.2	0.060	1.77	1.73	1.20	1.20	0.24	0.29
1.03	30	1.2	0.040	1.73	1.73	1.20	1.20	0.39	0.29
2.06	20	2.0	0.10	11.70	10.82	1.44	1.524	0.40	0.46

succeed even in the application of the model based on the rate eqn. 1 [1]. We always obtained values higher then experimental values [*i.e.*, $\varphi_e < (\varphi_e)_{lim}$]. Analogous results were obtained using eqn. 16 for $t_{sec}/t_0 = 1$ (see Tables VI–VIII), although the exclusion limit of the sorbent used is 1000 kilodaton and the relative molecular weights of the proteins examined are much smaller. On the other hand, excellent agreement between the calculated and experimental data was achieved for $t_{sec}/t_0 = 0.5$. This value is too small, in our opinion, because the column volume accessible to proteins would be only 20%. Nevertheless, it follows from these calculations that the concentration of salt at which a protein leaves the column is also nearly constant. In the work of Yamamoto *et al.* [13], the coefficient k'' has the real meaning of being the capacity factor of a salt, *e.g.*, sodium chloride, which is not equal to zero in IEC. On the other hand, its physical interpretation is unclear in HIC because the capacity factor of ammonium sulphate is

TABLE V

CALCULATED AND EXPERIMENTAL DATA FOR RIB

t_0 (min)	t_g (min)	φ_0 (mol dm^{-3})	g (mol dm^{-3} min^{-1})	t_R (min)		φ_e (mol dm^{-3})		$W_{1/2}$ (ml)	
				Exp.	Calc.	Exp.	Calc.	Exp.	Calc.
1.03	30	2.0	0.0667	7.12	6.59	1.86	1.846	0.56	0.52
1.03	20	2.0	0.100	6.25	6.13	1.88	1.890	0.39	0.42
1.03	20	1.8	0.090	4.25	4.79	1.80	1.80	0.43	0.76
1.03	30	1.8	0.060	4.37	4.74	1.80	1.80	0.62	0.76
1.03	30	1.6	0.053	2.32	2.19	1.60	1.60	0.38	0.32
1.03	20	1.6	0.080	2.25	2.19	1.60	1.60	0.34	0.32
1.03	30	2.2	0.073	9.33	9.13	1.88	1.899	0.56	0.49
1.03	20	2.2	0.110	7.80	7.84	1.89	1.891	0.37	0.40
1.03	20	2.5	0.125	9.67	9.91	1.92	1.890	0.34	0.37
1.03	30	2.5	0.083	12.17	12.27	1.905	1.897	0.44	0.46
2.06	20	2.2	0.110	9.88	8.90	1.78	1.888	0.28	0.40

TABLE VI

THE EXPERIMENTAL AND CALCULATED t_R AND φ_e VALUES (USING LSS THEORY) FOR LYS

t_g (min)	φ_0 (mol dm^{-3})	t_R (min)			φ_e (mol dm^{-3})		
		Exp.	Calc.		Exp.	Calc.	
			A[a]	B[b]		A[a]	B[b]
30	2.0	11.77	11.56	13.80	1.55	1.56	1.42
20	2.0	9.50	9.86	11.54	1.55	1.52	1.35
20	1.8	7.82	7.74	9.94	1.55	1.56	1.36
30	1.8	9.17	9.14	10.33	1.54	1.55	1.38
30	1.6	6.12	6.93	8.83	1.54	1.50	1.40
20	1.6	5.62	6.62	8.14	1.55	1.47	1.35

[a] $t_{sec}/t_0 = 0.5$.
[b] $t_{sec}/t_0 = 1.0$.

really zero, as was verified experimentally. Nevertheless, this correction is necessary. The reason probably lies in changes in protein conformation during separation, *i.e.*, different conformations for isocratic *vs.* gradient elution, as postulated by Hodder *et al.* [14].

A comparison of the experimentally obtained and calculated values of t_R and $W_{1/2}$ (see Tables IV and V) gives very good agreement. For $\varphi_0 < (\varphi_e)_{lim}$ the calculation is carried out as for isocratic conditions for the whole length of the column if the retention volume is smaller then 2.5 cm^3 $[(t_0 + t_D)F]$. If V_R is higher, the calculation is

TABLE VII

THE EXPERIMENTAL AND CALCULATED t_R AND φ_e VALUES (USING LSS THEORY) FOR CHYM

t_g (min)	φ_0 (mol dm^{-3})	t_R (min)			φ_e (mol dm^{-3})		
		Exp.	Calc.		Exp.	Calc.	
			A[a]	B[b]		A[a]	B[b]
30	2.0	14.15	14.05	14.83	1.39	1.40	1.35
20	2.0	10.85	11.36	12.72	1.42	1.37	1.23
20	1.8	9.33	9.77	11.22	1.41	1.37	1.24
30	1.8	11.82	11.62	13.52	1.39	1.40	1.29
30	1.6	8.98	8.81	10.72	1.39	1.40	1.30
20	1.6	7.43	7.90	9.39	1.41	1.37	1.25
30	2.2	15.50	16.11	17.21	1.43	1.39	1.27
20	2.2	11.90	12.65	13.41	1.44	1.36	1.22
20	2.5	13.27	14.20	14.87	1.47	1.35	1.20
30	2.5	17.55	18.51	19.47	1.46	1.38	1.25

[a,b] See Table VI.

TABLE VIII

THE EXPERIMENTAL AND CALCULATED t_R AND φ_e VALUES (USING LSS THEORY) FOR RIB

t_g (min)	φ_0 (mol dm^{-3})	t_R (min)			φ_e (mol dm^{-3})		
		Exp.	Calc.		Exp.	Calc.	
			A[a]	B[b]		A[a]	B[b]
30	2.0	7.12	7.58	8.95	1.86	1.83	1.70
20	2.0	6.25	7.07	8.06	1.88	1.80	1.64
30	2.2	9.33	9.69	11.57	1.88	1.86	1.71
20	2.2	7.80	8.53	9.55	1.89	1.82	1.64
20	2.5	9.67	10.52	11.47	1.92	1.75	1.63
30	2.5	12.17	12.74	14.13	1.91	1.86	1.70

[a,b] See Table VI.

carried out as for gradient conditions from the point in the column when the peak maximum is "matched" by the descending concentration of salt (the beginning of the gradient). Eqns. 10 and 11 were used for the calculation of σ^2 for connection of two identical columns (50 × 2 mm I.D.). In this instance the experimental values of t_R were always nearly 1 min higher. This difference was found repeatedly even for a 100-mm column. This disagreement could be removed applying another value of k''.

From Yamamoto *et al.*'s [13] conclusions on the influence of the gradient conditions selected on the resolution of a pair of proteins (R_s) it follows that (i) resolution increases with depression of the gradient slope, $R_s \approx [(t_g F)/\Delta\varphi]^{1/2}$, (ii) if $(\Delta\varphi/t_g F)$ is constant, R_s is independent of the length of column and (iii) if $(V_0\Delta\varphi/t_g F)$ is constant, R_s increases with $L^{1/2}$.

To obtain a better experimental verification of the given conclusions, the gradient conditions and a pair of proteins were chosen for which separation is more efficient. The results, including calculated data, are given in Table IX and confirm that the conclusions given above are valid for the system studied.

TABLE IX

THE CALCULATED AND EXPERIMENTAL DATA INCLUDING RESOLUTION FOR RIB AND BSA

L (mm)	t_g (min)	φ_0 (mol dm^{-3})	RIB				BSA				R_s	
			t_R (min)		$W_{1/2}$ (ml)		t_R (min)		$W_{1/2}$ (ml)		Exp.	Calc.
			Exp.	Calc.	Exp.	Calc.	Exp.	Calc.	Exp.	Calc.		
50	60	2.0	8.22	7.58	0.89	0.78	16.87	16.10	0.99	0.87	2.70	3.05
50	60	2.4	16.45	16.73	0.66	0.76	24.53	24.36	0.85	0.76	2.91	2.94
100	60	2.0	11.83	9.18	0.71	0.72	19.85	17.37	1.09	0.80	2.62	3.17
100	60	2.4	20.10	18.63	0.69	0.66	27.03	25.51	0.93	0.73	2.51	2.93
50	30	2.0	6.83	6.59	0.49	0.51	10.94	10.68	0.68	0.57	2.07	0.24

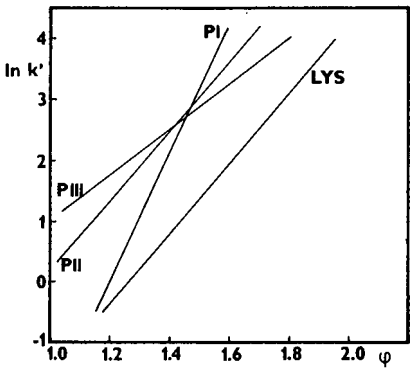

Fig. 2. Dependences of ln k' on φ (mol dm^{-3}) for hypothetical proteins and LYS.

In addition, we investigated the relationships between R_s and φ_0, t_g and L for different mutual positions of dependences ln $k' \approx \varphi$. We chose three pairs of hypothetical proteins, PI, PII and PIII, with lysozyme. The courses of ln $k' \approx \varphi$ are demonstrated in Fig. 2. Parameters a and b describing the relationship $\sigma^2 \approx \varphi$ were chosen to be identical with those for LYS.

The value of k'' [or $(\varphi_e)_{lim}$] and g_{crit} were chosen in the same way. The results of calculations are shown in Fig. 3. If $\varphi_0 > (\varphi_e)_{lim}$ (1.52 mol dm^{-3}), the suggested relationships correspond with the conclusions of Yamamoto *et al.* [13] and others [3–9]. It is also clear that a knowledge of $(\varphi_e)_{lim}$ is very important. With the pair PI–LYS and PII–LYS it is always advantageous to choose φ_0 near to $(\varphi_e)_{lim}$, where an optimum (not too significant) exists. For the pair PIII–LYS it is more advantageous to start the gradient below this limit value or to chose isocratac conditions and to profit from the influence of a longer column. This information was verified experimentally with the pair LYS–BSA, where the mutual position of the dependence ln $k' \approx \varphi$ is analogous to that of LYS–PIII (see Fig. 1). An increase in the column length (50, 100 and 150 mm) resulted in an increase in resolution (R_s = 0.56, 0.82 and 0.99, respectively) under isocratic elution conditions (φ = 1.4 mol dm^{-3}). On the other hand, this pair of proteins could not be separated with any gradient elution if $\varphi_0 \geqslant (\varphi_e)_{lim}$.

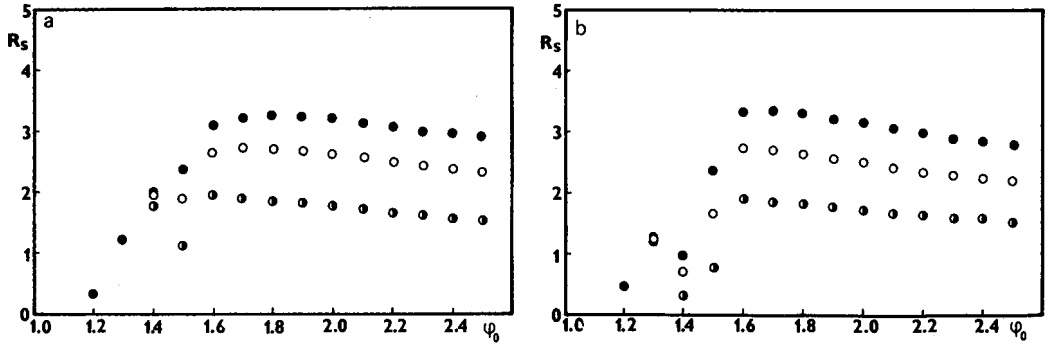

Fig. 3.

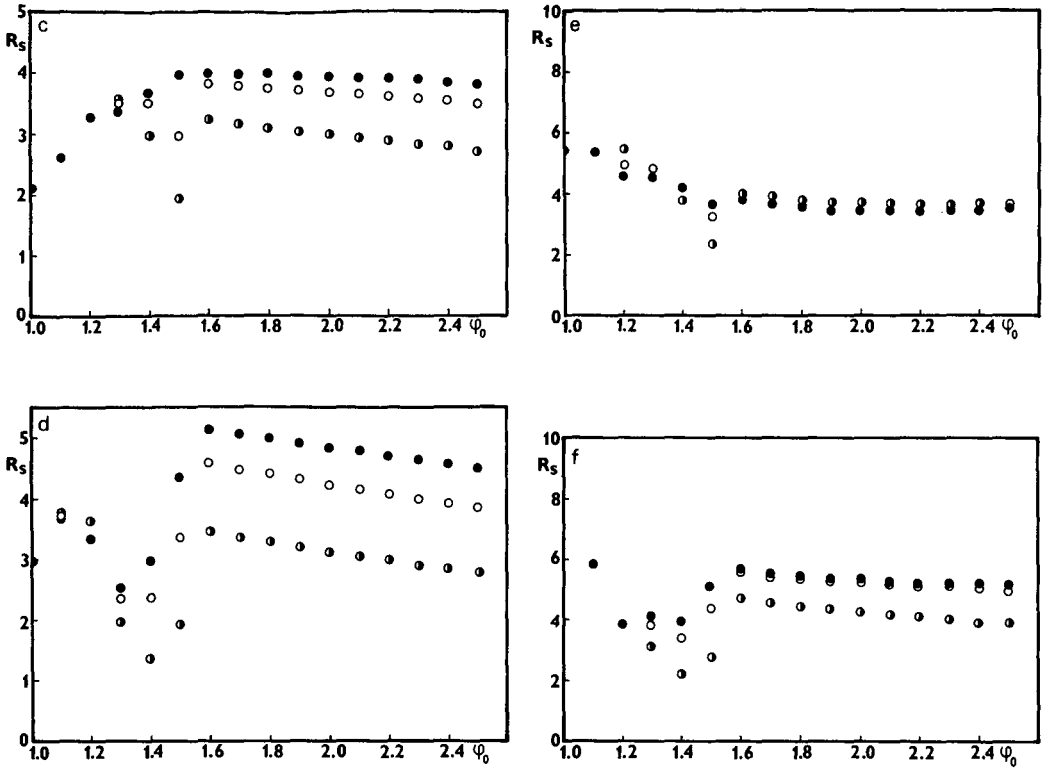

Fig. 3. Influence of φ_0 (mol dm^{-3}), t_g and L on the resolution of hypothetical proteins and LYS. (a) LYS–PI, L = 5 cm; (b) LYS–PI, L = 10 cm; (c) LYS–PII, L = 5 cm; (d) LYS–PII, L = 10 cm; (e) LYS–PIII, L = 5 cm; (f) LYS–PIII, L = 10 cm. In all instances: ●, 60 min; ○, 40 min; ◑, 20 min.

CONCLUSION

The strategy of the selection of gradient elution conditions, from the point of view of the resolution of proteins, following from the model used here does not differ in principle from those proposed by other workers [3–9,13]. From the experiments and calculations in this work it follows that in the HIC of proteins there can exist very gentle dependence of the salt concentration at which a protein leaves the column at $(\varphi)_e$ on the gradient steepness (g) and on the value of the product gt_0, so that this value of φ_e will be almost constant, $(\varphi_e)_{lim}$, for a given protein. For an unknown mixture of proteins it is not difficult to determine the values of $(\varphi_e)_{lim}$ for individual proteins if the quality of the separation allows the identification of individual peaks. One has only to carry out two or three gradient experiments with a high starting concentration of salt (φ_0), then φ_0 should be chosen to be close to the highest $(\varphi_e)_{lim}$. A knowledge of isocratic relationships ($\ln k' \approx \varphi$) even gives the chance to decide on isocratic elution in some special cases.

REFERENCES

1 I. Kleinmann, P. Šmídl, J. Plicka and V. Svoboda, *J. Chromatogr.*, 479 (1989) 327.
2 I. Kleinmann, P. Šmídl, J. Plicka and V. Svoboda, *J. Chromatogr.*, 523 (1990) 131.
3 P. Jandera and J. Churáček, *Kapalinová Chomatografie s Programovatelným Složením Mobilní Fáze, Pokroky Chemie*, Academia, Prague, 1984.
4 L. R. Snyder, M. A. Stadalius and M. A. Quarry, *Anal. Chem.*, 55 (1983) 1413.
5 M. A. Stadalius, M. S. Gold and L. R. Snyder, *J. Chromatogr.*, 296 (1984) 31.
6 M. A. Stadalius, M. S. Gold and L. R. Snyder, *J. Chromatogr.*, 327 (1985) 27.
7 M. A. Stadalius, M. A. Quarry and L. R. Snyder, *J. Chromatogr.*, 327 (1985) 93.
8 B. F. D. Ghrist, M. A. Stadalius and L. R. Snyder, *J. Chromatogr.*, 387 (1987) 1.
9 M. A. Stadalius, B. F. D. Ghrist and L. R. Snyder, *J. Chromatogr.*, 387 (1987) 21.
10 N. T. Miller and B. L. Karger, *J. Chromatogr.*, 326 (1985) 45.
11 V. Svoboda, *Radioisotopy*, 18 (1977) 775.
12 A. Katti, Y. F. Maa and Cs. Horváth, *Chromatographia*, 24 (1987) 646.
13 S. Yamamoto, K. Nakanishi and R. Matsuno, *Ion-Exchange Chromatography of Proteins* (*Chromatographic Science Series*, Vol. 43), Macel Dekker, New York, Basle, 1988.
14 A. N. Hodder, M. I. Aguilar and M. T. W. Hearn, *J. Chromatogr.*, 476 (1989) 391.

Journal of Chromatography, 523 (1990) 151–161
Elsevier Science Publishers B.V., Amsterdam

CHROM. 22 701

Determination of O-ethyl S-2-diisopropylaminoethyl methylphosphonothioate (VX) by thermospray liquid chromatography–mass spectrometry

E. R. J. WILS* and A. G. HULST
Prins Maurits Laboratory TNO, P.O. Box 45, 2280 AA Rijswijk (The Netherlands)
(First received January 30th, 1990; revised manuscript received July 4th, 1990)

ABSTRACT

The determination of the nerve agent O-ethyl S-2-diisopropylaminoethyl methylphosphonothioate (VX) by thermospray liquid chromatography–mass spectrometry was studied. The solvent system acetonitrile–methanol–0.25 *M* ammonium acetate was used on a reversed-phase C_{18} column. By selected ion monitoring at the protonated molecular ion of VX (*m/z* 268), the predominant peak in its thermospray mass spectrum, an amount of 200 pg could be detected. For the determination of VX in water at levels below 1 ng/ml, preconcentration by C_{18} cartridges was investigated. The applicability of the method was demonstrated by the determination of VX in spiked river waters. A concentration of 0.1 ng/ml could be detected starting from a water sample of 50 ml. A second application concerned the analysis of water extracts of spiked soil samples.

INTRODUCTION

Owing to its acetylcholinesterase-inhibiting properties O-ethyl S-2-diisopropylaminoethyl methylphosphonothioate (VX) is considered as a chemical warfare agent [1], the use of which is forbidden by the Geneva Protocol of 1925. The confirmed use of chemical weapons in the Iran–Iraq conflict [2] and their presumed proliferation [2,3] emphasizes the need for specific detection and identification methods for all compounds which are considered as chemical warfare agents. Unequivocal proof of the use of chemical weapons can only be based on spectrometric analyses. Owing to its sensitivity and selectivity, mass spectrometry is at present the most suitable technique for this purpose, especially if environmental samples need to be analysed.

The determination of VX and a number of its impurities have been studied in detail by gas chromatography–mass spectrometry (GC–MS) [4]. Using electron impact and chemical ionization, over twenty compounds were identified in an aged VX sample. VX is a fairly involatile compound which, after dispersion in the environment, will be retained in soil and surface water. The fate of VX in several types of soil has been studied [5,6]. In humic sand, humic loam and clayey peat, 90% of VX degraded within 2 days. VX is more stable in water. Below pH 8.0 the hydrolysis is fairly slow at 25°C ($t_{\frac{1}{2}}$ = 184 h at pH 8.0) [7]. In contrast to other organophosphorus nerve agents, no

determination of VX in water samples has been reported so far. Verweij *et al.* [8] isolated the nerve agents isopropyl methylphosphonofluoridate (sarin), 1,2,2-trimethylpropyl methylphosphonofluoridate (soman) and ethyl N,N-dimethylphosphoramidocyanidate (tabun) from water by adsorption on XAD-4 resin, followed by desorption with ethyl acetate and transfer of the ethyl acetate solution to a Tenax tube, which was analysed by a thermal desorption method. However, an attempt to determine VX by thermal desorption from Tenax proved to be unsuccessful [9]. Owing to the tendency of VX to adsorb strongly on any surface, Fowler and Smith [10] converted VX into the more volatile ethyl methylphosphonofluoridate in front of an adsorption tube filled with Chromosorb 106 in a procedure for the determination of VX in air at low concentrations by thermal desorption.

Instead of isolating VX from the aqueous phase, direct analysis of water samples by reversed-phase high-performance liquid chromatography (HPLC) may be performed. Sipponen [11] reported the determination of the nerve agents sarin, tabun and soman by HPLC using a detector based on the cholinesterase inhibition reaction. Detection limits in the range 10–200 pg were obtained. However, VX was not investigated and the described application concerned the analysis of urban air samples. As VX exhibits a relatively weak non-selective absorbance with a maximum at *ca.* 210 nm, the use of ultraviolet detectors is limited. Recently, a number of papers have been published describing the determination of VX-related organophosphorus pesticides [12–15] and hydrolysis products of pesticides and nerve agents in water [16] by thermospray liquid chromatography–mass spectrometry (TSP–LC–MS).

The determination of VX by TSP–LC–MS is described in this paper. In principle, no isolation step is necessary for the determination of compounds in aqueous samples by TSP–LC–MS. However, in order to obtain a low detection level, preconcentration will be necessary. Recently, the use of Sep-Pak C_{18} cartridges for the isolation and concentration of organophosphorus pesticides from water was demonstrated [17]. This was also investigated for VX.

EXPERIMENTAL

Materials

Ammonium acetate and ammonium formate (both analytical-reagent grade) were obtained from Aldrich (Milwaukee, WI, U.S.A.). Ammonia solution (25% in water), used to adjust the pH of the eluent, acetonitrile (gradient grade) and methanol (analytical-reagent grade) were purchased from Merck (Darmstadt, F.R.G.). Polyethylene glycols (PEG-200 and PEG-400) used for tuning and mass axis calibration were supplied by Fluka (Buchs, Switzerland). Tri-*n*-butyl phosphate was obtained from UCB (Leuven, Belgium).

Sep-Pak and Bond Elut C_{18} cartridges were purchased from Waters Assoc. (Milford, MA, U.S.A.) and Analytichem International (Harbor City, CA, U.S.A.), respectively.

VX was prepared in the laboratory and gave, in addition to a satisfactory elemental analysis, correct spectral (IR, NMR and mass) data. A stock solution of VX in water was prepared at a concentration of 4 μg/ml. At a pH of *ca.* 6 and when stored in a refrigerator at 4°C, no noticeable hydrolysis was observed over a period of 2 weeks. More dilute solutions were prepared freshly from this stock solution.

For all purposes water was purified in a Milli-Q water-purification system (Millipore, Bedford, MA, U.S.A.). Use of plastic tubes, containers, etc., with a high content of plasticizer was avoided as much as possible. Samples from the rivers Rhine and Meuse were taken in The Netherlands at Lobith and Keizersveer, respectively.

Soil samples were prepared as part of an international round-robin exercise coordinated by the Finnish Research Project for Chemical Warfare Verification [18]. The samples were spiked with VX (purity 94%) and some of its degradation products at a level of 100 mg/kg. The samples were prepared on September 21, 1989, stored at 5°C until September 25, 1989, and arrived at this laboratory on September 28, 1989. They were stored in a freezer at −25°C till the start of the analysis on October 13, 1989. The soil samples had the following chemical and physical characteristics: granulation, clay <2 μm 49.2%, silt 2–50 μm 16.5% and sand >50 μm 34.3%; moisture content at 105°C, 4.5%; pH, 6.8; and organic matter content, 3.2%.

Liquid chromatography

The LC system was assembled from a Waters Assoc. Model 510 solvent-delivery system, a Valco injector (Bester, Amsterdam, The Netherlands) with a 40-μl sample loop and a stainless-steel column (250 mm × 5 mm I.D.) which was packed in the laboratory with 7-μm LiChrosorb C_{18} particles (Merck). The connection between the column and the TSP interface consisted of a low-dead-volume tee, a Valco injector with a 5-μl sample loop for flow injections and a 2-μm screen filter (Waters Assoc.). A second solvent-delivery system (Waters Model 590) combined with a pulse damper (Touzart et Matignon, Vitry sur Seine, France) was connected to the low-dead-volume tee for post-column addition of an ammonium acetate solution or for the introduction of the calibration mixture.

TSP–LC–MS analyses were performed with mobile phases consisting of methanol–0.1 *M* ammonium acetate (80:20) or acetonitrile–methanol–0.25 *M* ammonium acetate (70:20:10) at a flow-rate of 1.2 ml/min. In both instances 0.05 *M* ammonium acetate was added post-column at a flow-rate of 0.5 ml/min. Injections directly into the TSP interface were carried out in a flow (1.2 ml/min) of 0.05 *M* ammonium acetate.

Mass spectrometry

A Nermag (Argenteuil, France) R 10-10 C quadrupole instrument, equipped with a TSP ion source (Nermag), was coupled with the LC system via a Vestec (Houston, TX, U.S.A.) TSP interface. The TSP source was equipped with a repeller and discharge ionization, whereas the mass spectrometer was fitted with the CONIPHOT detection system. Tuning and mass axis (m/z) calibration in the positive ion mode from m/z 60 to 800 were performed with a mixture of PEG-200 and PEG-400. Mass spectra were scanned over the mass range m/z 100–350 at a scan rate of 0.6 s. Single-ion detection experiments were carried out by monitoring the protonated molecular ion of VX at m/z 268 using an integration time of 0.6 s.

The temperature of the capillary tip was optimized before each set of experiments using background ions in the m/z 200–300 region. The ion block temperature was maintained at 250°C and the repeller voltage was adjusted between 120 and 200 V.

Determination of breakthrough volumes

Breakthrough volumes were measured by successively pressing portions of 20 ml of VX solution (4 μg/ml) through C_{18} cartridges by means of a syringe at a flow-rate of *ca.* 10 ml/min. After each portion, the effluent was analysed for VX using flow injections. Cartridges were prewetted by passing 5 ml of methanol and 10 ml of water through the cartridges.

RESULTS AND DISCUSSION

Thermospray mass spectrum of VX

The TSP mass spectrum of VX depends on the liquid composition. The protonated molecular ion at *m/z* 268 was obtained almost exclusively (Fig. 1A) by using ionization by the ammonium acetate buffer in mixtures with high contents of methanol or acetonitrile. No ammonium adduct ion could be observed, indicating that the proton affinity of VX is higher than that of ammonia (858 kJ/mol) [19]. Small fragments were observed at *m/z* 145, 146 and 188. In Table I the most probable

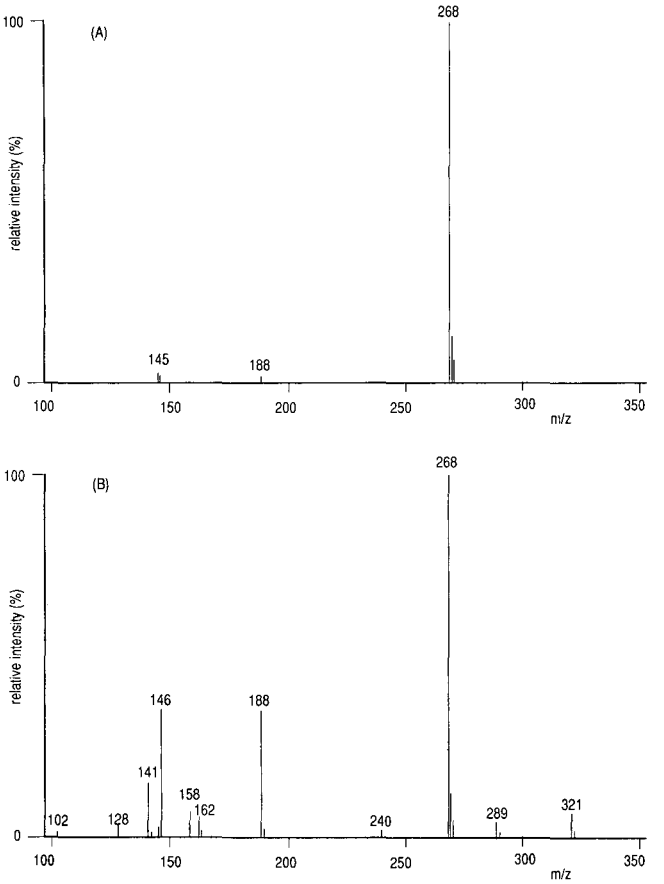

Fig. 1. Thermospray mass spectrum of VX (A) in a liquid composition consisting of acetonitrile–methanol–0.089 *M* ammonium acetate (50:14:36) and (B) in 0.1 *M* ammonium acetate.

TABLE I

STRUCTURES OF FRAGMENTS FOUND IN THE TSP MASS SPECTRA OF VX

i = Iso-.

m/z	Fragment	*m/z*	Fragment
102	$(iC_3H_7)_2NH\rceil H^+$	162	$(iC_3H_7)_2NCH_2CH_2SH\rceil H^+$
128	$(iC_3H_7)_2NCH{=}CH_2\rceil H^+$		
141	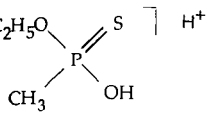	188	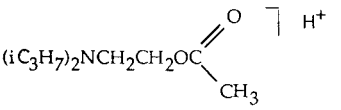
145			
146	$(iC_3H_7)_2NCH_2CH_2NH_2\rceil H^+$	240	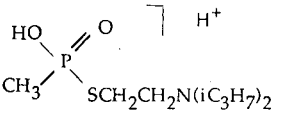
158	$(iC_3H_7)_2NCH_2CH_2OH\rceil H^+$		
	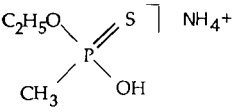	268	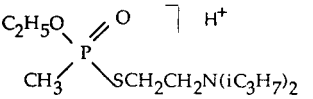
		289	$(iC_3H_7)_2NCH_2CH_2SCH_2CH_2N(iC_3H_7)_2\rceil H^+$
		321	$(iC_3H_7)_2NCH_2CH_2SSCH_2CH_2N(iC_3H_7)_2\rceil H^+$

structures of the ions are presented. The ion at *m/z* 188 cannot be readily explained from simple bond cleavages, or attributed to VX hydrolysis products. Using ammonium formate this ion shifted to *m/z* 174, indicating the formation of an ester between 2-diisopropylaminoethanol and either acetic or formic acid. Except for this unexpected ion, the spectra obtained by using both buffers were identical. In accordance with the results published by Voyksner and Haney [12] and Barceló [20], no enhancement of the sensitivity was observed by using ammonium formate.

More ions were observed in 0.1 *M* ammonium acetate solution (Fig. 1B). They correspond to the protonated molecular ions or ammonium adduct ions of known VX decomposition products [5–7] (see Table I). The relative intensities of the ions depended strongly on the experimental conditions, so the spectrum presented has to be regarded as an example. As already demonstrated by McFadden and Lammert [21], discharge ionization and variation of the repeller voltage may lead to fragmentation of analytes. This was also observed for VX. Using discharge ionization, the intensities of some ions (*m/z* 128, 146 and 162) became enhanced. The ion at *m/z* 128 may be derived from those at *m/z* 146 and 162 by the elimination of water and hydrogen sulphide, respectively. Unfortunately, analysis in a 100% aqueous solution can only be performed when VX is directly introduced by flow injection. This type of analysis will be limited to those samples in which the concentration of VX is sufficiently high in comparison with other constituents.

Liquid chromatography of VX

Water with a high content of organic modifier was used for the described determination of the organophosphorus nerve agents or pesticides by reversed-phase HPLC [11–15]. Similar conditions were chosen for VX. Owing to the basic diisopropylaminoethyl moiety, adjustment of the pH was necessary. At a pH of *ca.* 5, a broad, tailing peak was observed using a C_{18} column and methanol–0.1 *M* ammonium acetate (50:50) as the eluent, probably owing to an exchange reaction between VX and its protonated form. Increasing the pH led to longer retention times, so the methanol content was raised to 80%. A reasonably sharp peak was obtained when the pH of the eluent corresponded with the pK_a of VX (*ca.* 8.5) [7]. However, it was necessary to change the eluent composition owing to the co-elution of VX with the well known plasticizer tri-*n*-butyl phosphate (MW 266). Under the conditions used its TSP mass spectrum consisted mainly of the protonated molecular ion at *m/z* 267. This spectrum differed from that published by Barceló [13], which gave in addition to the ion at *m/z* 267 (relative intensity 40%) the ammonium adduct ion as the base peak. However, both spectra gave an isotope peak of the protonated molecular ion at *m/z* 268, which interfered with the protonated molecular ion of VX. Because tri-*n*-butyl phosphate is a water pollutant which has been found at relatively high levels (up to 10 ng/ml) in European rivers [22,23] chromatographic separation has to be achieved. In addition to its appearance in the environment, tri-*n*-butyl phosphate may also be considered as an analytical artifact [24] which is difficult to eliminate. Inspection of the mass spectrometer background at high multiplier gain revealed the presence of ions at *m/z* 267 and 268, probably due to tri-*n*-butyl phosphate originating from organic solvents, plastic tubing, etc. Therefore, another eluent composition was evaluated, consisting of acetonitrile, methanol and water. The eluent composition was optimized for the separation between tri-*n*-butyl phosphate and VX, leading to the mixture acetonitrile–methanol–0.25 *M* ammonium acetate (70:20:10). Because of the low water content, a relatively high ammonium acetate concentration was used, giving a good shielding of the acidic silanol groups of the column. The combination used also gave a short retention time, providing fast analyses. No adjustment of the pH with ammonia proved to be necessary when using such a high acetonitrile content. A typical chromatogram is presented in Fig. 2A.

In agreement with a recent paper [25], the chromatographic conditions described here may be used for several weeks without a noticeable decrease in efficiency, provided that the top of the column is repacked regularly. However, it must be noted that dissolution of silica material occurs under these conditions, which may ultimately lead to blocking of the TSP interface. During several weeks of operation a gradual increase in the optimum tip temperature occurred, caused by deposition of silica material at the heated capillary tip. This process could be reduced by setting the vaporizer temperature *ca.* 2°C below the optimum temperature.

Sensitivity

The sensitivity of the system was determined by single ion monitoring (SIM) at *m/z* 268 using ionization by the ammonium acetate buffer. Although VX could be determined using the above-described eluent composition, the high content of the organic modifier is a less preferential situation in TSP ionization [26]. In order to achieve a lower detection limit, the water content of the liquid in the TSP interface was

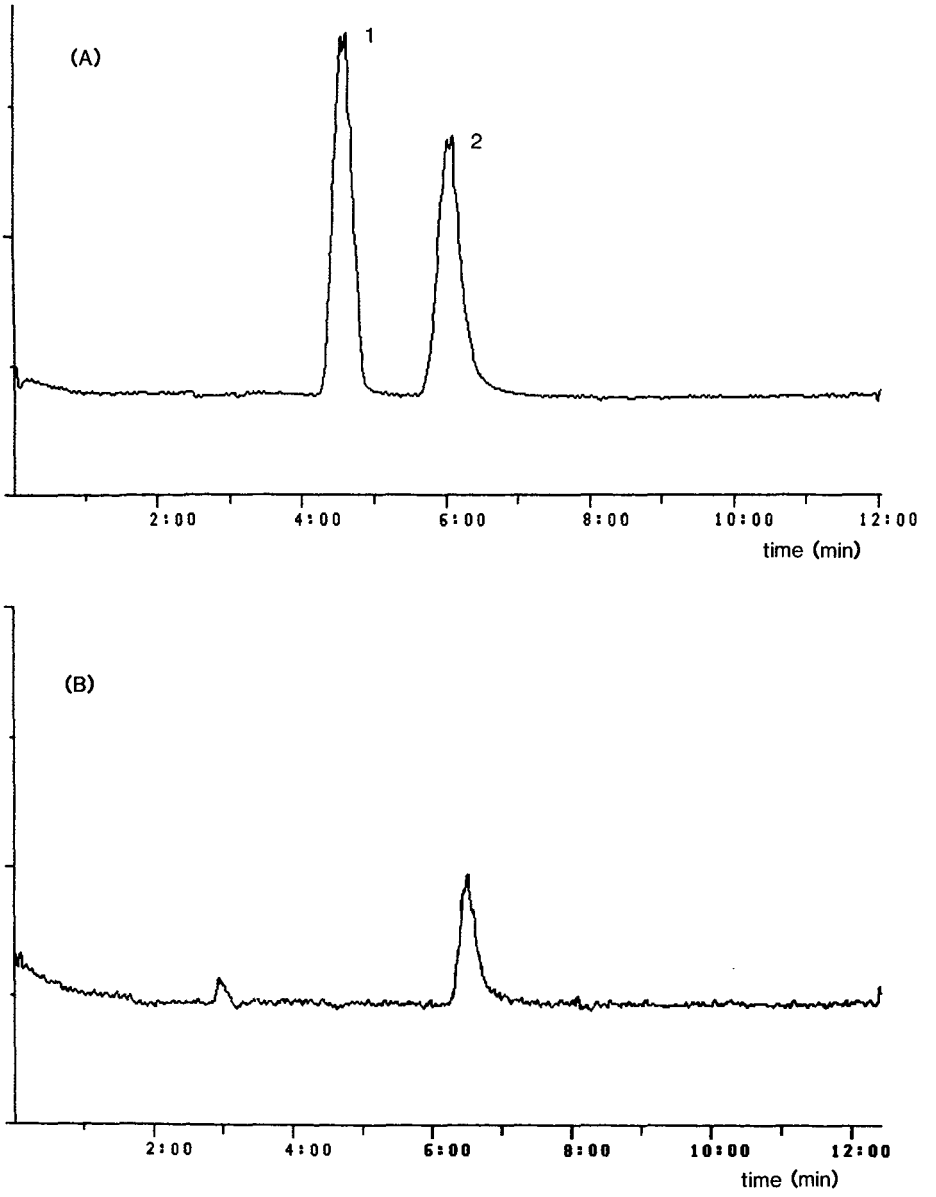

Fig. 2. Chromatographic behaviour of VX on a C_{18} column using acetonitrile–methanol–0.25 *M* ammonium acetate (70:20:10). (A) Separation between (1) tri-*n*-butyl phosphate and (2) VX. (B) Signal-to-noise ratio obtained after injecting 200 pg of VX.

increased by post-column addition of 0.05 *M* ammonium acetate, leading to acetonitrile–methanol–0.089 *M* ammonium acetate solution (50:14:36). Using an injection loop of 40 μl, an amount of 200 pg of VX dissolved in methanol could be detected with a signal-to-noise ratio above 10 (see Fig. 2B). The noise was partly

determined by the height of the mass spectrometer background signal at *m/z* 268. However, the result could be readily repeated on a day-to-day basis. Owing to the high percentage of organic solvents in the eluent, the degree of contamination of the ion source block increased daily, resulting in a gradual decrease in the signal-to-noise ratio after 1 week.

Preconcentration

The above-described sensitivity allows the determination of VX in water at concentrations down to 5 ng/ml. In order to detect VX in water below this level, preconcentration has to be carried out. The breakthrough volume of VX on Sep-Pak C_{18} cartridge was measured in demineralized water at pH 6.0 using a concentration of 4 μg/ml. After passing 60 ml through the cartridge, 1% of the original VX concentration was found in the effluent. A similar experiment was carried out with Rhine water (pH 7.5) spiked with VX at the same concentration. After 180 ml still no VX was observed in the effluent, indicating that the breakthrough volume is strongly dependent on the nature of the water. Based on these experiments, 50 ml was chosen as the maximum volume of water used for preconcentration experiments. The desorption of the Sep-Pak C_{18} cartridges with isopropanol and methanol was investigated. Methanol gave slightly better results. However, 2 ml of methanol were necessary to achieve an extraction efficiency above 80%. In order to reduce the volume of methanol to 1 ml, the cartridge was eluted in the reverse direction. In this way, recovery efficiencies of the procedure higher than 80% were normally obtained.

The possibility of sampling water in the field by C_{18} cartridges instead of transporting the water samples to a laboratory was investigated. Therefore, some preservation experiments were carried out. Decomposition of VX on Sep-Pak C_{18} cartridges was observed. The recovery efficiency decreased when the time between adsorption of VX and elution with methanol became longer than 15 min. After 1 day VX could no longer be detected. This was observed for a wide range of VX concentrations. Analysis by TSP–LC–MS showed that the following seven compounds were formed: ethylmethylphosphonic acid, ethylmethylthiophosphonic acid, S-2-diisopropylaminoethylmethylphosphonothioic acid, 2-diisopropylaminoethanol, 2-diisopropylaminoethanethiol, bis(2-diisopropylaminoethyl) sulphide and bis(2-diisopropylaminoethyl) disulphide. These decomposition products, due to the cleavage of the P–S, S–C and C–O bonds of VX, were also found during the hydrolysis of VX in the pH range 7–10 [7].

The preconcentration and preservation of VX were also investigated using Bond Elut C_{18} cartridges. Comparable adsorption and desorption efficiencies were obtained, but in contrast to Sep-Pak C_{18}, no decomposition was observed after storage overnight (18 h). Apparently Sep-Pak C_{18} cartridges contain active sites which catalyse the hydrolysis of VX. According to information given by the manufacturers, the difference between these two types of cartridges must be due to the procedures used for linking the C_{18} group to the silica surface. This led to a better shielding of the silanol groups in the case of the Bond Elut cartridges.

Applications

In order to investigate the applicability of the procedure, water samples from two major European rivers (Rhine and Meuse) were spiked with VX. In Fig. 3A the

chromatogram obtained using SIM at *m/z* 268 after concentration of 50 ml of Rhine water to 1 ml of methanol with a Bond Elut C_{18} cartridge is presented. Three peaks were observed, of which the middle one corresponded to tri-*n*-butyl phosphate. In Fig. 3B the result of the same experiment is presented after spiking Rhine water with VX at a level of 0.1 ng/ml. The contact time was *ca.* 15 min, in which hardly any hydrolysis of

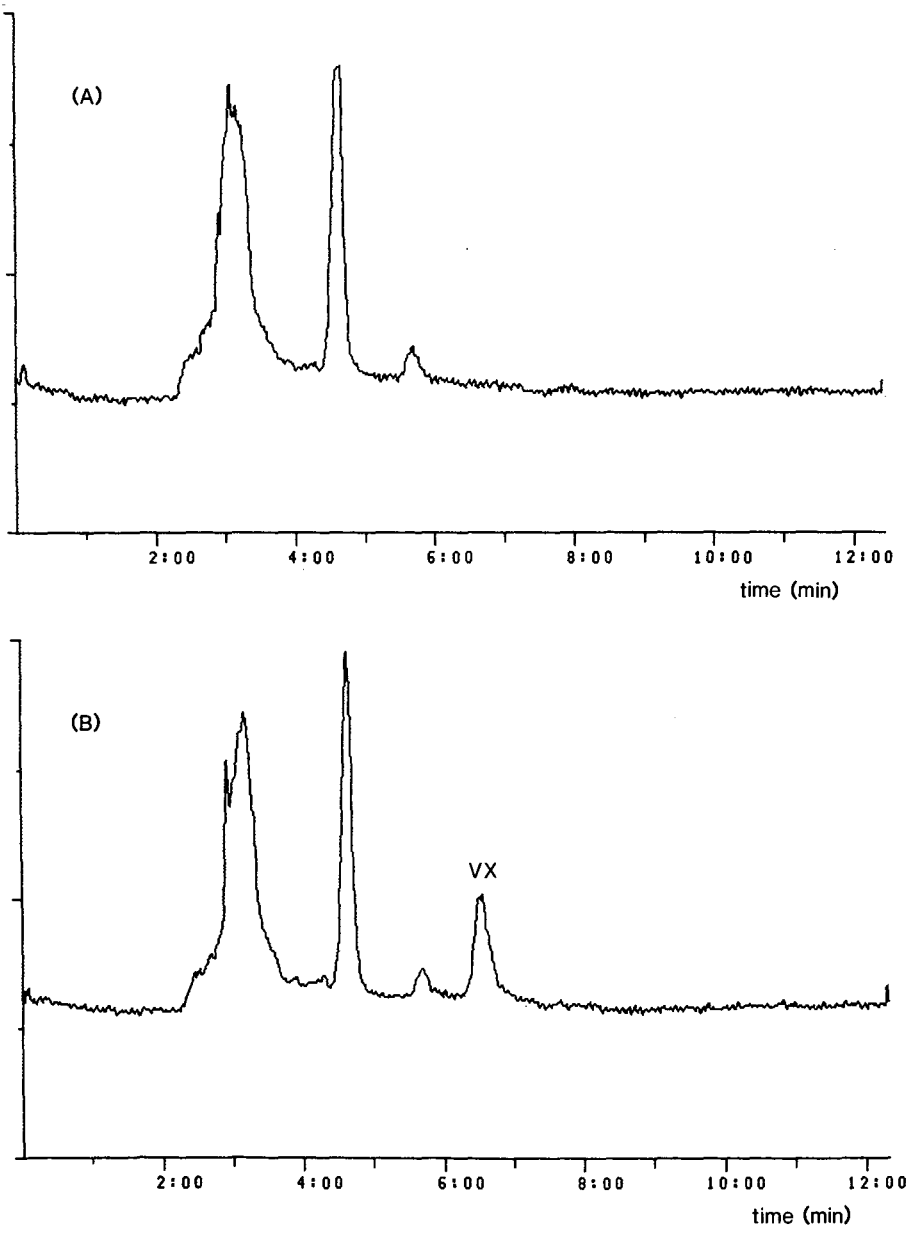

Fig. 3. Determination of VX in a 50-ml Rhine water sample. (A) Unspiked Rhine water; (B) Rhine water spiked with 0.1 ng/ml of VX.

the added VX took place. Based on the applied concentration step with an efficiency of 80% and the sample loop volume of 40 μl, the amount of VX injected corresponded to 160 pg. Similar results were obtained with water from the river Meuse. Both results demonstrate that it is possible to detect the presence of VX by TSP–LC–MS at a level of 0.1 ng/ml in *ca.* 15 min. Perhaps this level could be reduced even further by increasing the amount of water and/or further concentration of the methanol solution by evaporation. However, at lower levels problems with the selectivity are to be expected and more extensive clean-up procedures or techniques such as TSP–LC–MS–MS will be necessary.

VX has also determined successfully in water extracts of soil samples. Clayey soil samples spiked with VX were extracted as described by Verweij and Boter [5] by shaking at room temperature for 1 h either with an organic solvent mixture (chloroform–methanol) or with demineralized water. Extraction of the soil samples with water and determination of VX by TSP–LC–MS led to better quantitative results compared with the extraction with the organic solvent mixture and determination of VX by GC techniques (GC–MS and GC combined with a thermionic nitrogen–phosphorus detector). In three soil samples an average concentration of 3 mg/kg of VX was found in the water extracts, whereas in the organic solvent mixtures only 0.4 mg/kg of VX was found. Because also no interferences of soil constituents were observed, the analysis based on TSP–LC–MS provided a good alternative to the analysis based on GC techniques.

CONCLUSIONS

A rapid and simple procedure based on TSP–LC–MS was developed for the determination of the nerve agent VX. Combined with preconcentration, the procedure shows promise for the detection of VX in environmental samples at a relatively low level.

ACKNOWLEDGEMENTS

Water Transport Company Rijn-Kennemerland Ltd., Nieuwegein, The Netherlands, and Water Storage Corporation Brabantse Biesbosch Ltd., Werkendam, The Netherlands, are acknowledged for providing the water samples. Special thanks are due to L. Coppet of the DRET/CEB laboratory (Vert-le-Petit, France) for preparing the soil samples and to Mrs. M. Rautio of the Department of Organic Chemistry of the University of Helsinki (Finland) for organizing the round-robin verification exercise.

REFERENCES

1 J. A. F. Compton, *Military Chemical and Biological Agents, Chemical and Toxicological Properties*, Telford Press, Caldwell, NJ, 1987.
2 S. J. Lundin, in *SIPRI Yearbook 1989, World Armaments and Disarmament*, Oxford University Press, Oxford, 1989, pp. 99–132.
3 L. Ember, *Chem. Eng. News*, 64, No. 15 (1986) 8.
4 P. A. D'Agostino, L. R. Provost and J. Visentini, *J. Chromatogr.*, 402 (1987) 221.
5 A. Verweij and H. L. Boter, *Pestic. Sci.*, 7 (1976) 355.
6 J. Kaayk and C. Frijlink, *Pestic. Sci.*, 8 (1977) 510.
7 J. Epstein, J. J. Callahan and V. E. Bauer, *Phosphorus*, 4 (1974) 157.

8 A. Verweij, M. A. van Liempt-van Houten and H. L. Boter, *Int. J. Environ. Anal. Chem.*, 21 (1985) 63.
9 *Trace Analysis of Chemical Warfare Agents. C.4. Air Monitoring as a Means for the Verification of Chemical Disarmament. Part III. Further Development and Testing of Methods*, Ministry of Foreign Affairs of Finland, Helsinki, 1987.
10 W. K. Fowler and J. E. Smith, Jr., *J. Chromatogr.*, 478 (1989) 51.
11 K. B. Sipponen, *J. Chromatogr.*, 389 (1987) 87.
12 R. D. Voyksner and C. A. Haney, *Anal. Chem.*, 57 (1985) 991.
13 D. Barceló, *Biomed. Environ. Mass Spectrom.*, 17 (1988) 363.
14 A. Farran, J. de Pablo and D. Barceló, *J. Chromatogr.*, 455 (1988) 163.
15 L. D. Betowski and T. J. Jones, *Environ. Sci. Technol.*, 22 (1988) 1430.
16 E. R. J. Wils and A. G. Hulst, *J. Chromatogr.*, 454 (1988) 261.
17 J. Mañes Vinuesa, J. C. Moltó Cortés, C. Igualada Canas and G. Font Pérez, *J. Chromatogr.*, 472 (1989) 365.
18 *International Interlaboratory Comparison (Round Robin) Test for the Verification of Chemical Disarmament. F.1. Testing of Existing Procedures*, Ministry of Foreign Affairs of Finland, Helsinki, 1990.
19 A. G. Harrison, *Chemical Ionization Mass Spectrometry*, CRC Press, Boca Raton, FL, 1983, pp. 33–38.
20 D. Barceló, *Org. Mass Spectrom.*, 24 (1989) 219.
21 W. H. McFadden and S. A. Lammert, *J. Chromatogr.*, 385 (1987) 201.
22 A. P. Meijers and R. van der Leer, *Water Res.*, 10 (1976) 597.
23 J. I. Gómez-Belinchón, J. O. Grimalt and J. Albaigés, *Chemosphere*, 17 (1988) 2189.
24 B. S. Middleditch, *Analytical Artifacts* (*Journal of Chromatography Library*, Vol. 44), Elsevier, Amsterdam, 1989, p. 704.
25 B. Law and P. F. Chan, *J. Chromatogr.*, 467 (1989) 267.
26 D. J. Liberato and A. L. Yergey, *Anal. Chem.*, 58 (1986) 6.

Journal of Chromatography, 523 (1990) 163–172
Elsevier Science Publishers B.V., Amsterdam

CHROM. 22 784

Photochemical reaction coupled to solid-state peroxyoxalate chemiluminescence for the high-performance liquid chromatographic detection of compounds having weak chromophores

INGRID AICHINGER[a], GERALD GÜBITZ[a] and JOHN W. BIRKS*

Department of Chemistry and Cooperative Institute for Research in Environmental Sciences (CIRES), Campus Box 216, University of Colorado, Boulder, CO 80309 (U.S.A.)

(First received March 2nd, 1990; revised manuscript received August 30th, 1990)

ABSTRACT

The combination of a solid state peroxyoxalate chemiluminescence detection system with a post-column photochemical reactor is described for the detection of compounds exhibiting low UV absorbance. The photochemical reactor drives a sensitized photooxygenation reaction catalyzed by anthraquinones, whereby hydrogen is abstracted from analytes having weak C–H bonds to form H_2O_2. The H_2O_2 is detected by chemiluminescence in a detection system consisting of a short reaction column packed with bis-2,4,6-trichlorophenyloxalate and a quartz flow cell containing aminofluoranthene immobilized on glass beads. The applicability of this photochemical–chemiluminescence detection system is demonstrated for a variety of compounds of pharmaceutical interest.

INTRODUCTION

One of the limiting factors in current applications of high-performance liquid chromatography (HPLC) is the lack of sensitive and selective detectors for compounds having low UV extinction coefficients. Refractive index (RI) detectors have very poor sensitivity and almost no selectivity, while the use of electrochemical detectors is restricted to a small number of compounds having electrochemical activity.

Post-column reactions can be used to overcome some of these shortcomings. In recent years, photochemical reactions have been successfully applied to improve sensitivity and selectivity for a variety of compound classes [1–9]. Gandelman and Birks [10] developed a post-column photochemical reaction system using anthraquinones as "photooxygenation sensitizers" for the detection of "hydrogen atom-donating" compounds. The anthraquinone is spiked into the mobile phase of the HPLC system. When irradiated with UV light (366 nm), the electronically excited anthraquinone

[a] Present address: Institute of Pharmaceutical Chemistry, Karl Franzens University, Universitätsplatz 1, A-8010 Graz, Austria.

0021-9673/90/$03.50

molecule, Q*, abstracts a hydrogen atom from compounds having C–H bond strengths less than about 95 kcal mol^{-1} to form a semiquinone radical, QH·, as follows:

$$Q + h\nu \rightarrow Q^*$$
$$Q^* + RH \rightarrow QH\cdot + R\cdot$$

In the presence of oxygen, the semiquinone radical donates its hydrogen to O_2 to form the hydroperoxyl radical, $HO_2^{\cdot}$, which subsequently disproportionates to form H_2O_2:

$$QH\cdot + O_2 \rightarrow Q + HO_2^{\cdot}$$
$$HO_2^{\cdot} + HO_2^{\cdot} \rightarrow H_2O_2 + O_2$$

In the absence of competing reactions for HO_2 radicals, the concentration of H_2O_2 produced depends linearly on the concentration of the analyte, RH. As discussed below, linearity over more than two orders of magnitude was demonstrated. Details of the mechanism of this sensitized photoxygenation reaction have been discussed by Bolland and Cooper [11] and Wells [12,13]. In the absence of O_2, the semiquinone radicals disproportionate to Q and dihydroxyanthracene, QH_2, according to the reaction:

$$QH\cdot + QH\cdot \rightarrow Q + QH_2$$

Gandelman and Birks have developed detectors based on both aerobic [10] and anaerobic [14–16] reactions of anthraquinones for the detection of non-UV absorbing compounds. In the anaerobic system, the highly fluorescent dihydroxyanthracene, QH_2, is formed and detected by fluorescence, whereas in the aerobic system H_2O_2 is formed and detected by luminol chemiluminescence. The former detection system is referred to as "photoreduction fluorescence" (PRF) and the latter as "photooxygenation chemiluminescence" (POCL).

Here we report a simplification and improvement in the sensitivity of the POCL detection principle. The luminol chemiluminescence system for detection of H_2O_2 is replaced by a solid-state peroxyoxalate chemiluminescence system. In this system, the solid exalate ester is packed into a short column where it is delivered to the mobile phase by dissolution. The fluorophore required by the peroxyoxalate reaction for emission of light is immobilized on glass beads and packed in a flow cell contained in a photomultiplier tube housing [17]. Analytes eluting from the HPLC column produce H_2O_2 in the photochemical reactor. This H_2O_2 reacts with the oxalate ester to produce high energy intermediates which in turn excite the immobilized fluorophore. Emission of light by the fluorophore is detected by the photomultiplier tube. This solid-state chemiluminescence detection system has been successfully applied to the detection of H_2O_2 in surface water in connection with acid rain studies [18] and in combination with H_2O_2-producing immobilized enzyme reactors in flow injection analysis [19] and HPLC [20,21]. Poulsen and co-workers [22–24] also have applied this solid-state peroxyoxalate chemiluminescence system to the detection of anthraquinones separated by HPLC.

In this study, the POCL detection principle is adapted to detect hydrogen-atom-donating compounds using the photooxygenation sensitizers anthraquinone-2,6-disulfonate (AQDS) and 2-*tert.*-butylanthraquinone (t-BAQ) as additives to the mobile phase. The applicability of this approach has been investigated by examining a wide variety of compounds having only weak or no UV absorption. Detection limits were found to be in the range 200 pg to 5 ng.

EXPERIMENTAL

Chemicals

Anthraquinone-2,6-disulfonic acid disodium salt and (t-BAQ) were purchased from Aldrich. Bis-2,4,6-trichlorophenyl oxalate (TCPO) was synthesized according to the method of Mohan and Turro [25] and recrystalized from uvasol ethyl acetate and benzene. 3-Aminofluoranthene (Janssen, Beerse, Belgium) was immobilized on 40–80-μm controlled pore glass beads (350 Å pore size, Serva, Heidelberg, F.R.G.) as described by Gübitz *et al.* [17] Tris buffer (trizma base, reagent grade) was obtained from Sigma. HPLC-grade acetonitrile was purchased from Merck (Darmstadt, F.R.G.).

HPLC equipment

A Hitachi-Merck L-6000 HPLC pump was used for mobile phase delivery. Samples were injected by means of a Rheodyne 7125 injector with a 20-μl loop. Separations were carried out on a 250 × 4.6 mm I.D. LiChrosorb RP-18, 5-μm column or a 125 × 4.6 mm I.D. LiChrosorb-NH_2, 5-μm column (Merck). Flow-rates ranged from 0.5 to 1.0 ml min^{-1}.

Photochemical reactor

A 12.5-m length of PTFE tubing (0.33 mm I.D.) was crocheted into a cylinder [26], which surrounds a pyrex sleeve. This pyrex sleeve slides over an 8-watt "black lamp" (Sylvania Model E 8TS 1BLB). Aluminum foil was wrapped around the reactor to increase the photon flux, and the reactor was cooled by a fan.

TCPO delivery system

System A (Fig. 1a). A PTFE-coated column having an internal diameter of 3.6 mm and a length of 30 mm was packed with a mixture of finely ground TCPO and 40–80-μm glass beads, 70:30 (w/w). The reactor was inserted in line after the photochemical reactor, close to the detection cell.

System B (Fig. 1b). TCPO was dissolved from a TCPO column (40 × 4.6 mm I.D.) by acetonitrile–Tris buffer (99:1), delivered by a syringe pump at 0.25 ml min^{-1}. It was found that the three-way mixing tee should be installed as close as possible to the detector cell.

Detection cell

The detection cell was made from a 3-cm PTFE tube (1.2 mm I.D.) and packed with 40–80-μm glass beads immobilized with 3-aminofluoranthene. Underivatized beads were packed both in front of and following the immobilized fluorophore layer. The ends of the cell were connected with PTFE capillaries by means of Omnifit

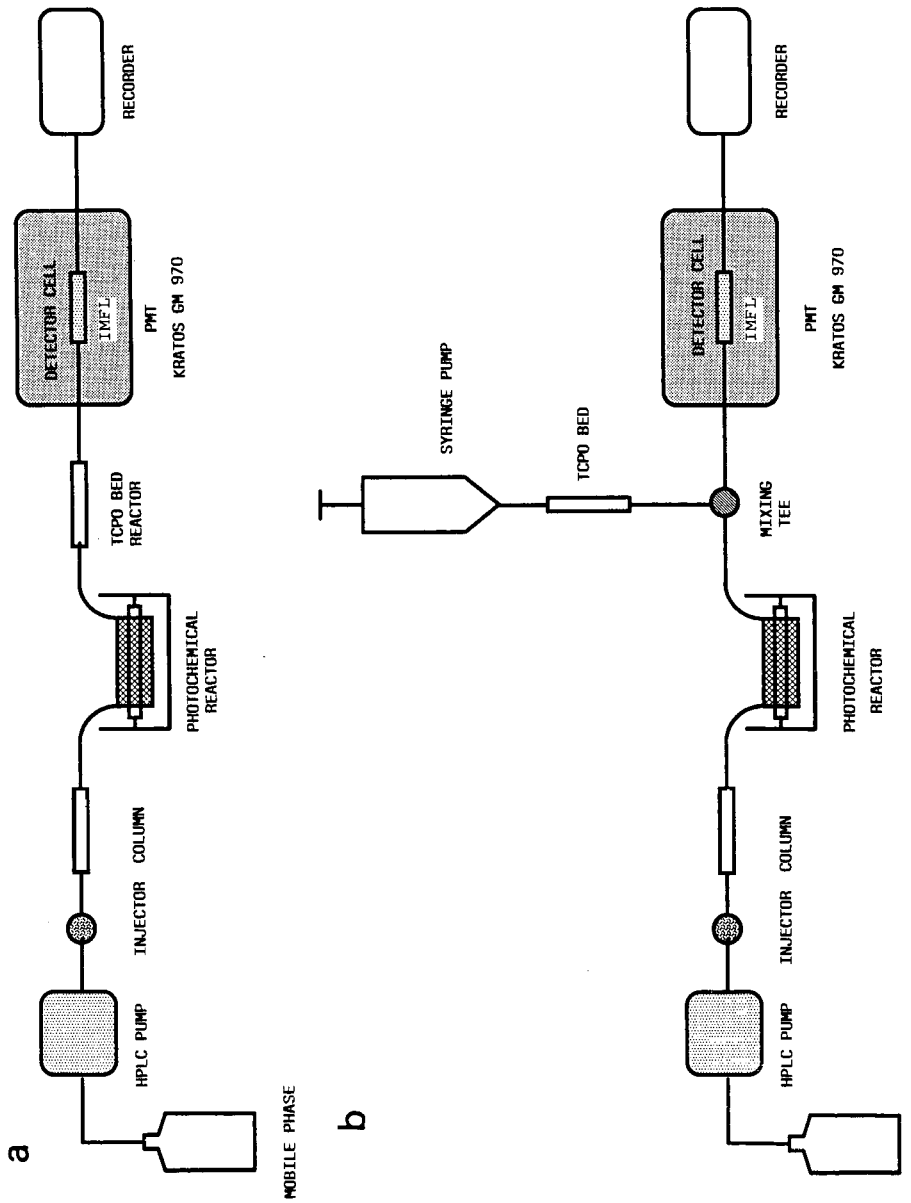

Fig. 1 (a) Instrumental setup for the in-line TCPO reactor (system A). One pump is required. (b) Instrumental setup for solid-state addition of TCPO using a separate TCPO reagent stream (system B). One mobile phase pump and one TCPO solvent addition pump are required. IMFL = Immobilized fluorophore; PMT = photomultiplier tube.

fittings. A frit cut from inert frit material was inserted at the outlet end of the cell. This cell was mounted directly in front of the photomultiplier tube of a Kratos FS 970 fluorescence detector in place of the original flow cell. The fluorimeter was operated with the light source off and without emission filters at a photomultiplier tube voltage of 900–1250 V.

RESULTS AND DISCUSSION

Detection system

As noted above, two different methods were used to deliver the oxalate ester (Fig. 1a and b). System A (Fig. 1a, solid TCPO reagent bed in line after the photoreactor) allows the elimination of one pump from the overall system. This is the simplest approach, but the mobile phase must be capable of solubilizing enough TCPO for good sensitivity. TCPO was mixed with glass beads in order to minimize the formation of a void volume and resulting degradation of chromatographic resolution as TCPO is consumed. System B (Fig. 1b, solid TCPO reagent bed not in line with the reactor) requires a second pump, but the reagent bed delivery of solvent for TCPO dissolution can be optimized. Another alternative, the use of a split flow system, has been described by Poulsen *et al.* [23]. In all cases, the fluorophore (3-aminofluoranthene) was used in an immobilized form, packed into the detector flow cell. This eliminates the need for a fluorophore delivery pump, minimizes the handling of toxic solutions, and minimizes the blank. It was found that the immobilized fluorophore could be used for months without loss in sensitivity.

The length of the photochemical reactor was optimized by determining the chemical yield of H_2O_2. This was done by comparing the signals for isopropanol standards with the signals of suitable H_2O_2 standards. A maximal signal-to-noise ratio was observed with a coil length of 12 m. When using a flow-rate of 0.5 ml min^{-1}, the residence time in the photochemical reactor was 240 s.

AQDS and t-BAQ were tested at various concentrations as photooxygenation sensitizers. The anthraquinones were added to the mobile phase to avoid the need for an additional pump. it has been found that anthraquinones in the mobile phase do not interfere with chromatographic separations at the concentrations used here [10]. Compared to AQDS, a higher chemical yield of H_2O_2 and enhanced sensitivity was obtained using t-BAQ. The signal-to-noise ratio was found to be optimal for a concentration of $4.8 \cdot 10^{-5}$ *M* t-BAQ.

The use of additional lamps arranged around the reactor resulted in an increase in the signals; however, because the background was also enhanced, the net signal-to-noise ratio was not improved. Improvement in sensitivity might be obtained by using a lamp with higher intensity in conjunction with further solvent purification to lower the background signal. Another approach, the use of immobilized anthraquinones packed in a quartz "photoreactor column", currently is under investigation as a potential means to lower background noise.

Limits of detection and reproducibility

Table I shows the limits of detection (signal-to-noise ratio 3) obtained for various analytes using systems A and B. Compared to RI detection, the sensitivity is about two orders of magnitude better. The detection limits obtained for cardiac

TABLE I

DETECTION LIMIT COMPARISONS FOR SYSTEMS A AND B

Conditions: HPLC flow-rate = 0.5 ml min^{-1}; mobile phase I = acetonitrile–water, 80:20; mobile phase II = acetonitrile–water, 53:47; mobile phase III = acetonitrile–water, 95:5; sensitizer = $4.8 \cdot 10^{-5}$ *M* 2-*tert.*-butylanthraquinone dissolved in the mobile phase; TCPO bed flow-rate in system B = 0.25 ml min^{-1}.

Compound	Mobile phase	Limit of detection (ng)	
		System A	System B
Isopropanol	I	5	2
Octanol	I	10	5
Nerol	III	30	0.5
Eugenol	III	50	1
Citronellol	III	50	1
Linalool	III	20	0.2
Anethol	I	10	5
Glucose	I	10	5
Fructose	I	10	5
Ascorbic acid	I	10	5
Hydrocortisone	I	10	2
Digoxin	I	10	2
Caffeine	II	5	2
Theophylline	II	10	4
Theobromine	II	5	2
Diprophylline	II	10	4
Etophylline	II	5	2
Proxyphylline	II	10	4
Aniline	I	0.5	0.2
Phenol	I	0.5	0.2
Thiamazol	I	10	4
Sulfaguanidine	I	10	4
Propylthiouracil	I	10	4
DOPA	I	1	0.5

glycosides, steroid hormones, purines, phenols and aromatic amines are slightly better or in the same range as UV detection, while the selectivity of detection is much greater. Alcohols or sugars, which cannot be detected with UV detectors because of the lack of chromophores show detection limits in the low nanogram range. We note that some compounds in Table I, *e.g.* aniline and phenol, also may be detected with high sensitivity using other detectors such as fluorescence or electrochemical detectors. Detection is two to three orders of magnitude more sensitive than the POCl system using luminol reported earlier [10]. This is due primarily to a lower background emission in the peroxyoxalate system when coupled to a photochemical reactor.

The POCL detection of glucose can be compared with enzymatic–chemiluminescence detection. Both detection techniques produce H_2O_2 as a surrogate analyte. In flow injection analysis, Pilosof and Nieman [27] obtained a detection limit of $7.5 \cdot 10^{-8}$ *M* or 13.5 ng (when corrected to $S/N = 3$) for glucose using luminol detection of H_2O_2 produced by reaction of glucose with glucose oxidase separated from the flow

stream by a microporous membrane. The detection limit reported here, is better when calculated as mass of analyte (5 ng), but poorer when calculated as concentration ($1.4 \cdot 10^{-6}$ *M*). Bostick and Hercules [28,29] reported limits of detection two times lower than those of Pilosof and Nieman using an immobilized enzyme technique. In recent work, Koerner and Nieman [30] detected β-D-glucosides by hydrolysis to β-D-glucose (using β-glucosidase) followed by an immobilized enzyme reactor and luminol chemiluminescence. Detection limits in chromatography as glucose was approximately 1 ng.

The optimal composition of the solvent for the chemiluminescence reaction was found to be 80–90% organic modifier. The application of the on-line TCPO reactor (system A) is therefore restricted to chromatography systems with this solvent composition range. With increasing water content, the mobile phase TCPO concentration decreases because of the insolubility in water, resulting in a decrease in sensitivity.

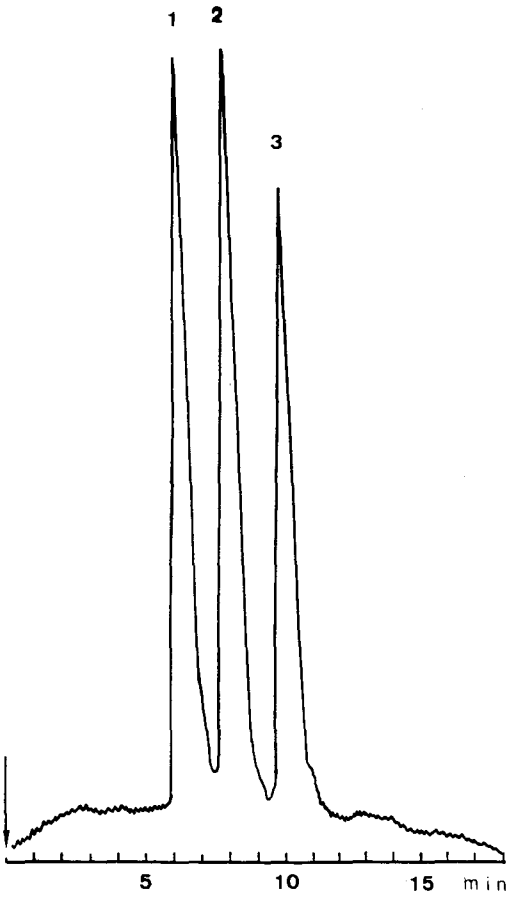

Fig. 2. Separation of terpene alcohols using system B; 1 = eugenol (25 ng), 2 = nerol (10 ng), 3 = citronellol (25 ng). Conditions: column, LiChrosorb RP-18, 5 μm, 250 × 4.6 mm I.D.; mobile phase, $4.8 \cdot 10^{-5}$ *M* 2-*tert.*-butylanthraquinone in 53% acetonitrile; flow-rate = 0.9 ml min^{-1}; TCPO bed flow-rate = 0.25 ml min^{-1}; TCPO delivery solvent, acetonitrile–tris buffer 99:1.

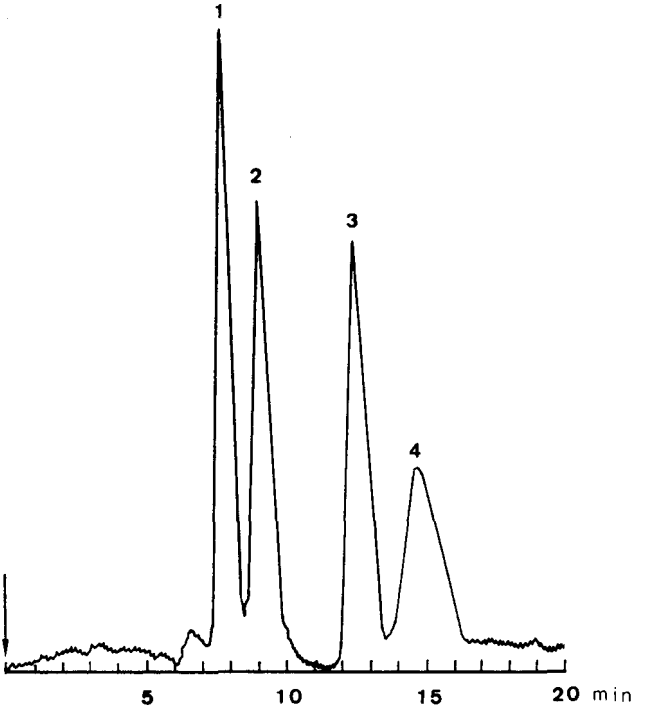

Fig. 3. Separation of purines using system B: 1 = caffeine (20 ng), 2 = theobromine (20 ng), 3 = diprophylline (40 ng), 4 = theophylline (100 ng). Conditions: column, LiChrosorb-NH_2, 5 μm, 125 × 4.6 mm I.D.; mobile phase, $4.8 \cdot 10^{-5}$ *M* 2-*tert.*-butyl-anthraquinone in 95% acetonitrile; flow-rate = 0.5 ml min^{-1}; TCPO bed flow-rate = 0.25 ml min^{-1}; TCPO delivery solvent, acetonitrile–tris buffer, 99:1.

This problem may be circumvented by using an oxalate ester of higher solubility, bis [4-nitro-2-(3,6,9-trioxadecyloxycarbonyl)phenyl] oxalate (TDPO) having a solubility in acetonitrile of 1 *M* for example [31], or by applying the dual pump system (system B), which is mobile phase independent. System B also makes possible the addition of catalyst to the reagent delivery solvent, which has been shown to enhance sensitivity and precision [22].

The linear range was checked by means of calibration curves for caffeine and eugenol. The calibration curves were found to be linear over a range of more than two orders of magnitude. The correlation coefficient for the range of 5–500 ng eugenol was 0.999. The relative standard deviation for 20 ng caffeine was 1.7% ($n=10$) and 0.9% ($n=7$) for 20 ng eugenol.

Chromatography

The presence of anthraquinone in the mobile phase did not interfere with the chromatographic separations. It can be assumed, however, that the quinones partition into the C_{18} stationary phase and modify its retention characteristics to some extent. For many separation problems, mobile phases containing 80–90% organic modifier can be applied. In these cases, system A, containing the peroxyoxalate reac-

tor in line, can be used. Mixing the TCPO with glass beads results in a negligible difference in band broadening relative to system B without an in-line TCPO bed.

Compatibility with the photocatalytic reaction system is another basic requirement for the mobile phase. The choice of the mobile phase is restricted to solvents which do not have abstractable hydrogen atoms. The addition of alcohols or cyclic ethers, for example, is not possible. Acetonitrile is the only solvent we have found to serve as a suitable organic modifer.

Fig. 2 shows the separation of some terpene alcohols. Because the mobile phase used was not compatible with the conditions required for the chemiluminescence reaction, the 2-pump system (system B) was applied. For the separation of purines shown in Fig. 3, a very high organic modifier concentration (95%) is required. This results in a more rapid dissolution of TCPO, and for this reason, system B is also preferable.

ACKNOWLEDGEMENTS

The authors thank the Austrian Fonds zur Förderung der wissenschaftlichen Forschung (FWF) for a visitor's grant to G. Gübitz, the Fulbright commission for a scholarship to I. Aichinger and the National Science Foundation for support of this project.

REFERENCES

1 A. H. M. T. Scholten, P. L. Welling, U. A. Th. Brinkman and R. W. Frei, *J. Chromatogr.*, 199 (1980) 239.
2 A. H. M. T. Scholten, U. A. Th. Brinkman and R. W. Frei, *Anal. Chim. Acta*, 114 (1980) 137.
3 J. W. Birks and R. W. Frei, *Trends Anal. Chem.*, 1 (1982) 361.
4 M. Uihlein and E. Schwab, *Chromatographia*, 15 (1982) 140.
5 P. J. Twitchett, P. L. Williams and A. C. Moffat, *J. Chromatogr.*, 149 (1978) 683.
6 I. S. Krull and W. R. LaCourse, in I.S. Krull (Editor), *Reaction Detection in Liquid Chromatography*, Marcel Dekker, New York, 1986, p. 303.
7 U. A. Th. Brinkman, *Chromatographia*, 24 (1987) 190.
8 R. Huber and K. Zech, in R. W. Frei and K. Zech (Editors), *Selective Sample Handling and Detection in HPLC (J. Chromatogr. Library*, Vol. 38A) Elsevier, Amsterdam, 1988, p. 413.
9 R. W. Schmid and C. Wolf, *J. Chromatogr.*, 478 (1989) 369.
10 M. S. Gandelman and J. W. Birks, *J. Chromatogr.*, 242 (1982) 21.
11 J. L. Bolland and H. R. Cooper, *Proc. Roy, Soc. (London), Ser. A*, 225 (1954) 405.
12 C. F. Wells, *Trans. Faraday Soc.*, 57 (1961) 1703.
13 C. F. Wells, *Trans. Faraday Soc.*, 57 (1961) 1719.
14 M. S. Gandelman and J. W. Birks, *Anal. Chem.*, 54 (1982) 2131.
15 M. S. Gandelman and J. W. Birks, U. A. Th. Brinkman and R. W. Frei, *J. Chromatogr.*, 282 (1983) 191.
16 M. S. Gandelman and J. W. Birks, *Anal. Chim. Acta*, 155 (1983) 159.
17 G. Gübitz, P. van Zoonen, C. Gooijer, N. H. Velthorst and R. W. Frei, *Anal. Chem.*, 57 (1985) 2071.
18 P. van Zoonen, D. A. Kamminga, C. Gooijer, N. H. Velthorst, R. W. Frei and G. Gübitz, *Anal. Chim. Acta*, 174 (1985) 151.
19 P. van Zoonen, D. A. Kamminga, C. Gooijer, N. H. Velthorst, R. W. Frei, E. Künssberg and G. Gübitz, *Anal. Lett.*, 19 (1986) 1949.
20 P. van Zoonen, C. Gooijer, N. H. Velthorst, R. W. Frei, J. H. Wolf, J. Gerrits and F. Flentge, *J. Pharm. Biomed. Anal.*, 5 (1987) 485.
21 H. Jansen, U. A. Th. Brinkman and R. W. Frei, *J. Chromatogr.* 440 (1988) 217.
22 J. R. Poulsen, J. W. Birks, G. Gübitz, P. van Zoonen, C. Gooijer, N. H. Velthorst and R. W. Frei, *J. Chromatogr.*, 360 (1986) 371.

23 J. R. Poulsen, J. W. Birks, P. van Zoonen, C. Gooijer, N. H. Velthorst and R. W. Frei, *Chromatographia*, 21 (1986) 587.
24 J. R. Poulsen and J. W. Birks, *Anal. Chem.*, 62 (1990) 1242.
25 A. G. Mohan and M. J. Turro, *J. Chem. Ed.*, 51 (1974) 528.
27 J. R. Poulsen, K. S. Birks, M. S. Gandelman and J. W. Birks, *Chromatographia*, 22 (1986) 231.
27 D. Pilosof and T. A. Nieman, *Anal. Chem.*, 54 (1982) 1698.
28 D. T. Bostick and D. M. Hercules, *Anal. Lett.*, 7 (1974) 347.
29 D. T. Bostick and D. M. Hercules, *Anal. Chem.*, 47 (1975) 447.
30 P. J. Koerner, Jr. and T. A. Nieman, *J. Chromatogr.*, 449 (1988) 217.
31 K. Imai, H. Nawa, M. Tanaka and H. Ogata, *Analyst*, 111 (1986) 209.

Journal of Chromatography, 523 (1990) 173–188
Elsevier Science Publishers B.V., Amsterdam

CHROM. 22 703

On-line sample clean-up of fermentation broths and substrates prior to the liquid chromatographic separation of carbohydrates

G. MARKO-VARGA*
Department of Analytical Chemistry, University of Lund, P.O. Box 124, 221 00 Lund (Sweden)
E. DOMINGUEZ[a] and B. HAHN-HÄGERDAL
Department of Applied Microbiology, University of Lund, P.O. Box 124, 221 00 Lund (Sweden)
L. GORTON
Department of Analytical Chemistry, University of Lund, P.O. Box 124, 221 00 Lund (Sweden)
and
H. IRTH, G. J. DE JONG, R. W. FREI[b] and U. A. Th. BRINKMAN
Department of Analytical Chemistry, Free University, De Boelelaan 1083, 1081 HV Amsterdam (The Netherlands)
(Received May 14th, 1990)

ABSTRACT

A coupled precolumn set-up is described for the clean-up of fermentation broths and substrates of hydrolysed lignocellulose prior to the analysis of carbohydrates. Matrix components cause severe problems owing to irreversible adsorption, increased back-pressure in the analytical column and interferences with the detection of the analytes. Sep-Pak (quaternary ammonium and amino) phases were used for the removal of brown reaction compounds and aldehydes. Non-polar (aromatic) compounds, phenolic acids and their derivatives and metal ions were removed using the hydrophobic polymer PLRP-S and a mixed cation–anion-exchange phase, respectively. Breakthrough volumes on the four precolumns were measured for fifteen model compounds normally present in hydrolysed lignocellulose. Applications to real samples illustrate the increased detectability in refractive index and UV detection and in detection systems using immobilized enzyme post-column reactors with UV and electrochemical detection.

INTRODUCTION

The increasing demand for the characterization and quantification of substrates and metabolites in complex biological matrices and for the screening of large numbers of samples has stimulated progress with new detection principles in these areas. The selectivity and sensitivity in column liquid chromatographic (LC) detection

[a] On leave from the Department of Pharmacy, Food Analysis and Nutrition, University of Alcala de Henares, Madrid, Spain.
[b] Author deceased.

0021-9673/90/$03.50

modes are crucial factors that have to be optimized in the study of sample composition in fermentation processes [1–3]. The concentration levels of interfering compounds vary strongly in the fermentation process as a result of the biological activity in the cells and the media. Often obtaining good resolution is the most time-consuming step in setting up a chromatographic system. There is therefore an increasing tendency to introduce selectivity in the sample preparation and/or in the detection step in order to facilitate the separation procedure [4]. A precolumn sample clean-up step before injection can be introduced by the use of solid-phase extraction [5–7] on either disposable or reusable precolumns in a coupled column set-up. With complex samples both pre- and post-column selectivity are required and can correspondingly be introduced.

Sample clean-up can be accomplished either (i) by sorption of the analyte on the clean-up phase and elution of most of the interfering compounds, which can be performed in one step or in several steps in which the eluent strength gradually increases linearly or in a step gradient, the strongest eluent desorbing the analyte, or (ii) by sorption of the interfering compounds on the precolumn, while the analyte has no affinity to bind to the column material and elutes directly. If there is a large variety of interfering compounds, several clean-up columns with different sorption characteristics have to be used.

Waste water from the pulp industry contains a hemicellulose fraction with high levels of lignocellulose, oligosaccharides and various monosaccharides as the major sugar constituents [8,9]. This fraction can be used as a substrate for ethanol production by fermentation with *Saccharomyces cereviseae* [10]. The acid hydrolysis of wood will produce a complex mixture, containing a wide variety of compounds present in the technical substrate used in the fermentation process (see Fig. 1). Moreover, during this fermentation step, the level of toxic compounds may be decreased or even reduced to zero, which is also beneficial from an environmental point of view. This paper describes the removal of a large number of interfering compounds present in a hydrolysed lignocellulose substrate and in fermentation broths that would otherwise severely disturb the determination of the carbohydrate composition. Fifteen test compounds (for structures, see Fig. 2) are sorbed in a coupled pre-column set-up.The precolumns used are both disposable cartridges and small stainless-steel columns packed with silica and/or polymer-based stationary phases. After passage through four precolumns, the sugars in hydrolysed waste water and in the fermentation broths can be introduced into a conventional LC system.

The sugars are monitored either directly with refractive index (RI) or UV (195 nm) detection or with a post-column detection [11,12] system using a co-immobilized enzyme reactor (CIMER) [2] and UV or electrochemical detection.

EXPERIMENTAL

Apparatus

A schematic diagram of the experimental LC set-up is given in Fig. 3. The apparatus consists of the three high-pressure pumps (two Model 2150 from LKB, Bromma, Sweden, and one Model 600 from Waters Assoc., Milford, MA, U.S.A.), four six-port valves [one Waters Assoc. U6K, one Rheodyne (Cotati, CA, U.S.A.) Model 7000 and two Rheodyne Model 7045], denoted I, II, III and IV in Fig. 3, two

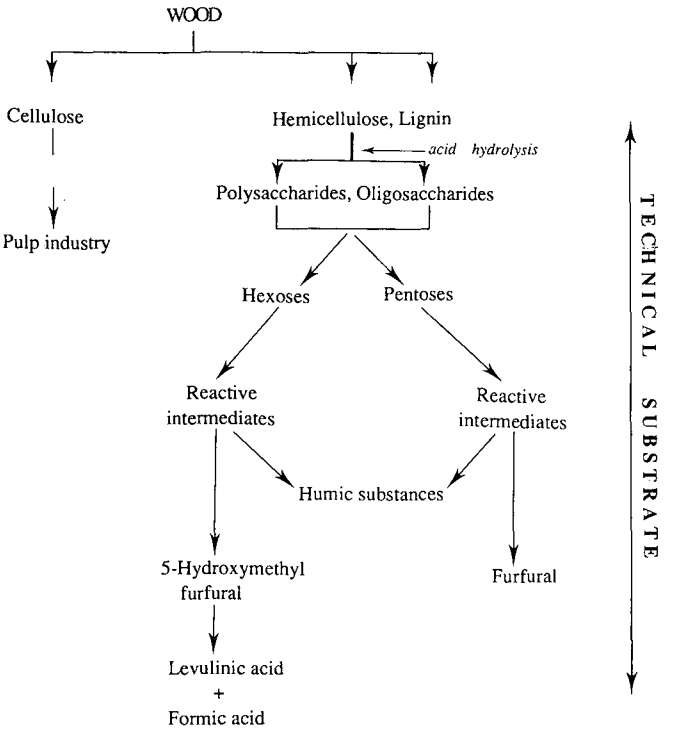

Fig. 1. Breakdown scheme of the acid hydrolysis of lignocellulose.

injection loops (1000 and 10 μl), a low-dead-volume mixing T-piece, a recorder (LKB 2210), an RI detector (Model 2142, LKB) and a UV spectrophotometer (Model SPD-6A, Shimadzu, Kyoto, Japan). The laboratory-built amperometric flow cell was a three-electrode cell of the wall-jet type using a modified graphite working electrode, a platinum auxiliary electrode and an Ag/AgCl reference electrode (Model K 801, Radiometer, Copenhagen, Denmark), kindly provided as a gift by Dr. T. Buch-Rasmussen (Radiometer). The working electrode was a chemically modified electrode (CME) modified with a phenoxazine derivative [13]; the mediator was immobilized by adsorption as described previously [14,15]. The applied potential used throughout this work was 0 mV *vs.* Ag/AgCl, controlled by a potentiostat (Zäta Elektronik, Lund, Sweden). The eluent and the reagent solution were pumped at a flow-rate of 0.6 and 0.1 ml/min, respectively, unless indicated otherwise. The CIMER was operated at room temperature; it has a volume of 295 μl (23.5 × 4.0 mm I.D.).

The analytical column (300 × 7.8 mm I.D.), a ligand-exchange column in Pb(II) form (Aminex HPX-87 P), was run at 65°C and was prethermostated as described previously [7]. Precolumn 3 (PLRP-S, Polymer Labs., Church Stretton, Shropshire, U.K.; particle size 10 μm, pore size 100 Å, 50 x 4.5 mm I.D., packed under high pressure) and precolumn 4 containing a 1:1 mixture of an anion- and cation-exchange support (Aminex A-29, Bio-Rad Labs., Richmond, CA, U.S.A., and Aminex HPX-87H, both with 9-μm particle size, 50 × 4.0 mm I.D., packed under

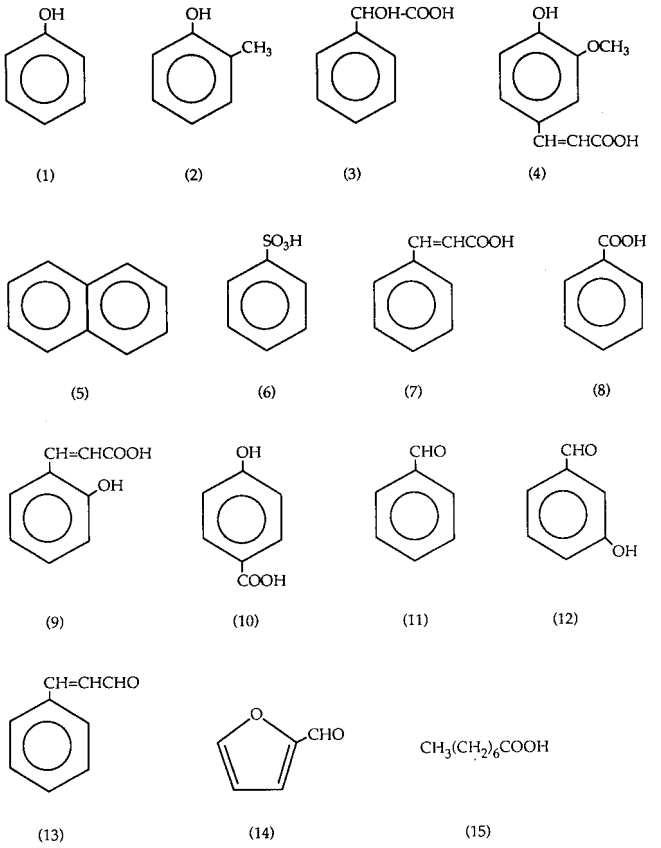

Fig. 2. Structures of the fifteen model compounds investigated. 1 = Phenol; 2 = *o*-cresol; 3 = mandelic acid; 4 = ferulic acid; 5 = naphthalene; 6 = benzenesulphonic acid; 7 = cinnamic acid; 8 = benzoic acid; 9 = *o*-coumaric acid; 10 = *p*-hydroxybenzoic acid; 11 = benzaldehyde; 12 = *m*-hydroxybenzaldehyde; 13 = cinnamaldehyde; 14 = furfural; 15 = caprylic acid.

high pressure) were all packed with polymer-based materials. Precolumns 1 and 2 were Sep-Pak (Waters–Millipore, Milford, MA, U.S.A.) cartridges packed with a quaternary ammonium (QMA) and a primary amino-type silica-based stationary phase, respectively, both with a particle size of 40 μm. Breakthrough curves for the different precolumn stationary phases were recorded using UV detection at 225 nm (standard solutions of the model compounds) or 600 nm (spent sulphite liquor).

Preparation of the CIMER

The co-immobilization of mutarotase [MT, E.C. 5.1.3.3, from porcine kidney, Sigma (St. Louis, MO, U.S.A.), cat. No. M-4007], glucose dehydrogenase [GDH, E.C. 1.1.1.47, from *Bacillus megaterium*, Merck (Darmstadt, F.R.G.), cat. No. 13732] and galactose dehydrogenase (GADH, E.C. 1.1.1.48, from recombinant *Escherichia coli* using *Pseudomonas fluorescens* gene, Sigma, cat. No. G-6637) was done covalently with glutaraldehyde as described previously [15]. The support used was a CPG-10 glass (particle size 37–74 μm, pore size 500 Å; Serva, Heidelberg, F.R.G.). In the

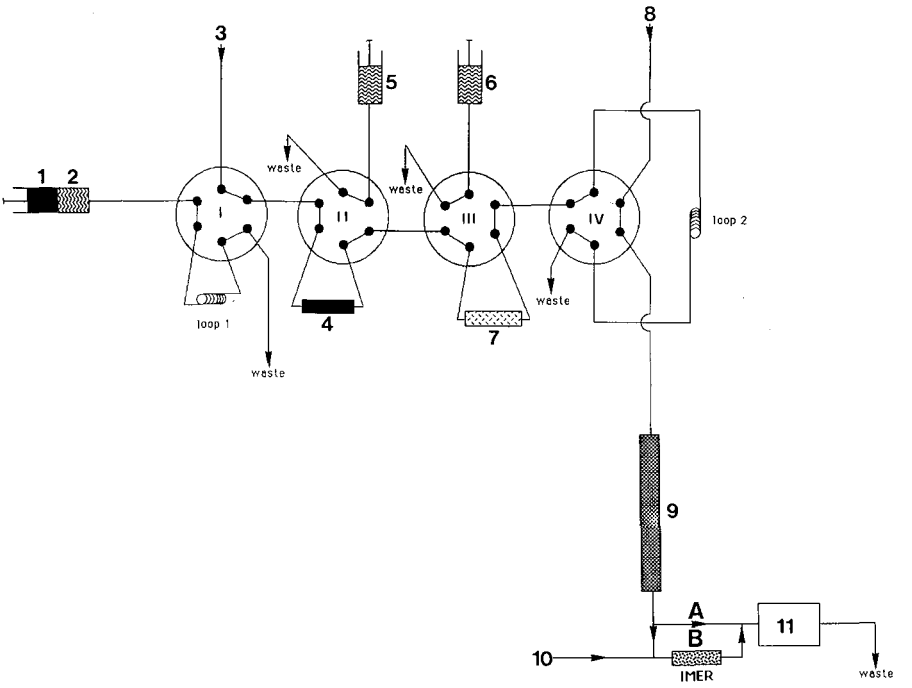

Fig. 3. Scheme of the precolumn and analytical system with (A) direct RI or UV monitoring and (B) CIMER post-column reaction detection. 1, Sep-Pak QMA precolumns; 2, Sep-Pak amino precolumn; 3, preconcentration pump; 4, PLRP-S precolumn; 5, regeneration solvent [methanol–water (80:20)]; 6, regeneration solvent (nitric acid); 7, mixed cation–anion-exchange precolumn; 8, LC pump; 9, analytical column; 10, reagent pump; 11, detector; I and IV, injectors; II and III, switch valves.

CIMER the sugars react with the cofactor NAD^+ (nicotinamide adenine dinucleotide), yielding stoichiometric amounts of NADH, reflecting the sugar levels in the sample [2]. The enzymatically produced NADH is monitored either by UV absorbance (340 nm) or by electrochemical detection, which involves two selective steps. In the amperometric detector cell, NADH is electrocatalytically oxidized at 0 mV *vs.* Ag/AgCl at an electrode chemically modified with a phenoxazine derivative [16].

Fermentation conditions

A slowly stirred 250-ml beaker sealed with a rubber stopper was inoculated with 145 g/l of baker's yeast, *Saccharomyces cereviseae* (dry weight). Spent sulphite liquor (SSL), sodium based, was kindly supplied by Modo (Örnsköldsvik, Sweden). The only pretreatment of the substrate was the adjustment of the pH to 6.0 with sodium hydroxide and the addition of fermentation nutrients: 0.25% (w/v) yeast extract (Difco, Detroit, MI, U.S.A.) and 0.025% (w/v) $(NH_4)_2HPO_4$. After 30 min and 4 h, samples were taken, diluted and filtered prior to analysis.

Clean-up procedure

The samples were diluted 25–200-fold with water before adjusting the pH to 6–7 with sodium hydroxide. The sample was then filtered through a 45-μm sterile mem-

brane filter to remove solids. Loop I (1000 μl) was filled by flushing a 1.5–2 ml sample through the QMA (precolumn 1) and amino (precolumn 2) clean-up columns (see Fig. 3). By switching valve I the sample was transported on-line onto the PLRP-S column (precolumn 3) and then onto the mixed anion–cation-exchange column (precolumn 4). The purified sample was trapped in a 10-μl loop connected to valve IV and injected into the analytical system.

Chemicals

HPLC-grade water was produced in a Milli-Q system (Millipore, Bedford, MA, U.S.A.) and was used throughout this work. Water was used as the mobile phase in the coupled clean-up precolumns and in the separation column. A 0.7 *M* phosphate buffer (pH 7.0) containing 14 m*M* NAD^+ and 7 m*M* EDTA was used as the reagent stream for the enzymatic reaction.

Model compounds

The model compounds and test mixtures were prepared by dissolving appropriate amounts in water and in water–ethanol mixtures. NADH was diluted with buffer (0.1 *M* phosphate buffer, pH 7.0) for the preparation of standard solutions that were run in the flow-injection mode. The NADH concentrations were determined by UV absorption spectrometry at 340 nm.

RESULTS AND DISCUSSION

Nature of the fermentation broth and substrate

The technical substrate, spent sulphite liquor (SSL), is a by-product from the sulphite pulping process. In this investigation it was used as a model substrate for the fermentation of lignocellulose hydrolysates, as it contains soluble sugars. SSL is in some ways comparable to other wood hydrolysates with a complex composition [17–20]. Lignin has a complicated aromatic polymer structure and consists of dehydrogenated polymers of coriphenyl, sinapyl and *p*-coumaryl alcohol. Its acid hydrolysis yields a wide variety of phenolic derivatives [20–22]. Further, the fermentation process itself can cause, depending on the microorganisms involved, a considerable increase in the complexity of the sample.

During the hydrolysis of wood, humic substances are produced, which are believed by some workers to be related to a direct decomposition product of lignin and by others to be compounds produced by microorganisms [20,23–25]. They are dark brown, amorphous and colloidal compounds with a complex composition and incompletely known structure. The major constituents are humic acids, which are polymers of hydroxyphenols and hydroxybenzoic acids, *i.e.*, aromatic polymers of high molecular weight to which an unusually large number of functional groups are attached. Humic substances are also coupled to proteins, peptides, amino acids and aliphatic and aromatic compounds [24].

The hydrolysis of wood further results in browning reactions, which are also very common in fruit juices, milk products, sugar cane molasses and microbial growth media. The compounds formed during browning reactions give rise to the dark brown colour of the SSL and, later, also of the broth. The presence of browning-reaction compounds is known to affect the growth and metabolism of various mi-

croorganisms [20,26]. Furfural, maltol and 5-hydroxymethylfurfural are examples of browning-reaction products known to inhibit fermentation processes [23]. Reactions of amines, amino acids and proteins with sugars, aldehydes and ketones, known as Maillard reactions, also produce browning compounds [27,28]. They involve a condensation reaction between the carbonyl groups of carbohydrates and the α-amino groups of amino acids or proteins. This initiates the formation of Schiff's bases, which further undergo a cyclization to the corresponding N-substituted glycosylamines [29]. These reactions can take place in both acidic and alkaline media. The browning reactions are mainly caused by monosaccharides, but can also proceed in the presence of reducing disaccharides such as maltose and lactose. Non-reducing sugars, oligosaccharides and polysaccharides cannot participate unless the glycosidic bonds are cleaved, releasing reducing (mono)saccharides [30]. Further series of rearrangements of the N-substituted glucosamine can occur and lead to 1-amino-1-deoxy-2-ketose derivatives, causing the formation of brown pigments. Caramelization is another process in which sugars, in the absence of proteins and amino acids heated over their melting-points, darken to a dark brown colour. These reactions take place under both alkaline and acidic conditions. The chemical composition of the reaction products is complex and little understood. Phenolic compounds can be catalysed enzymatically to form brown melanins by polyphenolic oxidase, also known as phenolase (E.C. 1.10.3.1).

Precolumn system

The matrix components in SSL cause major problems in sugar determination. Apart from obscuring the sugar peaks in both UV and RI detection, they cause severe problems due to irreversible adsorption and increased back-pressure and they also have an inhibitory effect on the enzyme activity in the CIMER [16]. We have developed a precolumn clean-up procedure in order to remove these matrix components. Fifteen model compounds known to be breakdown products in lignin hydrolysates were chosen to determine breakthrough volumes on the stationary phases investigated (for the overall scheme, see Fig. 4).

Removal of brown compounds (precolumn 1). The selective clean-up of humic-containing waters on both reusable [31] and disposable [32,33] precolumns has been reported. The removal of disturbing brown components such as humic substances and lignin breakdown products must essentially be complete. These compounds adsorb strongly to the polymeric stationary phase in the analytical column and interact with the analytes in an unpredictable way, which causes an increasing back-pressure and errors in quantitative evaluations.

The sorption capacity of the compounds causing the brown colour in SSL, which has a dry weight of 5 mg/ml, was determined for different disposable clean-up columns (Sep-Pak); the results are given in Table I. The anion-exchange material was found to have the highest capacity (27 ml/g), indicating the anionic characteristics of the brown compounds at pH 6.0. The smaller capacities for the QMA phase at lower dilution factors (50–100) can be explained by the fact that, despite the high dilution, overloading of the stationary phase rather than insufficient retention determines the breakthrough. The other ten Sep-Pak phases with varying functionalities did not exhibit sufficient affinity for the browning-reaction compounds ($V_b < 2$ ml, see Table I).

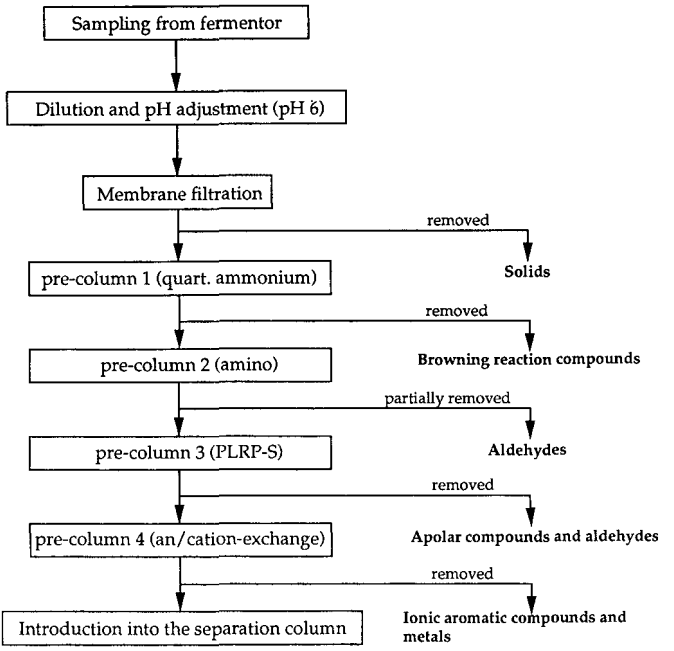

Fig. 4. Scheme of the clean-up procedure.

Sorption of aldehydes on the amino phase (precolumn 2). Many aldehydes have an inhibitory effect on the enzyme activity and also may interfere with the separation and UV or RI detection of the carbohydrates. Aromatic aldehydes are most often separated by reversed-phase chromatography using silica-based C_{18} supports [34,35]. They can also be oxidized on-line on a polymeric anion-exchange resin in the permanganate form [36], or reduced by immobilized borohydride on the same support [37]. These solid-phase extraction columns are used in the precolumn mode.

As aldehydes preferentially bind to amino-modified stationary phases, probably owing to Schiff's base formation, we investigated the use of a Sep-Pak amino-bonded stationary phase for their removal. This step was introduced to increase the sorption properties of interfering aldehydes. The breakthrough volumes on a precolumn (30 × 4.0 mm I.D.) packed with this stationary phase were 3–5 ml for all the aldehydes (0.1 m*M*) investigated (see Table II). No significant differences were found in the breakthrough volume using 1 m*M* concentrations of aldehydes, indicating that this breakthrough is caused by chromatographic elution.

Sorption of model compounds on the PLRP-S phase (precolumn 3). Breakthrough experiments were run with fifteen model compounds (see Fig. 2) in either pure water (the water-soluble compounds) and/or in ethanol–water (1:99 or 5:95, v/v) (all compounds). In actual practice, the ethanol content after fermentation is about 5%; consequently, the breakthrough was investigated under these conditions. The breakthrough volumes are given in Table II. The breakthrough volume of most of these compounds decreases when the alcohol level increases. All model compounds except caprylic acid have an aromatic skeleton with various functional groups at-

TABLE I

BINDING CAPACITY OF BROWNING-REACTION COMPOUNDS IN SSL ON DIFFERENT SEP-PAK STATIONARY PHASES

Column, 30 × 4.0 mm I.D.; particle size, 40 μm; flow-rate, 1.0 ml/min; pH of the sample solution, 6.0; relative standard deviation, 3–8% ($n = 5$).

Column type	Capacity (ml/g stationary phase)	Dilution factor of SSL sample
QMA	27	200
	14	100
	6	50
C_{18}	1	100
Primary amino	2	100
Florisil	1	100
Carboxymethyl	1	100
Silica	1	100
Cyano	1	100
Diol	1	100
Alumina A	0	100
Alumina B	1	100
Alumina N	1	100

tached to it. Benzenesulphonic acid is the only compound that has no affinity for the hydrophobic phase regardless of the eluent composition, *i.e.*, it is too strong an acid although it contains an aromatic ring. *o*-Cresol, with an additional methyl group, is more hydrophobic than phenol and is therefore retained more strongly on PLRP-S. *p*-Hydroxybenzoic acid, *o*-coumaric acid, mandelic acid and ferulic acid all contain a phenol structure with an additional carboxylic group. The introduction of a charged group increases the polarity of the molecule and decreases the binding strength. Mandelic acid contains an ethyl group between the aromatic ring and the carboxylic group which, as the breakthrough volumes show, does not seriously influence the hydrophobicity of the molecule compared with *p*-hydroxybenzoic acid. However, *o*-coumaric acid and ferulic acid are more strongly sorbed owing to the aliphatic double bonds in these molecules. The additional methoxy group in ferulic acid does not increase the hydrophobicity. The breakthrough volumes further show that the aldehyde group does not contribute as much to the polarity of the molecule as an alcohol or carboxylic group; all aldehydes except furfural show good binding properties for PLRP-S. As could be expected, naphthalene, which represents the hydrophobic class of compounds present in the broths, is the most strongly bound of all the compounds investigated.

Sorption of model compounds and metal ions on polymeric anion–cation-exchange resin (precolumn 4). All phenolic derivatives and acids except benzenesulphonic acid have pK_a values around 4 or higher (see Table II). When using pH 6 in our experiments, all acids will be deprotonated; consequently, they are well retained on the anion-exchange phase, as shown in Table II. As is to be expected, increasing the ionic strength in most instances decreased the sorption capacity owing to a competitive elution mechanism. The breakthrough volume for naphthalene and all aldehydes on this phase is low.

TABLE II

BREAKTHROUGH VOLUME (V_b) OF FIFTEEN MODEL COMPOUNDS ON PRIMARY AMINO, POLYMERIC (PLRP-S) AND POLYMERIC ANION-EXCHANGE SUPPORTS

Column size, 30 × 4.0 mm I.D.; analyte concentrations were 0.1 m*M*.

Analyte	pK_a	V_b (ml)						
		Amino[a]	PLRP-S			Aminex A-29		
			A[b]	B[c]	C[d]	A[b]	B[c]	D[e]
Phenol	9.98	–[f]	13	11	8	3	2	1
o-Cresol	10.20	–	37	30	26	2	1	1
Ferulic acid		–	n.d.[g]	24	13	n.d.	352	64
Mandelic acid	3.85	–	4	4	2	412	380	50
Benzenesulphonic acid	0.70	–	0	0	0	136	80	39
Cinnamic acid	3.89	–	n.d.	78	60	n.d.	486	148
o-Coumaric acid	4.61	–	n.d.	26	16	n.d.	324	62
Benzoic acid	4.19	–	n.d.	20	13	n.d.	209	106
p-Hydroxybenzoic acid	4.48/9.32	–	n.d.	2	1	n.d.	352	150
Caprylic acid	4.85	–	n.d.	20	10	n.d.	33	18
Benzaldehyde		5	n.d.	40	19	n.d.	0	0
Furfural		3	5	3	2	0.	0	0
m-Hydroxybenzaldehyde		4	n.d.	4	3	n.d.	2	1
Cinnamaldehyde		5	n.d.	62	28	n.d.	0	0
Naphthalene		–	n.d.	392	309	n.d.	3	3

[a] In water–ethanol (99:1, v/v) containing 1 m*M* sodium sulphite and 1 m*M* sodium acetate.
[b] In water.
[c] In water–ethanol (99:1, v/v).
[d] In water–ethanol (95:5, v/v).
[e] In water–ethanol (95:5, v/v) containing 1 m*M* sodium sulphite and 1 m*M* sodium acetate.
[f] Not determined.
[g] Not dissolvable.

Metal ions in the samples have to be quantitatively removed becaused the analytical column is a ligand-exchange column with Pb(II) ions bound on the sulphonated polystyrene–divinylbenzene support. If other cations such as (Ni(II), Fe(II) or Co(II), or higher concentration of H^+, are present, ion exchange will take place, which will result in a mixed ligand-exchange phase. This will influence the capacity factors of the analytes in an unpredictable way. In most instances the capacity factors will decrease and the support will swell, which results in an increased back-pressure [16]. The binding capacity of the cation exchanger packed in precolumn 4, which was determined by atomic absorption spectrometry, was 2.0 mmol/g phase for Fe(II), 2.1 mmol/g for Ni(II) and 2.2 mmol/g for Co(II). These values agree with the retention order found by others using polymeric supports for the ion chromatographic separations of metal ions [38]. The background levels of Ni(II), Fe(II) and Co(II) in the lignocellulose substrate used were 0.25, 3.6 and 0.5 ppm, respectively, which would theoretically allow more than 2400 injections (1000 μl) of undiluted substrate before regeneration of the ion-exchange column with nitric acid is required.

Performance of the clean-up procedure

The total analytical system including the CIMER was used to test the robustness of the coupled precolumn set-up (see Fig. 4). The diluted sample was introduced into loop 1 (1000 μl) by flushing 1.5–2.0 ml of sample through the QMA (precolumn 1) and amino (precolumn 2) clean-up columns. By switching valve I the sample is eluted on-line into the PLRP-S column (precolumn 3), where the more hydrophobic compounds are bound, and then into the mixed anion–cation-exchange column (precolumn 4) where the phenolic derivatives, acids and metal ions are retained. The purified sample is trapped in a 10-μl loop (loop 2) connected to valve IV and injected into the analytical system. Fig. 5 shows the peak profiles of different injection volumes which were recorded by placing an RI detector in series with the precolumn system. When the maximum sugar concentration was reached, the injection was performed. Depending on the complexity of the matrix, the QMA and amino Sep-Pak precolumns were exchanged after 3–10 injections. An attempt was made to regenerate the QMA phase, which was loaded with brown components, by washing with ethanol and phosphoric acid. The results were not encouraging: only about 15–30% of the sorbed material could be removed. Regeneration with more strongly acidic or alkaline solutions might destroy the bonded-phase material and was therefore not attempted. The PLRP-S (precolumn 3) was regenerated with 3 ml of methanol–water (80:20, v/v) and the mixed anion–cation exchanger (precolumn 4) by flushing with 1 ml of 1 *M* nitric acid. After each run the columns were equilibrated with 15 ml of water before re-use.

Table II shows that all the acidic test compounds investigated have breakthrough volumes higher than 10 ml for at least one of the stationary phases used. In all instances except phenol the breakthrough volume is even higher than 30 ml. As the total volume injected is only about 1 ml, a very efficient clean-up is obtained. For real samples, the efficiency of the sample clean-up procedure was studied by means of UV spectrometry. The samples that were analysed were fermented and unfermented hydrolysed lignocellulose (SSL). Untreated samples exhibited strong absorbance in the region of 230–270 nm. After the clean-up procedure, the absorbance in this wavelength range diminished by more than two orders of magnitude for both types of

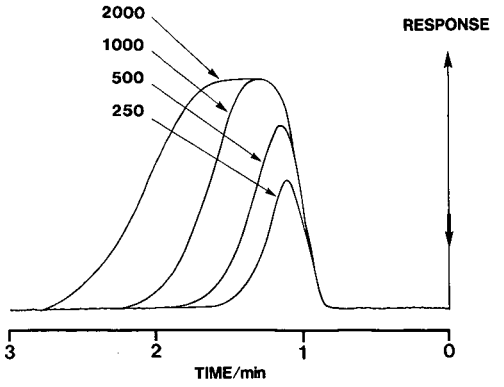

Fig. 5. Peak profiles of different injection volumes (250, 500, 1000 and 2000 μl) recorded by placing an RI detector (attenuation 64) in series with the precolumn system.

samples, which indicates that the aromatic sample constituents are efficiently removed.

The recovery of the whole procedure for cellobiose, glucose, xylose, galactose, arabinose and mannose (30 μM–25 mM) was 91% (relative standard deviation = 2–6%, $n = 30$) when comparing a direct injection of a SSL standard into valve 4 with a sample injected in valve 1 and running through the whole precolumn set-up. The resulting chromatograms for standard solutions are shown in Fig. 6. When using an RI detector several unknown peaks appear in the chromatogram, probably originating from the ion-exchange and amino precolumns, as they also appear when analysing reference solutions (see Fig. 6b). However, these peaks do not interfere with the analyte peaks; therefore, no attempt was made to eliminate this problem. Fig. 6 also demonstrates that, except for a shift in retention times, there is no major difference between direct injections and injections following the clean-up procedure.

Determination of sugars in fermentation broths and substrates

The usefulness of the precolumn clean-up procedure was investigated for the various detectors, *viz.*, RI and UV (190 nm) detection and post-column CIMER coupled to either a UV or an electrochemical detector. On comparing the chromatograms for crude and purified samples it is obvious that the clean-up is of major importance in RI detection. If the clean-up system is omitted, matrix components of the fermented sample interfere with the glucose and xylose peaks (see Fig. 7a); after clean-up, quantification of these sugars is possible (Fig. 7b). The peak heights for galactose and mannose without clean-up (see Fig. 7a) are much higher than those found after clean-up (Fig. 7b), which indicates that these peaks also contain components other than the sugars.

The sugars show only weak UV absorption below 200 nm. At 195 nm, impurities present in the eluent, including dissolved oxygen, cause severe problems with

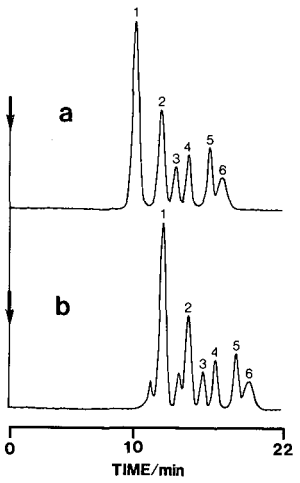

Fig. 6. Separation and RI detection (attenuation 4) of a standard sugar mixture. (a) 10-μl direct injection; (b) 10-μl injection after precolumn clean-up. Peaks: 1 = cellobiose, 20 mM; 2 = glucose, 2 mM; 3 = xylose, 1 mM; 4 = galactose, 1 mM; 5 = arabinose, 1 mM; 6 = mannose, 1 mM. LC conditions: flow-rate, 0.6 ml/min; mobile phase, water; temperature, 65°C; for other conditions, see Experimental.

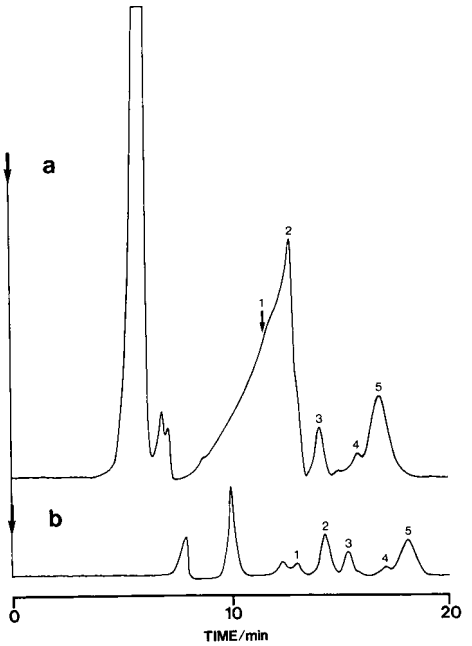

Fig. 7. Separation and RI (attenuation 2) detection of sugars present in fermented SSL diluted 25-fold, (a) before and (b) after precolumn clean-up. Peaks: 1 = glucose, 200 μM; 2 = xylose, 380 μM; 3 = galactose, 190 μM; 4 = arabinose, 75 μM; 5 = mannose, 220 μM. Conditions as in Fig. 6.

baseline stability, which reduces the detection sensitivity. When injecting crude samples it is impossible to quantify or even detect the sugars (Fig. 8a). However, when using the pre-column set-up, quantification is possible (Fig. 8b).

The precolumn set-up was also evaluated using the CIMER post-column detection mode (see Fig. 9) [39,40]. This combines the specificity of enzyme catalysis with the sensitivity of amperometric or UV (340 nm) detection of NADH. Amperometric detection is often preferable to UV detection as it is inherently more selective. After enzyme catalysis the chemically modified electrode (CME) eliminates many of the difficulties encountered in spectrophotometric detection, *e.g.*, overlapping of absorbing peaks, refractive index effects and turbidity. The performance of the CIMER is described in ref. 16.

All six sugars for which the CIMER was active showed a linear response over more than two orders of magnitude (30–200 μM to 5–25 mM). The upper linear range is determined by the amount of bound enzyme in the reactor and the NAD^+ concentration. For a substrate for which the enzyme has a high activity such as glucose it was $5 \cdot 10^{-3}$ M and for a substrate with a low activity such as mannose it was $25 \cdot 10^{-3}$ M. The limits of detection were determined by the noise of the CME and were $3 \cdot 10^{-5}$ M for glucose and $2 \cdot 10^{-4}$ M for mannose; all sugars had almost the same linear range as described previously [15]. When using the postcolumn detection modes, the band broadening increases only moderately compared with direct RI detection [7]. A comparison of CIMER–UV and CIMER–EC (see Fig. 9) with direct RI or UV detection (Figs. 7 and 8, respectively) shows the advantage of the former detection modes regarding selectivity and sensitivity.

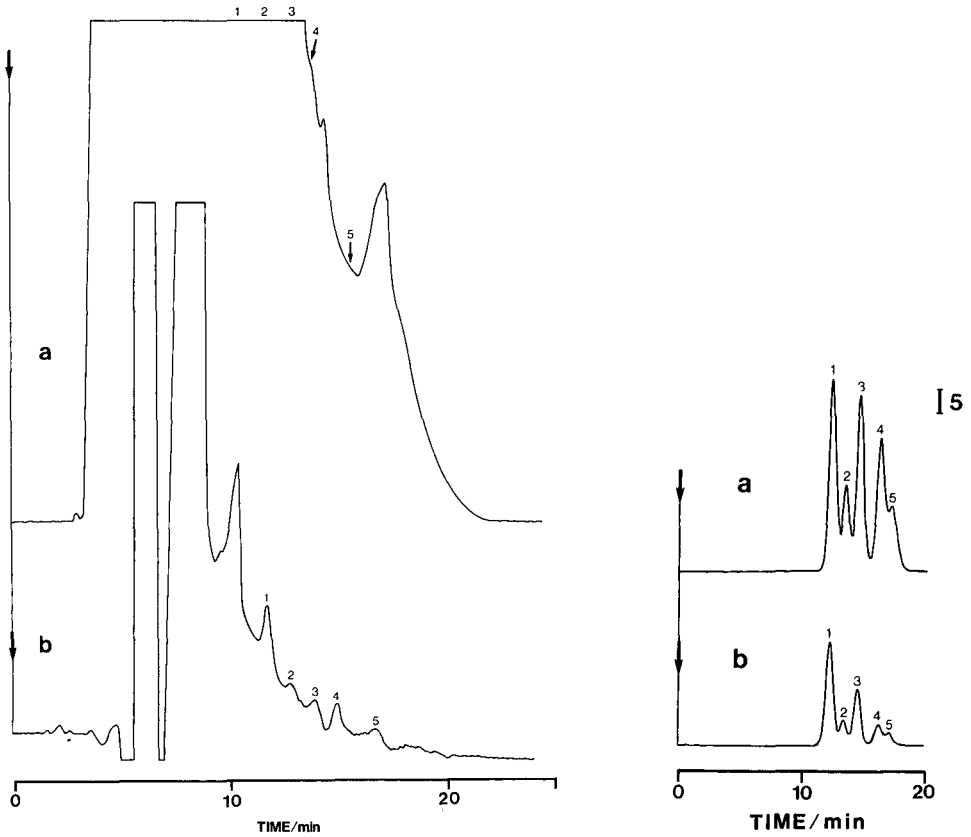

Fig. 8. Chromatogram of unfermented SSL diluted 100-fold using UV detection (195 nm; attenuation, 0.01 a.u.f.s.) (a) before and (b) after precolumn clean-up. Peaks: 1 = glucose, 150 μM; 2 = xylose, 170 μM; 3 = galactose, 200 μM; 4 = arabinose, 120 μM; 5 = mannose, 400 μM. Conditions as in Fig. 6.

Fig. 9. Chromatogram of fermented SSL diluted 200-fold using (a) CIMER–electrochemical detection at the start of the fermentation process and (b) CIMER–UV (340 nm, 0.1 a.u.f.s.) detection at the end of the fermentation process. Conditions: LC flow-rate, 0.7 ml/min; reagent flow-rate, 0.15 ml/min; amperometric oxidation potential at CME, 0 mV *vs.* Ag/AgCl. Peaks: (a) 1 = glucose, 65 μM; 2 = xylose, 180 μM; 3 = galactose, 78 μM; 4 = arabinose, 57 μM; 5 = mannose, 280 μM; (b) 1 = glucose, 100 μM; 2 = xylose, 190 μM; 3 = galactose, 97 μM; 4 = arabinose, 34 μM; 5 = mannose, 110 μM.

CONCLUSIONS

An on-line precolumn set-up has been designed which features four precolumns containing anion- and cation-exchange, amino-bonded silica and hydrophobic PLRP-S materials. If this set-up is combined with a CIMER postcolumn derivatization system, rapid analytical information on the carbohydrate composition in fermentation processes can be obtained. The whole set-up is simple to operate and can provide selective, rapid and reproducible process data.

Although one cannot readily conclude this from all the chromatograms in this paper (*cf.*, Figs. 7b and 9), the inherent selectivity of the CIMER post-column detec-

tion modes often is superior to RI and low-wavelength (190-nm) UV detection in the analysis of fermentation substrates and broths of widely different composition. The use of the precolumn clean-up system allowed the injection of at least 150 samples during a 3-week period with only minor (10%) decreases in enzyme activity, which compares favourably with previous experiments [16].

Further work on real samples with the described method is in progress.

ACKNOWLEDGEMENTS

The authors thank the Waters Division of Millipore in Sweden for the loan and support of chromatographic instrumentation and Pim Voogt (Amsterdam) for the high-pressure packing of the precolumns. Financial support from the Swedish Board for Technical Development (STU) and the National Energy Administration (STEV) is gratefully acknowledged.

REFERENCES

1 H. Senn, *Doctoral Thesis*, University of Basle, Zürich, 1989.
2 G. Marko-Varga, *Anal. Chem.*, 61 (1989) 831.
3 H. Engelhardt and P. Ohs, *Chromatographia*, 23 (1987) 657.
4 R. W. Frei, *Acta Pharm. Suec.*, 25 (1988) 97.
5 M. W. F. Nielen, A. J. Valk, R. W. Frei, U. A. Th. Brinkman, Ph. Musscle, R. de Nijs, B. Ooms and W. Smink, *J. Chromatogr.*, 393 (1987) 69.
6 L. Yago, *Int. Lab.*, Nov./Dec. (1985) 40.
7 G. Marko-Varga, *J. Chromatogr.*, 408 (1987) 157.
8 F. Tjerneld, I. Persson, P. Å. Albertsson and B. Hahn-Hägerdal, *Biotechnol. Bioeng.*, 15 (1985) 40.
9 T. Linden and B. Hahn-Hägerdal, *Biotechnol. Tech.*, 3 (1989) 189.
10 K. Skoog and B. Hahn-Hägerdal, *Enzyme Microb. Technol.*, 10 (1988) 66.
11 R. W. Frei, *Chromatographia*, 15 (1982), 161.
12 I. S. Krull (Editor), *Reaction Detection in Liquid Chromatography*, Marcel Dekker, New York, 1986.
13 L. Gorton, B. Persson, M. Polasek and G. Johansson, in A. Ivaska (Editor), *Proceedings of Electro-FinnAnalysis (1988)*, Plenum Press, New York, in press.
14 R. Appelqvist, *Doctoral Thesis*, University of Lund, Lund, 1987.
15 R. Appelqvist, G. Marko-Varga, L. Gorton, A. Torstensson and G. Johansson, *Anal. Chim. Acta*, 169 (1985) 237.
16 G. Marko-Varga, E. Dominguez, B. Hahn-Hägerdal and L. Gorton, *J. Chromatogr.*, 506 (1990) 423.
17 B. Sanchez and J. Bautista, *Enzyme Microb. Technol.*, 10 (1988) 315.
18 P. A. Pfeifer, G. Bonn and O. Bobleter, *Biotechnol. Lett.*, 6 (1984) 541.
19 A. V. Tran and R. P. Chambers, *Enzyme Microb. Technol.*, 8 (1986) 439.
20 C. H. Fuchsman, *Industrial Chemistry and Technology*, Academic Press, New York, 1980.
21 E. Burtscher, O. Bobleter, W. Schwald, R. Concin and H. Binder, *J. Chromatogr.*, 390 (1987) 401.
22 R. W. Thring, E. Chornet and R. P. Overend, *J. Chromatogr.*, 467 (1989) 441.
23 T. A. Clark and K. L. Mackie, *J. Chem. Technol. Biotechnol.*, 34B (1984) 101.
24 G. G. Choudry, *Humic Substances*, Gordon and Breach, New York, 1984.
25 H. L. Bohn, M. McNeal and G. A. O'Connor, *Soil Chemistry*, Wiley, New York, 1979.
26 N. Banerjee, R. Bhatnager and L. Viwanathan, *Enzyme Microb. Technol.*, 3 (1981) 24.
27 N. A. M. Eskin, H. M. Handerson and R. J. Townsend, *Biochemistry of Food*, Academic Press, New York, 1971.
28 L. C. Maillard, *C. R. Acad. Sci.*, 154 (1912) 66.
29 S. M. Partridge and R. C. Brimley, *Biochem. J.*, 51 (1952) 628.
30 M. Karel and T. P. Labuza, *J. Agric. Food. Chem.*, 16 (1968) 717.
31 G. Marko-Varga, I. Csiky and J. Å. Jönsson, *Anal. Chem.*, 56 (1984) 2066.
32 I. Csiky, G. Marko-Varga and J. Å. Jönsson, *Anal. Chim. Acta*, 178 (1985) 307.
33 E. Hoffmann, G. Marko-Varga, I. Csiky and J. Å. Jönsson, *Int. J. Environ. Anal. Chem.*, 25 (1986) 161.

34 E. Burtscher, H. Binder, R. Concin and O. Bobleter, *J. Chromatogr.*, 252 (1982) 167.
35 A. P. Cook, T. M. Macleod, J. D. Appleton and A. F. Fell, *J. Chromatogr.*, 467 (1989) 395.
36 K.-H. Xie, C. T. Santa Maria, I. S. Krull, U. Neue, R. King, B. Bildingmeyer and A. Newhart, *J. Liq. Chromatogr.*, 6 (1983) 2109.
37 I. S. Krull, K-H. Xie, S. Golgan, U. Neue, R. King and B. Bildingmeyer, *J. Liq. Chromatogr.*, 6 (1983) 605.
38 D. T. Gjerde and J. S. Fritz, *Ion Chromatography*, Hüthig, Heidelberg, 2nd ed., 1987.
39 K. Shimada, T. Oe and T. Nambara, *J. Chromatogr.*, 492 (1989) 345.
40 L. D. Bowers, in I. S. Krull (Editor), *Reaction Detection in Liquid Chromatography*, Marcel Dekker, New York, 1986, pp. 195-222.

Journal of Chromatography, 523 (1990) 189–200
Elsevier Science Publishers B.V., Amsterdam

CHROM. 22 705

Analysis of N- and O-glycosidically bound sialooligosaccharides in glycoproteins by high-performance liquid chromatography with pulsed amperometric detection

SUSUMU HONDA*, SHIGEO SUZUKI, SACHIKO ZAIKI and KAZUAKI KAKEHI
Faculty of Pharmaceutical Sciences, Kinki University, 3–4–1 Kowakae, Higashi-osaka (Japan)
(Received May 8th, 1990)

ABSTRACT

N-Glycosidically bound sialooligosaccharides in a model glycoprotein of serum type (porcine thyroglobulin) were released by pronase digestion, followed by hydrazinolysis. The resulting oligosaccharides were re-N-acetylated and reduced with sodium borohydride. On the other hand, O-glycosidically bound sialooligosaccharides were released from a mucin-type glycoprotein (bovine submaxillary mucin) with alkali in the presence of sodium borohydride. The reduced oligosaccharides thus obtained from both types of glycoproteins were analysed by high-performance liquid chromatography on a column of a latex-type pellicular anion-exchange resin with strong alkali as eluent. These sequential procedures were useful for mapping of oligosaccharides in glycoproteins.

INTRODUCTION

Glycoproteins have covalently bound oligosaccharide chains in their peptide backbones, which play an important role in cell-to-cell recognition (*e.g.*, ref. 1). As the structures of the oligosaccharides in glycoproteins are dependent on variations in the enzymatic processing environment, structural variations reflect the physiological and pathological conditions to which the precursor proteins have been exposed. Therefore, oligosaccharide mapping is important for biological and clinical studies involving biosynthesis and metabolism of glycoproteins. So far, high-performance liquid chromatography (HPLC) has been most widely used for this purpose, especially in the reversed-phase partition mode as N-pyridylglycamine derivatives (*e.g.*, ref. 2). It requires, however, multi-step derivatization and clean-up processes.

An alternative method is direct separation of oligosaccharides on a latex-type anion-exchange resin with strong alkali as eluent with pulsed amperometric detection using a gold electrode [3]. This method has been applied to the analysis of oligosaccharides released from glycoproteins [4–10]. Separation is rapid and the sensitivity is down to the picomole level. Although the use of strong alkali can cause degradation or isomerization, this method seems promising for pattern analysis of oligosaccharides in glycoproteins. This paper proposes general procedures for the analysis of N- and O-glycosidically bound sialooligosaccharides in glycoproteins, including liberation processes.

0021-9673/90/$03.50

EXPERIMENTAL

Streptomyces griseus Pronase P was obtained from Boehringer (Mannheim, F.R.G.). *Clostridium perfringens* neuraminidase and coffee bean α-galactosidase were purchased from Sigma (St. Louis, MO, U.S.A.). All enzymes were used without further purification. Anhydrous hydrazine was purchased from Aldrich (Milwaukee, WI, U.S.A.). All other reagents and carbohydrate samples were of the highest grade commercially available. Water was deionized and doubly distilled before use.

Thyroglobulin was prepared from porcine thyroid glands according to the method of Ui and Tarutani [11] and was subjected to exhaustive digestion with Pronase P. The digest was applied to a column of Sephadex G-25 (30 cm × 10 mm I.D.) and the column eluted with water. The fractions corresponding to 11–15 ml of eluate were collected and evaporated to dryness. The residue was divided into three fractions (neutral, monosialo- and disialoglycopeptide fractions) on a column (80 cm × 18 mm I.D.) of DEAE-Sephadex A-25 by isocratic elution with a 2 m*M* acetic acid–1 m*M* pyridine mixture (100 ml), followed by gradient elution with the same buffer to a 100 m*M* acetic acid–50 m*M* pyridine mixture according to the procedure of Fukuda and Egami [12]. Each fraction was deionized on a column of Sephadex G-25 in a similar manner to that for Pronase P digest. Each of the mono- and disialoglycopeptide fractions were further hydrazinolysed and re-N-acetylated by the method of Takasaki *et al.* [13], then reduced with 0.1 *M* sodium borohydride in 0.05 *M* sodium hydroxide for 6 h at 27°C. The reaction mixture was decationized by passing it through a column of Amberlite CG-120 (H^+ form), and the combined eluate and water washings were evaporated to dryness. The residue was dissolved in a small volume of methanol and the solution evaporated to dryness. The treatment with methanol and evaporation was repeated twice more to remove boric acid.

The residues finally obtained from the neutral glycopeptide and reduced sialooligosaccharide fractions were dissolved in water and 20-μl portions were analysed by HPLC with isocratic elution. For HPLC with gradient elution, a sample (50 μg) of thyroglobulin was directly hydrazinolysed (without being digested with Pronase P), re-N acetylated and reduced with sodium borohydride in a similar manner to that for the sialoglycopeptide fractions. The residue was dissolved in water and the whole solution injected into the HPLC system.

Bovine submaxillary mucin was isolated by the method of Tettamanti and Pigman [14]. It was treated with 1 *M* sodium borohydride in 0.05 *M* sodium hydroxide for 24 h at 45°C to liberate oligosaccharides as reduced forms, according to the procedure of Iyer and Carlson [15]. The reduced oligosaccharides from this mucin-type glycoprotein were analysed by HPLC with isocratic elution in a similar manner to that for thyroglobulin, after removal of boric acid by decationization and treatment with methanol. Erythrocyte ghost was prepared from porcine blood by the method of Dodge et al. [16] and treated with sodium borohydride in alkali in a similar manner to that for bovine submaxillary mucin. HPLC was performed by isocratic elution.

In all HPLC experiments with isocratic elution the HPLC system consisted of a Hitachi 655 dual plunger pump, a Rheodyne 7125 sample injector with a 20-μl loop, a Dionex HPIC-AG 6 guard column (5 cm × 4 mm I.D.), a Dionex HPIC-AS 6 analytical column (25 cm × 4 mm I.D.) and a Dionex triple pulse amperometric

detector equipped with a gold electrode (PAD II). In analytical HPLC (0.5–2.5 μg as saccharide for each run), all portions of the eluates were introduced to the detector, whereas in preparative HPLC (5–25 μg as saccharide for each run), the eluate for each sample was continuously divided into two portions (volume ratio 1:9) by use of a splitter, and the smaller portion was led into the detector for monitoring. The larger portion was fractionated, and the combined fractions for every peak were neutralized and deionized on a column of Sephadex G-25. In analytical HPLC with gradient elution, a Dionex pump capable of programmed gradient elution (GPM) was used, but other parts were the same as those for isocratic elution.

^{1}H NMR spectra of the major fractions from preparative HPLC were recorded in deuterium oxide at room temperature with a JEOL JNM GSX-500 spectrometer. The proton signals were referenced to the methyl proton signal of acetone (2.225 ppm) in δ (ppm). The water signal was eliminated by measuring the spectra in the homogate decoupling mode. Fast atom bombardment mass spectra were obtained in a glycerol matrix using a JEOL HX-100 spectrometer. Each sample was dissolved in aqueous 10% glycerol and a 2-μl portion of each sample solution was loaded on a stainless-steel sample plate. The energy of the primary xenon beam was 6 kV. Scanning was carried out every 10 s up to m/z 2000. The ion source had an accelerating potential of 5 kV. Calibration of mass number was carried out by using Ultra Mark (PCR Research Chemicals, FL, U.S.A.) as the mass reference.

RESULTS AND DISCUSSION

Problem of interference by amino acids and proteins

As the present system employed pulse amperometry on a gold electrode for detection, which is also sensitive to amino group-containing substances, interference by amino acids and proteins was examined. Fig. 1a and b shows the chromatograms obtained with 0.5 *M* sodium hydroxide after injection of a mixture of 1 μmol each of eighteen kinds of amino acids and 5 μg of bovine serum albumin, respectively.

The amino acid mixture gave intense peaks (not assigned) at *ca.* 5 and 13 min together with a few peaks near the void volume, but the protein sample gave no peaks within 30 min except for a few small ones near the void volume. These results indicate that in the analysis of oligosaccharides from glycoproteins amino acids must be removed before HPLC analysis. However, this problem was solved simply by passing sample solutions through a Sephadex G-25 column (30 cm × 1.0 cm I.D.) and collecting the 11–15-ml fraction of the aqueous eluate.

Separation of oligosaccharides derived from glycoproteins

Oligosaccharide chains in glycoproteins can be either N- and O-glycosidically bound to the polypeptide cores. In this work procine thyroglobulin and bovine submaxillary mucin were used, respectively, as the models of these two types.

Oligosaccharide in porcine thyroglobulin. Three fractions corresponding to neutral, monosialo- and disialoglycopeptides were obtained by clean-up of the Pronase P digest of porcine thyroglobulin on a column of Sephadex GA-25, followed by fractionation on a column of DEAE-Sephadex A-25.

Analysis of the neutral glycopeptide fraction by isocratic elution gave three major peaks and one minor peak, as shown in Fig. 2a.

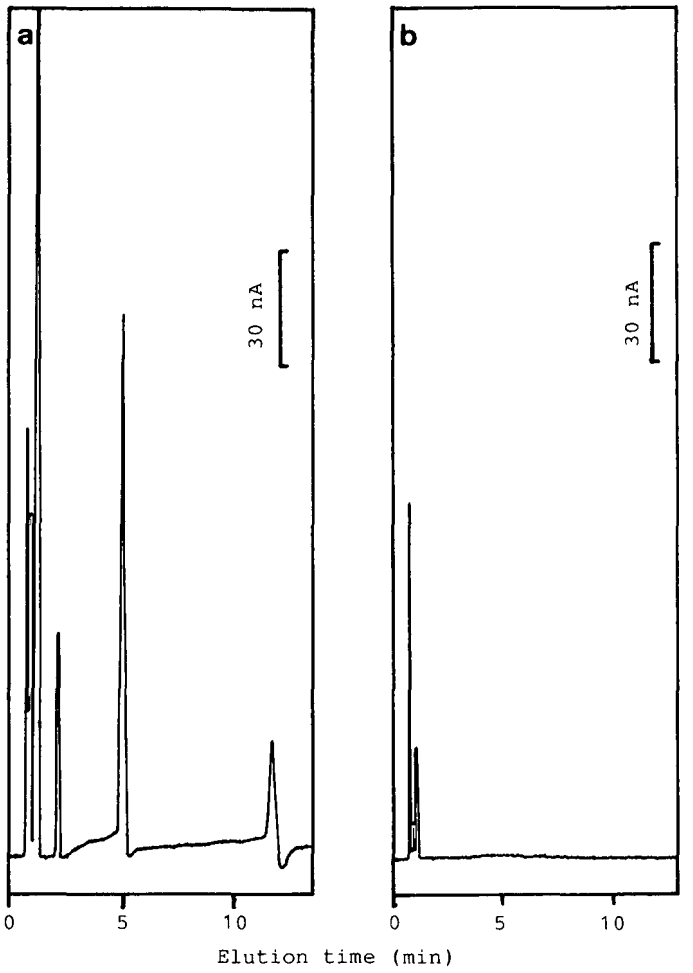

Fig. 1. Analysis of (a) a mixture of amino acids (1 μmol each) and (b) bovine serum albumin (5 μg). Column, Dionex HPIC AS-6 (25 cm × 4 mm I.D.); flow-rate, 1.0 ml/min; detection, pulsed amperometry on a gold electrode; E_1 = +0.05 V (0.6 s), E_2 = +0.60 V (0.12 s), E_3 = −0.80 V (0.42 s).

The compounds corresponding to the major peaks were isolated by preparative HPLC, followed by deionization. The ^{1}H NMR spectra of the compounds giving peaks 1 (**1**) and 2 (**2**) indicated the presence of seven and eight anomeric protons (H-1s), respectively, whose chemical shifts (Table I) are consistent with those of the hepta- and octasaccharides of high-mannose type shown above the elution profile. Each of them also showed the presence of two N-acetyl groups giving the signals of the methyl protons at 2.04 and 2.06 ppm together with two β-methylene protons (ca. 2.8 ppm) in the asparagine residue. The chemical shifts of the anomeric protons and the protons at C-2 (H-2s) of individual monosaccharide residues were in good agreement with those in the literature [17]. The spectrum of the compound corresponding to peak 3 (**3**) showed the presence of two N-acetyl and two methylene groups. It also

gave complex signals of H-1 and H-2 protons which could be assigned as shown in Table I.

The multiplicity of the signals in the 5.0–4.9 ppm region indicated the presence of three isomers of high mannose-type nonasaccharides linked to asparagine, differing in the position of attachment of the D-mannose residues. Substitution of the A-, B- and C-mannose residues by the D-mannose residue resulted in a downfield shift of the anomeric protons as given in statics and from the intensities of these signals the molar ratio of the A-, B- and C-bound positional isomers were estimated to be 23:13:64. Peak 4 is probably a $Man_8GlcNAc_2Asn$ analogue, judging from the k' value, although the ^1H NMR data were not conclusive owing to limited availability of the sample.

The mono- and disialoglycopeptides gave multiple peaks due to heterogeneity of the peptide moity, because the peptide linkages were not hydrolysed completely. Therefore, each of the sialoglycopeptide fractions was submitted to sequential hydrazinolysis, re-N-acetylation and borohydride reduction, then fractionated on a column of DEAE-Sephadex. The amount of desialylated products appearing at the void volume was roughly calculated to be less than 10% of the starting fraction on a weight basis for both sialoglycopeptide fractions. This result confirms that the partial degradation was almost negligible and this series of derivatizations gave reliable oligosaccharide mapping. Fig. 2b and c show the chromatograms for reduced mono- and disialooligosaccharide fractions, respectively. They also include the proposed structures of the compounds giving the major peaks. The compound corresponding to peak 5 (**5**) from the reduced monosialooligosaccharide, as its ^1H NMR spectrum (Table II) was in good agreement with that in the literature [17].

The compound giving peak 6 (**6**) was thought to have an additional α-Gal residue linked to the peripheral Gal residue in **5**, because digestion of **6** with coffee bean α-galactosidase removed peak 6 from the elution profie and yielded a peak identical with peak 5. Further, **6** gave a ^1H NMR spectrum identical with that of **5**, except for the presence of additional H-1 signal at 5.135 ppm with a coupling constant of 3.5 Hz and a slightly upfield shift of the H-1 signal of the 6′-GlcNAc residue from 4.471 to 4.446 ppm. This situation was the same as that for the tetra-antennary oligosaccharide reported by Dorland *et al.* [18], which has also a peripheral α-Gal residue linked to the Gal residue. The minor peaks in Fig. 2b are considered to arise from isomerically monosialylated bi- and triantennary oligosaccharides, although the positions of attachment of the NeuNAc residue are not known.

Peak 7 from the reduced disialooligosaccharide fraction was assignable to the biantennary oligosaccharide in which both peripheral Gal residues are sialylated. Peak 8 from the same fraction is presumably due to a mixture of triantennary oligosaccharides having two NeuNAc residues at different Gal residues, because partial desialylation with *Clostridium perfringens* neuraminidase gave peaks identical with one of the minor peaks from the reduced monosialooligosaccharide fraction.

Hence the present system allowed excellent separations of neutral glycopeptides and also reduced sialooligosaccharides, possibly owing to slight difference in hydrophilicity. The reproducibility of the retention times was fairly high, the relative standard deviation being less than 0.1% for these peaks.

With thyroglobulin oligosaccharides, prior fractionation on an anion-exchange column was essential, as isocratic elution could not separate, in one run, all types of

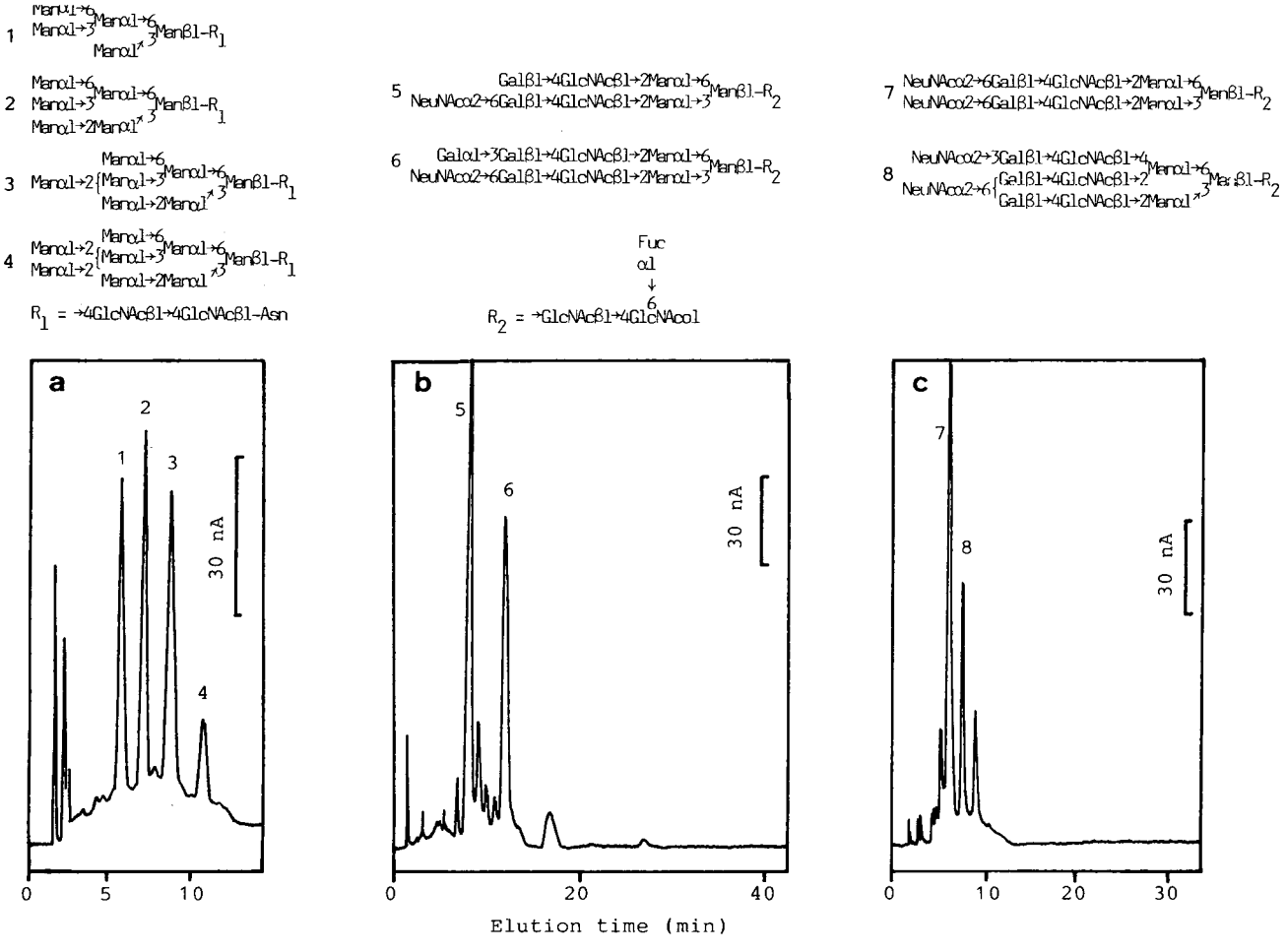

Fig. 2. Analysis of the (a) neutral glycopeptides, (b) reduced monosialo- and (c) reduced disialooligosaccharides, derived from porcine thyroglobulin. Eluent: (a) 0.5, (b) 0.5 and (c) 0.8 *M* sodium hydroxide solutions. Other conditions as in Fig. 1. Sample scale: 11–30 μg as glycoprotein.

TABLE I

ASSIGNMENT OF THE CHEMICAL SHIFTS OF REPRESENTATIVE PROTON SIGNALS OF MAJOR NEUTRAL GLYCOPEPTIDES DERIVED FROM PORCINE THYROGLOBULIN

Numbering of monosaccharide residue:

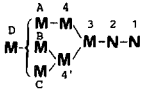

M = mannose; N = N-acetylglucosamine.

Signal	Monosaccharide residue	1 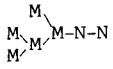	2 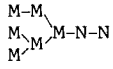	3 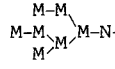	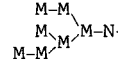	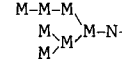
H-1	1	5.072	5.072	5.072	5.072	5.072
NAc	1	2.037	2.038	2.037	2.037	2.037
	2	2.063	2.063	2.064	2.064	2.064
H-1	4	5.094	5.348	5.340	5.340	5.340
	4′	4.870	4.874	4.871	4.871	4.871
	A	5.094	5.094	*5.404*	5.093	5.093
	B	4.907	4.909	4.908	*5.149*	4.908
	C		5.054	5.056	5.056	*5.304*
	D			5.043	5.043	5.043
H-2	3	4.25	4.23	4.23	4.23	4.23
	4	4.07	4.11	4.09	4.09	4.09
	4′	4.15	4.15	4.15	4.15	4.15
	B	3.99	3.99	3.99	3.99	3.99
	C		4.07	4.07	4.07	4.07
	D			4.07	4.07	4.07

TABLE II

ASSIGNMENT OF THE CHEMICAL SHIFTS OF REPRESENTATIVE PROTON SIGNALS OF MAJOR SIALOOLIGOSACCHARIDES DERIVED FROM PORCINE THYROGLOBULIN

Numbering of monosaccharide residue:

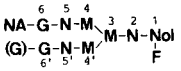

M = mannose; N = N-acetylglucosamine; Nol = N-acetylgucosaminitol; F = fucose; G = galactose.

Signal	Monosaccharide residue	**5**	**6**
		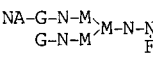	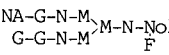
H-1	4	5.138	5.139
	4′	4.927	4.929
	5	4.609	4.607
	5′	4.581	4.583
	6	4.446	4.446
	6′	4.471	4.446
	Fuc	4.897	4.898
	α-Gal		5.135
H-2	3	4.26	4.26
	4	4.19	4.20
	4′	4.11	4.11
H-3ax	NeuNAc	1.777	1.777
H-3eq	NeuNAc	2.668	2.669
H-5	Fuc	4.11	4.11
H-6	Fuc	1.212	1.212
NAc	1	2.018	2.017
	2	2.076	2.074
	5	2.058	2.058
	5′	2.044	2.043
	NeuNAc	2.035	2.035

saccharides differing in the number of sialic acid residues. Gradient elution alleviated the problem of prior fractionation, and simultaneous gradient separation of neutral, mono-and disialooligosaccharides was accomplished, although with lower reproducibility of retention times (*e.g.*, the relative standard deviation for peak 1 was 5.3%, $n = 5$). Fig. 3 shows an example of the separation of all the oligosaccharides with gradient elution.

The sample was prepared by direct hydrazinolysis, re-N-acetylation and borohydride reduction, and gradient elution was performed by adding 0.1 *M* sodium hydroxide containing 0.5 *M* sodium acetate to 0.1 *M* sodium hydroxide in 200 min. Peaks were tentatively assigned by comparing the elution pattern with those obtained by isocratic elution of neutral glycopeptide and reduced mono- and disialooligosaccharide fractions. Neutral, high-mannose-type oligosaccharides were eluted first at *ca.* 20 min, reduced monosialooligosaccharides followed in the range of 35–40 min and reduced disialooligosaccharides appeared after 45 min. The unassigned peaks

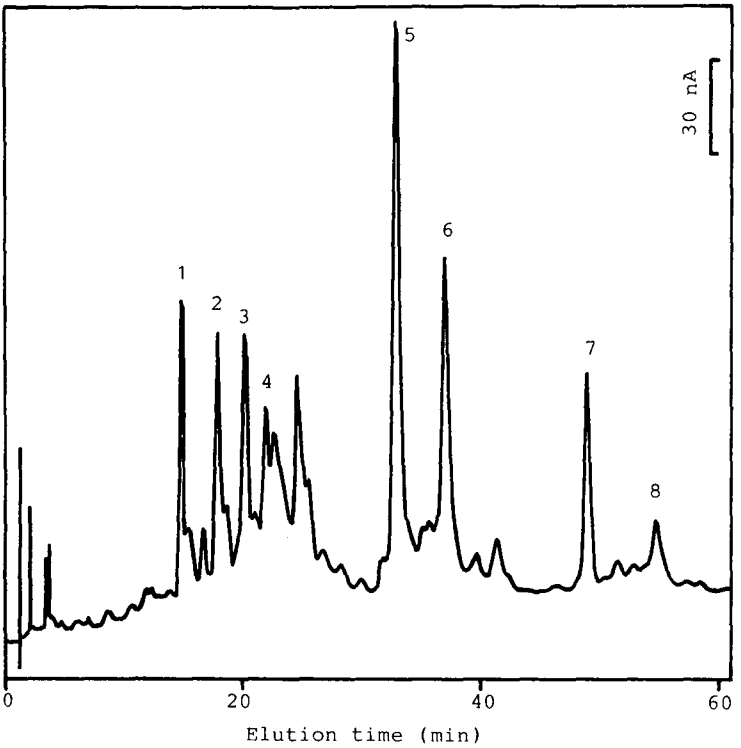

Fig. 3. Analysis of the reduced neutral and sialooligosaccharides derived from porcine thyroglobulin. Gradient elution from 0.1 *M* sodium hydroxide to 0.1 *M* sodium hydroxide containing 0.5 *M* sodium acetate in 200 min. Other conditions as in Fig. 1. Sample scale: 50 μg as glycoprotein. Numbering of peaks as in Fig. 2.

between 22 and 23 min were presumably due to oligopeptides formed by partial degradation of the polypeptide core, which escaped clean-up with Sephadex G-25 and Amberlite CG-120 columns. Such compounds would be difficult to remove by this clean-up procedure, and digestion of glycoprotein samples with Pronase P prior to hydrazinolysis is desirable to eliminate the problem of non-carbohydrate contaminants.

Oligosaccharides from bovine submaxillary mucin. Bovine submaxillary mucin contains large amounts of NeuNAc and NeuNGc-containing di- and trisaccharides, which can be easily released as reduced forms with dilute alkali containing sodium borohydride. Fig. 4 shows the separation of the reduced oligosaccharides obtained after clean-up on a column of Sephadex G-25, using 0.3 *M* sodium hydroxide.

Fast atom bombardment mass spectrometry (FAB-MS) of the substance corresponding to peak 1 gave an intense signal at *m/z* 513 together with a weak signal at 716. They can be assigned to the $[M-H]^-$ ions resulting from NeuNAcα2→6GalNAc–OH (disaccharide a) and GlcNAcβ1→3(NeuNAcα2→6)GalNAc–OH (trisaccharide a) reported by Tsuji and Osawa [19]. The compound giving peak 2 gave a

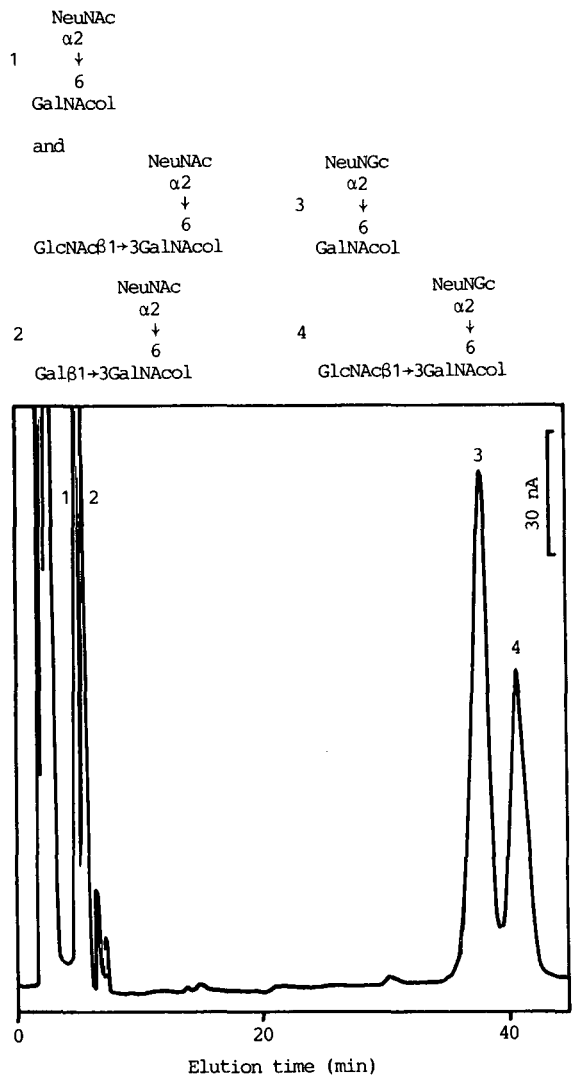

Fig. 4. Analysis of the reduced oligosaccharides derived from bovine submaxillary mucin. Eluent: 0.3 *M* sodium hydroxide solution. Other conditions as in Fig. 1. Sample scale: 11 μg as glycoprotein.

signal at *m/z* 674, which similarly resulted from Galβ1→3(NeuNAcα2→6)GalNAc–OH (trisaccharide b). Slowly eluting peaks 3 and 4 are considered to be due to the NeuNGc analogues of disaccharide a and trisaccharide a, respectively, because the isolated compounds corresponding to these peaks gave signals at *m/z* 529 and 732 respectively, in FAB-MS. Although the separation of faster eluting oligosaccharide was not efficient under these conditions, use of lower concentrations of sodium hydroxide gave better resolution.

The O-glycosidically bound oligosaccharides are widely distributed, ranging from soluble glycoproteins inside and outside cells to insoluble ones on cell surface.

As a representative of the latter type of glycoproteins, porcine erythrocyte membrane was treated with sodium borohydride in dilute alkali in the same manner as described for bovine submaxillary mucin, although in suspension. Analysis of the released oligosaccharides by the present system with 0.5 *M* sodium hydroxide as eluent (Fig. 5) yielded two later eluting peaks (peaks 1 and 2), which are presumably due to sialooligosaccharides.

The amounts of these oligosaccharides were too low to allow definitive assignment by ^{1}H NMR spectrometry. However, as the main oligosaccharides in glycophorin, the major erythrocyte membrane glycoprotein, has been reported to have O-glycosidically bound oligosaccharides, Galβ1→3(NeuNGcα2→6)GalNAc and Galβ1→3GlcNAcβ1→4GlcNAcβ1→3Galβ1→3(NeuNGcα2→6)GalNAc [20], peaks 1 and 2 might be assigned to these NeuNGc-containing oligosaccharides. Although further studies are required for unequivocal assignment, it is clear that the present method is also useful for pattern analysis of oligosaccharides on cell surfaces.

The results obtained here by using model proteins of serum type and mucin type demonstrate the usefulness of these procedures for the analysis of both N- and O-glycosidically bound sialooligosaccharides derived from these glycoproteins. Conversion to borohydride-reduced derivatives is quantitative, as is well established, and eliminates the problem of the presence of anomers and avoids on-column epimerization and degradation. In addition, the sensitivity was not lowered by this treatment, permitting analysis at the several tens of micrograms level as glycoprotein.

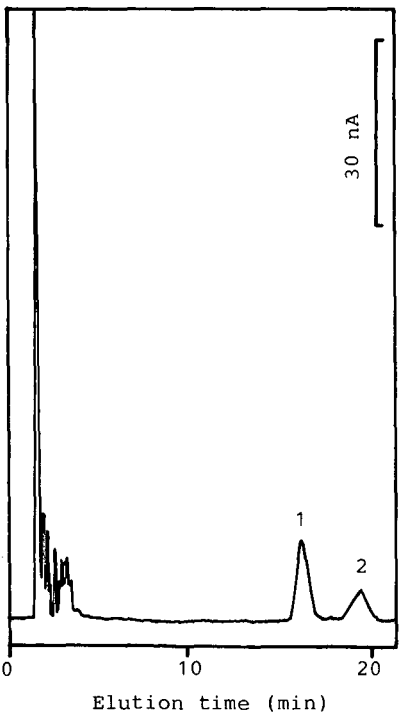

Fig. 5. Analysis of the reduced oligosaccharides derived from porcine erythrocyte ghost. Eluent: 0.5 *M* sodium hydroxide solution. Other conditions as in Fig. 1. Sample scale: 73 μl as blood.

ACKNOWLEDGEMENT

The authors wish to express their gratitude to Professor Y. C. Lee from The Johns Hopkins University, for useful discussion throughout the work.

REFERENCES

1 T. W. Rademachen, R. B. Parekh and R. A. Dwek, *Annu. Rev. Biochem.*, 57 (1988) 785.
2 N. Tomiya, J. Awaya, M. Kurono, S. Endo, Y. Arata and N. Takahashi, *Anal. Biochem.*, 171 (1988) 73.
3 R. D. Rocklin and C. A. Pohl, *J. Liq. Chromatogr.*, 6 (1983) 1577.
4 M. R. Hardy and R. R. Townsend, *Proc. Natl. Acad. Sci. U.S.A.*, 85 (1988) 3289.
5 R. R. Townsend, M. R. Hardy, O. Hindsgaul and Y. C. Lee, *Anal. Biochem.*, 174 (1988) 459.
6 R. R. Townsend, M. R. Hardy, D. A. Cummings, J. P. Carver and B. Bendiak, *Anal. Biochem.*, 182 (1989) 1.
7 R. R. Townsend, M. R. Hardy and Y. C. Lee, *Methods Enzymol.*, 179 (1989) 65.
8 M. R. Hardy and R. R. Townsend, *Carbohydr. Res.*, 188 (1989) 1.
9 W. T. Wang and D. Zopf, *Carbohydr. Res.*, 189 (1989) 1.
10 L. J. Basa and M. W. Spellman, *J. Chromatogr.*, 499 (1990) 205.
11 N. Ui and O. Tarutani, *J. Biochem. (Tokyo)*, 50 (1961) 508.
12 M. Fukuda and F. Egami, *Biochem. J.*, 123 (1971) 407.
13 S. Takasaki, T. Mizuochi and A. Kobata, *Methods Enzymol.*, 83 (1982) 263.
14 G. Tettamanti and W. Pigman, *Arch. Biochem. Biophys.*, 124 (1968) 41.
15 R. N. Iyer and D. M. Carlson, *Arch. Biochem. Biophys.*, 142 (1971) 101.
16 J. T. Dodge, C. Mitchell and D. J. Hanahan, *Arch. Biochem. Biophys.*, 100 (1963) 119.
17 J. F. G. Vliegenthart, L. Dorland and H. van Halbeek, *Adv. Carbohydr. Chem., Biochem.*, 41 (1983) 209.
18 L.Dorland, H. van Halbeek and J. F. G. Vliegenthart, *Biochem. Biophys. Res. Commun.*, 122 (1984) 859.
19 T. Tsuji and T. Osawa, *Carbohydr. Res.*, 151 (1986) 391.
20 I. Kawashima, K. Fukuda, M. Tomita and A. Hamada, *J. Biochem. (Tokyo)* 91 (1982) 865.

Journal of Chromatography, 523 (1990) 201–216
Elsevier Science Publishers B.V., Amsterdam

CHROM. 22 747

High-performance reversed-phase ion-pair chromatographic study of myo-inositol phosphates

Separation of myo-inositol phosphates, some common nucleotides and sugar phosphates

MIKLÓS PATTHY*
Institute for Drug Research, Szabadságharcosok útja 47–49, 1045 Budapest (Hungary)
TAMÁS BALLA
Department of Physiology, Semmelweis University Medical School, 1088 Budapest (Hungary)
and
PÉTER ARÁNYI
Institute for Drug Research, Szabadságharcosok útja 47–49, 1045 Budapest (Hungary)
(First received April 4th, 1990; revised manuscript received July 20th, 1990)

ABSTRACT

A detailed study of all the major chromatographic variables affecting the retention behaviour and separation of myo-inositol phosphates in reversed-phase ion-pair chromatographic systems was carried out. The parameters studied included the eluent concentration of the pairing ion, the eluent concentration of the organic modifier and the buffer salt, the pH of the eluent, the minimum column plate count necessary for the separation of the inositol trisphosphate isomers and isocratic and gradient modes of separation. The retention behaviour of some common nucleotides and sugar phosphates was also investigated as these phosphates present chromatographic interference problems in biochemical studies based on the cellular incorporation of $[^{32}P]P_i$. The separation methods developed appear to be superior to established anion-exchange separation techniques in terms of separation speed and "mildness" of the chromatographic conditions.

INTRODUCTION

Considerable interest in the cellular production and metabolism of myo-inositol phosphates has developed since the demonstration that activation of some plasma-membrane receptors leads to the production of inositol 1,4,5-trisphosphate [Ins(1,4,5)P_3], a second messenger that promotes the mobilization of intracellular calcium stores. It is now clear that the metabolism of Ins(1,4,5)P_3 is complex, proceeding by two main routes, resulting in several closely related myo-inositol phosphates. (For a detailed review of the biosynthesis and degradation of the myo-inositol phosphates, see ref. 1.)

0021-9673/90/$03.50

Currently, several methods exist for the separation of myo-inositol phosphates, such as open-bed anion exchange [2], anion exchange in cartridges [3], gas–liquid chromatography [4], high-voltage paper electrophoresis [5], high-performance liquid chromatography (HPLC) using strong anion-exchange packing materials [6,7] and a combination of anion exchange and gas chromatography [8].

However, gas chromatographic methods involve laborious sample preparation (usually with more than one derivate), and open-bed and cartridge separation techniques and high-voltage paper electrophoresis lack the separation efficiency necessary for the analysis of complex samples. High-performance anion-exchange methods, although frequently used, may cause difficulties because polyvalent ions (*e.g.*, polyphosphoinositols) adsorb very strongly on ion exchangers and, as a result, long elution times (1–2 h) and high buffer salt concentrations (1–2 *M*) are needed for the separation, putting a great strain on the whole of the chromatographic system.

High-performance reversed-phase ion-pair chromatography (RP-IPC) has been successfully used in the separation of various ionic compounds [9–11]. The separation speed, efficiency and "mildness" of the chromatographic conditions (*e.g.*, lower buffer salt concentrations and column back-pressures) make this approach an attractive alternative to established anion-exchange HPLC methods.

Two laboratories have used RP-IPC for the separation of myo-inositol phosphates. They developed isocratic methods for the separation of Ins(1,4)P_2 and Ins (1,4,5)P_3 [12], Ins(1,4)P_2 (eluted near the front), InsP_3 isomers and Ins(1,3,4,5)P_4 [13] and also some adenine nucleotides, 2-3-bisphosphoglycerate, D-fructose-1,6-diphosphate (FDP), InsP_3 isomers and Ins(1,3,4,5)P_4 [14]. All these separations were made after studying some characteristics of the RP-IPC systems used.

In order to exploit the full separation potential of RP-IPC (isocratic and gradient), we carried out a detailed study of all the major chromatographic variables that affect the retention (and separation) of some of the more common inositol phosphates Ins(1)P_1, Ins(1,4)P_2, Ins(1,4,5)P_3, Ins(1,3,4)P_3 and Ins(1,3,4,5)P_4. The data obtained can be best used in experiments involving the cellular incorporation of [^{3}H]inositol but, as ample reference has also been made to the retention behaviour of some prominent nucleotides and sugar phosphates in various RP-IPC systems, they can also be used in biochemical studies based on the incorporation of [^{32}P]P_i.

EXPERIMENTAL

Chemicals

Materials and their sources were as follows. Tetrabutylammonium hydrogensulphate (TBAHS) was obtained from Sigma (St. Louis, MO, U.S.A.) and potassium dihydrogenphosphate (LiChropur) and acetonitrile (LiChrosolv) from Merck (Darmstadt, F.R.G.). The Nucleosil 100-5 C_{18} (5 μm) column packing material was the product of Macherey, Nagel & Co. (Düren, F.R.G.). D-Myo-[2-^{3}H]inositol 1-phosphate, D-myo-[2-^{3}H]inositol 1,4-bisphosphate, D-myo-[2-^{3}H]inositol 1,4,5-trisphosphate, D-myo-[2-^{3}H]inositol 1,3,4,5-tetrakisphosphate (all potassium salts) and myo-[2-^{3}H]inositol were supplied by Amersham International (Amersham, U.K.). D-Myo-[2-^{3}H]inositol 1,3,4-trisphosphate was from New England Nuclear (Boston, MA, U.S.A.). Adenosine-5′-monophosphoric acid (AMP), adenosine-5′-diphosphate (ADP), adenosine-5′-triphosphate (ATP), adenosine-3′,5′-cyclic monophosphate (c-

AMP), guanosine-5′-diphosphate (GDP) and guanosine-5′-triphosphate (GTP) were obtained from Calbiochem (La Jolla, CA, U.S.A.). Glucose-6-phosphate (G6P), FDP and aldolase (from rabbit muscle) were purchased from Boehringer (Mannheim, F.R.G.). The glucose–hexokinase reagent kit was supplied by Baker Instruments (Allentown, PA, U.S.A.). All other chemicals were of analytical-reagent grade.

Chromatography

For isocratic separation of the compounds studied, the HPLC system included a Varian 8500 pulse-free pump equipped with a stop-flow septumless injector (Varian, Palo Alto, CA, U.S.A.). For gradient separations two Varian 8500 pumps were used. The chromatographic support (Nucleosil 100-5 C_{18}, 5 μm) was packed in stainless-steel columns by Bio-Separation Technologies (Budapest, Hungary). The column dimensions and the composition of the mobile phases are specified in the figure legends. The flow-rate was 1 ml/min and fractions of 0.33 or 0.50 ml were collected. All separations were carried out at ambient temperature. The radioactivity of the eluted fractions was determined with a liquid scintillation counter (Wallac 1410; Pharmacia–LKB, Turku, Finland). Detection of FDP [15] and G6P [16] in the eluted fractions was performed by established enzymatic methods.

The elution of the nucleotides was monitored with a Variscan (Varian) absorbance monitor (at 254 nm) and a Kipp and Zonen (Delft, The Netherlands) BD 40 recorder. Inositol phosphates were injected as obtained from the supplier. The activity of the individual phosphates placed on the column varied between $1 \cdot 10^4$ and $2 \cdot 10^4$ dpm. The nucleotides (0.1 mg/ml solutions) and the sugar phosphates (100 mg/ml solutions) were dissolved in the mobile phase. The amount of the individual nucleotides placed on the column varied between 2 and 5 μg. The amount of FDP or G6P injected was 2 mg. The UV absorbances obtained after the enzymatic procedures with an aliquot of the eluted fraction were measured with a CentrifiChem System 400 spectrophotometer (Union Carbide, Rye, NY, U.S.A.) at 240 nm (FDP) and 340 nm (G6P).

RESULTS AND DISCUSSION

Dependence of k′ on the concentration of the pairing ion in the eluent

The capacity factor (k') was calculated using the equation $k' = (t_R - t_0)/t_0$, where t_0 and t_R are the retention times of an unretained solute (the first baseline disturbance observed after the injection of 100 μl of distilled water) and the solute in question, respectively. Of various quaternary amines, TBAHS proved to be the most efficient as the pairing ion for the separation of inositol phosphates [13]. From eluents containing no TBAHS, inositol phosphates (IPs) and other organic phosphates are very poorly retained or not retained at all.

All the k' *vs.* TBAHS concentration plots in Fig. 1. have a similar convex shape. We found that the position of the retention maxima for both IPs and nucleotides was primarily determined by the nature and concentration of the organic modifier in the eluent, and that changes in salt concentration and pH had hardly any effect on the position of the maxima observed. When identical acetonitrile concentrations (*e.g.*, 15%) were used for IPs and nucleotides, the maxima appeared at the same TBAHS concentration (10–15 m*M*). With higher acetonitrile concentrations (20%) the maxi-

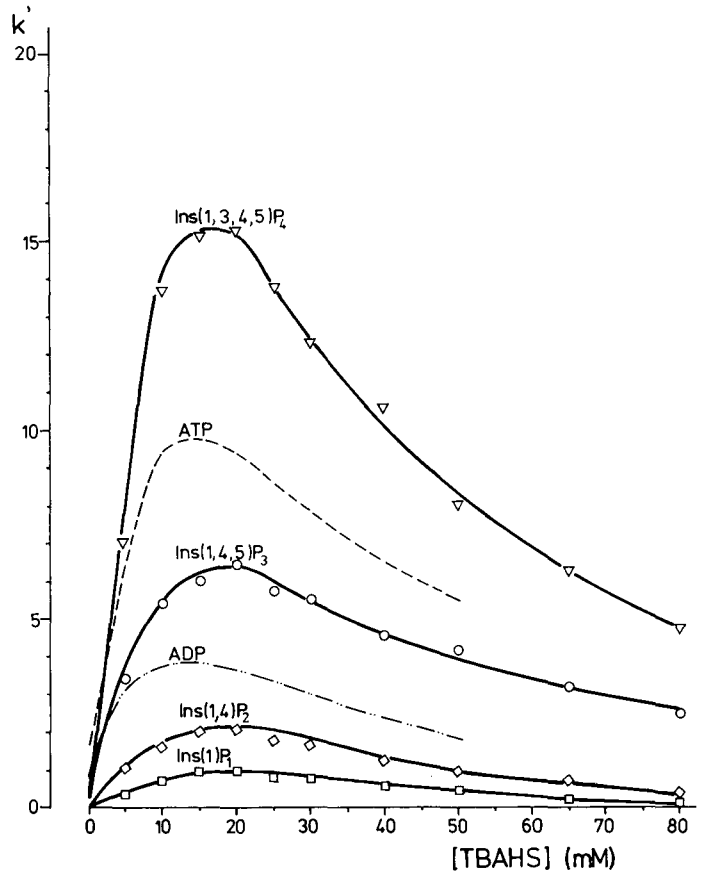

Fig. 1. Dependence of k' on the concentration of TBAHS in the eluent. Column: Nucleosil C_{18} (5 μm), 150 × 4.0 mm I.D., with a 20 × 4.0 mm I.D. precolumn ($t_0 = 1.32$ min). The eluent for IPs consisted of 20% (v/v) acetonitrile, 25 m*M* KH_2PO_4 and 0–80 m*M* TBAHS, the pH of the aqueous part being adjusted to 7.0 using 20% (w/v) KOH solution. The eluent for adenine nucleotides consisted of 15% acetonitrile, 20 m*M* KH_2PO_4 and 0–80 m*M* TBAHS, the pH of the aqueous part being adjusted to 5.2 using 20% (w/v) KOH solution.

ma appeared at higher TBAHS concentrations (15–20 m*M*), irrespective of pH and/or salt concentration changes in the eluent (see the IP curves in Fig. 1). In aqueous buffers with a very low (1%) concentration of methanol, adenine nucleotides exhibited retention maxima at 0.3 m*M* TBAHS [17].

Thus, the eluent concentration of the organic modifier and the TBAHS concentration at which retention maxima are obtained run parallel with each other (zero concentrations excluded). As limited changes in the eluent pH and salt concentration do not affect the amount of the pairing ion adsorbed [18], maximum retention of IPs (and/or nucleotides) can be achieved at any practical TBAHS concentration in the eluent (*e.g.*, in the range 0.3–30 m*M*), depending on the concentration of the organic modifier used (which influences the adsorption of TBAHS on the surface).

For our experiments a TBAHS concentration of 10 m*M* was preferred as RP-

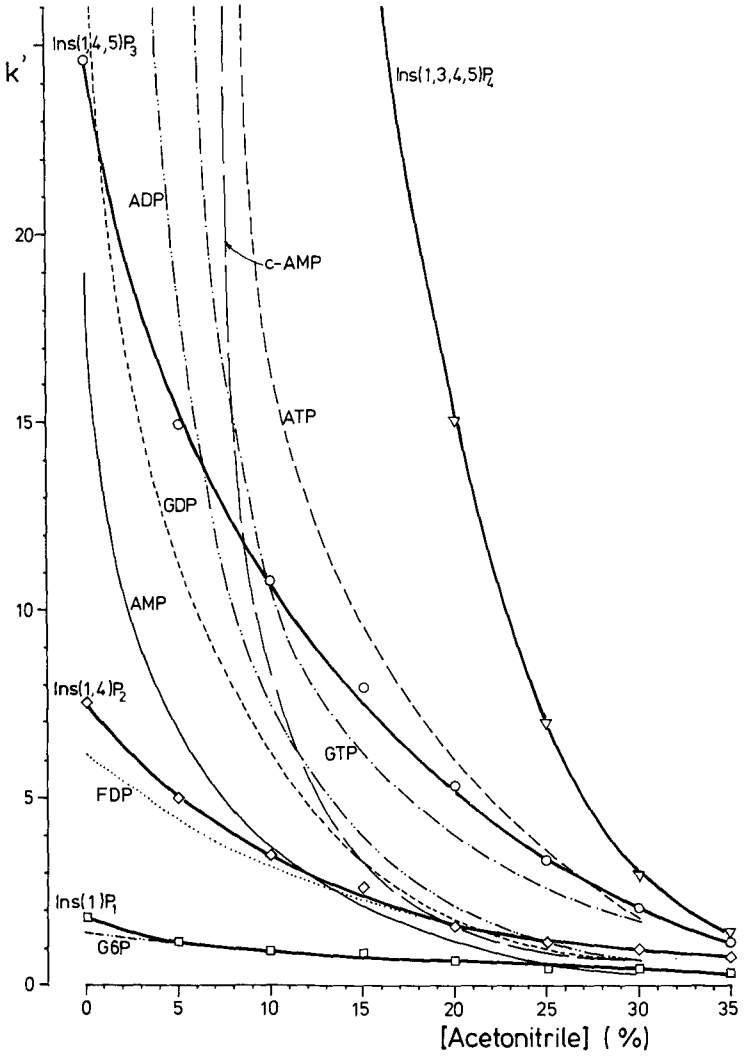

Fig. 2. Dependence of k' on acetonitrile volume percentage in the eluent. Column as in Fig. 1. The eluent consisted of 25 m*M* KH_2PO_4, 10 m*M* TBAHS and 0–35% (v/v) acetonitrile. The pH of the aqueous part was adjusted to 5.0.

IPC systems with much lower pairing ion concentrations are more sensitive to temperature changes and require long re-equilibration times [11,17], which is a disadvantage especially when gradient elution is used. These TBAHS concentrations are too low for micelle formation to be considered as an explanation for the falling side of the k' *vs.* TBAHS concentration curves [10]. The explanation may be related to an increased coverage of the adsorbent surface by the pairing ion [9] and an increased competition by the counter ion of the pairing ion with the sample anions for retention on the surface [19].

Dependence of k' on acetonitrile admixture

An increase in the acetonitrile content in the eluent [in the range 5–30% (at constant pH, TBAHS and phosphate concentrations)] decreases the retention of nucleotides to a greater extent than that of IPs (the retention of c-AMP is affected most, see Fig. 2).These selectivity changes indicate that, although the dominant mechanism of the RP-IPC process with TBAHS as pairing ion is mostly ion exchange [18] or ion interaction [20], non-specific (apolar or hydrophobic) interactions also have an important role.

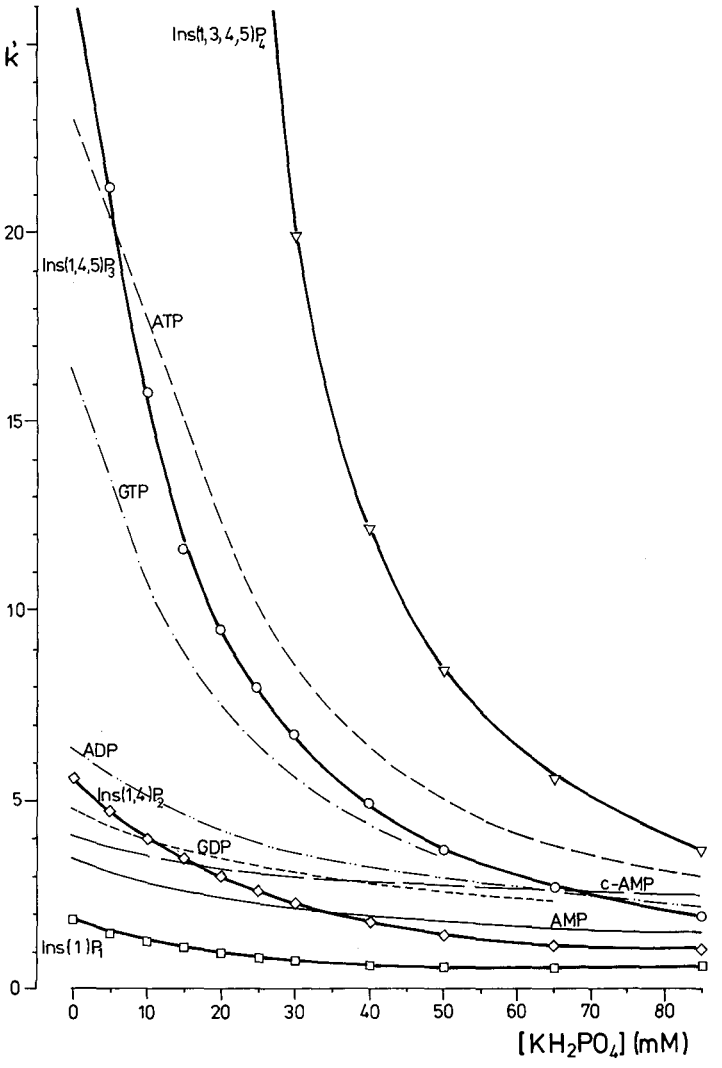

Fig. 3. Dependence of k' on phosphate concentration in the eluent. Column as in Fig. 1. The eluent consisted of 15% acetonitrile, 10 m*M* TBAHS and 0–85 m*M* KH_2PO_4. The pH of the aqueous part was adjusted to 5.0.

Owing to the heterocyclic ring system in their molecules, non-specific interactions are stronger with nucleotides and become significant with eluents containing less than about 10% of acetonitrile. With c-AMP, which has the smallest phosphate moiety of the nucleotides, non-specific interactions appear to be especially strong in eluents containing less than 7% acetonitrile, but their significance is greatly reduced in eluents with over 20% of acetonitrile.

With eluents containing more than 35% of acetonitrile, ionic interactions also approach zero, as acetonitrile concentrations higher than 35% seem to flatten the adsorption isotherm of the pairing ion to such an extent that a 10 m*M* eluent concentration of TBAHS (in our case) cannot provide the surface concentration of the pairing ion necessary for a reasonable retention of the ion pairs formed.

As shown in Fig. 2, sugar phosphates behave very similarly to their inositol phosphate counterparts. The separation of G6P from Ins(1)P_1 is only possible with eluents having a low phosphate concentration and containing no acetonitrile at all. Myo-inositol was invariably eluted with or very near the front.

Dependence of k' on the phosphate concentration of the eluent

As shown in Fig. 2, the retention of IPs is governed mostly by ionic interactions, whereas that of the nucleotides is determined by both ionic and non-specific interactions. An increase in the eluent phosphate concentration, therefore, will cause a more pronounced reduction in the retention of IPs (as it would in ion-exchange systems, in general).

When the phosphate concentration in the eluent is increased in the range 0–50 m*M*, the retention of c-AMP is hardly influenced, whereas the k' values of IPs decrease considerably (see Fig. 3). The effective phosphate concentration range is pushed downward in eluents containing more than 15% of acetonitrile, and extended to higher phosphate (or counter ion) concentrations if less than 15% of acetonitrile is used in the eluent.

The eluent strength in most RP-IPC systems is determined by both the volume percentage of the organic modifier and the salt concentration in the mobile phase (at a rough estimate, a 1% change in the eluent acetonitrile concentration equals, in our case, a 5 m*M* change in eluent phosphate concentration). However, eluents of the same average strength may exhibit different selectivity characteristics, depending on the acetonitrile to phosphate concentration ratio in the eluent (see the discussion on Figs. 4 and 5).

It should also be mentioned that phosphate concentrations below 15 m*M* resulted in much poorer than expected column efficiencies (especially when eluent pH was below 4.0). The apparent efficiency improves with increasing phosphate concentration in the range 0–40 m*M*, but at higher concentrations the effect is negligible. In addition, phosphate concentrations higher than 30–40 m*M* caused substantial "quenching" by reducing the solubility of scintillants {a scintillant to eluent ratio of 5:1 was used for the detection of IPs; the cocktail consisted of 6g of 2,5-diphenyloxazole, 0.6 g of 1,4-di[2-(5-phenyl)oxazoyl]benzene and 150 g of naphthalene dissolved in 1800 ml of dioxane and 150 ml of toluene}. Therefore, unless special selectivity effects require differently, the practical phosphate concentration range in RP-IPC eluents for the separation of radiolabeled IPs and nucleotides appears to be 15–40 m*M*.

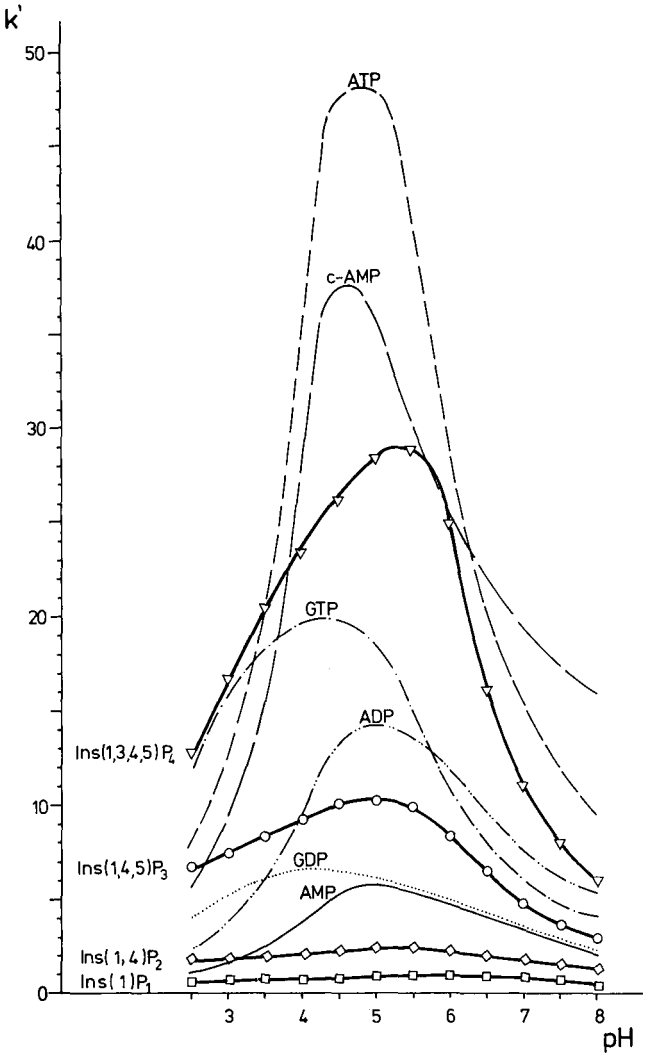

Fig. 4. Dependence of k' on mobile phase pH. Column as in Fig. 1. The eluent consisted of 3% acetonitrile, 10 m*M* TBAHS and 100 m*M* KH_2PO_4. The pH of the aqueous part varied between 2.5 and 8.0.

Dependence of k' on mobile phase pH

Ins(1,4,5)P_3-like phosphates have a polyphosphate–polyester character, whereas ATP-like phosphates have a polyphosphate–monoester type group with $pK_a \approx 6.5$ [21] in their molecules. Conflicting data have been published on the pH dependence of the retention of both IPs and adenine nucleotides in RP-IPC systems. Shayman and BeMent [13] reported a narrow pH optimum (maximum retention) for IPs and ATP at pH 3.5. Sulpice *et al.* [14], however, reported an increase in retention for Ins(1,4,5)P_3 in the pH range 3.5–8.0, with pH 8.0 resulting in the highest retention. For adenine nucleotides the maximum retention was reported to be at *ca.* pH 6.5. On the other

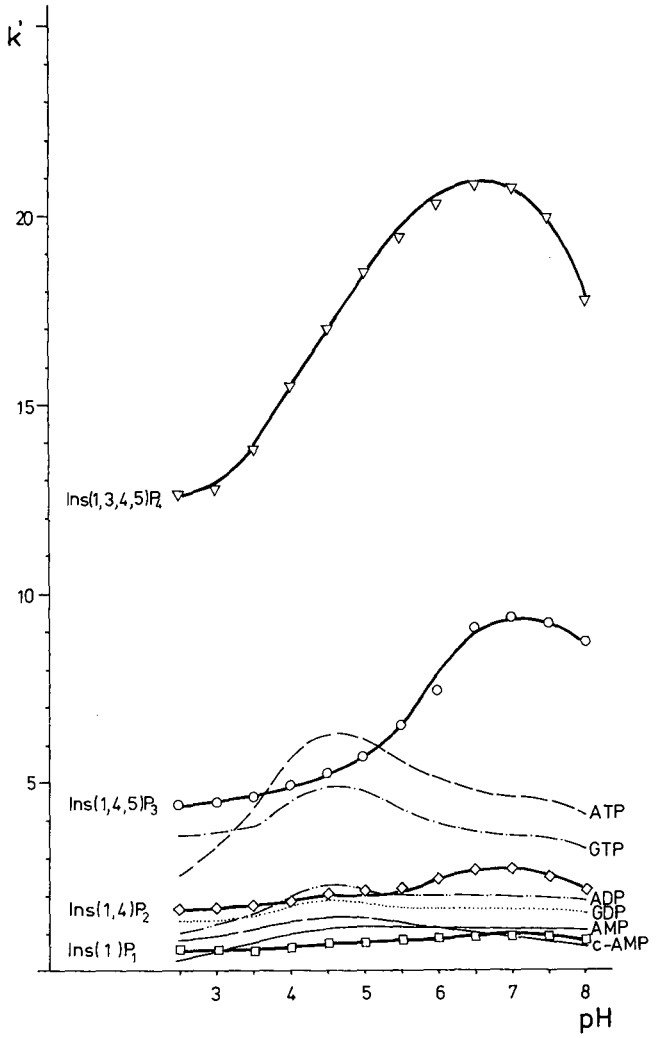

Fig. 5. Dependence of k' on mobile phase pH. Column as in Fig. 1. The eluent consisted of 20% acetonitrile, 10 mM TBAHS and 15 mM KH_2PO_4. The pH of the aqueous part varied between 2.5 and 8.0.

hand, Ingebretsen *et al.* [17] found maxima in the k' *vs.* pH plots of adenine nucleotides at pH 5.0.

All three groups of workers used tetrabutylammonium as pairing ion in phosphate buffer and acetonitrile [13, 14] as organic modifier. There were, however, substantial differences in the concentrations of the organic modifier and the buffer salt in the eluents used by Ingebretsen *et al.* and Sulpice *et al.* (the latter eluent components influence ionic equilibria in aqueous–organic mixtures as both of these modify the pK_a of the solute of interest [22], especially when the eluent pH is established near the pK_a of the solute). In an attempt to explain the discrepancies in the results published by the above workers, we used two eluents with different acetonitrile to phosphate

concentration ratios for studying the pH dependence of the retention of the compounds concerned.

Fig. 4 shows the k' *vs.* pH plots when an eluent with a relatively high phosphate concentration (100 m*M*) and low acetonitrile concentration (3%, v/v) was used, and Fig. 5 presents the k' *vs.* pH curves of the same compounds obtained with an eluent of moderate phosphate and acetonitrile concentrations (15 m*M* and 20%, respectively). In each k' *vs.* pH study the TBAHS, phosphate and acetonitrile concentrations were held constant. The pH of the KH_2PO_4 buffer (which at first decreased on addition of TBAHS) was adjusted using 20% (w/v) potassium hydroxide solution.

Inspection of the data in Fig. 4 shows that, using an organic solvent to counter ion concentration ratio similar to that reported by Ingebretsen *et al.*, we confirmed a maximum retention for adenine nucleotides at about pH 5, although for acids with $pK_a \approx 6.5$ the retention maxima were expected to be at a higher pH.

The chromatographic conditions under which the data in Fig. 5 were obtained were similar to those used by Sulpice *et al.* (there was some difference in the TBAHS concentrations, but these only affect the absolute and not the relative k' values). The k' *vs.* pH plots for the IPs in Fig. 5 are similar to that reported for Ins(1,3,4)P_3 by Sulpice *et al.*, but we failed to confirm the retention maxima (at pH 6.5) of adenine nucleotides which they reported. In our hands, the k' *vs.* pH plots for the nucleotides showed maxima at pH 4.5. We confirmed, however, that the k' *vs.* pH curves of IPs and nucleotides show opposing tendencies in the pH range 5.5–7.0 under such conditions.

Our k' *vs.* pH data (for IPs and ATP) and the results published by Shayman and BeMent [13] are, on the other hand, difficult to reconcile, irrespective of the chromatographic conditions used. The pK_a values of these phosphates make the retention maxima (reported at pH 3.5) very unlikely.

When the respective plots in Figs. 4 and 5 are compared, it is notable that the position of the maxima of the nucleotide curves is much less influenced by the organic solvent to counter ion concentration ratio in the eluent than the position of the maxima of the IP curves.

If we accept $k' = 20$ as a practical maximum for the retention of the compound eluted last in an isocratic system, we have pH 3 and pH 7 (in Figs. 4 and 5) to compare the retention behaviours of the compounds studied in eluents of similar average elution strength. The influence of pH (alone) on retention can be studied when elution orders obtained at pH 3 and 7 in the same figure (Fig. 4 or Fig. 5) are compared.

When we compare the elution orders obtained at the same pH, but in different figures (Figs. 4 and 5; *i.e.*, at different acetonitrile to phosphate concentration ratios in the eluent), we see that at both pH 3 and 7 the retentions of c-AMP and some IPs [Ins(1,4)P_2 and Ins(1,4,5)P_3] are affected most, as was found earlier (at pH 5.0) on studying the plots in Figs. 2 and 3.

The combined effect of the eluent pH and acetonitrile to phosphate concentration ratio on RP-IPC selectivity in the separation of IPs and nucleotides can be studied by comparing the elution order at pH 3 in Fig. 4 with that at pH 7 in Fig. 5, and similarly the elution order at pH 7 in Fig. 4 with that at pH 3 in Fig. 5. In the latter instance the relative retentions of eight solutes out of ten are affected considerably, demonstrating the combined power of these eluent parameters to influence the selectivity in RP-IPC.

Separation of myo-inositol phosphates and some isomers

One problem in the isocratic RP-IPC separation of the IPs mentioned comes from the fact that Ins(1)P_1 is poorly retained (or not retained at all) from solvents that elute Ins(1,3,4,5)P_4 in a reasonable length of time (at $k' \leqslant 15$). On the other hand, if Ins(1)P_1 has a satisfactory retention ($k' \approx 1.5$–2.0), Ins(1,3,4,5)P_4 does not elute from the column in the solvent used.

Another problem is the separation of isomers. Whereas the RP-IPC separation of the IPs presented in Figs. 1–5 was relatively easy, the Ins(1,3,4)P_3 and Ins(1,4,5)P_3 isomers showed very close similarities in chromatographic behaviour throughout the retention studies (Figs. 1–5). The same applies to inositol bisphosphate isomers [although authentic isomers were not available, our Ins(1,4)P_2 probably contained a mixture of positional isomers]. In other words, the selectivity factor, α ($\alpha = k'_2/k'_1$, where k'_1 and k'_2 are the k' values of peaks 1 and 2, with peak 2 eluting later), for the isomers is low in the RP-IPC systems studied.

When the α values for peaks 1 and 2 (*e.g.*, the inositol trisphosphate isomers) are in the range 1.105–1.109 (which was typical in most of the RP-IPC systems studied), and we have a tolerably high retention for peak 2 ($10 < k'_2 < 15$), a plate count of at least 4500 is needed for a baseline separation of these peaks (we pretested the efficiency of the RP-IPC columns using AMP and ATP as test compounds in the eluent employed, and an average plate count of 4500 was considered to be the necessary minimum).

When the k' values are below the range suggested, columns with even higher plate counts are necessary for the separation of the isomers. In this work, we used columns with an average plate count of about 7500 (for AMP and ATP). Such col-

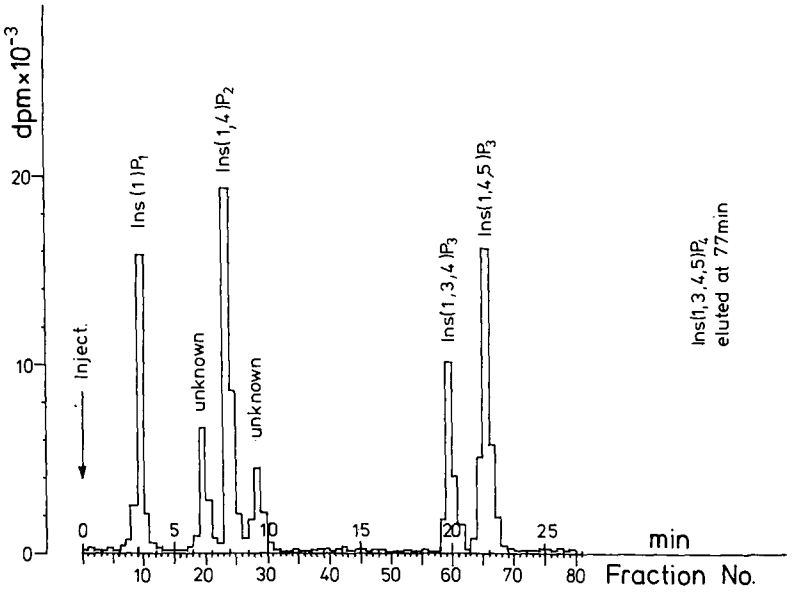

Fig. 6. Separation of myo-inositol phosphates in an isocratic RP-IPC system. Column: Nucleosil C_{18} (5 μm), 200 × 4.0 mm I.D., with a 20 × 4.0 mm I.D. precolumn ($t_0 = 1.66$ min). The eluent consisted of 12% acetonitrile, 10 m*M* TBAHS and 15 m*M* KH_2PO_4. The pH of the aqueous part was adjusted to 5.0.

umns also facilitated the separation of what we assume to be inositol bisphosphate isomers [we could not even speculate, however, whether our systems can separate Ins(1)P_1 and Ins(4)P_1, a major inositol phosphate in cells, as the former eluted in a single peak and the latter was not available]. In order to maintain the required column efficiency, columns should be checked for plate counts every 2–3 days during a series of analyses and, if necessary, the precolumn should be replaced.

A representative chromatogram of [^{3}H]IPs obtained in an isocratic system is shown in Fig. 6. A poor retention for Ins(1)P_1 and a very strong retention for Ins (1,3,4,5)P_4 are the weak points of the isocratic RP-IPC system. The separation of the isomers, however, is excellent. An obvious answer to the problem presented in Fig. 6 is a gradient mode of elution.

Gradient elution is not very common with RP-IPC systems as RP-IPC ionic equilibria ("disturbed" by a gradual increase in the volume percentage of the organic modifier) are time consuming to restore. In the RP-IPC separation of IPs and nucleotides, however, the eluent strength can also be increased by the use of salts (see Fig. 3) and a "mixed gradient" (with increasing acetonitrile and phosphate concentrations by the stronger eluent, eluent B) can be accomplished in a shorter span of acetonitrile concentrations than a "normal" gradient in which eluent strength is increased by acetonitrile alone. Also, a smaller change in acetonitrile concentrations disturbs the basic equilibrium in an RP-IPC process (the partition of the pairing ion between the stationary and the mobile phases) to a lesser extent, as was discussed in relation to

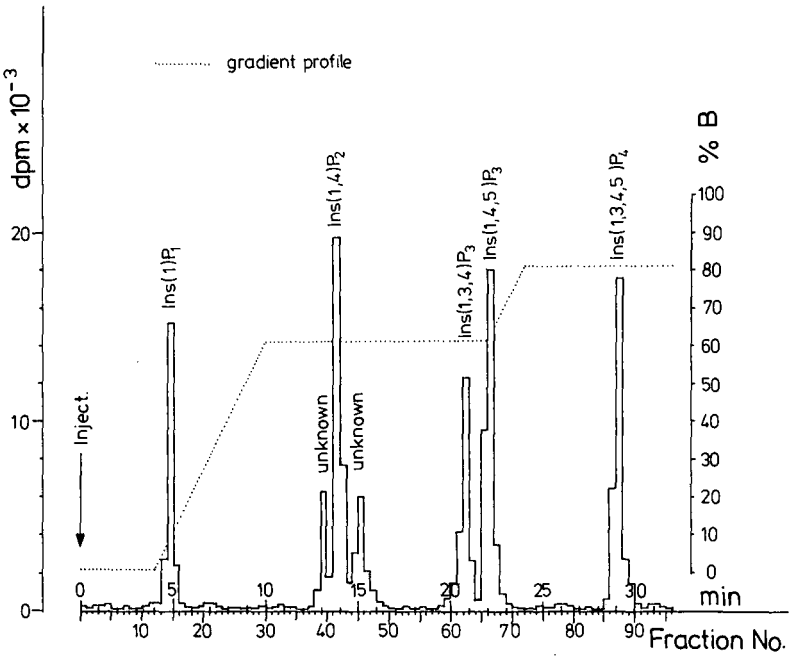

Fig. 7. Separation of myo-inositol phosphates in a gradient RP-IPC system. Column as in Fig. 6. Eluent A consisted of 10 m*M* TBAHS and 15 m*M* KH_2PO_4, the pH being adjusted to 5.0. Eluent B consisted of 30% acetonitrile, 10 m*M* TBAHS and 35 m*M* KH_2PO_4, the pH of the aqueous part being 5.0. The gradient was 1% B (4 min), 1–61% B (6 min), hold (12 min), 61–81% B (2 min), hold (8 min).

Fig. 1. With a mixed gradient (and a relatively high pairing ion concentration), a re-equilibration period of 20 min between chromatographic runs was sufficient and permitted reproducible gradient RP-IPC separations. Day-to-day and run-to-run system reproducibilities (gradient runs) were checked through the retention of AMP, ATP and Ins(1,4,5)P_3 and were, on average, within 2% and 0.2%, respectively.

A representative gradient separation of all the [^{3}H]IPs studied is shown in Fig. 7. The peaks marked "unknown" are thought to be inositol bisphosphate isomers. For the separation of the isomers we chose isocratic conditions (actually "near-isocratic" conditions as there is always a delay in eluent strength during gradient elution). As shown, the retention of Ins(1)P_1 is satisfactory, the isomers are well resolved and the last peak is eluted within 30 min. [^{3}H]Inositol leaves the column unretained and is eluted in the first 4 min even if a relatively large amount of activity is placed on the column. The chromatographic conditions presented in Fig. 7 are likely to provide satisfactory separations of [^{3}H]inositol phosphates also in biological samples.

Separation of myo-inositol phosphates, some common nucleotides and sugar phosphates

The technique of ^{32}P labeling is said to be less expensive and more efficient than ^{3}H labeling, and can be used with all types of cells without permeabilization treatments [14]. However, these advantages are considerably diminished by the fact that ^{32}P labeling leads to a large number of highly labeled phosphorylated compounds in cell or tissue extracts (nucleotides, dinucleotides, sugar phosphates, etc.), among

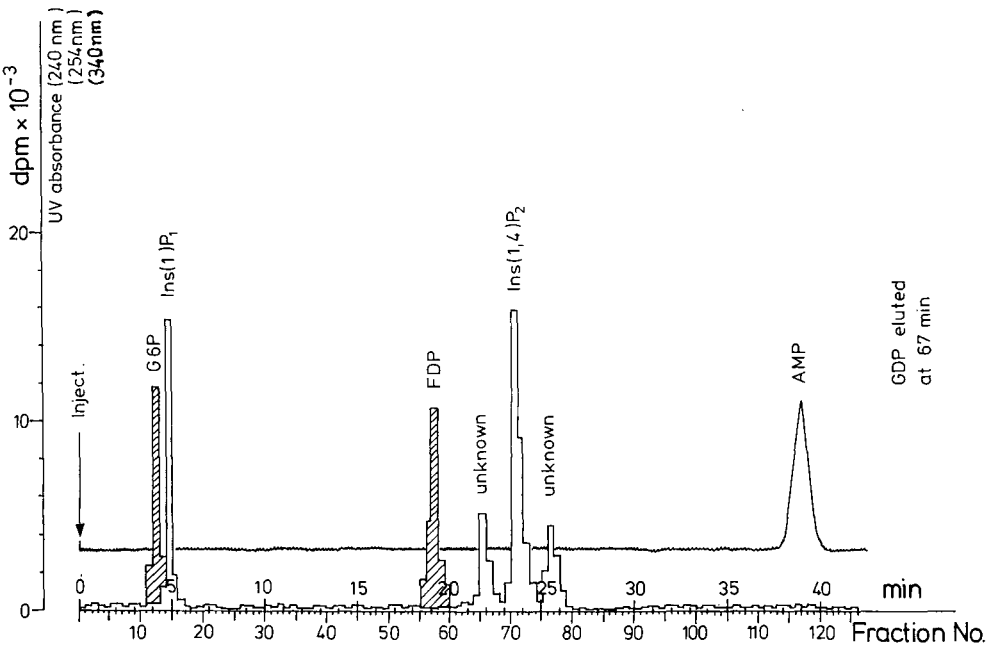

Fig. 8. Separation of some early eluting IPs, nucleotides and sugar phosphates in an isocratic RP-IPC system. Column as in Fig. 6. The eluent consisted of 10 m*M* TBAHS and 15 m*M* KH_2PO_4. The pH of the eluent was adjusted to 5.0.

which IPs represent only a few percent of the total radioactivity. In such instances, the separation of IPs from the interfering compounds is a challenging task even if efficient extraction and concentration steps are combined with efforts to reduce selectively the amount of nucleotides in the extracts [14,23,24]. The retention and separation studies in this work provide some means for controlling elution orders and peak spacing in order to cope with such interference problems.

An isocratic RP-IPC system for the separation of some early eluting phosphates is presented in Fig. 8. Ins(1)P_1 and G6P are partially resolved, but Ins(1,4)P_2 is well separated from both FDP and the nucleotides. This isocratic system was used as the initial step in the gradient separation of all the compounds studied (see Fig. 9). Between the peaks of Ins(1)P_1 and FDP, ample space is left for some (unknown) early eluting phosphorylated compounds in a biological sample. Another function of the relatively long (12 min) initial step is to "preserve" the elution order shown in Fig. 8 during the steep gradient step, by which Ins(1,4)P_2 can be eluted before a group of (otherwise interfering) nucleotides. This objective is also helped by a substantial delay in elution strength (the actual elution strength appearing on the surface of the adsorbent is well below that indicated by the gradient profile for a given moment of the separation). While maintaining a satisfactory resolution for all the compounds of

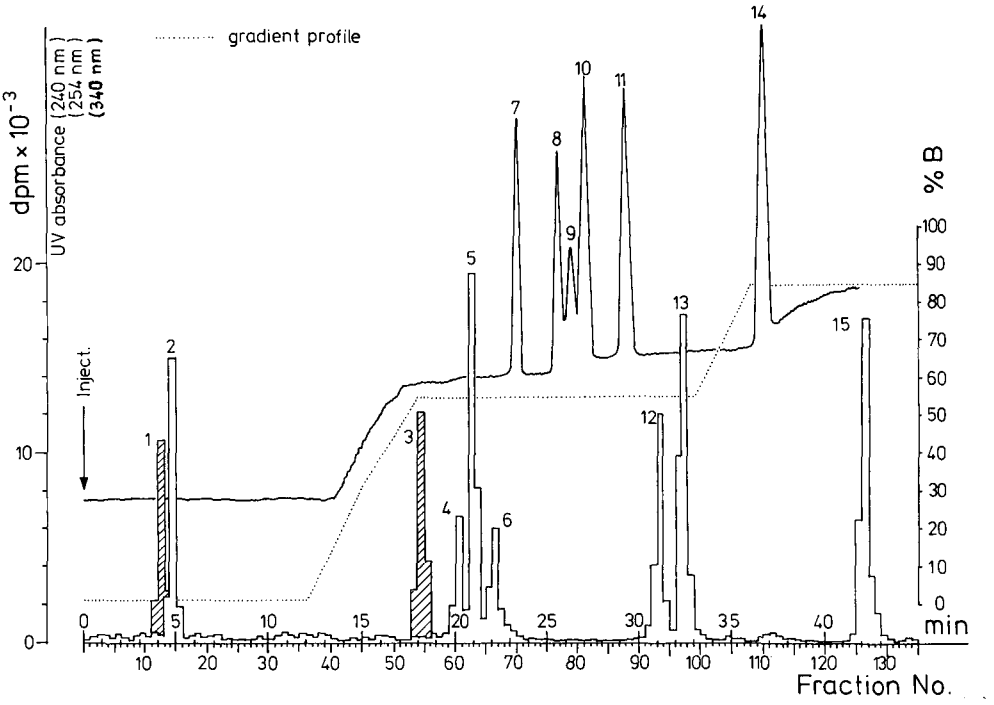

Fig. 9. Separation of myo-inositol phosphates, some common nucleotides and sugar phosphates in a gradient RP-IPC system. Column as in Fig. 6. Eluents A and B as in Fig. 7. The gradient was 1% B (12 min), 1–31% B (3 min), 31–55% B (3 min), hold (15 min), 55–85% B (3 min), hold (6 min). The compounds separated were (1) G6P, (2) Ins(1)P_1, (3) FDP, (4 and 6) unknowns, (5) Ins(1,4)P_2, (7) AMP, (8) GDP,(9) c-AMP, (10) ADP, (11) GTP, (12) Ins(1,3,4)P_3, (13) Ins(1,4,5)P_3, (14) ATP and (15) Ins(1,3,4,5)P_4.

interest, the whole RP-IPC gradient run takes less than 45 min at a flow-rate of 1 ml/min, providing a faster separation of these compounds than the anion exchange HPLC methods published so far.

CONCLUSIONS

The results of this study provide further evidence of the usefulness of the RP-IPC approach in the separation of myo-inositol phosphates, nucleotides and sugar phosphates. The RP-IPC system selectivity, which is very good for Ins(1)P_1, Ins(1,4)P_2, Ins(1,4,5)P_3, Ins(1,3,4,5)P_4 and all the nucleotides examined, can be influenced considerably by changing the pH and the organic modifier to buffer salt concentration ratio in the eluent. For the separation of inositol trisphosphate isomers, columns with plate counts of at least 4500 are needed.

Isocratic RP-IPC systems are useful only if two to five closely related IPs are to be separated. However, under proper chromatographic circumstances, gradient RP-IPC separations can also be carried out reproducibly, followed by a 20-min re-equilibration period. Complex gradient separations can be accomplished in less than 45 min under mild chromatographic conditions (using less than 50 m*M* phosphate in the eluent), so RP-IPC is likely to become a useful alternative to established anion-exchange HPLC separation techniques in the determination of myo-inositol phosphates and other organic phosphates in biological samples.

ACKNOWLEDGEMENTS

The authors thank Mrs. E. Blazsek for excellent technical assistance and Mrs. Á. Csikós for typing the manuscript. They also thank S. Juhász of B.S.T. (Budapest, Hungary) for packing the chromatographic columns.

REFERENCES

1 P. W. Majerus, T. M. Connolly, V. S. Bansal, R. C. Inhorn, T. D. Ross and D. L. Lips, *J. Biol. Chem.*, 263 (1988) 3051–3054.
2 M. J. Berridge, *Biochem. J.*, 212 (1983) 849–858.
3 K. A. Wreggett and R. F. Irvine, *Biochem. J.*, 245 (1987) 655–660.
4 A. L. Leavitt and W. R. Sherman, *Methods Enzymol.*, 89 (1982) 9–18.
5 B. W. Agranoff, P. Murthy and E. B. Seguin, *J. Biol. Chem.*, 258 (1983) 2076–2078.
6 R. F. Irvine, E. E. Anggard, A. J. Letcher and C. P. Downes, *Biochem. J.*, 229 (1985) 505–511.
7 N. M. Dean and J. D. Moyer, *Biochem. J.*, 242 (1987) 361–366.
8 G. P. Heathers, T. Juehne, L. J. Rubin, P. B. Corr and A. S. Evers, *Anal. Biochem.*, 176 (1989) 109–116.
9 C. T. Hung and R. B. Taylor, *J. Chromatogr.*, 202 (1980) 333–345.
10 R. S. Deelder and J. H. M. van den Berg, *J. Chromatogr.*, 218 (1981) 327–339.
11 M. Patthy and R. Gyenge, *J. Chromatogr.*, 449 (1988) 191–205.
12 J. Poggioly, J.-C. Sulpice and G. Vassort, *FEBS Lett.*, 206 (1986) 292–297.
13 J. A. Shayman and D. M. BeMent, *Biochem. Biophys. Res. Commun.*, 151 (1988) 114–122.
14 J.-C. Sulpice, P. Gascard, E. Journet, F. Rendu, D. Renard, J. Poggioly and F. Giraud, *Anal. Biochem.*, 179 (1989) 90–97.
15 V. Jagannathan, K. Singh and M. Damodaran, *Biochem. J.*, 63 (1956) 94–105.
16 R. J. L. Bondar and D. C. Mead, *Clin. Chem.*, 20 (1974) 586–590.
17 O. C. Ingebretsen, A. M. Bakken, L. Segadal and M. Farstad, *J. Chromatogr.*, 242 (1982) 119–126.
18 J. C. Kraak, K. M. Jonker and J. F. K. Huber, *J. Chromatogr.*, 142 (1977) 671–688.

19 Q. Xianren and W. Baeyens, *J. Chromatogr.*, 456 (1988) 267–285.
20 B. A. Bidlingmeyer, *J. Chromatogr. Sci.*, 18 (1980) 525-539.
21 H. Sigel, K. Becker and D. B. McCormick, *Biochim. Biophys. Acta*, 148 (1967) 655–664.
22 J. L. M. van de Venne, J. L. H. M. Hendrikx and R. S. Deelder, *J. Chromatogr.*, 167 (1978) 1–16.
23 J. L. Meek, *Proc. Natl. Acad. Sci. U.S.A.*, 83 (1986) 4162–4166.
24 G. W. Mayr, *Biochem. J.*, 254 (1988) 585–591.

Journal of Chromatography, 523 (1990) 217–225
Elsevier Science Publishers B.V., Amsterdam

CHROM. 22 735

Controlling the retention of clopenthixol and other basic drug substances by reversed-phase ion-pair chromatography on bonded-phase materials using two counter-ions of opposite charge

PER HELBOE

Drug Standardization Laboratory, National Board of Health, 378 Frederikssundsvej, DK-2700 Brønshøj (Denmark)

(First received May 22nd, 1990; revised manuscript received July 30th, 1990)

ABSTRACT

In the reversed-phase chromatography of nitrogen-containing bases on chemically bonded ODS-silica, peak tailing and prolonged retention are often considerable problems. These effects are due to residual silanols on the surface of the column material and may be remedied by adding suitable amines or quaternary ammonium ions to the eluent as anti-tailing agents. However, further addition of an anionic compound is often needed to achieve a suitable retention. The retention mechanism in such systems is complex as interaction takes place between the anionic compound and the solute molecules, anti-tailing agent and column packing material. The influence of the nature of the anti-tailing agent and anionic counter-ion on the retention of *cis*- and *trans*-clopenthixol and of other basic drug substances was investigated and it was found that both the retention and the selectivity were greatly affected.

INTRODUCTION

Nitrogen-containing basic compounds constitute a major proportion of the drug substances used in modern therapy. Therefore, the determination of such compounds is an important topic in drug analysis. The relatively polar characteristics of such substances, which are readily soluble in *e.g.*, aqueous methanol, makes high-performance liquid chromatography (HPLC) on chemically bonded materials an obvious possibility. However, it was shown in 1978 by Wahlund and Sokolowski [1] that peak tailing and even prolonged retention are often seen when chromatographing nitrogen-containing bases on bonded-phase materials. This problem is probably due to the presence of residual silanol groups on the surface of the column material [2,3]. The peak tailing may be prevented by the addition to the eluent of a suitable anti-tailing agent to mask the residual silanols. The most efficient anti-tailing agents were shown to be long-chain dimethylalkylamines and trimethylalkylammonium compounds [*e.g.*, 1, 4–8]. By removing totally the effect of residual silanols, the retention of nitrogen-containing compounds will be strongly dependent on the pH of the eluent, as the ionized form of the solute will, at the concentration of methanol used in

0021-9673/90/$03.50

this study, have only a minor affinity to the apolar stationary phase. This means that at low pH such compounds can be expected to elute close to the void volume and the same situation will take place for quaternary ammonium compounds independent of pH. To achieve a suitable retention, it is possible to use a further additive to the eluent, an anionic compound suitable for the formation of ion pairs with the ionized amine or quaternary ammonium compound. This technique has previously been shown to result in efficient separations and good peak shapes [6–10].

In a previous investigation [7], several basic drug substances were investigated with a view to comparing he possible standardization of reversed-phase HPLC methods using bonded-phase materials and two counter ions of opposite charge in the eluent relative to systems based on dynamically modified silica. Several antidepressant and neuroleptic drugs were investigated, including *cis-* and *trans*-clopenthixol, imipramines and structurally related compounds. For all compounds it was found that an efficient separation with excellent peak shape was obtainable. However, the separation of *cis- trans*-clopenthixol required an analysis time of about 30 min (capacity factor, k', for the *trans* compound being *ca.* 20). The aim of this work was to investigate the influence of variations in methanol concentration and in the nature (alkyl chain length) of the two counter ions of opposite charge on the retention and selectivity of the basic drug substances previously investigated.

EXPERIMENTAL

Chemicals

The drug substances were of pharmacopoeial quality. Decyltrimethylammonium (DeTMA) bromide was obtained from Pfaltz & Bauer (Stamford, CT, U.S.A.), dodecyltrimethylammonium (DTMA) bromide and tetradecyltrimethylammonium (TTMA) bromide from Sigma (St. Louis, MO, U.S.A.) and octadecyltrimethylammonium (STMA) bromide and all sodium alkanesulphonates from Fluka (Buchs, Switzerland). All other chemicals, including cetyltrimethylammonium (CTMA) bromide, were of analytical-reagent grade from E. Merck (Darmstadt, F.R.G.).

Apparatus

The individual chromatographic systems were tested on a liquid chromatograph consisting of a Kontron Model 410 LC pump, a Kontron Model 735 LC UV detector (operated at 254 nm) and a Rheodyne Model 7125 injection valve. Chromatograms were recorded on a Kipp & Zonen Model BD-8 recorder. Retention data were collected on a Hewlett-Packard Model 3359A laboratory data system.

Chromatography

All experiments were performed on a 120 × 4.6 mm I.D. column from Knauer (Berlin, F.R.G.) psacked by the dilute slurry technique with chemically bonded LiChrosorb RP-18 ODS-silica (5 μm) (E. Merck).

The eluents used were methanol–water–0.2 *M* potassium phosphate buffer (pH 4.0) (60:35:5) with the addition of 2.5 m*M* alkyltrimethylammonium bromide and 5 m*M* sodium alkanesulphonate and systems with various amounts of methanol.

The chromatographic system, including column, eluent, pump and injection valve, was thermostated at 30°C.

RESULTS AND DISCUSSION

The test substances investigated were *cis*- and *trans*-clopenthixol and several other neuroleptic and antidepressant drug substances which had been examined in a previous investigation [7]. In particular, the separation of the former substances was found to be important as the use in therapy has recently changed from the mixture of the two compounds to the pure *cis* compound, which almost solely possesses the biological effect. Therefore, a method that is able to detect a small amount of *trans*-clopenthixol in *cis*-clopenthixol (*e.g.*, less than 1%) is needed. In a previous investigation [7] a fully satisfactory separation was achieved, the resolution between the two compounds being 1.6. However, a drawback was the time of analysis, which was *ca.* 30 min ($k' \approx 20$). The eluent used for that separation was methanol–water–0.2 *M* potassium phosphate buffer (pH 4.0) (60:35:5) with the addition of 2.5 m*M* DTMA bromide and 5 m*M* sodium decanesulphonate. An obvious possibility for improving the method was to adjust the retention by increasing the concentration of methanol in the eluent to achieve a time of analysis of, *e.g.*, *ca.* 10 min ($k' \approx 6$). This could be expected to work without problems from experience with reversed-phase chromatography in general, as the resolution would be expected to be sufficient provided that the separation factor is not affected. Calculating from the values of k' and assuming a constant separation factor (α), the resolution in an improved system should be *ca.* 1.45 [11]. However, by increasing the percentage of methanol to 65% the time of analysis was reduced to *ca.* 15 min and the resoltuion in this separation was 1.3. Another possibility for reducing the retention in a reversed-phase ion-pair chromatographic separation would be to reduce the carbon chain length in the alkanesul-

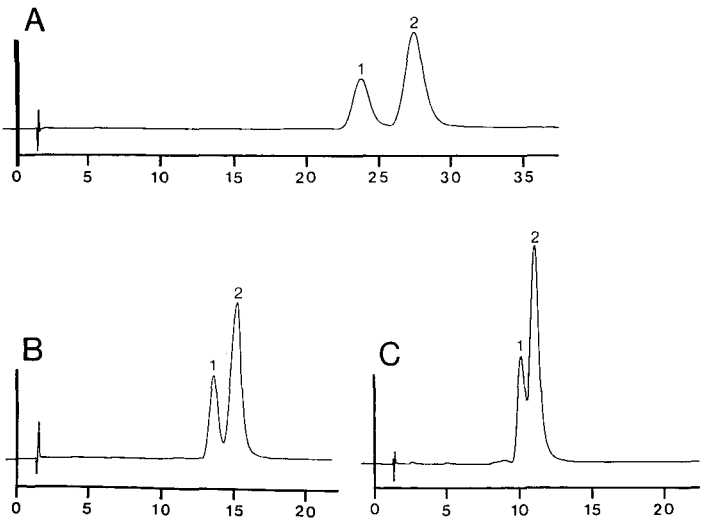

Fig. 1. Separation of (1) *cis* and (2) *trans*-clopenthixol using three different eluents. Column: LiChrosorb RP-18 (120 × 4.6 mm I.D.). Eluents: methanol–water–0.2 *M* potassium phosphate buffer (pH 4.0), A and C (60:35:5), B (65:30:5), with the addition of 2.5 m*M* DTMA bromide and 5 m*M* sodium decanesulphonate (A and B) or sodium hexanesulphonate (C). Flow-rate: 1 ml/min. Detection: UV, 254 nm, 0.32 a.u.f.s. Time scales in min.

phonate used as the counter ion. By using the original methanol concentration of 60% and substituting hexanesulphonate for decanesulphonate as the counter ion, a time of analysis of *ca.* 15 min was achieved but in this instance the resoltuion had been reduced to 0.7. The chromatograms are shown in Fig. 1.

The retention mechanism in these chromatographic systems is complex. The alkanesulphonate interacts both with the anti-tailing quaternary ammonium ions and with solute ions. Further, the two surfactants may be co-adsorbed on to the column material [12,13]. As the concentration of alkanesulphonate is twice that of the quaternary ammonium compound, there will always be counter ions present to form ion pairs with solute ions and the effect of variations in the nature of the counter ions can be expected to be as in reversed-phase ion-pair chromatography in general. The affinity of the quaternary ammonium ions to residual silanols is even more pronounced than that to alkanesulphonates, as it appears that the anti-tailing effect is not reduced by their presence [7]. The effect on retention and selectivity of variations in the nature of both quaternary ammonium ions and alkanesulphonates was investigated and a study was also made of the influence of variations in the concentration of methanol in the eluent.

Nature of quaternary ammonium compound and alkanesulphonate

The effect of alkyltrimethylammonium compounds with alkyl carbon chain lengths varying from 10 to 18 and of alkanesulphonates with carbon chain lengths varying from 4 to 12 were investigated. Some of the results obtained are given in Table I, which shows the effects of variations in the quaternary ammonium compound using 5 m*M* decanesulphonate as the anionic counter ion. Correspondingly, variations in the nature of the alkanesulphonates were investigated using 2.5 m*M* DTMA bromide as the anti-tailing agent.

From the variations in the quaternary ammonium compounds it appears that the retention of the basic compounds decreases with increasing alkyl chain length. This occurs because the affinity of the anti-tailing agent to silanol groups increases with increasing apolar moiety in the molecule, an effect which is well known from chromatography on dynamically modified silica [8]. The influence of the residual silanols is never totally removed, as shown by the results when no alkanesulphonate is present in the eluent. In such a case the retention of imipramine when, *e.g.*, DeTMA is used as the anti-tailing agent is $k' = 3.66$ and an asymmetry fractor of 3.7, whereas the results when using STMA is $k' = 0.28$ and asymmetry factor of 1.6. The tailing has thus been reduced to a level which is acceptable by increasing the alkyl chain length of the quaternary ammonium compound; *cf.*, previous investigations discussing the anti-tailing effects in reversed-phase chromatography using eluents containing two counter ions [7,8]. However, the retention is still considerable, taking into account that the substance is considerably ionized. The retention and the remaining tendency for tailing are due to a remaining interaction with silanol groups.

An increase in the alkyl chain length of the alkanesulphonate has the effect, well known in regular reversed-phase ion-pair chromatography, that the retention of cationic solutes increases [e.g., 14]. A linear relationship in ion-pair chromatography between log k' and carbon number in the counter ion has previously been predicted from theory and shown by experiments [15,16]. From the results of this study, it appears that such a linear relationship also seems to exist, as shown in Fig. 2. It is

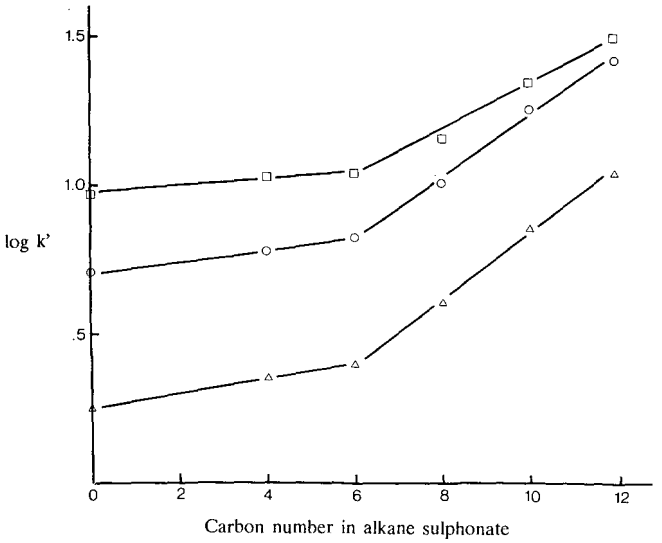

Fig. 2. Relationship between retention (log k') of (△) imipramine, (○) *cis*-clopenthixol and (□) prochlorperazine and carbon number in the alkanesulphonate added to the eluent. Column: LiChrosorb RP-18 (120 × 4.6 mm I.D.). Eluent: methanol–water–0.2 *M* potassium phosphate buffer (pH 4.0) (60:35:5) with the addition of 2.5 m*M* DTMA bromide and 5 m*M* sodium alkanesulphonate with carbon number 4–12.

seen, however, that a change in the linearity appears at six carbon atoms, or alternatively a curved plot approximation might be drawn. The background for this change relative to previously reported results [15,16] has not yet been elucidated. A possible explanation might be that sulphonate ions containing eight carbon atoms and more are adsorbed to some extent on the surface of the column material, thereby enhancing the retention when forming ion pairs with solute molecules. It has been shown by Knox and Hartwick [17] that a change in chain length or in concentration of a sulphonate counter ion will cause a change in surface concentration and, thereby, in surface charge. Further, such adsorbed sulphonate ions will also be able to form ion pairs with DTMA ions, thus increasing the amount of apolar stationary phase, as discussed below.

As mentioned previously, the additives in the eluent may interact with each other, forming ion pairs. The interaction is more pronounced the longer the chain length of the two counter ions. For the most lipophilic counter ions it appears that such ion pairs are adsorbed on the surface of the column packing material, thereby increasing the amount of apolar stationary phase. From Table I it is seen that this effect is reflected by an increased retention of the neutral solute benzene. The strongly lipophilic nature of the ion pairs between quaternary ammonium ions and alkanesulphonates was also demonstrated by solubility problems when using both types with long alkyl chains. Thus it was not possible to perform a planned experiment using STMA bromide and dodecanesulphonate as the ion pairs caused precipitation in the eluent. For other combinations it was found that only by using a chromatographic system which was thermostated at 30°C was it possible to prevent the precipitation which occurred in the eluents at room temperature.

TABLE I

RETENTION AND SELECTIVITY (SEPARATION FACTOR, α, RELATIVE TO ONE COMPOUND IN EACH GROUP) OF TEN TEST SUBSTANCES AND OF BENZENE

Eluent: methanol–water–0.2 m*M* potassium phosphate buffer (pH 4.0) with the addition of 2.5 m*M* alkyltrimethylammonium bromide and 5 m*M* alkanesulphonate as indicated.

Compound	Parameter	Quaternary ammonium compound, 2.5 *M* (5 m*M* decanesulphonate in eluent)					Alkanesulphonate, 5 m*M* (2.5 m*M* DTMA in eluent)					
		C_{10}	C_{12}	C_{14}	C_{16}	C_{18}	C_0	C_4	C_6	C_8	C_{10}	C_{12}
Imipramine	k'	10.85	7.16	3.68	2.07	1.03	1.80	2.22	2.50	4.06	7.16	11.05
Desipramine	α	1.03	1.08	1.11	1.13	1.24	0.71	0.77	0.86	0.97	1.08	1.20
Imipramine N-oxide	α	0.68	0.78	1.02	1.14	1.96	2.65	2.25	1.85	1.23	0.78	0.60
cis-Clopenthixol	k'	25.73	17.61	8.89	4.57	2.41	5.18	5.98	6.80	10.11	17.61	26.69
trans-Clopenthixol	α	1.14	1.16	1.20	1.25	1.33	1.09	1.10	1.10	1.12	1.16	1.21
Chlorpromazine	k'	20.28	14.01	7.68	4.37	2.90	4.02	4.85	5.29	7.54	14.01	22.64
Prochlorperazine	α	1.64	1.60	1.63	1.57	1.53	2.33	2.20	2.11	1.92	1.60	1.40
Perphenazine	α	1.13	1.07	1.03	0.95	0.78	0.99	1.06	1.11	1.10	1.07	1.04
Amitriptyline	k'	13.33	8.83	4.48	2.43	1.23	1.89	2.49	3.00	4.75	8.83	13.94
Nortriptyline	α	0.97	0.91	0.89	0.84	0.79	1.17	1.26	1.15	1.01	0.91	0.84
Benzene	k'	3.04	3.06	3.04	3.16	3.58	2.89	3.01	2.94	2.97	3.06	3.09

It appears from Table I that not only the retention is greatly influenced by the nature of the two counter ions of opposite charge in the eluent. Large variations in selectivity are also seen, *e.g.*, for *cis*- and *trans*-clopenthixol it appears that an increased separation is obtained by increasing the alkyl chain length of both types of additives. However, the effects of the two additives on retention are opposite. The purpose of a separation method for these two compounds, as mentioned above, was to achieve an effective separation within *ca.* 10 min. It was found that the optimum combinations of additives for this particular separation was the addition to the eluent of 2.5 m*M* CTMA bromide and 5 m*M* sodium dodecanesulphonate. Fig. 3 shows the separation of *ca.* 1% of *trans*-clopenthixol in *cis*-clopenthixol.

Methanol concentration

As mentioned previously, the influence of variations in the concentration of methanol in the eluent is not as simple as expected for plain reversed-phase chromatographic systems. Examples of such a relationship are shown in Table II. It appears that the mean retention of the compounds decreases as expected with an increase in the amount of methanol in the eluent. However, the selectivity towards the individual groups of compounds is influenced to different extents and several pairs of substances reverse the order of elution during the series of experiments. For *cis*- and *trans*-clopenthixol it is seen that there is a general decrease in separation with increasing modifier concentration and this excludes the possibility, as indicated also by the preliminary investigations, of reducing the time of analysis by increasing the percentage of methanol in the eluent.

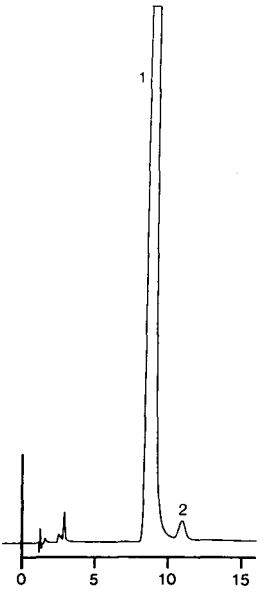

Fig. 3. Separation of 1% *trans*-clopenthixol (2) in *cis*-clopenthixol (1). Column: LiChrosorb RP-18 (120 × 4.6 mm I.D.). Eluent: methanol–water–0.2 *M* potassium phosphate buffer (pH 4.0) (60:35:5) with the addition of 2.5 m*M* CTMA bromide and 5 m*M* sodium dodecanesulphonate. Flow-rate 1 ml/min. Detection: UV, 254 nm, 0.32 a.u.f.s. Time scale in min.

TABLE II

RETENTION AND SELECTIVITY (SEPARATION FACTOR, α, RELATIVE TO ONE COMPOUND IN EACH GROUP) OF TEN TEST SUBSTANCES

Eluent: methanol–water–0.2 *M* potassium phosphate buffer (pH 4.0) with the addition of 2.5 m*M* alkyltrimethylammonium bromide and 5 m*M* alkanesulphonate as indicated. Methanol concentration varied from 50% to 70%.

Compound	Parameter	Additive									
		DTMA + C_8-sulphonate					STMA + C_8-sulphonate				
		50%	55%	60%	65%	70%	50%	55%	60%	65%	70%
Imipramine	k'	8.09	6.17	4.27	3.24	2.53	0.81	0.82	0.84	0.88	0.86
Desipramine	α	1.08	0.97	0.90	0.81	0.72	1.26	1.10	0.95	0.83	0.74
Imipramine N-oxide	α	1.76	1.82	1.88	1.83	1.76	3.89	3.61	3.44	3.14	2.88
cis-Clopenthixol	k'	26.46	17.75	10.77	7.24	4.81	2.67	2.29	2.28	2.21	1.99
trans-Clopenthixol	α	1.23	1.19	1.15	1.12	1.10	1.34	1.30	1.24	1.18	1.14
Chlorpromazine	k'	19.86	14.07	8.74	6.56	4.93	2.71	2.42	2.29	2.14	1.90
Prochloroperazine	α	2.04	2.13	2.23	2.31	2.27	2.54	2.03	2.19	2.28	2.38
Perphenazine	α	1.14	1.11	1.08	0.97	0.90	0.82	0.85	0.90	0.93	0.95
Amitriptyline	k'	10.36	7.50	4.92	3.57	2.66	1.07	0.98	0.97	0.98	0.86
Nortriptyline	α	1.09	0.99	0.93	0.84	0.77	1.26	1.12	1.00	0.87	0.83

CONCLUSION

Reversed-phase ion-pair liquid chromatographic separations of nitrogen-containing basic drug substances using two counter ions of opposite charge in the eluent were investigated. It was found that both the retention and selectivity are greatly influenced by the nature of the two additives and by the concentration of methanol in the eluent. It was shown that by choosing a suitable combination of the two types of additive it is possible to obtain an efficient separation within a reasonable time. This was demonstrated on the two closely related compounds *cis*- and *trans*-clopenthixol.

REFERENCES

1 K.-G. Wahlund and A. Sokolowski, *J. Chromatogr.*, 151 (1978) 299.
2 B. L. Karger, J. N. LePage and N. Tanaka, in Cs. Horváth (Editor), *High-Performance Liquid Chromatography Advances and Perspective*, Vol. 1, Academic Press, New York, 1980, p. 159.
3 A. Nahum and Cs. Horváth, *J. Chromatogr.*, 203 (1981) 53.
4 A. Sokolowski and K.-G. Wahlund, *J. Chromatogr.*, 189 (1980) 299.
5 B.-A. Persson, S.-O. Jansson, M.-L. Johansson and P.-O. Lagerström, *J. Chromatogr.*, 316 (1984) 291.
6 P. Helboe, *J. Chromatogr.*, 245 (1982) 229.
7 S. H. Hansen, P. Helboe and M. Thomsen, *J. Chromatogr.*, 409 (1987) 71.
8 P. Helboe, S. H. Hansen and M. Thomsen, *Adv. Chromatogr.*, 28 (1988) 195.
9 J. A. DeSchutter and P. DeMoerloose, *J. Pharm. Biomed. Anal.*, 6 (1988) 879.
10 J. A. DeSchutter and P. DeMoerloose, *J. Chromatogr.*, 437 (1988) 83.
11 L. R. Snyder and J. J. Kirkland, *Introduction to Modern Liquid Chromatography*, Wiley, New York, 1979, pp. 34*ff*.
12 J. Rodakiewicz-Nowak, *J. Colloid Interface Sci.*, 91 (1983) 368.
13 W.-Y. Lin, M. Tang, J. S. Stranahan and N. Deming, *Anal. Chem.*, 55 (1983) 1872.
14 P. Helboe and M. Thomsen, *Int. J. Pharm.*, 2 (1979) 317.
15 C. Horvath, W. Melander, I. Molnar and P. Molnar, *Anal. Chem.*, 49 (1977) 2295.
16 B. A. Bidlingmeyer, S. N. Deming, W. P. Price, B. Sachok and M. Petrusek, *J. Chromatogr.*, 186 (1979) 419.
17 J. H. Knox and R. A. Hartwick, *J. Chromatogr.*, 204 (1981) 3.

Journal of Chromatography, 523 (1990) 227–233
Elsevier Science Publishers B.V., Amsterdam

CHROM. 22 690

Chromatographic behaviour of aromatic acids in reversed-phase high-performance liquid chromatography

B. RITTICH* and M. PIROCHTOVÁ

Institute of Systematic and Ecological Biology, Czechoslovak Academy of Sciences, Poříčí 3b, 603 00 Brno (Czechoslovakia)

(First received January 5th, 1990; revised manuscript received June 21st, 1990)

ABSTRACT

Using reversed-phase high-performance liquid chromatography, the effect of the pH of the mobile phase on the retention of indole-3-acetic acid and some derivatives of benzoic acid was investigated. The capacity factors of the neutral form (log k'_n), and the anionic form (log k'_{ia}) and the pK_A^* values of solutes in given mobile phases were determined. The log k'_n values were correlated with 1-octanol–water partition coefficients (log P_{oct}). Both the log k'_n and log k'_{ia} values of the acids tested were correlated with their fungicidal activities examined against *Fusarium moniliforme* CCMF-180 and *Penicillium expansum* CCMF-567. Significant linear relationships between fungicidal activities and log k'_{ia} were found.

INTRODUCTION

Auxins are a group of plant hormones among which indole-3-acetic acid (IAA) is considered to be the major but perhaps not the sole active substance [1]. This compound has been identified in different plant materials [1,2].

Reversed-phase high-performance liquid chromatography (RP-HPLC) on silica gel with chemically bonded alkyl chains has proved to be a valuable method for separating polar ionogenic compounds [3–5]. However, substances such as benzoic and phenolic acids [6,7] present in plant can interfere with the determination of IAA. The chromatographic behaviour of ionizable compounds can be varied by changing either the pH or the modifier content of the mobile phase. The chromatographic separation of IAA, benzoic and phenolic acids is usually carried out on octadecylsilica (C_{18}) column eluted with mixtures of water and a water-miscible organic modifier [8–14].

The partition coefficient between 1-octanol and water, P_{oct}, is a good descriptor of the hydrophobicity of compounds and it can be used as an alternative method to control their chromatographic behaviour [15–17].

The aim of this work was to study the effect of the pH of the mobile phase in RP-HPLC on the chromatographic behaviour of IAA and some benzoic acids.

0021-9673/90/$03.50

THEORETICAL

The solute retention in HPLC is expressed by the capacity factor k'. Total protonation of carboxylic groups with $pK_A < 3.5$ in RP-HPLC requires an eluent with pH <2. However, this is not feasible owing to instability of the matrix of an alkyl-bonded stationary phase. For these compounds only the distribution coefficient can be measured. The distribution coefficient is defined as the ratio of the concentrations of a solute in the organic and aqueous phases at a given pH. The partition coefficient is defined as the ratio of the concentrations of the same form of the solute in the two phases. The capacity factor of a monoprotic acid can be expressed [3,4,18] as

$$\log k' = \log (k'_n + k'_{ia} K_A/[H^+]) - \log (1 + K_A/[H^+]) \quad (1)$$

where k'_n is the capacity factor of the neutral form, k'_{ia} the capacity factor of the anionic form of the acid, K_A the dissociation constant of the acid in the eluent and $[H^+]$ the concentration of solvated protons. Eqn. 1 represents the relationship between the capacity factor of a partially dissociated weak acid and the hydrogen ion concentration in the eluent. For $pH \ll pK_A$, eqn. 1 can be simplified to eqn. 2, assuming that k'_{ia} is negligible compared with k'_n:

$$\log k' = \log k'_n - \log (1 + K_A/[H^+]) \quad (2)$$

When the capacity factor is measured at various pH values (at the same ratio of water and modifier), it is possible from delogarithmed and linearized eqns. 1 and 2 to determine the pK_A value of a solute in a given mobile phase:

$$k' = k'_n + (k'_{ia} - k')K_A/[H^+] \quad (3a)$$

$$k' = k'_n - k'K_A/[H^+] \quad (3b)$$

Hydrogen ion concentration plays an important role in eqns. 1 and 2. pH is generally reported as the pH of an aqueous buffer component before it is mixed with an organic modifier, or as the operational pH of the water–organic mixture as measured by a glass electrode. Generally, the latter approach is preferred when the pH of the mixture has to be finally adjusted. The thermodynamically valid pH value in mixed media, pH*[a], is expressed as

$$pH^* = pH^{app} - \delta \quad (4)$$

where pH^{app} is the apparent pH (measured by a pH meter) of the mixed medium and δ is a correction factor, which is available for the methanol–water system in the literature [19,20].

As pH* values are available, the pK_A^* values can be determined chromatographically using eqns. 3a and 3b.

---

[a] The symbol marked with an asterisk refers to a water–organic mixture.

EXPERIMENTAL

Chemicals and equipment

Indole-3-acetic acid and benzoic acid derivatives were obtained from Lachema (Brno, Czechoslovakia), Fluka (Buchs, Switzerland) and Merck (Darmstadt, F.R.G.). They all were of analytical-reagent grade and used without further purification. The compounds used are listed in Tables I and IV. Solvents were redistilled before use.

Chromatography was performed on a Varian LC 8500 chromatograph with a UV-50 variable-wavelength detector (200–900 nm) using a CGC column (150 × 3.3 mm I.D.) (Tessek, Prague, Czechoslovakia) packed with Separon SCX-C_{18} (particle size 5 μm) silica gel with a C_{18} chemically bonded non-polar stationary phase and a Micro Pak CH-10 column (250 × 2.2 mm I.D., Merck, Darmstadt) packed with LiChrosorb RP-18 stationary phase (particle size 10 μm).

Conditions

Methanol–water (2:3) with the pH adjusted with sulphuric acid was used for studying the influence of mobile phase pH on the retention of tested acids. The separation of benzoic acids on the Micro Pak CH-10 column was carried out with methanol–water–acetic acid (30:65:5 and 40:55:5) as mobile phase at a flow-rate of 1.0 ml/min. Capacity facors were evaluated from the retention time of the solute, t_R, and the retention time of an unretarded component, $t_{R,0}$.

The pK_A values of acids [16,21], correction factor δ [19] and log P_{oct} values determined in the 1-octanol–water system [22–24] were taken from the literature.

RESULTS AND DISCUSSION

The values of K_A^* for methanol–water (2:3) as the mobile phase with different adjusted pH* values were calculated using eqn. 3b from the slope of the k' *vs.* $k'/[H^+]$ dependence. However, eqn. 3b is valid only for undissociated acids. It is assumed that this condition is satisfied for mobile phases with adjusted pH 2.59 and 3.15 (with respect to low k'_{ia} values determined in a mobile phase with pH 4.36 this assumption was fulfilled; see below). As the k'_{ia} values were not available for the mobile phase with pH 4.36, eqn. 3b was used also for the calculation of K_A^* and k'_n. These values were considered only as guesses and were used for the calculation of k'_{ia} values using eqn. 1 (first step). The k'_{ia} values obtained were used for the recalculation of the K_A^* and k'_n values using eqn. 3a (for the mobile phase of pH 4.36 only) (second step). The results are given in Table I. There were no significant differences between the first and second steps in the K_A^* values and in the k'_n values. A significant linear relationship was found between the pK_A values determined in water and pK_A^* (eqns. 5 and 6) (Table II). As the pK_A^* value of 4-hydroxybenzoic acid was outside the regression curve, it was excluded from the tested set.

The pK_A values of benzoic and 2-hydroxybenzoic acid were similar to those given by Van de Venne *et al.* [5]. The log k' and log k'_n values were correlated with the log P_{oct} values (Table III). A dominant influence of the values of the correlation coefficients was exhibited by 2-hydroxybenzoic acid, which had a lower pK_A value than the other acids. The chromatographic behaviour of this acid was evidently influenced (with regard to poor buffering of mobile phase) by the local changes of

TABLE I

THE EFFECT OF pH OF THE MOBILE PHASE ON THE SEPARATION OF AROMATIC ACIDS

System: Separon SGX-C_{18} column, methanol–water (2:3) mobile phase. k' = Capacity factor (uncorrected value); k'_n = capacity factor of the neutral form of an acid; k'_{ia} = capacity factor of the anionic form of an acid (for pH* = 4.36); K_A^* = dissociation constant determined chromatographically using methanol–water (2:3) mobile phase; K_A = dissociation constant determined in water [14].

Compound	No.	Log k'			Log k'_n		Log k'_{ia}		pK_A^*		pK_A
		I[a]	II[a]	III[a]	a[b]	b[b]	a[b]	b[b]	a[b]	b[b]	
IAA	I	0.215	0.268	0.276	0.276	0.276	−2.112	−1.824	4.98	5.04	4.65
$HOOCC_6H_4R$: R =											
H	II	0.310	0.386	0.417	0.412	0.412	−1.521	−1.222	4.73	4.72	4.19
2-OH	III	0.093	0.042	0.523	0.528	0.529	−1.912	−1.620	3.92	3.91	2.97
3-OH	IV	−0.319	−0.227	−0.214	−0.213	−0.213	−2.585	−2.720	4.72	4.72	4.06
4-OH	V	−0.444	−0.418	−0.411	−0.412	−0.412	−2.070	−1.765	5.27	5.26	4.48
2-OCH_3	VI	0.033	0.090	0.143	0.125	0.125	−1.645	−1.326	4.78	4.77	4.04
3-OCH_3	VII	0.401	0.488	0.508	0.506	0.506	−1.849	−1.525	4.72	4.72	4.27
4-OCH_3	VIII	0.447	0.542	0.558	0.558	0.558	−2.011	−1.698	4.70	4.70	4.36

[a] I, pH* = 4.36; II, pH* = 3.15; III, pH* = 2.59.
[b] a = 1st step of calculation; b = 2nd step of calculation (the procedure is given in the text).

mobile phase pH due to the mentioned acid injection. This influence was much stronger at higher mobile phase pH. The mobile phase without buffer was used in order to attempt to avoid the effect of the association of the acid anions with buffer cations on chromatographic retention [5].

Methanol–water–acetic acid mobile phases of various composition were used to determine the log k' values of the set of benzoic acid derivatives (Table IV). Significant linear relationships between log P_{oct} and log k' were calculated (eqns. 15 and 16, Table III). The influence of the "ortho effect" on chromatographic behaviour was not important. The relationships were calculated only for uncorrected log k' values because the pK_A^* values for given mobile phases were not available.

TABLE II

VALUES OF REGRESSION COEFFICIENTS FOR EQNS. 5 AND 6

n = Number of compounds in the set; r = correlation coefficient; s = standard deviation; t_a, t_b = Student's characteristics for the coefficients a and b of the regression equation $Y = a + bX$ (the coefficients were tested on hypothesis $a = 0$, $b = 0$).

Compound Nos.	Equation	n	r	s	t_a	t_b
I–IV, VI–VIII	pK_A = −2.979 + 1.517pK_A^{*a} (5)	7	0.962	0.145	3.634[c]	8.627[d]
I–IV, VI–VIII	pK_A = −2.717 + 1.459pK_A^{*b} (6)	7	0.966	0.137	3.662[c]	9.180[d]

[a] 1st step of calculation.
[b] 2nd step of calculation.
[c] Statistically significant difference ($P < 0.05$).
[d] Statistically significant difference ($P < 0.01$).

TABLE III

REGRESSION EQUATIONS FOR THE LOG P_{oct}–LOG k' CORRELATIONS

Systems: A = CGC glass column packed with Separon SGX-C_{18}, methanol–water (2:3) mobile phase; B = Micro Pak CH-10 column packed with LiChrosorb RP-18, methanol–water–acetic acid (30:65:5) mobile phase. n, r, s and t_b as in Table II.

Compound Nos.	System	pH*	Equation: log P_{oct} =		n	r	s	t_b
II–VIII	A	4.36	1.695 + 0.813log k'	(7)	7	0.836	0.186	3.733[b]
II, IV–VIII	A		1.628 + 0.801log k'	(8)	6	0.988	0.048	14.262[c]
II–VIII	A	3.15	1.599 + 0.844log k'	(9)	7	0.948	0.107	7.323[c]
II, IV–VIII	A		1.575 + 0.765log k'	(10)	6	0.986	0.052	13.069[c]
II–VIII	A	2.59	1.575 + 0.828log k'	(11)	7	0.958	0.097	8.192[c]
II, IV–VIII	A		1.559 + 0.753log k'	(12)	6	0.981	0.048	11.460[c]
II–VIII	A	–	1.557 + 0.830log k'_n[a]	(13)	7	0.962	0.093	8.594[c]
II, IV–VIII	A	–	1.562 + 0.756log k'_n[a]	(14)	6	0.983	0.056	12.051[c]
II–VIII, X–XIII	B	2.51	1.204 + 1.176log k'	(15)	13	0.966	0.099	13.001[c]
II, IV, V, VII, VIII	B		1.217 + 1.248log k'	(16)	10	0.974	0.096	12.916[c]

[a] 2nd step of calculation.
[b] Statistically significant difference ($P < 0.05$).
[c] Statistically significant difference ($P < 0.01$).

TABLE IV

BENZOIC ACID DERIVATIVES: RP-HPLC CAPACITY FACTORS (LOG k'), 1-OCTANOL–WATER PARTITION COEFFICIENTS (LOG P_{oct}) AND pK_A VALUES

Systems: B = Micro Pak CH-10 column packed with LiChrosorb RP-18, methanol–water–acetic acid (30:65:5) mobile phase; C = Micro Pak CH-10 column packed with LiChrosorb RP-18, methanol–water–acetic acid (40:55:5) mobile phase.

Substituent	Compound No.	Log k'		Log P_{oct}[c]	pK_A
		B[a]	C[b]		
H	II	0.627	0.269	1.87	4.19
2-OH	III	0.701	0.362	2.18[d]	2.97
3-OH	IV	0.112	−0.262	1.36[e]	4.06
4-OH	V	−0.026	−0.368	1.31	4.48
2-OCH_3	VI	0.417	0.000	1.59	4.04
3-OCH_3	VII	0.761	0.321	2.02	4.33
4-OCH_3	VIII	0.695	0.291	1.96	4.53
2-CH_3	IX	0.898	0.400	–	3.91
3-CH_3	X	0.963	0.460	2.37	4.27
4-CH_3	XI	0.940	0.366	2.27	4.36
2-Cl	XII	0.657	0.173	1.98	2.92
3-Cl	XIII	1.103	0.610	2.68	3.82
4-Cl	XIV	–	0.616	2.65	3.98
2-NO_2	XV	0.898	−0.281	–	3.91
3-NO_2	XVI	0.604	0.238	1.83	3.49
4-NO_2	XVII	0.660	0.291	1.89	3.43

[a] pH* = 2.51.
[b] pH* = 2.55.
[c] From ref. 22.
[d] From ref. 23.
[e] From ref. 24.

TABLE V

RELATIONSHIP BETWEEN THE FUNGICIDAL ACTIVITY OF AROMATIC ACIDS AND THEIR CAPACITY FACTORS IN ANIONIC FORM

Log $1/C_{ia} = a + b \log k'_{ia}$. C_{ia} = Fungicidal activity of the anionic form of acid; other symbols as in Table II.

Compound Nos.	a	b	Fungi[a]	n	r	s	t_b	Eqn. No.[c]
I–IV, VI–VIII	2.829	0.224	F	7	0.940	0.040	6.769[b]	17
	2.836	0.201	P	7	0.923	0.041	5.859[b]	18

[a] F = *Fusarium moniliforme* CCMF-180; P = *Penicillium expansum* CCMF-567.
[b] Statistically significant difference ($P < 0.01$).
[c] In eqns. 17 and 18 the k'_{ia} values obtained in the 2nd step of their calculation were used.

For the mutual correlations of physico-chemical parameters, the limit of the allowable precision of a correlation was taken to be a value of the correlation coefficient [25] of $r \geqslant 0.9$.

Both log k'_n and log k'_{ia} values of the tested acids were correlated with their fungicidal activities [26] examined against *Fusarium moniliforme* CCMF-180 and *Penicillium expansum* CCMF-567. Non-significant linear relationship between fungicidal activities and log k'_n values were found ($r = 0.468$ and 0.446, respectively). In contrast, significant relationships between fungicidal activities and log k'_{ia} were found (Table V). This result agrees with the well known experience that salts of benzoic acid derivatives are fungicidally active [27]. It is interesting that IAA, a plant growth regulator, was also fungicidally active.

REFERENCES

1 T. C. Moore, *Biochemistry and Physiology of Plant Hormones*, Springer, New York, 1979.
2 R. S. Bandurski and A. Schulze, *Plant Physiol.*, 60 (1977) 211.
3 Cs. Horváth, W. Melander and J. Molnár, *Anal. Chem.*, 49 (1977) 142.
4 Cs. Horváth and W. Melander, *J. Chromatogr. Sci.*, 15 (1977) 393.
5 J. L. Van de Venne, J. L. H. M. Hendrikx and R. S. Deelder, *J. Chromatogr.*, 167 (1978) 1.
6 R. S. Bandurski and A. Schulze, *Plant Physiol.*, 54 (1974) 257.
7 D. Fengel and G. Wegener, *Wood*, Walter de Gruyter, Berlin, New York, 1983.
8 M. Wurst, Z. Přikryl and J. Vokoun, *J. Chromatogr.*, 286 (1984) 237.
9 E. Tillberg, *Plant Physiol.*, 76 (1984) 84.
10 G. Guinn, D. L. Brummett and R. C. Beier, *Plant Physiol.*, 81 (1986) 997.
11 R. Kysilka and M. Wurst, *J. Chromatogr.*, 446 (1988) 315.
12 A. Tsantili-Kakoulidou, N. El Tayar, H. Van de Waterbeemd and B. Testa, *J. Chromatogr.*, 389 (1987) 33.
13 B. Jende-Strid, in H. F. Linskens and J. F. Jackson (Editors), *Modern Methods of Plant Analysis*, Springer, Heidelberg, 1988, p. 109.
14 J. A. Delcour, C. J. A. Vinkx, S. Vanhamel and G. G. A. G. Block, *J. Chromatogr.*, 467 (1989) 149.
15 B. Rittich, M. Polster and O. Králík, *J. Chromatogr.*, 197 (1980) 43.
16 T. Hanai, K. C. Tran and J. Hubert, *J. Chromatogr.*, 239 (1982) 385.
17 K. Miyake, F. Kitaura, N. Mizuno and H. Terada, *J. Chromatogr.*, 389 (1987) 47.
18 S. H. Unger and T. F. Feuerman, *J. Chromatogr.*, 176 (1979) 426.
19 C. L. De Ligny and M. Rehbach, *Recl. Trav. Chim. Pays-Bas*, 79 (1960) 727.
20 R. G. Bates, M. Paabo and R. G. A. Robinson, *J. Phys. Chem.*, 67 (1963) 1833.
21 R. C. Weast (Editor), *Handbook of Chemistry and Physics*, Chemical Rubber, Cleveland, OH, 49th ed., 1968, p. D-90.

22 C. Hansch and A. Leo, *Substituent Constants for Correlation Analysis in Chemistry and Biology*, Wiley, New York, 1979.
23 T. Hanai and J. Hubert, *J. Chromatogr.*, 239 (1982) 527.
24 R. F. Rekker, *The Hydrophobic Fragmental Constant*, Elsevier, Amsterdam, 1977.
25 O. Exner, *Correlation Analysis of Chemical Data*, Plenum Press and SNTL, New York, 1988, p. 228.
26 B. Rittich, K. Jurtíková, P. Doležal, M. Pirochtová and J. Hřib, *Quant. Struct.–Act. Relat.*, submitted for publication.
27 B. Melicher (Editor), *Chemická Léčiva (Chemical Drugs)*, Avicenum, Prague, 3rd ed., 1987.

Journal of Chromatography, 523 (1990) 235–246
Elsevier Science Publishers B.V., Amsterdam

CHROM. 22 712

Liquid chromatographic determination of free and total fatty acids in milk and milk products as their 2-nitrophenylhydrazides

HIROSHI MIWA* and MAGOBEI YAMAMOTO

Faculty of Pharmaceutical Sciences, Fukuoka University, 8–19–1, Nanakuma, Jonan-ku, Fukuoka 814–01 (Japan)

(First received May 1st, 1990; revised manuscript received July 23rd, 1990)

ABSTRACT

A high-performance liquid chromatographic (HPLC) method with direct derivatization is described for the determination of both free fatty acids and total fatty acids in milk and milk products. The method is based on the reaction of these acids with 2-nitrophenylhydrazine hydrochloride with and without saponification of the samples, and there are no sample work-up steps. The derivatized fatty acids were separated into two groups, short-chain fatty acids ($C_{2:0}$–$C_{6:0}$) and long-chain fatty acids ($C_{8:0}$–$C_{22:6}$), as their hydrazides, by a simple solvent extraction. The HPLC of each acid group was performed isocratically with short retention times on a YMC-FA column. The results showed good recovery and reproducibility using 2-ethylbutyric acid and margaric acid as internal standards for the two acid groups. The method is simple, rapid and reliable and has advantages with regard to resolution, analysis time and sensitivity over previous methods.

INTRODUCTION

Free fatty acids (FFA) in milk and milk products contribute to their desirable flavour, but when present in excessive amounts can impart a rancid flavour. Elevated FFA levels are generally caused by the natural milk lipase and/or by the heat-stable bacterial lipase [1]. The determination of total fatty acids (TFA), *i.e.*, the sum of FFA and esterified fatty acids (EFA) in milk and milk products, is necessary to investigate whether they are contaminated with other fats and oils.

Although gas–liquid chromatography (GLC) is a popular means for the determination of FA, several inherent advantages of high-performance liquid chromatography (HPLC) make it more convenient. The main problem in these chromatographic methods is that the quantitative isolation of FFA is required prior to suitable derivatization. Common isolation procedures involve the use of potassium hydroxide–silicic acid [2], anion-exchange [3] and alumina columns [4]. These procedures may result in loss of sample or in hydrolysis of the endogenous EFA such as glycerides owing to the relatively long contact with the strong alkali used in the isolation procedures.

We have previously described a direct derivatization method with 2-nitrophe-

0021-9673/90/$03.50

nylhydrazine hydrochloride (2-NPH · HCl) for the determination of FFA in serum and of TFA in fats and oils without the need for any isolation procedures [5–7]. The aims of this study were to improve the method for the direct derivatization of both FFA and TFA in milk and milk products and to determine FA hydrazides such as short-chain FA (SCFA) ($C_{2:0}$–$C_{6:0}$) and long-chain FA (LCFA) ($C_{8:0}$–$C_{22:6}$) hydrazides using isocratic HPLC.

EXPERIMENTAL

Reagent solutions

All FA solutions in ethanol were obtained from Yamamura Chemical Labs. (Kyoto, Japan). 2-NPH · HCl (Tokyo Kasei Kogyo, Tokyo, Japan) solutions (0.02 *M*) were prepared by dissolving the reagent in 0.1 *M* hydrochloric acid–ethanol (1:1, v/v) and 0.3 *M* hydrochloric acid-ethanol (1:1, v/v) for determining the FFA and TFA, respectively. A 1-ethyl-3-(3-dimethylaminopropyl)carbodiimide hydrochloride (1-EDC · HCl) (Sigma, St. Louis, MO, U.S.A.) solution (0.25 *M*) was prepared by dissolving the reagent in a solution of pyridine (3%, v/v) in ethanol. A potassium hydroxide solution (10%, w/v) in methanol–water (1:1, v/v) and a potassium hydroxide (0.4 *M*)–ethanol (1:1, v/v) solution were prepared. All the reagent solutions were stable for at least 3 months when kept below 5°C. These solutions were also commercially available from the Yamamura Chemical Labs. All other chemicals were of analytical-reagent grade, unless stated otherwise. As the samples, commercially available milk and milk products wer used.

Determination of FFA in milk and milk products

For samples, 100 μl of milk, about 20 mg of butter and cheese and about 50 mg of condensed milk, ice cream and yogurt were measured exactly. To the milk product samples, 100 μl of water were added. To each sample, 200 μl of ethanol containing 20 nmol of 2-ethylbutyric acid and 20 nmol of margaric acid as internal standards, 200 μl of 2-NPH · HCl solution and 200 μl of 1-EDC · HCl solution were successively added and the mixture was heated at 80°C for 5 min. After the addition of 200 μl of potassium hydroxide solution, the mixture was further heated at 80°C for 5 min and then cooled. The resulting hydrazide mixture was neutralized by adding 4 ml of 1/30 *M* phosphate buffer (pH 6.4)–0.5 *M* hydrochloric acid (7:1, v/v) and the LCFFA hydrazides were extracted with 5 ml of *n*-hexane. About a 3-ml portion of the residual aqueous layer was taken and the SCFFA hydrazides were extracted twice with 4 ml of diethyl ether.

The *n*-hexane layer and the combined ether layer were evaporated with a stream of nitrogen at room temperature. Each residue was dissolved in 200 μl of methanol and filtered through a YMC Top-Filter (pore size 0.45 μm) (Yamamura Chemical Labs.). An aliquot of 10–20 μl was injected into the chromatograph.

Determination of TFA in milk and milk products

For samples, 10 μl of milk, about 1 mg of butter and cheese, about 2 mg of condensed milk and ice cream and about 10 mg of yogurt were measured exactly. Each sample was dissolved in 200 μl of ethanol containing 400 nmol of 2-ethylbutyric acid and 200 nmol of margaric acid as internal standards and was saponified with 100

μl of 0.4 *M* potassium hydroxide–ethanol (1:1, v/v) solution at 80°C for 20 min. To the saponified sample, 200 μl of 2-NPH · HCl solution and 200 μl of 1-EDC · HCl solution were added and the mixture was heated at 80°C for 5 min. After the addition of 200 μl of potassium hydroxide solution, the mixture was further heated at 80°C for 5 min and then cooled. The resulting hydrazide mixture was treated in the same way as in the determination of FFA in milk and milk products.

The *n*-hexane layer and combined ether layer were evaporated with a stream of nitrogen at room temperature. Each residue was then dissolved in 200 μl of methanol and an aliquot of 2–10 μl was injected into the chromatograph.

HPLC analysis

Chromatographic analyses were carried out using a Shimadzu (Kyoto, Japan) LC-6A liquid chromatograph equipped with an ERC-3310 on-line degasser (Erma, Tokyo, Japan) and a Shimadzu SPD-6AV variable-wavelength UV–visible detector. The detector was set at 400 nm and the detector signals were recorded on a Rikadenki (Tokyo, Japan) multi-pen recorder. The column temperature was kept constant at 35°C using a Shimadzu GTO-6A column oven. The column consisted of a BBC-4-C_8 guard column (particle size 5 μm, 10 × 4 mm I.D.) and a YMC-FA (C_8) main column (particle size 5 μm, 250 × 6 mm I.D.), packed at Yamamura Chemical Labs.

The separations of the SCFA and LCFA hydrazides were achieved isocratically using acetonitrile–methanol–water as the eluent at a flow-rate of 1.2 ml/min. The pH of the eluents was maintained at about 4.5 by adding 0.1 *M* hydrochloric acid. The acetonitrile–methanol–water (30:20:50, v/v/v) eluent for the determination of SCFA was filtered through a Nuclepore filter (pore size 2 μm) (Nomura Micro Science, Osaka, Japan). The acetonitrile–methanol–water (75:11:14, v/v/v) eluent for the determination of LCFA was filtered through a Fluoropore filter (pore size 0.45 μm) (Sumitomo Electric, Osaka, Japan).

RESULTS AND DISCUSSION

Sample preparation

The major problems arising in the direct derivatization of FA in saponified and unsaponified milk and milk products are the presence of protein-bound acids and the pH of the reaction mixture. The protein-bound acids in milk and milk products were deproteinized by the ethanol contained in the reaction mixture. The reaction mixture was maintained at a constant pH by the addition of hydrochloric acid because an increase in the pH of the reaction mixture decreased the yields of the hydrazides [5,6]. The experiments established that the FFA and EFA in milk and milk products could be converted into their hydrazides in high yields.

The SCFA in milk and milk products are important from the standpoint of flavour and as a criterion of quality deterioration, whereas the LCFA are of widespread interest in human health and nutrition [8,9]. Therefore, the FA derivatized with 2-NPH · HCl were classified for each purpose into the two groups, SCFA and LCFA, according to previously described methods [5,6] with a slight modification.

Chromatographic conditions

The two principal parameters for the elution volumes of FA hydrazides were

the number of carbon atoms and the number of unsaturated bonds in the FA chain [7]. Acetonitrile and methanol have different effects on the two parameters. Therefore, the conditions for HPLC separations of the SCFA and LCFA hydrazides were investigated using a YMC-FA column and different eluents consisting of acetonitrile, methanol and water in various proportions.

Fig. 1 shows a typical separation of SCFA hydrazides ($C_{2:0}$–$C_{6:0}$) including *iso*

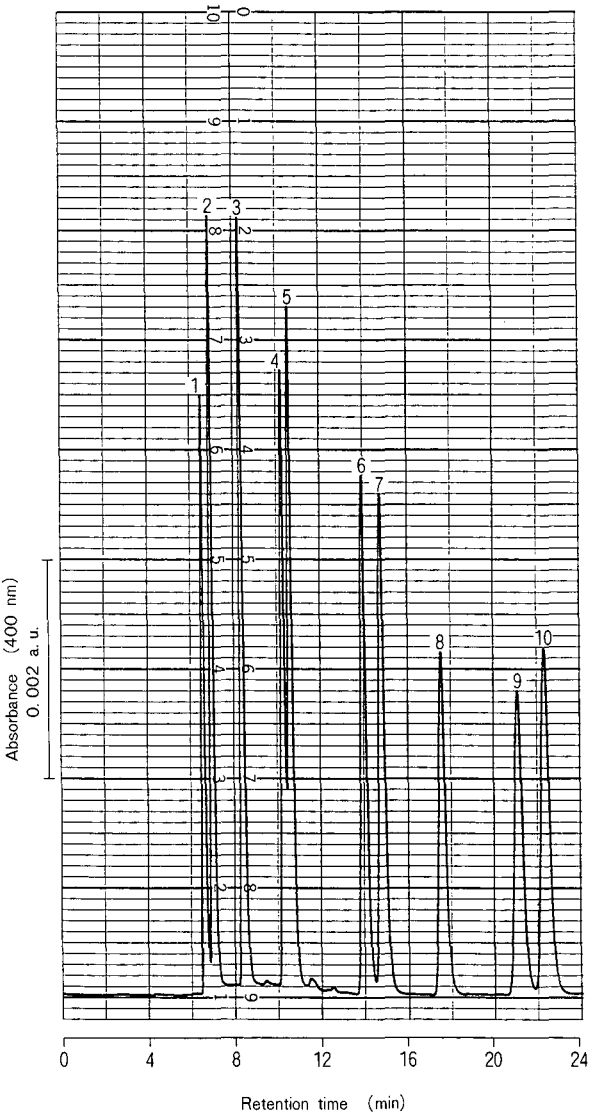

Fig. 1. Chromatogram of the 2-nitrophenylhydrazides of a standard mixture of ten fatty acids obtained with visible detection. Peaks: 1 = lactic; 2 = acetic; 3 = propionic; 4 = isobutyric; 5 = *n*-butyric; 6 = isovaleric; 7 = *n*-valeric; 8 = 2-ethylbutyric (internal standard); 9 = isocaproic; 10 = *n*-caproic acid hydrazide. Each peak corresponds to 150 pmol.

isomers and lactic acid hydrazide by HPLC with acetonitrile–methanol–water (30:20:50, v/v/v) as the eluent and detection in the visible range. The *iso* isomers were eluted faster than the normal isomers. Fig. 2 shows a chromatogram of a mixture of

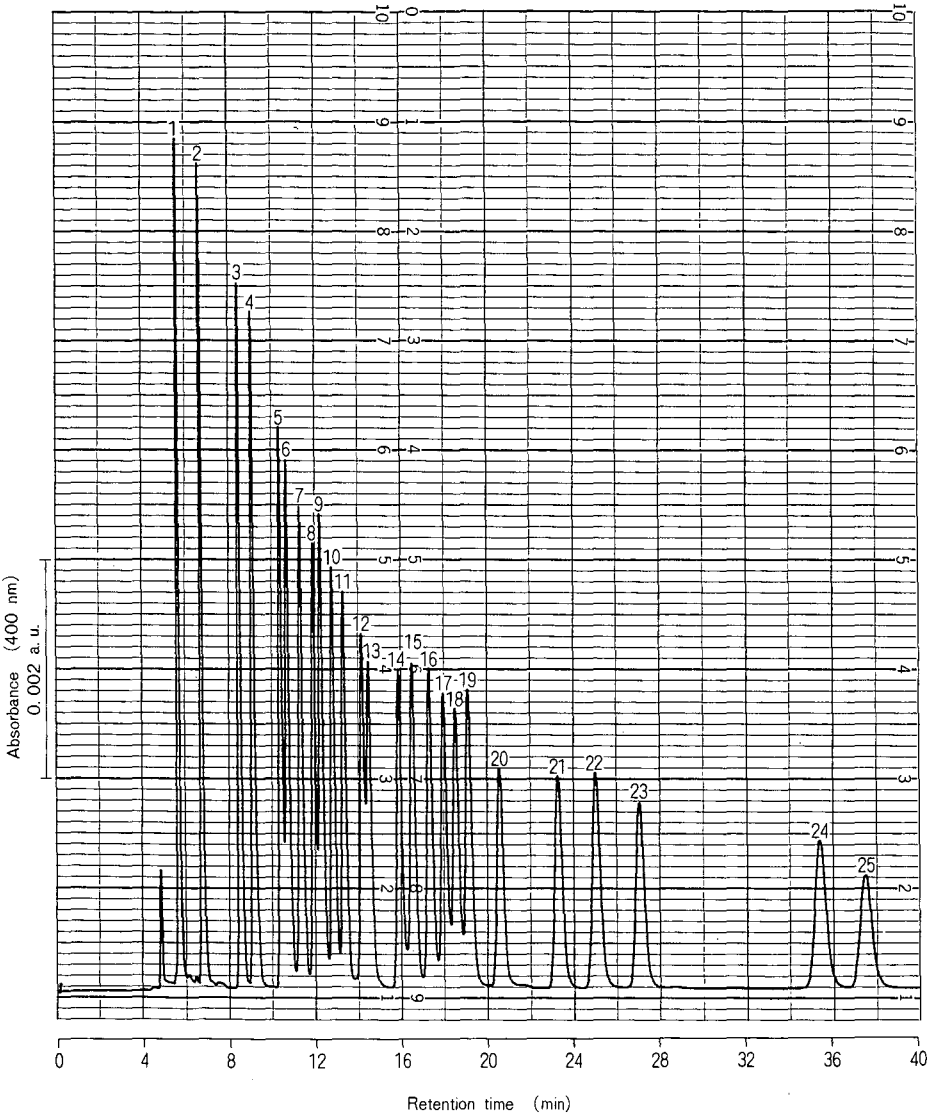

Fig. 2. Chromatogram of the 2-nitrophenylhydrazides of a standard mixture of 25 fatty acids obtained with visible detection. Peaks: 1 = caprylic ($C_{8:0}$); 2 = capric ($C_{10:0}$); 3 = lauric ($C_{12:0}$); 4 = myristoleic ($C_{14:1}$); 5 = eicosapentaenoic ($C_{20:5}$); 6 = linolenic ($C_{18:3}$); 7 = myristic ($C_{14:0}$); 8 = docosahexaenoic ($C_{22:6}$); 9 = palmitoleic ($C_{16:1}$); 10 = aracidonic ($C_{20:4}$); 11 = linoleic ($C_{18:2,cis,cis}$); 12 = linoelaidic ($C_{18:2,trans,trans}$); 13 = eicosatrienoic ($C_{20:3}$); 14 = palmitic ($C_{16:0}$); 15 = docosatetraenoic ($C_{22:4}$); 16 = oleic ($C_{18:1,cis}$); 17 = elaidic ($C_{18:1,trans}$); 18 = eicosadienoic ($C_{20:2}$); 19 = margaric ($C_{17:0}$) (internal standard); 20 = docosatrienoic ($C_{22:3}$); 21 = stearic ($C_{18:0}$); 22 = eicosaenoic ($C_{20:1}$); 23 = docosadienoic ($C_{22:2}$); 24 = arachidic ($C_{20:0}$); 25 = erucic ($C_{22:1}$) acid hydrazide. Each peak corresponds to 150 pmol.

saturated and mono- and polyunsaturated LCFA hydrazides ($C_{8:0}$–$C_{22:6}$), including *cis–trans* isomers, obtained by using acetonitrile–methanol–water (75:11:14, v/v/v) as the eluent and detection in the visible range. The retention times increased with increasing chain length for the LCFA hydrazides and inversely with the degree of unsaturation for the unsaturated LCFA hydrazides. The *trans* isomers were eluted after the corresponding *cis* isomers. These chromatographic behaviours of the hydrazine derivatives agree with those of other FA derivatives [10–14], and lead to the occurance of several pairs of FA which are difficult to separate.

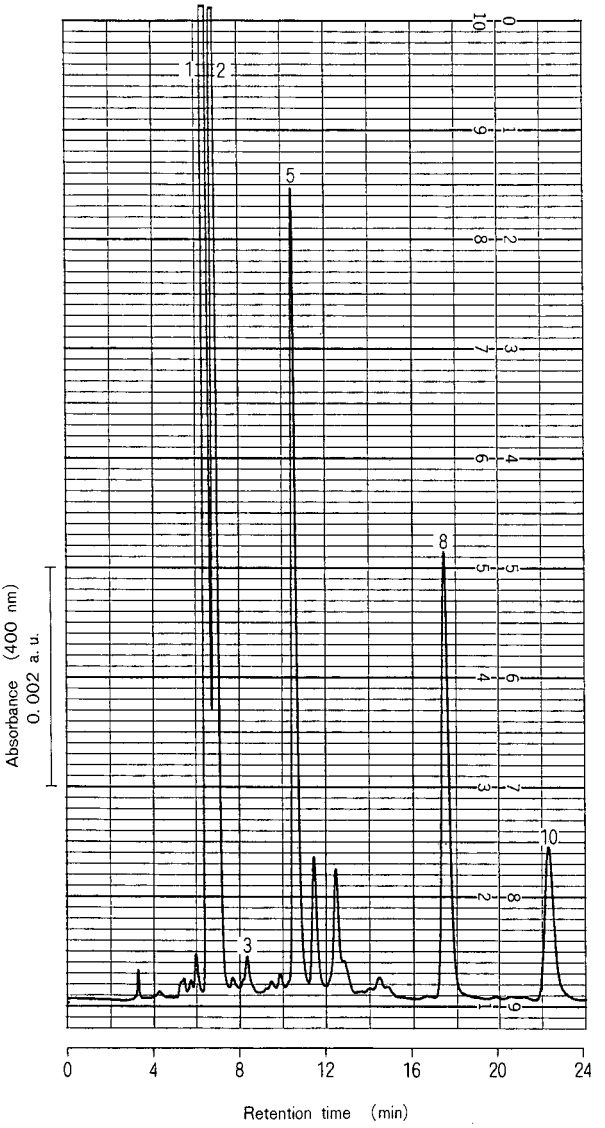

Fig. 3. Short-chain free fatty acid profile of butter. Peaks as in Fig. 1.

However, the excellent resolution of critical pairs and triplets, such as eicosapentaenoic ($C_{20:5}$) and linolenic ($C_{18:3}$) acids, docosahexaenoic ($C_{22:6}$) and palmitoleic ($C_{16:1}$) acids, arachidonic ($C_{20:4}$) and linoleic ($C_{18:2}$) acids and palmitic ($C_{16:0}$), docosatetraenoic ($C_{22:4}$) and oleic ($C_{18:1}$) acids could be accomplished by elution in the isocratic mode, which is a distinct advantage over gradient elution techniques [10–14].

Quantitative analysis

To construct calibration graphs for quantification, increasing amounts of mixtures of the SCFA and LCFA were derivatized in the presence of 2-ethylbutyric acid and margaric acid as internal standards and analysed. The relationships between the relative peak heights and the amounts of the SCFA were linear at least over the range

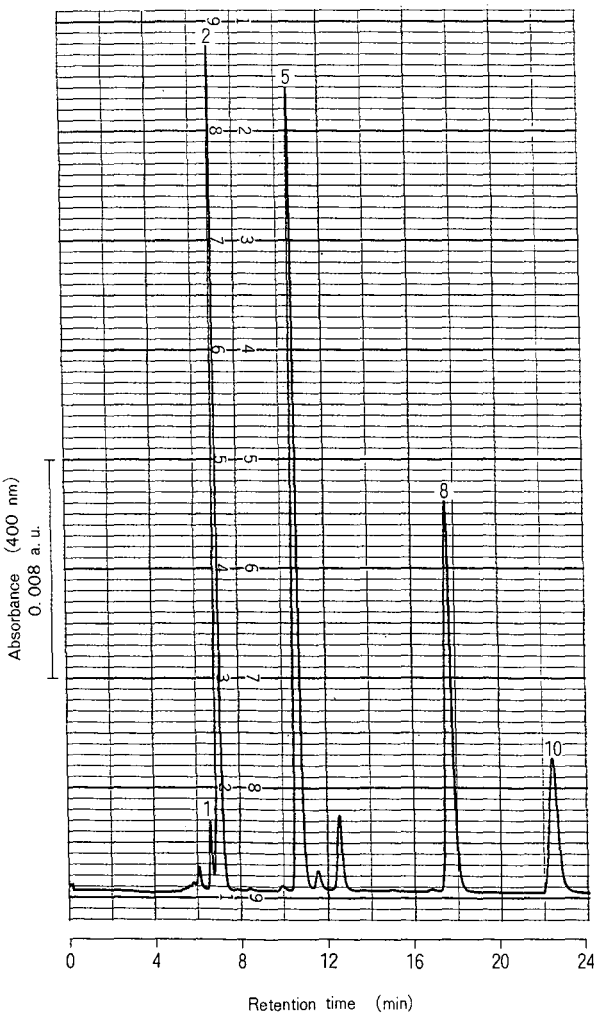

Fig. 4. Short-chain total fatty acid profile of butter. Peaks as in Fig. 1.

2 pmol–5 nmol per injection with correlation coefficients of 0.999–1.000. The calibration graphs for the LCFA were linear over a wide concentration range, 1 pmol–5 nmol per injection, with correlation coefficients of 0.999–1.000. The limits of detection, based on a signal-to-noise ratio of 2, were 1–2 pmol and 500 fmol–1 pmol per injection for the SCFA and LCFA, respectively.

Recovery and reproducibility were investigated six times in butter by adding known mixtures of the SCFA and LCFA. In this experiment, the recoveries of FFA were in the range 95.2–104.3% [coefficients of variation (C.V.) = 1.1–4.2%] when the

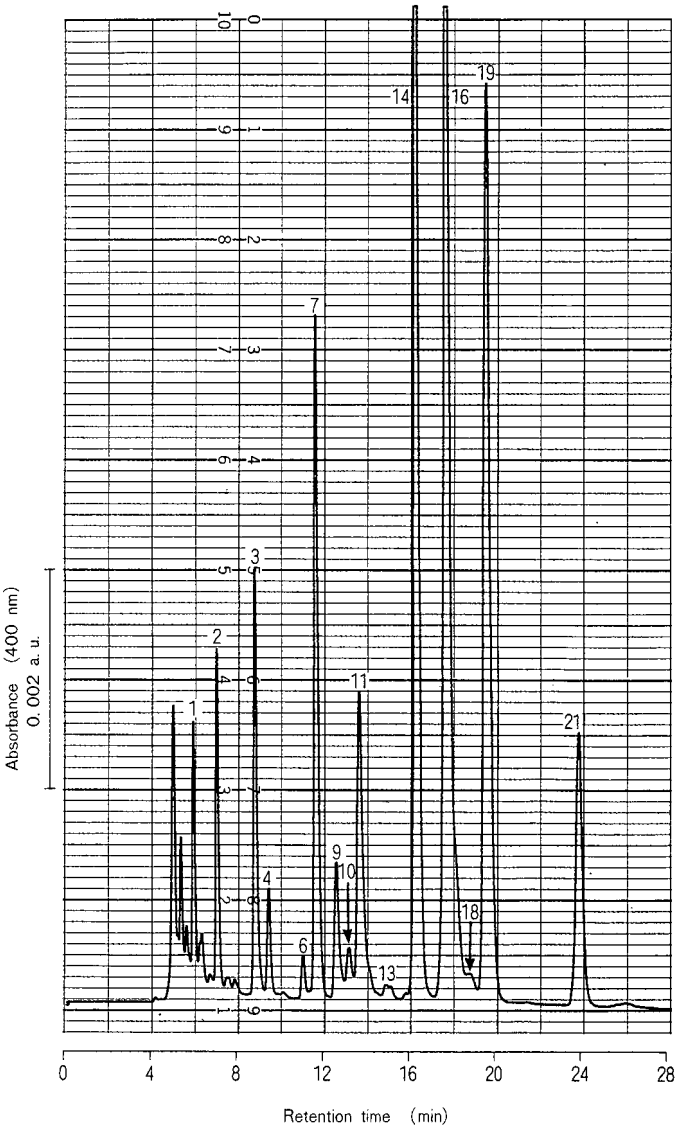

Fig. 5. Long-chain free fatty acid profile of butter. Peaks as in Fig. 2.

following amounts of FA were added: $C_{4:0}$, $C_{6:0}$, $C_{16:0}$, $C_{18:0}$, $C_{18:1}$ and $C_{18:2}$ = 20 nmol; others = 5 nmol. The recoveries of TFA were in the range 96.4–103.3% (R.S.D 0.5–3.9%) when the following amounts of FA were added: $C_{4:0}$, $C_{6:0}$, $C_{16:0}$, $C_{18:0}$, $C_{18:1}$ and $C_{18:2}$ = 200 nmol; others = 50 nmol.

The within-run precision was evaluated by assaying the same butter sample nine times for FFA and TFA. The precision (C.V.) ranged from 0.4 to 4.5% and from 0.6 to 3.7% for the FFA and TFA, respectively. These results indicate that the method has a satisfactory precision for the determination of FFA and TFA in milk and milk products.

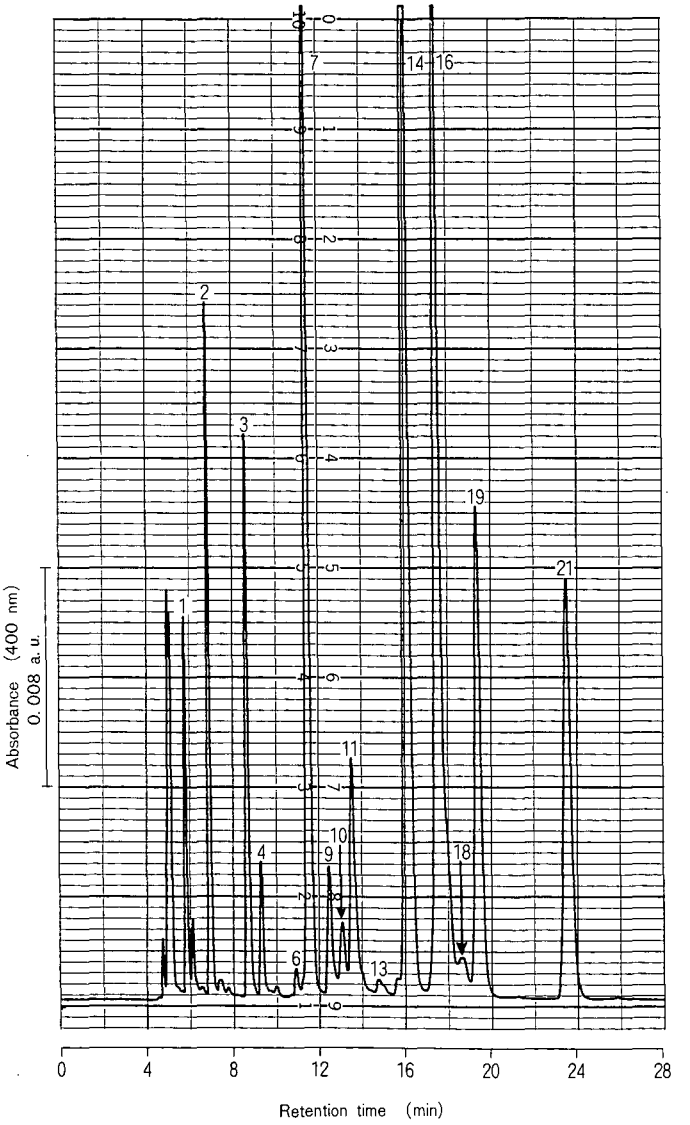

Fig. 6. Long-chain total fatty acid profile of butter. Peaks as in Fig. 2.

Applicability

We applied the method to the determination of FFA and TFA in milk and milk products. The FFA and TFA profiles of SCFA and LCFA in butter are shown in Figs. 3–6. The chromatograms of LCFFA and LCTFA monitored by the visible absorbance showed a very clean background. In the HPLC of SCFFA and SCTFA some unknown peaks were found on the chromatograms, but the hydrazides were completely separated from the unknown peaks, with the exception of acetic acid hydrazide. All the FA in the samples were easily identified by comparison of the retention times of their hydrazides with those of standards, because the FA derived from milk and milkproducts varied from C_4 to C_{20} [2–4, 15–18].

Tables I and II give the amounts of SCFFA and SCTFA in milk and milk products. The SCFFA, butyric acid ($C_{4:0}$) and caproic acid ($C_{6:0}$) are largely responsible for the rancid flavour, and the total $C_{4:0}/C_{6:0}$ ratio is very significant for determining the criterion of contamination. Tables I and II indicate that there is a large difference between the free and total lactic acid estimates. One possible explanation for the difference is the decomposition of lactose which may be present in the samples by heating with potassium hydroxide. Other differences between the SCFFA and SCTFA were accounted for the EFA. The FA compositions of LCFFA and LCTFA in the samples are given in Tables III and IV. In all the samples, the chain length of

TABLE I

AMOUNTS OF SCFFA IN MILK AND MILK PRODUCTS

SCFFA	Amount of SCFFA (nmol/g)[a]					
	Milk	Condensed milk	Butter	Cheese	Ice cream	Yogurt
Lactic	459.10[b]	733.75	5.39[c]	80.03[c]	649.50	64.26[c]
n-Butyric	162.89[b]	128.17	873.95	532.21	51.39	112.49
n-Caproic	39.20[b]	41.60	328.00	168.00	18.80	40.00

[a] Mean results ($n = 3$).
[b] nmol/ml
[c] μmol/g.

TABLE II

AMOUNTS OF SCTFA IN MILK AND MILK PRODUCTS

SCTFA	Amount of SCTFA (nmol/g)[a]					
	Milk	Condensed milk	Butter	Cheese	Ice cream	Yogurt
Lactic	15.29[b]	28.43	38.55	194.13	85.67	88.63
n-Butyric	15.55[b]	31.78	484.99	235.58	20.45	9.20
n-Caproic	5.29[b]	10.60	165.09	81.04	24.58	2.95

[a] Mean results ($n = 3$).
[b] μmol/ml.

TABLE III

LCFFA COMPOSITIONS OF MILK AND MILK PRODUCTS

LCFFA	LCFFA composition (mol%)[a]					
	Milk	Condensed milk	Butter	Cheese	Ice cream	Yogurt
$C_{8:0}$	3.69	3.76	1.48	1.78	1.57	5.05
$C_{10:0}$	5.77	5.59	3.58	3.90	4.75	5.71
$C_{12:0}$	5.69	5.56	5.78	6.99	5.07	6.05
$C_{14:0}$	12.16	12.07	14.27	11.81	10.68	14.18
$C_{14:1}$	1.34	1.39	1.36	1.00	0.79	1.12
$C_{16:0}$	28.32	26.64	31.88	26.68	28.57	31.43
$C_{16:1}$	1.93	2.15	2.08	1.76	1.52	1.44
$C_{18:0}$	9.34	8.83	9.91	13.99	22.64	9.34
$C_{18:1c}$	25.15	25.97	22.71	16.79	19.69	20.54
$C_{18:2c,c}(n\text{-}6)$	4.87	5.91	5.03	12.16	3.34	3.70
$C_{18:3}(n\text{-}3)$	0.53	0.65	0.58	1.45	1.38	0.44
$C_{20:2}(n\text{-}6)$	0.57	0.53	0.48			
$C_{20:3}(n\text{-}6)$	0.24	0.21	0.20	0.20		
$C_{20:4}(n\text{-}6)$	0.40	0.74	0.66	1.49		1.00
Total (μmol/g)	1.013[b]	1.680	9.554	6.899	1.281	0.560

[a] Mean results ($n=3$).
[b] μmol/ml.

TABLE IV

LCTFA COMPOSITIONS OF MILK AND MILK PRODUCTS

LCTFA	LCTFA composition (mol%)[a]					
	Milk	Condensed milk	Butter	Cheese	Ice cream	Yogurt
$C_{8:0}$	3.43	3.20	3.76	3.19	4.18	3.31
$C_{10:0}$	6.85	5.65	7.04	6.01	7.45	5.68
$C_{12:0}$	5.81	5.31	6.51	6.29	6.54	5.22
$C_{14:0}$	16.78	16.31	18.04	16.78	16.06	15.70
$C_{14:1}$	1.29	1.49	1.59	1.22	1.11	1.27
$C_{16:0}$	30.44	29.98	31.62	29.81	28.18	30.73
$C_{16:1}$	1.50	1.82	1.57	1.45	1.37	1.58
$C_{18:0}$	11.16	10.42	9.45	11.90	13.76	11.80
$C_{18:1c}$	17.23	20.15	15.33	18.12	16.34	18.65
$C_{18:2c,c}(n\text{-}6)$	3.90	3.80	3.38	3.35	2.64	4.15
$C_{18:3}(n\text{-}3)$	0.39	0.34	0.34	0.69	1.11	0.29
$C_{20:2}(n\text{-}6)$	0.14	0.19	0.19	0.10	0.12	0.30
$C_{20:3}(n\text{-}6)$	0.24	0.31	0.24	0.24	0.23	0.32
$C_{20:4}(n\text{-}6)$	0.93	1.03	0.94	0.85	0.91	1.00
Total (mmol/g)	0.140[b]	0.334	2.300	0.938	0.454	0.088

[a] Mean results ($n=3$).
[b] mmol/ml.

the LCFA extends from C_8 to C_{22}, and the amounts of LCTFA were at least 100 times higher than those of LCFFA.

The individual levels of SCFFA and LCFFA in the butter sample were consistent with those reported by Wood and Lindsay [18].

CONCLUSION

The FFA in milk and milk products can be reacted directly with 2-NPH · HCl without hydrolytic or oxidative degradation. This method also allows the direct derivatization of TFA after saponification of milk and milk products, and there are no work-up steps involving evaporation of solvent or aqueous washes where SCFA could be lost. The HPLC analyses described here permit the isocratic separations of both SCFA and LCFA in samples with good accuracy, precision and sensitivity owing to the minimum sample preparation required.

The simplicity and rapidity of this method are particularly suitable for routine determinations of FFA and TFA in milk and milk products.

REFERENCES

1 H. C. Deeth, C. H. Fitz-Gerald and A. F. Wood, *Aust. J. Dairy Technol.*, 34 (1979) 146.
2 R. D. McCarthy and A. H. Duthie, *J. Lipid Res.*, 3 (1962) 117.
3 I. Hornstein, J. A. Alford, L. E. Elliott and P. F. Crowe, *Anal. Chem.*, 32 (1960) 540.
4 H. C. Deeth, C. H. Fitz-Gerald and A. J. Snow, *N. Z. J. Dairy Sci. Technol.*, 18 (1983) 13.
5 H. Miwa and M. Yamamoto, *J. Chromatogr.*, 421 (1987) 33.
6 H. Miwa, M. Yamamoto, T. Nishida, K. Nunoi and M. Kikuchi, *J. Chromatogr.*, 416 (1987) 237.
7 H. Miwa and M. Yamamoto, *J. Chromatogr.*, 351 (1986) 275.
8 R. G. Ackman, *Perspective on Eicosapentaenoic Acid (EPA)*, 1 (1986) 4.
9 W. E. M. *Lands, Fish and Human Health*, Academic Press, New York, 1986.
10 R. Wood and T. Lee, *J. Chromatogr.*, 254 (1983) 237.
11 H. Tsuchiaya, T. Hayashi, M. Sato, M. Tatsumi and N. Takagi, *J. Chromatogr.*, 309 (1984) 43.
12 J. D. Baty, S. Pazouki and J. Dolphin, *J. Chromatogr.*, 395 (1987) 403.
13 T. Hanis, M. Smrz, P. Klir, M. Macek, J. Klima, J. Base and Z. Deyl, *J. Chromatogr.*, 452 (1988) 443.
14 G. Kargas, T. Rudy, T. Spennetta, K. Takayama, N. Querishi and E. Shrago, *J. Chromatogr.*, 526 (1990) 331.
15 D. D. Bills, L. L. Khatri and E. A. Day, *J. Dairy Sci.*, 46 (1963) 1342.
16 M. Iyer, T. Richardson, C. H. Amundson and A. Boudreau, *J. Dairy Sci.*, 50 (1967) 285.
17 E. S. Humbert and R. C. Lindsay, *J. Dairy Sci.*, 52 (1969) 1862.
18 A. H. Wood and R. C. Lindsay, *J. Dairy Sci.*, 63 (1980) 1058.

Journal of Chromatography, 523 (1990) 247–255
Elsevier Science Publishers B.V., Amsterdam

CHROM. 22 693

Separation of phenylamine- and naphthylaminesulphonic acids by reversed-phase high-performance liquid chromatography

HANFA ZOU*, YUKUI ZHANG, XIBING WEN and PEICHANG LU
Dalian Chromatographic R & D Centre of China, Dalian Institute of Chemical Physics, Academia Sinica, Dalian 116011 (China)
(First received March 20th, 1990; revised manuscript received July 10th, 1990)

ABSTRACT

Mixtures of singly and multiply substituted phenylamine- and naphthylaminesulphonic acids, important intermediates in the synthesis of dyestuffs, were separated by reversed-phase liquid chromatography with UV detection. Linear regression analysis according to the retention equation $\ln k' = \ln k'_w + cC_b$ [where k'_w is the extrapolated capacity factor at $C_b = 0$ and c is mainly determined by molecular interaction between the solute and the eluent; they are constants for a given solute at a given column system; C_b is the concentration of organic modifier (v/v)] with and without experimental data at $C_b = 0$ being taken into account was carried out. The regression coefficient in the former situation is much lower than that in the latter. A linear relationship between $\ln k'_w$ (without taking the data at $C_b = 0$ into account) and the $\ln k'_w$ measured at $C_b = 0$ was obtained. The effect of the eluent acidity on k' is complex, indicating that the negatively charged, neutral and positively charged solutes simultaneously contribute to the retention. The retention value increases with increasing concentration of sodium chloride, but the linear regression analysis according to Horváth's equation $\ln k' = A + Bm$ (where A and B are constants related to the physico-chemical behaviour of a given column system and m is the concentration of the inorganic salt) is not good, which may be caused by masking of the ionized silanol group and changing the eluent surface tension simultaneously.

INTRODUCTION

High-performance liquid chromatography (HPLC) is the method of choice for the routine determination of ionic aromatic sulphonates [1–5]. Separations on ion exchangers are unsatisfactory because of the poor recovery of the analytes [6] and the use of a silica column with an aqueous phase leads to irreproducible retention times [1] and unstable baselines [7]. Reversed-phase columns, in contrast, give reproducible separations and stable baselines. Several separations in the ion-pair mode have been reported [8–10], but the use of an ion-pair reagent seems to shorten the column lifetime. Better, predictable and more economical separations are observed using reversed-phase columns with inorganic electrolytes as the mobile phase. We have extended this idea to determine individual phenylamine- and naphthylaminesulphonic acids and -sulphonates in complex mixtures by isocratic elution from reversed-phase columns. The effects of the concentration of organic modifier, inorganic salt and acidity on the retentions of the phenylamine- and naphthylaminesulphonic acids were investigated.

0021-9673/90/$03.50

EXPERIMENTAL

Materials

The compounds analysed (Table I) were obtained from the Dyestuff Laboratory, Chemical Engineering Department, Dalian University of Science and Technology. Standard solutions were prepared in 10 mmol/l sodium phosphate buffer (pH 6.8). Doubly distilled water was used throughout. The reagents used were of analytical-reagent grade.

Apparatus and assay conditions

HPLC was done at room temperature using stainless-steel columns (200 × 4.0 mm I.D.) that contained a reversed-phase packing material of 5-μm mean particle diameter (Polygosil 5 C_{18}) obtained from Macherey-Nagel (Düren, F.R.G.). The mobile phase was delivered by a BT-3020 pump (Biotronik, F.R.G.). The eluates were detected with a UV detector (Knauer) set at 254 nm. Samples were loaded with a Model 7125 syringe-loading sample injector (Rheodyne, U.S.A.). The flow-rate of the eluent was 1.0 ml/min. The eluent pH was measured with an SA-720 pH meter (Orion, U.S.A.). All the experimental data were processed with an NEC-APCIV personal computer.

TABLE I

PHENYLAMINE- AND NAPHTHYLAMINESULPHONIC ACIDS ANALYSED AND THEIR CAPACITY FACTORS WITH AQUEOUS BUFFER CONTAINING 10 mmol/l NaH_2PO_4 (pH 6.8) AS THE ELUENT

No.	Solute	Capacity factor (k')
1	Phenylamine-2-sulphonic acid	2.31
2	Phenylamine-3-sulphonic acid	1.03
3	Phenylamine-4-sulphonic acid	0.484
4	Phenylamine-2,5-disulphonic acid	0.078
5	5-Methylphenylamine-2-sulphonic acid	8.29
6	4-Methylphenylamine-3-sulphonic acid	2.87
7	4-Methoxyphenylamine-3-sulphonic acid	1.43
8	6-Chlorophenylamine-3-sulphonic acid	8.64
9	4-Chlorophenylamine-3-sulphonic acid	1.87
10	1,3-Diaminophenyl-4-sulphonic acid	0.510
11	1,3-Diaminophenyl-4,6-disulphonic acid	0.093
12	1,3-Diamino-2,4,6-trimethylphenyl-5-sulphonic acid	1.72
13	1,4-Diaminophenyl-2-sulphonic acid	0.612
14	2,2'-Diaminodiphenyl-4,4'-disulphonic acid	1.08
15	Naphthylamine-4-sulphonic acid	14.44
16	Naphthylamine-5-sulphonic acid	4.37
17	Naphthylamine-7-sulphonic acid	18.56
18	Naphthylamine-8-sulphonic acid	29.85
19	2-Aminonaphthalene-1-sulphonic acid	15.66
20	2-Aminonaphthalene-5-sulphonic acid	10.73
21	2-Aminonaphthalene-4,8-disulphonic acid	0.179
22	2-Aminonaphthalene-3,6-disulphonic acid	1.07
23	2-Aminonaphthalene-4,6,8-trisulphonic acid	0.027
24	2-Aminonaphthalene-3,6,8-trisulphonic acid	0.032

RESULTS AND DISCUSSION

It was known [2,7] that ionic aryl sulphonates can be separated by reversed-phase HPLC. We confirmed this and showed that singly and multiply substituted phenylamine- and naphthylaminesulphonic acids can be separated from the intermediates of synthetic dyestuffs and determined (Fig. 1, Table I). Figs. 1 and 2 show the separation of singly and multiply substituted phenylamine- and naphthylaminesulphonic acids.

Effect of molecular structure on the capacity factor, k'

From the retention data shown in Table I, the rules for the effect of molecular structure on the retention values can be deduced as follows:

(a) It is easy to separate the *o*-, *m*- and *p*-isomers of phenylamine- and naphthylaminesulphonic acids by reversed-phase (RP) HPLC. The retention data for the singly amino- and sulphonic acid-substituted phenylamine- and naphthylaminesulphonic acid isomers (Nos. 1–3 and 15–20 in Table I) support this idea.

(b) The retention order of the *o*-, *m*- and *p*-phenylaminesulphonic acid isomers is *o*- > *m*- > *p*-. The fact that the *o*-isomer has the largest retention may be due to the intramolecular hydrogen-bonding interaction, which will decrease the interaction between the solute and the mobile phase. The retention of the *m*-isomer is larger than that of the *p*-isomer, possibly owing to electrostatic effects of the substituted functional

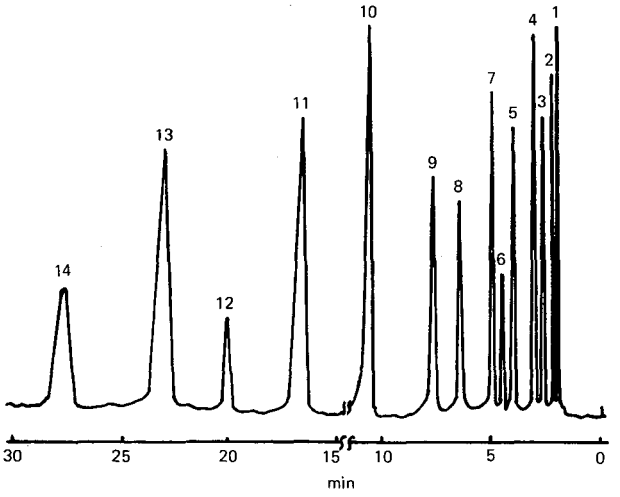

Fig. 1. Typical chromatogram of a mixture of phenylamine- and naphthylaminesulphonic acids. Mobile phase containing 10 mmol/l sodium phosphate buffer (pH 6.8). The flow-rate of the eluent was changed from 1.0 to 1.8 ml/min after sample injection at 13 min. For other conditions, see Experimental. Peaks: 1 = 2-aminonaphthalene-4,6,8-trisulphonic acid; 2 = 2-aminonaphthalene-4,8-disulphonic acid; 3 = 1,3-diaminophenyl-4-sulphonic acid; 4 = 1,4-diaminophenyl-2-sulphonic acid; 5 = 2-aminonaphthalene-3,6-disulphonic acid; 6 = 4-methoxyphenylamine-3-sulphonic acid; 7 = 1,3-diamino-2,4,6-trimethylphenyl-5-sulphonic acid; 8 = phenylamine-2-sulphonic acid; 9 = 4-methylphenylamine-3-sulphonic acid; 10 = naphthylamine-5-sulphonic acid; 11 = 6-chlorophenylamine-3-sulphonic acid; 12 = 2-aminonaphthalene-6-sulphonic acid; 13 = naphthylamine-4-sulphonic acid; 14 = naphthylamine-7-sulphonic acid.

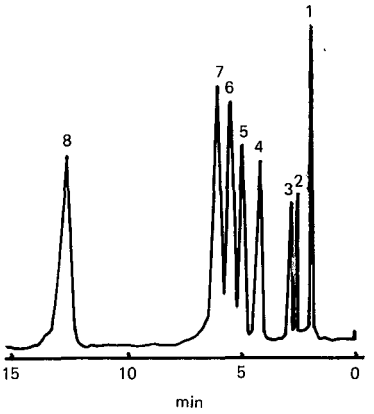

Fig. 2. Chromatogram of a mixture of eight phenylamine- and naphthylaminesulphonic acids. Mobile phase: methanol–phosphate buffer (15:85) containing 10 mmol/l NaH_2PO_4 (pH 6.8). Other experimental conditions as in Fig. 1. Peaks: 1 = 2-aminonaphthalene-3,6,8-trisulphonic acid; 2 = phenylamine-3-sulphonic acid; 3 = 1,3-diamino-2,4,6-trimethylphenyl-5-sulphonic acid; 4 = 4-methylphenylamine-3-sulphonic acid; 5 = 2-aminonaphthalene-6-sulphonic acid; 6 = 4-nitrophenylamine-2-sulphonic acid; 7 = 2-aminonaphthalene-1-sulphonic acid; 8 = naphthylamine-8-sulphonic acid.

groups, the explanation of which is as follows: the sulphonic acid group is an electronwithdrawing group in a conjugate molecule, which will attract the lone pair of electrons of the amino group in the *m*-isomer more strongly than that in the *p*-isomer. Therefore, the hydrogen-bonding interaction between the *p*-isomer and the mobile phase is stronger than that between the *m*-isomer and the mobile phase, which makes the retention of the *m*-isomer larger than that of the *p*-isomer. On the other hand, the retention of naphthylamine-8-sulphonic acid is the largest of all of the isomers of amino- and sulphonic acid-substituted naphthalenes, which means that the intramolecular hydrogen-bonding interaction between the 1- and 8-substituted groups is the strongest of all such hydrogen-bonding interactions of the tested solutes.

(c) In reversed-phase chromatography the retention of a solute increases with increasing number of non-polar groups such as CH_3, $=CH_2$ and C_6H_5, and decreases with increasing number of polar groups such as NH_2, OH and SO_3H. From the retention values in Table I, it can be seen that the negative effect of the SO_3H group on the retention value is larger than that of the NH_2 group, and the positive effects of a phenyl ring and a naphthyl ring on the retention values are approximately equal to the negative effects of two and three SO_3H groups, respectively, phenylamine-sulphonic acids substituted with NH_2 and SO_3H groups with no intramolecular hydrogen-bonding interactions still show a slight retention and naphthylaminesulphonic acids substituted with three SO_3H and one NH_2 groups show no retention under the experimental conditions used.

Effect of the organic modifier concentration on k'

The effect of variation of varying the organic modifier concentration with methanol-to-buffer volume ratios (v/v) in the range 0–0.25 on *k'* are shown in Table II.

TABLE II

CAPACITY FACTORS OF EIGHT PHENYLAMINE- AND NAPHTHYLAMINESULPHONIC ACIDS MEASURED AT DIFFERENT CONCENTRATIONS OF METHANOL IN THE MOBILE PHASE CONTAINING 10 mmol/l NaH_2PO_4 (pH 6.8)

Solute	Methanol-to-buffer ratio (v/v)					
	0	0.05	0.1	0.15	0.2	0.25
2-Aminonaphthalene-3,6,8-trisulphonic acid	0.03	0.02	0	0	0	0
Phenylamine-3-sulphonic acid	1.03	0.59	0.44	0.33	0.26	0.21
4-Methylphenylamine-3-sulphonic acid	2.97	1.05	0.77	0.57	0.42	0.32
4-Methoxyphenylamine-2-sulphonic acid	6.62	2.93	1.86	1.25	0.93	0.74
4-Nitrophenylamine-2-sulphonic acid	9.51	4.54	2.95	1.97	1.60	1.11
2-Aminonaphthalene-6-sulphonic acid	12.02	4.84	2.72	1.66	1.28	0.86
2-Aminonaphthalene-1-sulphonic acid	15.95	6.32	3.63	2.35	1.74	1.13
Naphthylamine-8-sulphonic acid	30.00	14.03	8.72	6.01	4.71	3.64

The effect of the organic modifier concentration on k' in RP-HPLC can be described as [11–13]:

$$\ln k' = \ln k'_w + cC_b \quad (1)$$

where k'_w is the capacity factor extrapolated at $C_b = 0$, c is a constant mainly determined by the molecular interaction between the solute and the eluent and C_b is the concentration of the organic modifier. The results of linear regression analysis of the experimental data shown in Table II according to eqn. 1, either not taking or taking into account the k' value at $C_b = 0$, are given in Table III. It can be seen that the

TABLE III

COEFFICIENTS OF LINEAR REGRESSION ANALYSIS OF THE EXPERIMENTAL DATA IN TABLE II

Solute	Not taking account of data at $C_b = 0$			Taking account of data at $C_b = 0$		
	Ln k'_w	c	r	Ln k'_w	c	r
Phenylamine-3-sulphonic acid	−0.2954	−5.184	0.9976	−0.1252	−6.112	0.9840
4-Methylphenylamine-3-sulphonic acid	0.3384	−5.966	0.9997	0.7317	−8.106	0.9564
4-Methoxyphenylamine-2-sulphonic acid	1.343	−6.891	0.9909	1.629	−8.455	0.9747
4-Nitrophenylamine-2-sulphonic acid	1.802	−6.934	0.9948	2.036	−8.156	0.9811
2-Aminonaphthalene-6-sulphonic acid	1.899	−8.418	0.9906	2.207	−10.10	0.9785
2-Aminonaphthalene-1-sulphonic acid	2.187	−8.357	0.9951	2.492	−10.02	0.9803
Naphthylamine-8-sulphonic acid	2.882	−6.626	0.9891	3.154	−8.109	0.9745

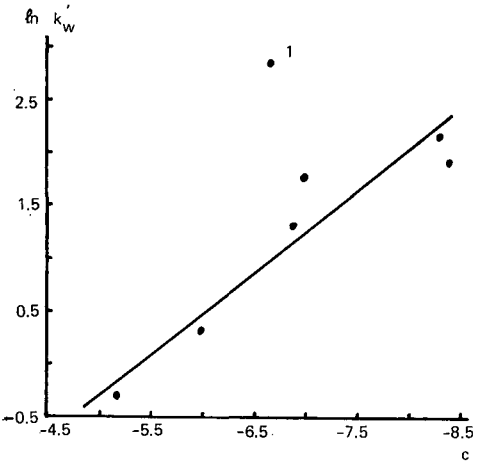

Fig. 3. Linear regression of ln k'_w *vs.* c for the six solutes excluding naphthylamine-8-sulphonic acid shown in Table III. Ln $k'_w = -3.766 - 0.7155c$, $r = 0.9343$. Point 1 represents naphthylamine-8-sulphonic acid.

regression coefficients in the former instance are much higher than those in the latter, which means that the change of k' value in the C_b range 0–0.05 is different from that in the range 0.05–0.25. There are many reports [12,14,15] that there is a linear relationship between ln k'_w and c for the same class or related compounds. Fig. 3 shows the relationship between ln k'_w and c for phenylamine- and naphthylamine sulphonic acids, and it can be seen that it is approximately linear except for naphthylamine-8-sulphonic acid, which means that the interaction behaviour of this acid is different from that of the other compounds in Table III. This may be due to the difference in the hydrogen-bonding interactions between the naphthylamine-8-sulphonic acid and the

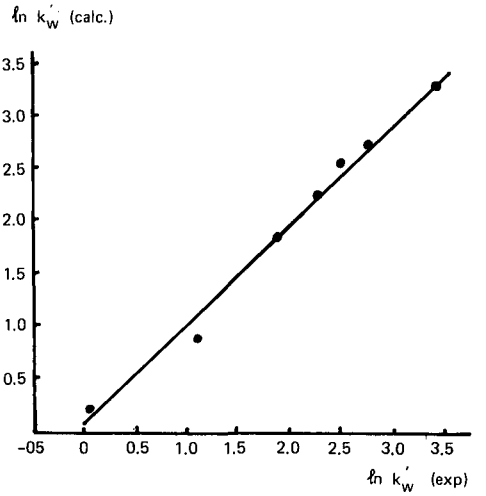

Fig. 4. Linear relationship between ln k'_w experimentally observed at $C_b = 0$ and the value extrapolated from the retention equation ln $k' = \ln k'_w + cC_b$.

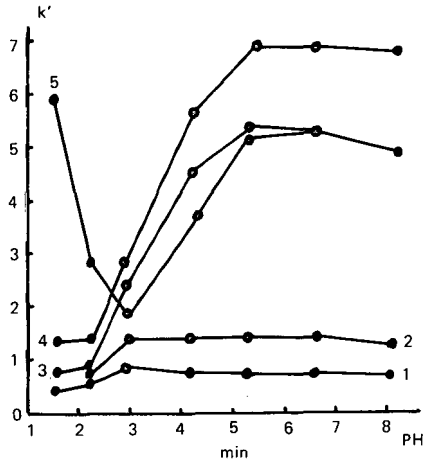

Fig. 5. Graphs showing the effect of the eluent pH on the capacity factors for five phenylamine and naphthylamine sulphonic acids. Mobile phase: methanol–phosphate buffer (0.075:0.925) containing 0.4 mol/l NaCl and 10 mol/l NaH_2PO_4. For other conditions, see Experimental. Solutes: 1 = phenylamine-3-sulphonic acid; 2 = 4-chlorophenylamine-3-sulphonic acid; 3 = 2-aminonaphthalene-6-sulphonic acid; 4 = 2-aminonaphthalene-5-sulphonic acid; 5 = 4-nitrophenylamine-2-sulphonic acid.

other compounds in the experimental column system. Some workers [14–16] used the extrapolated capacity factor ln k'_w (or log k'_w) to predict the *n*-octanol–water partition coefficient (log P_{oct}). We applied a linear regression between the extrapolated capacity factors ln k'_w on the left in Table III and those calculated from k'_w at $C_b = 0$ in Table II; the results are shown in Fig. 4 and indicate that the interaction behaviour in the real buffer system is parallel to that of the extrapolated system for the same class or related compounds.

Effect of pH of the eluent on k'

The effects of varying the eluent pH on the capacity factors of five phenylamine- and naphthylaminesulphonic acids are shown in Fig. 5. Solutions covering the pH range 1.4–8.2 were adjusted by adding 6 mol/l HCl to an eluent containing 10 mmol/l KH_2PO_4 and 0.4 mol/l NaCl with $C_b = 0.075$, where the high concentration of NaCl is intended to minimize the effect on the capacity factor of ionic strength changes caused by variations in pH. Over this pH range, the solutes containing NH_2 and SO_3H groups can exist in three different ionization states:

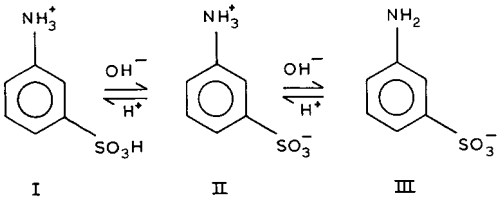

I II III

The pK_a value of the NH_2 group is *ca.* 4.5 and that of the SO_3H group is 1–2.5. In the pH range 5–8.2 there is no serious change in the capacity factors of any of the solutes,

TABLE IV

CAPACITY FACTORS OF 7 PHENYLAMINE- AND NAPHTHYLAMINESULPHONIC ACIDS MEASURED AT DIFFERENT CONCENTRATIONS OF INORGANIC SALT IN THE MOBILE PHASE CONTAINING 10 mmol/l NaH_2PO_4 (pH 6.8) WITH $C_b = 0.08$

Solute	NaCl (mmol/l)					
	0	0.91	50	10.9	350	609
2-Aminonaphthalene-3,6,8-trisulphonic acid	0.03	0.07	0.12	0.14	0.17	0.19
Phenylamine-3-sulphonic acid	0.55	0.57	0.64	0.68	0.74	0.78
4-Methylphenylamine-3-sulphonic acid	0.91	0.99	1.09	1.17	1.32	1.40
4-Methoxyphenylamine-2-sulphonic acid	2.29	2.49	2.78	2.95	3.36	3.63
4-Nitrophenylamine-2-sulphonic acid	3.58	3.88	4.26	4.55	4.94	5.22
2-Aminonaphthalene-6-sulphonic acid	3.36	3.58	3.98	4.27	4.66	4.97
2-Aminonaphthalene-1-sulphonic acid	4.61	5.00	5.56	5.93	6.67	7.27

because they exist in form III. However, with decrease in the pH of the eluent, the NH_2 group becomes partly ionized to NH_3^+. In the pH range 3–5, solutes 3, 4 and 5 in Fig. 5 exist in forms II and III and the capacity factor decreases, but there is no serious change in the capacity factors for solutes 1 and 2, which means these two solutes are still in form III. With a further decrease in pH value to 1.4–3, the NH_2 group in solutes 3, 4 and 5 is fully ionized to NH_3^+, and the SO_3^- of solute 5 is partly non-ionized as SO_3H, which means that solutes 3 and 4 exist in form II and solute 5 in the forms I and II. However, solutes 1 and 2 may exist in forms II and III.

Effect of inorganic salt concentration on k'

The variation of k' with varying concentration of the inorganic salt is shown in Table IV. The capacity factors of the phenylamine- and naphthylaminesulphonic acids increase with increasing concentration of NaCl in the eluent. According to Horváth *et al.* [17], the effect of the inorganic salt concentration on k' in RP-HPLC can be expressed as

$$\ln k' = A + Bm \tag{2}$$

TABLE V

COEFFICIENTS OF LINEAR REGRESSION ANALYSIS OF THE EXPERIMENTAL DATA IN TABLE IV

Solute	*A*	*B*	*r*
2-Aminonaphthalene-3,5,7-sulphonic acid	−2.599	1.865	0.7117
Phenylamine-3-sulphonic acid	−0.5220	0.5071	0.8929
4-Methylphenylamine-3-sulphonic acid	0.0116	0.6111	0.9062
4-Methoxyphenylamine-2-sulphonic acid	0.9343	0.6569	0.9142
4-Nitrophenylamine-2-sulphonic acid	1.377	0.5193	0.8814
2-Aminonaphthalene-6-sulphonic acid	1.308	0.5260	0.8773
2-Aminonaphthalene-1-sulphonic acid	1.643	0.6468	0.9167

where A and B are constants related to the physico-chemical behaviour of a given column system and m is the concentration of the inorganic salt. Table V gives the coefficients of the linear regression analysis of the experimental data in Table IV. It can be seen that the regression coefficient is about 0.9, which means that the linear relationship represented by eqn. 2 is not very good. We consider that the k' values of the solutes are affected not only by the surface tension of the eluent with varying salt concentration, but also by the interaction between the NH_2 and SO_3^- groups and ionized silanol groups [18]. With increasing NaCl concentration, the ionized silanol group is partly masked, which will decrease the replusive interaction between the ionized silanol group and the SO_3^- group of the solute and increase its capacity factor. Therefore, the linear relationship in eqn. 2 is not good enough to describe the effects of the NaCl concentration on k'.

CONCLUSION

The proposed method enabled us to determine the phenylamine- and naphthylaminesulphonic acids in the synthesis of dyestuffs on a reversed-phase column. The retention values are affected by the concentration of organic modifier and inorganic salt and the pH of the eluent. A linear relationship between the experimentally measured $\ln k'_w$ values and those extrapolated from the retention equation $\ln k' = \ln k'_w + cC_b$ was observed.

REFERENCES

1 U. Streule and A. V. Wattenwyl, *Chromatographia*, 12 (1979) 25.
2 P. Jandera and J. Churacek, *J. Chromatogr.*, 197 (1980) 181.
3 S. K. Lee and T. L. Yeh, *J. Chromatogr.*, 260 (1983) 97.
4 A. T. Hunter, *J. Chromatogr.*, 319 (1985) 319.
5 H. Zou, Y. Zhang, X. Wen and P. Lu, *Fenxi Huaxue*, in press.
6 Y. Yoshii, A. Ito and O. Manabe, *Bunseki Kagaku*, 26 (1977) 179.
7 H. Grossenbacher, T. Thurnheer, D. Zurrer and A. M. Cook, *J. Chromatogr.*, 360 (1986) 219.
8 C. Bandi and T. Venturini, *J. Chromatogr. Sci.*, 19 (1981) 308.
9 N. P. Crosby, *Food Sci. Technol.*, 11 (1984) 323.
10 T. Li, Z. Wu and Y. Liu, *SEPU*, 5 (1987) 216.
11 R. Kaliszan, K. Osmialowski, S. A. Tomellini, S.-H. Hsu, S. D. Fazio and R. A. Hartwick, *J. Chromatogr.*, 352 (1986) 141.
12 Th. Braumann, G. Weber and L. H. Grimme, *J. Chromatogr.*, 261 (1983) 329.
13 P. Lu, H. Zou and Y. Zhang, *Sci. Sin. Ser. B*, in press.
14 W. E. Hammers, G. J. Meurs and C. L. de Ligny, *J. Chromatogr.*, 247 (1982) 1.
15 M. Harnisch, H. J. Mockel and G. Schulze, *J. Chromatogr.*, 282 (1983) 315.
16 Th. Braumann and B. Jastorff, *J. Chromatogr.*, 329 (1985) 321.
17 Cs. Horváth, W. Melander and I. Molnar, *J. Chromatogr.*, 125 (1976) 129.
18 K. E. Bij, Cs. Horváth, W. Melander and A. Nahum, *J. Chromatogr.*, 203 (1981) 65.

Journal of Chromatography, 523 (1990) 257–264
Elsevier Science Publishers B.V., Amsterdam

CHROM. 22 714

Use of β-diketonate anions as eluent in non-suppressed ion chromatography

Acetylacetonate eluent for the separation of fluoride and chloride

NAOKI HIRAYAMA*, MASAHIRO MARUO, AKINOBU SHIOTA and TOORU KUWAMOTO
Department of Chemistry, Faculty of Science, Kyoto University, Kitashirakawa-Oiwake-cho, Sakyo-ku, Kyoto 606 (Japan)

(First received May 14th, 1990; revised manuscript received July 27th, 1990)

ABSTRACT

β-Diketones in aqueous solution exist in different chemical states owing not only to keto–enol tautomerism but also to dissociation equilibria. The use of acetylacetonate anion as the eluent in ion chromatography was effective for the elution of weakly retained anions such as fluoride and chloride. Further, by using the chelate-forming ability of β-diketones, it was found that the influence of metal cations in the sample solution on the ion chromatograms is eliminated.

INTRODUCTION

Non-suppressed ion chromatography (IC) was developed for the separation and determination of various anions [1,2], and has been widely applied to the separation and determination of many kinds of anions and cations by selecting suitable eluent ions [3,4].

Fluoride and chloride anions have been often determined by using non-suppressed IC [3,4]. However, because fluoride, in particular, is weakly retained on the anion-exchange resin, it is necessary to select an eluent with a weak driving strength to separate the fluoride peak from first system (dip) peak. Therefore, two methods can be considered: the use of a low-concentration eluent or the selection of an eluent anion with a weak driving strength. In the former instance, the sample peak is broadened because of the lack of an exchangeable eluent anion for the sample anion on the resin. The latter, however, is suitable, as hydroxide [5] and nicotinate [6] anions are useful eluents.

Further, the baseline level often fluctuates for some time after the injection of sample solutions containing metal cations. Hence it is necessary to remove or mask these metal cations in order to eliminate this phenomenon.

β-Diketones (1,3-diones), which are well known chelating reagents with metal

0021-9673/90/$03.50

cations [7], exist in different forms owing not only to keto–enol tautomerism but also to dissociation equilibria, as follows:

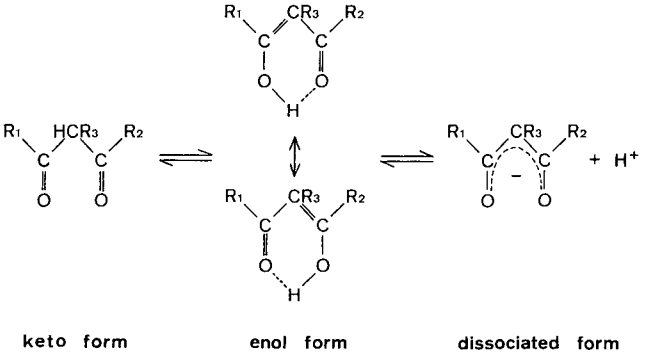

It was considered that the dissociated from (β-diketonate anion) could be used as an eluent in non-suppressed IC because the driving strength of the enol group is relatively small. Moreover, by changing the side-chains (R_1, R_2 and R_3) of these reagents, one can control the driving strength of the β-diketonate anion in IC.

In addition, β-diketonate anions react with many metal ions, as follows:

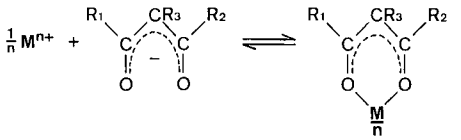

Therefore, it is possible to eliminate the influence of metal ions in sample solutions without pretreatment by using β-diketonate anions as the eluent.

In this work, the acetylacetonate anion ($R_1 = R_2 = CH_3$, $R_3 = H$), which is simplest β-diketonate anion, was selected as the eluent and applied to the determination of fluoride and chloride anions.

EXPERIMENTAL

Apparatus

A Tosoh Model HLC-601 ion chromatograph system was used, consisting of a computer-controlled pump, a conductivity detector, a sample injector (100 μl) and an oven. An anion-exchange column (50 mm × 4.6 mm I.D.) packed with Tosoh TSKgel IC-Anion-PW (polymethacrylate gel, capacity 0.03 ± 0.003 mequiv./g) was used for the separation of anions. The flow-rate was maintained at 1.0 ml/min under a pressure of 40–60 kg/cm^2. The separation column and the conductivity detector were placed in an oven regulated at 30°C. The data were recorded with a Shimadzu Chromatopack C-R1A recorder.

Eluents

Acetylacetone (2,4-pentanedione, Hacac, pK_a = 8.99 [8]) was purified by the method of Steinbach and Freiser [9]. A 100-ml volume of analytical-reagent grade

TABLE I

COUNTER CATIONS USED, STABILITY CONSTANTS OF $M(acac)_i^{(n-i)+}$ COMPLEXES AT 25°C [8] AND REAGENTS USED

Cation	Log β_1[a]	Log β_2[a]	Log β_3[a]	Reagent
Li^+	–			LiCl
Na^+	–			NaCl
Mg^{2+}	3.65	6.25		$MgCl_2$
Al^{3+}	8.6[b]	16.5[b]	22.3[b]	$AlCl_3 \cdot 6H_2O$
K^+	–			KCl
Ca^{2+}	–	–		$CaCl_2 \cdot 2H_2O$
Cr^{3+}	–	–	–	$CrCl_3 \cdot 6H_2O$
Mn^{2+}	4.21	7.30		$MnCl_2 \cdot 4H_2O$
Fe^{2+}	5.07[b]	8.67[b]		$FeSO_4 \cdot 7H_2O$
Fe^{3+}	9.8[b]	18.8[b]	26.2[b]	$FeCl_3 \cdot 6H_2O$
Co^{2+}	5.40	9.54		$CoCl_2 \cdot 6H_2O$
Ni^{2+}	6.00	10.60		$NiCl_2$
Cu^{2+}	8.25	15.05		$CuCl_2 \cdot 2H_2O$
Zn^{2+}	5.06	9.00		$ZnCl_2$

[a] $\beta_i = [M(acac)_i^{(n-i)+}]/[M^{n+}][acac^-]^i$ (M^{n+} is the metal ion).
[b] at 30°C.

acetylacetone was shaken with 10 ml of dilute ammonia (1:10) and shaken with two 10-ml portions of distilled water. This solution were distilled at 136°C.

Acetylacetone–sodium hydroxide (sodium acetylacetonate, Naacac) solutions as eluents were prepared by dissolving the purified acetylacetone in distilled water and adding 1 *M* sodium hydroxide solution to control the eluent pH.

Sodium salicylate (NaSa), sodium benzoate (NaBz) and sodium acetate (NaOAc) eluents were prepared by dissolving analytical-reagent grade reagents in distilled water.

All of these eluent solutions were deaerated before use.

Standard sample solutions

Stock standard solutions of 100 m*M* sodium fluoride, chloride, nitrite, bromide nitrate and carbonate were prepared by from analytical-reagent grade salts. Working standard solutions were obtained by diluting the stock solutions with distilled water.

Counter cations used in the investigation are shown in Table I. Stock standard solutions of 100 mequiv./l of each cation were prepared by from analytical-reagent grade reagents as shown in Table I. Working standard solutions were obtained by diluting the stock solutions with distilled water. The stability constants (β_i) of metal complexes with $acac^-$ are given in Table I [8].

River water

As an example of an application, river-water samples collected from the Otada river and the Muko river (both in Nishinomiya City, Hyogo, Japan) on May 2nd, 1990, were used after filtration through a 0.2-μm Millipore filter.

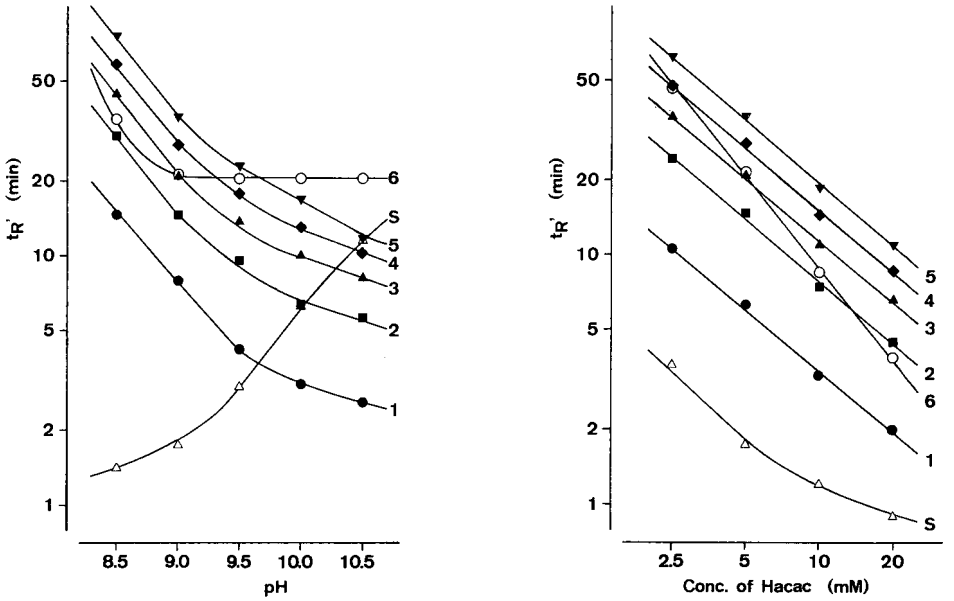

Fig. 1. Relationship between retention times (t_R') of anions and eluent pH. Sample: 1 = fluoride; 2 = chloride; 3 = nitrite; 4 = bromide; 5 = nitrate; 6 = carbonate. S = second system peak. Eluent: 5.0 m*M* Hacac–NaOH.

Fig. 2. Relationship between retention times and concentration of Hacac. Sample: 1 = fluoride; 2 = chloride; 3 = nitrite; 4 = bromide; 5 = nitrate; 6 = carbonate. S = second system peak. Eluent: Hacac–NaOH (pH 9.0).

RESULTS AND DISCUSSION

Optimum chromatographic conditions

In non-suppressed IC, it is necessary to consider two system (dip) peaks [10], the first being due to the difference in the conductance of the eluent and sample water band, and the latter to the compensation for the first system peak. In order to reduce the errors in quantitative analysis, the selection of optimum chromatographic conditions such that the position of the sample anion peak is separated from those of the system peaks was investigated.

Fig. 1 shows the relationship between the retention times of sample anions and eluent pH at a fixed eluent concentration (5.0 m*M*). With increasing eluent pH, the fluoride peak was eluted rapidly and near to the first system peak, and the second system peak overlapped with several peaks of the sample anions. On the other hand, with decreasing pH, the degree of dissociation of Hacac was decreased and the retention times were increased.

Fig. 2 shows the relationship between the retention times and the concentration of Hacac at a fixed eluent pH (9.0). With decreasing concentration, the retention time increased. On the other hand, with increasing concentration, the fluoride peak was near to the second system peak and the peaks of chloride and carbonate overlapped.

Based on these results, the optimum eluent pH and concentration of Hacac

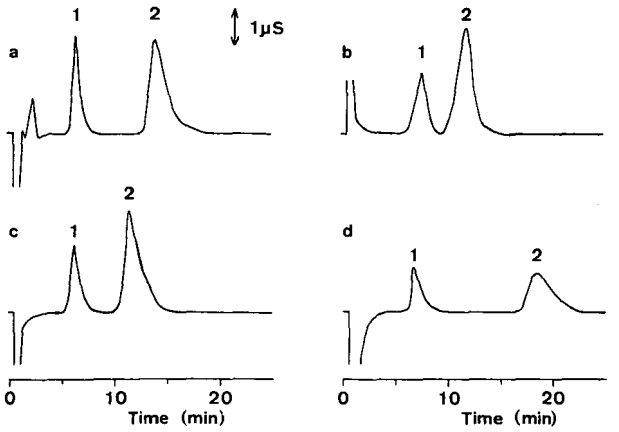

Fig. 3. Ion chromatograms obtained with different eluent anions. Sample: 1 = 0.5 m*M* (9.5 μg/ml) fluoride; 2 = 0.5 m*M* (17.8 μg/ml) chloride. Eluent: (a) 5.0 m*M* Hacac–NaOH (pH 9.0); (b) 0.5 m*M* NaSa (pH 6.2); (c) 1.5 m*M* NaBz (pH 6.5); (d) 5.0 m*M* NaOAc (pH 7.7).

were selected as 9.0 and 5.0 m*M*, respectively. Under these optimum conditions, the detection limits (signal-to-noise ratio = 2) of fluoride and chloride were 1.2 μ*M* (23 ng/ml) and 1.5 μ*M* (55 ng/ml), respectively.

Comparison between elution behaviour of Naacac and other eluents

Fig. 3 shows ion chromatograms of fluoride and chloride obtained using several eluents having similar driving strengths, and Table II gives data for the elution behaviour of fluoride.

As the driving strength of Sa^- is high, the concentration has to be low for the separation of the fluoride peak and the first system peak. Therefore, leading of the peak shape occurred owing to the lack of an exchangeable eluent anion for the sample anion on the resin, and the values of the plate number (*N*) and symmetry (*S*) became worse.

Bz^- has suitable driving strength for the elution of fluoride. However, the peak was broadened and the *N* value became poorer because of some interaction between Bz^- and the resin.

TABLE II

COMPARISON OF ELUTION BEHAVIOUR WITH DIFFERENT ELUENTS

Sample: 0.5 m*M* (9.5 μg/ml) fluoride.

Eluent	Retention time, t'_R (min)	Plate number, *N*	Symmetry, *S*	Peak area[a], *Y*
5.0 m*M* Naacac (pH 9.0)	6.09	412	1.11	1.70
0.5 m*M* NaSa (pH 6.2)	7.39	203	0.52	1.55
1.5 m*M* NaBz (pH 6.5)	5.77	212	1.67	1.52
5.0 m*M* NaOAc (pH 7.7)	6.30	255	2.00	1.00

[a] Relative value with *Y*(NaOAc) = 1.

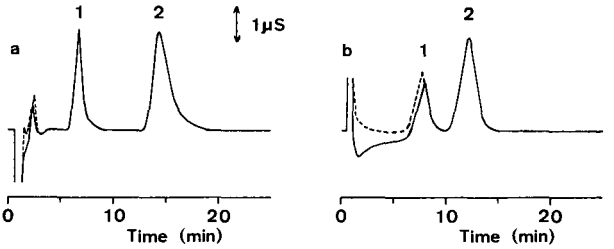

Fig. 4. Ion chromatograms obtained with iron (III) cation present in the sample. Sample: 1 = 0.5 m*M* (9.5 μg/ml) fluoride; 2 = 0.5 m*M* (17.8 μg/ml) chloride. Cations: solid lines, 0.5 m*M* Na^+ and 0.17 m*M* (0.5 mequiv./l) Fe^{3+}; dashed lines, 1.0 m*M* Na^+. Eluent: (a) 5.0 m*M* Hacac–NaOH (pH 9.0); (b) 0.5 m*M* NaSa (pH 6.2).

AcO^- has a low driving strength and can be used at high concentrations as an eluent. However, because the driving strength is too low, tailing occurred on the fluoride peak and the *N* and *S* values became worse. Moreover, the peak area (*Y*) of fluoride became small because the AcO^- anion has a relativley high conductivity.

Finally, $acac^-$ was found to be suitable as an eluent with regard to *N*, *S* and *Y* values. This result seems to be due to the following reasons: (1) $acac^-$ has suitable driving strength for the separation of fluoride and the first system peak (referring to N); (2) uncharged Hacac was adsorbed on the resin and suppressed the interaction between charged $acac^-$ and the resin (referring to *S*); and (3) the conductivity of $acac^-$ is suitable for the detection of fluoride (referring to *Y*).

TABLE III

COMPARISON OF THE DEVIATION OF THE BASELINE ON CHROMATOGRAM CAUSED BY METAL CATIONS IN THE SAMPLE WITH SEVERAL ELUENTS

Sample: 0.5 m*M* (9.5 μg/ml) fluoride and 0.5 m*M* (17.8 μg/ml) chloride [or 0.25 m*M* (24.0 μg/ml) sulphate]. Cation: 0.5 m*M* Na^+ and 0.5 mequiv./l metal cation.

Cation	Deviation (ratio to peak height of 0.5 m*M* F^-, %)			
	5.0 m*M* Naacac (pH 9.0)	0.5 m*M* NaSa (pH 6.2)	1.5 m*M* NaBz (pH 6.5)	5.0 m*M* NaOAc (pH 7.7)
Li^+	0.0	0.0	−0.5	−0.8
Na^+	0.0	0.0	−0.5	−0.8
Mg^{2+}	−6.8	0.0	+4.7	−4.9
Al^{3+}	0.0	−8.1	−6.3	−0.8
K^+	0.0	0.0	−0.5	−0.8
Ca^{2+}	0.0	+2.5	+6.8	−20.3
Cr^{3+}	0.0	−3.1	−5.3	+4.1
Mn^{2+}	−13.9	+1.9	+10.5	−13.8
Fe^{2+}	0.0	−5.0	−1.1	−7.3
Fe^{3+}	+0.3	−9.3	−4.7	−7.3
Co^{2+}	−0.7	+0.6	+7.4	−17.1
Ni^{2+}	−0.7	0.0	+2.6	−3.3
Cu^{2+}	0.0	−4.3	−4.7	0.0
Zn^{2+}	−1.1	−8.1	−4.7	−9.8

Hence it was concluded that $acac^-$ is the preferred eluent for the separation and determination of fluoride and chloride anions.

Comparison between the influence of metal cations in the sample on Naacac and other eluents

Fig. 4 shows chromatograms of fluoride and chloride in the presence of Fe^{3+} in the sample with Naacac and NaSa eluents. With NaSa as eluent, Fe^{3+} influenced the baseline and the fluoride peak. In contrast, with Naacac as eluent, Fe^{3+} did not interfere.

Table III shows the influences of fourteen metal cations in the sample on the baselines of chromatograms obtained with the use of four eluents. With three eluents (not Naacac), several cations influenced the baselines. On the other hand, with Naacac as eluent, only Mg^{2+} and Mn^{2+}, which have relatively low stability constants of their complexes with $acac^-$ (see Table I [8]), influenced the baselines. It was concluded that most of the metal cations form acac chelates and elute rapidly from the column, and that $acac^-$ is the preferred eluent for eliminating the influence of metal cations in the sample.

Application to river-water samples

The Otada river, a branch stream of the Muko river, contains relatively large amounts of fluoride and calcium owing to the presence of biotite granite, in which calcium fluoride is enriched [11,12]. To evaluate this method, fluoride and chloride were measured in several samples collected from the two rivers. The results, shown in Table IV, were compared with those given in a previous paper [11].

It has been speculated that high concentrations of chloride in samples 6–9 and

TABLE IV

CONCENTRATIONS OF FLUORIDE AND CHLORIDE ANIONS IN THE OTADA AND MUKO RIVERS

River	Sample No.	Previous paper [11]		This method	
		F^- (μg/ml)[a]	Cl^- (μg/ml)[b]	F^- (μg/ml)	Cl^- (μg/ml)
Otada	1	1.89	4.6	1.30	3.81
	2	0.96	5.6	1.17	5.58
	3	1.05	8.9	1.40	9.45
	3	1.78	2.9		
	5	2.46	4.8		
	6			2.03	114
	7	1.66	142		
	8			1.64	65.1
	9	2.25	640	1.70	154
	10	2.18	3.2	1.49	3.26
	11	1.58	160		
Muko	12			0.22	44.1
	13			0.52	41.7

[a] Direct photometric method with lanthanum–alizarin complexone chelate [13].
[b] Mercury(II) thiocyanate method.

11 (Otada river) are caused by mineral spring water located at the river side [11,12], and that samples 12 and 13 (Muko river) are contaminated by domestic sewage. The present results agreed approximately with those obtained previously [11] and hence this ion chromatographic method seems very useful for the determination of fluoride and chloride in natural water samples containing metal cations without pretreatment of the sample solution or intricate handling.

CONCLUSION

The use of $acac^-$ as the eluent has been shown to be useful for the separation and determination of fluoride and chloride, which are retained very weakly on anion-exchange resins. This eluent has a relatively low driving strength and was very effective for separating the fluoride peak from the first (or second) system peak. Fluoride and chloride were measured with relatively high sensitivities by using this eluent. Further, because $acac^-$ is a very effective chelating reagent, it successfully eliminated the influence of metal cations in the sample solution on the baseline of the chromatogram. In addition, Hacac is a very weak acid (pK_a = 8.99 [8]) and it is considered that Hacac–NaOH solution can also be used as the eluent in suppressed IC.

ACKNOWLEDGEMENTS

The authors thank Professor Yuzuru Kusaka (Kōnan University, Hyogo, Japan) for expert advice and providing useful data. This work was financially supported by the Nippon Life Insurance Foundation, No. C88110012.

REFERENCES

1 D. T. Gjerde, J. S. Fritz and G. Schmuckler, *J. Chromatogr.*, 186 (1979) 509.
2 D. T. Gjerde, G. Schmuckler and J. S. Fritz, *J. Chromatogr.*, 187 (1980) 442.
3 J. G. Tarter (Editor), *Ion Chromatography*, Marcel Dekker, New York, Basle, 1987.
4 D. T. Gjerde and J. S. Fritz, *Ion Chromatography*, Hüthig, Heidelberg, 2nd ed., 1987.
5 T. Okada and T. Kuwamoto, *Anal. Chem.*, 55 (1983) 1001.
6 J. S. Fritz, D. L. Duvall and R. E. Barron, *Anal. Chem.*, 56 (1984) 1177.
7 R. C. Mehrotra, R. Bohra and D. P. Gaur, *Metal β-Diketonates and Allied Derivatives*, Academic Press, London, 1978.
8 S. Kotrlý and L. Šůcha, *Handbook of Chemical Equilibria in Analytical Chemistry*, Ellis Horwood, Chichester, 1985.
9 J. F. Steinbach and H. Freiser, *Anal. Chem.*, 25 (1953) 881.
10 T. Okada and T. Kuwamoto, *Anal. Chem.*, 56 (1984) 2073.
11 Y. Kusaka and T. Sagawa, *Mem. Kōnan Univ., Sci. Ser.*, 16 (1973) 21.
12 Y. Kusaka and T. Sagawa, *Nippon Kagaku Kaishi*, (1974) 2322.
13 H. Hashitani, H. Yoshida and H. Muto, *Bunseki Kagaku*, 16 (1967) 44.

Journal of Chromatography, 523 (1990) 265–272
Elsevier Science Publishers B.V., Amsterdam

CHROM. 22 704

Extraction and clean-up procedure for polychlorinated dibenzo-*p*-dioxins and dibenzofurans in fly ash from municipal solid waste incinerators

B. JIMÉNEZ*, M. J. GONZÁLEZ and L. M. HERNÁNDEZ
Instituto de Quimica Orgánica General (C.S.I.C.), C/ Juan de la Cierva 3, 28006 Madrid (Spain)
(First received March 5th, 1990; revised manuscript received July 18th, 1990)

ABSTRACT

An exhaustive extraction and a good clean-up method for analysis of polychlorinated dibenzo-*p*-dioxins (PCDDs) and polychlorinated dibenzofurans (PCDFs) in incinerator fly ash is presented. After Soxhlet extraction of the fly ash with benzene, a multi-step clean-up is necessary to remove all interferences from the sample. The principal problem is the separation of PCDDs and PCDFs from the polychlorinated biphenyls. There are two key conditions: the alumina activation and the polarity of the solvents used. The recovery of the PCDDs and PCDFs is good, ranging from 87.1 to 118 percent.

INTRODUCTION

Polychlorinated dibenzo-*p*-dioxins (PCDDs) and polychlorinated dibenzofurans (PCDFs) have been the subject of much concern in recent years. Some of these compounds, especially the 2,3,7,8-substituted congeners, have extraordinarily toxic properties and are teratogenic, mutagenic and potentially carcinogenic [1]. Since PCDDs were found in fly ash from the Amsterdam municipal incinerator [2], investigations have been carried out [3,4] on the emissions from municipal incinerators from different parts of the world.

Because of the high toxicity of these compounds, it is necessary to have an effective method for their identification and determination at parts per trillion (ppt) levels. The determination of ppt concentrations of chemical residues generally requires the use of either highly selective sample purification procedures or very specific detectors [5,6].

We describe here an extraction and exhaustive clean-up procedure for PCDDs and PCDFs in fly ash from Spanish municipal solid waste (MSW) incinerators.

EXPERIMENTAL AND RESULTS

The chromatographic adsorbents used were basic alumina 100–200 mesh (Bio-Rad, AG10, Ref. 33197) and acid silica gel, 100–200 mesh (Bio-Rad, Biosil-A, Ref.

0021-9673/90/$03.50

131.1340). The gels were rinsed with 300 ml of dichloromethane and the dichloromethane-saturated material was dried in a glass tube furnace under a continuous purge of dry nitrogen initially at 50°C, increased to 180°C over a period of 25 min and maintained there for 90 min. The adsorbents were then activated for an additional 90 min at 300°C. The adsorbents were stored in a glass bottle in a desiccator over phosphorus pentoxide until used. Alumina needed additional activation prior to its use.

Concentrated sulphuric acid on silica (44%), 1 *M* sodium hydroxide on silica (33%) and silver nitrate on silica (10%) were prepared as described previously [7,8].

Chromatographic and extraction solvents, including *n*-hexane, dichloromethane, benzene, toluene and carbon tetrachloride were of glass-distilled pesticide grade (Merck).

Gas chromatography (GC) was performed using a Perkin-Elmer Model 8310B instrument equipped with a ^{63}Ni electron-capture detector. A fused-silica WCOT capillary column (50 m × 0.22 mm I.D.) covered with BP-5, obtained from Chrompack, was used. The chromatographic conditions were as follows: detector temperature, 350°C; injector temperature 300°C; column temperature programme, 100°C for 3 min, increased at 20°C/min to 180°C, then at 2°C/min to 250°C, held for 45 min, increase at 2°C/min to 280°C, held for 20 min. The carrier gas (nitrogen) flow-rate was 0.35 ml/min.

PCDDs and PCDFs used as reference standards for GC were obtained from Wellington Labs. (Ontario, Canada).

Fly ash samples were taken from Spanish municipal incinerators located in Cádiz, Alava, Gerona, Barcelona, Melilla, Pontevedra and Palma de Mallorca. Samples were stored in closed containers at room temperature and protected from light.

All glassware was cleaned using the following procedure: (1) rinsing with soap and tap water; (2) rinsing with acetone; (3) ultrasonic agitation for 1 h in a 2% aqueous solution of detergent; (4) rinsing with copious amounts of tap water; (5) rinsing with deionized water; and (6) heating in a general laboratory oven for 2 h at 130°C.

Extraction

A variety of methods have been used for the extraction of PCDDs and PCDFs from fly ash. Extraction efficiencies of PCDDs and PCDFs have been compared [9] using seven different extraction methods and it was concluded [9] that generally Soxhlet extraction with benzene or toluene gives the best results. We therefore tried Soxhlet extraction with benzene and toluene and, although both solvents gave good results, benzene was selected because its evaporation time is shorter than that of toluene, which reduces the preanalytical treatment time.

The fly ash was extracted with 200 ml of benzene for 36 h and the benzene extract was evaporated to dryness.

Fly ash extracts contain a complex mixture of PCDDs, PCDFs and other extractable organic compounds. These compounds include polycyclic aromatic hydrocarbons (PAHs) and numerous chlorinated compounds [10–12]. The complexity of the mixture makes the identification and determination of the individual isomers very difficult.

Clean-up

In order to avoid the above interferences, it was necessary to develop a multi-step clean-up method which is very effective at removing PAHs and clorinated compounds and also yields a high recovery and good precision for PCDDs and PCDFs.

Procedure

Removal of benzene-extractable compounds other than PCDDs and PCDFs is accomplished by passing the extract of the residue through the first (A) of the column systems (see Fig. 1) prepared as follows. A glass-wool plug is inserted into the end of the column to serve as a bed support and the following materials are then placed in sequence in the column: 1.0 g of silica (bottom layer); 2.0 g of 33% 1 *M* sodium hydroxide on silica; 1.0 g of silica; 4.0 g of 44% concentrated sulphuric acid on silica; and 1.0 g of silica (top layer). The packed column is prewashed with 30 ml of *n*-hexane and the effluent is discarded. The extract of the residue (1.5 ml) is then passed through the column followed by three 1.5-ml *n*-hexane rinses of the boiling glass vessel. Following these rinses, an additional 55 ml of *n*-hexane is passed through the column.

The total effluent is then evaporated to dryness under a stream of nitrogen. The residue is passed through a dual column system consisting of an chromatographic column draining into a bottom column (B and C, respectively, in Fig. 1) to remove common chemical interferences with PCDDs and PCDFs.

Column B is packed with 1.5 g of silica gel containing 10% (w/w) silver nitrate and column C is packed with 6 g of basic alumina. A glass-wool plug is placed at the bottom of each column (B and C) and, after depositing the reagents, the columns are prewashed with 30 ml of *n*-hexane, the washings being discarded.

The residue from column A is transferred to silver nitrate–silica column (B) using three 1.5-ml portions of *n*-hexane. A 45-ml volume of *n*-hexane is used as the eluent. The eluate is collected on the top of the basic alumina column. Now the problem is to separate the PCDDs and PCDFs from polychlorinated biphenyls (PCBs) into the alumina column. First, we tried 50 ml of *n*-hexane–carbon tetrachloride (50:50, v/v) to remove PCBs, and finally 22.5 ml of *n*-hexane–dichloromethane (50:50, v/v) for eluting PCDDs and PCDFs as described previously [6]. However,

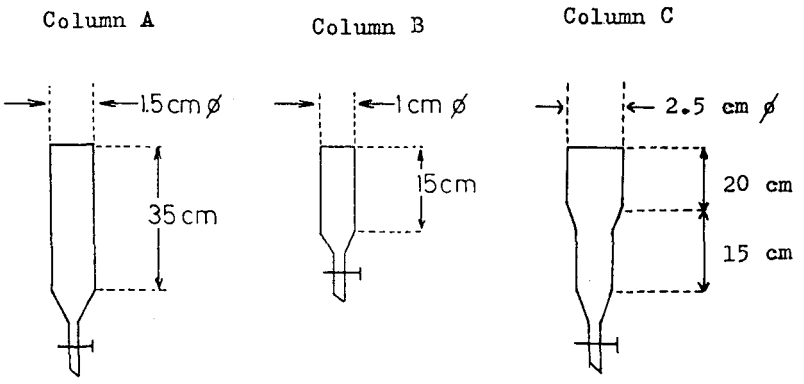

Fig. 1. Liquid chromatographic clean-up columns. ∅ = Diameter.

these solvents did not solve the problem; the PCDDs and PCDFs fraction contained too much impurities, principally PCBs. It was therefore necessary to investigate the polarity of the solvents. The solvents proposed by Albro *et al.* [13]were investigated. Two fractions of 25 ml were tried: *n*-hexane–dichloromethane (98:2, v/v) to elute PCBs and *n*-hexane–dichloromethane (80:20, v/v) to elute PCDDs and PCDFs. The two fractions contained too much impurities and the separation was poor.

In view of these results, the alumina activation was investigated. Three experiments were designed with (1) alumina activated at 600°C for 16 h [14], (2) alumina activated at 130°C for 8 h [15] and (3) alumina activated at 130°C for 18 h [13,16]. For all three experiments 6 g of basic alumina and 10 ml of solvent per gram of alumina were used. The fractionation scheme is shown in Fig. 2.

The best results for the removal of all impurties were obtained using alumina using alumina activated at 130°C for 18 h. The results confirmed the significance of the alumina activation conditions. This is important for removing all impurities and for obtaining a good separation of PCDDs and PCDFs from PCBs. Up to this stage of our investigations we have only achieved the first objective. The polarity of the solvents was then investigated using alumina activated at 130°C for 18 h.

Three different experiments were carried out in order to establish the influence of solvent polarity and the amount of solvent on the production of the different fractions (Fig. 3). For this investigation a mixture of known standards containing

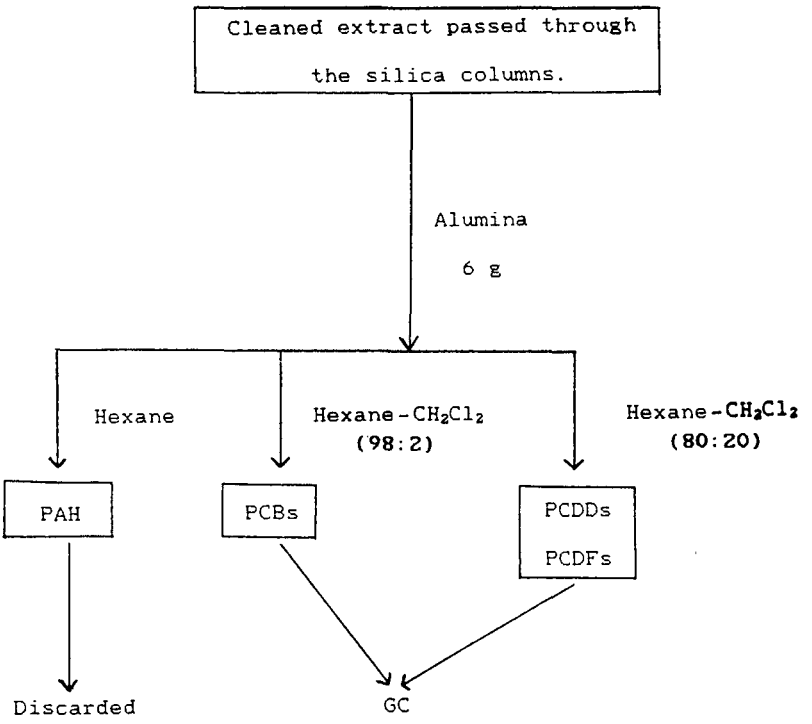

Fig. 2. Fractionation scheme.

Experiment	1	2	3
Fraction 1	Hexane-CCl_4 (50:50) 50 ml	Hexane-CCl_4 (50:50) 40 ml	Hexane-CCl_4 (75:25) 50 ml
Fraction 2	Hexane-CH_2Cl_2 (80:20) 50 ml	Hexane-CH_2Cl_2 (80:20) 40 ml	Hexane-CH_2Cl_2 (80:20) 50 ml

Fig. 3. Scheme of three experiments to study the effects of polarity and amount of solvent. Fraction 1 for PCBs and fraction 2 for PCDDs and PCDFs.

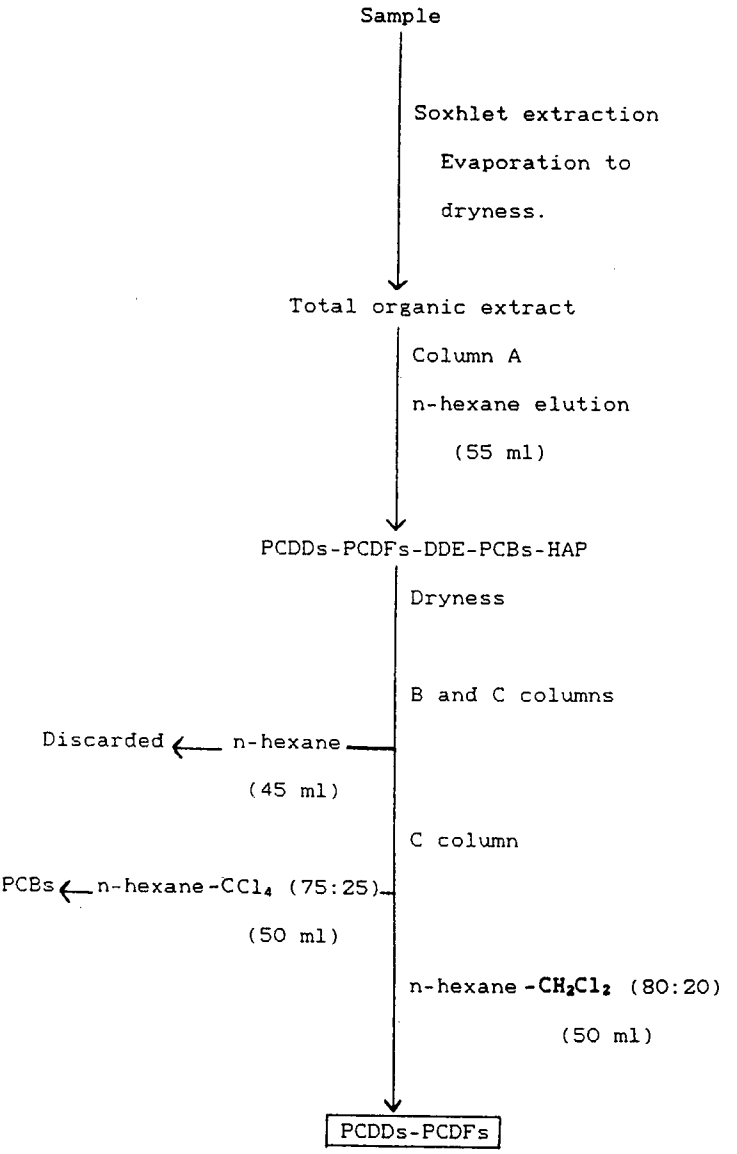

Fig. 4. Definitive procedure for extraction and clean-up.

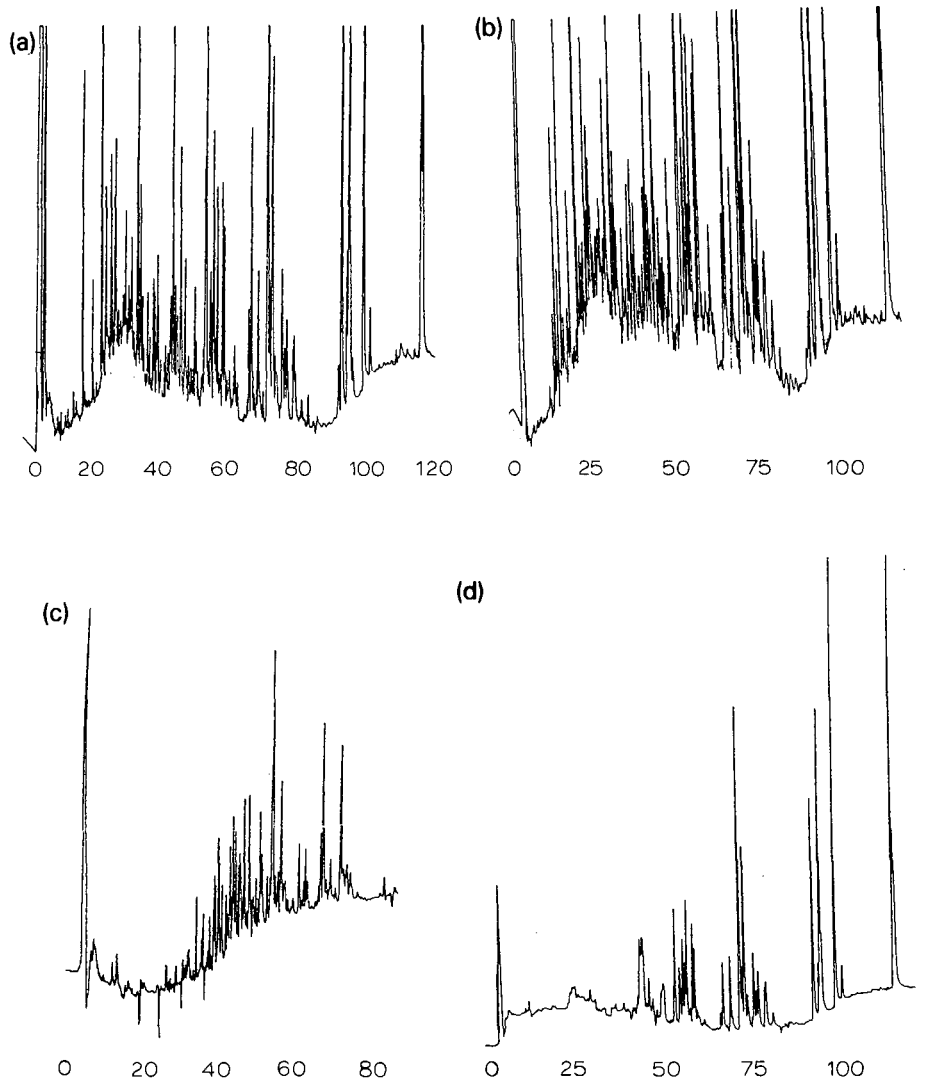

Fig. 5. Chromatograms corresponding to the different steps of the clean-up procedure. (b) Total organic extract from fly ash containing PCDDs, PCDFs and other extractable organic compounds. (a) Organic extract passed through the first column (A). (c) fraction of PCBs obtained from the alumina column (B). (d) Final fraction obtained from the alumina column, containing the PCDDs and PCDFs. Time scales in min.

PCBs, PCDDs and PCDFs was used. Fig. 3 shows that although the amount of solvent is not important, the polarity of the solvent is a key factor. Using the solvents in experiment 3 a good separation can be obtained, PCBs eluting in a fraction apart from PCDDs and PCDFs. The recommended procedure for extraction and clean-up based on this investigation is shown in Fig. 4.

The chromatograms in Fig. 5 show the different fractions obtained during the

TABLE I

RECOVERY OF PCDD AND PCDF ISOMERS

PeCDD = pentachloro dibenzo-*p*-dioxin; PeCDF = pentachloro dibenzo-*p*-furan; HxCDD = hexachloro dibenzo-*p*-dioxin; HxCDF = hexachloro dibenzo-*p*-furan; TCDD = tetrachloro dibenzo-*p*-dioxin; HpCDD = heptachloro dibenzo-*p*-dioxin; OCDD = octachloro dibenzo-*p*-dioxin.

Experiment No.	Isomers	Recovery (%)
1	1,2,3,7,8-PeCDD 1,2,3,7,8-PeCDF 2,3,4,7,8-PeCDF	109.11
	1,2,3,4,7,8-HxCDD 1,2,3,6,7,8-HxCDD 1,2,3,7,8,9-HxCDD 1,2,3,4,7,8-HxCDF 1,2,3,6,7,8-HxCDF 1,2,3,7,8,9-HxCDF 2,3,4,6,7,8-HxCDF	101.84
2	2,3,7,8-TCDD	87.1
3	1,2,3,4,6,7,8-HpCDD	95.16
4	OCDD	118

extraction and clean-up process. The benzene extract (Fig. 5b) from fly ash contains the PCDDs, PCDFs and all impurities. Fig. 5a corresponds to the benzene extract passed through the first silica column (A). The PCB fraction is in Fig. 5c and finally, the fraction containing the PCDDs and PCDFs exhaustively cleaned-up is in Fig. 5d. It can also be seen that PCDDs and PCDFs are separated according to their degree of chlorination.

DISCUSSION

An effective extraction and clean-up method for PCDDs and PCDFs has been devised. A multi-step clean-up is necessary to remove all interferents from these samples. Whereas the first step of the clean-up is commonly used with good results [7], the main problem is the separation of PCDDs and PCDFs from PCBs in the final step, and this separation has been achieved with the proposed method. There are two key conditions: the alumina activation and the polarity of the solvents.

The recovery for PCDDs and PCDFs isomers with different chlorine contents was checked with four experiments. Fly ash with all extractable organic compounds previously extracted was used. From Table I it can be seen that high recoveries were obtained for all isomers, ranging from 87.1 to 118%. Values higher than 100% have been explained elsewhere [17]. This effect is suspected to be related to the injection of samples into the gas chromatograph. Recoveries are probably influenced by errors associated with the measurement and handling of small injection volumes.

REFERENCES

1 A. W. M. Hay, *Chlorinated Dioxins and Related Compounds. Impact on the Environment*, Pergamon Press, Oxford, 1982.
2 K. Olie, P. C. Vermeulen and O. Hutzinger, *Chemosphere*, 8 (1977) 455.
3 H. R. Buser, H. P. Bosshardt and C. Rappe, *Chemosphere*, 7 (1978) 417.
4 G. A. Eiceman, R. E. Clement and F. W. Karasek, *Anal. Chem.*, 51 (1979) 2343.
5 R. W. Baughman and M. S. Meselson, *Environ. Health Perspect.*, 5 (1973) 27.
6 K. Li, C. Chiu and R. C. Lao, *Chemosphere*, 14 (1985) 803.
7 L. L. Lamparski, T. J. Nestrick and R. H. Stehl, *Anal. Chem.*, 51 (1979) 1453.
8 L. L. Lamparski and T. J. Nestrick, *Anal. Chem.*, 52 (1980) 2045.
9 R. M. M. Kooke, J. W. A. Lustenhouwer and O. Hutzinger, *Anal. Chem.*, 53 (1981) 461.
10 F. W. Karasek and A. C. Viau, *J. Chromatogr.*, 265 (1983) 79.
11 M. F. Gonnord and F. W. Karasek, *Tech. Sci. Munic.*, 77 (1982) 221.
12 G. A. Eiceman, A. C. Viau and F. W. Karasek, *Anal. Chem.*, 52 (1980) 1492.
13 P. W. Albro, J. S. Schroeder, D. J. Harvan and B. J. Corbelt, *J. Chromatogr.*, 197 (1984) 155.
14 G. F. Van Ness, I. G. Solch, M. L. Taylor and T. O. Tiernan, *Chemosphere*, 9 (1980) 553.
15 G. Bertoni, D. Brocco, V. Di Palo, A. Liberti, M. Pozzansini and F. Bruner, *Anal. Chem.*, 50 (1978) 732.
16 P. W. Albro and C. E. Parker, *J. Chromatogr.*, 197 (1980) 155.
17 H. Valente and K. M. Aldous, *Anal. Chem.*, 60 (1988) 1478.

Journal of Chromatography, 523 (1990) 273–280
Elsevier Science Publishers B.V., Amsterdam

CHROM. 22 755

Gas chromatographic determination of airborne dialkyltin dichlorides as hydride derivatives

SINIKKA VAINIOTALO* and LEILA HÄYRI[a]

Department of Industrial Hygiene and Toxicology, Institute of Occupational Health, Topeliuksenkatu 41 a A, SF-00250 Helsinki (Finland)

(First received May 22nd, 1990; revised manuscript received August 9th, 1990)

ABSTRACT

A sampling and analysis method for airborne dibutyltin and dioctyltin dichlorides was developed. The air samples were collected on glass-fibre filters. The chlorides were desorbed with *n*-hexane and converted into hydrides using sodium borohydride. The hydride derivatives were analysed by capillary gas chromatography with flame ionization detection (FID). The identity of dibutyltin and dioctyltin dihydrides in standard solutions was confirmed by gas chromatography–mass spectrometry (GC–MS) and GC–Fourier transform infrared spectrometry. The presence of tin compounds in the fumes released from heated PVC plastics (at 225°C) was shown by GC–MS. The detection limit of the method was 0.02 μg/ml (for tin), corresponding to a concentration of 0.0003 mg/m^3 in an air sample of 120 l. The sensitivity of the method was about 50 times better with FID compared with optimum electron-capture detection conditions. This method can also be applied to the determination of dimethyltin dichloride.

INTRODUCTION

Organotin compounds are used as stabilizers for halogen-containing polymers such as poly(vinyl chloride) (PVC). They account for about 30% of the total stabilizer consumption. Dibutyltin and dioctyltin compounds are the most widely used, but methyltin compounds are also very effective. These disubstituted organotin compounds have the general formular R_2SnX_2, with X representing any of a number of chemical groups such as mercaptide, thioglycolate, maleate or carboxylate. The amount of the stabilizer in the plastics ranges from 0.5 to 5% of the polymer weight.

Organotin compounds act as stabilizers in several ways, but in all instances they slow down the dehydrochlorination of PVC. They function, for example, as HCl scavengers and as blocking agents on weak sites in the polymer molecules [1]. Dialkyltin dichlorides are formed in both of these reactions [2]. These compounds may volatilize into the workplace atmosphere during high-temperature processing (usually at 150–200°C). As alkyltin compounds with different substituents X give the same

[a] Present address: Orion Corporation, Orion Pharmaceutica, P.O. Box 65, SF-02101 Espoo, Finland.

0021-9673/90/$03.50

reaction product R_2SnCl_2, this can be used as an indicator of air impurity during the processing of tin-stabilized PVC.

Several methods have been used to measure organotin compounds, including spectrophotometry, atomic absorption spectrometry (AAS), polarography and gas chromatography (GC). In high-performance liquid chromatography (HPLC), detection has been carried out with AAS or with a fluorescence detector after post-column derivatization. In GC method the tin compounds have been analysed as hydrides or after alkylation with detection methods based on electron-capture detection (ECD), flame photometry, AAS, flame ionization detection (FID) or mass spectrometry (MS) [3].

To monitor the release of these dialkyltin dichlorides into the air, a sensitive and selective method of analysis utilizing common analytical instruments was required. GC equipment is commonly used in organic analytical chemistry, but these organotin chlorides are not very volatile and they are also adsorbed on the column [4]. Because hydride formation is a rapid and simple method of rendering these compounds volatile and non-adsorbing, GC after hydridation was chosen as the method for the analysis. The hydride derivatives have been detected with electron-capture [4] and flame ionization [5] detectors. In this study, the responses of alkyltin dihydrides in these two detection systems were compared. An air sampling method for dioctyl and dibutyltin dichlorides was also tested. In addition, the formation and release of dialkyltin dichlorides in air was elucidated by heating tin-stabilized PVC in a dynamic system.

EXPERIMENTAL

Reagents

Dioctyltin dichloride was purchased from Riedel-de Haën (Hannover, F.R.G.), dibutyltin dichloride from Aldrich-Chemie (Steinheim, F.R.G.) and dimethyltin dichloride from Merck-Schuchardt (Hohenbrunn, F.R.G.). Sodium borohydride ($NaBH_4$) was obtained from BDH (Poole, U.K.), *n*-hexane (HPLC grade) from Rathburn Chemicals (Walkerburn, U.K.) and *n*-heptane from J.T. Baker (Deventer, The Netherlands).

Analysis procedure

A 2-ml volume of dialkyltin dichloride–*n*-hexane solution and 1 ml of $NaBH_4$–ethanol solution were shaken in a test-tube and allowed to stand for 15 min. The $NaBH_4$ solution was prepared by adding 1 g of $NaBH_4$ to 40 ml of ethanol and shaking the mixture in an ultrasonic bath. This solution remained turbid. A 5-ml volume of water was added to the test-tube to remove the reagent. The *n*-hexane layer was separated and 1 μl was injected into the GC system.

The stabilities of the stock standard solution, of the untreated samples during storage and of the tin hydrides during storage were tested. The desorption efficiency, the reproducibility and the detection limits of the method were also tested. The identity of the hydrides in the standard solutions was confirmed with GC–MS and GC–Fourier transform infrared spectrometry (GC–FT-IR).

Gas chromatography

The GC equipment consisted of a Hewlett-Packard Model 5790 gas chromatograph with a ^{63}Ni electron-capture detector and a Hewlett-Packard Model 5890 gas chromatograph with a flame ionization detector. The injector temperature was 230°C for both instruments and the detector temperature was 280°C in the flame ionization apparatus. The gas flows were hydrogen 30, air 410 and make-up (helium) 26 ml/min. The optimum detector temperatures were tested for the EC detector. An argon–methane (5%) flow of 60 ml/min was used.

The column for the determination of dioctyl- and dibutyltin dihydrides (Oc_2SnH_2 and Bu_2SnH_2) was a fused-silica capillary column coated with a 0.17-μm film of HP-5 (25 m × 0.3 mm I.D.). The oven temperature programme was 50°C (held for 0.5 min), increased at 3.5°C/min to 75°C and then at 30°C/min to 200°C (held for 2 min) for Bu_2SnH_2 and 90°C (held for 0.5 min), increased at 4°C/min to 190°C and then at 30°C/min to 250°C (held for 2 min) for Oc_2SnH_2. The splitless injection mode was used with a splitless period of 0.5 min. The flow of the carrier gas (helium) was 4 ml/min. Dimethyltin dihydride (Me_2SnH_2) was analysed with a silica capillary column coated with a 5-μm film of DB-1 (30 m × 0.5 mm I.D.). The split injection mode (splitting ratio *ca.* 8:1) was used with a carrier gas flow-rate of 4.4 ml/min. The temperature programme was 30°C (held for 6 min), increased at 40°C to 200°C (held for 1 min).

GC–MS

The mass spectrometer was a Hewlett-Packard 5970 A quadrupole mass-selective detector equipped with a Hewlett-Packard Model 5890 gas chromatograph. The electron impact spectra were achieved at an ionization potential of 70 eV and an emission current of 300 μA. The columns and the GC oven temperature programmes were as described above.

GC–FT-IR

For IR analysis a Nicolet 20 SCX FT-IR spectrometer with an MCT detector, a GC light-pipe interface and a Hewlett-Packard Model 5890 gas chromatograph were used.

Degradation experiments and sampling tests

The formation and release of dialkyltin dichlorides and the sampling procedures were tested by heating PVC plastics containing about 1.5% of dibutyl and dioctyltin mercaptides in a dynamic system at 225°C. The temperature chosen was close to the PVC processing temperatures, which are usually 150–200°C but may sometimes exceed 200°C. Slices of PVC film were placed in a glass tube (150 cm × 1.4 cm I.D.) in an even layer (0.3 g/cm). The tube was heated by a ring oven (10 cm × 1.8 cm I.D.), which was moved along the tube at a speed of 1.34 mm/min. The degradation products were conducted to a chamber [poly(methyl methacrylate), 32 × 50 × 70 cm] with an air flow of 0.5 l/min, this air flow being mixed with an air flow of 8 l/min immediately before the chamber to dilute and cool the fumes. The temperature of the air just before the inlet never exceeded 28°C.

Concentrations of 2–8 mg/m^3 for dibutyltin dichloride and up to 1 mg/m^3 for dioctyltin dichloride were measured in the chamber. The air samples were sucked

through the holes in the chamber. Several sampling devices were connected in series, and these permitted separate GC analyses to test the breakthrough. The sampling tests were carried out with both glass-fibre filters and Tenax tubes, because preliminary tests showed that these samplers adsorbed both dioctyl and dibutyl dichlorides. The sampling recovery was not studied as it was not possible to produce constant, known concentrations of the chlorides in the air. The identities of the tin compounds found were confirmed by GC–MS.

RESULTS AND DISCUSSION

Analysis

The reproducibility of the method was good: the relative standard deviation was 3% for Bu_2SnH_2 and 2% for Oc_2SnH_2 at a concentration of 8 μg/ml ($n=4$). The linearity was also good. The correlation coefficient was 0.9 for Oc_2SnH_2 and 1.0 for Bu_2SnH_2 for standard solutions in the range 0.02–100 μg/ml. The detection limit (calculated in terms of tin) was 0.02 μg/ml for Bu_2SnCl_2 and Oc_2SnCl_2 and 1.5 μg/ml for Me_2SnCl_2. These figures correspond to air concentrations of 0.0003 and 0.025 mg/m^3, respectively, for an air sample of 120 l.

The stock standard solutions (chlorides) were tested and found to be stable for at least 7 weeks. The Bu_2SnH_2 solution could be stored for at least 2 weeks, but the Oc_2SnH_2 derivative was stable for only 1 week. All of the solutions were stored in glass vials in a refrigerator at 4°C.

Gas chromatography

The responses of the electron-capture and flame ionization detectors were compared by injecting the same amount of dialkyltin dihydrides under identical GC conditions into both gas chromatographs. The flame ionization detector showed a

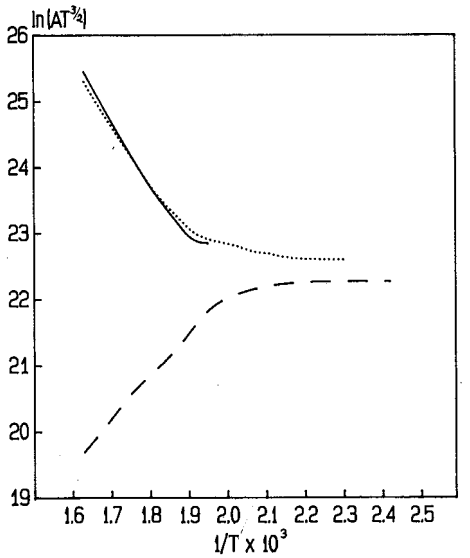

Fig. 1. ECD response of (—) dioctyltin dihydride, (...) dibutyltin dihydride and (---) dimethyltin dihydride.

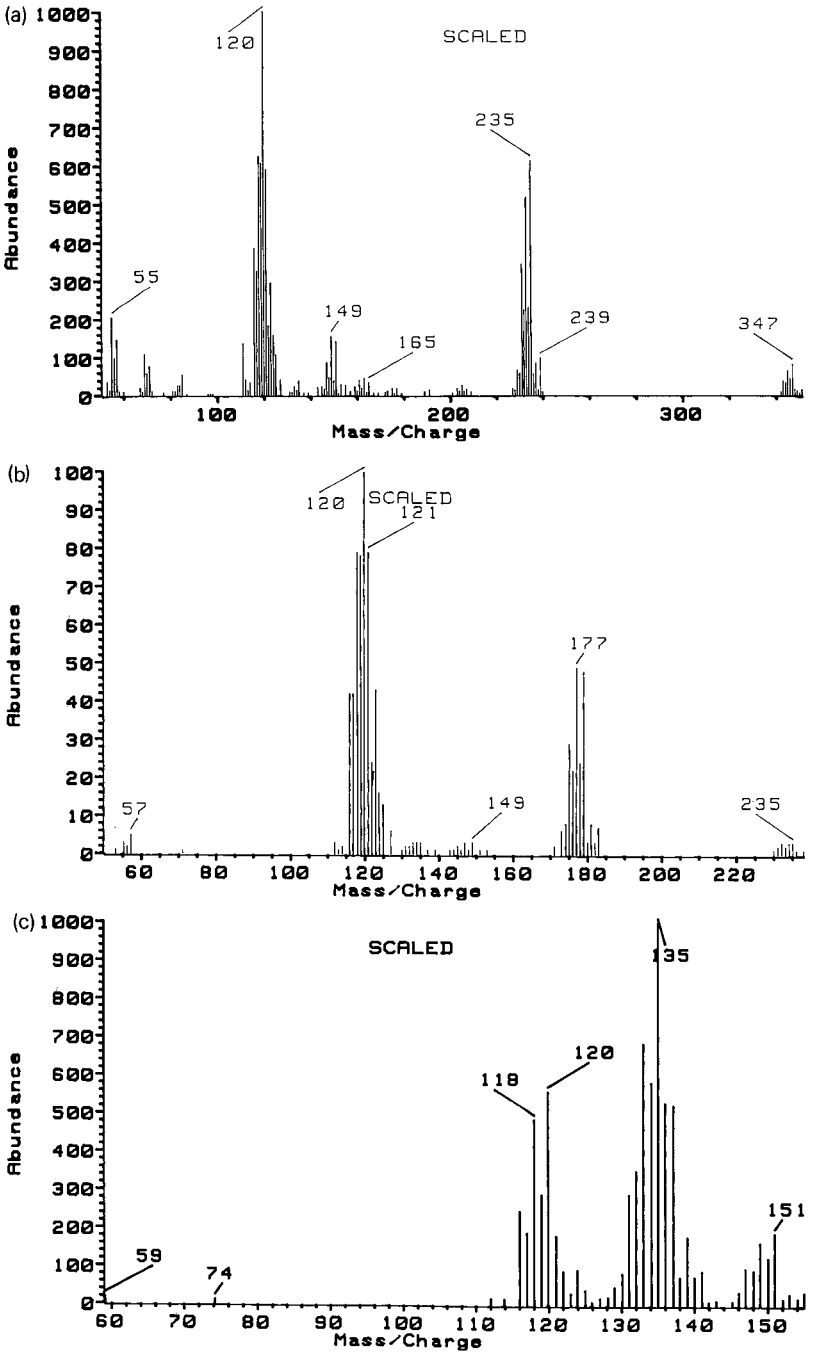

Fig. 2. Mass spectra of (a) dioctyltin dihydride, (b) dibutyltin dihydride and (c) dimethyltin dihydride.

greater sensitivity for all three compounds. The FID response of Oc_2SnH_2 and Bu_2SnH_2 was about 50 times that using ECD (340°C), or 10 times in the case of Me_2SnH_2 (at a detector temperature of 170°C). The retention times were 19.1, 6.2 and 5.1 min for the octyl, butyl and methyl compounds, respectively, under the conditions described above. Because the methyl derivative was not separated from the *n*-hexane solvent, it was prepared in *n*-heptane. Using split injection a sharp peak eluting before the solvent was obtained.

Because the response of the electron-capture detector is markedly temperature dependent, the optimum operating temperatures for the electron-capture detector were determined by plotting the Ln $AT^3/^2$ against $1/T$ for the dialkyltin dihydrides (Fig. 1), where A is the peak area for a fixed mass of dialkyltin dihydride injected at the different detector temperatures T (K). For Bu_2SnH_2 and Oc_2SnH_2 the optimum temperature was 340°C ($10^3/T = 1.63$). The mechanism of the response appeared to be dissociative, as indicated by the negative slope. For Me_2SnH_2 the response was highest below 190°C ($10^3/T = 2.16$), and the positive slope indicated a non-dissociative mechanism.

GC–MS

GC–MS was used to confirm the presence of dialkyltins in the standard solutions and in the degradation products of the PVC plastics. The mass spectra showed a typical tin pattern (Fig. 2) of ten isotopes of tin, ^{120}Sn being the most abundant. Fragmentation of Bu_2SnH_2 and Oc_2SnH_2 began principally with the loss of the alkyl group. Ions of m/z 347 and 235 could also be found, indicating a loss of hydrogen before the loss of the alkyl groups. However, the abundances were much lower than those of the fragments $[BuSnH_2]^+$ and $[OcSnH_2]^+$. No obvious peak of molecular ions could be observed. In the mass spectrum of Me_2SnH_2 the molecular ion was also absent or negligible, but the fragment $[Me_2SnH]^+$ of m/z 151 was found. The mass spectra indicated that fragmentation may begin in different ways, with loss of either hydrogen or the methyl group. The base peak was m/z 150, $[MeSn]^+$, but m/z 120 $[Sn]^+$ in the case of butyl of octyl hydrides.

GC–FT-IR

The GC–FT-IR spectra of Oc_2SnH_2 and Bu_2SnH_2 are shown in Fig. 3. A strong absorption band (stretching) from the tin–hydrogen bond of the butyl compound could be seen with a wavenumber of 1840 cm^{-1}. In the literature this band is reported to be between 1832 and 1845 cm^{-1} [6]. The tin–hydrogen band of the octyl hydride was at 1839 cm^{-1}, compared with 1830–1836 cm^{-1} reported in the literature [6].

Sampling and degradation experiments

Sampling was performed with glass-fibre filters (SKC 225L-16, diameter 13 mm) with an air flow of 2 l/min. After sampling the filters could be stored in test-tubes in a refrigerator for 2 weeks without any loss of the chlorides. The desorption efficiency was found to be >99% for the octyl compound and >98% for the butyl compound when the desorption liquid was 2 ml of *n*-hexane and the desorption time was 1 h. These test samples were prepared at a concentration of 8 μg/ml (calculated as hydrides) by spiking filters with the standard solutions. The filters for desorption tests were analysed immediately after drying at room temperature.

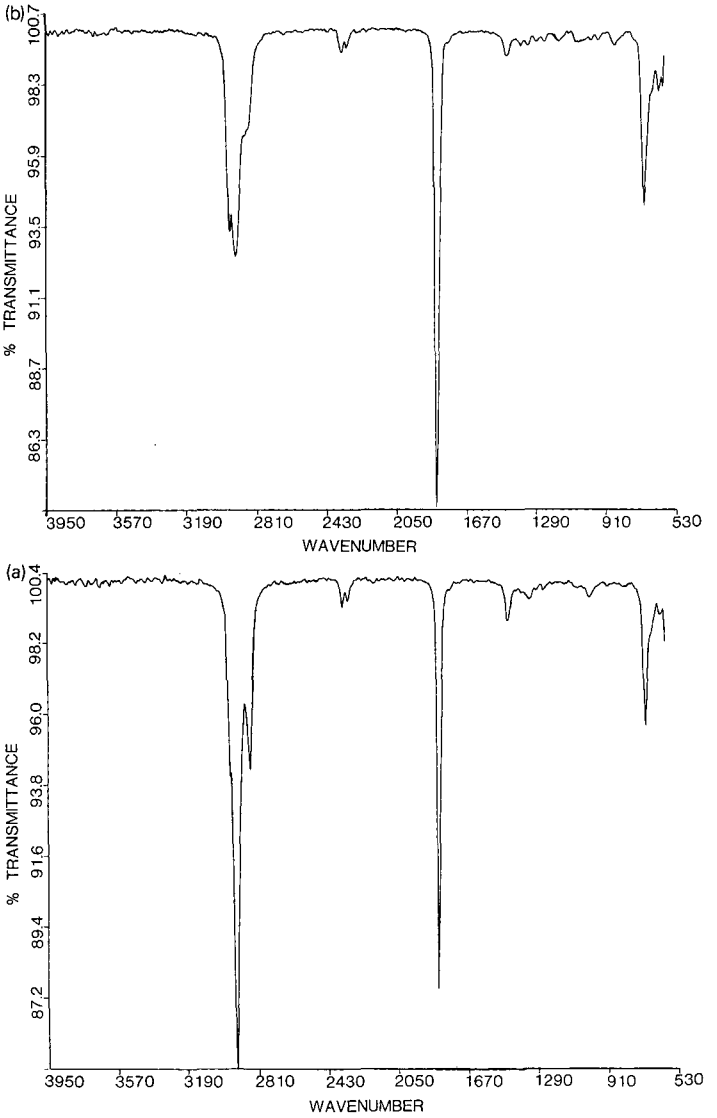

Fig. 3. GC–FT-IR spectra of (a) dioctyltin dihydride and (b) dibutyltin dihydride.

The glass-fibre filter was shown to have a considerably better sampling efficiency than the Tenax tube, which may indicate that the chlorides were in the aerosol phase. Usually filters are used for the collection of aerosols and solid adsorbents (such as Tenax) for the collection of gas-phase compounds. In the filter sampling, after a sampling time of 1 h, the breakthrough was $<5\%$ for the butyl compound; for the octyl compound it was 1.1% after 2 h. The breakthrough was calculated as the ratio of the amount found in the second filter to the sum of the amounts in the first and second filters.

The samples from the degradation experiments analysed by GC–MS revealed the same mass spectra of tin compounds as the standard solutions. A typical GC–FID

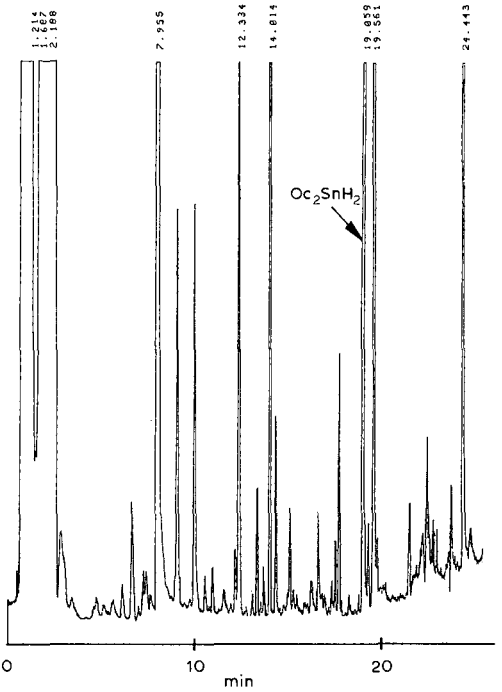

Fig. 4. GC–FID of the fumes of tin-stabilized PVC heated at 225°C.

trace originating from PVC fumes is shown in Fig. 4. The other peaks were well separated from the tin compounds and no interfering substances were eluted at the same time as the tin compounds. The ECD trace of these fumes was more complex than obtained with FID, indicating that the selectivity of ECD is not useful for the determination of organotins in these kinds of matrices. It is also possible that the sample contains interfering compounds at such low concentrations that they are not found by GC–MS (or GC–FID), despite having a high ECD response. Therefore, although the ECD method is not insensitive, FID is preferable for the fumes studied here.

This GC–FID application was shown to be simple and sensitive for the measurement of low air concentrations of tin compounds in the complex mixtures formed during thermal processing of PVC plastics. With this method concentrations substantially lower than the current hygienic standard for organic tin compounds in the working atmosphere (0.1 mg/m^3, calculated as tin) [7] can be measured.

REFERENCES

1 J. Stepek and H. Daoust, *Additives for Plastics*, Springer, New York, 1983, pp. 155–159.
2 K. Kircher, *Chemische Reaktionen bei der Kunststoffverarbeitung*, Carl Hanser, Munich, Vienna, 1982, pp. 248–252.
3 J. Ashby, S. Clark and P. J. Craig, *Spec. Publ. R. Soc. Chem.*, No. 66 (1988) 263.
4 Y. Hattori, A. Kobayashi, S. Takemoto, K. Takami, Y. Kuge, A. Sukimae and M. Nagamoto, *J. Chromatogr.*, 315 (1984) 341.
5 A. Woollins and W. R. Cullen, *Analyst* (London), 104 (1984) 1527.
6 *Gmelin's Handbuch der anorganischen Chemie, Ergänzungswerk zur 8. Auflage*, Band 35, Teil 4, Springer, Berlin, 1976, pp. 105 and 112.
7 ACGIH, *Threshold Limit Values and Biological Exposure Indices for 1989–1990*, American Conference of Governmental Industrial Hygienists, Cincinnati, OH, 1989.

Journal of Chromatography, 523 (1990) 281–292
Elsevier Science Publishers B.V., Amsterdam

CHROM. 22 716

Use of crown ethers in the isotachophoretic determination of metal ions

KEIICHI FUKUSHI*
Kobe University of Mercantile Marine, Fukae, Higashinada, Kobe 658 (Japan)
and
KAZUO HIIRO
Department of Industrial Chemistry, Ube Technical College, Tokiwadai, Ube 755 (Japan)
(First received March 27th, 1990; revised manuscript received June 21st, 1990)

ABSTRACT

The effects of crown ethers on the effective mobilities of various metal ions in capillary isotachophoresis were studied. The effective mobilities of thallium, lead and silver ions decreased when the concentration of crown ethers in an ordinary leading electrolyte was increased up to 50 m*M*. Thus, by use of 18-crown-6, ammonium and thallium ions and thallium and lead ions were completely separated and could be determined. Similarly, by use of 15-crown-5, potassium and thallium ions and ammonium and silver ions were completely separated and could be determined.

INTRODUCTION

It is necessary to adjust the effective mobilities of analyte ions for the isotachophoretic separation of ions that have similar ionic mobilities. Use of cyclodextrins for this purpose was described in a previous paper [1].

Crown ethers have also been used for the same purpose. Alkali and alkaline earth metal ions have been separated or determined by use of 18-crown-6 in the leading electrolyte as a complexing agent for these ions [2–8]. However, there is no report concerning the isotachophoretic separation of heavy metal ions by use of crown ethers. It can be presumed that thallium, lead and silver ions also form inclusion complexes with crown ethers in the separating columns according to the formation constants of the metal–crown ether complexes [9] and that their effective mobilities decrease [1,2,10].

Isotachophoretic separations of ammonium and thallium ions and of potassium and thallium ions are difficult with ordinary leading electrolytes, because their ionic mobilities are very similar in aqueous solutions [11]. Further, there are slight differences between the ionic mobilities of thallium and lead ions and of ammonium and silver ions in aqueous solutions [11]. These ions can be determined accurately and precisely if large differences between their effective mobilities can be obtained.

We therefore studied the effects of 18-crown-6 and 15-crown-5 on the effective

0021-9673/90/$03.50

mobilities of ammonium, lead, potassium, thallium and silver cations. The results of these experiments were applied to subsequent simultaneous determinations by capillary isotachophoresis: ammonium and thallium ions and thallium and lead ions with ordinary leading electrolytes containing appropriate amounts of 18-crown-6 and potassium and thallium ions and ammonium and silver ions with leading electrolytes containing 15-crown-5.

EXPERIMENTAL

Apparatus

A Shimadzu Model IP-2A isotachophoretic analyser was used with a potential-gradient detector. The main column was a fluorinated ethylene–propylene (FEP) copolymer tube (12 cm × 0.5 mm I.D.) and the precolumn was a polytetrafluoroethylene (PTFE) tube (10 cm × 1.0 mm I.D.). A Hamilton Model 1701-N microsyringe was used for the injection of samples into the isotachophoretic analyser. Distilled, demineralized water was obtained from a Yamato-Kagaku Model WG-25 automatic still and a Nihon Millipore Milli-QII system.

Reagents

All reagents were of analytical-reagent grade and used without further purification. Distilled, demineralized water was used throughout. 18-Crown-6 and 15-crown-5 were obtained from Aldrich (Milwaukee, WI, U.S.A.). Standard solutions of various cations were prepared by dissolving their chlorides or nitrates in water; nitrates were used for the preparation of mixed solutions of ammonium and silver ions to prevent the precipitation of silver chloride.

Procedures

Inject 5-μl volumes of solutions containing 1.0 mM of each cation into the isotachophoretic analyser. As leading electrolyte use an aqueous solution containing 5 mM hydrochloric acid, 0.01 wt.-% Triton X-100 and an appropriate amount of crown ether (this leading electrolyte had already been found to be suitable for the isotachophoretic determination of cations [7]), and as terminating electrolyte 10 mM histidine adjusted to pH 4.0 with 0.5 M hydrochloric acid. For the determination of silver ion, use perchloric acid instead of hydrochloric acid to prevent the precipitation of silver chloride in the separating column. Maintain the migration current at 200 μA for the first 7 min in the former electrolyte system and 13 min in the latter, then reduce it to 100 μA. Increase the concentration of 18-crown-6 or 15-crown-5 in the leading electrolyte up to 50 mM.

Calculate the potential unit (PU) value [12], which is generally used as a parameter for the identification of the analyte ions, defined by

$$PU = (PG_A - PG_L)/(PG_T - PG_L) \quad (1)$$

where PG is the potential gradient. The subscripts denote the analyte (A), leading (L) and terminating (T) ions, respectively. The relationship between the PU value and the effective mobility of the analyte ion ($\bar{m}_A$) [12] is given by

$$PU = (a - 1)^{-1}\,\bar{m}_L/\bar{m}_A - (a - 1)^{-1} \quad (2)$$

where $\bar{m}$ is the effective mobility and $a = \bar{m}_L/\bar{m}_T$. Eqn. 2 indicates that the PU value becomes larger when the effective mobility of the analyte ion ($\bar{m}_A$) becomes smaller, and the former becomes smaller when the latter becomes larger. That is, the change in the effective mobility of the analyte ion can be obtained indirectly in terms of the PU value.

RESULTS AND DISCUSSION

Effective mobilities of analyte ions

When analyte ions (A^+ and B^+) form 1:1 complexes (AN^+ and BN^+) with an electrically neutral ligand N, their complex formation constants (K_{AN} and K_{BN}) are defined by

$$K_{AN} = [AN^+]_A/([A^+]_A[N]_A) \tag{3}$$

and

$$K_{BN} = [BN^+]_B/([B^+]_B[N]_B) \tag{4}$$

where the subscripts A and B denote the quantities related to each sample zone. Then the effective mobilities of A^+ and B^+ ($\bar{m}_A$ and $\bar{m}_B$) in their sample zones in the presence of ligand N are expressed as follows [10]:

$$\begin{aligned}\bar{m}_A &= (m_A[A^+]_A + m_{AN}[AN^+]_A)/([A^+]_A + [AN^+]_A) \\ &= (m_A + m_{AN}K_{AN}[N]_A)/(1 + K_{AN}[N]_A)\end{aligned} \tag{5}$$

$$\begin{aligned}\bar{m}_B &= (m_B[B^+]_B + m_{BN}[BN^+]_B)/([B^+]_B + [BN^+]_B) \\ &= (m_B + m_{BN}K_{BN}[N]_B)/(1 + K_{BN}[N]_B)\end{aligned} \tag{6}$$

where m_A, m_B, m_{AN} and m_{BN} are the ionic mobilities of the free analyte ions A^+, B^+ and the complexed analyte ions AN^+ and BN^+, respectively. Eqns. 5 and 6 indicate that cations A^+ and B^+ can be separated from each other even when they have the same ionic mobilities ($m_A = m_B$) if the complex formation constants with N are appreciably different ($K_{AN} \neq K_{BN}$): if $K_{AN} > K_{BN}$, $\bar{m}_A < \bar{m}_B$ and if $K_{AN} < K_{BN}$, $\bar{m}_A > \bar{m}_B$. In addition, $\bar{m}_A$ and $\bar{m}_B$ decrease with increasing $[N]_A$ and $[N]_B$, respectively.

In this study, N corresponds to crown ethers. The stabilities of inclusion complexes of analyte ions with crown ethers generally depend on (1) the kinds and location of the heteroatom in the crown ring, (2) the number of heteroatoms, (3) the relationship between the diameter of the cation and that of the cavity of the crown ether, (4) the charge of the cation, (5) the flexibility of the crown ring and (6) the intensity of interaction between the heteroatom and solvent, etc. [13].

Moreover, when analyte ions (A^+ and B^+) also form 2:1 (crown ring:cation) complexes (AN_2^+ and BN_2^+) with electrically neutral ligand N, their complex formation constants (K_{AN_2} and K_{BN_2}) are defined by

$$\begin{aligned}K_{AN_2} &= [AN_2^+]_A/([AN^+]_A[N]_A) \\ &= [AN_2^+]_A/(K_{AN}[A^+]_A[N]_A^2)\end{aligned} \tag{7}$$

and

$$K_{BN_2} = [BN_2^+]_B/([BN^+]_B[N]_B)$$
$$= [BN_2^+]_B/(K_{BN}[B^+]_B[N]_B^2) \quad (8)$$

Then the effective mobilities of A^+ and B^+ ($\bar{m}_A$ and $\bar{m}_B$) in their sample zones in the presence of ligand N are expressed as follows:

$$\bar{m}_A = (m_A[A^+]_A + m_{AN}[AN^+]_A + m_{AN_2}[AN_2^+]_A)/([A^+]_A + [AN^+]_A + [AN_2^+]_A)$$
$$= (m_A + m_{AN}K_{AN}[N]_A + m_{AN_2}K_{AN}K_{AN_2}[N]_A^2)/(1 + K_{AN}[N]_A + K_{AN}K_{AN_2}[N]_A^2) \quad (9)$$

$$\bar{m}_B = (m_B[B^+]_B + m_{BN}[BN^+]_B + m_{BN_2}[BN_2^+]_B)/([B^+]_B + [BN^+]_B + [BN_2^+]_B)$$
$$= (m_B + m_{BN}K_{BN}[N]_B + m_{BN_2}K_{BN}K_{BN_2}[N]_B^2)/(1 + K_{BN}[N]_B + K_{BN}K_{BN_2}[N]_B^2) \quad (10)$$

where m_{AN_2} and m_{BN_2} are the ionic mobilities of the complexed analyte ions AN_2^+ and BN_2^+, respectively. In this case, $\bar{m}_A$ and $\bar{m}_B$ depend on not only K_{AN} and K_{BN} but also K_{AN_2} and K_{BN_2} compared with the case previously described.

Determination of ammonium and thallium ions

The limiting molar conductivity of ammonium ion is approximately equal to that of thallium ion, *i.e.*, 73.5 and 74.7 S cm^2 mol^{-1}, respectively, at 25°C in aqueous solution [11]. Therefore, it is difficult to separate these ions from each other with ordinary leading electrolytes.

Fig. 1 shows the effect of 18-crown-6 concentration on the *PU* values of several cations (concentration 1.0 m*M*). The *PU* value of lead ion greatly increased with increasing 18-crown-6 concentration up to 1.0 m*M*, but then reached an almost constant value. The *PU* values of both potassium and thallium ions increased with increasing 18-crown-6 concentration up to 50 m*M*; the magnitude of the increase for potassium ion was the same as that for thallium ion. The magnitude of the increase in the *PU* value for ammonium ion was smaller than that for any other cation. When various cations form 1:1 complexes with crown ethers and their complex formation constants are given in Table I [9]. It is concluded that (1) the dependence of the increase in the *PU* value on the 18-crown-6 concentration, thallium ion $\approx$ potassium ion $>$ ammonium ion, is in line with the order of magnitude of the complex formation constant with 18-crown-6 [1,2,10] and (2) at 18-crown-6 concentrations of 1.0 m*M* or above, lead is present mostly in the complexed form because of the large complex formation constant with 18-crown-6, so that the *PU* value of lead ion is almost constant [2,10].

Linear calibration graphs were obtained for ammonium and thallium ions up to 3.0 m*M* by using the leading electrolyte containing 20 m*M* 18-crown-6. The regression equations of these graphs for ammonium and thallium ions were $y = 9.6x$ and $y = 12.9x - 0.2$, respectively, where x is the concentration of the ion in m*M* and y the zone length in mm when the recording speed is adjusted to 40 mm/min, and the correlation coefficients were 0.998 and 1.000, respectively. The relative standard deviations were obtained by calculating the zone length per 1.0 m*M* at each point on the calibration graphs and were 0.036 and 0.028 ($n = 6$), respectively. The limits of

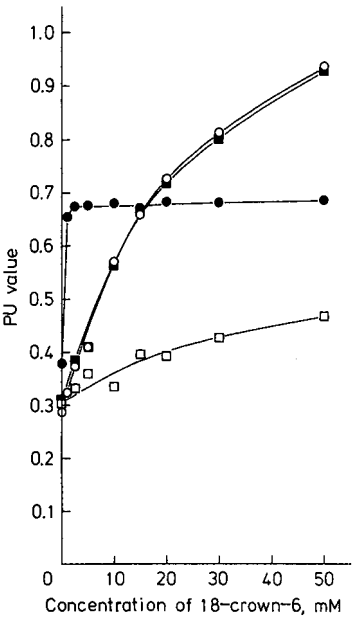

Fig. 1. Effect of 18-crown-6 concentration on the *PU* values of ammonium, lead, potassium and thallium ions. □ = NH_4^+; ● = Pb^{2+}; ■ = K^+; ○ = Tl^+.

determination for ammonium and thallium ions were $1.0 \cdot 10^{-2}$ and $7.8 \cdot 10^{-3}$ m*M*, respectively, corresponding to a 0.1-mm zone length. When 5-μl volumes of mixed solutions containing various concentrations of ammonium and thallium ions were injected and analysed by use of the calibration graphs, the error in the determination of these ions was less than $\pm 20\%$, as shown in Table II. The isotachopherogram of mixture 2 in Table II is shown in Fig. 2. Completely separated zones with sharp boundaries for the ammonium and thallium ions were obtained with the leading electrolyte containing 20 m*M* 18-crown-6, while the mixed zone of these ions was formed without 18-crown-6.

Determination of thallium and lead ions

There is a slight difference between the limiting molar conductivities of thallium and lead (69.5 S cm^2 mol^{-1}) ions [11]. If the difference between the effective mobilities of these ions increases further, these ions can be determined accurately.

As the *PU* value of lead ion greatly increased with increasing 18-crown-6

TABLE I

COMPLEX FORMATION CONSTANTS (LOG *K*) OF VARIOUS CATIONS WITH CROWN ETHERS IN AQUEOUS SOLUTION (25°C)

Crown ether	NH_4^+	Pb^{2+}	K^+	Tl^+	Ag^+
18-Crown-6	1.23	4.27	2.03	2.27	1.50
15-Crown-5	1.71	1.85	0.74	1.23	0.94

TABLE II

ANALYTICAL RESULTS FOR AMMONIUM AND THALLIUM IONS

Mixture No.	Added (mM)		Found (mM)		Error (%)	
	NH_4^+	Tl^+	NH_4^+	Tl^+	NH_4^+	Tl^+
1	0.50	3.0	0.51	3.2	+2.0	+6.7
2	1.0	1.0	0.97	1.0	−3.0	0.0
3	1.0	2.5	0.80	2.5	−20	0.0
4	1.5	2.0	1.5	2.1	0.0	+5.0
5	2.0	1.5	2.0	1.5	0.0	0.0
6	2.5	1.0	2.4	1.0	−4.0	0.0
7	3.0	0.50	3.0	0.53	0.0	+6.0

concentration up to 1.0 mM, as mentioned above, the variations of the PU values of thallium and lead ions were investigated when the 18-crown-6 concentration was increased up to 1.0 mM in 0.1 mM steps. The PU value of thallium ion increased slightly with increasing 18-crown-6 concentration up to 0.5 mM, but then almost levelled off, as shown in Fig. 3. On the other hand, the PU value of lead ion increased with increasing 18-crown-6 concentration, but only slightly when the concentration was >0.4 mM.

Linear calibration graphs were obtained for thallium and lead ions with the leading electrolyte containing 0.8 mM 18-crown-6. The regression equations for thallium and lead ions were $y = 8.6x - 0.5$ and $y = 22.5x - 0.5$, respectively, and the correlation coefficients were 0.999 and 1.000, respectively. The relative standard deviations were 0.048 and 0.028, respectively. The limits of determination for thallium and lead ions were $1.2 \cdot 10^{-2}$ and $4.4 \cdot 10^{-3}$ mM, respectively. The error in the simultaneous determination of these ions was less than $\pm 20\%$, as shown in Table III. The isotachopherogram of mixture 2 in Table III is shown in Fig. 4. The difference

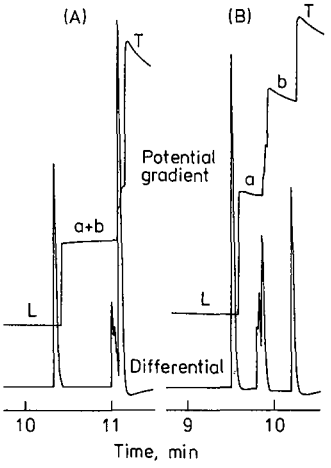

Fig. 2. Isotachopherograms for the separation of ammonium and thallium ions. (A) Without 18-crown-6; (B) 20 mM 18-crown-6. L = Leading ion; a = NH_4^+; b = Tl^+; T = terminating ion.

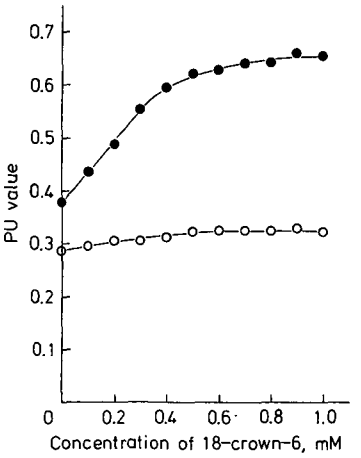

Fig. 3. Effect of 18-crown-6 concentration on the *PU* values of thallium and lead ions. ○ = Tl^+; ● = Pb^{2+}.

between the step heights of thallium and lead ions increased further by use of the leading electrolyte containing 0.8 m*M* 18-crown-6.

The volume of sample (mixed solution containing 1.0 m*M* of thallium and lead ions) injected into the isotachophoretic analyser was increased up to 50 μl. When the leading electrolyte containing 0.8 m*M* 18-crown-6 was used, the zone lengths for both thallium and lead ions increased in proportion to the volume up to 40 μl. On the other hand, when the leading electrolyte without 18-crown-6 was used, both zone lengths increased in proportion to the volume up to 15 μl. That is, by using the former leading electrolyte, the amounts of those ions which could be determined were increased about 2.7 times compared with the use of the latter.

The solubilities of thallium monochloride at 20°C and lead dichloride at 25°C in water are 0.325 and 1.08 g per 100 g, respectively [14]. In this study, the concentrations of the analyte ions were less than 3.0 m*M*. Therefore, thallium monochloride and lead dichloride are not precipitated in the separation column.

TABLE III

ANALYTICAL RESULTS FOR THALLIUM AND LEAD IONS

Mixture No.	Added (m*M*)		Found (m*M*)		Error (%)	
	Tl^+	Pb^{2+}	Tl^+	Pb^{2+}	Tl^+	Pb^{2+}
1	0.50	3.0	0.48	2.9	−4.0	−3.3
2	1.0	1.0	1.2	1.0	+20	0.0
3	1.0	2.5	1.0	2.5	0.0	0.0
4	1.5	2.0	1.7	2.0	+13	0.0
5	2.0	1.5	2.2	1.5	+10	0.0
6	2.5	1.0	2.9	1.0	+16	0.0
7	3.0	0.50	3.4	0.53	+13	+6.0

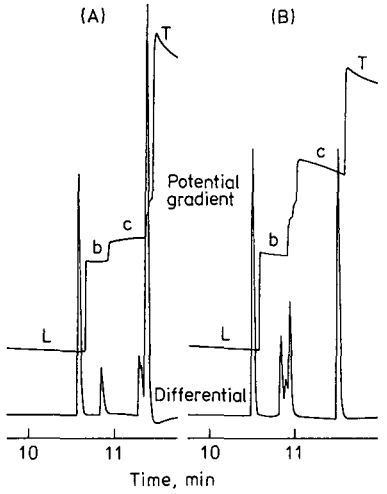

Fig. 4. Isotachopherograms for the separation of thallium and lead ions. (A) Without 18-crown-6; (B) 0.8 m*M* 18-crown-6. L = Leading ion; b = Tl^+; c = Pb^{2+}; T = terminating ion.

Determination of potassium and thallium ions

The limiting molar conductivity of potassium ion (73.5 S cm^2 mol^{-1}) is approximately equal to that of thallium ion [11], so it is difficult to separate these ions with ordinary leading electrolytes.

Fig. 5 shows the effect of 15-crown-5 concentration on the *PU* values of several cations. The *PU* values of both potassium and thallium ions increased almost linearly with increasing 15-crown-5 concentration up to 50 m*M*; the magnitude of the increase for thallium ion was larger than that for potassium ion. The *PU* value of lead ion also increased with increasing 15-crown-5 concentration, but only slightly when the latter was >30 m*M*. The *PU* value of ammonium ion increased slightly with increasing

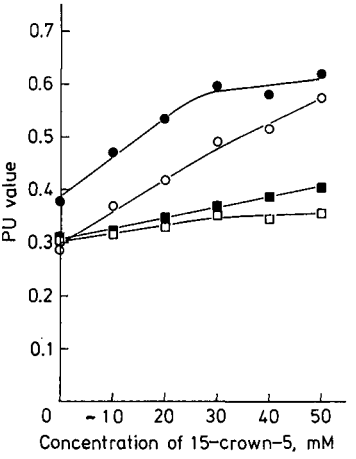

Fig. 5. Effect of 15-crown-5 concentration on the *PU* values of ammonium, potassium, thallium and lead ions. □ = NH_4^+; ■ = K^+; ○ = Tl^+; ● = Pb^{2+}.

TABLE IV

CAVITY DIAMETERS OF CROWN ETHERS AND IONIC RADII OF VARIOUS CATIONS

Crown ether	Cavity diameter (Å)	Cation	Ionic radius (Å)
18-Crown-6	2.6–3.2	NH_4^+	1.45
15-Crown-5	1.7–2.2	Pb^{2+}	1.18
		K^+	1.33
		Tl^+	1.49
		Ag^+	1.13

15-crown-5 concentration up to 30 m*M*, but then almost levelled off. In this instance, the dependence of the increase in the *PU* value on the 15-crown-5 concentration is not necessarily in line with the order of magnitude of the complex formation constant with 15-crown-5 shown in Table I. Cations with diameters larger than those of crown rings also form 2:1 (crown ring:cation) complexes [*e.g.*, K^+(benzo-15-crown-5)$_2$ complex] [13]. Cavity diameters of crown ethers [13] and ionic radii of various cations [15,16] are shown in Table IV. Because the ionic radii of both thallium and ammonium ions are larger than that of potassium ions, it can be presumed that these cations also form 2:1 complexes with 15-crown-5. Therefore, the dependences of the increases in the *PU* value on the 15-crown-5 concentration cannot be compared with one another on the basis of only the order of magnitude of the complex formation constants given in Table I.

Linear calibration graphs were obtained for potassium and thallium ions by using the leading electrolyte containing 50 m*M* 15-crown-5. The regression equations for potassium and thallium ions were $y = 10.5x - 0.1$ and $y = 12.0x - 0.3$, respectively, both correlation coefficients being 1.000. The relative standard deviations were 0.0072 and 0.031, respectively. The limits of determination for potassium and thallium ions were $9.5 \cdot 10^{-3}$ and $8.3 \cdot 10^{-3}$ m*M*, respectively. The error in the simultaneous determination of these ions was less than $\pm 16\%$, as shown in Table V. The isotachopherogram of mixture 2 in Table V is shown in Fig. 6. Completely separated zones with sharp boundaries for the potassium and thallium ions were obtained with

TABLE V

ANALYTICAL RESULTS FOR POTASSIUM AND THALLIUM IONS

Mixture No.	Added (m*M*)		Found (m*M*)		Error (%)	
	K^+	Tl^+	K^+	Tl^+	K^+	Tl^+
1	0.50	3.0	0.48	3.1	−4.0	+ 3.3
2	1.0	1.0	0.98	0.98	−2.0	− 2.0
3	1.0	2.5	0.97	2.5	−3.0	0.0
4	1.5	2.0	1.5	2.1	0.0	+ 5.0
5	2.0	1.5	2.0	1.6	0.0	+ 6.7
6	2.5	1.0	2.5	1.1	0.0	+10
7	3.0	0.50	2.9	0.58	−3.3	+16

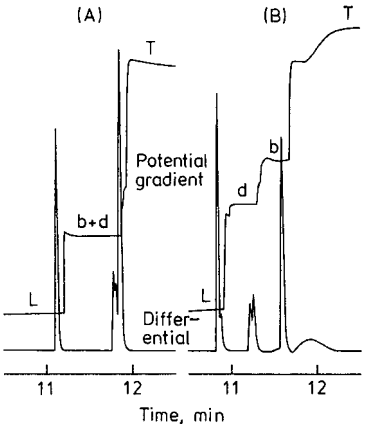

Fig. 6. Isotachopherograms for the separation of potassium and thallium ions. (A) Without 15-crown-5; (B) 50 m*M* 15-crown-5. L = Leading ion; b = Tl^+; d = K^+; T = terminating ion.

the leading electrolyte containing 50 m*M* 15-crown-5, whereas a mixed zone of these ions was formed without 15-crown-5.

Determination of ammonium and silver ions

There is a small difference between the limiting molar conductivities of ammonium and silver (61.9 S cm^2 mol^{-1}) ions [11]. If the difference between the effective mobilities of these ions increases further, greater amounts of these ions can be determined accurately.

Fig. 7 shows the effects of 18-crown-6 and 15-crown-5 concentrations on the *PU* values of ammonium and silver ions. The *PU* value of silver ion increased to similar extents with increasing 18-crown-6 and 15-crown-5 concentrations up to 50 m*M*. In contrast, the *PU* value of ammonium ion increased with increasing 18-crown-6

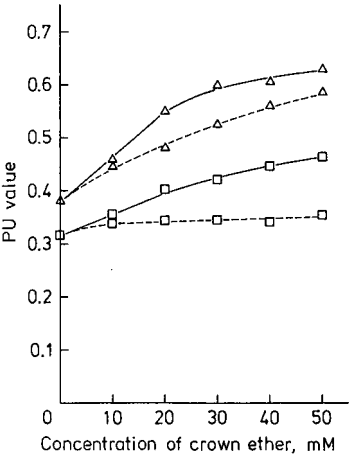

Fig. 7. Effect of crown ether concentration on the *PU* values of ammonium and silver ions. □ = NH_4^+; △ = Ag^+; solid lines, 18-crown-6; dashed lines, 15-crown-5.

TABLE VI

ANALYTICAL RESULTS FOR AMMONIUM AND SILVER IONS

Mixture No.	Added (m*M*)		Found (m*M*)		Error (%)	
	NH_4^+	Ag^+	NH_4^+	Ag^+	NH_4^+	Ag^+
1	0.50	3.0	0.53	3.1	+6.0	+3.3
2	1.0	1.0	0.86	0.97	−14	−3.0
3	1.0	2.5	0.91	2.5	−9.0	0.0
4	1.5	2.0	1.6	2.0	+6.7	0.0
5	2.0	1.5	2.2	1.6	+10	+6.7
6	2.5	1.0	2.7	1.1	+8.0	+10
7	3.0	0.50	3.2	0.50	+6.7	0.0

concentration up to 50 m*M*, whereas it remained almost constant with increasing 15-crown-5 concentration. Therefore, the leading electrolyte containing 50 m*M* 15-crown-5 was adopted for the simultaneous determination of ammonium and silver ions. It is concluded that the dependence of the increase in the *PU* value for ammonium ion on the 18-crown-6 concentration is almost identical with that for silver ion, as are the magnitudes of their complex formation constants with 18-crown-6 [1,2,10]. On the other hand, the dependences of increase in the *PU* value on the 15-crown-5 concentration cannot be compared with each other on the basis of only the order of magnitude of the complex formation constant shown in Table I, as described in the previous section.

Linear calibration graphs were obtained for ammonium and silver ions by use of the leading electrolyte containing 50 m*M* 15-crown-5. The regression equations for

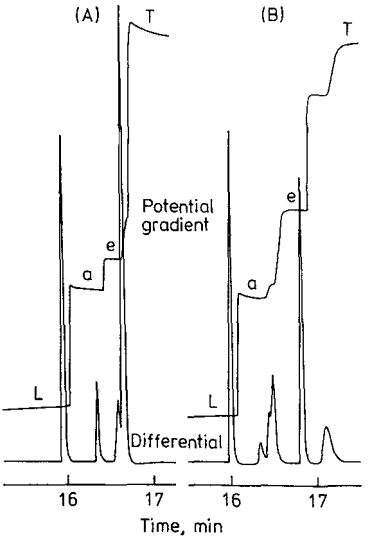

Fig. 8. Isotachopherograms for the separation of ammonium and silver ions. (A) Without 15-crown-5; (B) 50 m*M* 15-crown-5. L = Leading ion; a = NH_4^+; e = Ag^+; T = terminating ion.

ammonium and silver ions were $y = 9.0x + 0.1$ and $y = 11.2x - 0.3$, respectively, both correlation coefficients being 0.999. The relative standard deviations were 0.046 and 0.051, respectively. The limits of determination for ammonium and silver ions were $1.1 \cdot 10^{-2}$ and $8.9 \cdot 10^{-3}$ mM, respectively. The error in the simultaneous determination of these ions was less than $\pm 14\%$, as shown in Table VI. The isotachopherogram of mixture 2 in Table VI is shown in Fig. 8. The difference between the step heights of ammonium and silver ions increased further by using the leading electrolyte containing 50 mM 15-crown-5.

REFERENCES

1 K. Fukushi and K. Hiiro, *J. Chromatogr.*, 518 (1990) 189.
2 M. Tazaki, M. Takagi and K. Ueno, *Chem. Lett.*, (1982) 639.
3 F. S. Stover, *J. Chromatogr.*, 298 (1984) 203.
4 F. S. Stover, *J. Chromatogr.*, 368 (1986) 476.
5 K. Fukushi and K. Hiiro, *Talanta*, 35 (1988) 55.
6 K. Fukushi and K. Hiiro, *Fresenius' Z. Anal. Chem.*, 332 (1988) 125.
7 K. Fukushi and K. Hiiro, *Talanta*, 35 (1988) 799.
8 A. A. G. Lemmens, F. M. Everaerts, J. W. Venema and H. D. Jonker, *J. Chromatogr.*, 439 (1988) 423.
9 R. Oda, in R. Oda, T. Shono and I. Tabushi (Editors), *Crown Ether no Kagaku* (*Crown Ether Chemistry*), Kagaku-Dojin, Kyoto, 1978, p. 9.
10 M. Tazaki, T. Hayashita, Y. Fujino and M. Takagi, *Bull. Chem. Soc. Jpn.*, 59 (1986) 3459.
11 Chemical Society of Japan, *Kagaku Binran*, Maruzen, Tokyo, 3rd ed., 1984, p. II-460.
12 H. Miyazaki and K. Kato, *Tosoku-Denki-Eido-Ho* (*Isotachophoresis*), Kodansha Scientific, Tokyo, 1980, p. 30.
13 K. Takemoto, M. Miyata and K. Kimura, *Hosetsu-Kagobutsu* (*Inclusion Compounds*), Tokyo-Kagaku-Dojin, Tokyo, 1989, p. 18.
14 M. Oki, T. Osawa, M. Tanaka and H. Chihara (Editors), *Kagaku-Dai-Jiten* (*Encyclopedic Dictionary of Chemistry*), Tokyo-Kagaku-Dojin, Tokyo, 1st ed., 1989, pp. 319 and 321.
15 T. Shono, in R. Oda, T. Shono and I. Tabushi (Editors), *Crown Ether no Kagaku* (*Crown Ether Chemistry*), Kagaku-Dojin, Kyoto, 1978, p. 112.
16 R. Kiriyama and H. Kiriyama, *Kozo-Muki-Kagaku* (*Structural Inorganic Chemistry*), Kyoritsu-Shuppan, Tokyo, 1985, p. 237.

Journal of Chromatography, 523 (1990) 293–299
Elsevier Science Publishers B.V., Amsterdam

CHROM. 22 737

Note

Chromatographic behaviour of cyclodextrin complexes of nucleotides, nucleosides and their bases

MANABU SENO*, MEILING LIN and KAZUTOSHI IWAMOTO
Institute of Industrial Science, University of Tokyo, 7–22–1, Roppongi, Minato-ku, Tokyo 106 (Japan)
(First received April 3rd, 1990; revised manuscript received August 2nd, 1990)

The α-, β- and γ-cyclodextrins (CDs) are cyclic oligosaccharides containing six, seven and eight glucose units, respectively. The specific ability of CDs to form inclusion complexes with a variety of molecules and ions has been utilized in high-performance liquid chromatography (HPLC) for the separation of optical, geometrical and structural isomers [1–3]. In recent years, preparations of CD-bonded stationary phases [1–8] and applications of mobile phases containing CDs in reversed-phase liquid chromatography (RP-LC) [9–11] have been widely studied. Cline Love and Arunyanart [12] dealt with the latter method to determine the stability constants (K) of the inclusion complexes of benzene, phenol, *o*, *m*- and *p*-nitrophenol, naphthalene and biphenyl with β-CD according to a three-phase model of micellar chromatography [13,14]. Moreover, the separations of structural isomers of hydroxy-, methoxy- and amino-substituted benzoic acids using a mobile phase containing β-CD or a β-CD-immobilized stationary phase were reported by Bazánt *et al.* [15].

We have recently used α-, β- and γ-CDs as mobile phase components and studied the separation of NADH and NADP using a reversed-phase chromatographic system. The capacity factors (k'_2) of inclusion complexes of NADH and NADP with CDs, and their stability constants were determined based on a model consisting of three reversible processes [16].

This paper reports the results of further studies on the determination of the capacity factors of inclusion complexes of nucleotides (AMP, ADP and ATP), nucleosides (adenosine, uridine and thymidine) and bases (adenine, uracil and thymine) with CDs, and their stability constants by chromatography [16–20]. This method is useful for the analysis, separation and purification of these nucleotides, nucleosides and bases.

EXPERIMENTAL

Reagents

AMP (adenosine 5′-monophosphate), ADP (adenosine 5′-diphosphate) and ATP (adenosine 5′-triphosphate) were obtained from Sigma, adenosine, uridine,

0021-9673/90/$03.50

adenine, uracil and thymine from Wako and thymidine and α-, β- and γ-CDs from Tokyo Kasei. All materials were used without further purification.

Apparatus and procedures

A Bionert LC system (Japan Spectroscopic) equipped with a Model 875-UV Intelligent UV–VIS detector operating at 254 nm, an SIC Chromatocorder 12 and a Model 880-PU Intelligent pump were employed. A Hitachi Gel 3056 ODS reversed-phase column (150 × 4 mm I.D.; 5 μm particle diameter) was used.

The CD mobile phase was prepared by dissolving an appropriate weight of CD in 0.05 *M* Na_2HPO_4–NaH_2PO_4 buffer (pH 6) and filtering through a poly(vinylidene fluoride) membrane filter (Millipore, pore size 0.65 μm). All the chromatographic experiments were carried out at a constant flow-rate of 1.0 ml/min and at room temperature. A 3-μl sample solution containing 50 μg/ml of solute was injected into the column. The void volume of the column with a mobile phase containing different concentrations of CD was determined by using analytical-reagent grade potassium nitrate [17].

RESULTS AND DISCUSSION

An example of separations of nucleotides (ADP and ATP), nucleosides (uridine and thymidine) and bases (uracil and thymine) using 0.05 *M* phosphate buffer (pH 6) solution with or without β-CD is shown in Fig. 1. By adding β-CD to the mobile phase the retention times of these solutes were considerably reduced, and the peaks of ADP

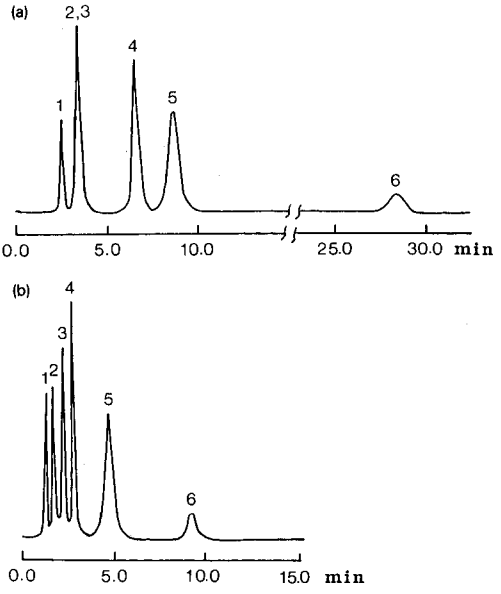

Fig. 1. Separation of nucleotides, nucleosides and bases by using a mobile phase of 0.05 *M* phosphate buffer (pH 6), (a) with and (b) without CD. Column, Hitachi Gel 3056 ODS-C_{18}; flow-rate, 1.0 ml/min. Peaks: 1 = ATP; 2 = ADP; 3 = uracil; 4 = uridine; 5 = thymine; 6 = thymidine.

and uracil were separated from one another. Similar behaviour was observed on addition of α- and γ-CD to the phosphate buffer mobile phase.

The stability constant and capacity factor of a CD inclusion complex can be calculated by using eqn. 1, which was derived earlier [16] on the basis of a three reversible reaction model consisting a reversible complex formation process between the guest molecule and CD in the mobile phase, and two reversible adsorption processes between the guest molecule and the inclusion complex on the stationary phase of an ODS column:

$$k' = \frac{k'_1 + k'_2 K[\mathrm{CD}]}{1 + K[\mathrm{CD}]} \tag{1}$$

where k' is the experimentally determined capacity factor, K is the stability constant of the inclusion complex and k'_1 and k'_2 are the capacity factors of the free guest molecule and its inclusion complex, respectively. If k'_2 is small enough to be ignored, the value of K is obtained from straight lines obtained by plotting $1/k'$ *vs.* [CD]. If k'_2 cannot be neglected, eqn. 1 is rearranged to

$$\frac{k'_1 - k'_2}{k' - k'_2} = 1 + K[\mathrm{CD}] \tag{2}$$

and by assigning an appropriate value of k'_2 to obtain a straight line of $(k'_1 - k'_2)/(k' - k'_2)$ *vs.* [CD], the value of K is determined from the slope of the line.

The retention volumes of nucleotides (AMP, ADP and ATP), nucleosides (adenosine, uridine and thymidine) and their bases (adenine, uracil and thymine) were measured at different concentrations of α-, β- and γ-CD in 0.05 *M* phosphate buffer (pH 6). The relationships between the capacity factors of nucleotides, nucleosides and bases and the concentration of α-, β- or γ-CD in the mobile phase are shown in Figs. 2, 3 and 4, respectively. Similar relationships were observed previously for NADH and NADP [16]. With an increasing concentration of α-, β- or γ-CD, the k' values of nucleotides, nucleosides and their bases are reduced, suggesting that α-, β- and γ-CDs

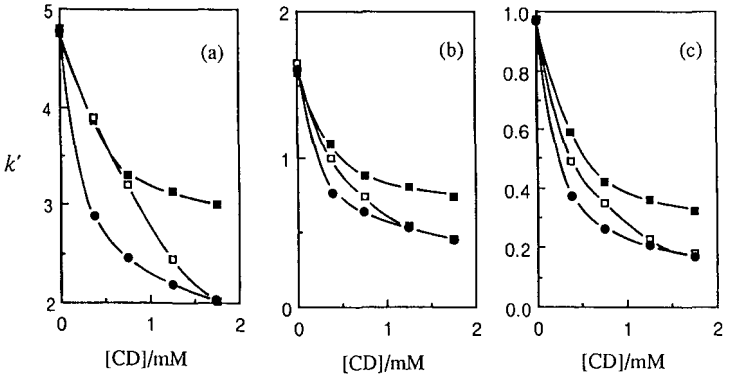

Fig. 2. Relationships between the capacity factors, k', of (a) AMP, (b) ADP and (c) ATP and the concentrations of (□) α-CD, (●) β-CD and (■) γ-CD. Conditions as in Fig. 1.

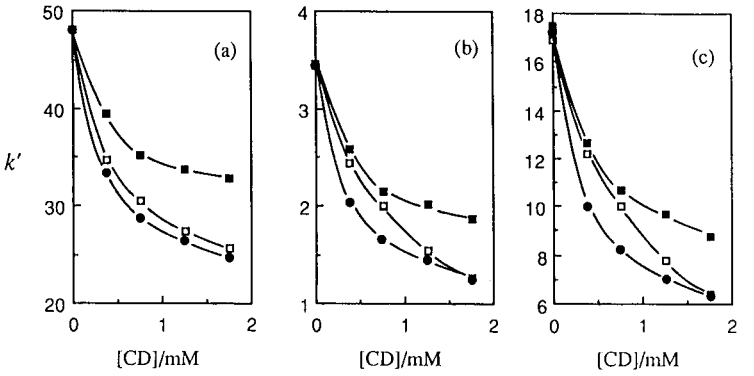

Fig. 3. Relationships between the capacity factors, k', of (a) adenosine, (b) uridine and (c) thymidine and the concentrations of (□) α-CD, (●) β-CD and (■) γ-CD. Conditions as in Fig. 1.

form inclusion complexes with these compounds. Addition of β-CD reduces the k' values more than additions of α- and γ-CDs, and the effects decrease in the order β-CD > α-CD > γ-CD.

Plots of $1/k'$ *vs.* [α-CD] for AMP, ADP, ATP, uridine, thymidine, uracil and thymine give good linear relationships. In these instances the values of k'_2 are adequately small. The stability constants of these compounds with α-CD were calculated from these compounds with α-CD were calculated from these plots and the results are given in Table I. The partition coefficients k_1 and k_2 were determined from the capacity factors k'_1 and k'_2, respectively [16], and these values are also given in Table I. The order of the partition coefficients k_1 is adenine > adenosine ≫ AMP > ADP > ATP in the purine series and thymidine > thymine > uridine > uracil in the pyrimidine series. On the other hand, the order is adenosine > thymidine > uridine in the nucleoside series and adenine > thymine > uracil in the base series.

ATP was eluted more rapidly than ADP and both were eluted faster than AMP. This is because of the larger number of phosphate groups in the compounds, which

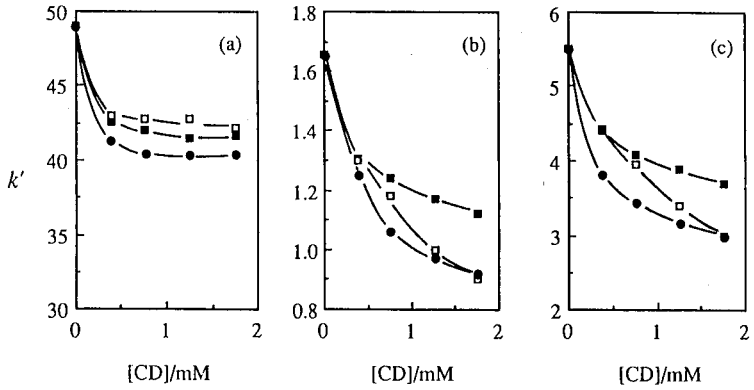

Fig. 4. Relationships between the capacity factors, k', of (a) adenine, (b) uracil and (c) thymine and the concentrations of (□) α-CD, (●) β-CD and (■) γ-CD. Conditions as in Fig. 1.

TABLE I

PARTITION COEFFICIENTS, k_1 AND k_2, AND STABILITY CONSTANTS, K (l mmol^{-1}) OF NUCLEOTIDES, NUCLEOSIDES AND BASES WITH α-, β- AND γ-CD

Compound	α-CD			β-CD			γ-CD		
	k_1	k_2	K	k_1	k_2	K	k_1	k_2	K
Nucleotides									
AMP	8.51	0.0	0.93	8.51	2.96	3.13	8.51	4.66	2.27
ADP	3.00	0.0	1.54	3.00	0.53	3.76	3.00	1.00	2.52
ATP	1.77	0.0	2.51	1.77	0.11	4.52	1.77	0.35	2.80
Nucleosides									
Adenosine	87.70	34.72	1.67	87.70	37.00	2.94	87.70	53.35	2.49
Uridine	6.32	0.0	0.97	6.32	1.75	3.57	6.32	2.70	2.29
Thymidine	31.28	0.0	0.93	31.28	8.13	3.08	31.28	10.96	1.74
Bases									
Adenine	89.62	—[a]	—[a]	89.62	—[a]	—[a]	89.62	—[a]	—[a]
Uracil	3.03	0.0	0.44	3.03	1.39	2.68	3.03	1.86	2.67
Thymine	10.05	0.0	0.45	10.05	4.75	3.50	10.05	5.85	1.98

[a] The peak of adenine was so broad and diffuse that k' was difficult to determine.

influences their hydrophilicity and solubility. The retention order of AMP, ADP, and ATP is analogous to that obtained on a μBondapak C_{18} reversed-phase column by using 0.05 *M* ammonium dihydrogenphosphate buffer as the mobile phase at pH 6.0 and a flow-rate of 2 ml/min [21]. In the pyrimidine series, the nucleosides were retained more strongly than their bases on the ODS columns; even so, the nucleosides have a higher hydrophilicity than their bases owing to the hydroxyl group on the ribose ring [21–23]. In reversed-phase chromatography, the elution characteristics are usually dependent on the hydrophobic interaction between the hydrophobic surface of the stationary phase and the substrate molecules in the aqueous phase and, therefore, the retention order observed for the nucleosides and the bases can be explained by this theory [24–26]. Adenosine and adenine have substantial hydrophobic interactions between their purine ring and the stationary phase of column compared with the pyrimidine ring series, as the purine ring is more hydrophobic than the pyrimidine ring. In the same manner, thymidine and thymine are more hydrophobic and retained more strongly than uridine and uracil because of the methyl group on their ring.

With adenosine, the plot of $1/k'$ *vs.* [CD] was not linear, indicating that k'_2 is not negligibly small. The k'_2 values of the inclusion complexes of the nucleotides, the nucleosides and their bases with β- and γ-CD also cannot be neglected. The values of k'_2 were therefore assigned to give a linear relationship between $(k'_1 - k'_2)/(k' - k'_2)$ and the concentration of [CD] in the mobile phase according to eqn. 2. The stability constants of all the nucleotides, nucleosides and bases with β- and γ-CDs together with that of adenosine with α-CD were determined from the slopes of these plots and the results are also given in Table I. The elution peak of adenine was very broad and diffuse, probably because it is slightly soluble in aqueous solution. Hence it was difficult to determine its stability constant.

The stability constants of these nucleotides, nucleosides and bases with β-CD are larger than those with α- and γ-CDs. This indicates that these nucleotides, nucleosides

and bases are liable to form more stable inclusion complexes with β-CD. The relative stabilities of CD inclusion complexes are governed by factors such as hydrogen bonding, hydrophobic interactions and solvation effects and also the space-filling ability of the guest molecules [27–31]. It was confirmed that a better fit of the substrate molecule in the cavity results in stronger complex formation [32]. The cavity sizes of α-, β- and γ-CDs are reported to be 0.45–0.57, 0.70–0.78 and 0.85–0.95 nm [33–35], respectively, and the sizes of adenine, thymine and uracil are estimated to be about 0.70, 0.66 and 0.58 nm, respectively, from the CPK model. The experimental results and the calculated data confirm that these nucleotides, nucleosides and bases form inclusion complexes with β- and γ-CDs by incorporating their purine or pyrimidine ring into the cavity of the respective CD. On the other hand, the inner diameter of the cavity of α-CD is to small to incorporate the purine and pyrimidine rings completely. Probably these rings are partly incorporated into the cavity of α-CD. This explains the small K values of inclusion complexes with α-CD shown in Table I.

The adsorption of the inclusion complexes of these nucleotides, nucleosides and bases on the ODS stationary phase is weak compared to that of the corresponding free solutes, that is, $k_1 > k_2$. The partition coefficients k_2 of γ-CD complexes are larger than those of β-CD complexes, and those of α-CD complexes are nearly zero except for adenosine. Adenosine is more hydrophobic than the other nucleosides, as suggested by its large value of k_1 [26], so that it is assumed that its α-CD inclusion complex is strongly adsorbed on the column and the k_2 value of adenosine is far from zero. The value of k_2 is clearly dependent on the molecular weight or the cavity size of CD and an increase in the molecular weight enhances the affinity of CD complexes to the ODS column.

REFERENCES

1 D. W. Armstrong and W. Demond, *J. Chromatogr.*, 22 (1984) 411.
2 D. W. Armstrong, A. Alak, K. Bui, W. Demond and T. Ward, *J. Inclus. Phenom.*, 2 (1984) 533.
3 D. W. Armstrong, T. J. Ward, R. D. Armstrong and T. E. Beesley, *Science (Washington, D.C.)*, 232 (1986) 1132.
4 D. W. Armstrong, W. DeMond, A. Alak, W. L. Hinze, T. E. Riehl and K. H. Bui, *Anal. Chem.*, 57 (1985) 234.
5 D. W. Armstrong, X. Yang, S. M. Han and R. A. Maenges, *Anal. Chem.*, 59 (1987) 2594.
6 H. J. Issaq, *J. Liq. Chromatogr.*, 11 (1988) 2131.
7 K. Fujimura, T. Ueda and T. Ando, *Anal. Chem.*, 55 (1983) 446.
8 S. El, Gezawi, N. Omar, N. El. Rabbat and J. H. Perrin, *J. Pharm. Biomed. Anal.*, 6 (1988) 393.
9 M. Gadag, G. Szepesi and L. Huszar, *J. Chromatogr.*, 436 (1988) 31.
10 C. A. Chang, Q. Wu and L. Tan, *J. Chromatogr.*, 316 (1986) 199.
11 K. Shimada, T. Masue, K. Toyoda, M. Takani and T. Nambara, *J. Liq. Chromatogr.*, 11 (1988) 1475.
12 L. J. Cline Love and M. Arunyanart, (*ACS Symposium Series*, No. 297), American Chemical Society, Washington, DC, 1986, p. 226.
13 D. W. Armstrong and F. Nome, *Anal. Chem.*, 53 (1981) 1662.
14 D. W. Armstrong and G. Y. Stine, *J. Am. Chem. Soc.*, 105 (1983) 2962.
15 L. Bazánt, M. Wurst and E. Smolková-Keulemansová, *J. Chromatogr.*, 445 (1988) 337.
16 M. Seno, M. L. Lin and K. Iwamoto, *J. Chromatogr.*, 508 (1990) 127.
17 J. Zukowski, D. Sybilska and J. Jurczak, *Anal. Chem.*, 57 (1985) 2215.
18 J. Debowski and D. Sybilska, *J. Chromatogr.*, 353 (1986) 409.
19 A. Manop and L. J. Cline Love, *Anal. Chem.*, 56 (1984) 1557.
20 K. Uekama, F. Hirayama, S. Nasu, N. Matsuo and T. Irie, *Chem. Pharm. Bull.*, 26 (1978) 3477.
21 F. S. Anderson and R. C. Murphy, *J. Chromatogr.*, 121 (1976) 251.
22 P. R. Brown and E. Grushka, *Anal. Chem.*, 52 (1980) 1210.

23 P. J. M. Van Haastert, *J. Chromatogr.*, 210 (1981) 229.
24 Cs. Horváth, W. R. Melander and I. Molnár, *J. Chromatogr.*, 125 (1976) 129.
25 Cs. Horváth, W. R. Melander and I. Molnár, *Anal. Chem.*, 49 (1977) 142.
26 W. Hiroo, *J. Chromatogr.*, 322 (1985) 255.
27 F. Cramer, *Rev. Pure Appl. Chem.*, 5 (1955) 143.
28 C. Van Hooidonk and J. C. A. E. Breebaart-Hansen, *Recl. Trav. Chim. Pays-Bas*, 90 (1971) 680.
29 F. Cramer and W. Dietsche, *Chem. Ber.*, 92 (1959) 1739.
30 J. Debowski, J. Jurczak and D. Sybilska, *J. Chromatogr.*, 282 (1983) 83.
31 D. W. Armstrong, *J. Liq. Chromatogr.*, 7 (1984) 353.
32 F. Cramer and F. M. Henglein, *Chem. Ber.*, 90 (1957) 2561.
33 W. J. James, D. French and R. E. Rundle, *Acta Crystallogr.*, 12 (1958) 385.
34 J. Szejtli, *Cyclodextrins and Their Inclusion Complexes*, Akadémiai Kiadó, Budapest, 1982, p. 25.
35 J. A. Thoma and L. Stewart, in R. L. Whistler and E. F. Paschall (Editors), *Starch, Chemistry and Technology*, Academic Press, New York, 1965, pp. 209–249.

Journal of Chromatography, 523 (1990) 300–304
Elsevier Science Publishers B.V., Amsterdam

CHROM. 22 821

Note

Chromatographic separation of β-substituted 3-(3,4-dihydroxyphenyl)alanine derivatives

PATRICK CAMILLERI*, CATHERINE A. DYKE, CHRISTINE ECKERS and ANTHONY N. SHAW

SmithKline Beecham Pharmaceuticals, The Frythe, Welwyn, Herts AL6 9AR (U.K.)

(First received May 15th, 1990; revised manuscript received September 13th, 1990)

Hydroxyphenylalanine compounds such as *ortho-*, *meta-* and *para*-tyrosine, dihydroxyphenylalanine and iodotyrosine derivatives have been analysed either by ion-exchange [1] or high-performance liquid chromatography (HPLC) [2–4]. As these molecules show significant absorption at wavelengths between 240-280 nm, they can be detected at low concentrations by spectrometric detection without the need for derivatisation [5–7].

In the present study we report the reversed-phase HPLC analysis of a number of closely related β-substituted dihydroxyphenylalanine derivatives. This chromatographic method was investigated as a possible final purification step in the isolation of (2*S*,3*S*)-2-amino-3-(3,4-dihydroxy phenylalanine)-4-pentynoic acid (**2**) which was prepared from the corresponding methyl ester (**1**). The dihydroxy phenylalanine derivative (**2**) was required as part of a program aimed at the design of mechanism based inhibitors of dopamine β-hydroxylase [8].

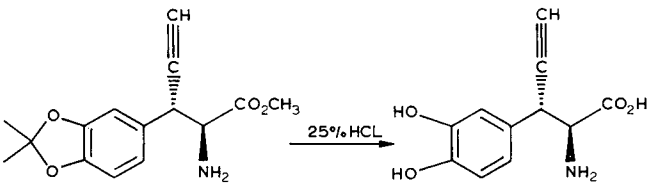

(1) (2)

EXPERIMENTAL

Chemicals

Compound **1** was synthesised by the Medicinal Chemistry Section of SmithKline Beecham (Welwyn, U.K.). All reagents used in the synthesis of **2** from **1** were purchased from Aldrich (U.K.) and were used without further purification.

0021-9673/90/$03.50

Water used in HPLC analysis was double-distilled deionised quality. Methanol, acetic acid, formic acid and phosphoric acid were AnalaR grade purchased from BDH (U.K.). Trifluoroacetic acid was obtained from Aldrich.

Acid hydrolysis of 1

A solution of **1** (461 mg, 1.67 mmol) and L-ascorbic acid (5 mg, 0.11 mmol) in 5 ml of 6.9 *M* aqueous hydrochloric acid was heated under argon at 80–90°C for 3 h, then at 115°C for 1.5 h. After cooling the solution was loaded on to an ion-exchange column (600 × 30 mm) packed with a strongly acidic cation-exchange resin [Bio-Rad 50W-X2 (H)] and **1** was eluted with 1 *M* aqueous pyridine. All fractions containing materials active to ninhydrin after spot testing on a thin-layer chromatography plate (LiChrosorb RP-8; BDH) were combined and solvent was removed under reduced pressure. The ion-exchange process was repeated two more times. After removing the eluting solvent, the residue was dissolved in water and the solvent removed under vacuum. This process was repeated another time and finally the residue was dissolved in water and freeze dried to leave a cream-coloured solid (265 mg) which was analysed by HPLC.

HPLC

Chromatographic analysis was performed on a Perkin-Elmer Series 4 liquid chromatograph equipped with a Perkin-Elmer ISS-100 autoinjector. A Kratos Spectroflow 783 variable-wavelength absorbance detector was set at 280 nm.

Reversed-phase analysis was carried out on a μBondapak C_{18} column (30.0 × 3.9 mm I.D., 10 μm) supplied by Millipore (Sweden). Four mobile phases were used with this column. Each contained 2.5% methanol as one of the components. The remaining 97.5% consisted of one of the following four acids: acetic (0.0164 *M*, pH 3.01), formic (0.0217 *M*, pH 2.28), phosphoric (0.0102 *M*, pH 1.83) and trifluoroacetic (0.0088 *M*, pH 1.73). These molarities correspond to solutions of these acids in water in the ratio of 0.1 to 99.9 (v/v).

Mass spectral characterisation

MS data were obtained with a Finnigan TSQ46 mass spectrometer, mass range 125–650 a.m.u. The vapouriser temperature was set at 120°C. Ammonium acetate (0.1 *M*) was added before detection.

RESULTS AND DISCUSSION

The acid hydrolysis of the methyl ester **1** gave four major products, denoted by peaks A–D in Fig. 1, and a number of minor impurities. The chromatographic separation of the four major components was found to be best when either 0.1% trifluoroacetic acid or 0.1% phosphoric acid was used in the mobile phase. In contrast, 0.1% acetic acid or formic acid gave shorter retention times and a decrease in the resolution of peaks B and C. In all cases the addition of 2.5% methanol as the cosolvent in the mobile phase was necessary to give sharp peaks. 0.1% trifluoroacetic acid was chosen as the mobile phase in preference to phosphoric acid as this acid had no adverse effects on the mass spectral identification of components A–D.

The mass spectra obtained for compounds A–D are shown in Fig. 2. None of the

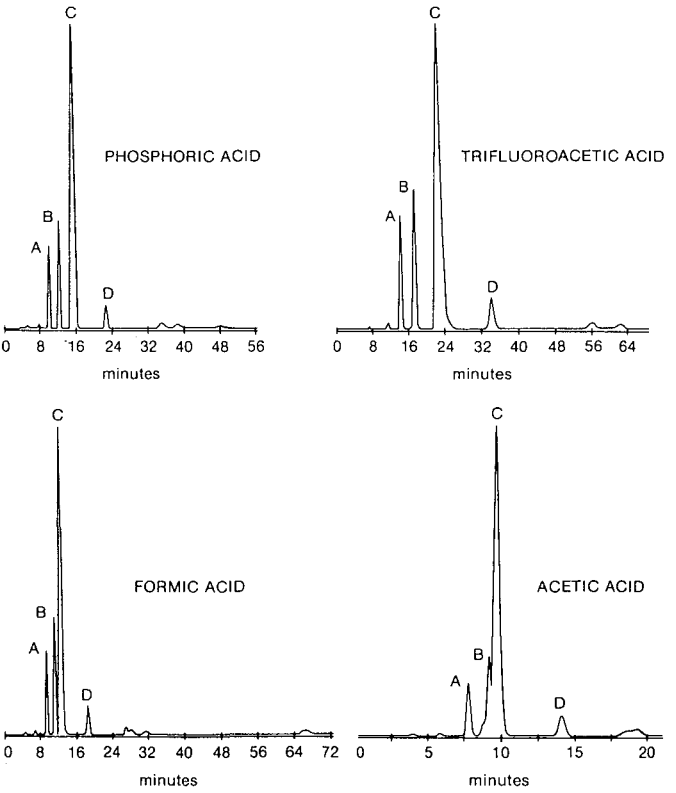

Fig. 1. HPLC analysis of the reaction mixture from the hydrolysis of **1** using 0.1% (a) phosphoric acid, (b) trifluoroacetic acid, (c) formic acid and (d) acetic acid in the mobile phase. For peaks A–D, see text.

molecules corresponds to starting material **1**. Peak D was identified as compound **5** which is a product from the partial hydrolysis of **1** (*m/z* 262 $(M+1)^+$, 234, 218). The dioxan ring in **5** is still intact. Peak C indeed corresponds to the desired amino acid **2** (*m/z* 222 $(M+1)^+$), whereas peaks A and B are due to isomeric compounds **3** and **4** (*m/z* 240 $(M+1)^+$, 223; 196) which arise from the addition of a water molecule across the acetylenic bond of either **1** or **2**.

The order of elution of compounds **2** to **5** is related to their hydrophobicity. Thus compound **5** which lacks the two hydroxyl groups on the aromatic moiety has the longest retention time. The ethynyl group in **2** makes this molecule more hydrophobic than **3** or **4** which have a keto or an aldehyde substituent in the β-position of the amino acid group. Peaks A and B were tentatively assigned to the structures **3** and **4** shown as **3** is expected [9] to be slightly more hydrophobic than **4**.

The pK_1 and pK_2 values of dihydroxyphenylalanine have been reported as 2.31 and 8.71, respectively [10]. The corresponding pK values of **2–5** are expected to be lower than those for dihydroxyphenylalanine due to the electron-withdrawing nature of the substituents in the β-position of the amino acid groups in these compounds. Under the acidic conditions used to separate these molecules the amino group is

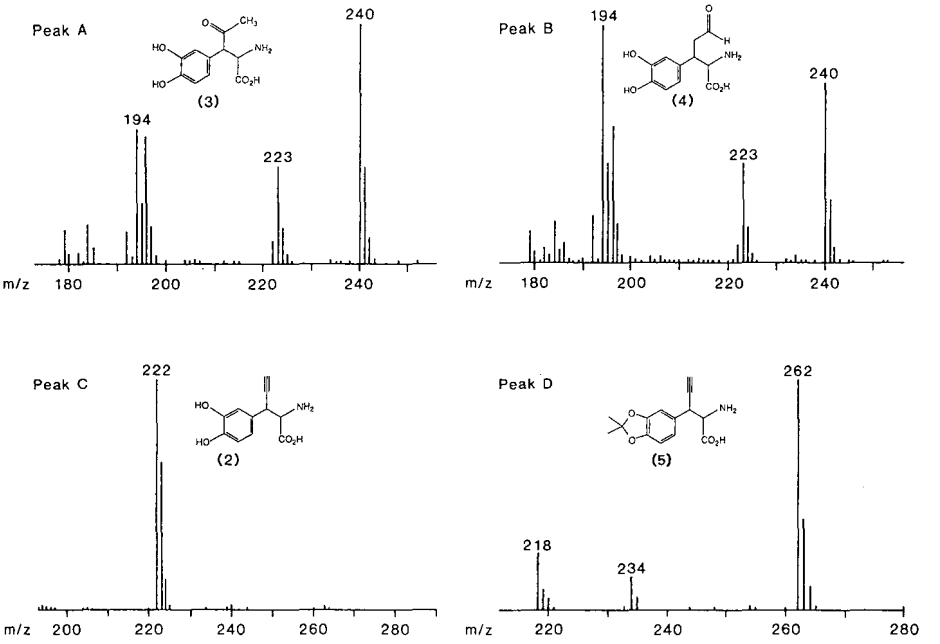

Fig. 2. Mass spectral characterisation of compounds corresponding to peaks A–D (see text). Stereochemistry has been omitted from the structures.

protonated in all cases. The pK_a value of the carboxyl group is around 2 so that its extent of ionisation to the carboxylate form will be low at pH values lower than 2. However, it is only in the case when either 0.1% trifluoroacetic acid (pK_a = 0.25) or 0.1% phosphoric acid (pK_a = 2.15) is used in the mobile phase that the pH of the eluent is lower than 2. As both acetic (pK_a = 4.76) and formic (pK_a = 3.75) are weaker acids than phosphoric or trifluoroacetic the pH of the mobile phase containing 0.1% of the former two acids is higher than the pK_a of the carboxylic group in compounds **2**–**5**, giving rise to longer retention times and poorer resolution.

In conclusion, 0.1% trifluoroacetic acid in the eluent has allowed facile separation of **2** from other components obtained in the hydrolysis of **1**. As the preparation of analytically pure **2** for biological testing proved to be difficult by other purification methods such as crystallisation or column chromatography, the HPLC method outlined was suitable for scaling up using a preparative column of the same stationary phase to prepare a chromatographically pure sample of **2** for biological testing.

REFERENCES

1 S. Ishimitsu, S. Fujimoto and A. Ohara, *Chem. Pharm. Bull.*, 28 (1980) 990.
2 M. T. W. Hearn and W. S. Hancock, *J. Liq. Chromatogr.*, 2 (1979) 217.
3 S. Ishimitsu, S. Fujimoto and A. Ohara, *Chem. Pharm. Bull.*, 30 (1982) 1889.
4 A. Hisaka, S. Kasamatsu, N. Takenaga and M. Ohtawa, *J. Chromatogr.*, 494 (1989) 183.
5 C. L. Zimmerman, *Anal. Biochem.*, 75 (1976) 77.
6 J. M. Wilkinson, *J. Chromatogr. Sci.*, 16 (1978) 547.

7 E. A. Bump and D. J. Reed, *Anal. Biochem.*, 78 (1977) 527.
8 L. I. Kruse, C. Kaiser, W. E. De Wolf, P. A. Chambers, P. J. Goodhart, M. Ezikial and E. H. Ohlstein, *J. Med. Chem.*, 31 (1988) 704.
9 C. Hansch and A. Leo, *Substituent Constants for Correlation Analysis in Chemistry and Biology*, Wiley, New York, 1979.
10 J. E. Gorton and R. F. Jameson, *J. Chem. Soc., A*, (1968) 2615.

Journal of Chromatography, 523 (1990) 305–311
Elsevier Science Publishers B.V., Amsterdam

CHROM. 22 829

Note

Determination of sterigmatocystin in fermentation broths by reversed-phase high-performance liquid chromatography using post-column fluorescence enhancement

FRANK L. NEELY* and CURT S. EMERSON
Lilly Research Laboratories, a Division of Eli Lilly and Company, Indianapolis, IN 46254 (U.S.A.)
(First received July 2nd, 1990; revised manuscript received September 18th, 1990)

Sterigmatocystin is a highly toxic [1] and carcinogenic [2] compound produced by certain species of *Aspergillus*, *Cheatomium*, *Bipolaris* and *Penicillium*. Sterigmatocystin is often found in foodstuffs [3–14] as a metabolite of the ubiquitous *A. versicolor* and has been observed as a contaminant in the fermentation process. Due to the toxicity of sterigmatocystin, the fermentation broth produced by these organisms may present handling and safety problems. As a result, a rugged method for the determination of sterigmatocystin in culture is a necessity. Thin-layer chromatography (TLC) has been widely utilized for the determination of sterigmatocystin [9,10,15–20], but is not easily automated for routine analysis. In addition, the fluorescence intensity of the aluminum chloride derivatized sterigmatocystin has bene observed to decay with time [17]. Reversed- and normal-phase high-performance liquid chromatography (HPLC) has also been utilized extensively [21–30], but the resolution of sterigmatocystin from matrix components is often difficult. This problem may be avoided with extensive sample cleanup or by converting the sterigmatocystin to a fluorescent derivative The commonly utilized acetyl derivative of sterigmatocystin may be prepared by the reaction of sterigmatocystin with acetic anhydride and pyridine. The utility of this approach, however, is limited by the relatively long reaction time, sensitivity of the reaction to water, and the gradual decomposition of the acetyl derivative [21]. In this paper, we report an HPLC method for the determination of sterigmatocystin in fermentation broths utilizing a post-column reaction to produce a fluorescent derivative. This method offers enhanced selectivity and sensitivity over UV detection and is easily automated for routine analysis.

EXPERIMENTAL

Chemicals

Sterigmatocystin was obtained from Sigma (St. Louis, MO, U.S.A.). Standards were prepared by dissolving the appropriate amount of material in HPLC-grade

0021-9673/90/$03.50

methanol. All solvents were of HPLC grade and were purchased from Fisher Scientific (Springfield, NJ, U.S.A.). All other chemicals were of reagent grade and were filtered prior to use.

Apparatus

A Perkin-Elmer Series 4 liquid chromatograph with a Perkin-Elmer LC-420 autosampler was used as the chromatographic system. A Brownlee Newguard RP-18 guard column (15 × 3.2 mm I.D., 7 μm) (Applied Biosystems, Foster City, CA, U.S.A.) was used prior to the Beckman Ultrasphere C_{18} analytical column (Beckman Instruments, Fullerton, CA, U.S.A.). The particle size of the 25 cm × 4.6 mm I.D. analytical column was 5 μm. The aluminum chloride solution was delivered to the mixing tee by a Beckman 1108 solvent delivery module. The reaction coil, consisting of 0.010-in. diameter stainless-steel tubing, was heated by an FH40 heater controlled by a FH50 controller module from FIAtron (Oconomowoc, WI, U.S.A.). The fluorescence of the eluate was monitored with a Waters Model 420 fluorescence detector. The excitation filter was 254 nm and the emission filter was 455 nm. Alternatively, the absorbance was monitored with a Kratos Model 773 absorbance detector.

Extraction of sterigmatocystin

The fermentation broth was filtered with a Whatman No. 1 filter. A 5-g portion of the damp filter cake was extracted with 10 ml of methanol and homogenized. The supernatant solution was then filtered with a 0.45 μm LID/X filter obtained from Genex (Gaithersburg, MD, U.S.A.). The filtered solution was then used for analysis. Alternatively, 10 ml of methanol was added to a 3 g portion of whole broth. The suspension was homogenized and filtered as above.

Chromatographic conditions

The mobile phase consisted of methanol–water (88:12). The flow-rate of the mobile phase was 0.5 ml/min. For samples with late-eluting peaks, a cleaning gradient consisting of methanol was employed for 3 min after the elution of sterigmatocystin. A 5% (w/w) solution of anhydrous aluminum chloride in methanol was delivered at a flow-rate of 0.5 ml/min to the mixing tee. Unless otherwise specified, the injection volume was 50 μl. Optimization experiments were performed in the flow injection mode.

Thin-layer chromatography

Whatman LK-5D silica TLC plates were washed with methanol and dried in an oven at 60°C prior to use. The samples were spotted with 5-μl Drummond microcaps and developed with carbon tetrachloride–chloroform–acetic acid (49.5:49.5:1, v/v/v). This solvent composition was found to provide improved resolution over the AOAC method [31]. Otherwise, the method was unchanged. The TLC plates were scanned after derivatization with aluminum chloride with a CAMAG TLC Scanner II with mercury source ad a 460 nm emission cutoff filter.

RESULTS AND DISCUSSION

Sterigmatocystin reacts with aluminum chloride in solution to give a fluorescent product, 1,3,8-trihydroxyxanthone [32]. The extent of this reaction was found to be

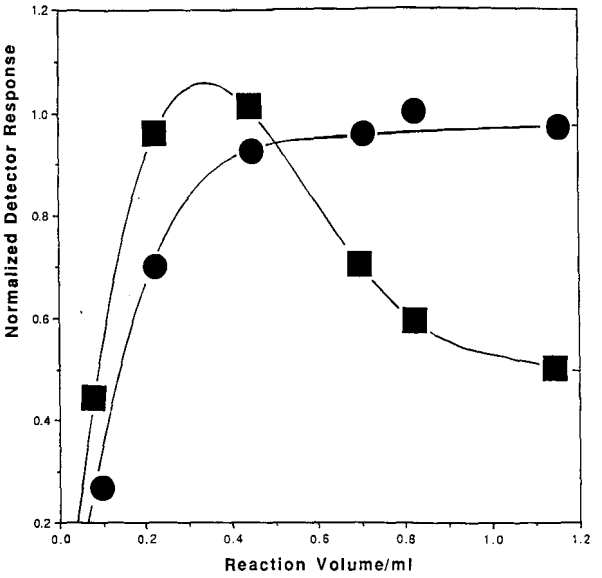

Fig. 1. Plot of normalized peak area (circles) and height (squares) as a function of post-column reactor volume in ml. The mobile phase and reagent solution flow-rates were held constant at 0.5 ml/min.

dependent on reaction time, temperature, $AlCl_3$ concentration and solvent composition. Fig. 1 shows a plot peak height and area as a function of reactor volume at 25°C. The area of the peak increased as the reactor volume was increased from 0.08 to 0.4 ml. With reactor volumes greater than 0.4 ml, no increase in peak area was observed. Over the domain 0.08 to 0.4 ml, the plot of peak height matched that of peak area. With greater reactor volumes, however, the peak height decreased, probably as a result of longitudinal diffusion in the post-column reactor.

The temperature of the reaction coil had a significant effect on the detector response. At 30 and 35°C, the fluorescence intensity was enhanced 20 and 31%, respectively, over the signal at 25°C. Further increase in temperature to 50°C did not result in any signal enhancement, suggesting that the reaction had reached completion.

Francis *et al.* [24] has observed that the fluorescence intensity of 1,3,8-trihydroxyxanthone on TLC plats decayed upon exposure to atmospheric water. Similarly, the intensity of the fluorescence signal in the flowstream was inversely proportional to the aqueous composition of the mobile phase. Table I lists the relative peak areas for sterigmatocystin as a function of the mobile phase composition obtained in the flow injection mode.

Fig. 2 shows a comparison of the fluorescence and absorbance chromatograms of a typical sample of fermentation extract. The fluorescence chromatogram displayed no interferences with the sterigmatocystin peak. In contrast, the absorbance chromatogram displayed poor resolution. Abramson and Thorsteinson [21] have also observed poor resolution of sterigmatocystin from barley extracts with a similar chromatographic system. The gradient pogram was designed to ensure the complete elution of matrix components but is not necessary for less complex samples.

TABLE I

EFFECT OF WATER ON SIGNAL INTENSITY

Mobile phase composition: methanol–water	Relative response
100:0	1.00
95:5	0.94
90:10	0.91
85:15	0.78
80:20	0.76
70:30	0.73
60:40	0.66
50:50	0.63

The retention time of the sterigmatocystin was highly reproducible. A series of 12 injections of a 0.82-ppm sample solution gave an average retention time of 9.78 min with a coefficient of variation (C.V.) of 0.2%. The C.V. of the area of the standards was 2.1%. The response of the detector was linear over the domain 0.1 to 15 ppm. At concentrations in excess of 30 ppm, the calibration plot bowed toward the concentration axis. A detection limit of 0.09 ppm was determined on the basis of signal-to-noise

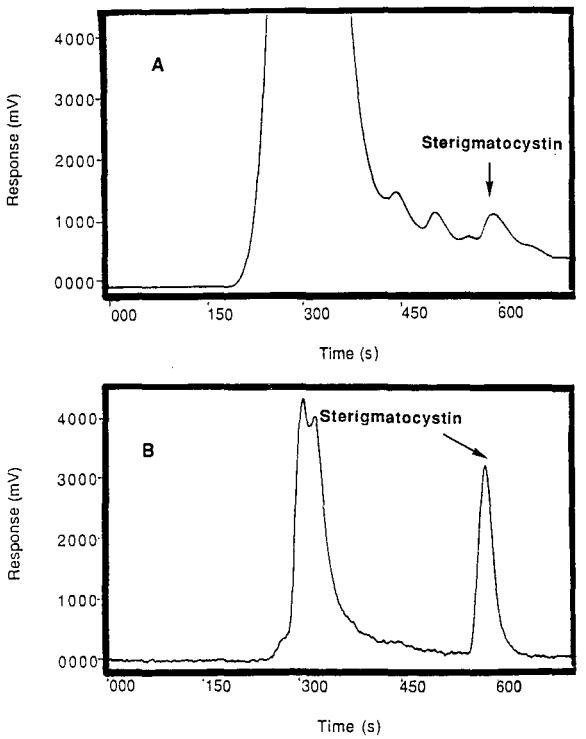

Fig. 2. Typical chromatograms of a fermentation extract containing 2 ppm sterigmatocystin. (A) Absorbance detection at 325 nm. (B) Post-column derivatization with fluorescence detection.

TABLE II

RECOVERY OF STERIGMATOCYSTIN FROM SPIKED BROTH SAMPLES

Initial (μg)[a]	Added (μg)	Recovery (%)
1.20	0.94	95
1.20	1.13	91
1.20	1.50	93
1.20	2.25	89
1.20	4.30	89
1.20	8.00	89

[a] Mass of sterigmatocystin initially present in a 1.5-ml aliquot of fermentation extract.

ratio. Table II lists the recovery of sterigmatocystin spiked into the sample solution. Over the domain of 0.94 to 8.00 μg spiked, the recovery ranged from 95 to 89%, indicating quantitative recovery. In addition, the quantitative recovery suggests that unresolved matrix components do not quench the fluorescence of the derivatized sterigmatocystin.

To further determine the specificity of the sterigmatocystin peak, several emission cutoff filters were substituted for the 455-nm filter normally employed. A standard and a "worst-case" sample, prepared by mixing broths obtained at the conclusion of several fermentations, were run with each filter. Table III lists the peak areas of the samples and standards as a fuction of cutoff wavelength. The ratio of the sample area to standard area was invariant with emission cutoff filter. Therefore, an interfering peak must possess the identical emission spectrum as well as retention time and reaction specificity to be mistaken for sterigmatocystin.

The HPLC method was validated by comparison to the AOAC standard TLC method [31]. About fifty samples of fermentation origin were analyzed by both methods. Fig. 3 depicts a scatter diagram of the HPLC data *versus* TLC data with a best-fit line. A near ideal slope of 1.01 was obtained by a simple regression. The intercept of the plot corresponded to 0.06 ppm, which is most likely an artifact of the densitometer. In all cases studied, the HPLC data agreed with the TLC data within experimental error of both methods.

TABLE III

PEAK AREA AS A FUNCTION OF EMISSION FILTER

Emission filter (nm)	Standard area ($\times 10^3$)	Sample area ($\times 10^3$)	Ratio
530	1320	662	0.50
495	2840	1330	0.47
455	3840	1870	0.49
525	4063	2039	0.50

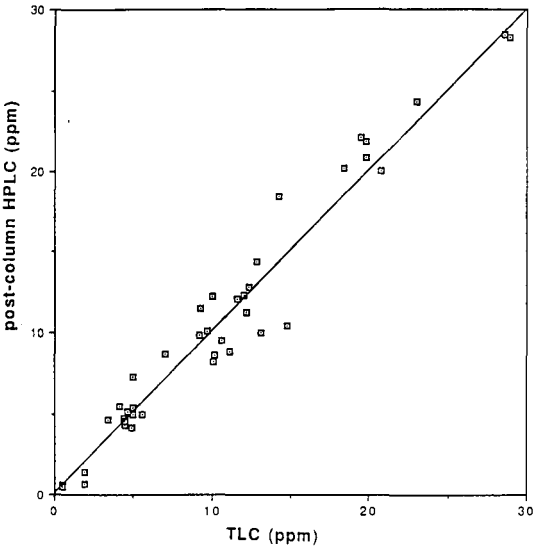

Fig. 3. Comparison of post-column HPLC method with AOAC TLC method. Data were obtained from samples of fermentation extract. Line: HPLC = 1.01 · TLC + 0.63; correlation coefficient = 0.96.

CONCLUSIONS

A rapid and reliable chromatographic system has been demonstrated for the analysis of sterigmatocystin. Comparison of the HPLC method with the AOAC planar chromatographic method gave an excellent correlation, suggesting that no interferences were present in the HPLC assay. The use of post-column derivatization eliminates uncertainty resulting from incomplete derivatization and decomposition of the derivative. Although the assay was developed for samples of sterigmatocystin in culture, the post-column derivatization scheme may be easily adapted for other applications. Indeed, the water dependence of the fluorescence intensity suggests that aluminum chloride derivatization is well suited for normal-phase chromatography. This phenomenon is not a problem for reversed-phase applications because the sterigmatocystin elutes long after the void volume of the column and reactor.

REFERENCES

1 I. F. H. Purchase and J. J. van der Watt, in I. F. H. Purchase (Editor), *Mycotoxins in Human Health*, Macmillan, New York, 1971.
2 I. F. H. Purchase and J. J. van der Watt, *Food Cosmet. Toxicol.*, 7 (1970) 289.
3 K. Ohtsubu, M. Saito and H. Kimura, *Food Cosmet. Toxicol.*, 16 (1978) 143.
4 P. T. Curry, R. N. Reed, R. M. Martino and R. M. Kitchin, *Mutation Res.*, 137 (1984) 111.
5 N. Ueda, K. Fugie, K. Gotoh-Mimura, S. S. Chattopadhyay and T. Sugiyama, *Mutation Res.*, 139 (1984) 302.
6 D. Abramson and T. Thorsteinson, *J. Assoc. Off. Anal. Chem.*, 72 (1989) 342.
7 D. Abramson, R. N. Sinha and J. T. Mills, *Cereal Chem.*, 60 (1983) 350.

8 P. M. Scott, W. van Walbeek, B. Kennedy and D. Anyeti, *J. Agric. Food Chem.*, 20 (1972) 1103.
9 A. Athnasios and G. O. Kuhn, *J. Assoc. Off. Anal. Chem.*, 60 (1977) 104.
10 G. M. Shannon and O. L. Shotwell, *J. Assoc. Off. Anal. Chem.*, 59 (1976) 963.
11 O. J. Francis, Jr., G. P. Kirshenheuter, G. M. Ware, A. S. Carman and S. S. Kuan, *J. Assoc. Off. Anal. Chem.*, 71 (1988) 725.
12 O. J. Francis, Jr., L. J. Lipinski, J. A. Gaul and A. D. Campbell, *J. Assoc. Off. Anal. Chem.*, 65 (1982) 672.
13 R. Schidt, J. Mondani, E. Ziegenhagen and K. Dose, *J. Chromatogr.*, 207 (1985) 435.
14 W. J. Hurst, K. P. Snyder and R. A. Martin, Jr., *J. Chromatogr.*, 392 (1987) 389.
15 V. Betina, *J. Chromatogr.*, 477 (1989) 187.
16 J. R. Spilmann, Jr., *J. Assoc. Off. Anal. Chem.*, 68 (1985) 452.
17 O. J. Francis, Jr., G. M. Ware, A. S. Carman and S. S. Kuan, *J. Assoc. Off. Anal. Chem.*, 68 (1985) 643.
18 P. Golinski and J. Grabarkkiewicz-Szczesna, *J. Assoc. Off. Anal. Chem.*, 67 (1984) 1108.
19 K. Y. Lee, C. F. Poole and A. Zlatkis, *Anal. Chem.*, 52 (1980) 879.
20 L. J. Vorster and I. F. H. Purchase, *Analyst (London)*, 93 (1968) 694.
21 D. Abramson and T. Thorsteinson, *J. Assoc. Off. Anal. Chem.*, 72 (1989) 342.
22 D. L. Orti, J. Grainger, D. L. Ashley and R. H. Hill, Jr., *J. Chromatogr.*, 462 (1989) 269.
23 S. P. McCormick, E. Bowers and D. Bhatnagar, *J. Chromatogr.*, 441 (1988) 400.
24 O. J. Francis, Jr., G. P. Kirschenheuter, G. M. Ware, A. S. Carman and S. S. Kuan, *J. Assoc. Off. Anal. Chem.*, 71 (1988) 725.
25 W. J. Hurst, K. P. Snyder and R. A. Martin, Jr., *J. Chromatogr.*, 392 (1987) 389.
26 P. Lepom, *J. Chromatogr.*, 354 (1986) 518.
27 O. J. Francis, Jr., L. L. Lipinski, J. A. Gaul and A. D. Campbell, *J. Assoc. Off. Anal. Chem.*, 65 (1982) 672.
28 R. Schmidt, J. Mondani, E. Zeigenhagen and K. Dose, *J. Chromatogr.*, 207 (1981) 435.
29 K. Ito, A. Yamanti, T. Hamasaki and Y. Hatsuda, *Agric. Biol. Chem.*, 40 (1976) 2099.
30 M. E. Stack, S. Nesheim, N. L. Brown and A. L. Pohland, *J. Assoc. Off. Anal. Chem.*, 59 (1976) 966.
31 W. Horwitz (Editor), *Official Methods of Analysis of the Association of Official Analytical Chemists*, Association of Official Analytical Chemists (AOAC), Washington, DC, 13th ed., 1980.
32 J. E. Davies, D. Kirkaldy and J. C. Roberts, *J. Chem. Soc.*, (1960) 2169.

Journal of Chromatography, 523 (1990) 312–316
Elsevier Science Publishers B.V., Amsterdam

CHROM. 22 702

Note

Isolation of a fibrinogen-converting enzyme ficozyme from the venom of *Bothrops asper* by one-step affinity chromatography on Blue Sepharose

H. FOŘTOVÁ, J. E. DYR* and J. SUTTNAR
Institute of Hematology and Blood Transfusion, U Nemocnice 1, CS-128 20 Prague 2 (Czechoslovakia)
(First received March 8th, 1990; revised manuscript received July 9th, 1990)

Based on the conversion of fibrinogen to fibrin, very specific enzymes with limited action, cleaving off only fibrinopeptides from fibrinogen, are widely used for the determination of the amount and functional properties of fibrinogen. Such enzymes should meet the following requirements: they must catalyse the splitting off of fibrinopeptides, they must not be inhibited by plasmatic inhibitors including heparin and they must have neither fibrinogenolytic nor prothrombin-converting activity. The main drawbacks to the use of thrombin (the physiological activator in the conversion off fibrinogen to fibrin) for the determination off fibrinogen are that it is inhibited by plasmatic inhibitors, including heparin, and also activates prothrombin [1]. Some snake venoms contain enzymes which specifically cleave of fibrinopeptides from fibrinogen [2]. For example, bathroxobin, isolated from the venom of *Bothrops atrox*, releases fibrinopeptides A only and is used in the kinetic method for the determination of fibrinogen [3].

Snake venoms represent a very complex mixture, including about 80 protein components [4] of various biological activities: procoagulant [2], fibrinogenolytic [2], prothrombin-converting [2,5] and many others [2,6]. To obtain an enzyme of desirable purity using common separation methods, multi-step procedures are usually necessary. This paper describes a one-step dye-ligand affinity chromatographic method for the isolation of a fibrinogen-converting enzyme (ficozyme) from the snake venom of *Bothrops asper*.

EXPERIMENTAL

Affinity chromatography was carried out on Blue Sepharose and gel filtration chromatography on Superose 12 HR 10/30 using the fast protein liquid chromatographic (FPLC) system (all from Pharmacia, Uppsala, Sweden).

The protein concentrations in the individual fractions were determined from the absorbances at 280 nm, assuming an absorbance of 10.0 for a solution of 10 mg/ml and a 1-cm light path.

0021-9673/90/$03.50

Fibrinogen-converting activity was tested as follows: 50 μl of tested fraction, 50 μl of buffer [50 m*M* Tris–HCl (pH 7.4)–0.1 *M* NaCl] and 100 μl of human fibrinogen (3 mg/ml) (Kabi, Sweden) were mixed in a test-tube and the clotting time was recorded as the time of visible clot formation.

Fibrinogenolytic activity was determined as the time necessary to dissolve the fibrin gel prepared in the same way as for the determination of the fibrinogen-converting activity.

Prothrombin-converting activity and the influence of plasmatic inhibitors were tested using a slight modification of the method for the kinetic determination of fibrinogen [3]. A 100-μl volume of the test fraction were placed in a 1-cm spectrophotometric cuvette and diluted with 2 ml of buffer [0.1 *M* Tris (pH 7.5)–polyethyleneglycol 6000 (2 g per 100 ml)–Brij 35 (1 g per 100 ml)–$CaCl_2$ (50 mg per 100 ml)] and 50 μl of human plasma were added. The absorbance at 340 nm was monitored and the increase in absorbance per minute was determined from the linear part of the curve. For the testing of prothrombin-converting activity either hirudin (1 U/ml, final concentration) or oxalate plasma free from coagulation factors [removed by adsorption on $BaSO_4$ (100 mg per 100 ml of plasma)] were added. For the testing of the influence of plasmatic inhibitors either 50–200 μl of serum or 50 μl of heparin (0.1–20 IU/ml, final concentration) were added.

The release of fibrinopeptides was determined using reversed-phase high-performance liquid chromatography (RP-HPLC) on a CGC C_{18} (10 μm) (150 × 3 mm I.D.) according to Suttnar *et al.* [7]. Sodium dodecyl sulphate polyacrylamide gel electrophoresis (SDS-PAGE) was performed on 5–15% gradient polyacrylamide gel essentially according to Laemmli and Favre [8].

The rates of hydrolysis of chromogenic substrates for thrombin (TS), kallikrein (PK) and plasmin (S2251) by the isolated fractions (100 μl) were measured spectrophotometrically under the following conditions: substrate concentration, 0.1 m*M*; ionic strength, 0.15 *M*; temperature, 25°C; total volume, 2.5 ml; Tris–imidazole buffer, pH 7.4 (S2251) and pH 8.4 (TS, PK).

Phenylmethanesulphonyl fluoride (PMSF) (Sigma, St. Louis, MO, U.S.A.) and hirudin (Sigma) were used as received.

RESULTS AND DISCUSSION

Dye-ligand affinity chromatography of the crude venom of *Bothrops asper* was performed on a column of Blue Sepharose (20 × 2.6 cm I.D.) equilibrated with buffer A [50 m*M* imidazole (pH 6.3)–0.1 *M* NaCl). A 500 -mg amount of lyophilized crude venom of *B. asper* was dissolved in 5 ml of buffer A; insoluble material was removed by centrifugation (15 000 *g* for 20 min) and the soluble portion was applied to the column. During isocratic elution the venom was separated into three peaks (Fig. 1). The fraction containing ficozyme (indicated by the hatched area) constituted about 2.0% of the venom proteins. It exhibited a specific activity of 300 batroxobin units [9] per mg (BU/mg). The separation resulted in an overall 55-fold purification at a 90% yield. Proteins that were more strongly adsorbed on Blue Sepharose were eluted at a higher ionic strength [buffer B: 50 m*M* imidazole (pH 6.3)–1 *M* NaCl].

The crude ficozyme split off only fibrinopeptides A from fibrinogen as indicated by RP-HPLC. Only the peak of fibrinopeptide A was detected by HPLC of the

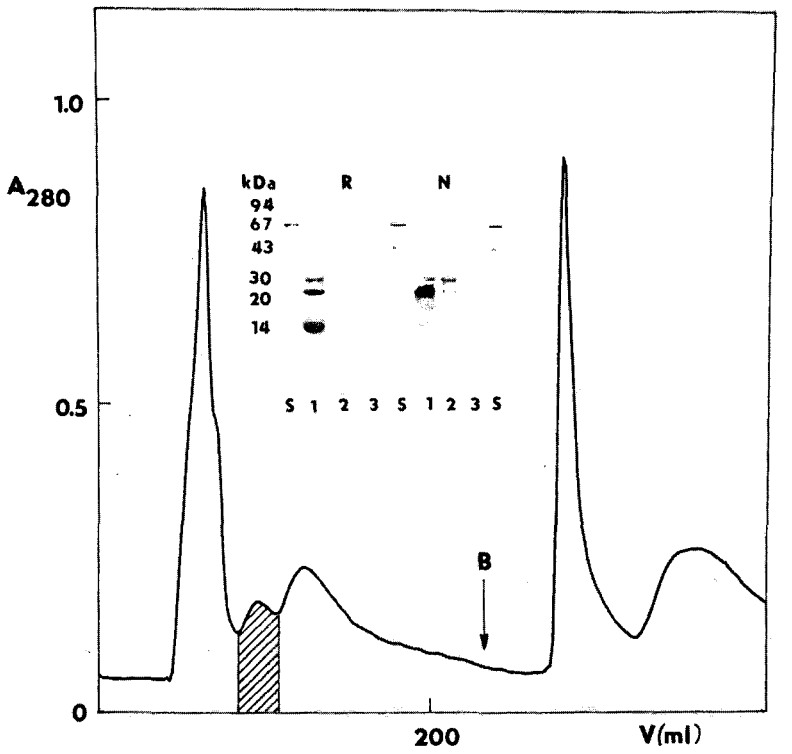

Fig. 1. Elution profile of crude *Bothrops asper* venom (500 mg in 5 ml) on Blue Sepharose. Column 20 × 2.6 cm I.D.; flow-rate, 1.5 ml/min; starting buffer, 50 m*M* imidazole (pH 6.3)–0.1 *M* NaCl; buffer B: 50 m*M* imidazole (pH 6.3)–1 *M* NaCl. The fraction containing ficozyme is hatched. The inset shows SDS gradient (5–15%) PAGE of the crude *B. asper* venom (1), the hatched crude fraction (2) and ficozyme further purified (3) by gel filtration on Superose 12. R = reduced, N = non-reduced samples; S = molecular mass markers. The gel was stained with Coomassie Brilliant Blue R-250.

supernatant of a sample taken after incubation of the ficozyme with fibrinogen for a time equal to ten times the clotting time. SDS-PAGE of the reduced precipitate of the sample showed more than 95% of intact α-, β- and γ-chains of fibrinogen, indicating a negligible fibrinogenolytic activity of ficozyme.

The fraction was not significantly inhibited with either plasmatic inhibitors or heparin. Its prothrombin-converting activity was also negligible and the presence of neither serum nor hirudin had any significant effect on the kinetic assay for fibrinogen determination.

However, gel filtration chromatography on Superose 12 performed in 50 m*M* Tris–HCl (pH 7.4)–0.1 *M* NaCl and SDS-PAGE revealed the size heterogeneity of the ficozyme fraction. The maximum degree of fibrinogen-converting activity (1800 BU/mg) was found in a fraction with a molecular mass of 34 kilodalton (calculated from the elution volume). SDS-PAGE showed that the fraction having the highest activity consisted of a major protein band of higher molecular mass (Fig. 1). The discrepancy between the results obtained with gel filtration and SDS-PAGE may indicate either

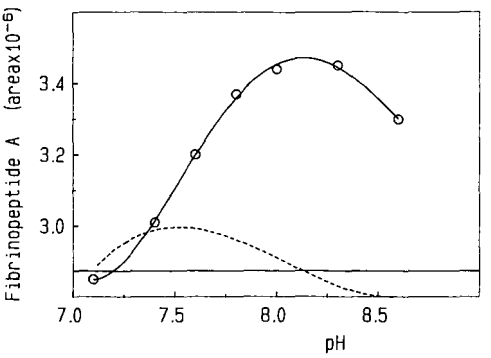

Fig. 2. pH dependence of the initial release of fibrinopeptide A (full line, expressed as the area of the peak of fibrinopeptide A) from fibrinogen at high fibrinogen concentration (20 μM). Reaction conditions: 50 mM Tris–HCl, ionic strength 0.15 M adjusted with NaCl; temperature, 30°C. A ficozyme concentration corresponding to 0.01 BU was used. The broken line is the first derivative of the pH dependence curve.

an unusual shape of the molecule or protein–Superose matrix interaction. The crude fraction had activities towards the low-molecular-mass chromogenic peptide substrates TS and PK of 0.57 and 0.39 μmol/s · mg, respectively, and the purified ficozyme 6.75 and 4.83 μmol/s · mg, respectively. Both fractions were free from S-2251 activity.

The fibrinopeptide-releasing activity of purified ficozyme was inhibited by the serine protease inhibitor PMSF. Incubation of ficozyme with PMSF (at a final concentration of 0.26 mg/ml, *i.e.*, 1.5 mM) for 30 min caused a decrease in its activity to 60% of the original level and at a final concentration of 0.52 mg/ml, *i.e.*, 3 mM, to 40%. Repeated addition of PMSF (with an increase in its concentration of 1 mM each time) at 30-min intervals for 3 h resulted in the complete inhibition of the activity of ficozyme. Ficozyme was not inhibited by antithrombin III (0.05–0.25 μM), antithrombin III (0.25 μM) simultaneously with heparin (5 IU/ml), iodacetamide (1–5 mM), 5.5′-dithiobis(2-nitrobenzoic acid) (0.25–5 mM), EDTA (2.5–12.5 mM) or *o*-phenantroline (5–10 mM). The results show that ficozyme was not inhibited by thiol protease and metalloprotease inhibitors, suggesting that it was a serine protease.

The effect of changing pH on the fibrinopeptide A-releasing activity of ficozyme is shown in Fig. 2. The optimum pH under the present consitions was found to be 8.1.

The results show that by using very simple one-step affinity chromatography on Blue Sepharose it is possible to isolate a fibrinogen-converting enzyme that has suitable characteristics for the determination of the concentration and functional properties of plasma fibrinogen.

ACKNOWLEDGEMENT

The authors are indebted to Prof. F. Kornalík for the provision of crude venom of *B. asper* and for helpful discussions.

REFERENCES

1 J. W. Fenton, II, *Ann. N.Y. Acad. Sci.*, 485 (1986) 5.
2 F. Kornalík, *Pharmacol. Ther.*, 29 (1985) 353.
3 U. Becker, K. Bartl and A. W. Wahlefeld, *Thromb. Res.*, 35 (1984) 475.
4 J. E. Dyr, J. Suttnar and F. Kornalík, *Folia Haematol.*, 115 (1988) 203.
5 J. E. Dyr, B. Blombäck, B. Hessel and F. Kornalík, *Biochim. Biophys. Acta*, 990 (1989) 18.
6 J. E. Dyr, B. Hessel, J. Suttnar, F. Kornalík and B. Blombäck, *Toxicon*, 27 (1989) 359.
7 J. Suttnar, J. E. Dyr, H. Fořtová and J. Pristach, *Biochem. Clin. Bohemoslov.*, 18 (1989) 17.
8 U. K. Laemmli and M. Favre, *J. Mol. Biol.*, 80 (1973) 575.
9 K. Stocker and G. H. Barlow, *Methods Enzymol.*, 45 (1976) 214.

Journal of Chromatography, 523 (1990) 317–320
Elsevier Science Publishers B.V., Amsterdam

CHROM. 22 790

Note

High-performance liquid chromatographic enantioseparation of intermediates relating to the total synthesis of (−)-physostigmine

THOMAS B. K. LEE and GEORGE S. K. WONG*
Chemical Research Department, Hoechst-Roussel Pharmaceuticals Inc., Somerville, NJ 08876 (U.S.A.)
(Received July 31st, 1990)

(−)-Physostigmine (**1**) is a clinically useful anticholinesterase agent which has been used in the treatment of myasthenia gravis and glaucoma. More recently, selected (−)-physostigmine analogues have also shown promise as Alzheimer's disease therapeutic agents. Our interests in new (−)-physostigmine analogues have led us to develop a stereoselective synthesis of (−)-physostigmine [1] (Fig. 1). To facilitate our synthetic effort and to ensure a high optical purity of the synthetic material, we required analytical high-performance liquid chromatographic (HPLC) enantioseparation of the intermediates as shown in the scheme. We report herein the application of derivatized cellulose-based chiral stationary phase (CSP) to the separation of these intermediates.

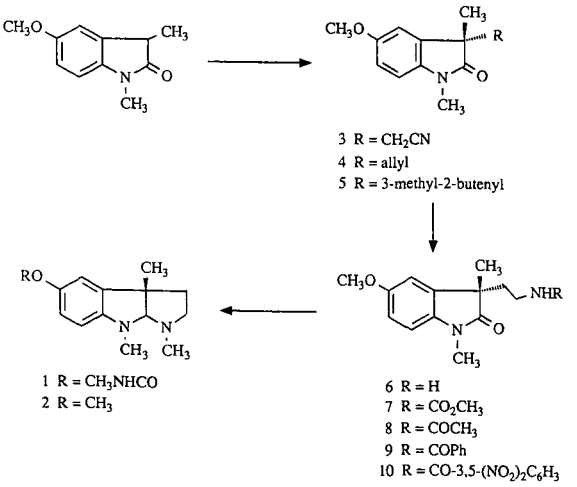

Fig. 1. Stereoselective synthesis of (−)-physostigmine. Ph = Phenyl.

0021-9673/90/$03.50

EXPERIMENTAL

Apparatus

The chromatography was performed with a M-6000A pump (Waters Assoc., Milford, MA, U.S.A.), a SF 769 variable-wavelength detector (Kratos, Ramsey, NJ, U.S.A.), and a 3390 integrator (Hewlett-Packard, Palo Alto, CA, U.S.A.).

The prepacked columns used were Daicel Chiracel OD and OJ columns (25 cm × 4.6 mm I.D.) and were purchased from Daicel Chemical Industries.

Materials

Racemic forms of compounds **1–10** were prepared according to literature procedures [1,2]. HPLC-grade hexanes and 2-propanol were purchased from Fisher Scientific (Pittsburgh, PA, U.S.A.).

RESULTS AND DISCUSSIONS

The results and the conditions for the chromatographic separation of the intermediates on Chiralcel OD/OJ columns are presented in Tables I–III. Complete resolution can be observed for (±)-oxindoles **3–5** and (±)-esermethole (**2**). Attempts to separate (±)-amine **6** directly on a Crownpak CR(+) column (Daicel) have not been completely successful. Since (±)-amine **6** cannot be assayed directly on these Chiralcel columns, it is therefore derivatised as carbamate **7**, or as amides **8–10** before being analysed. Of these, only the carbamate **7** and the dinitro substituted benzoyl amide **10** can be resolved. It is also interesting to note that the resolution of (±)-physostigmine (**1**) and amide **10** is improved when isopropanol is replaced by ethanol as the solvent modifier.

The mechanism responsible for the separation is complex and is probably due to a combination of hydrogen bonding, and dipole-dipole interaction of the sub-

TABLE I

HPLC SEPARATION OF (±)-PHYSOSTIGMINE AND (±)-ESERMETHOLE ON CHIRALCEL COLUMNS

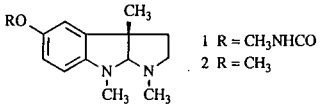

1 R = CH_3NHCO
2 R = CH_3

Mobile phases: A = isopropanol–hexane (5:95); B = ethanol–hexane (3:97); C = isopropanol–hexane (2:98). α = Separation factor; R_s = resolution factor.

Compound	Column	Mobile phase	Flow-rate (ml/min)	α	R_s	Less polar enantiomer
1	OD	A	0.5	1.11	<0.7	*S*
1	OJ	A	0.8	1.12	0.95	*S*
1	OJ	B	1.0	1.14	1.28	*S*
2	OD	C	0.6	1.36	<0.7	–
2	OJ	A	0.6	1.41	2.36	*S*

TABLE II

HPLC SEPARATION OF (±)-OXINDOLES ON CHIRALCEL COLUMNS

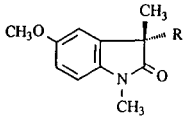

3 R = CH_2CN
4 R = allyl
5 R = 3-methyl-2-butenyl

Mobile phases: A = isopropanol–hexane (10:90); B = isopropanol–hexane (1:99); C = isopropanol–hexane (2:98). α = Separation factor; R_s = resolution factor.

Compound	Column	Mobile phase	Flow-rate (ml/min)	α	R_s	Less polar enantiomer
3	OD	A	1.0	1.32	3.32	*R*
3	OJ	A	1.0	1.04	<0.6	–
4	OD	B	0.7	1.0	<0.4	–
4	OJ	C	0.6	1.17	1.57	*R*
5	OJ	A	0.5	1.66	2.43	*R*

strates with the chiral stationary phases. Additional π–π interaction of the phenyl moeity of the substrate with that of the CSP may also be important for chiral recognition [3,4].

CONCLUSION

Both the Chiralcel OD and OJ columns are well suited for the analytical separation of chiral oxindoles. We have shown that by a proper choice of the CSP, enantiomers of all critical intermediates in the synthesis of (−)-physostigmine can be

TABLE III

HPLC SEPARATION OF (±)-1,3-DIMETHYL-5-METHOXYOXINDOLYLETHYLAMINE DERIVATIVES ON CHIRALCEL COLUMNS

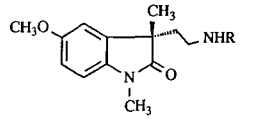

6 = H
7 = CO_2CH_3
8 = $COCH_3$
9 = COPh
10 = CO-3,5-$(NO_2)_2C_6H_3$

Mobile phases: A = isopropanol–hexane (10:90); B = isopropanol–hexane (15:85); C = isopropanol–hexane (20:80); D = ethanol–hexane (10:90). α = Separation factor; R_s = resolution factor.

Compound	Column	Mobile phase	Flow-rate (ml/min)	α	R_s	Less polar enantiomer
7	OD	A	1.0	1.90	2.24	*R*
7	OJ	A	0.6	1.08	0.87	*R*
8	OD	B	1.0	1.00	<0.4	–
9	OD	A	1.0	1.00	<0.4	–
9	OJ	A	1.0	1.00	<0.4	–
10	OD	C	0.8	1.32	1.03	*S*
10	OD	D	1.5	1.41	3.84	*S*

separated. This chiral HPLC method will facilitate our synthetic efforts and unambiguous determination of the optical purity of the synthetic material.

REFERENCES

1 T. B. K. Lee and G. S. K. Wong, *J. Org. Chem.*, (1990) in press.
2 P. L. Julian and J. Pikl, *J. Am. Chem. Soc.*, 57, (1935) 563.
3 Y. Okamoto, M. Kawashima and K. Hatada, *J. Chromatogr.*, 363 (1986) 173.
4 Y. Okamoto, R. Aburatani and K. Hatada, *J. Chromatogr.*, 389 (1987) 95.

Journal of Chromatography, 523 (1990) 321–326
Elsevier Science Publishers B.V., Amsterdam

CHROM. 22 748

Note

Simultaneous determination of thimerosal and chlorhexidine in solutions for soft contact lenses and its applications in stability studies

OLIVER YOA-PU HU*
School of Pharmacy, National Defense Medical Center, P.O. Box 90048-508, Taipei (Taiwan)
and
SHIANG-YI WANG, YAW-JU FANG, YUEN-HUA CHEN and MING-LU KING
Research and Development Department, Kingdom Pharmaceutical Co. Ltd., Taipei (Taiwan)
(First received March 1st, 1990; revised manuscript received July 25th, 1990)

Chlorhexidine, hexamethylenebis[5-(4-chlorophenyl)biguanide] (**I**), is a disinfectant which is effective against a wide range of vegetative Gram-positive and Gram-negative bacteria. Thimerosal, ethyl(sodium *o*-mercaptobenzoato)mercury (**II**), is an effective antibacterial and antifungal agent (Fig. 1). Both drugs are widely used together or alone as preservatives in pharmaceutical formulations, particularly, in liquid formulations such as ophthalmic solutions and storage and rinsing solutions for contact lenses.

Thimerosal is known to be unstable in aqueous solution [1,2]. It has also been reported that the presence of halides can have an adverse influence on the stability of

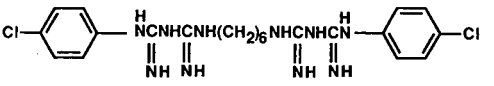

CHLORHEXIDINE
(I)

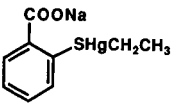

THIMEROSAL
(II)

Fig. 1. Structures of thimerosal and chlorhexidine.

0021-9673/90/$03.50

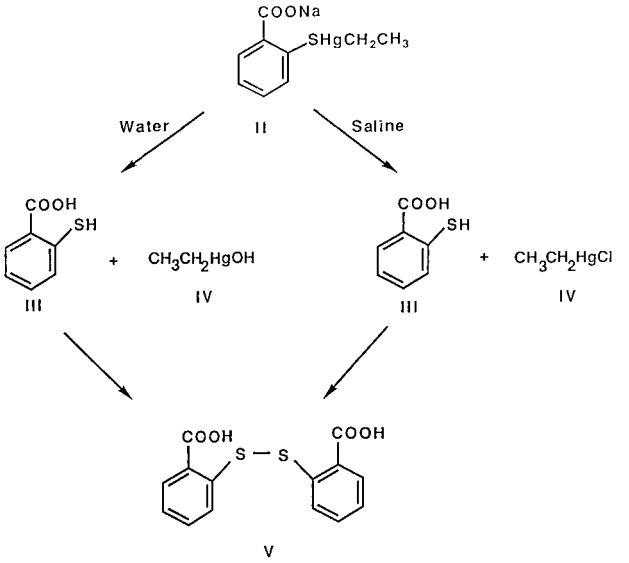

Fig. 2. Reaction scheme of the decomposition of thimerosal in aqueous solution. **II** = Thimerosal; **III** = thiosalicylic acid; **IV** = ethylmercury hydroxide; **V** = 2,2′-dithiosalicylic acid.

thimerosal [3,5], which also can be adsorbed from solutions stored in plastic containers [6]. The decomposition of thimerosal in aqueous solution has been studied [2], and it was shown that the major degradation products were thiosalicylic acid (**III**) and ethylmercury hydroxide (**IV**). Thiosalicylic acid in turn can undergo oxidative degradation irreversibly to 2,2′-dithiosalicylic acid (**V**) [7] (Fig. 2.).

In the past, chlorhexidine and thimerosal in pharmaceutical products have been determined by various conventional methods, such as UV spectrophotometry [8], polarography [9,10] and colorimetry [11,13] for thimerosal and colorimetry [14,15], gas chromatography [16–18] and by catalytic oxidation of [^{14}C]chlorhexidine [19] for chlorhexidine. These procedures are often tedious and time consuming.

Although a number of high-performance liquid chromatographic (HPLC) procedures such as the anion-exchange HPLC [20], HPLC with a radial-compression column [21], HPLC with electrochemical detection [22] and HPLC with atomic absorption [23] have been developed for the determination of thimerosal in dosage forms, there was no specific and accurate method available for simultaneous determination of thimerosal and chlorhexidine in soft contact lens storage and rinsing solutions.

This paper describes a stability-indicating method which rapidly and simultaneously determines thimerosal and chlorhexidine gluconate in solutions. The method has been successively applied in a stability study of contact lens storage and rinsing solutions containing thimerosal and chlorhexidine.

EXPERIMENTAL

Apparatus

The HPLC apparatus consisted of a Model 880-PU pump (JASCO, Tokyo, Japan), a SIC (Tokyo, Japan) Autosampler 23 automatic sampler, a JASCO 870-UV variable-wavelength UV detector and a SIC Chromatocorder 12 integrator. A 7-μm Nucleosil C_{18} column was used. For the column system a precolumn (7-μm Nucleosil C_{18}; Inpac International, Taipei, Taiwan) was also used.

Chemicals and reagents

Thimerosal and chlorhexidine (as gluconate) were purchased from E. Merck (Darmstadt, F.R.G.). Softline "Kingdom" storage and rinsing solution (thimerosal 0.0025%, chlorhexidine 0.0125%) was obtained from Kingdom Pharmaceutical (Taipei, Taiwan). All chemicals were of analytical-reagent grade and all solvents were of HPLC grade.

Chromatography

The assays for thimerosal and chlorhexidine were performed using the 7-μm Nucleosil C_{18} column and a mobile phase of 0.1 *M* KH_2PO_4 (pH 3.5)–methanol (40:60), prepared as follows. A 13.6-g amount of potassium dihydrogenphosphate was placed in a 1000-ml volumetric flask, 800 ml of distilled water were added and after dissolution, the solution was diluted to volume with distilled water. The final pH was 3.5, adjusted with phosphoric acid. This solution was mixed with 1500 ml of methanol and the mixture was degassed and filtered through a 0.45-μm membrane filter prior to use. A flow-rate of 1.0 ml/min, a UV detector wavelength of 254 nm (0.04 a.u.f.s.), ambient temperature and an injection volume of 20 μl were used in all the assays.

Precision, reproducibility, linearity and accuracy

Thimerosal (500.2 mg) and chlorhexidine gluconate (20%) (1089.9 mg) were weighed and transferred with the aid of *ca.* 30 ml of distilled water into a 100-ml volumetric flask. They were mixed well until all the ingredients had dissolved, then diluted to volume with distilled water. An aliquot of appropriate volume of the thimerosal and chlorhexidine gluconate solution was diluted with distilled water to make a series of diluted solutions covering the ranges 2–150 μg/ml of thimerosal and 2.72–436 μg/ml of chlorhexidine gluconate. A 50-μl volume of methylparaben (3 mg/ml), as internal standard, was added to each 1 ml of sample in the above sample solutions.

Stability study

Samples of the commercial product (Softlite "Kingdom" storage and rinsing solution), which were in their original containers kept in an environmental chamber of 45°C for periods of up to 3 months, were used as analytical samples. A 9.5-ml volume of these samples was transferred into a 10-ml volumetric flask containing 0.5 ml of internal standard solution (methylparaben, 3 mg/ml). The HPLC determinations were conducted at specific time intervals (0, 18, 30, 44, 61, 93 days). The same solution, kept in an environmental chamber at 4°C, was used as a control in the assays.

RESULTS AND DISCUSSION

A typical chromatogram of simultaneously determined thimerosal, thimerosal decomposition products and chlorhexidine gluconate is shown in Fig. 3. Under the

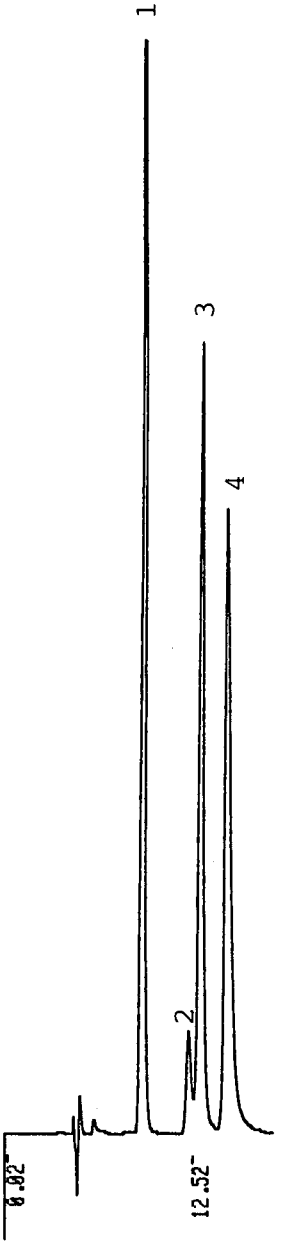

Fig. 3. Chromatogram of methylparaben, thiosalicylic acid, 2,2′-dithiosalicylic acid, thimerosal, and chlorhexidine. Peaks: 1 = methylparaben (3 μg); 2 = thiosalicylic acid (20 ng) and 2,2′-dithiosalicylic acid (20 ng); 3 = thimerosal (0.5 μg); 4 = chlorhexidine gluconate (2.5 μg). Time scale in min.

TABLE I

BETWEEN-DAY ACCURACY AND PRECISION OF THE DETERMINATION OF THIMEROSAL AND CHLORHEXIDINE GLUCONATE IN AQUEOUS SOLUTION BY HPLC

Compound	Actual concentration (μg/ml)	Measured concentration (mean ±S.D., $n = 3$)	R.S.D. (%) ($n = 3$)	Concentration determined expressed as % of the standard
Thimerosal	50.0	51.5 ± 0.40	0.77	103
Chlorhexidine gluconate	136	138 ± 2.50	1.81	101

assay conditions described, the retention times determined were 11.4 min (thimerosal), 14.9 min (chlorhexidine gluconate), 7.8 min (methylparaben) and 10.9 min (thiosalicylic acid, 2,2′-dithiosalicylic acid). The chromatogram clearly demonstrates that thiosalicylic acid and 2,2′-dithiosalicylic acid can be separated well from thimerosal and chlorhexidine gluconate. The sample was completely eluted in 20 min. The limit of detection of the assay was 0.1 μg for thimerosal and 0.2 μg for chlorhexidine gluconate.

Excellent linearity of the calibration graphs was observed over the range 2–150 μg/ml for thimerosal and 2.72–436 μg/ml for chlorhexidine gluconate. The within-day ($n = 3$) and between-day ($n = 10$) calibration graphs for chlorhexidine gluconate and thimerosal all had correlation coefficients of 0.999. Table I demonstrates the accuracy and precision of the determination of thimerosal and chlorhexidine gluconate in aqueous solution. The reproducibility of the method was determined by analysing the results of three replicate injections of a solution containing 50 μg/ml of thimerosal and 136 μg/ml of chlorhexidine gluconate. Thimerosal, which eluted first, was determined with a relative standard deviation (R.S.D.) of 0.77%. Chlorhexidine gluconate, which had the longest retention time, was determined with an R.S.D. of 1.81%.

In the stability study, the concentrations of thimerosal and chlorhexidine gluconate in the Softlite "Kingdom" storage and rinsing solution with time revealed that their contents in stability test samples at 45°C did not decrease significantly ($P > 0.05$) and no signs of thiosalicylic acid or 2,2′-dithiosalicylic acid were detected.

The proposed procedure offers a rapid and sensitive method for the routine simultaneous determination of thimerosal and chlorhexidine gluconate. Also, after a series of tests, the method was found to be insensitive to small variations of pH, in the ionic strength of the KH_2PO_4 solution and hence in minor variations in the composition of the mobile phase.

We conclude that the stability-indicating assay procedure presented here is accurate and precise for the simultaneous determination of thimerosal and chlorhexidine gluconate in solutions, and that the Softline storage and rinsing solution is stable for at least 3 months at 45°C.

REFERENCES

1 K. Tsuji, Y. Yamawaki and Y. Miyazaki, *Arch. Pract. Pharm.*, 24 (1951) 110.
2 F. Tanaka and M. Mitsuno, *Annu. Rep. Takeda Res. Lab.*, 10 (1951) 65.
3 K. Horworka and B. Horworka, R. Meyer, *Pharmazie*, 28 (1973) 136.
4 E. Ludtke and R. Pohloudek-Fabini, *Pharmazie*, 32 (1977) 625.

5 E. Ludtke, H. Darsow and R. Pohloudek-Fabini, *Pharmazie*, 32 (1977) 99.
6 N. E. Richardson, D. J. G. Davies, B. J. Meakin and D. A. Norton, *J. Pharm. Pharmacol.*, 29 (1977) 717.
7 M. Kharasch, *U.S. Pat.*, 2 012 820 (1935).
8 F. Neuwald and G. Schmitzek, *Pharm. Ztg.*, 112 (1967) 1308.
9 E. B. Beyer, *J. Assoc. Off. Anal. Chem.*, 52 (1969) 844.
10 T. Omura, S. Morishita and Y. Ueda, *Bunseki Kagaku*, 19 (1970) 941.
11 A. R. Neurath, *Cesk. Farm.*, 10 (1961) 75.
12 J. Viska and A. Okac, *Cesk. Farm.*, 15 (1966) 356.
13 J. Viska and A. Okac, *Cesk. Farm.*, 16 (1967) 29.
14 C. Andermann, M. O. Bubler and M. Erhart, *J. Pharm. Sci.*, 69 (1980) 215.
15 S. Pinzauti, E. LaPorta, M. Casini and C. Betti, *Pharm. Acta Helv.*, 57 (1982) 334.
16 K. Siefert, D. Casagrande, H. Silberman, *J. Chromatogr.*, 109 (1975) 193.
17 E. Cropper, R. Platt, A. Puttnam, *J. Soc. Cosmet. Chem.*, 26 (1975) 355.
18 B. F. Holmes, in E. Read (Editor), *Methodological Surveys in Biochemistry*, Vol. 7, Ellis Horwood, Chichester, 1978, p. 328.
19 D. L. Mackeen and K. Green, *J. Pharm. Pharmacol.*, 30 (1978) 678.
20 C. C. Fu and M. J. Sibley, *J. Pharm. Sci.*, 66 (1977) 738.
21 S. W. Lam, R. C. Meyer and L. T. Takahashi, *J. Parent. Sci. Technol.*, 35 (1981) 262.
22 G. C. Visor, R. A. Kenley, J. S. Fleitman, D. A. Neu and I. W. Partridge, *Pharm. Res.*, 2 (1985) 73.
23 W. Holak, *J. Liq. Chromatogr.*, 8 (1985) 563.

Author Index

Erratum

J. Chromatogr., 515 (1990) 451–457

Page 451, Abstract, 4th line, "dipeptides" should read "dipeptide amides".

END OF SYMPOSIUM PAPERS

Vol. 523

journal of
chromatography news section

ANNOUNCEMENTS OF MEETINGS

2nd INTERNATIONAL SYMPOSIUM ON SUPERCRITICAL FLUIDS, BOSTON, MA, U.S.A., MAY 19–21, 1991

The widespread interest in processing with supercritical fluids provided the impetus for organizing the 1st International Symposium on Supercritical Fluids held in Nice, France in October, 1988. Our objective for the 2nd International Symposium scheduled for 19–21 May, 1991, is to provide a forum for presenting state-of-the-art information on this emerging technology. We are encouraging participants to submit their most recent research work on fundamentals (*e.g.*, thermodynamics, high-pressure phase and reaction behavior, physico-chemical properties determination) as well as their most recent development work (*e.g.*, processing techniques, novel applications in areas such as materials science, etc.).

The proceedings will be published in advance of the conference and distributed to participants when they register.

Space is provided for companies to exhibit their products and manufacturing information concerning processing with supercritical fluids.

For further details contact: Symposium Chairman, Professor Mark A. HcHugh, Department of Chemcial Engineering, The Johns Hopkins University, Baltimore, Maryland 21218, U.S.A. Tel.: (301) 338-8752; Fax: (301) 338-5508 or (508) 794-9580.

4th EUROPEAN CONFERENCE ON THE SPECTROSCOPY OF BIOLOGICAL MOLECULES, HESLINGTON, U.K., 1–6 SEPTEMBER, 1991

The 4th European Conference on the Spectroscopy of Biological Molecules, ECSBM '91, will be held at the University of York, U.K., September 1–6, 1991.

This international conference will focus mainly on the structure and dynamics of biological and related systems as determined from Raman and IR spectroscopic methods. However, it also will provide a critically comparative review of recent progress in this field as achieved through the application of other methods, particularly NMR, CD, optical absorption and fluorescence, and X-ray crystallography. Topics to be included are: proteins — structure, conformation and dynamics; chromophoric proteins — haem systems, rhodopsins, photosynthetic systems, etc.; enzymes — reaction kinetics and mechanism; substrate/inhibitor interactions; nucleic acids — structure, conformation and dynamics; drug interactions; protein–nucleic acid interactions; biomembranes — lipids, organization, interactions with proteins; carbohydrates — oligo- and polysaccharides; biomedical/biotechnological applications; experimental methods; theoretical methods; and other topics.

The scientific programme will include invited lectures and poster sessions, with an emphasis on providing opportunities for discussion. There will be no parallel sessions.

Submission of oral and poster papers is invited in all the topic areas of the conference. The Organizing Committee will select the oral presentations and will issue invitations in December 1990.

A major exhibition of spectroscopic instrumentation and equipment will be held in conjunction with the scientific programme.

For further details contact: Professor R.E. Hester, ECSBM '91 Heslington, York, YO1 5DD, U.K.

Announcements are included free of charge. Information on planned events should be sent well in advance (preferably 6 months or more) to: Journal of Chromatography, News Section, P.O. Box 330, 1000 AH Amsterdam, The Netherlands, Fax: (31) 20-5862845.

CALENDAR OF FORTHCOMING EVENTS

Jan. 15–17, 1991
Park City, UT, U.S.A.

1991 Symposium on Supercritical Fluid Chromatography
Contact: Dr. M.L. Lee, Department of Chemistry, Brigham Young University, Provo, UT 84602, U.S.A. Tel.: (801) 378-2135; Fax: (801) 378–5474. (Further details published in Vol. 504, No. 2.)

Jan. 22–24, 1991
Paris, France

Congrès de Chromatographies en Phases Liquide et Supercritique
Contact: Société Française de Chimie, Division "Chimie Analytique", Congrès CPL/CPS, 250 rue Saint-Jacques, 75005 Paris, France. Tel.: (1) 43252078; Fax: (1) 40468380.

Jan. 22–24, 1991
Fort Lauderdale, FL, U.S.A.

***7th International Symposium on Separation Science and Biotechnology**
Contact: Janet E. Cunningham, Barr Enterprises, P.O. Box 279, Walkersville, MD 21793, U.S.A. Tel.: (301) 898-3772; Fax: (301) 898-5596.

Feb. 2–6, 1991
Salt Lake City, UT, U.S.A.

***2nd International Symposium on Field-Flow Fractionation**
Contact: Julie Westwood, FFF Research Center, Department of Chemistry, University of Utah, Salt Lake City, UT 84112, U.S.A. Tel.: (801) 581-5419. (Further details published in Vol. 513.)

Feb. 3–6, 1991
San Diego, CA U.S.A.

HPCE '91, 3rd International Symposium on High Performance Capillary Electrophoresis
Contact: HPCE '91, Ms. Shirley E. Schlessinger, Symposium Manager, 400 East Randolph Drive, Suite 1015, Chicago, IL 60601, U.S.A. (Further details published in Vol. 504, No. 2.)

Feb. 10–15, 1991 Melbourne, Australia	**POLYMER '91, Polymer Materials: Preparation, Characterization and Properties** Contact: POLYMER '91 Secretary, P.O. Box 224, Belmont, Vic. 3216, Australia.
March 1, 1991 Cardiff, U.K.	***Symposium on Gas Headspace Vapour Analyzers and Monitors** Contact: Dr. J.D.R. Thomas, School of Chemistry and Applied Chemistry, University of Wales College of Cardiff, P.O. Box 912, Cardiff CF1 3TB, U.K. Tel.: (0222) 87400, ext. 5853; Fax: (0222) 371921.
March 4–7, 1991 Les Diablerets, Switzerland	**4th Hans Wolfgang Nürnberg Memorial Workshop on Toxic Metal Compounds (Interrelation Between Chemistry and Biology)** Contact: Dr. Ernest Merian, Im Kirsgarten 22, CH-4106 Therwil, Switzerland.
March 4–8, 1991 Chicago, IL, U.S.A.	***42nd Pittsburgh Conference and Exposition on Analytical Chemistry and Applied Spectroscopy** Contact: Mrs. Alma Johnson, Program Secretary, The Pittsburgh Conference, 300 Penn Center Blvd., Suite 332, Pittsburgh, PA 15235, U.S.A. (Further details published in Vol. 513.)
March 11–13, 1991 Lausanne, Switzerland	**2nd Soil Residue Analysis Workshop** Contact: Professor J. Tarradellas, IGE-EPFL, 1015 Lausanne, Switzerland.
March 19–21, 1991 Washington, DC, U.S.A.	***International Electrophoresis Society Meeting** Contact: Mrs. Janet Cunningham, IES Symposium Manager, Barr Enterprises, P.O. Box 279, Walkersville, MD 21793, U.S.A. Tel.: (301) 898-3772; Fax: (301) 898-5596. (Further details published in Vol. 513.)
March 26, 1991 Maarssen, The Netherlands	***4th Symposium on Fast Protein Liquid Chromatography** Contact: Marianne Wobma, Pharmacia Nederland BV, Houttuinlaan 4, 3447 GM Woerden, The Netherlands. Tel.: (03480) 77631. (Further details published in Vol. 513.)
April 28–May 1, 1991 Boston, MA, U.S.A.	***3rd International Symposium on Pharmaceutical and Biomedical Analysis** Contact: Ms. Shirley E. Schlessinger, Symposium Manager PBA '91, 400 East Randolph Drive, Suite 1015, Chicago, IL 60601, U.S.A. Tel.: (312) 527-2011. (Further details published in Vol. 513.)
May 13–15, 1991 Arlington, VA, U.S.A.	***8th International Symposium on Preparative Chromatography** Contact: Janet E. Cunningham, Barr Enterprises, P.O. Box 279, Walkersville, MD 21793, U.S.A. Tel.: (301) 898-3772; Fax: (301) 898-5596. (Further details published in Vol. 513.)

May 19–21, 1991
Boston, MA, U.S.A.

***2nd International Symposium on Supercirtical Fluids**
Contact: Mark A. McHugh, Department of Chemical Engineering, The John Hopkins University, Baltimore, MD 21218, U.S.A. Tel.: (301) 338-8752; Fax: (301) 338-5508 or (508) 794-9580.

May 21, 1991
Washington, DC,
U.S.A.

***CHROMEXPO-91 (Chromatography Exhibition, Poster Session, Educational Seminars)**
Contact: Janet E. Cunningham, Barr Enterprises, P.O. Box 279, Walkersville, MD 21793, U.S.A. Tel.: (301) 898-3772; Fax: (301) 898-5596.

May 27–31, 1991
Rome, Italy

2nd International Symposium on Chiral Discrimination
Contact: Professor D. Misiti or Professor F. Gasparrini, Laboratori di Chimica Organica, Facoltà di Farmicia, Università "La Sapienza", Piazzale Aldo Moro 5, 00185 Rome, Italy. Tel.: (06) 4452900; fax: (06) 49912780. (Further details published in Vol. 477, No. 2.)

May, 27–31, 1991
Ghent, Belgium

IVth International Symposium on Quantitative Luminescence Spectrometry in Biomedical Sciences
Contact: Dr. Willy R.G. Baeyens, Symposium chairman, State University of Ghent, Pharmaceutical Institute, Harelbekestraat 72, B-9000 Ghent, Belgium. (Further details published in Vol. 483.)

June 3–7, 1991
Basel, Switzerland

HPLC '91, 15th International Symposium on Column Liquid Chromatography
Contact: Secretariat HPLC '91, Convention Center Basel, Congress Department, P.O. Box, CH-4021 Basel, Switzerland. (Further details published in Vol. 477, No. 2.)

June 4–6, 1991
Egham, U.K.

***5th International LIMS Conference**
Contact: The Conference Registrar, 5th International LIMS Conference, P.O. Box 341, High Wycombe, Buckinghamshire HP11 2QG, U.K. Tel.: (0494) 24769.

June 9–14, 1991
Bergen, Norway

XXVII Colloquium Spectroscopicum Internationale
Contact: Secretariat XXVII CSI, HSD Congress-Conference, P.O. Box 1721 Nordnes, N-5024 Bergen, Norway. Tel.: (475) 318414; Telex: 42607 hsd n, Fax: (475) 324555. (Further details published in Vol. 508, No.2.)

June 10–13, 1991
San Francisco,
CA, U.S.A.

***5th Annual Seminar on Analytical Biotechnology**
Contact: Janet E. Cunningham, Barr Enterprises, P.O. Box 279, Walkersville, MD 21793, U.S.A. Tel.: (301) 898-3772; Fax: (301) 898-5596.

July 16–18, 1991 London, U.K.	**Two-Dimensional Polyacrylamide Gel Electrophoresis** Contact: Conference Secretariat 2-D PAGE 1991, Department of Cardiothoracic Surgery, National Heart & Lung Institute, Dovehouse Street, London SW3 6LY, U.K. (Further details published in Vol. 504, No. 2.)
Aug. 17–22, 1991 Budapest, Hungary	**33rd IUPAC Congress** Contact: 33rd IUPAC Congress, E. Pungor, c/o Hungarian Academy of Sciences, Gellèrt ter 4, H-1111 Budapest, Hungary.
Aug. 21–24, 1991 Kumamoto, Japan	**5th International Conference on Flow Analysis** Contact: Professor Ishibashi, Department of Applied Analytical Chemistry, Faculty of Engineering 36, Kyushu University, Hokazaki, Higashiku, Fukuoka 812, Japan. (Further details published in Vol. 475.)
Aug. 25–31, 1991 Makuhari, Japan	**ICAS '91, IUPAC International Congress on Analytical Sciences** Contact: ICAS '91 Secretariat, The Japan Society for Analytical Chemistry, 1-26-2 Nishigotande, Shinagawa, Tokyo 141, Japan. Tel.: (813) 490-3351; fax: (813) 490-3572. (Further details published in Vol. 483.)
Sept. 1–6, 1991 Lubeck-Travemunde, F.R.G.	**8th International Conference on Fourier Transform Spectroscopy** Contact: Gesellschaft Deutscher Chemiker, Abt. Tagungen, P.O. Box 900440, D-6000 Frankfurt 90, F.R.G. Tel.: 17-366/360; Fax: (79) 17475; Telex: 4170497 gdch d.
Sept. 2–6, 1991 Warsaw, Poland	**8th Danube Symposium on Chromatography** Contact: 8th Danube Symposium on Chromatography, Janusz Lipkowski, Institute of Physical Chemistry of the Polish Academy of Sciences, Kasprzaka 44/52, 01-224 Warsaw, Poland. (Further details published in Vol. 502, No. 2.)
Sept. 4–6, 1991 Bilthoven, The Netherlands	**3rd Workshop on Chemistry and Fate of Modern Pesticides** Contact: Pesticides Workshop Office, Dr. P. van Zoonen, RIVM, P.O. Box 1, 3720 Bilthoven, The Netherlands. (Further details published in Vol. 472, No. 2.)
Sept. 24–25, 1991 Baden Baden, F.R.G.	***Short Course on Sample Handling in Liquid Chromatography** Contact: Workshop Office, IAEAC, M. Frei-Häusler, Postfach 46, CH-4123 Allschwil 2, Switzerland. Tel.: (004161) 632789 and (004161) 732950.
Sept. 24–28, 1991 Yokohama, Japan	**9th International Symposium on Affinity Chromatography and Biological Recognition** Contact: Professor Ken-ichi Kasai, Faculty of Pharmaceutical Sciences, Teikyo University, Sagamiko, Tsukui, Kanagawa 199-01, Japan.

Sept. 26–27, 1991 Baden Baden, F.R.G.	***5th Symposium on Handling of Environmental and Biological Samples in Chromatography** Contact: Workshop Office, IAEAC, M. Frei-Häusler, Postfach 46, CH-4123 Allschwil 2, Switzerland. Tel.: (004161) 632789 and (004161) 732950. (Further details published in Vol. 513.)
Oct. 14–18, 1991 Budapest, Hungary	**ECASIA 91, 4th European Conference on Applications of Surface and Interface Analysis** Contact: ECASIA 91, MTA ATOMKI, Pf. 51, H-4001 Debrecen, Hungary. Tel.: (36) 52-16181; Telex: 72210 (atom h); Fax: (36) 52-16181.
Oct. 20–23, 1991 Washington, DC, U.S.A.	***11th International Symposium on High-Performance Liquid Chromatography of Proteins, Peptides and Polynucleotides** Contact: Janet E. Cunningham, Barr Enterprises, P.O. Box 279, Walkersville, MD 21793, U.S.A. Tel.: (301) 898-3772; Fax: (301) 898-5596. (Further details published in Vol. 513.)
Jan. 6–11, 1992 California, U.S.A.	***1992 Winter Conference on Plasma Spectrochemistry** Contact: 1992 Conference on Plasma Spectrochemistry, Attn.: R. Barnes, c/o ICP Information Newsletter, Department of Chemistry, GRC Towers, University of Massachusetts, Amherst, MA 01003-0035, U.S.A. Tel.: (413) 545-2294; Fax: (413) 545-4490; BITNET: RBARNES@UMASS. (Further details published in Vol. 513.)
Feb. 18–21, 1992 Antwerp, Belgium	**2nd International Symposium on Hyphenated Techniques in Chromatography** Contact: Dr. R. Smits, p.a. BASF Antwerpen N.V., Scheldelaan B-2040 Antwerp, Belgium. Tel.: (32) 5682831; Fax: (323) 5683355; Telex: 31047 basant b. (Further details published in Vol. 508, No. 2.)
May 17–22, 1992 Kyoto, Japan	**4th International Conference on Fundamentals of Adsorption** Contact: Prof. M. Suzuki, Conference Chairman, Institute of Industrial Science, University of Tokyo, 7-22-1 Roppongi, Minatoku, Tokyo 106, Japan. (Further details published in Vol. 508, No. 2.)

* Indicates new or amended entry

PUBLICATION SCHEDULE FOR 1990

Journal of Chromatography and Journal of Chromatography, Biomedical Applications

MONTH	J	F	M	A	M	J	J	A	S	O	N	D
Journal of Chromatography	498/1 498/2 499	500 502/1	502/2 503/1 503/2 504/1	504/2 505/1	505/2 506 507 508/1	508/2 509/1 509/2 510	511 512 513	514/1 514/2 515	516/1 516/2 517 518/1	518/2 519/1	519/2 520 521/1 521/2 522	523
Cumulative Indexes, Vols. 451–500		501										
Bibliography Section		524/1		524/2		524/3		524/4		524/5		524/6
Biomedical Applications	525/1	525/2	526/1	526/2 527/1	527/2	528/1 528/2	529/1	529/2 530/1	530/2	531 532/1	532/2 533	534

INFORMATION FOR AUTHORS

(Detailed *Instructions to Authors* were published in Vol. 522, pp. 351–354. A free reprint can be obtained by application to the publisher, Elsevier Science Publishers B.V., P.O. Box 330, 1000 AH Amsterdam, The Netherlands.)

Types of Contributions. The following types of papers are published in the *Journal of Chromatography* and the section on *Biomedical Applications*: Regular research papers (Full-length papers), Review articles and Short Communications. Short Communications are usually descriptions of short investigations and reflect the same quality of research as Full-length papers, but should preferably not exceed six printed pages. Letters to the Editor can comment on (parts of) previously published articles, or they can report minor technical improvements of previously published procedures; they should preferably not exceed two printed pages. For review articles, see inside front cover under Submission of Papers.

Submission. Every paper must be accompanied by a letter from the senior author, stating that he is submitting the paper for publication in the *Journal of Chromatography*. Please do not send a letter signed by the director of the institute or the professor unless he is one of the authors.

Manuscripts. Manuscripts should be typed in double spacing on consecutively numbered pages of uniform size. The manuscript should be preceded by a sheet of manuscript paper carrying the title of the paper and the name and full postal address of the person to whom the proofs are to be sent. As a rule, papers should be divided into sections, headed by a caption (*e.g.*, Abstract, Introduction, Experimental, Results, Discussion, etc.). All illustrations, photographs, tables, etc., should be on separate sheets.

Introduction. Every paper must have a concise introduction mentioning what has been done before on the topic described, and stating clearly what is new in the paper now submitted.

Abstract. Full-length papers and Review articles should have an abstract of 50–100 words which clearly and briefly indicates what is new, different and significant. (Notes and Letters to the Editor are published without an abstract.)

Illustrations. The figures should be submitted in a form suitable for reproduction, drawn in Indian ink on drawing or tracing paper. Each illustration should have a legend, all the *legends* being typed (with double spacing) together on a *separate sheet*. If structures are given in the text, the original drawings should be supplied. Coloured illustrations are reproduced at the author's expense, the cost being determined by the number of pages and by the number of colours needed. The written permission of the author and publisher must be obtained for the use of any figure already published. Its source must be indicated in the legend.

References. References should be numbered in the order in which they are cited in the text, and listed in numerical sequence on a separate sheet at the end of the article. Please check a recent issue for the layout of the reference list. Abbreviations for the titles of journals should follow the system used by *Chemical Abstracts*. Articles not yet published should be given as "in press" (journal should be specified), "submitted for publication" (journal should be specified), "in preparation" or "personal communication".

Dispatch. Before sending the manuscript to the Editor please check that the envelope contains four copies of the paper complete with references, legends and figures. One of the sets of figures must be the originals suitable for direct reproduction. Please also ensure that permission to publish has been obtained from your institute.

Proofs. One set of proofs will be sent to the author to be carefully checked for printer's errors. Corrections must be restricted to instances in which the proof is at variance with the manuscript. "Extra corrections" will be inserted at the author's expense.

Reprints. Fifty reprints of Full-length papers, Notes and Letters to the Editor will be supplied free of charge. Additional reprints can be ordered by the authors. An order form containing price quotations will be sent to the authors together with the proofs of their article.

Advertisements. Advertisement rates are available from the publisher on request. The Editors of the journal accept no responsibility for the contents of the advertisements.

For Superior Chiral Separation From Analytical To Preparative.

The finest from DAICEL·····

Why look beyond DAICEL? We have developed the finest CHIRALCEL, CHIRALPAK and CROWNPAK with up to 17 types of HPLC columns, all providing superior resolution of racemic compounds.

NEW CHIRALPAK AS

● CHIRALPAK AS

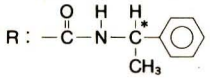

for β-Lactam antibiotics

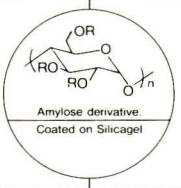

NEW CHIRALPAK AD

● CHIRALPAK AD

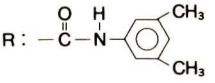

4-Acetoxy-2-azetidine

Eluent : Hexane/Ethanol = 8/2
Flow rate : 1.0mℓ/min
Temperature : r.t.
Detection : UV254nm

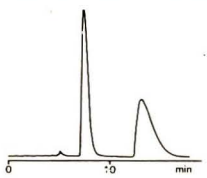

Oxyphencyclimine

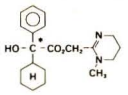

Eluent : Hexane/2-Propanol = 9/1
Flow rate : 1.0mℓ/min
Temperature : r.t.
Detection : UV254nm

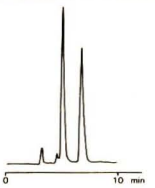

Ofloxacine methyl ester

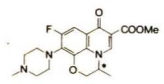

Eluent : Hexane/EtOH = 8/2
Flow rate : 1.2mℓ/min
Temperature : 40°C
Detection : UV254nm

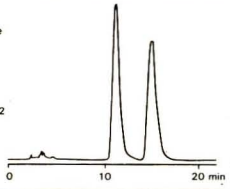

Verapamil

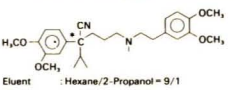

Eluent : Hexane/2-Propanol = 9/1
Flow rate : 1.0mℓ/min
Temperature : r.t.
Detection : UV254nm

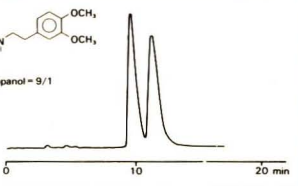

Analytical column 0.46cm × 25cm(10μm)

- CHIRALCEL OA
  OB
  OC
  OD
  OJ
  OF
  OG
  OK
- CHIRALPAK AS
  AD

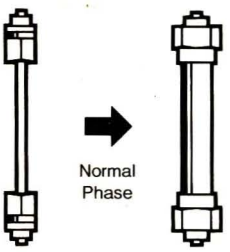

Semi-preparative column 2cm × 25cm(10μm)

You can have Pure enantiomer quickly!!

■Separation Service

- A pure enantiomer separation in the amount of 100g ~ 10kg is now available.
- Please contact us for additional information regarding the manner of use and application of our chiral columns and how to procure our separation service.

DAICEL CHEMICAL INDUSTRIES, LTD.

chiral chemicals division.
8-1, Kasumigaseki 3-chome, Chiyoda-ku, Tokyo 100, Japan Phone: 03 (507) 3151 FAX: 03 (507) 3193

DAICEL(U.S.A.), INC.
Fort Lee Executive Park
Two Executive Drive, Fort Lee,
New Jersey 07024
Phone: (201) 461-4466
FAX: (201) 461-2776

DAICEL(U.S.A.), INC.
23456 Hawthorne Blvd.
Bldg. 5, Suit 130
Torrance, CA 90505
Phone: (213) 791-2030
FAX: (213) 791-2031

DAICEL(EUROPA)GmbH
Oststr. 22
4000 Düsseldorf 1, F.R. Germany
Phone: (211) 369848
Telex: (41) 8588042 DCEL D
FAX: (211) 364429

DAICEL CHEMICAL(ASIA)PTE. LTD.
65 Chulia Street #40-07
OCBC Centre, Singapore 0104
Phone: 5332511
FAX: 5326454